



**HAL**  
open science

# An integrated method for the transient solution of reduced order models of geometrically nonlinear structural dynamic systems

Fritz Adrian Lülfi

► **To cite this version:**

Fritz Adrian Lülfi. An integrated method for the transient solution of reduced order models of geometrically nonlinear structural dynamic systems. Structural mechanics [physics.class-ph]. Conservatoire national des arts et métiers - CNAM, 2013. English. NNT : 2013CNAM0884 . tel-00957455

**HAL Id: tel-00957455**

**<https://theses.hal.science/tel-00957455>**

Submitted on 10 Mar 2014

**HAL** is a multi-disciplinary open access archive for the deposit and dissemination of scientific research documents, whether they are published or not. The documents may come from teaching and research institutions in France or abroad, or from public or private research centers.

L'archive ouverte pluridisciplinaire **HAL**, est destinée au dépôt et à la diffusion de documents scientifiques de niveau recherche, publiés ou non, émanant des établissements d'enseignement et de recherche français ou étrangers, des laboratoires publics ou privés.

École Doctorale du Conservatoire National des Arts et Métiers  
Laboratoire de Mécanique des Structures et des Systèmes Couplés

**THÈSE DE DOCTORAT**

*présentée par* : Dipl.-Ing. **Fritz Adrian LÜLF**

*soutenue le* : **5 décembre 2013**

*pour obtenir le grade de* : **Docteur du Conservatoire National des Arts et Métiers (ED 415)**

*Discipline / Spécialité* : **Mécanique**

**An integrated method for the transient solution of reduced order  
models of geometrically nonlinear structural dynamic systems**

**MEMBRES DU JURY:**

Hermann G. MATTHIES	Président du jury	TU Braunschweig
Roger OHAYON	Directeur de thèse	CNAM/LMSSC Paris
Duc-Minh TRAN	Encadrant de thèse	ONERA/DADS
Jean-Pierre GRISVAL	Examineur	ONERA/DADS
Georges JACQUET-RICHARDET	Rapporteur	INSA/LaMCoS Lyon
Fabrice THOUVEREZ	Rapporteur	ECL/LTDS Lyon

*"A study of finite deformation will require that cherished assumptions be abandoned and a fresh start made with an open (but not empty!) mind."  
Javier Bonet and Richard D. Wood*

# Remerciements

Dans l'esprit de Bonnet et Wood je remercie tout le personnel du *Département Aéroélasticité et Dynamique des Structures* de m'avoir accueilli au sein de leur équipe avec convivialité et pour l'enthousiasme que nous avons partagé pendant ces trois années passées.

Je tiens à remercier particulièrement mon directeur de thèse

**Roger Ohayon**  
et  
**Duc Minh Tran,**

mon encadrant, de m'avoir fait confiance pour réaliser ce travail, de m'avoir corrigé pendant les moments les plus cruciaux et de leur aide lors la réalisation de mes travaux. Vous m'avez permis d'acquérir beaucoup de nouvelles compétences en mécanique et au delà.

Je remercie également M. Jean-François Deü et M. Jean-Sébastien Schotté pour leurs cours en dynamique non-linéaire et interaction fluide-structure.

Mein besonderer Dank gilt Herrn Prof. Matthias (PhD) und seinen Mitarbeitern am Institut für wissenschaftliches Rechnen der Technischen Universität Braunschweig, wo ich einen sehr lehrreichen Forschungsaufenthalt verbringen konnte. Außerdem wurde ich durch sie auch im Laufe zahlreicher Konferenzen und Seminare immer wieder mit richtungsweisenden Denkanstößen angeregt.

Mein herzlichster Dank geht auch an meine Familie und meine Freunde in Deutschland und in Frankreich, die mich in der herausfordernden Zeit meiner Promotion begleitet haben.

Zu guter letzt richte ich meinen innigsten Dank an Ann Jeanine. Du bist mit Deinem Pragmatismus immer zur Stelle, wenn ich mit meinem nicht mehr weiter weiß.

---

# Abstract

In the context of modern structural dynamics transient simulations require that nonlinear phenomena, e.g. vibrations with finite amplitude, are taken into account in a rigorous manner in order to comply with the ever tightening requirements of accuracy. For the description of the dynamic behaviour of a geometrically nonlinear structure much evolved formulations are available. The direct transient solutions of finite element problems based on these formulations remain costly despite the constant growth of available computational power. When the reduction of the computational cost is required, especially when these solutions have to be obtained repeatedly as it is the case during e.g. optimisation or coupling with another numeric solver, the introduction of a reduced model of the geometrically nonlinear structure becomes necessary. The model reduction techniques are well developed for linear systems but in the context of the dynamics of geometrically nonlinear structures they have yet to reach their full potential.

This work creates a method that yields rapid, accurate and parameterisable transient solutions of geometrically nonlinear structures under external excitation. The structures are supposed to be already discretised and their dynamic equilibrium is described with a matrix equation.

The projection on a reduced basis is used to create a reduced model of the geometrically nonlinear structure. Also reduction methods that do not rely on a projection, like the Nonlinear Normal Modes and the Proper Generalised Decomposition, are explored.

The choice of the projection on a reduced basis entails the choice of an approach that is used to create the reduced basis. A number of common reduced bases are presented and the choice between them is based on numerical experiments. The objective of these simulations is two-fold. They determine which of the reduced bases is best suited for a certain combination of nonlinearity and external forcing, and they determine to which extent these bases possess an inherent robustness. The bases' capabilities are evaluated with respect to the quality of the reconstructed transient solution when they are used to reduce the test-case for which they were originally created. Their inherent robustness is evaluated on the basis of reconstructed transient solutions when the reduced bases are applied to the same system under a differently parameterised excitation. A novel type of multi-criteria decision analysis error metric is proposed to this effect.

The test-cases are combinations of a locally and an entirely nonlinear academic system under excitations of either harmonic or impulse type. A nonlinear Newmark scheme with inflation of the nonlinear terms is used to obtain transient solutions and to limit the error to the introduction of the reduced basis.

One of the results of this comprehensive study is a mapping of the different bases' performances against the combinations of the type of nonlinearity and the type of excitation. From this it becomes evident that, depending on the application, not all bases are equally well suited for reducing a given type of nonlinearity. The results show clearly that the choice of the most appropriate reduced basis depends foremost on the type of excitation and only second to that on the nonlinearity of the system.

A lack of robustness is observed for all reduced bases. The results concerning the bases' robustness indicate the tendencies in sensitivity of the resulting bases with respect to changes in the parameters describing the excitation. They show that the bases should be established at the most critical values of the parameters, e.g. the highest amplitude of the external forcing. A pronounced similarity of the vectors forming the

---

different bases is also established.

However, the obtained results also show that the introduction of the reduced basis alone is not sufficient to allow for the nonlinear evolution of the transient solution. The use of an inflation formulation of the nonlinear terms is not feasible under performance considerations. From these findings three requirements are identified for the algorithm that is to yield a rapid, accurate and parameterisable transient solution. The solution algorithm has to be adapted in order to allow for the nonlinear evolution of the transient solution, the reduced solution has to be rendered independent from the full order model by introducing an autonomous formulation of the nonlinear terms and the reduced basis has to be adapted to external parameters.

Each of these three requirements is addressed with a specific method. The choice of the respective method is based on the presentation of several common approaches for addressing the same requirement and the exploration of their respective qualities with numerical experiments.

For adapting the solution algorithm the update of the reduced basis is introduced. This method is specially conceived and expanded with the augmentation of the reduced bases. The augmentation flattens jumps in the physical quantities that occur when the update is performed in intervals. This original method is chosen over the quasistatic correction and the Least-Squares Petrov-Galerkin method, both from literature.

For expressing the nonlinear terms with an autonomous formulation the polynomial formulation is selected. It expresses the nonlinear terms for the nonlinear internal forces and the tangent stiffness matrix with a sum of tensor vector products. A dedicated identification approach based on static nonlinear solutions allows the determination of tensors. During numerical tests the polynomial formulation shows a much higher degree of accuracy in reproduced the nonlinear terms than approaches such as the direct linearisation or the linear interpolation.

For adapting the reduced basis to external parameters an interpolation approach is taken from literature. This approach transforms the reduced bases in a tangent space where the actual interpolation takes place. Upon retransformation the interpolated basis for a given set of parameters becomes available.

The integrated method is the central result of this work. It allows reaching the initially stated aim of obtaining a rapid, accurate and parameterisable transient solution of a geometrically nonlinear structure. The integrated method is created by uniting the three selected methods of update and augmentation of the reduced basis, the polynomial formulation of the nonlinear terms and the interpolation for adapting the reduced basis. A Newmark-type time-marching solution algorithm forms the common backbone for the three methods. The application of the integrated method on test-cases with geometrically nonlinear finite elements confirms that this method responds to the initial aim of an rapid, accurate and parameterisable transient solution.

The integrated method, as it presented in this work, can be seen as one particular realisation of a more general framework. This framework covers all aspects of the reduction of nonlinear systems by projection on a reduced basis with the aim of obtaining a transient solution. The methods that are actually used for the integrated method are only examples that prove to be preferable for the application at hand. It is believed that for any application a comparable integrated method can be conceived.

The entire work is wrapped in a detailed development of discrete geometrically nonlinear structural dynamics. The discrete nonlinear dynamics form the application of the integrated method. It is extensively described in order identify the limits of the safe application of the integrated method. The finite element test-cases on which the integrated method is applied are comprehensively characterised to demonstrate the kind of problems for which the integrated method is conceived.

**Keywords :** structural dynamics, geometric nonlinearities, model reduction, reduced bases, linear normal modes, proper orthogonal decomposition, basis update, parameters

---



# Résumé

Dans le contexte des structures modernes les calculs en dynamique transitoire nécessitent la prise en compte rigoureuse des phénomènes nonlinéaires, comme par exemple les vibrations avec des grandes amplitudes, pour répondre aux exigences d'exactitude de plus en plus sévères. Pour décrire la dynamique d'une structure géométriquement nonlinéaire des formulations très évoluées sont disponibles. Les simulations temporelles directes des modèles éléments finis de ces formulations sont encore très coûteuses, malgré les progrès constants sur la puissance des moyens de calcul. Afin de réduire les coûts de calcul, surtout quand ces calculs doivent être réalisés plusieurs fois dans le cadre d'une optimisation ou par exemple en couplage avec une simulation d'aérodynamique, la construction des modèles réduits de la structure nonlinéaire s'avère nécessaire. Les techniques de réduction de modèle sont bien développées pour des systèmes linéaires mais dans le contexte de la dynamique d'une structure géométriquement nonlinéaire, qui pose des challenges spécifiques, elles ne sont pas encore arrivées à la fin de leur potentiel.

Ce travail aboutit à la création d'une méthode qui permet des solutions transitoires accélérées, fidèles et paramétrables d'une structure géométriquement nonlinéaire soumise à une excitation externe. La structure est supposée d'être déjà discrétisée et son équilibre dynamique doit être décrit par une équation matricielle.

La projection sur une base réduite est introduite afin d'obtenir un modèle réduit. D'autres méthodes de réduction, qui ne s'appuient pas sur une projection, comme les Modes Nonlinéaires Normales et la Décomposition Généralisée Propre, sont également considérées.

Le choix de l'introduction de la projection sur une base réduite entraîne le choix d'une approche qui fournit la base réduite. Quelques approches communes pour la création d'une base réduite sont présentées et le choix est basé sur des expériences numériques. L'objectif de cette étude numérique est double. Elle vise de déterminer laquelle des différentes méthodes de création engendre la base de projection la mieux adaptée pour une combinaison donnée de la nonlinéarité et de l'excitation et jusqu'à quelle mesure les bases sont robustes face à un changement des paramètres externes. Les qualités des bases réduites sont évaluées avec la solution transitoire reconstruite, qui est obtenue quand les bases sont utilisées pour réduire les cas test pour lequel elles étaient construites au préalable. Leur robustesse inhérente est déterminée également avec les solutions transitoires reconstruites, quand les bases sont utilisées pour réduire le même cas-test avec des paramètres différents. A cet effet une nouvelle mesure d'erreur est proposée. Elle est inspirée de l'aide à la décision multicritère.

Les cas test académiques sont constitués d'un système localement ou entièrement non-linéaire et soumis à une excitation harmonique ou impulsionnelle. Un algorithme du type Newmark avec inflation des termes nonlinéaires est utilisé pour obtenir des solutions transitoires dont l'erreur est limitée à l'introduction de la base.

Un des résultats de cette étude complète est un classement de la performance des bases réduites différentes pour les différents types de nonlinéarité et d'excitation. De là il devient évident, que, selon l'application, pas toutes les bases réduites ne sont aussi bien adaptées pour réduire un certain type de nonlinéarité. Ces résultats montrent clairement que le choix de la méthode la plus appropriée dépend d'abord du type d'excitation et seulement secondairement de la non-linéarité du système. Un manque de robustesse est constaté pour toutes les bases pour des changements des paramètres de l'excitation. Ceci peut être atténué si les bases

---

sont construites avec la valeur la plus critique du paramètre par exemple avec la plus grande force appliquée. Une adaptation de la base de réduction s'avère donc nécessaire. La ressemblance prononcée des vecteurs des différentes bases réduites est également démontrée.

Cependant il est aussi mis en évidence d'une manière très claire que la simple introduction d'une base réduite n'est pas suffisante pour prendre en compte le comportement nonlinéaire. L'utilisation de l'inflation des termes nonlinéaires n'est pas faisable sous en considérant la performance. A partir de ces résultats trois exigences à une méthode pour une solution transitoire rapide, d'une qualité haute et paramétrable sont déduites. L'algorithme de solution doit permettre un suivi de l'évolution nonlinéaire de la solution transitoire, la solution réduite doit être rendue indépendante du modèle grand-ordre en éléments finis en remplaçant les termes nonlinéaires avec une formulation autonome et la base réduite doit être adaptée à des paramètres externes.

Trois méthodes spécifiques sont préparées et chacune de ces méthodes répond à une des trois exigences.

Pour la prise en compte de l'évolution nonlinéaire la méthode de la mise-à-jour et augmentation de la base réduite est conçue et enrichie d'une manière expresse. L'augmentation lisse des sauts qui apparaissent dans les déplacements physiques quand la mise-à-jour est effectuée en intervalles. Cette méthode novatrice est préférée à la correction quasistatique et la méthode Petrov-Galerkin aux moindres carrées, les deux prises de la littérature.

Pour l'expression des termes nonlinéaires avec une formulation autonome la formulation polynomiale est choisie. Elle exprime les termes nonlinéaires des forces internes et de la matrice de raideur tangente avec une somme des produits tenseur vecteur. Une approche d'identification dédiée et basée sur des solutions nonlinéaires statiques permet la détermination des tenseurs. Lors des tests numériques la formulation polynomiale produit un degré d'exactitude beaucoup plus élevé lors de la reproduction des termes nonlinéaires que d'autres approches comme la linéarisation directe ou l'interpolation linéaire.

Pour l'adaptation des bases réduites à des paramètres externes une approche d'interpolation est prise de la littérature. Cette approche transforme les bases réduites dans un espace tangent, où l'interpolation proprement dite a lieu. Après re-transformation la base interpolée devient disponible.

La méthode intégrée est le résultat central de ce travail. Elle permet d'atteindre le but initial d'une solution transitoire accélérée, fidèle et paramétrable d'une structure géométriquement nonlinéaire. La méthode intégrée est créée par l'unification des trois méthodes choisies: la mise-à-jour et augmentation de la base réduite, la formulation polynomiale des termes nonlinéaires et l'interpolation de la base réduite à des paramètres externes. Un algorithme de type Newmark forme le cadre de la méthode intégrée. L'application de la méthode intégrée sur des cas test en éléments finis géométriquement nonlinéaires confirme qu'elle répond au but initial d'obtenir des solutions transitoires accélérées, fidèles et paramétrables.

La méthode intégrée, tel qu'elle est présentée dans ce travail, peut être vue comme une réalisation particulière d'un *framework* beaucoup plus général. Ce *framework* couvre tous les aspects de la réduction des systèmes nonlinéaires par projection sur une base réduite dans le but d'obtenir une solution transitoire. Les méthodes qui sont spécifiquement choisies pour être utilisées dans la méthode intégrée ne sont que des exemples qui se présentaient comme préférable pour l'application traitée. Il est envisageable qu'une méthode intégrée comparable peut être conçue pour n'importe quelle application.

Les travaux centraux entiers sont entourés d'une description détaillée des éléments finis géométriquement non linéaires. La dynamique des structures géométriquement nonlinéaires fournit l'application de la méthode intégrée. Elle est décrite en détail pour marquer les limites d'une application assurée et testée de la méthode intégrée. Les cas test en éléments finis pour lesquels la méthode intégrée est appliquée sont caractérisés d'une manière complète pour démontrer le type des problèmes pour lesquels la méthode intégrée est conçue.

**Mots clés :** dynamique de structures, nonlinéarités géométriques, réduction du modèle, bases réduites, modes propres, décomposition orthogonale propre, mise-à-jour de la base réduite, paramètres

# Contents

ABSTRACT	V
RÉSUMÉ	IX
LIST OF TABLES	XV
LIST OF FIGURES	XVII
NOMENCLATURE	XXI
1 INTRODUCTION	1
1.1 Exploring the motivation for reduction in the domain of structural dynamics and identifying its three central aims	2
1.2 Assessing the state of the art	3
1.2.1 Reducing the model to accelerate the solution	3
1.2.2 Ensuring accuracy of the reduced model by taking into account the nonlinear behaviour	4
1.2.3 Parameterising the reduced model	4
1.2.4 Identifying the lack of an integrated method and making its construction the primary objective	5
1.3 Going beyond the state of the art and defining the aims and the outline of this work	5
1.3.1 Stressing the explorative character of the study	6
1.3.2 Identifying and presenting the overall framework for the construction of the integrated method	6
1.4 Highlighting the achievements and providing the manuscript's outline	8
2 LAYING THE FOUNDATIONS OF GEOMETRICALLY NONLINEAR STRUCTURAL DYNAMICS	11
2.1 Expanding the continuous description of the dynamic equilibrium	12
2.1.1 Expanding the dynamic equilibrium formulation	12
2.1.2 Introducing the principle of virtual work	13
2.1.3 Considering initial and boundary conditions	14
2.1.4 Uniting the previous definitions in the Total Lagrangian formulation	15
2.2 Discretising the equilibrium formulation	18
2.2.1 Discretising the Total Lagrangian formulation	19
2.2.2 Developing the nonlinear bar element	21
2.2.3 Developing the nonlinear volume element	23
2.3 Providing the basic matrix equation	32
3 CHOOSING A REDUCTION APPROACH AND A COMPATIBLE TRANSIENT SOLUTION PROCEDURE	35
3.1 Selecting a reduction approach	36

3.1.1	Defining the purpose of the reduction approach . . . . .	36
3.1.2	Surveying some reduction approaches . . . . .	37
3.1.3	Choosing the reduction approach . . . . .	49
3.2	Obtaining transient solutions of full order and reduced order systems . . . . .	50
3.2.1	Obtaining a transient solution of full order nonlinear systems . . . . .	51
3.2.2	Obtaining a transient solution of reduced order nonlinear systems . . . . .	56
3.2.3	Identifying of the requirement for an autonomous formulation of the nonlinear terms . . . . .	60
3.3	Creating some common reduced bases . . . . .	61
3.3.1	Linear Normal Modes . . . . .	62
3.3.2	Ritz-vectors . . . . .	66
3.3.3	Orthogonal Decomposition . . . . .	68
3.3.4	A Priori Reduction . . . . .	74
3.3.5	Centroidal Voronoi Tessellation . . . . .	77
3.3.6	Local Equivalent Linear Stiffness Method . . . . .	78
3.3.7	Homogenising the constitution of the reduced bases . . . . .	82
4	COMPARING THE REDUCED BASES AND TESTING THEIR ROBUSTNESS . . . . .	85
4.1	Preparing the studies . . . . .	86
4.1.1	Defining the studies' aims and scope . . . . .	86
4.1.2	Defining the criteria for judging the capabilities of the reduced bases . . . . .	87
4.1.3	Setting up the test-cases . . . . .	93
4.2	Conducting the studies and analysing the results . . . . .	101
4.2.1	Comparison of the reduced bases . . . . .	101
4.2.2	Robustness of the reduced bases . . . . .	118
4.3	Discussing the outcome of the numerical study . . . . .	133
5	ADDRESSING THE IDENTIFIED REQUIREMENTS OF AN ADAPTED SOLUTION ALGORITHM, OF THE AUTONOMY OF THE NONLINEAR TERMS AND OF PARAMETERISATION . . . . .	135
5.1	Adapting the solution algorithm . . . . .	137
5.1.1	Describing and testing the quasi-static correction . . . . .	137
5.1.2	Introducing and discussing the Least-Squares Petrov-Galerkin method . . . . .	146
5.1.3	Updating the reduced basis . . . . .	154
5.1.4	Outcome of the adaptation of the solution algorithm . . . . .	170
5.2	Replacing the inflation of the nonlinear terms with an autonomous formulation . . . . .	170
5.2.1	Presenting the linear interpolation and the direct linearisation . . . . .	171
5.2.2	Developing the polynomial formulation of the reduced nonlinear forces vector . . . . .	173
5.2.3	Considering neuronal networks as an additional approach . . . . .	189
5.2.4	Selecting an autonomous formulation by performing a numerical study . . . . .	189
5.2.5	Outcome of the requirement to replace the inflation of the nonlinear terms with an autonomous formulation . . . . .	192
5.3	Adapting reduced basis to external parameters . . . . .	192
5.3.1	Defining the problem of the adaptation of the reduced basis to external parameters . . . . .	193
5.3.2	Presenting the interpolation method . . . . .	194
5.3.3	Presenting the sensitivity analysis method . . . . .	198
5.3.4	Presenting the interlaced snapshot method . . . . .	199
5.3.5	Evaluating the adaptation methods by means of a numerical study . . . . .	200
5.3.6	Outcome for the requirement of parameterising the reduced system . . . . .	208
5.3.7	Abusing the interpolation approaches in tangent spaces as an autonomous formulation . . . . .	208
6	CREATING THE INTEGRATED METHOD FROM THE APPROACHES ADDRESSING THE IDENTIFIED REQUIREMENTS AND APPLYING IT TO NONLINEAR FINITE ELEMENT TEST-CASES . . . . .	211
6.1	Uniting the three elements and applying the integrated method . . . . .	212

6.1.1	Describing the integrated method . . . . .	212
6.1.2	Integrating the autonomous formulation and the update and augmentation on the academic test-cases . . . . .	219
6.2	Applying the integrated method to geometrically nonlinear bar elements . . . . .	229
6.2.1	Describing and characterising the test-case with nonlinear bar elements . . . . .	229
6.2.2	Applying the integrated method to the finite element test-case with bar elements . . . . .	233
6.3	Applying the integrated method to geometrically nonlinear volume elements . . . . .	245
6.3.1	Describing and characterising the test-case with nonlinear volume elements . . . . .	246
6.3.2	Prestressing the finite element test-case with volume elements . . . . .	261
6.3.3	Applying the integrated method to the finite element test-case with volume elements . . . . .	269
6.4	Outcome of the application of the integrated method . . . . .	286
7	CONCLUSION . . . . .	289
7.1	Concluding the work . . . . .	290
7.1.1	Discussing the obtained results . . . . .	290
7.1.2	Critical review of the major decisions . . . . .	293
7.2	Outlook for further research directions . . . . .	295
	BIBLIOGRAPHY . . . . .	297
A	PERFORMING AUXILIARY STUDIES TO ENHANCE THE COMPARISON OF THE REDUCED BASES . . . . .	325
A.1	Performing additional work on reduced bases . . . . .	326
A.1.1	Calibrating the Orthogonal Decomposition methods . . . . .	326
A.1.2	Exploring similarities between the mode shapes of the LELSM-vectors and the LNM . . . . .	329
A.2	Performing long-running simulations to explore computational performance and algorithmic dissipation . . . . .	332
A.2.1	Exploring the computational performance . . . . .	332
A.2.2	Exploring the algorithmic dissipation . . . . .	339
A.3	Solving with a constant tangent stiffness matrix . . . . .	340
B	TESTING LNM AND RITZ-VECTORS WITH SECOND ORDER TERMS . . . . .	341
B.1	Recalling the main methods . . . . .	342
B.1.1	Linear Normal Modes with Second Order Terms . . . . .	342
B.1.2	Ritz-vectors with Second Order Terms . . . . .	343
B.2	Choice of modes to be included . . . . .	343
B.3	Applying the SOT . . . . .	344
B.3.1	Overall Reduction Time . . . . .	344
B.3.2	Harmonic Excitation . . . . .	345
B.3.3	Impulse Excitation . . . . .	346
B.4	Outcome of the study on Second Order Terms . . . . .	346
C	IMPROVING THE CENTROIDAL VORONOI TESSELLATION . . . . .	347
C.1	General improvements and considerations of the CVT . . . . .	348
C.1.1	Classic Formulation . . . . .	348
C.1.2	Distance determination with Modal Assurance Criterion . . . . .	348
C.1.3	Adapting the CVT for systems under impulse excitation . . . . .	349
C.2	Presenting the numerical results justifying the replacement of the Euclidian norm with the MAC . . . . .	349
D	BROADENING THE DESCRIPTION OF THE NONLINEAR NORMAL MODES . . . . .	353
D.1	Surveying the historical development of the Nonlinear Normal Modes . . . . .	354
D.2	Exploring the interaction of Nonlinear Normal Modes . . . . .	355

## Contents

---

D.3	Sketching the analytical approach for obtaining Nonlinear Normal Modes . . . . .	356
D.4	Sketching the numerical approach for obtaining Nonlinear Normal Modes . . . . .	357
D.5	Describing the actual implementation of the numeric algorithm . . . . .	359

# List of Tables

2.1	The distribution of the nodes on the hexahedron in local coordinates . . . . .	25
2.2	The physical displacements of the nodes on the hexahedron . . . . .	25
2.3	The physical coordinates of the nodes on the hexahedron . . . . .	27
2.4	The Gauss-points and -weights . . . . .	32
3.1	The integration parameters for the nonlinear Newmark scheme . . . . .	59
4.1	The criteria selected for the score and their associated weights . . . . .	91
4.2	The comparison of the reduced bases . . . . .	119
4.3	The different configurations for the study of the robustness of the methods . . . . .	121
4.4	The numerical values of the different configurations for the study of the robustness of the methods . . . . .	121
4.5	The robustness of the reduced bases - table one . . . . .	131
4.6	The robustness of the reduced bases - table two . . . . .	132
5.1	The error metrics for the solutions of the entirely nonlinear system obtained with a constant reduced basis and with an updated and augmented reduced basis . . . . .	165
5.2	The error metrics and the combined numbers of jumps for the locally nonlinear system under harmonic excitation reduced with $r = 11$ LNM at given displacements . . . . .	167
5.3	The error metrics and the combined numbers of jumps for the entirely nonlinear system under harmonic excitation reduced with $r = 11$ LNM at given displacements . . . . .	168
5.4	The error metrics for the solutions of the entirely nonlinear system obtained with different constant reduced basis and with an updated and augmented reduced basis . . . . .	169
5.5	The nine points of the stencil for testing the reduced basis adaptation methods . . . . .	201
6.1	The error metrics for the different solutions of the entirely nonlinear test-case under harmonic excitation . . . . .	220
6.2	The error metrics for the transient solutions of the academic systems obtained with different combinations of methods . . . . .	228
6.3	The convergence of nonlinear transient solutions of the finite element test-case with bar elements for different discretisations . . . . .	231
6.4	The linear and nonlinear static displacements at the free end of the finite element test-case with bar elements for different values of Young's modulus . . . . .	231
6.5	The comparison of the interpolated modes with the reference modes for the finite element test-case with bar elements . . . . .	236
6.6	The error metrics for the transient solutions of the finite element test-case with bar elements obtained with different combinations of methods . . . . .	240
6.7	The error metrics for the transient solutions of the finite element test-case with bar elements with different constant reduced basis and with an updated and augmented reduced basis . . . . .	243

6.8	The comparison of the linear and the nonlinear static solution of the finite element test-case with volume elements obtained MatLab . . . . .	255
6.9	The overall solution times for static solutions of the finite element test-case with volume elements . . . . .	256
6.10	The linear static displacements at the free end of the finite element test-case with volume elements for different discretisations . . . . .	256
6.11	The nonlinear static displacements at the free end of the finite element test-case with volume elements for different discretisations . . . . .	257
6.12	The linear static displacements at the free end of the finite element test-case with volume elements for different values of Young's moduli . . . . .	257
6.13	The nonlinear static displacements at the free end of the finite element test-case with volume elements for different values of Young's modulus . . . . .	257
6.14	The comparison of the linear and the nonlinear static solutions obtained with NASTRAN and MatLab . . . . .	259
6.15	The comparison of the linear and the nonlinear static solution of the finite element test-case with volume elements obtained NASTRAN . . . . .	262
6.16	The comparison of the interpolated modes with the reference modes for the finite element test-case with volume elements . . . . .	269
6.17	The orders of magnitude in the polynomial approximation of the finite element test-case with volume elements . . . . .	275
6.18	The numerical results for the application of the integrated method with LNM on the finite element test-case with volume elements . . . . .	283
6.19	The computational performance results for the application of the integrated method with LNM on the finite element test-case with volume elements . . . . .	284

# List of Figures

2.1	The nonlinear bar element before and after deformation . . . . .	22
2.2	The nonlinear volume hexahedron element and the position of its nodes . . . . .	24
4.1	The locally nonlinear system . . . . .	96
4.2	The entirely nonlinear system . . . . .	97
4.3	The first two column vectors of the different reduced bases for the locally nonlinear system under harmonic excitation . . . . .	103
4.4	The first two column vectors of the different reduced bases for the locally nonlinear system under impulse excitation . . . . .	104
4.5	The first two column vectors of the different reduced bases for the entirely nonlinear system under harmonic excitation . . . . .	105
4.6	The first two column vectors of the different reduced bases for the entirely nonlinear system under impulse excitation . . . . .	106
4.7	The time histories of the 16 <sup>th</sup> degree of freedom of the locally nonlinear system under harmonic excitation obtained with different reduced bases at $r = 4$ . . . . .	108
4.8	The time histories of the 16 <sup>th</sup> degree of freedom of the locally nonlinear system under impulse excitation obtained with different reduced bases at $r = 4$ . . . . .	109
4.9	The time histories of the 16 <sup>th</sup> degree of freedom of the entirely nonlinear system under harmonic excitation obtained with different reduced bases at $r = 4$ . . . . .	110
4.10	The time histories of the 16 <sup>th</sup> degree of freedom of the entirely nonlinear system under impulse excitation obtained with different reduced bases at $r = 4$ . . . . .	111
4.11	The phase space representation of the 16 <sup>th</sup> degree of freedom of the entirely nonlinear system under harmonic excitation obtained with different reduced bases at $r = 4$ . . . . .	112
4.12	The relative energy of the entirely nonlinear system under harmonic excitation obtained with different reduced bases at $r = 4$ . . . . .	114
4.13	The score for different reduced basis for the locally nonlinear system under harmonic excitation . . . . .	116
4.14	The score for different reduced basis for the locally nonlinear system under impulse excitation . . . . .	116
4.15	The score for different reduced basis for the entirely nonlinear system under harmonic excitation . . . . .	117
4.16	The score for different reduced basis for the entirely nonlinear system under impulse excitation . . . . .	117
4.17	The relative performance for studying the robustness of LNM bases for the locally nonlinear system under harmonic excitation . . . . .	123
4.18	The relative performance for studying the robustness of LNM bases for the locally nonlinear system under impulse excitation . . . . .	123
4.19	The relative performance for studying the robustness of LNM bases for the entirely nonlinear system under harmonic excitation . . . . .	124
4.20	The relative performance for studying the robustness of LNM bases for the entirely nonlinear system under impulse excitation . . . . .	125

List of Figures

---

4.21	The relative performance for studying the robustness of POD bases for the locally nonlinear system under harmonic excitation . . . . .	127
4.22	The relative performance for studying the robustness of POD bases for the locally nonlinear system under impulse excitation . . . . .	127
4.23	The relative performance for studying the robustness of POD bases for the entirely nonlinear system under harmonic excitation . . . . .	128
4.24	The relative performance for studying the robustness of POD bases for the entirely nonlinear system under impulse excitation . . . . .	129
5.1	The overall reduction time for the locally non-linear system under harmonic excitation solved with the quasi-static correction . . . . .	141
5.2	The overall reduction time for the entirely non-linear system under harmonic excitation solved with the quasi-static correction . . . . .	141
5.3	The overall reduction time for the locally non-linear system under impulse excitation solved with the quasi-static correction . . . . .	142
5.4	The overall reduction time for the entirely non-linear system under impulse excitation solved with the quasi-static correction . . . . .	142
5.5	The R2MSE for the locally non-linear system under harmonic excitation solved with the quasi-static correction . . . . .	143
5.6	The R2MSE for the locally non-linear system under impulse excitation solved with the quasi-static correction . . . . .	144
5.7	The R2MSE for the entirely non-linear system under harmonic excitation solved with the quasi-static correction . . . . .	144
5.8	The R2MSE for the entirely non-linear system under impulse excitation solved with the quasi-static correction . . . . .	145
5.9	The overall reduction time for the large variant of the locally non-linear system under harmonic excitation solved with the LSPG method . . . . .	150
5.10	The overall reduction time for the large variant of the entirely non-linear system under harmonic excitation solved with the LSPG method . . . . .	151
5.11	The R2MSE for the large variant of the locally non-linear system under harmonic excitation solved with the LSPG method . . . . .	152
5.12	The R2MSE for the large variant of the entirely non-linear system under harmonic excitation solved with the LSPG method . . . . .	152
5.13	The four possible positions of the basis update in the nonlinear Newmark scheme . . . . .	156
5.14	The time histories of the 16 <sup>th</sup> degree of freedom of the entirely nonlinear system for different positions of the basis update (LNM with $r = 3$ ) . . . . .	157
5.15	The R2MSE and the MAC of the entirely nonlinear system under harmonic excitation reduced with the LNM at $r = 3$ . . . . .	158
5.16	The evolution of the norm of the derivation of the initial residual for the locally nonlinear system . . . . .	159
5.17	The evolution of error metrics for the reduced solution for the locally nonlinear system . . . . .	160
5.18	The time histories of the 16 <sup>th</sup> degree of freedom of the entirely nonlinear system with the basis update triggered by the rate of change of the generalised initial residual and showing characteristic jumps . . . . .	162
5.19	The time histories of the 16 <sup>th</sup> degree of freedom of the entirely nonlinear system obtained with a constant reduced basis and with an updated and augmented reduced basis . . . . .	165
5.20	The time histories of the 16 <sup>th</sup> degree of freedom of the entirely nonlinear system obtained with a constant reduced basis and with an updated and augmented reduced basis . . . . .	169
5.21	The overview of the possible operations based on the polynomial formulation of the nonlinear terms . . . . .	188
5.22	The overall reduction time for the autonomous solutions of the entirely nonlinear system under harmonic excitation . . . . .	190

5.23	The mean of the R2MSE for the autonomous solutions of the entirely nonlinear system under harmonic excitation . . . . .	191
5.24	The absolute error of the solutions obtained with the reference bases as a function of $\hat{f}_E$ and $\Omega$	204
5.25	The relative error obtained with the interpolation method . . . . .	205
5.26	The relative error obtained with the sensitivity analysis method . . . . .	206
5.27	The relative error obtained with the interlaced snapshots method's first option . . . . .	207
5.28	The relative error obtained with the interlaced snapshots method's second option . . . . .	207
6.1	The time histories of the 16 <sup>th</sup> degree of freedom of the entirely nonlinear system under harmonic excitation obtained with different reduced solutions with LNM at $r = 8$ . . . . .	221
6.2	The time history of the 16 <sup>th</sup> degree of freedom of the entirely nonlinear system under harmonic excitation obtained with the integrated method with LNM at $r = 8$ . . . . .	222
6.3	The R2MSE for the locally non-linear system under harmonic excitation for different autonomous approximations with constant and updated LNM bases . . . . .	225
6.4	The R2MSE for the locally non-linear system under harmonic excitation for different autonomous approximations with static and updated POD bases . . . . .	225
6.5	The R2MSE for the entirely non-linear system under harmonic excitation for different autonomous approximations with constant and updated LNM bases . . . . .	226
6.6	The R2MSE for the entirely non-linear system under harmonic excitation for different autonomous approximations with constant and updated POD bases . . . . .	226
6.7	The finite element test-case with nonlinear bar elements . . . . .	230
6.8	The mean and the variance of the R2MSE as a function of the order $r$ of the reduced model of the finite element test-case with bar elements . . . . .	232
6.9	The set-up for prestressing the finite element test-case with nonlinear bar elements . . . . .	234
6.10	The interpolation of the first mode of the finite element test-case with bar elements . . . . .	235
6.11	The interpolation of the 15 <sup>th</sup> mode of the finite element test-case bar volume elements . . . . .	235
6.12	The time histories of the generalised coordinates $q_1$ and $q_{r+1}$ of the finite element test-case with bar elements . . . . .	238
6.13	The time histories of $u_{100}$ of the finite element test-case with bar elements for different reduced solution procedures . . . . .	240
6.14	The score of different reduced solution procedures for the finite element test-case with bar elements . . . . .	242
6.15	The time histories of the three reduced solutions and the reference solution of the finite element test-case with bar elements . . . . .	243
6.16	An early interval in the time histories of the three reduced solutions and the reference solution	244
6.17	A late interval in the time histories of the three reduced solutions and the reference solution	244
6.18	The finite element test-case with nonlinear volume elements . . . . .	248
6.19	The maximum static deformations for the test with a single volume element . . . . .	250
6.20	The norm of the nonlinear tangent stiffness matrix for the test with a single volume element	250
6.21	The number of Newton-Raphson iterations for the test with a single volume element . . . . .	251
6.22	The maximum static nonlinear deformation for the test with a single volume element . . . . .	252
6.23	The resulting static displacements for the multiple elements test . . . . .	253
6.24	The norm of the nonlinear tangent stiffness matrix for the test with multiple volume elements	254
6.25	The number of Newton-Raphson iterations for the test with multiple volume elements . . . . .	254
6.26	The maximum static nonlinear deformation for the test with multiple volume elements . . . . .	255
6.27	The mean and the variance of the R2MSE as a function of the order $r$ of the reduced model of the finite element test-case with volume elements . . . . .	258
6.28	The comparison of the linear static deformations obtained with MatLab and NASTRAN . . . . .	260
6.29	The comparison of the nonlinear static deformations obtained with MatLab and NASTRAN	261
6.30	The Campbell diagram of the finite element test-case with volume elements under prestress	268
6.31	The interpolation of the first mode of the finite element test-case with volume elements . . . . .	270
6.32	The R2MSE for the finite element test-case with volume element for different reduced bases	271

6.33	The R2MSE for the robustness of the Linear Normal Modes for the non-linear finite element system under harmonic excitation . . . . .	272
6.34	The R2MSE of the robustness of the Proper Orthogonal Decomposition for the non-linear finite element system under harmonic excitation . . . . .	273
6.35	The time histories of the physical displacements of the node on the blade's tip for different solutions . . . . .	274
6.36	The mean of the R2MSE for different solutions of the finite element test-case with volume elements . . . . .	275
6.37	The overall solution times for different solutions of the finite element test-case with volume elements . . . . .	277
6.38	The physical displacements at $t = 1.5$ of the finite element test-case with volume elements at $r = 8$ . . . . .	279
6.39	The evolution of the R2MSE for different solutions of the finite element test-case with volume elements at $r = 8$ . . . . .	280
6.40	The evolution of the MAC for different solutions of the finite element test-case with volume elements at $r = 8$ . . . . .	281
6.41	The evolution of the relative energy for different solutions of the finite element test-case with volume elements at $r = 8$ . . . . .	282
6.42	The R2MSE and solution times of the combinations of formulations of the reduced nonlinear forces vector and the reduced basis . . . . .	286

# Nomenclature

## Mathematical operators and symbols

$e$	Euler's number
$i$	imaginary unit
$\mathbb{R}$	space of real numbers
$\square^T$	transpose operation
$\square^{-1}$	inverse operation
tr	trace operation
$\bar{\square}$	mean value of the set $\square$
$\tilde{\square}$	tangential value to the function $\square$
$\hat{\square}$	reduced equivalent of the term $\square$
$\otimes$	connection between tensor and vector entities
$\square!$	factorial
$\delta$	Dirac function
$\delta_{ij}$	Kronecker operator
$\mathcal{O}(\square)$	of order $\square$
$\frac{d}{d\square}$	total derivation with respect to $\square$
$\frac{\partial}{\partial\square}$	partial derivation with respect to $\square$
$\nabla$	Nabla (or Del) operator with the respective partial differential operators as components
$\delta\square$	virtual variation of $\square$
$\Delta\square$	increment of $\square$
$\triangle\square$	difference of $\square$
$\{\dots\}$	set of items
$[\dots]$	set of items assembled to a vector or matrix
$\emptyset$	empty set
$(\square)$	iteration or counting index if it is used as sub- or superscript
$ \square $	absolute value of $\square$ for a scalar
$\ \square\ $	norm of $\square$ for a vector or matrix two-norm if not specified otherwise

---

## Greek characters

$\alpha$	parameter of the Proper Generalized Decomposition algorithm
$\alpha$	parameter of the HHT- $\alpha$ -method
$\alpha_M$	parameter of the generalised $\alpha$ -method
$\boldsymbol{\alpha}$	vector of factors for the interpolation of the reduced basis
$\beta$	parameter of the Newmark schemes
$\gamma$	parameter of the Newmark schemes
$\delta_j$	quadrature weight for averaging over a time period
$\epsilon$	damping coefficient
$\epsilon$	convergence threshold for the time-marching solution algorithms
$\epsilon$	threshold for A Priori Reductions
$\epsilon$	convergence threshold for the time-marching solution algorithms
$\epsilon_r$	threshold for initialising the update of the reduced basis
$\zeta$	third direction of the local coordinate space of an element
$\eta$	second direction of the local coordinate space of an element
$\eta_{ij}^{(t \rightarrow t + \Delta t)}$	nonlinear part of the incremental step in the Green-Lagrange strain
$\Theta$	combined space time domain of a problem
$\lambda$	eigenvalue
$\lambda$	Lamé's first parameter
$\mu$	Lamé's second parameter
$\boldsymbol{\mu}$	vector of the parameters defining an operating point
$\boldsymbol{\mu}_0$	vector of the parameters defining the actual operating point of the system
$\nu$	Poisson's ratio of a Hooke-material
$\xi$	first direction of the local coordinate space of an element
$\rho$	density of a material
$\sigma$	stress
$\hat{\sigma}$	index set
$\boldsymbol{\Sigma}$	centre matrix of the singular value decomposition
$\phi$	column-vector of the projection basis $\boldsymbol{\Phi}$
$\hat{\phi}$	eigenvectors in the orthogonal decomposition procedures
$\check{\phi}_{i,k}$	Second Order Term
$\boldsymbol{\Phi}$	generic projection basis, trial space
$\boldsymbol{\Psi}$	secondary, left-hand projection basis, test space

---

$\omega$	eigenfrequency
$\Omega$	frequency of the external forcing
$\Omega$	spatial domain of the system
$\partial\Omega$	boundary of the spatial domain of the system
$\Omega_a$	rotational speed to which the system is subjected for prestressing

## Latin characters

$A$	surface of the system
$A$	section area of a bar element
$\mathbf{a}$	prestressing acceleration vector
$\mathbf{a}_N$	nodal prestressing acceleration vector
$\mathbf{A}$	generic SPD matrix
$\mathbf{A}^{(h)}$	tensor of order $h + 1$ containing the coefficients of a polynomial nonlinear forces vector
$\mathbf{b}$	initial conditions in state space representation
$\mathbf{B}_L$	linear strain interpolation matrix
$\mathbf{B}_{NL}$	nonlinear strain interpolation matrix
$c$	generic damping coefficient
$c_j$	parameter in the calculation of Ritz-vectors
$C_{ijkl}$	constititional term of the discrete material formulation
$\hat{c}_j^{(i)}$	cosine terme in the Harmonic Balance method
$c$	parameter in the calculation of greedy indices
$\mathbf{C}$	damping matrix of the discrete system
$\mathbf{C}$	matrix expression of the linear stress-strain relation
$d$	degree of the polynomial formulation of the nonlinear forces vector
$\mathbf{D}$	the skew-symmetric matrix of gyroscopic coupling
$\mathbf{D}$	matrix differential operator linking the strain to the displacements
$e$	error metric for the quality of a solution originating from a reduced system
$e_a$	Modal Assurance Criterion (MAC)
$e_d$	relative oscillation deviation
$e_{ij}^{(t \rightarrow t + \Delta t)}$	linear part of the incremental step in the Green-Lagrange strain
$e_r$	relative root mean square error (R2MSE)
$\bar{e}_r$	relative error metric
$E$	Young's modulus of a Hooke-material
$E$	energy
$E_r$	energy ratio
$\Delta E$	energy difference
$\mathbf{E}$	material matrix of a Hooke-material
$\mathbf{f}$	vector of generic external forces
$\mathbf{f}_0$	vector of the preloading forces
$\mathbf{f}_E$	vector of the external forces without inertial forces
$F$	integral accounting for the work done by the external forces
$F$	monodimensional nucleus function in the Proper Generalized Decomposition algorithm
$\mathbf{F}_E$	external forces vector formulation in the Harmonic Balance method

---

$g$	nonlinear internal forces
$g$	norm of the nonlinear internal forces vector used for bar elements
$G$	Green-Lagrange strain tensor
$\mathbf{g}$	vector of nonlinear internal forces in the discrete system
$\mathbf{G}$	matrix representing the direct linearisation of the nonlinear forces vector
$\tilde{\mathbf{G}}$	reduced matrix representing the direct linearisation of the nonlinear forces vector
$h$	energy level in Rosenberg's introduction of the NNMs
$h_i$	interpolation function
$h_j$	Hardy's multiquadrics radial basis function
$H$	periodicity condition
$\mathbf{H}$	matrix of the eigenproblem for the realignment of the A Priori basis
$i$	generic counting index primarily used for the degrees of freedom of the high-fidelity system
$I_y$	second moment of area of a beam
$\mathbf{I}$	identity matrix
$j$	generic counting index
$j$	factor in the Harmonic Balance method
$\mathbf{J}$	factor matrix in the Harmonic Balance method
$\mathbf{J}$	Jacobian for the nonlinear element
$k$	generic counting index primarily used for the degrees of freedom of the reduced order system
$\mathbf{K}$	stiffness matrix of the discrete system
$\mathbf{K}_c$	skew-symmetric matrix of centrifugal acceleration
$\mathbf{K}_a$	SPD matrix of centrifugal softening
$l$	generic counting index
$L$	length
$m$	generic counting index
$m$	number of solution snapshots
$m$	number of precomputed reduced bases
$m$	counter for the retainer that prohibits the update of the reduced basis
$m_r$	threshold for the retainer
$\mathbf{m}$	index mask obtained from the greedy algorithm
$\mathbf{M}$	mass matrix of the discrete system
$n$	dimension of the high-fidelity system
$n$	normal to associate a direction to the surface of a body
$n_g$	number of the evaluations of the vector of the nonlinear internal forces $\mathbf{g}$
$\mathbf{n}$	normal vector to associate a direction to the surface of a body
$\mathbf{N}$	basis normalisation matrix
$\mathbf{N}$	displacement interpolation matrix
$o$	generic counting index
$p$	generic counting index

---

$p$	generic real value
$\mathbf{p}$	vector in the calculation of greedy indices
$\mathbf{P}$	matrix in the calculation of greedy indices
$q$	generalised coordinate (displacement in the reduced system)
$\dot{q}$	velocity in the reduced system
$\ddot{q}$	acceleration in the reduced system
$\mathbf{q}$	vector of the displacements of the reduced system
$\dot{\mathbf{q}}$	vector of the velocities of the reduced system
$\ddot{\mathbf{q}}$	vector of the accelerations of the reduced system
$\mathbf{q}_E$	generalised multiplier for the quasistatic correction
$\mathbf{Q}$	matrix in the Harmonic Balance method
$\mathbf{Q}$	matrix in the calculation of greedy indices
$\mathbf{Q}$	orthogonal matrix of a QR-factorisation
$\mathbf{Q}$	pure rotation matrix
$r$	dimension of the reduced order system
$r_a$	radius if the system is subjected for prestressing
$R$	main radius of the radial interpolation function
$\mathcal{R}o$	Rossby-number, a measure for the contribution of the Coriolis-forces
$\mathbf{r}$	vector of the residual
$\mathbf{R}$	upper triangular matrix of a QR-factorisation
$s$	generic counting index
$s$	generic real value
$\hat{s}_j^{(i)}$	sine term in the Harmonic Balance method
$\mathbf{s}$	vector of the tangential step in the phase-space
$S_{ij}^{0 \rightarrow t + \Delta t}$	second Piola-Kirchhoff stress
$\mathbf{S}$	Jacobian matrix of the system in the nonlinear Newmark iteration
$t$	time
$t_0$	start time of a simulation
$t_e$	end time of a simulation
$T$	period of an oscillation
$u$	displacement
$u$	nodal displacement in the first direction of Cartesian space
$u_i$	generic displacement
$\dot{u}$	velocity
$\ddot{u}$	acceleration
$\bar{U}$	energy potential in Rosenberg's introduction of the NNMs
$\mathbf{u}$	vector of the physical displacements
$\dot{\mathbf{u}}$	vector of the velocities
$\ddot{\mathbf{u}}$	vector of the accelerations
$\mathbf{U}$	left matrix of the singular value decomposition
$v$	nodal displacement in the second direction of Cartesian space
$v$	velocity in Peshek's analytical construction of a NNM
	$v = \dot{u}$
$v_r$	variance of the relative root mean square error $e_r$
$\mathbf{v}$	velocities in Peshek's analytical construction of a NNM

---

	$\mathbf{v} = \dot{\mathbf{u}}$
$V$	volume of the system
$V_k$	Voronoi region
$\mathbf{V}^T$	right matrix of the singular value decomposition
$w$	nodal displacement in the third direction of Cartesian space
$w_i$	Gauss weight
$W$	work
$x$	first direction in Cartesian space
$x_i$	generic direction in Cartesian space
$x_i$	mass-normalised displacement in Rosenberg's introduction of the NNMs
$x_1$	first spatial coordinate
$x_2$	second spatial coordinate
$x_3$	third spatial coordinate
$X$	deformation gradient
$X$	function for the slave displacements in Peshek's analytical construction of a NNM
$X_i$	spatial coordinate in Rosenberg's introduction of the NNMs
$\mathbf{X}$	deformation gradient
$y$	second direction in Cartesian space
$Y$	function for the slave velocities in Peshek's analytical construction of a NNM
$z$	third direction in Cartesian space
$\mathbf{z}$	phase space representation of the kinematic configuration variables
	$\mathbf{z} = [\mathbf{u}, \dot{\mathbf{u}}]^T$

## List of abbreviations

<b>2PK</b>	second Piola-Kirchhoff stress
<b>APR</b>	A Priori Reduction
<b>BFGS</b>	Broyden-Fletcher-Goldfarb-Shanno method
<b>CFD</b>	Computational Fluid Dynamics
<b>CVT</b>	Centroidal Voronoi Tessellation
<b>DOF</b>	Degree Of Freedom
<b>FEM</b>	Finite Element Method
<b>FOM</b>	Full Order Model
<b>GNAT</b>	Gauss-Newton with approximated tensors (method)
<b>POD</b>	Global POD (Proper-Orthogonal Decomposition)
<b>GPS</b>	Global Positioning System
<b>HBM</b>	Harmonic Balance Method
<b>HHT</b>	Hilber-Hughes-Taylor $\alpha$ -method
<b>LELSM</b>	Local Equivalent Linear Stiffness Method
<b>LNM</b>	Linear Normal Mode
<b>LSPG</b>	Least Squares Petrov-Galerkin
<b>MatLab</b>	Matrix Laboratory
<b>NASTRAN</b>	Nasa Structural Analysis System
<b>NNM</b>	Non-Linear Normal Mode
<b>POD</b>	Proper-Orthogonal Decomposition
<b>MAC</b>	Modal Assurance Criterion

**R2MSE** Relative Root Mean Square Error  
**ROM** Reduced Order Model  
**SOD** Smooth Orthogonal Decomposition  
**SOT** Second Order Terms  
**SPD** symmetric positive definite  
**SVD** singular value decomposition  
**SVK** Saint Venant-Kirchhoff (material model)



# Chapter 1

## Introduction

---

The paramount aim of this work is to obtain a rapid, accurate and parameterisable transient solution of a geometrically nonlinear structure under external excitation. This is achieved by developing a numerical method for constructing an autonomous and parameterisable reduced order model of the structure and for solving this reduced model to obtain a transient solution with a numerical effort that is less than the effort required for the transient solution of the full order model.

The introduction starts with a brief motivation for the striving for a reduced model. The central interest of a reduced model is the resulting lean computational effort that accelerates the solution and enables a variety of follow-on applications, e.g. optimisations. From this strive the three central aims of rapidity, accuracy and parameterisation are derived and their fulfilment identified as essential for a successful reduced solution. For each of these aims the state of the art of the available methods and approaches is assessed. There is a multitude of sophisticated and specific approaches available that each addresses at least one of these aims. However, the review of literature also reveals the lack of a single integrated method that combines approaches for all three aims. The development of such an integrated method that responds to all three aims at the same time is identified as the approach to be followed with this study.

The introduction also stresses that this work is aimed at being an explorative study based only on numerical experiments. The exclusive concentration on already discretised problems allows the seamless integration of the different specific methods on matrix level. The approach that is taken and its different stages are presented as the conclusion of the introduction.

## 1.1 Exploring the motivation for reduction in the domain of structural dynamics and identifying its three central aims

The constant strive for increasing the performance of structural elements in turbo-machinery with respect to weight, life-cycle numbers and thermal stress leads routinely to operating points that are well beyond the limits of the applicability of linear approximations. This imposes the exclusively nonlinear simulation of such structures to identify possible occurrences of unwanted vibrations, resonances and even contacts during non-stationary operating phases (e.g. Griffin [84] and Sanliturk et al. [199]). Such behaviour may occur due to aerodynamic phenomena as stall and surge (Mansoux et al. [143]). The existing, sophisticated methods for the transient solution of nonlinear structural dynamic problems require highly specific information for the description of the structure and the investment of considerable numerical efforts in order to yield meaningful results. Usually, neither is available in the early stages of the design process where the unwanted vibrations and resonances can be detected and countered most effectively.

The consequence is that early in the design process only relatively simple approximations of the dynamic behaviour of the structural element are available to generate information that drives design decisions. This is due to the limited definition of the structure and the resulting large number of possible alternatives. High-fidelity numerical simulations are used only relatively late in the design process when the design is essentially finalised and close to being frozen. This late in the design process the availability of information is also high because most to the design parameters are determined. At this point the willingness to invest considerable numerical effort is often higher, as it allows understanding the structure's transient dynamics in a small number of well-defined circumstances.

The diametrically opposed distribution of the importance of the decisions and the availability of pertinent and precise information along the time-scale of the design process poses a major problem (Balci [19], Keane and Nair [114], Kellner et al. [115]). The early and important design decisions, which are based on limited information, may turn out to be sub-optimal as more precise information become available later in the design process. Such a sub-optimal initial decision is usually costly to correct towards the end of the design process.

A common tendency in all major industries seems hence to be to bring forward the use of high-fidelity simulation on the time-scale of the design process (Kellner et al. [115], Chen and White [60]). This leads to the three central aims of the reduction. Solutions are required that preserve the nonlinear nature of the structure. This property of accuracy is required in order to obtain pertinent results that can be used to drive the design process. The solutions have also to be adaptable to external parameters, as prescribed by e.g. the operating point of the turbine, because many decisive parameters are only vaguely defined in the early stages of the design process thus covering large areas of possible design alternatives and conditions. Above all, the solutions are required to be obtained rapidly, with a lean computational effort so that different solutions can be obtained fast, e.g. for parameter studies, identification (Kerschen et al. [118]) or optimisations (Rao and Savsani [185]). Reduced models with an accelerated solution can also be used for integration with other codes, simulating e.g. another physic like a fluid flow for aeroelastic applications (Tran [226]), or for pinpointing pertinent information in an otherwise unwieldy full order system. This thinking seems to persist despite the constant growth of available computational power.

At the present time only algorithms and methods exist that respond to no more than two of these three aims. This leads to situations in which the solutions are often obtained with a purely linear approximation, with negligence of the external parameters or not in the required quantity because their computational cost is deemed too high. In all cases the occurrence of unwanted vibrations, resonance and contacts cannot be excluded and if such phenomena are discovered in later design stages they have to be eliminated with a much higher effort than it would have been possible early on in the design process.

### 1.2 Assessing the state of the art

Commonly, the requirement for a computationally lean solution is addressed with a reduced order model of the matrix formulation of the structure's dynamic equilibrium describing the structure's dynamics. A reduced order model is a numerical tool that alleviates the computational burden without changing the physics of the underlying problem.

In the previous section the three central aims of a reduction are derived from the application of the reduced solutions during the design process. These aims are

- a lean computational effort and a pronounced acceleration of the solution time compared to the high-fidelity simulation.
- a high accuracy of the reduced solution, by taking into account the nonlinear behaviour of the structural element.
- the possibility to adapt the reduced order model as a function of external parameters.

A considerable number of highly sophisticated and successful approaches exists in literature of which each can achieve at least one of these three aims. Their current mainstays and most recent developments are assessed below.

#### 1.2.1 Reducing the model to accelerate the solution

The ever-growing need for the numerical treatment of discrete dynamic models of geometrically nonlinear structures continues to outpace the growth of reasonably affordable computational power. The huge matrices emerging from the fine discretisation of such structures pose considerable challenges with respect to their computational tractability and the meaningful exploitation of the obtained results. Reduced models have gained considerable attention, as they allow meeting these two challenges.

As an answer to the challenge of a reasonable computational tractability the reduced model of a discretised structure allows for a rapid transient solution of its dynamic behaviour. Focussing on the characteristic behaviour of the structure by means of the reduced model allows for the selective extraction of pertinent information. Furthermore, the introduction of parameters into reduced systems enables affordable repeated solutions, as required for a whole range of applications. Repeated solutions are required for e.g. optimisation (Buhl et al. [42], Jung and Gea [112]), for virtual prototyping and monitoring (Kerschen et al. [118]) and long running solutions for life cycle simulations (Meyer and Matthies [146, 147]).

The mainstay of the reduction in the domain of structural dynamics is the projection on a reduced basis. The approach of reducing a structural dynamic system by projection on a reduced basis goes back to the very beginning of modal decomposition (e.g. Bathe [22]). The first application of this approach to nonlinear structural dynamic systems was probably made by Nickell [161], who proposed the use of the Linear Normal Modes of the underlying linear structure to this effect. However, the Linear Normal Modes dismiss the nonlinearity. Subsequently many authors proposed reduced bases specifically for the use with arbitrary systems to circumvent this constraint. Notable among these is Sirovich [207, 208, 209], who rendered the approach of the Karhunen-Loève decomposition numerically feasible by introducing the notion of snapshots, creating thus the Proper Orthogonal Decomposition. This technique gives the least error in the Root Mean Square Sense as shown by Bellizzi and Sampaio [31]. Wilson et al. [241] devised a numerical approach on the basis of the Lanczos algorithm for approximating Linear Normal Modes that have yet to converge and thus replicate the nonlinearity of the system.

An approach that does not project the nonlinear system on a reduced basis is Nonlinear Normal Modes. Nonlinear Normal Modes go back to the idea of Rosenberg [190], who suggested to represent the system's motion as closed loops on hyperplanes in the phase-state-space. This approach was recently cast in a numerical algorithm by Kerschen et al. [117] and Peeters et al. [170]. The interpretation and presentation of the system's behaviour in the phase-state-space allows for direct and visual access to the system's charac-

teristics in terms of bifurcations, attractors and stable orbits, but does not yield an efficient formulation for a fast solution because of its implicit nature.

Another approach without a reduced basis is the Proper Generalized Decomposition, presented by e.g. Chinesta et al. [62] as a multidimensional projection. The solution is presented as a sum of products of nucleus functions. Each nucleus function is an exclusive function of the quantity of interest. This allows including external parameters describing the system alongside the physical displacements of the system, as additional dimensions in a reduced model. Following the recent efforts by Ammar et al. [7, 9] the Proper Generalised Decomposition is in vivid development at this time.

### 1.2.2 Ensuring accuracy of the reduced model by taking into account the nonlinear behaviour

The aim of including the nonlinear behaviour of the structural element in the reduced model is automatically fulfilled by the explicitly nonlinear approach of the Nonlinear Normal Modes. Also the Proper Generalised decomposition can handle nonlinear behaviour in an intrinsic manner.

However, the projection on a reduced basis commonly implies that a single reduced basis can be found to be optimal in a given sense. This reduced basis remains constant throughout the transient solution, i.e. it does not follow the nonlinear evolution of the transient solution. The present state of research in the domain of reduction by projection on a reduced basis provides a variety of reduced bases that are conceived specifically for the use on nonlinear systems, but which remain constant nonetheless. The first propositions for alleviating this constraint are the repeated construction of Linear Normal Modes as tangent modes by Slaats et al. [210].

Another approach, which does not adapt the reduced basis but the solution algorithm, is the Least-Squares Petrov-Galerkin method by Carlberg et al. [55], which projects the system on its own, semi-reduced residual. This particular approach allows for a reduced system with a bound error but requires either an evaluation of the full order system for each iteration or the construction of a dedicated substitution system that approximates the residual, the so-called hyper-reduction.

In the same category of special solution algorithms falls the quasistatic correction that is presented by Hansteen and Bell [92]. This approach recovers components of the external excitation of the structural element and uses these forces for an additional static solution. The result of this static solution is added to the transient solution at each time-step.

### 1.2.3 Parameterising the reduced model

The requirement that the reduced model has to accept external parameters is also fulfilled by the Proper Generalised Decomposition. For the Nonlinear Normal Modes such a parameterisation is yet to be found. For the projection on a reduced basis approach the reduced basis has to be adapted in order to fulfil this requirement.

One type of available approaches covers reduced bases that can be considered as averaged for several values of the parameters. The prototypical approach in this group is the Global Proper Orthogonal Decomposition approach as it used by e.g. Taylor and Glauser [220]. This approach combines reduced bases for several sets of external parameters. It is only available for Proper Orthogonal Decomposition bases.

Another type of available approaches adapts the reduced bases as a function of the external parameters. This includes using the derivations of the column vectors of the reduced bases with respect to the external parameters as done with e.g. the sensitivity analysis method by Hay et al. [95]. A more sophisticated approach aims at the interpolation of the reduced bases for different sets of external parameters in a tangent space. Together with the necessary transformations into and from the tangent space this is proposed by Amsallem and Farhat [10].

### **1.2.4 Identifying the lack of an integrated method and making its construction the primary objective**

All the different approaches that are presented above and many more are highly specific for one of the three aims. For example, the work of Amsallem and Farhat [10] for adapting the reduced basis as a function of external parameters is applied to linearised problems only. At the same time, e.g. the Least-Squares Petrov-Galerkin method by Carlberg et al. [55], which is specifically designed for the reduction of nonlinear systems, has no provisions for adapting the reduced basis as a function of external parameters. The same goes for the overwhelming majority of the presented approaches. All of them are highly specific and successful for their given aims, but currently there is no method known to the author that answers to all three identified aims at the same time.

The most promising method with this ambition is probably the Proper Generalised Decomposition (PGD). However, this method presents a radical departure from the common approach of a projection on a flat space, because the PGD reduces on a curved space. This property has yet to supersede the established procedures as they are common in the engineering community and prevalent in commercially available codes. As a rather recent method the Proper Generalised Decomposition also lacks the pervasiveness and the sound validation by a long research history as it is the case for e.g. the reduction by projection on a reduced basis. Furthermore, the Proper Generalised Decomposition is a monolithic approach and does not allow assembling different methods that respond to the different requirements in a single integrated method.

Here, the integrated character of the method lies in covering all aspects related to the reduced order model of the structural elements. Sayma et al. [200] and Vahdati et al. [230] propose an integrated method that integrates simulations for different physics without any reduction. The integrated method as it is developed here is only concerned with the consistent and comprehensive treatment of the reduction of a structural dynamic system.

The multitude of methods that have been and are developed around the reduction by projection on a reduced basis offers all elements that are required to respond to the three aims of accelerating the solution time, ensuring the accuracy by accounting for the nonlinear behaviour and allowing a parameterisation of the reduced model. For each of these three aims several dedicated methods are available. Also available are a multitude of different common method for creating reduced bases, specifically adapted solution algorithms, which take the nonlinear behaviour of the system into account, and methods that handle the parameterisation of the reduced bases.

However, there seems to be no integrated method that combines these approaches in order to achieve all three aims at once. Also, there is no framework available that allows combining different approaches, each achieving one aim, in an interchangeable manner in order to construct an integrated method for a given problem. Providing such a framework and describing an integrated method is the primary motivation and the overall aim of this work.

A first tentative approach at combining different methods is made by Grolet and Thouverez [85]. They use the Harmonic Balance Method in conjunction with the Proper Generalised Decomposition in order to obtain reduced periodic solutions of geometrically nonlinear structures. The strive for steady state periodic solution distinguishes their approach from the presented work.

## **1.3 Going beyond the state of the art and defining the aims and the outline of this work**

The requirement for a transient solution of a geometrically nonlinear structure, which is obtained from a parameterisable reduced order model, with a computational effort that is less than the effort required by the geometrically nonlinear finite element solution, is identified. Many methods proposed in literature address at least one but not more than two of the aims that are to be achieved by the introduction of the

### 1.3. GOING BEYOND THE STATE OF THE ART AND DEFINING THE AIMS AND THE OUTLINE OF THIS WORK

---

reduced order model with a highly specific approach. The domain is lacking a single integrated method that merges approaches for all three aims and provides a consistent framework for combining these approaches (Mignolet et al. [149]). This lack seems to persist already for a certain time (Noor [163]).

The overall aim of this work is the creation of an integrated method that allows obtaining the transient solution of a geometrically nonlinear structure under external forcing, while considerably reducing the computational effort, taking into account the nonlinear behaviour and allowing the parameterisation of the reduced model. This integrated method is to serve as an exemplary realisation of a framework that allows combining methods corresponding to these three aims as necessary. To develop such a numerical method that allows constructing a reduced, parameterisable model of a geometrically nonlinear structure with the aim of obtaining a transient dynamic solution in less computational time is the step to be taken beyond the state of the art.

#### 1.3.1 Stressing the explorative character of the study

The field of structural dynamics has the distinction of being one of the domains with the longest research history. This puts current research in the favourable position of being able to draw on a stable and consolidated understanding of the mathematical means and models that are used to describe the encountered physical phenomena. This understanding allows to relieve the effort on the tip of the wedge of knowledge that has been driven deep into this particular field of research since its inception and to reorient research to the wedge's flanks with the aim of broadening and widening the available knowledge. In fact, widening the available knowledge is the central ambition of this work.

Current research in structural dynamics seems more focused on solution procedures than on the decryption of the underlying physical phenomena. Another major branch of research is currently aimed at coupling structural problems with other domains, e.g. fluid dynamics or heat phenomena. So researchers are currently pushing the lateral boundaries of the domain of structural dynamics instead of driving the wedge deeper into the domain.

This work inscribes itself in this direction of research which defines its means and conduct. There is no intention to develop strict theoretical proves or predictions. All decisions are based on numerical experiments that are designed with circumspection and whose results are gauged with specifically defined criteria. The integration of the different approaches in a single integrated method is done on discrete level. Operating on matrix equations allows the direct application of the already established methods and ensures their seamless integration.

The selection of approaches and methods is limited to approaches and methods that address single structures. Techniques that are devised for assemblies or multiple sub-structures are not considered because the main focus of this work is the reduced model of a single structure.

#### 1.3.2 Identifying and presenting the overall framework for the construction of the integrated method

In a first step the framework is identified in which the construction of the integrated method is to take place. To this effect the concepts of projection on a reduced basis, Nonlinear Normal Modes and Proper Generalised Decomposition are reviewed against a set of criteria. This set of criteria allows assessing their suitability and their potential for achieving the aims of rapidity, accuracy and parameterisation of the solution, either as an intrinsic property or by accommodating specific methods. The concept of reduction by projection on a reduced basis responds best to these requirements and its selection leads to the necessity of the choice of an approach for generating a reduced basis.

The approach of a reduction by projection on a reduced basis is intimately linked with the solution algorithm that is used to obtain the reduced solution. In this work the focus is put on the Newmark scheme family of nonlinear solvers. It is a well proven method and together with its most recent developments, it

### 1.3. GOING BEYOND THE STATE OF THE ART AND DEFINING THE AIMS AND THE OUTLINE OF THIS WORK

---

is omnipresent in commercial software. It is shown that the full order system and the reduced order model have the exact same structure. Both descriptions of the system's dynamics can hence be solved by the same type of Newmark scheme. Therefore it is desirable to maintain a Newmark-type solution scheme as the backbone of the integrated method that is developed. Also, being based on a Newmark-type solution algorithm should certainly facilitate the introduction and distribution of the integrated method. The classic Newmark scheme and one of its variants is used to obtain reduced transient solutions. The fact that two different Newmark-type algorithms are used as the backbone of the integrated method, anticipates the future endorsement of other solution algorithms as the backbone of the integrated method.

For the choice of the reduced basis several common approaches for creating reduced bases are presented. The actual choice is based on the accuracy of the reconstructed transient solutions of a series of unified test-cases of academic nature. The test-cases are combinations of a locally and an entirely nonlinear system under a harmonic or an impulse excitation. This arrangement ensures avoiding that the selected test-case may favour a specific reduced basis. The reconstructed transient solutions are obtained with a nonlinear Newmark scheme that includes a constant reduced basis and an inflation type, non-autonomous formulation of the nonlinear terms to ensure that the appearing errors are exclusively introduced by the projection of the system on the reduced basis. Relative error metrics are developed that combine the elementary error metrics of Relative Mean Deviation, Relative Oscillation Deviation, Relative Root Mean Square Error and energy difference in order to avoid the bias of some error metrics towards certain reduced bases. The reduced bases are compared amongst each other on the grounds of the relative error metric, for finding the most suited one for reducing the nonlinear test-cases. The established reduced bases are then used again and unchanged to reduce the same test-case with a differently parameterised excitation in order to assess the bases' robustness.

The results show that a simple reduction by projection on a constant basis does not yield a sufficiently accurate transient solution with any reduced basis. Also, all unchanged bases do not offer enough robustness to reduce a differently parameterised test-case. The inspection of the solution algorithm shows that a different formulation is required for the nonlinear terms to allow the benefits of a reduced solution to unfold to full effect. Furthermore, the employed inflation formulation is bound to become infeasible for the numerical efforts of the finite element test-case. Because all reduced bases fall short of the applied error threshold the decision is made to continue the development of a reduced, autonomous and parameterisable model of a geometrically nonlinear structure independently from a specific basis and that possible improvements have to be introduced in the solution algorithm itself.

Three areas of improvements in the existing algorithm for obtaining reduced transient solutions are determined to remedy the identified shortcomings of this method. These areas are the development of an approach for the update of the reduced basis as a function of the reduced solution and its inclusion in the algorithm for the reduced transient solution, the introduction of an autonomous expression that replaces the inflation of the nonlinear terms and the introduction a method that adapts the reduced order model as a function of external parameters, such as the rotating speed of the turbine blade.

For all of these three improvements different alternatives are either already available in literature or developed specifically. To separate the errors that are introduced or prevented by their introduction, the improvements are introduced one at a time. For each of the three improvement areas the solutions obtained with the different alternatives are evaluated with the same error metrics and test-cases that are developed for the choice of the reduced basis beforehand. This is done for consistency and because it allows to assess the error of the different alternatives for different reduced bases. The alternatives that perform best against the criteria are then retained for being merged in the integrated method.

The academic nature of the test-cases that are used until this point allows a pertinent classification of the type of nonlinearity for which a given reduced basis is preferably to be used because for such systems the nonlinear terms are formulated analytically and are thus of a single category. The analytic formulation of the nonlinear terms is also numerically very fast and not comparable in computational efforts with corresponding finite element formulations. Geometrically nonlinear finite element test-cases are thus devised that are representative for a turbine blade. They are used to confirm the results obtained from the entirely nonlinear academic system under harmonic excitation, as the corresponding combination of type of nonlin-

#### 1.4. HIGHLIGHTING THE ACHIEVEMENTS AND PROVIDING THE MANUSCRIPT'S OUTLINE

---

earity and excitation for a turbine blade at its operating point, and the possible gains in computation time are determined if the inflation formulation for the nonlinear terms can be replaced.

In the final step the integrated method, which allows to construct a reduced model of a geometrically nonlinear structure, by projecting it on a reduced basis, to adapt it to external parameters and solves it with autonomous expressions for the nonlinear terms while updating the reduced basis to make it follow the evolution of the reduced solution, is created by merging the previously selected approaches. The integrated method is applied on the nonlinear finite element test-cases and tested with respect to error of the reconstructed solution and computational performance to allow gauging the trade-off between loss in quality and gain in speed.

### **1.4 Highlighting the achievements and providing the manuscript's outline**

The manuscript opens in the following chapter 2 with laying the foundations of geometrically nonlinear structural dynamics. The continuous Total Lagrangian formulation is presented and transformed in a discrete formulation. Geometrically nonlinear bar and volume elements are provided and it is shown that the dynamic equilibrium of a geometrically nonlinear structure can be written in a single matrix equation. This equation serves as the jump-off and hinging point for the following developments.

In chapter 3 the reduction approach is chosen and compatible transient solution procedures are presented. The approaches of projection on a reduced basis, the Nonlinear Normal Modes and the Proper Generalised Decomposition, that have been identified during the assessment of the state of the art, are detailed. The choice is based on criteria that gauge the reduction approaches' potential to yield a rapid, accurate and parameterisable transient solution.

The selection of the reduction by projection on a reduced basis determines the following course of action decisively. It allows the choice of the Newmark-type family of time-marching solution algorithms as backbone for the integrated method. The straightforward introduction of the reduced basis is demonstrated with two variants of the Newmark algorithm. This proves that even the backbone of the integrated method can be changed readily as required by the problem at hand. The requirement of disconnecting the reduced solution entirely from the full order finite element method by replacing the nonlinear terms with autonomous formulations is identified by the inspection of the algorithms.

In line with the choice of the reduction by projection on a reduced basis several common reduced bases are created. The approaches for their creation are detailed and improved where necessary. In particular the performance of the Centroidal Voronoi Tessellation is boosted by introducing the Modal Assurance Criterion as a measure of closeness during the determination of the regions.

In chapter 4 the reduced bases are tested and their robustness is investigated. The numeric tests are performed on academic test-cases. They have the double objective of comparing the reduced bases among each other in their capacity to reduce a geometrically nonlinear structure and to investigate their robustness if the original reduced basis is applied to reduce a differently parameterised test-case. To judge the performances of the reduced bases without any bias the novel multi-criteria decision analysis criteria of score and relative performance are developed. The judgement of the bases' performance is based on the time histories of the transient solutions. The transient solutions are obtained with reduced Newmark algorithm. In order to limit the origin of the observed errors exclusively to the introduction of the reduced basis the solutions are obtained without autonomous formulations for the nonlinear terms.

The intention at this point is to identify a reduced basis that performs exceptionally well and can be used to reduce geometrically nonlinear structures without further adaptation. However, the obtained results show clearly that such a basis is not among the study's candidate bases. No basis performs sufficiently well with respect to the developed criteria. A good quality of the reconstructed solution usually comes with a pronounced lack of robustness, so that no reduced basis can fulfil the two requirements at the same time.

#### 1.4. HIGHLIGHTING THE ACHIEVEMENTS AND PROVIDING THE MANUSCRIPT'S OUTLINE

---

The decision is made at this point not to propose a new reduced basis but to improve the solution algorithm in order to make up for the poor performance of the reduced bases. In order to organise the improvement of the solution algorithm two requirements that have to be addressed by the solution algorithm are identified. They are derived from the results of the numeric tests. In order to improve the quality of the reconstructed solution the solution algorithm has to adapt the reduced basis in a way that makes it follow the nonlinear evolution of the solution. Also, the reduced basis has to be adapted as a function of the external parameters to ensure its applicability for a wide range of sets of external parameters.

In chapter 5 the identified requirements of adapting the solution algorithm, of replacing the nonlinear terms with autonomous formulations and of adapting the reduced basis as a function of external parameters are addressed. The requirement of the autonomous formulations is identified during the introduction of the reduced basis into the solution algorithm. The two other requirements are derived from the numerical results of the tests of the reduced bases in the previous chapter. For all three requirements a number of candidate approaches is presented and tested on the academic test-cases. This allows exploring their respective properties and to make a justified decision as to which approach is to be retained for the integrated method. At the same time it is the intention to provide a large toolbox of different approaches. Within the proposed framework of the integrated method this allows replacing an approach, which is retained here, with another approach that might be more suitable for a given problem.

Adapting the solution algorithm centres on approaches that allow the Newmark-family type of time-marching solution algorithms to take the nonlinear evolution of the transient solution into account. Included are the quasistatic correction, the Least-Square Petrov-Galerkin approach and the update of the reduced basis. The update of the reduced basis is developed extensively and improved by the addition of the augmentation. The augmentation of the updated basis with the jumps of the physical quantities of displacement, velocity and acceleration, is a novel aspect of the common sense approach of updating the reduced basis and an original contribution.

For the autonomous formulation of the nonlinear terms the direct linearisation and the polynomial formulation are studied. The polynomial formulation replaces the nonlinear terms by tensor products of the generalised coordinates. While it is an approach available in literature, it is extensively investigated and modified in order to become compatible with the update of the reduced basis.

Adapting the reduced bases as a function of external parameters draws on an interpolation approach from literature. The reduced bases form a data-base, are transformed in a tangent space and interpolated there. The result is retransformed and made available for the reduced transient solution. Due to the update of the reduced basis only the initial reduced basis at the beginning of the transient solution has to be adapted.

After choosing all components that respond to the different requirements the retained approaches are assembled in the integrated method. This integrated method forms the central result of this work and it is described in chapter 6. The integrated method is constructed around the backbone of a reduced Newmark-type time-marching algorithm. The reduction is achieved by projecting the dynamic equilibrium on a reduced basis. The reduced basis is updated and augmented in a dynamic fashion in order to follow the nonlinear evolution of the solution. The update and augmentation method is inserted as a self-contained block into the solution algorithm. The reduced nonlinear terms required for the transient solution are expressed with the polynomial formulation as an integral part of the solution algorithm. The interpolation is used to adapt the initial reduced basis to external parameters. This integrated method responds to the three initially identified requirements and allows for a rapid, accurate and parameterisable reduced transient solution.

The integrated method is thoroughly tested. The initial application and testing takes place with the academic test-cases that are used to investigate the reduced bases. In order to demonstrate the applicability of the integrated method to finite element problems two such test-cases are solved. The test-cases are built with the geometrically nonlinear bar and volume elements that are introduced in the first chapter. All test-cases are extensively characterised because their characteristics determine the area of safe application of the integrated method.

In the conclusion in chapter 7 the central results and decisions are reviewed. An outlook on future

#### 1.4. HIGHLIGHTING THE ACHIEVEMENTS AND PROVIDING THE MANUSCRIPT'S OUTLINE

research is given.

## Chapter 2

# Laying the foundations of geometrically nonlinear structural dynamics

---

In this chapter the formulations of the dynamic equilibrium of geometrically nonlinear structural systems are introduced. First this is done in a continuous and then in a discrete manner. The nonlinearities are distributed over the entire structure and they are moderate, so that they allow a description of the structure's behaviour with the assumption of finite displacements. Beyond the assumption of finite displacements no other nonlinearities are considered.

The gradual expansion of the terms of the continuous formulation is aimed at introducing the Total-Lagrangian formulation. The choice for executing the continuous description in a Total-Lagrangian formulation with a linear material law is driven by the requirement for a purely geometrically nonlinear system that is to serve as a test-case.

The discrete formulation is developed alongside to render the continuous formulation computationally tractable and to yield a single matrix equation that describes the dynamic equilibrium. The detailed discrete descriptions of nonlinear bar and volume elements follow. These are required to build finite element test-cases to which the methods to be developed are applied. They are also used to highlight how the continuous formulation is reflected in the discrete formulation.

Finally, all discrete nonlinear terms of the dynamic equilibrium are condensed in a single matrix equation. This equation serves as the jump-off and hinging point for the following choice of a reduction method and a compatible transient solution procedure.

## 2.1 Expanding the continuous description of the dynamic equilibrium

In this section the dynamic equilibrium of a geometrically nonlinear structure is developed in continuous formulation. The involved terms are expanded gradually with the aim of preparing them for a discretisation. This expansion is the necessary prerequisite for the availability of the discrete formulation that is to be developed in the following section.

### 2.1.1 Expanding the dynamic equilibrium formulation

There is a number of standard volumes available on all angles of structural dynamics. The formulations below are mainly taken from Bathe [22] and Zienkiewicz et al. [247], which are rather common starting points for ventures into nonlinear structural dynamics. Additional information is available from Holzapfel [100], Wriggers [245] and Amabili [6].

The dynamic equilibrium of the displacements of the structure  $u(x, t)$  at the space position  $x$  at time  $t$ , can be written as

$$\rho \ddot{u} + \nabla S = f_E \quad \text{in } \Theta = (t_0, t_e] \times \Omega(t). \quad (2.1)$$

It expresses the equilibrium of forces in the entire spatial domain  $\Omega$ , occupied by the structure, over the time domain between  $t_0$  and  $t_e$ . The product of the material's density  $\rho$  with the accelerations  $\ddot{u}$  denotes the inertial forces. Overdots represent derivations with respect to time. The external forces that are acting on the body are expressed by  $f_E$ . The internal forces are expressed with the second Piola-Kirchhoff (2PK) stress tensor  $S$  as a combination of a strain measure with a material description. The displacements are defined as the differences between the space positions of a material point in two configurations

$$u = x^{(t)} - x^{(0)}. \quad (2.2)$$

The notion of configurations is a cornerstone of the nonlinear formulation of the dynamic equilibrium and expanded in more detail below.

The dynamic equilibrium is expressed in an inertial reference frame<sup>1</sup>. There are no damping terms included in equation (2.1) because a continuous formulation of damping at this stage would obscure the intention of presenting a geometrically nonlinear system. An empirical damping term is later added on matrix level.

Supposing a homogeneous, isotropic, non-dissipative, and linearly elastic material the 2PK stress tensor can be expressed as

$$S = \frac{E\nu}{(1+\nu)(1-2\nu)} \text{tr}(G) + 2\frac{E}{2(1+\nu)} G. \quad (2.3)$$

The material's properties are introduced by means of the Young's modulus  $E$  and the Poisson's ratio  $\nu$ . This description represents the engineering point of view. It is used exclusively throughout the remainder of this

---

<sup>1</sup>A prestressing due to a rotation is introduced later on matrix level to provide external parameters. It is treated in the dedicated section 6.3.2.2.

work<sup>2</sup>. The internal strains are expressed with the Green-Lagrange strain tensor  $G$ . Its components are

$$G_{ij} = \frac{1}{2} \left( \frac{\partial u_i}{\partial x_j} + \frac{\partial u_j}{\partial x_i} + \frac{\partial u_k}{\partial x_i} \frac{\partial u_k}{\partial x_j} \right). \quad (2.4)$$

The displacements are defined as in equation (2.2). Material points in the initial configuration of the system are labelled by  $x^{(0)}$ , while those of the deformed configuration at the instant  $t$  are labelled with  $x^{(t)}$ . The use of the Einstein summation convention in equation (2.4) stipulates summations over repeated indices. This concerns the nonlinear part, where a summation over the index  $k$  is implied. This leads to  $\sum_{k=1}^3 \frac{\partial u_k}{\partial x_i} \frac{\partial u_k}{\partial x_j}$  for the nonlinear part.

With the introduction of the deformation gradient

$$X_{ij} = \frac{\partial x_i^{(t)}}{\partial x_j^{(0)}}, \quad (2.5)$$

the Green-Lagrange strain tensor  $G$  becomes

$$G = \frac{1}{2} (X^T X - I), \quad (2.6)$$

which is more suited for discretisation purposes. Furthermore, the deformation gradient from equation (2.5) allows a link between the 2PK-stress, exclusively used for calculation and without a tangible physical meaning, and the physical Cauchy stress  $\sigma$ . This link is established by

$$\sigma = \frac{1}{\det X} X S X^T. \quad (2.7)$$

Reinserting all expanded terms from equations (2.3) to (2.7) into the initial equation (2.1) yields an equilibrium formulation that is almost ready for discretisation. The next step is the application of the principle of virtual work to reduce the degree of derivation of the displacements  $u$ . This is necessary because the order of derivation of the displacements  $u$  with respect to the spatial coordinates  $x$  is currently two. In equation (2.1). The  $\nabla$ -operator is applied to a strain measure, which, in itself, is a derivation of the displacement with respect to a spatial coordinate.

### 2.1.2 Introducing the principle of virtual work

The principle of virtual work is an application of the variational principle (e.g. Bathe [22]). This principle states that every displacement field  $u$  that is a solution of equation (2.1) remains a solution, regardless of the fact that the equation is multiplied with the virtual displacement field  $\delta u$ .

The equilibrium of a mechanical system, be it a single finite element or a whole body, can be expressed through the principle of virtual work in which the spatial derivations of the internal stresses  $\nabla S$  and the external forces  $f_E$  acting within and upon the system, respectively, multiplied with a virtual displacement field  $\delta u$  cancel each other out. That is, they are in perfect equilibrium, as indicated by e.g. Bonet and Wood [40, 5.23]. This translates into the sum of virtual works, performed by the real stresses and real forces on

---

<sup>2</sup>the factors 2 and  $\frac{1}{2}$  in equation (2.3) are kept to ensure compatibility with the common notation using Lamé constants  $\lambda$  and  $\mu$ . The Lamé constants are preferred for description of structural dynamics that is slanted towards the mathematical aspects. They are defined as  $\lambda = \frac{E\nu}{(1+\nu)(1-2\nu)}$  and  $\mu = \frac{E}{2(1+\nu)}$  (Zienkiewicz et al. [247])

the virtual displacements, being zero.

Equation (2.8) contains equation (2.1) in parentheses. It is multiplied with the virtual displacement field  $\delta u$ . The integrals are performed over the volume  $V$  of the body, which corresponds to the spatial domain occupied by the system.

$$\delta W = \int_V \delta u (\rho \ddot{u} - \nabla S - f_E) dV = 0. \quad (2.8)$$

Expanding equation (2.8) yields the spatial virtual work equation that states the equilibrium of a deformable system as in Bonet and Wood [40, 5.27]:

$$\int_V \delta u \rho \ddot{u} dV - \int_V \delta G S dV = \int_V \delta u f_E dV. \quad (2.9)$$

where  $\delta G$  is the virtual strain resulting from the virtual displacements  $\delta u$ . The additional term  $\int_V \delta u S dV$ , introduced through the integration by parts, is disposed of by additional considerations involving the properties of the  $\delta u$ .

The transition from equation (2.8) to equation (2.9) consists basically in a partial integration which is balanced by the introduction of the border terms. The aim of the partial integration is to shift one degree of derivation from the physical terms to the virtual terms; still with the ultimate intention to prepare the equilibrium for discretisation.

Equation (2.9), with its even distribution of derivations, could now be used for discretisation. However, the implications of the introduction of nonlinear stress and strain measurements and the integrations performed in equation (2.9) require considerable additional efforts that have to be directed at further expanding the terms as a preparation for numerical treatment. Additionally, the notion of configurations has to be introduced. Configurations govern the distinction between significant deformation states of the system. These deformation states serve as references to define the descriptions of the equilibrium and e.g. determine over which volume  $V$  the integrals in equation (2.9) are performed.

### 2.1.3 Considering initial and boundary conditions

Before continuing with the ongoing expansion of equation (2.1) a brief consideration of the initial and boundary conditions that can be applied is in order. These conditions are necessary for a meaningful solution and are important in the context of the introduction of a simulation time, at whose beginning the system's state is defined by the initial conditions. The boundary conditions are supposed to be constant during the entire simulated time  $(t_0, t_e]$ . Boundary conditions that evolve over time, and, even more, boundary conditions that are unknown, lead to the separate class of contact nonlinearities, which is not considered in the scope of this work.

As equation (2.1) is a second order differential equation in time, the two initial conditions for the displacements and the velocities have to be given as

$$u(x, 0) = u_0 \quad (2.10)$$

$$\dot{u}(x, 0) = \dot{u}_0. \quad (2.11)$$

Anticipating the definition of the different configurations in the following section, this would be the initial or reference configuration. If the  $u_0$  are all zero, this state is also called the undeformed configuration.

Boundary conditions on the boundary  $\partial\Omega$  of the domain are given either for the displacements or for the

applied forces. Prescribing displacements reads

$$u(\partial\Omega_u, t) = u_{\partial\Omega_u} \quad \forall t \in (t_0, t_e], \quad (2.12)$$

which is a Dirichlet boundary condition and translates to a clamping from the engineering point of view. Applying forces translates to

$$S(\partial\Omega_f, t) n = f_E(t) \quad \forall t \in (t_0, t_e], \quad (2.13)$$

which is a Neumann boundary condition and expresses external forcing. The normal  $n$  is introduced to associate a direction to the surface of the body.

For the boundaries of the system the conditions

$$\partial\Omega_u \cup \partial\Omega_f = \partial\Omega \quad (2.14)$$

$$\partial\Omega_u \cap \partial\Omega_f = \emptyset \quad (2.15)$$

have to be fulfilled. This condition prescribes boundary conditions to be set for the entire boundary of the system.

The formulation of the dynamic equilibrium, as it is presented in equation (2.1), does not yet contain any velocity dependent damping. Such effects are included later<sup>3</sup>, in a somewhat artificial manner, on matrix level once the problem is discretised. Damping effects on the boundary of the domain, as e.g. friction, are therefore not considered.

### 2.1.4 Uniting the previous definitions in the Total Lagrangian formulation

Transient solutions of structural dynamic systems are commonly solved with time-marching algorithms<sup>4</sup>. From an instant  $t \geq t_0$ , at which the state of the structure in  $u$  and  $\dot{u}$  is known, the next state at the instant  $t + \Delta t$  is calculated. The distance covered in time is the time-step  $\Delta t$ .

Geometrically nonlinear formulations drop one of the central assumptions of linear formulations, the one of infinitesimally small displacements. This is one of the major characteristics of geometrically nonlinear formulations because geometrically nonlinear formulations keep the assumptions of an ideally elastic material (see equation (2.3)) and of constant boundary conditions (see equations (2.12) and (2.13)). Allowing finite displacements implies that the body's volume  $V^{(t)}$  at the instant  $t$  is different from its volume  $V^{(0)}$  at the instant  $t_0$ . It also implies that the volume  $V^{(t+\Delta t)}$  at the instant  $t + \Delta t$  is as much an unknown as the displacements  $u(t + \Delta t)$ . This renders the evaluation of the integrals over the volume in equation (2.9) rather difficult. To simplify the representation, the inertial terms are dropped for now and later added again on matrix level.

To tackle this problem, the notion of configurations is introduced. It allows to unite specific measures of stress and strain and to understand them as a kind of transformation between a reference configuration and the current configuration. A multitude of approaches exists that differs in the choice of the reference configuration and the choice of the transformations between this reference configuration and the current, or deformed, configuration.

The notion of configurations delivers also a strong argument for neglecting mass and inertial terms for

---

<sup>3</sup>see section 2.3 on page 32

<sup>4</sup>Refer to section 3.2 for a selection of time-marching algorithms. Especially the presented nonlinear Newmark scheme and its variants are rather common in the context of structural dynamics.

now. The mass and inertial terms can simply be described in the reference configuration once the transformation of the stress and strain measures is performed. As this section is preoccupied with these transformations the mass and inertial terms are not detailed as they can be determined later in the reference configuration and reintroduced into the discrete description of the system's dynamics on matrix level.

The Total Lagrangian formulation is chosen here because it is one of the rather well understood standard approaches for metal-like materials<sup>5</sup> and allows to build on a robust basis, which is in widespread use, for applying further methods, which remains the ultimate aim of this research. This specific formulation takes the initial state at  $t_0$  as reference configuration. The transformations between this state and the deformed configuration at  $t + \Delta t$  are the previously introduced terms  $S$  and  $G$  for expressing the stresses and strains<sup>6</sup>. The measures  $S$  and  $G$  are work-conjugate because they are defined between the same configurations and thus yield a meaningful definition of work.

For the Total Lagrangian formulation the equivalent formulation of the principle of virtual work (2.9) reads, following the formulation of Bathe [22, 6.14],

$$\int_{V^{(0)}} \delta G_{ij}^{(0 \rightarrow t+\Delta t)} S_{ij}^{(0 \rightarrow t+\Delta t)} dV^{(0)} = \int_{V^{(t+\Delta t)}} f_E^{(t+\Delta t)} \delta u dV^{(t+\Delta t)} \quad (2.16)$$

where the work-conjugate quantities of the Second Piola-Kirchhoff stress  $S_{ij}^{(0 \rightarrow t+\Delta t)}$  and the virtual Green-Lagrange strain  $\delta G_{ij}^{(0 \rightarrow t+\Delta t)}$  have been introduced in order to allow for the treatment of finite displacements. Their superscripts  $(0 \rightarrow t + \Delta t)$  indicate that they are formulated between the initial, reference configuration at the instant  $t_0$  and the current, deformed configuration at the instant  $t + \Delta t$ . The inertial terms have been omitted. First, this is done for clarity and second, Bathe [22] states explicitly that the inertial efforts do not influence the formulation internal equilibrium. Ultimately, inertial efforts can simply be added to equation (2.16) as additional external forces that are defined in the reference configuration and that are acting on the volume of the body.

The Second Piola-Kirchhoff stress, in indicial notation, reads

$$S_{ij}^{(0 \rightarrow t+\Delta t)} = \frac{\rho^{(0)}}{\rho^{(t+\Delta t)}} \frac{\partial x_i^{(0)}}{\partial x_k^{(t+\Delta t)}} \sigma_{kl}^{(t+\Delta t)} \frac{\partial x_j^{(0)}}{\partial x_l^{(t+\Delta t)}}. \quad (2.17)$$

by inverting equation (2.7). This is basically a transformation of the basic Cauchy stress  $\sigma_{kl}^{(t+\Delta t)}$  between the reference configuration  $t_0$  and the deformed configuration of the system at  $t + \Delta t$ . It uses the transformation tensor formed by the partial derivatives  $\frac{\partial x_i^{(0)}}{\partial x_j^{(t+\Delta t)}}$  from equation (2.5). Again, the  $x_i^{(0)}$  are coordinates in the reference configuration and  $x_j^{(t+\Delta t)}$  are coordinates in the deformed configuration. Later, during the discretisation, this transformation will foremost affect the interpolation functions  $N$  as they can be expressed depending either on the  $x_i^{(0)}$  or on the  $x_i^{(t+\Delta t)}$ . The ratio of the densities  $\frac{\rho^{(0)}}{\rho^{(t+\Delta t)}}$  reflects the change in volume during the deformation. It is related to  $\det X$  in equation (2.7).

In anticipation of a solution that will use time integration between the instants  $t$  and  $t + \Delta t$  the second

<sup>5</sup>Other e.g. rubber-like materials and fluids may be solved more appropriately with e.g. the Updated Lagrangian formulation

<sup>6</sup>The Updated Lagrangian formulation follows the same approach but takes the state  $t$ , which is preceding the instant  $t + \Delta t$  as reference. This requires the use of other measures for the stresses and the strains. While the Total Lagrangian formulation requires considerable computation for the necessary transformations while allowing the integrations to be performed over the initial volume, it is the opposite for the Updated Lagrangian formulation, which does not require any transformation, but its integrations are performed over the deformed system, which comes at a comparable computational cost; see Bathe [22] and Krenk [123]).

## 2.1. EXPANDING THE CONTINUOUS DESCRIPTION OF THE DYNAMIC EQUILIBRIUM

Piola-Kirchhoff stress can be expanded to:

$$S_{ij}^{(0 \rightarrow t+\Delta t)} = S_{ij}^{(0 \rightarrow t)} + S_{ij}^{(t \rightarrow t+\Delta t)} \quad (2.18)$$

The same expansion can be applied to the Green-Lagrange strain, which is the work-conjugate strain measure to the second Piola-Kirchhoff stress. The Green-Lagrange strain  $G_{ij}^{(0 \rightarrow t+\Delta t)}$  from equation (2.4) can be written as

$$G_{ij}^{(0 \rightarrow t+\Delta t)} = \frac{1}{2} \left( \frac{\partial u_i^{(t+\Delta t)}}{\partial x_j^{(0)}} + \frac{\partial u_j^{(t+\Delta t)}}{\partial x_i^{(0)}} + \frac{\partial u_k^{(t+\Delta t)}}{\partial x_i^{(0)}} \frac{\partial u_k^{(t+\Delta t)}}{\partial x_j^{(0)}} \right), \quad (2.19)$$

which is then also expanded into:

$$G_{ij}^{(0 \rightarrow t+\Delta t)} = G_{ij}^{(0 \rightarrow t)} + G_{ij}^{(t \rightarrow t+\Delta t)}, \quad (2.20)$$

where the latter, incremental step  $G_{ij}^{(t \rightarrow t+\Delta t)}$ , is, in turn, decomposed into a linear  $e_{ij}^{(t \rightarrow t+\Delta t)}$  and a nonlinear  $\eta_{ij}^{(t \rightarrow t+\Delta t)}$  part. The two parts  $e_{ij}^{(t \rightarrow t+\Delta t)}$  and  $\eta_{ij}^{(t \rightarrow t+\Delta t)}$  read

$$G_{ij}^{(t \rightarrow t+\Delta t)} = e_{ij}^{(t \rightarrow t+\Delta t)} + \eta_{ij}^{(t \rightarrow t+\Delta t)} \quad (2.21)$$

$$e_{ij}^{(t \rightarrow t+\Delta t)} = \frac{1}{2} \left( \frac{\partial u_i^{(t \rightarrow t+\Delta t)}}{\partial x_j^{(0)}} + \frac{\partial u_j^{(t \rightarrow t+\Delta t)}}{\partial x_i^{(0)}} + \frac{\partial u_k^{(0 \rightarrow t)}}{\partial x_i^{(0)}} \frac{\partial u_k^{(t \rightarrow t+\Delta t)}}{\partial x_j^{(0)}} + \frac{\partial u_k^{(t \rightarrow t+\Delta t)}}{\partial x_i^{(0)}} \frac{\partial u_k^{(0 \rightarrow t)}}{\partial x_j^{(0)}} \right) \quad (2.22)$$

$$\eta_{ij}^{(t \rightarrow t+\Delta t)} = \frac{1}{2} \frac{\partial u_k^{(t \rightarrow t+\Delta t)}}{\partial x_i^{(0)}} \frac{\partial u_k^{(t \rightarrow t+\Delta t)}}{\partial x_j^{(0)}} \quad (2.23)$$

The property of nonlinearity of these two parts is defined with respect to the displacements  $u_k^{(t \rightarrow t+\Delta t)}$ . So,  $\eta_{ij}^{(t \rightarrow t+\Delta t)}$  is nonlinear in  $u_k^{(t \rightarrow t+\Delta t)}$  while  $e_{ij}^{(t \rightarrow t+\Delta t)}$  is linear in  $\partial u_k^{(t \rightarrow t+\Delta t)}$ , it contains various nonlinearities of the form  $u_k^{(0 \rightarrow t)} u_k^{(t \rightarrow t+\Delta t)}$ .

Separating incremental steps ( $t \rightarrow t + \Delta t$ ) from initial displacement steps ( $0 \rightarrow t$ ) yields the equation of virtual work

$$\begin{aligned} & \int_{V^{(0)}} \frac{\partial \delta u_i^{(t \rightarrow t+\Delta t)}}{\partial x_j} S_{ij}^{(t \rightarrow t+\Delta t)} dV^{(0)} + \int_{V^{(0)}} \delta \eta_{ij}^{(t \rightarrow t+\Delta t)} S_{ij}^{(0 \rightarrow t)} dV^{(0)} \\ & = \int_{V^{(0)}} f_E^{(t+\Delta t)} dV^{(0)} - \int_{V^{(0)}} \delta e_{ij}^{(t \rightarrow t+\Delta t)} S_{ij}^{(0 \rightarrow t)} dV^{(0)}, \end{aligned} \quad (2.24)$$

where the equality of  $\delta G_{ij}^{(0 \rightarrow t+\Delta t)} = \delta G_{ij}^{(t \rightarrow t+\Delta t)}$  (Bathe [22, p. 524]) has been exploited. This is the equivalent of equation (2.16) in the reference configuration (0).

This equation (2.24) is the complete continuous formulation of the equation of motion in a Total Lagrangian formulation. The inertial terms that are omitted in equation (2.16) have to be added and the equation has to be further linearised and discretised in order to allow for a numerical solution. The nonlinearities, introduced in the equations above, reside in the stresses  $S$  as they are transformed between the reference and the deformed configuration.

## 2.2 Discretising the equilibrium formulation

The central idea of the discretisation is to solve the underlying equation of the problem only at distinct spatial locations and interpolate between these locations with relatively simple functions. This avoids the search for one single and exceedingly complex function that covers the entire system. In the context of structural dynamics the dynamic equilibrium from equation (2.1) has to be solved for the displacements  $u$ . The distinct spatial locations are to become the nodes of a finite element mesh (Belytschko et al. [34]).

The first step is to approximate the displacements  $u(x_1, x_2, x_3, t)$  as the product of a vector with the nodal displacements and the displacement interpolation matrix  $\mathbf{N}$ . This is written as

$$u(x_1, x_2, x_3, t) \approx \mathbf{N}(x_1, x_2, x_3) \mathbf{u}(t). \quad (2.25)$$

It is the last time that the displacement field will appear as a continuous entity. The discrete displacements of all nodes are arranged in the vector  $\mathbf{u}$  in a suitable order

$$\mathbf{u}(t) = [u_1(t) \quad u_2(t) \quad u_3(t) \quad \dots \quad u_n(t)]^T \quad (2.26)$$

for the system which is supposed to possess  $n$  nodal degrees of freedom. This vector is called the vector of nodal displacements. The discrete nodal displacements are smeared over the volume of the system between the nodes by means of the displacement interpolation matrix  $\mathbf{N}(x_1, x_2, x_3)$ . The interpolation matrix contains relatively simple interpolation functions. It proves advantageous for further developments to use the discretisation to separate time and space. Hence, the vector of nodal displacements  $\mathbf{u}(t)$  depends exclusively on the time  $t$  and the displacement interpolation matrix  $\mathbf{N}(x_1, x_2, x_3)$  is time-invariant.

It is worth repeating and noting that the nodal displacements  $\mathbf{u}(t)$  do not represent absolute positions in space. On the contrary, in accordance with the notion of configurations, which was introduced in the preceding section, they represent incremental displacements between a reference configuration of the system and the deformed configuration. This is obvious for completely linear systems, where the displacements take place around an origin representing the static equilibrium state of the system. But when the description of the displacements is done in a geometrically nonlinear manner, the notion of the reference configuration becomes very important, as shown in section 2.1.4. The interpolation matrix  $\mathbf{N}$  has to be constructed accordingly to allow for a correct representation of the deformed continuous system by means of the nodal degrees of freedom. This somewhat dilutes the intention to strictly separate time- and space-dependent variables that is introduced with equation (2.25). However, the interpolation matrix  $\mathbf{N}$  has to follow the nonlinear deformations of the system and these deformations evolve with the time.

The approach of interpolating the nodal displacements to approximate the displacement field  $u$  can also be applied to the geometry of the finite element itself. The so-called mapping of finite elements is a transformation between the global coordinate space  $x_1, x_2$  and  $x_3$ , that contains the physical coordinates of the element's nodes, and a local, normalised coordinate space of the finite element. Within this local coordinate space, that is limited to each finite element, the coordinates  $\xi, \eta$  and  $\zeta$  range from  $-1$  to  $1$  each. In the case of so-called iso-parametric elements the mapping between the local and the global coordinate system is done with functions of the same order as the interpolation functions for the field variable. This course of

action proved advantageous because, the computational effort needed during the numerical solution for the transformations between the two systems is more than compensated for by the gain due to the application of standardised integration techniques, which are adapted for a normalised coordinate space. The mapping is an underlying layer of abstraction that transforms the physical quantities of geometry, which are of primary concern during structural analysis, to a formulation that is much more easily to handle numerically.

In the following the continuous formulations that are prepared for the discretisation in section 2.1.4 are briefly revisited and a first, generic discretisation is sketched. This sketch is performed without any theoretical rigour because it serves only to set the frame for the following introduction of two specific geometrically nonlinear finite elements: the nonlinear bar element and the nonlinear volume element. Especially the volume element serves to illustrate all aspects of a nonlinear finite element, from the iso-parametric mapping to the element's tangent stiffness matrix. The elements are chosen because they do not include rotations among their nodal degrees of freedom  $u_i$ , which would complicate the construction of the interpolation matrix  $N$  unnecessarily. Furthermore, these two types of elements will be used later to build nonlinear test-cases. The presentation of the elements is the final step in introducing the concept of geometric nonlinearity in structural dynamics. Once this final step is taken, the entire content of this chapter is condensed in a single matrix equation in final section 2.3.

### 2.2.1 Discretising the Total Lagrangian formulation

In the first part of this section it is sketched how the continuous formulation of the dynamic equilibrium in equation (2.1) is discretised. The sketching process remains on matrix level and sets the frame for the formulation of single elements in the next section. In a second part, the split in terms for time intervals from  $(t_0 \rightarrow t)$  and in terms for the time interval from  $(t \rightarrow t + \Delta t)$  is revisited and justified. This serves as a preparation for the incremental solution algorithm that is presented in the chapter 3 that follows.

#### 2.2.1.1 Establishing the discrete equilibrium formulation

In agreement with the ultimate aim of a numerical solution the overall stiffness matrix is introduced as a central part of the discretisation. It consists of a linear part  $\mathbf{K}_L^{(t_0 \rightarrow t)}$  and a nonlinear part  $\mathbf{K}_{NL}^{(t_0 \rightarrow t)}$ . The intention is to separate at least one instance of  $\mathbf{u}$  as a multiplicative factor in the formulation of the elastic, nonlinear internal forces

$$\mathbf{g}(\mathbf{u}) = \left( \mathbf{K}_L^{(t_0 \rightarrow t)} + \mathbf{K}_{NL}^{(t_0 \rightarrow t)} \right) \mathbf{u}. \quad (2.27)$$

Here, both terms  $\mathbf{K}_L^{(t_0 \rightarrow t)}$  and  $\mathbf{K}_{NL}^{(t_0 \rightarrow t)}$  are highly nonlinear in the spatial coordinates  $\mathbf{x}$ . But only  $\mathbf{K}_{NL}^{(t_0 \rightarrow t)}$  depends on  $\mathbf{u}$  and is hence termed the nonlinear part.

The linear part of the overall stiffness matrix is defined as

$$\mathbf{K}_L^{(t_0 \rightarrow t)} = \int_{V^{(t_0)}} \left( \mathbf{B}_L^{(t_0 \rightarrow t)} \right)^T \mathbf{C}^{(t_0)} \mathbf{B}_L^{(t_0 \rightarrow t)} dV^{(t_0)}. \quad (2.28)$$

The matrix  $\mathbf{C}^{(t_0)}$  regroups the components in  $E$  and  $\nu$  from the linear constitutional relation that is introduced in equation (2.3). The constitutional relation is defined in the reference configuration. The matrix  $\mathbf{B}_L^{(t_0 \rightarrow t)}$  contains the derivation of the interpolation matrix  $N$  with respect to the spatial coordinates  $\mathbf{x}$ . It contains all necessary elements for the transformation between the configurations  $t_0$  and  $t$ . This allows to perform the integrations of equation (2.9) over the undeformed volume  $V^{(t_0)}$ . This necessity of performing the transformation renders the linear part of the overall stiffness matrix highly nonlinear in the spatial co-

## 2.2. DISCRETISING THE EQUILIBRIUM FORMULATION

ordinates  $\mathbf{x}$ . Its name comes hence from the fact that it does not depend on the displacements  $\mathbf{u}$  so that the part of the internal forces expressed by  $\mathbf{K}_L^{(t_0 \rightarrow t)} \mathbf{u}$  is linear in  $\mathbf{u}$ .

The nonlinear part  $\mathbf{K}_{NL}^{(t_1 \rightarrow t_2)}$  of the stiffness matrix for the Total Lagrangian formulation is

$$\mathbf{K}_{NL}^{(t_0 \rightarrow t)} = \int_{V^{(t_0)}} \left( \mathbf{B}_{NL}^{(t_0 \rightarrow t)} \right)^T \mathbf{S}^{(t_0 \rightarrow t)} \mathbf{B}_{NL}^{(t_0 \rightarrow t)} dV^{(t_0)}. \quad (2.29)$$

This part differs according to the chosen formulation,. The term  $\mathbf{S}^{(t_0 \rightarrow t)}$  is the discrete representation of the 2PK stresses. The matrix  $\mathbf{B}_{NL}$  is a function of  $\mathbf{u}$ , which renders the expression  $\mathbf{K}_{NL}^{(t_0 \rightarrow t)} \mathbf{u}$  nonlinear in  $\mathbf{u}$ . It also remains highly nonlinear in the spatial coordinates  $\mathbf{x}$ .

Reintroducing the inertial effects, which were omitted in the final phase of the continuous formulation in the previous section, requires the definition of a mass matrix. This mass matrix, multiplied with the accelerations  $\ddot{\mathbf{u}}$ , the second order time derivations of the displacements, is to yield the inertial forces. It is defined as

$$\mathbf{M}^{(0)} = \int_{V^{(0)}} \mathbf{N}^T \rho^{(0)} \mathbf{N} dV^{(0)}. \quad (2.30)$$

Again, the integration is performed over the reference configuration as the used density of the material  $\rho^{(0)}$  is taken in the reference configuration. This is plausible because the matrices  $\mathbf{B}_L^{(t_0 \rightarrow t)}$  and  $\mathbf{B}_{NL}^{(t_0 \rightarrow t)}$  provide all necessary transformations to relay all calculations to the reference configuration.

The same goes for the external forces, which are expressed in the vector

$$\mathbf{f}_E^{(t+\Delta t)} = \int_{V^{(0)}} \mathbf{N}^T f_E^{(t+\Delta t)} dV^{(0)} + \int_{A^{(0)}} \mathbf{N}^T \mathbf{n} f_E^{(t+\Delta t)} dA^{(0)}. \quad (2.31)$$

It covers surface forces and all additional volume forces that are not of inertial nature.

With the definitions of the internal forces, the mass matrix and the external forces, the very first equation (2.1) can be rewritten in matrix form

$$\mathbf{M} \ddot{\mathbf{u}} + \mathbf{g}(\mathbf{u}) = \mathbf{f}_E(t), \quad (2.32)$$

which is as far as the discretisation on matrix level goes. Only a small addition to this principal matrix equation is made in section 2.3 in order to account for damping.

### 2.2.1.2 Preparing the discrete formulation for a numerical solution

Equation (2.24) saw the separation of the terms for the internal forces leading to components for time interval  $(0 \rightarrow t)$  and to incremental components for  $(t \rightarrow t + \Delta t)$ . This is not an arbitrary distinction but a preparation for the later use of the discrete formulation in a time-marching solution algorithm<sup>7</sup>. Within such an algorithm the nonlinear system is linearised at the instant  $t$  and iterations are made to extend the solution from the instant  $t$  to the next instant  $t + \Delta t$ . It becomes again evident that all previous efforts are solely directed towards a numerical solution.

Resulting from the separations of stress and strain in parts from  $(t_0 \rightarrow t)$  and from  $(t \rightarrow t + \Delta t)$  in

<sup>7</sup>Refer to section 3.2 for time-marching solution algorithms

## 2.2. DISCRETISING THE EQUILIBRIUM FORMULATION

---

equation (2.18), the incremental displacement  $\Delta \mathbf{u}$  in equation (2.33) represents an incremental displacement which is the difference between  $\mathbf{u}^{(t)}$  and  $\mathbf{u}^{(t+\Delta t)}$ . The formulation

$$\Delta \mathbf{u} = \mathbf{u}^{(t \rightarrow t+\Delta t)} = \mathbf{u}^{(t_0 \rightarrow t+\Delta t)} - \mathbf{u}^{(t_0 \rightarrow t)}, \quad (2.33)$$

is introduced in anticipation of the resolution of the equation above with a nonlinear Newmark algorithm in section 3.2. It is worth noting that the linearisation is only applied to the incremental terms, which span the displacements from  $t$  to  $t + \Delta t$ , while terms that link the current configuration  $t$  to the reference configuration  $t_0$  are not affected. This reflects the fact that the linearisation between the instants  $t$  and  $t + \Delta t$  is basically an expansion of the incremental terms, which neglects higher order terms under the assumption that the increment  $\Delta \mathbf{u}$  in the time-step  $\Delta t$  is sufficiently small.

The incremental displacement  $\Delta \mathbf{u}$  is introduced by the linearisation

$$\mathbf{g}(\mathbf{u}^{(t+\Delta t)}) \approx \mathbf{g}(\mathbf{u}^{(t)}) + \left( \mathbf{K}_{NL}^{(t_0 \rightarrow t)} + \mathbf{K}_L^{(t_0 \rightarrow t)} \right) \Delta \mathbf{u}. \quad (2.34)$$

Then  $\Delta \mathbf{u}$  can be calculated from

$$\begin{aligned} M^{(0)} \ddot{\mathbf{u}}^{(t+\Delta t)} + \left( \mathbf{K}_{NL}^{(t_0 \rightarrow t)} + \mathbf{K}_L^{(t_0 \rightarrow t)} \right) \Delta \mathbf{u} &= \mathbf{f}_E^{(t+\Delta t)} - \mathbf{g}(\mathbf{u}^{(t)}) \\ &= \mathbf{r}^{(t+\Delta t)}. \end{aligned} \quad (2.35)$$

It is still stipulated in this formulation that the external forces  $\mathbf{f}_E^{(t+\Delta t)}$  do not depend on  $\mathbf{u}^{(t+\Delta t)}$  and are thus deformation-independent. The residual  $\mathbf{r}^{(t+\Delta t)}$  plays a prominent role in developing a time-marching solution algorithm.

Albeit this high level equation gives a well-arranged and generic view of the nonlinear formulation it is not to be forgotten that the underlying operations, such as establishing the matrices  $\mathbf{B}_L$  and  $\mathbf{B}_{NL}$ , now regrouped in the vector  $\mathbf{g}(\mathbf{u})$  via the corresponding linear and nonlinear stiffness matrices, require extensive computation. However, due to its clearness in representation the vector  $\mathbf{g}(\mathbf{u})$  presents well the interest of splitting the nonlinear terms in the two time intervals  $(t_0 \rightarrow t)$  and  $(t \rightarrow t + \Delta t)$  and to separate  $\mathbf{u}$  as a multiplicative factor in the formulation of the internal forces  $\mathbf{g}(\mathbf{u})$  in equation (2.27).

### 2.2.2 Developing the nonlinear bar element

As a first step towards the application of the developed methods to a finite element test-case the methods are applied on a nonlinear bar element under compression and tension. The bar element allows to demonstrate the basic principle of discretisation, smearing the nodal displacements over the volume with the interpolation functions to approximate the continuous field. Also, the geometry of the bar element is very simple, so that the basic principle of discretisation can be exposed without diluting its prominence with other necessary operations, such as numerical integration schemes. For a complete presentation of such operations the volume element is presented in the next section.

In Ihlenburg [104] the author of Ihlenburg [103] compares two possible descriptions, taken from Bonet and Wood [40] and Krenk [123], of a geometrically nonlinear bar element. In order to anticipate the volume finite elements that are to be developed later, the Total Lagrangian formulation with the Green-Lagrange strain and the second Piola-Kirchhoff stress is chosen. Directly formulating the element's matrices allows avoiding lower-level aspects of the finite element method, in particular the basis functions and their integration with Gauss-points, that would, for now, only add an unnecessary layer of complication.

## 2.2. DISCRETISING THE EQUILIBRIUM FORMULATION

The matrices are given for a single bar element. The assembly to the global system's matrices follows the standard procedure of the finite element method. The values for the geometric properties  $L$  for the length and  $A$  for the section area as well as for the material's properties  $\rho$  for the density and  $E$  for the Young's modulus are to be understood as specific for the element under consideration. The used material law is a simple linearly elastic one, characterised only by the Young's modulus.

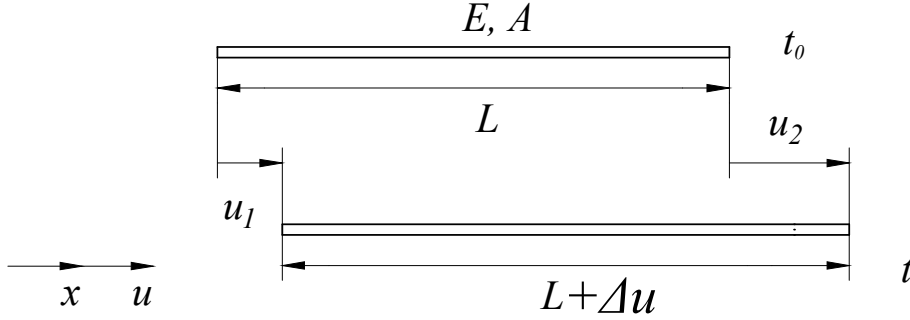


Figure 2.1: The nonlinear bar element before and after deformation

Figure 2.1 displays the element. Its displacement field  $u(x, t)$  is a function of time  $t$  and the only spatial direction  $x$ . The discretisation of this field requires the introduction of the nodal displacements  $u_1(t)$  and  $u_2(t)$  that describe the displacements of the two extremities of the bar. With the introduction of the interpolation matrix  $N = [1 - \frac{x}{L}, \frac{x}{L}]$  the bar's displacement field is approximated as

$$u(x, t) \approx \mathbf{N} \mathbf{u} \quad (2.36)$$

$$= \begin{bmatrix} 1 - \frac{x}{L} & \frac{x}{L} \end{bmatrix} \begin{bmatrix} u_1(t) \\ u_2(t) \end{bmatrix}. \quad (2.37)$$

This approximation follows the exact course of action that is initiated by the equation (2.25). Following through with this course of action with equation (2.30) yields the mass matrix of the element

$$\mathbf{M} = \frac{\rho EA}{6} \begin{bmatrix} 2 & -1 \\ -1 & 2 \end{bmatrix}. \quad (2.38)$$

The nonlinear forces vector is given as

$$\mathbf{g} = EA \frac{(L + \Delta u)^2 - L^2}{2L^2} \begin{bmatrix} -1 \\ 1 \end{bmatrix}, \quad (2.39)$$

where the lengthening of the element  $\Delta u$  is the difference of the displacements of its two nodes  $u_2 - u_1$ .

The nonlinear tangent stiffness matrix of the element is given as

$$\bar{\mathbf{K}} = \frac{EA}{L^3} \left( \begin{bmatrix} L^2 & -L^2 \\ -L^2 & L^2 \end{bmatrix} + \begin{bmatrix} (L\Delta u + \Delta u L + (\Delta u)^2) & - (L\Delta u + \Delta u L + (\Delta u)^2) \\ - (L\Delta u + \Delta u L + (\Delta u)^2) & (L\Delta u + \Delta u L + (\Delta u)^2) \end{bmatrix} + \frac{g}{EA} \begin{bmatrix} L^2 & -L^2 \\ -L^2 & L^2 \end{bmatrix} \right), \quad (2.40)$$

where  $g$  represents the norm of the nonlinear internal force from equation (2.39), which is considered to be constant throughout the element.

This concludes already the preparation of a geometrically nonlinear bar element for its application as a finite element. With the equations developed above, a complete discrete description of the nonlinear bar element is prepared and will be used as numerical test-case later on.

### 2.2.3 Developing the nonlinear volume element

The preceding continuous formulation of the nonlinear behaviour is now used in the finite element method. This section sketches the calculations that are necessary to be performed in order to obtain the nonlinear stiffness matrix and the vector of nonlinear internal forces of a single hexahedron element. The sketch follows closely the approach presented in preceding sections. However, the introduction of the interpolation functions now takes place on the level of local coordinates. The material law is added explicitly to relate stress with strain expressions. These combinations are consecutively assembled and prepared for numerical integration. With the numerical integrations performed, the expressions for the mass matrix  $\mathbf{M}$ , the tangent stiffness matrix  $\mathbf{K}_{NL}$  and the vector of the nonlinear internal forces  $\mathbf{g}(\mathbf{u})$  are obtained. This allows using the nonlinear volume element in a discrete formulation such as equation (2.32). Typical finite element procedures beyond the level of a single nonlinear element are not treated as part of this section. Such assembly procedures are described, together with the finite element itself, in dedicated literature such as Wriggers [245], Zienkiewicz et al. [247] or Bathe [22].

The finite volume element is chosen because it allows building complex test-cases.

#### 2.2.3.1 Introducing mapping and presenting the interpolation functions

Figure 2.2 shows the hexahedron with its nodes and the global coordinate system  $x, y$  and  $z$ . The first step to be taken is the so-called mapping, the transformation of the description to the local coordinate system.

On element level its geometry and its deformation are described in terms of the local coordinates  $\xi, \eta$  and  $\zeta$ , all three ranging from  $-1$  to  $1$ . The relation to the physical variables of geometry  $x, y$  and  $z$  and displacements  $u, v$  and  $w$  is established with interpolation functions  $h_i(\xi, \eta, \zeta)$ , where there is one  $h_i$  for every node of the element.

For the physical coordinates  $x, y$  and  $z$  the mapping is expressed as

$$x(\xi, \eta, \zeta) = \sum_{i=1}^8 h_i(\xi, \eta, \zeta) x_i \quad (2.41)$$

$$y(\xi, \eta, \zeta) = \sum_{i=1}^8 h_i(\xi, \eta, \zeta) y_i \quad (2.42)$$

$$z(\xi, \eta, \zeta) = \sum_{i=1}^8 h_i(\xi, \eta, \zeta) z_i, \quad (2.43)$$

which represents the sums of the products of the interpolation functions with the nodal values.

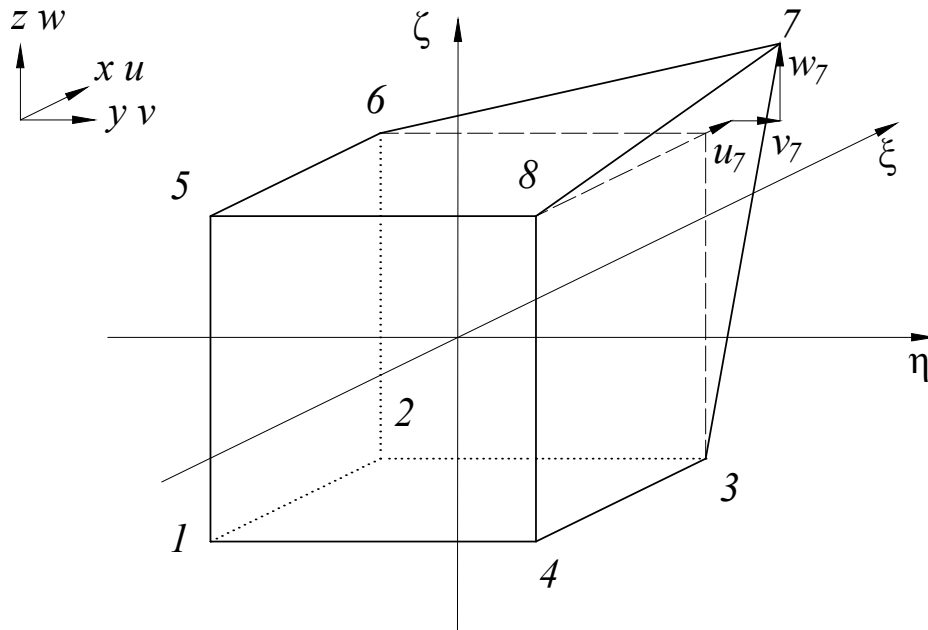


Figure 2.2: The nonlinear volume hexahedron element and the position of its nodes

For the hexahedron-element there are eight nodes to be defined. Table 2.1 attributes to each node its position in the basic hexahedron in terms of the local coordinates  $\xi$ ,  $\eta$  and  $\zeta$ .

There is one corresponding interpolation function for the mapping for each of the eight nodes. These interpolation functions attain 1 as value at the position of the node and 0 at all other nodes. For linear interpolation functions and the chosen hexahedron these functions are

$$h_i(\xi, \eta, \zeta) = \frac{1}{8} (1 + \xi_i \xi) (1 + \eta_i \eta) (1 + \zeta_i \zeta) \quad (2.44)$$

with  $i \in \{1, \dots, 8\}$ . This allows expressing the absolute values of the geometry and the displacements as function of the local coordinates. In order to be able to express also the derivations of these functions in the space of the localised coordinates the derivations of the interpolation functions from (2.44) with respect to the local coordinates are given as

$i$	$\xi_i$	$\eta_i$	$\zeta_i$
1	-1	-1	-1
2	1	-1	-1
3	1	1	-1
4	-1	1	-1
5	-1	-1	1
6	1	-1	1
7	1	1	1
8	-1	1	1

Table 2.1: The distribution of the nodes on the hexahedron in local coordinates

$$\frac{\partial h_i}{\partial \xi}(\eta, \zeta) = \frac{1}{8} (\xi_i) (1 + \eta_i \eta) (1 + \zeta_i \zeta) \quad (2.45)$$

$$\frac{\partial h_i}{\partial \eta}(\xi, \zeta) = \frac{1}{8} (1 + \xi_i \xi) (\eta_i) (1 + \zeta_i \zeta) \quad (2.46)$$

$$\frac{\partial h_i}{\partial \zeta}(\xi, \eta) = \frac{1}{8} (1 + \xi_i \xi) (1 + \eta_i \eta) (\zeta_i). \quad (2.47)$$

Again these three derivations exist for every of the eight nodes in the hexahedron-element, given in table 2.1, leading to  $i \in \{1, \dots, 8\}$ .

### 2.2.3.2 Expressing physical variables

The physical variables of the hexahedron-element, namely its displacements  $u$ ,  $v$  and  $w$  and its geometry  $x$ ,  $y$  and  $z$ , are expressed as functions of the local coordinates  $\xi$ ,  $\eta$  and  $\zeta$  by summing over the product of their nodal values with the interpolation functions.

The physical displacements of the nodes of the element are supposed to be known and are given in table 2.2.

$i$	$u_i$	$v_i$	$w_i$
1	$u_1$	$v_1$	$w_1$
2	$u_2$	$v_2$	$w_2$
3	$u_3$	$v_3$	$w_3$
4	$u_4$	$v_4$	$w_4$
5	$u_5$	$v_5$	$w_5$
6	$u_6$	$v_6$	$w_6$
7	$u_7$	$v_7$	$w_7$
8	$u_8$	$v_8$	$w_8$

Table 2.2: The physical displacements of the nodes on the hexahedron

Here the displacements are designated  $u$ ,  $v$  and  $w$  to be in accordance with figure 2.2. These designations distinguish between displacements in  $x$ ,  $y$  and  $z$ -direction, respectively. However, these designations are only used on element level and for illustration purposes. If the elements are later assembled and share the degrees of freedom of the node at which they are connected, all degrees of freedom, regardless of their

## 2.2. DISCRETISING THE EQUILIBRIUM FORMULATION

---

direction or nature, i.e. translation or even rotation, are given a unique  $u_i$  identification. The subscript  $i$  is sequential and assigned by an algorithm that tries to optimise the bandwidth of the resulting global matrices in the case of a high-performance commercial finite element code. This allows to regroup all physical displacements in a single vector  $\mathbf{u}$ .

In order to describe the displacement fields all over the hexahedron-element the three sums are build

$$u(\xi, \eta, \zeta) = \sum_{i=1}^8 h_i(\xi, \eta, \zeta) u_i \quad (2.48)$$

$$v(\xi, \eta, \zeta) = \sum_{i=1}^8 h_i(\xi, \eta, \zeta) v_i \quad (2.49)$$

$$w(\xi, \eta, \zeta) = \sum_{i=1}^8 h_i(\xi, \eta, \zeta) w_i, \quad (2.50)$$

where the interpolation functions  $h_i$  are defined in equation (2.44) in conjunction with table 2.1. This implies that the three displacement fields for the three spatial directions can be expressed independently from each other. For numerical efficiency these sums are naturally obtained by vector multiplications. For e.g. equation (2.48) this vector form reads

$$u(\xi, \eta, \zeta) = [h_1(\xi, \eta, \zeta), h_2(\xi, \eta, \zeta), \dots, h_7(\xi, \eta, \zeta), h_8(\xi, \eta, \zeta)] \begin{bmatrix} u_1 \\ u_2 \\ u_3 \\ u_4 \\ u_5 \\ u_6 \\ u_7 \\ u_8 \end{bmatrix}, \quad (2.51)$$

and serves as blueprint for the vector forms of equations (2.49) and (2.50). The spatial derivations of the displacement fields are obtained in exactly the same manner

$$\frac{\partial u}{\partial \xi} = \sum_{i=1}^8 \frac{\partial h_i}{\partial \xi} u_i \quad \frac{\partial u}{\partial \eta} = \sum_{i=1}^8 \frac{\partial h_i}{\partial \eta} u_i \quad \frac{\partial u}{\partial \zeta} = \sum_{i=1}^8 \frac{\partial h_i}{\partial \zeta} u_i \quad (2.52)$$

$$\frac{\partial v}{\partial \xi} = \sum_{i=1}^8 \frac{\partial h_i}{\partial \xi} v_i \quad \frac{\partial v}{\partial \eta} = \sum_{i=1}^8 \frac{\partial h_i}{\partial \eta} v_i \quad \frac{\partial v}{\partial \zeta} = \sum_{i=1}^8 \frac{\partial h_i}{\partial \zeta} v_i \quad (2.53)$$

$$\frac{\partial w}{\partial \xi} = \sum_{i=1}^8 \frac{\partial h_i}{\partial \xi} w_i \quad \frac{\partial w}{\partial \eta} = \sum_{i=1}^8 \frac{\partial h_i}{\partial \eta} w_i \quad \frac{\partial w}{\partial \zeta} = \sum_{i=1}^8 \frac{\partial h_i}{\partial \zeta} w_i. \quad (2.54)$$

Here all terms, except the nodal values  $u_i$ ,  $v_i$  and  $w_i$ , are a function of the local coordinates  $\xi$ ,  $\eta$  and  $\zeta$ . The nodal values are supposed to be known and come from table 2.2 while the spatial derivations of the interpolation functions come from equations (2.45) to (2.47).

In anticipation of the transformation of integrations between the physical volume of the element and the unit space of the local coordinates of the hexahedron, the same spatial derivations have to be defined for the geometry. The physical coordinates of the nodes are supposed to be known and are shown in table 2.3.

$i$	$x_i$	$y_i$	$z_i$
1	$x_1$	$y_1$	$z_1$
2	$x_2$	$y_2$	$z_2$
3	$x_3$	$y_3$	$z_3$
4	$x_4$	$y_4$	$z_4$
5	$x_5$	$y_5$	$z_5$
6	$x_6$	$y_6$	$z_6$
7	$x_7$	$y_7$	$z_7$
8	$x_8$	$y_8$	$z_8$

Table 2.3: The physical coordinates of the nodes on the hexahedron

The spatial derivations of the geometry and thus the equivalences to equations (2.52) to (2.54) for the geometry read

$$\frac{\partial x}{\partial \xi} = \sum_{i=1}^8 \frac{\partial h_i}{\partial \xi} x_i \quad \frac{\partial x}{\partial \eta} = \sum_{i=1}^8 \frac{\partial h_i}{\partial \eta} x_i \quad \frac{\partial x}{\partial \zeta} = \sum_{i=1}^8 \frac{\partial h_i}{\partial \zeta} x_i \quad (2.55)$$

$$\frac{\partial y}{\partial \xi} = \sum_{i=1}^8 \frac{\partial h_i}{\partial \xi} y_i \quad \frac{\partial y}{\partial \eta} = \sum_{i=1}^8 \frac{\partial h_i}{\partial \eta} y_i \quad \frac{\partial y}{\partial \zeta} = \sum_{i=1}^8 \frac{\partial h_i}{\partial \zeta} y_i \quad (2.56)$$

$$\frac{\partial z}{\partial \xi} = \sum_{i=1}^8 \frac{\partial h_i}{\partial \xi} z_i \quad \frac{\partial z}{\partial \eta} = \sum_{i=1}^8 \frac{\partial h_i}{\partial \eta} z_i \quad \frac{\partial z}{\partial \zeta} = \sum_{i=1}^8 \frac{\partial h_i}{\partial \zeta} z_i, \quad (2.57)$$

where again all terms, except the nodal values  $x_i$ ,  $y_i$  and  $z_i$ , are a function of the local coordinates  $\xi$ ,  $\eta$  and  $\zeta$ .

### 2.2.3.3 Establishing the matrices

With most descriptive preparations performed, the element's mass and stiffness matrix can be build. Establishing the stiffness matrix of an element requires the definition of several sub-matrices. These go by a variety of names and their physical meaning is not explored in particular. The stiffness matrix also requires the description of the law governing the behaviour of the material that constitutes the element. This stress-strain-relation is supposed to be linear.

**2.2.3.3.1 Prescribing a linear stress-strain-relation** The stress-strain relation that describes the material of the element allows expressing the internal stresses as a function of displacements. This form of the stress-strain relation is used in the so-called Voith-notation (Zienkiewicz et al. [247]) of the stress and strain calculation, which requires

$$\hat{\sigma} = C\hat{\epsilon}. \quad (2.58)$$

## 2.2. DISCRETISING THE EQUILIBRIUM FORMULATION

---

For an ideally elastic, isotropic material e.g. Zienkiewicz et al. [247] gives the required matrix as

$$\mathbf{C} = \frac{E}{(1+\nu)(1-2\nu)} \begin{bmatrix} 1-\nu & \nu & \nu & 0 & 0 & 0 \\ \nu & 1-\nu & \nu & 0 & 0 & 0 \\ \nu & \nu & 1-\nu & 0 & 0 & 0 \\ 0 & 0 & 0 & \frac{1-2\nu}{2} & 0 & 0 \\ 0 & 0 & 0 & 0 & \frac{1-2\nu}{2} & 0 \\ 0 & 0 & 0 & 0 & 0 & \frac{1-2\nu}{2} \end{bmatrix}, \quad (2.59)$$

in which the parameters  $E$  and  $\nu$  describe the Young's modulus and the Poisson's ratio, respectively. The vector  $\hat{\epsilon}$  regroups the strains and is defined as

$$\hat{\epsilon} = \begin{bmatrix} \hat{\epsilon}_1 \\ \hat{\epsilon}_2 \\ \hat{\epsilon}_3 \\ \hat{\epsilon}_4 \\ \hat{\epsilon}_5 \\ \hat{\epsilon}_6 \end{bmatrix} = \begin{bmatrix} \frac{\partial u}{\partial \xi} \\ \frac{\partial v}{\partial \eta} \\ \frac{\partial w}{\partial \zeta} \\ \frac{1}{2} \left( \frac{\partial u}{\partial \eta} + \frac{\partial v}{\partial \xi} \right) \\ \frac{1}{2} \left( \frac{\partial v}{\partial \zeta} + \frac{\partial w}{\partial \eta} \right) \\ \frac{1}{2} \left( \frac{\partial u}{\partial \zeta} + \frac{\partial w}{\partial \xi} \right) \end{bmatrix} \quad (2.60)$$

in the so-called engineering formulation (Bathe [22]), where the spatial derivations are defined in equations (2.52) to (2.54). This makes the strain  $\hat{\epsilon}$  a function of the local coordinates  $\xi$ ,  $\eta$  and  $\zeta$ . Application of equation (2.58) yields the vector of the Cauchy-stress  $\hat{\sigma}$ , which can be written in components as

$$\hat{\sigma} = \begin{bmatrix} \hat{\sigma}_1 \\ \hat{\sigma}_2 \\ \hat{\sigma}_3 \\ \hat{\sigma}_4 \\ \hat{\sigma}_5 \\ \hat{\sigma}_6 \end{bmatrix}, \quad (2.61)$$

and can also be arranged in the matrix form

$$\boldsymbol{\sigma} = \begin{bmatrix} \hat{\sigma}_1 & \hat{\sigma}_4 & \hat{\sigma}_6 \\ \hat{\sigma}_4 & \hat{\sigma}_2 & \hat{\sigma}_5 \\ \hat{\sigma}_6 & \hat{\sigma}_5 & \hat{\sigma}_3 \end{bmatrix}. \quad (2.62)$$

**2.2.3.3.2 Developing the deformation Gradient and second Piola-Kirchhoff stress** The deformation gradient, originally introduced in equation (2.5) and required for the nonlinear description, is given in its

discrete form by e.g. Krenk [123] as

$$\mathbf{X} = \begin{bmatrix} 1 & 0 & 0 \\ 0 & 1 & 0 \\ 0 & 0 & 1 \end{bmatrix} + \begin{bmatrix} \frac{\partial u}{\partial \xi} & \frac{\partial u}{\partial \eta} & \frac{\partial u}{\partial \zeta} \\ \frac{\partial v}{\partial \xi} & \frac{\partial v}{\partial \eta} & \frac{\partial v}{\partial \zeta} \\ \frac{\partial w}{\partial \xi} & \frac{\partial w}{\partial \eta} & \frac{\partial w}{\partial \zeta} \end{bmatrix} \quad (2.63)$$

where the spatial derivations are defined in equations (2.52) to (2.54). Together with the matrix form of the Cauchy stress  $\hat{\boldsymbol{\sigma}}$  from equation (2.62) the deformation gradient  $\mathbf{X}$  is used to define the second Piola-Kirchhoff stress  $\mathbf{S}$ . The 2PK stress  $\mathbf{S}$ , which is given in its continuous form in equation (2.3), becomes

$$\mathbf{S} = \det(\mathbf{X}) \mathbf{X} \boldsymbol{\sigma} \mathbf{X}^T, \quad (2.64)$$

when discretised. This  $3 \times 3$ -matrix is not directly of need in the calculations to follow. It is instead used in the form of one matrix

$$\tilde{\mathbf{S}} = \begin{bmatrix} \begin{bmatrix} \mathbf{S} \end{bmatrix} & \begin{bmatrix} 0 & 0 & 0 \\ 0 & 0 & 0 \\ 0 & 0 & 0 \end{bmatrix} & \begin{bmatrix} 0 & 0 & 0 \\ 0 & 0 & 0 \\ 0 & 0 & 0 \end{bmatrix} \\ \begin{bmatrix} 0 & 0 & 0 \\ 0 & 0 & 0 \\ 0 & 0 & 0 \end{bmatrix} & \begin{bmatrix} \mathbf{S} \end{bmatrix} & \begin{bmatrix} 0 & 0 & 0 \\ 0 & 0 & 0 \\ 0 & 0 & 0 \end{bmatrix} \\ \begin{bmatrix} 0 & 0 & 0 \\ 0 & 0 & 0 \\ 0 & 0 & 0 \end{bmatrix} & \begin{bmatrix} 0 & 0 & 0 \\ 0 & 0 & 0 \\ 0 & 0 & 0 \end{bmatrix} & \begin{bmatrix} \mathbf{S} \end{bmatrix} \end{bmatrix} \quad (2.65)$$

and its vector form

$$\hat{\mathbf{S}} = \begin{bmatrix} \hat{S}_1 \\ \hat{S}_2 \\ \hat{S}_3 \\ \hat{S}_4 \\ \hat{S}_5 \\ \hat{S}_6 \end{bmatrix} = \begin{bmatrix} S_{11} \\ S_{22} \\ S_{33} \\ 2S_{12} \\ 2S_{23} \\ 2S_{31} \end{bmatrix}. \quad (2.66)$$

This concludes the description of physical entities, especially the stress measure, in matrix form. The next step is the definition of the interpolation and transformation matrices.

**2.2.3.3.3 Defining the interpolation and transformation matrices** The interpolation matrix regroups the interpolation functions from equation (2.44) to allow for an approximation of the displacement field in the form of a matrix-vector product with the nodal displacements, as introduced in equation (2.25).

## 2.2. DISCRETISING THE EQUILIBRIUM FORMULATION

The direct interpolation matrix is defined as

$$\mathbf{N} = \begin{bmatrix} h_1(\xi, \eta, \zeta) & 0 & 0 & h_8(\xi, \eta, \zeta) & 0 & 0 \\ 0 & h_1(\xi, \eta, \zeta) & 0 & \dots & 0 & h_8(\xi, \eta, \zeta) \\ 0 & 0 & h_1(\xi, \eta, \zeta) & & 0 & h_8(\xi, \eta, \zeta) \end{bmatrix}, \quad (2.67)$$

with the interpolation function being defined by equation (2.44).

The linear strain displacement transformation matrix is defined as

$$\mathbf{B}_L(\xi, \eta, \zeta) = \mathbf{B}^{(1)}(\xi, \eta, \zeta) + \mathbf{B}^{(2)}(\xi, \eta, \zeta) \quad (2.68)$$

with

$$\mathbf{B}^{(1)} = \begin{bmatrix} \frac{\partial h_1}{\partial \xi} & 0 & 0 & \dots & \frac{\partial h_8}{\partial \xi} & 0 & 0 \\ 0 & \frac{\partial h_1}{\partial \eta} & 0 & & 0 & \frac{\partial h_8}{\partial \eta} & 0 \\ 0 & 0 & \frac{\partial h_1}{\partial \zeta} & \dots & 0 & 0 & \frac{\partial h_8}{\partial \zeta} \\ \frac{\partial h_1}{\partial \eta} & \frac{\partial h_1}{\partial \xi} & 0 & & \frac{\partial h_8}{\partial \eta} & \frac{\partial h_8}{\partial \xi} & 0 \\ 0 & \frac{\partial h_1}{\partial \zeta} & \frac{\partial h_1}{\partial \eta} & & 0 & \frac{\partial h_8}{\partial \zeta} & \frac{\partial h_8}{\partial \eta} \\ \frac{\partial h_1}{\partial \zeta} & 0 & \frac{\partial h_1}{\partial \xi} & & \frac{\partial h_8}{\partial \zeta} & 0 & \frac{\partial h_8}{\partial \xi} \end{bmatrix}, \quad (2.69)$$

where the spatial derivations of the interpolation functions are taken from equations (2.45) to (2.47), and

$$\mathbf{B}^{(2)} = [\mathbf{B}_1^{(2)}, \mathbf{B}_2^{(2)}, \dots, \mathbf{B}_8^{(2)}], \quad (2.70)$$

where

$$\mathbf{B}_i^{(2)} = \begin{bmatrix} \begin{pmatrix} \frac{\partial u}{\partial \xi} \\ \frac{\partial u}{\partial \eta} \\ \frac{\partial u}{\partial \zeta} \end{pmatrix} \frac{\partial h_i}{\partial \xi} & \begin{pmatrix} \frac{\partial v}{\partial \xi} \\ \frac{\partial v}{\partial \eta} \\ \frac{\partial v}{\partial \zeta} \end{pmatrix} \frac{\partial h_i}{\partial \xi} & \begin{pmatrix} \frac{\partial w}{\partial \xi} \\ \frac{\partial w}{\partial \eta} \\ \frac{\partial w}{\partial \zeta} \end{pmatrix} \frac{\partial h_i}{\partial \xi} \\ \begin{pmatrix} \frac{\partial u}{\partial \xi} \\ \frac{\partial u}{\partial \eta} \\ \frac{\partial u}{\partial \zeta} \end{pmatrix} \frac{\partial h_i}{\partial \eta} + \begin{pmatrix} \frac{\partial u}{\partial \eta} \\ \frac{\partial u}{\partial \zeta} \\ \frac{\partial u}{\partial \xi} \end{pmatrix} \frac{\partial h_i}{\partial \xi} & \begin{pmatrix} \frac{\partial v}{\partial \xi} \\ \frac{\partial v}{\partial \eta} \\ \frac{\partial v}{\partial \zeta} \end{pmatrix} \frac{\partial h_i}{\partial \eta} + \begin{pmatrix} \frac{\partial v}{\partial \eta} \\ \frac{\partial v}{\partial \zeta} \\ \frac{\partial v}{\partial \xi} \end{pmatrix} \frac{\partial h_i}{\partial \xi} & \begin{pmatrix} \frac{\partial w}{\partial \xi} \\ \frac{\partial w}{\partial \eta} \\ \frac{\partial w}{\partial \zeta} \end{pmatrix} \frac{\partial h_i}{\partial \eta} + \begin{pmatrix} \frac{\partial w}{\partial \eta} \\ \frac{\partial w}{\partial \zeta} \\ \frac{\partial w}{\partial \xi} \end{pmatrix} \frac{\partial h_i}{\partial \xi} \\ \begin{pmatrix} \frac{\partial u}{\partial \xi} \\ \frac{\partial u}{\partial \eta} \\ \frac{\partial u}{\partial \zeta} \end{pmatrix} \frac{\partial h_i}{\partial \zeta} + \begin{pmatrix} \frac{\partial u}{\partial \zeta} \\ \frac{\partial u}{\partial \xi} \\ \frac{\partial u}{\partial \eta} \end{pmatrix} \frac{\partial h_i}{\partial \xi} & \begin{pmatrix} \frac{\partial v}{\partial \xi} \\ \frac{\partial v}{\partial \eta} \\ \frac{\partial v}{\partial \zeta} \end{pmatrix} \frac{\partial h_i}{\partial \zeta} + \begin{pmatrix} \frac{\partial v}{\partial \zeta} \\ \frac{\partial v}{\partial \xi} \\ \frac{\partial v}{\partial \eta} \end{pmatrix} \frac{\partial h_i}{\partial \xi} & \begin{pmatrix} \frac{\partial w}{\partial \xi} \\ \frac{\partial w}{\partial \eta} \\ \frac{\partial w}{\partial \zeta} \end{pmatrix} \frac{\partial h_i}{\partial \zeta} + \begin{pmatrix} \frac{\partial w}{\partial \zeta} \\ \frac{\partial w}{\partial \xi} \\ \frac{\partial w}{\partial \eta} \end{pmatrix} \frac{\partial h_i}{\partial \xi} \end{bmatrix}, \quad (2.71)$$

and  $i \in \{1, \dots, 8\}$ . The spatial derivations in parentheses in equation (2.71) are defined by the terms in equations (2.52) to (2.54).

The nonlinear strain displacement transformation matrix is defined as

$$\mathbf{B}_{NL}(\xi, \eta, \zeta) = \begin{bmatrix} \begin{bmatrix} 0 & 0 \\ \tilde{\mathbf{B}}_{NL} & 0 \\ 0 & 0 \end{bmatrix} \\ \begin{bmatrix} 0 & 0 \\ 0 & \tilde{\mathbf{B}}_{NL} \\ 0 & 0 \end{bmatrix} \\ \begin{bmatrix} 0 & 0 \\ 0 & 0 \\ 0 & 0 \end{bmatrix} \end{bmatrix} \quad (2.72)$$

with

$$\tilde{\mathbf{B}}_{NL}(\xi, \eta, \zeta) = \begin{bmatrix} \frac{\partial h_1}{\partial \xi} & 0 & 0 & \frac{\partial h_2}{\partial \xi} & 0 & 0 & \dots & \frac{\partial h_7}{\partial \xi} & 0 & 0 & \frac{\partial h_8}{\partial \xi} \\ \frac{\partial h_1}{\partial \eta} & 0 & 0 & \frac{\partial h_2}{\partial \eta} & 0 & 0 & \dots & \frac{\partial h_7}{\partial \eta} & 0 & 0 & \frac{\partial h_8}{\partial \eta} \\ \frac{\partial h_1}{\partial \zeta} & 0 & 0 & \frac{\partial h_2}{\partial \zeta} & 0 & 0 & \dots & \frac{\partial h_7}{\partial \zeta} & 0 & 0 & \frac{\partial h_8}{\partial \zeta} \end{bmatrix}, \quad (2.73)$$

where it should be kept in mind that there are no trailing zeros.

**2.2.3.3.4 Defining the Jacobi matrix** The Jacobian  $\mathbf{J}$ , which allows to switch from physical coordinates  $x, y$  and  $z$  to local coordinates  $\xi, \eta$  and  $\zeta$  for the necessary integrations, is defined as

$$\mathbf{J} = \begin{bmatrix} \frac{\partial x}{\partial \xi} & \frac{\partial y}{\partial \xi} & \frac{\partial z}{\partial \xi} \\ \frac{\partial x}{\partial \eta} & \frac{\partial y}{\partial \eta} & \frac{\partial z}{\partial \eta} \\ \frac{\partial x}{\partial \zeta} & \frac{\partial y}{\partial \zeta} & \frac{\partial z}{\partial \zeta} \end{bmatrix} \quad (2.74)$$

where the spatial derivations of the element's geometry are given by equations (2.55) to (2.57).

#### 2.2.3.4 Integrating the element matrices numerically

The numerical integration yields the  $24 \times 24$ -matrices that describe the element's mass and its nonlinear stiffness. The square matrices are of dimension 24 because there are three translational degrees of freedom to every one of the eight corner nodes.

Computationally, the numerical integration is achieved by Gaussian summation. This technique evaluates combinations of the matrices above at defined points, called the Gauss-points  $\hat{\xi}_i, \hat{\eta}_i$  and  $\hat{\zeta}_i$ , multiplying the results with weights  $\hat{w}_i$  and summing over the different Gauss points (e.g. Zienkiewicz et al. [247]). The ensemble of the Gauss- points and their associated -weights is presented in table 2.4.

The mass matrix  $\mathbf{M}$  from equation (2.30) is integrated as

$$\mathbf{M} = \sum_{i=1}^3 \sum_{j=1}^3 \sum_{k=1}^3 \hat{w}_i \hat{w}_j \hat{w}_k \left( \mathbf{N}(\hat{\xi}_i, \hat{\eta}_j, \hat{\zeta}_k) \right)^T \rho \mathbf{N}(\hat{\xi}_i, \hat{\eta}_j, \hat{\zeta}_k) \det \left( \mathbf{J}(\hat{\xi}_i, \hat{\eta}_j, \hat{\zeta}_k) \right) \quad (2.75)$$

### 2.3. PROVIDING THE BASIC MATRIX EQUATION

---

$i$	$\hat{\xi}_i$	$\hat{\eta}_i$	$\hat{\zeta}_i$	$\hat{w}_i$
1	$\frac{-1}{\sqrt{3}}$	$\frac{-1}{\sqrt{3}}$	$\frac{-1}{\sqrt{3}}$	1
2	0	0	0	2
3	$\frac{1}{\sqrt{3}}$	$\frac{1}{\sqrt{3}}$	$\frac{1}{\sqrt{3}}$	1

Table 2.4: The Gauss-points and -weights

with the interpolation matrix  $\mathbf{N}$  from equation (2.67) and  $\rho$  as the uniform density of the material.

The nonlinear stiffness matrix of the element is composed of two parts

$$\mathbf{K}_{NL} = \sum_{i=1}^3 \sum_{j=1}^3 \sum_{k=1}^3 \hat{w}_i \hat{w}_j \hat{w}_k \left( \mathbf{K}_{NL}^{(1)} \left( \hat{\xi}_i, \hat{\eta}_j, \hat{\zeta}_k \right) + \mathbf{K}_{NL}^{(2)} \left( \hat{\xi}_i, \hat{\eta}_j, \hat{\zeta}_k \right) \right) \det \left( \mathbf{J} \left( \hat{\xi}_i, \hat{\eta}_j, \hat{\zeta}_k \right) \right), \quad (2.76)$$

with

$$\mathbf{K}_{NL}^{(1)} = \left( \mathbf{B}_L \left( \hat{\xi}_i, \hat{\eta}_j, \hat{\zeta}_k \right) \right)^T \mathbf{C} \mathbf{B}_L \left( \hat{\xi}_i, \hat{\eta}_j, \hat{\zeta}_k \right), \quad (2.77)$$

where  $\mathbf{B}_L$  is the linear strain displacement transformation matrix from equation (2.68), and

$$\mathbf{K}_{NL}^{(2)} = \left( \mathbf{B}_{NL} \left( \hat{\xi}_i, \hat{\eta}_j, \hat{\zeta}_k \right) \right)^T \tilde{\mathbf{S}} \left( \hat{\xi}_i, \hat{\eta}_j, \hat{\zeta}_k \right) \mathbf{B}_{NL} \left( \hat{\xi}_i, \hat{\eta}_j, \hat{\zeta}_k \right), \quad (2.78)$$

where  $\mathbf{B}_{NL}$  is the nonlinear strain displacement transformation matrix from equation (2.72) and  $\tilde{\mathbf{S}}$  the adapted matrix form of the second Piola-Kirchhoff stress from equation (2.65).

The nonlinear internal forces are calculated with the vector form of the second Piola-Kirchhoff stress from equation (2.66) as

$$\mathbf{g}(\mathbf{u}) = \sum_{i=1}^3 \sum_{j=1}^3 \sum_{k=1}^3 \hat{w}_i \hat{w}_j \hat{w}_k \left( \mathbf{B}_L \left( \hat{\xi}_i, \hat{\eta}_j, \hat{\zeta}_k \right) \right)^T \tilde{\mathbf{S}} \det \left( \mathbf{J} \left( \hat{\xi}_i, \hat{\eta}_j, \hat{\zeta}_k \right) \right). \quad (2.79)$$

This concludes the calculations on element level. Global matrices and the global vector of the nonlinear internal forces are obtained by the direct stiffness approach (e.g. Bathe [22]) and the computational tool of scatter vectors. The terms  $\mathbf{M}$  and  $\mathbf{g}(\mathbf{u})$ , that are made available by the numerical integration of the discrete formulation, can now be assembled in the discrete expression of the dynamic equilibrium in equation (2.32). The  $\mathbf{K}_{NL}$  from equation (2.76) is made available in forethought for the time-marching solution algorithms in section 3.2.

## 2.3 Providing the basic matrix equation

The ultimate step in the development of the discrete description of the dynamic equilibrium of a geometrically nonlinear structure is the establishment of a single matrix equation. This matrix equation condenses the preceding sections' content. It serves as the common basis for the transient solution and the reduction

### 2.3. PROVIDING THE BASIC MATRIX EQUATION

---

of the full order system and the solution of the reduced system. All further work and developments hinge upon this equation; hence it is inspected more closely.

Beginning with the continuous formulation of the dynamic equilibrium in equation (2.1) the terms are gradually expanded and, with the introduction of the principle of virtual work, prepared for discretisation. Finally, the discrete dynamic equilibrium formulation is obtained with equation (2.32). It reads

$$\mathbf{M}\ddot{\mathbf{u}} + \mathbf{g}(\mathbf{u}) = \mathbf{f}_E(t). \quad (2.80)$$

It conveys the exact same statement as the continuous formulation, i.e. the equilibrium of the inertial, the internal and the external forces. Details on how the inertial and internal nonlinear forces  $\mathbf{g}(\mathbf{u})$  are created have been presented with the nonlinear bar element and the nonlinear volume element in the preceding section 2.2.

The continuous and the discrete formulation of the dynamic equilibrium have the property of being conservative. They do not include any damping terms. This is intended, as there is no damping present, neither in the initial formulation, nor in the stress-strain relation of the linear elastic material used. However, a conservative system is neither physically correct nor desirable for a numerically stable transient solution.

Because the inclusion of damping effects on material level is complex and presents a field of research in its own right, a somewhat artificial damping term is added on matrix level. This term depends on the velocities  $\dot{\mathbf{u}}$  and is expressed with the damping matrix  $\mathbf{C}$ . In order to express a physical meaning of the damping forces the matrix  $\mathbf{C}$  has to be symmetric positive-definite (SPD). In the framework of Rayleigh damping (e.g. Wilson [240]) this can be achieved by expressing the damping matrix as a fraction of a linear tangent stiffness matrix

$$\mathbf{C} = \epsilon \bar{\mathbf{K}} \quad (2.81)$$

with  $\epsilon$  chosen so that  $\mathcal{O}(\mathbf{C}) \ll \mathcal{O}(\mathbf{K})$ . Such a damping does not cover the description of phenomena as e.g. viscoelasticity. The damping is simply linear and empirical.

Adding the damping effects to equation (2.80) yields the full order, nonlinear, non-conservative, dynamic system, which is completely discretised in space

$$\mathbf{M}\ddot{\mathbf{u}} + \mathbf{C}\dot{\mathbf{u}} + \mathbf{g}(\mathbf{u}) = \mathbf{f}_E(t). \quad (2.82)$$

Where the  $n \times n$  matrices  $\mathbf{M}$  and  $\mathbf{C}$  represent the mass and the damping terms, respectively. The  $n \times 1$  vector  $\mathbf{f}_E$  describes the external forces, which are exclusively a function of the time  $t$ , and all nonlinearities reside in the  $n \times 1$  vector  $\mathbf{g}$ , which is an exclusive function of the displacements  $\mathbf{u}$ . Overdots represent derivations with respect to time. Equation (2.82) is the starting point for the solution and the reduction.

The equation (2.82) is only valid in an inertial reference frame.

Later on, equation (2.82) will also be made depending on parameters  $\boldsymbol{\mu}$ . From the engineering point of view, these parameters may describe the operating point of the structure.



## Chapter 3

# Choosing a reduction approach and a compatible transient solution procedure

---

With a single matrix equation describing the dynamic equilibrium of a discretised, geometrically nonlinear system available, a choice of the reduction approach to be applied has to be made. Strongly depending on this choice is the selection of a compatible time-integration procedure that is to provide the transient solutions of the full order and of the reduced order system alike.

In a first step different reduction approaches are surveyed, some of which are a pure reduction while others are monolithic reduction-solution-approaches. Based on the criteria that are defined, the approach of reduction by projection on a reduced basis is selected. Because the projection on a reduced basis provides only the reduction, this approach demands the additional choice of a time-integration procedure. With the nonlinear Newmark scheme a robust and common procedure is presented. It is also demonstrated that this solution procedure is oblivious to the size of the system it solves. This proves to be important because the matrix description of the reduced dynamic system, as it is created by the projection on a reduced basis, has the exact same structure as the single matrix equation. Thus, the nonlinear Newmark scheme can provide transient solutions for the full order and for the reduced order system.

From this possibility the requirement for an autonomous formulation of the nonlinear terms in the reduced order system is derived. This requirement is however skipped for now because it would interfere with the thorough testing of the reduced bases that will take place in the following chapter 4. The current chapter 3 concludes with the presentation of reduced bases to complete the presentation of the reduction by projection approach and to prepare candidate bases for the following testing.

## 3.1 Selecting a reduction approach

The chapter 2 above treats the discretisation of the continuous formulation of the dynamic equilibrium (2.1), with an infinite number of degrees of freedom, to the matrix equation (2.82) with a finite number of  $n$  degrees of freedom. However, this finite number  $n$  is still substantial for engineering applications.

This large number of degrees of freedom limits the application of high fidelity, full order models for several applications, e.g. optimisation or control, despite the continuous growth of available computation power. At the same time, a sparse discretisation with a low number  $n$  of discrete degrees of freedom is contradictory to the basic idea of discretisation and is bound to yield poor results. To avoid having to make the major trade-off between poor results and a too costly computation, the number of degrees of freedom  $n$  has to be reduced to a lesser number  $r$ , while retaining the governing characteristics of the system. This is done with model reduction techniques.

These techniques are inserted into the solution workflow after the discretisation and prior to the actual solution, e.g. a time integration. As at this point the properties of the full order system (2.82) are known, the model reduction techniques can draw on them and be adapted in an optimal manner to the system under consideration. This circumvents the inconvenience of a sparse discretisation.

### 3.1.1 Defining the purpose of the reduction approach

The objective of the reduction of a discrete system is to condense the number of degrees of freedom by looking for relations between the different degrees of freedom. Carlberg et al. [55] use the image of a large  $n$ -dimensional space which contains all the full order system's degrees of freedom and which encloses a much smaller reduced space in which the actual solution to the system resides. Even though mathematically complete and correct, this image remains very tangible from an engineer's point of view and defines the reduction as a transformation between the two spaces.

Reduced models can be desirable for various reasons. They can, for example, be used to reduce the computational burden in a design process, they can be designed as fast executing replacements of the full order systems in embedded control applications, or they can be used to extract pertinent information which is hidden in the full order system. Irrespective of the aim pursued with it, the reduced model is never an end in itself. Its development is always geared towards gaining computational speed.

In the context of this work the reduced model is to replace the full order model during a numerical simulation that aims at establishing the structure's transient response to an external excitation evolving in time. This replacement is made to considerably reduce the computational effort required to obtain an approximated solution with an acceptable level of error.

The central property of a reduced model at this point is the fact that the reduced model does not change the physics of the underlying problem. This is opposite to an approach proposed by e.g. Bui-Thanh et al. [43], who propose a goal-oriented reduction approach. In their work the entire full order model is directly reduced to the cost-function that is required for an optimisation. This cost-function does not contain any information about the physical properties of the full order system.

The motivation behind the reduction lies in the desire to reduce the computational burden of the solution of a high-fidelity system be it to speed up the solution process, e.g. to enable near-real-time solutions or allow for optimisations. The ratio between gain in computational effort and error committed defines the success of the application of the reduced model. Both criteria are explored further over the course of this work. The order  $r$  of the reduced order system defines its size and has to be aptly chosen so that the reduced order model can retain the crucial properties of the full order model. At the same time, however, the computational cost of the necessary transformations between the reduced order and the full order model, deflations and inflations, must not exceed the gains through the simplified solution of the reduced order system.

### 3.1. SELECTING A REDUCTION APPROACH

---

Amsallem and Farhat [13] put it right by defining that “a ‘sufficiently accurate’ [reduced order model] is a lower-dimensional computational model which can faithfully reproduce the essential features of a higher-dimensional model at a fraction of its computational cost.”

#### 3.1.2 Surveying some reduction approaches

A comparison of reduction approaches is performed by Besselink et al. [37]. They focus on model-based reduction techniques for linear, time-invariant dynamic systems from structural dynamics, control and numerical mathematics. Their work provides decision guidelines for the selection of a reduction approach for different applications. Some of their criteria and considerations are also applied here.

The starting point for the reduced transient solution of a full order, nonlinear, non-conservative, dynamic system, which is completely discretised in space, is equation (2.82).

The main challenge of every model reduction technique is to find an adequate way to establish a reduced order model of the system with only  $r$  degrees of freedom. The reduced order model is constructed by applying relations to be found in such a way that these relations express the  $n$  degrees of freedom  $u_i$  of the full order system as functions of the  $r$  generalised degrees of freedom  $q_k$  of the reduced order system, with  $k \in \{1, \dots, r\}$  and  $r \ll n$ .

Using these relations, the full order system is first deflated to the reduced order system, then solved and then again inflated to full order to allow for a physical interpretation. The inflation step is necessary for at least some physical degrees of freedom of interest because the reduced order model’s degrees of freedom can be deprived of any physical meaning.

To obtain a reduced model there are methods that are independent of the chosen time-integration algorithm and methods that perform the reduction and the solution of the reduced system in a monolithic and interdependent fashion. As major representatives of the first type of methods the projection on a reduced basis and the Guyan reduction are included in the presentation of common reduction approaches. These projection based methods define a reduced basis on which the system (2.82) is projected. This introduces a clear separation of the reduction and the solution. The second type of methods, of which most emerged recently, does not build on a projection but strives for other means of relating the full order degrees of freedom  $\mathbf{u}$  to the generalised coordinates  $\mathbf{q}$ . Most notable among these are the Proper Generalised Decomposition, outlined by e.g. Ammar et al. [7, 9], and the Non-Linear Normal Modes, going back to Rosenberg [190] and recently rediscovered with success by Peeters et al. [169] and Kerschen et al. [117]. These direct methods are monolithic techniques because their approach includes and prescribes a certain algorithm for obtaining the transient solution. Their different approach renders the comparability with projection based reduction techniques somewhat difficult.

##### 3.1.2.1 Projection on a reduced basis

The projection based methods have in common that they define a subspace, represented by the reduced basis  $\Phi$ , which is used as a basis onto which the discrete equations describing the nonlinear dynamic system are projected.

For projection based reduction methods the reduced order model is introduced by means of expressing the physical displacements  $\mathbf{u}$  of the full order system in the reduced basis  $\Phi$ , yielding

$$\mathbf{u} = \Phi \mathbf{q} \tag{3.1}$$

with  $\mathbf{q}$  as the  $r \times 1$  vector of generalised coordinates. The reduced basis  $\Phi$  is an  $n \times r$  matrix. Introducing

### 3.1. SELECTING A REDUCTION APPROACH

---

this relation into equation (2.82) gives their respective counterparts in generalised coordinates

$$M\Phi\ddot{q} + C\Phi\dot{q} + g(\Phi q) = f_E. \quad (3.2)$$

This, in turn, yields  $n$  equations for the  $r$  generalised degrees of freedom and thus an over determined system. To counter the over determination, additional delimiters can be introduced by defining a matrix  $\Psi$  so that the number of equations is also reduced. The matrix  $\Psi$  is also of size  $n \times r$ . If equation (3.2) is left-multiplied with the transpose of  $\Psi$ , it becomes

$$\Psi^T M \Phi \ddot{q} + \Psi^T C \Phi \dot{q} + \Psi^T g(\Phi q) = \Psi^T f_E. \quad (3.3)$$

This yields a system of order  $r$  which is intended to be solved faster by an appropriate algorithm than the  $n$  equations of the full order high-fidelity system.

In detail this operation is to yield either reduced matrices of  $r \times r$  dimension, or even diagonal matrices. Diagonal matrices result in completely decoupling the equations defining the reduced degrees of freedom and turn the reduced system into  $r$  equations, which are completely independent from each other. But this is only possible in the linear case and with a specific  $\Psi$  such that

$$\Psi^T M \Phi = \text{diag} \quad (3.4)$$

$$\Psi^T C \Phi = \text{diag} \quad (3.5)$$

and

$$\Psi^T K \Phi = \text{diag} \quad (3.6)$$

enforce the orthogonality of  $\Phi$  and  $\Psi$ . Dinkler [70] stresses this aspect and requires even a dedicated normalisation should the initial  $\Phi$  not be ortho-normal.

The two matrices, which are both of  $n \times r$ , are commonly denominated as the trial and the test space:

- $\Phi$  as the basis of the trial space, or the right-hand reduced basis, and
- $\Psi$  as the basis of the test space, or the left-hand reduced basis.

Choosing  $\Psi = \Phi$  classes the reduction as a so-called Galerkin projection, whereas  $\Psi \neq \Phi$  leads to the class of so-called Petrov-Galerkin projections, which have some application later in the course of this work<sup>1</sup>. For the time being it is assumed that only Galerkin projections with  $\Psi = \Phi$  take place.

**3.1.2.1.1 Reducing the static matrices** Supposing, as stipulated before, that the full order mass matrix  $M$  and the full order damping matrix  $C$  depend neither on the displacements  $\mathbf{u}$  nor on the time  $t$  allows them to be converted permanently into the reduced  $r \times r$  matrices. For the mass matrix this yields

$$M \xrightarrow{\Phi} \begin{matrix} \Phi^T M \Phi \\ r \times n n \times n n \times r \\ r \times r \end{matrix} = \tilde{M}, \quad (3.7)$$

---

<sup>1</sup>Refer to the Least-Squares Petrov-Galerkin method in section 5.1.2.

### 3.1. SELECTING A REDUCTION APPROACH

---

and for the damping matrix

$$\underset{n \times n}{C} \xrightarrow{\Phi} \underset{r \times n \times n \times n \times r}{\Phi^T C \Phi} = \underset{r \times r}{\tilde{C}}. \quad (3.8)$$

**3.1.2.1.2 Reducing the vectors** A similar operation can be performed for the vectors in the discrete formulation of the dynamic equilibrium in equation (2.82). For the vector of external forces this is a simple premultiplication with the  $\Phi^T$ . This yields

$$\underset{n}{f_E}(t) \xrightarrow{\Phi} \underset{r \times n}{\Phi^T} \underset{n}{f_E}(t) = \underset{r}{\tilde{f}_E}(t), \quad (3.9)$$

and can be done prior to the transient solution because the time history of  $f_E$  is supposed to be known and the reduced basis  $\Phi$  is supposed to be constant.

For the vector of nonlinear internal forces a similar reduction can be imagined. In its conceptual form it reads

$$\underset{n}{g}(u) \xrightarrow{\Phi} \underset{r \times n}{\Phi^T} \underset{n}{g}(\Phi q) = \underset{r}{\tilde{g}}(q). \quad (3.10)$$

Unfortunately, such a reduction by projection on a reduced basis of  $g(u)$  to obtain  $\tilde{g}(q)$  is not easily feasible. The finite element formulation that is developed in section 2.2 proves to be far too complicated for a reduction by projection of the vector of internal forces. In order to enable such a reduction a specific formulation of the vector of the nonlinear internal forces is required<sup>2</sup>. At the same time, a reduction of the vector of nonlinear internal forces as in equation (3.10) is of central importance for the transient solution of the reduced system with the same type of time-marching algorithm as the algorithms used for the full order system<sup>3</sup>.

**3.1.2.1.3 Writing the dynamic equilibrium in reduced form** The introduction of the reduced matrices  $\tilde{M}$ ,  $\tilde{C}$  and vectors  $\tilde{g}$  and  $\tilde{f}_E$  makes it possible to write equation (2.82) in its reduced form:

$$\tilde{M}\ddot{q} + \tilde{C}\dot{q} + \tilde{g}(q) = \tilde{f}_E. \quad (3.11)$$

It is evident that the structures of equation (2.82), describing the full order system, and the equations of the reduced order system above are identical. This implies that the same solution techniques can be used for a full order system as well as for a completely reduced system.

The inflation to the full order system is done by applying equation (3.1) to the solution of the reduced order system. This relation between the  $u_i$  of the full order system and the  $q_k$  of the reduced order system is assured through the columns  $\phi$  of the matrix  $\Phi$ . This gives, as defined in equation (3.1), for the degrees of freedom of the full order system:

$$u_i = \sum_{k=1}^r \phi_{ik} q_k, \quad (3.12)$$

<sup>2</sup>Refer to section 3.2.3 for the identification of the requirement of such an autonomous formulation

<sup>3</sup>Refer to section 3.2.1.1 for the algorithm for the transient solution of the full order system and to section 3.2.2.1 for the reduced equivalent.

### 3.1. SELECTING A REDUCTION APPROACH

---

with  $\phi_{ki}$  as the  $k$ -th element of the  $i$ -th row of the reduction matrix  $\Phi$ .

**3.1.2.1.4 Giving an overview over some common reduced bases** For the creation of the bases of projection based reduction techniques there is a wealth of varieties available. The selection used in this study is by no means exhaustive and comprises

- the Linear Normal Modes (LNM), also known as Modal Decomposition (Bathe [22]), as one of the basics of reduction in structural dynamics, and their extensions in the form of obtaining them at maximum displacements and developing them into second order terms as done by Slaats et al. [210], among others.
- the Ritz-vectors, introduced by Wilson et al. [241] as an extension of the Lanczos algorithm (Lanczos [130]) for the estimation of eigenvectors. And with applications in the work of Kapania and Byun [113], who uses Ritz-vectors as reference for comparisons, and Burton and Rhee [47], who pushed this approach further by comparing a Ritz-vector dependent linear based reduction of nonlinear systems to Non-Linear Normal Modes. Recently this approach was extended to an enhanced order reduction method for forced nonlinear systems by AL-Shudeifat et al. [3], who used Ritz-vectors to enhance a reduced basis that comes from a Proper Orthogonal Decomposition procedure.
- the Proper Orthogonal Decomposition (POD), as the great classic of reduction and several of its variants. Originally used for experimental data, Sirovich [207] enabled the application of this method in a numerical context by introducing the concept of snapshots and making the POD procedure computationally tractable. And despite its relative age this method still spawns considerable research activity. Two of the most recent examples in this field are conducted by Amsellem [12], using it for the very sophisticated Least-Squares Petrov-Galerkin approach for the solution of nonlinear systems, and Bellizzi and Sampaio [30], creating the Smooth Orthogonal Decomposition by including the velocities.
- the A Priori Reduction (APR), which limits itself to the solution of the reduced system and, following its first application in thermo-mechanics by Ryckelynck [197], was soon adapted to more general problems and eventually applied to structural dynamics by Ryckelynck et al. [196]. However, its principle is still largely and effectively applied to fluid dynamics, as e.g. by Ammar et al. [8].
- the Centroidal Voronoi Tessellation (CVT), which employs a tessellation algorithm to group the snapshots of the solution around characteristic deformations. These characteristic deformations, which are the centroids of these groups, are then used as vectors of the projection basis. In this respect it resembles the POD, yet with the difference of working even more directly on the solution which is to be known beforehand. An overview of this technique is given by Du et al. [71].
- the Local Equivalent Linear Stiffness Method (LELSM) that creates equivalent linear stiffnesses for localised nonlinearities and uses an iterative approach for solving the amplitude dependency of this equivalent stiffness. The updated LELSM modes are the LNM of this specially constructed equivalent linear system. A starting point for this method is available from AL-Shudeifat and Butcher [2].

From literature review it becomes obvious that most of the techniques and advances in reduction techniques originate from the field of fluid dynamics, where research and innovation were and remain vivid, and that the resulting methods are only consecutively transferred to applications in structural dynamics.

#### 3.1.2.2 Guyan Reduction

The Guyan reduction was proposed by Guyan [90] and stands in-between a pure reduction by projection on a reduced basis and the concept of introducing master and slave coordinates, as it will be presented later in detail in the section 3.1.2.4, dedicated to the Nonlinear Normal Modes. Below, it is presented in its original intention as a reduction approach for linear systems. Since its inception, it has however undergone an enormous transformation as becoming the basis of sub-structuring techniques, e.g. the Craig-Bampton

### 3.1. SELECTING A REDUCTION APPROACH

---

method (Bampton and Craig [20]). This branch of development is not considered because the idea of sub-structuring, coupling different structures at their mutual interfaces, does not lend itself to the reduction of a single, uniform structure.

Being given  $n$  physical displacements  $u_i$  the Guyan reduction splits them into  $r$  master coordinates  $q_k$  and  $n - r$  slave coordinates  $\tilde{u}_l$ , which are not forced by the excitation. Then the slave coordinates  $\tilde{\mathbf{u}}$  are expressed as functions of the master coordinates  $\mathbf{q}$  with a coordinate transformation involving information from the equilibrium formulation, i.e. the mass and the stiffness matrix. The generalised coordinates  $\mathbf{q}$  are a subset of the physical displacements  $\mathbf{u}$ .

The following separation of the displacements  $\mathbf{u}$  in master coordinates  $\mathbf{q}$  and slave coordinates  $\tilde{\mathbf{u}}$  requires the assumption of a linear, conservative, and static system as

$$\mathbf{K}\mathbf{u} = \mathbf{f}_E. \quad (3.13)$$

This can easily be obtained by linearising the basic equation (2.82) at any given displacement and neglecting time dependent terms. By presuming that the lines of equation (3.13) can be shifted without problems the lines corresponding to forced and free nodes can be separated from each other

$$\begin{bmatrix} \mathbf{K}_{qq} & \mathbf{K}_{q\tilde{u}} \\ \mathbf{K}_{q\tilde{u}}^T & \mathbf{K}_{\tilde{u}\tilde{u}} \end{bmatrix} \begin{bmatrix} \mathbf{q} \\ \tilde{\mathbf{u}} \end{bmatrix} = \begin{bmatrix} \mathbf{f}_{E,q} \\ \mathbf{0} \end{bmatrix}. \quad (3.14)$$

The slave coordinates  $\tilde{\mathbf{u}}$  are not subjected to the external forcing.

The mass matrix  $\mathbf{M}$  and the stiffness matrix  $\mathbf{K}$  are split up in parts corresponding to the two sets of displacements. The part of the external forces that corresponds to the slave coordinates  $\mathbf{f}_{E,\tilde{u}}$  has to be zero.

Combining the two matrix equations in (3.14) into a single one yields

$$[\mathbf{K}_{qq} - \mathbf{K}_{q\tilde{u}}\mathbf{K}_{\tilde{u}\tilde{u}}^{-1}\mathbf{K}_{q\tilde{u}}^T] \mathbf{q} = \mathbf{f}_{E,q}, \quad (3.15)$$

from which the equivalent stiffness matrix of the reduced system can be obtained as

$$\tilde{\mathbf{K}} = [\mathbf{K}_{qq} - \mathbf{K}_{q\tilde{u}}\mathbf{K}_{\tilde{u}\tilde{u}}^{-1}\mathbf{K}_{q\tilde{u}}^T]. \quad (3.16)$$

This entity is known as the Schur-complement of  $\mathbf{K}$  in a more mathematical context (Strang [218]).

The mass matrix can be split in much the same way. Supposing

$$\mathbf{M} = \begin{bmatrix} \mathbf{M}_{qq} & \mathbf{M}_{q\tilde{u}} \\ \mathbf{M}_{q\tilde{u}}^T & \mathbf{M}_{\tilde{u}\tilde{u}} \end{bmatrix}, \quad (3.17)$$

an equivalent reduced mass matrix can be obtained as

$$\tilde{\mathbf{M}} = \mathbf{M}_{qq} - \mathbf{M}_{q\tilde{u}}\mathbf{K}_{\tilde{u}\tilde{u}}^{-1}\mathbf{K}_{q\tilde{u}}^T - (\mathbf{K}_{\tilde{u}\tilde{u}}\mathbf{K}_{q\tilde{u}}^T)^T (\mathbf{M}_{q\tilde{u}}^T - \mathbf{M}_{\tilde{u}\tilde{u}}\mathbf{K}_{\tilde{u}\tilde{u}}^{-1}\mathbf{K}_{q\tilde{u}}^T) \quad (3.18)$$

by using a transformation consideration on the level of total energy in the system.

This approach becomes especially accessible if the reduction is formulated in terms of quantities introduced in equation (3.1), i.e. by introducing a reduced basis  $\Phi$ . In equation (3.14) the physical coordinates

are split in forced and unforced displacements to become

$$\mathbf{u} = \begin{bmatrix} \mathbf{q} \\ \tilde{\mathbf{u}} \end{bmatrix}. \quad (3.19)$$

To handle the reduction and the inflation the reduced basis has to comply with equation (3.1), which requires  $\mathbf{u} = \Phi \mathbf{q}$ , so that

$$\Phi = \begin{bmatrix} \mathbf{I} \\ -\mathbf{K}_{\tilde{\mathbf{u}}\tilde{\mathbf{u}}}^{-1} \mathbf{K}_{q\tilde{\mathbf{u}}} \end{bmatrix}, \quad (3.20)$$

for the Guyan reduction.

Because of the fact that the master coordinates  $\mathbf{q}$  retain their physical meaning the Guyan reduction is especially suited for coupling different physics. If e.g. a structure is embedded in a fluid and both domains discretised in space, the interface displacements of the structure become the master coordinates  $\mathbf{q}$ . The internal displacements of the structure, that do not interact with the fluid, become slave coordinates  $\tilde{\mathbf{u}}$ . Furthermore, as the part of the external forcing corresponding to the slave coordinates  $\mathbf{f}_{E,q}$  has to be all zero, only the displacements subjected to a forcing from the surrounding fluid are retained. This effectively reduces the structural model to just the displacements that are of interest for the fluid simulation and alleviates the coupled code from the need to calculate the internal displacements of the structure.

#### 3.1.2.3 Truncated Harmonic Balance

The Harmonic Balance Method (HBM) assumes the time history of the displacements  $\mathbf{u}(t)$  to be represented by a Fourier series and introduces the thus obtained formulations into the equation of the system. This seemingly simple idea requires nevertheless extensive computations and is straightforward only for linear systems. It supposes the response to be of the same frequency as the excitation but with an amplitude and a phase to be determined.

The creation of this method is attributed to Bailey [18] and has since been widely applied to electric networks, by e.g. El-Rabaie et al. [73], and such systems as the Duffing oscillator by Beléndez et al. [27] and Özis and Yildirim [165]. For applications in aerodynamics, the Harmonic Balance Method lends itself naturally to basically harmonic problems such as helicopter rotors, as proven by Ekici et al. [72]. Applications in nonlinear structural dynamics comprise e.g. rotor-stator contact problems, as investigated by Groll and Ewins [86] and problems with discontinuities, as investigated by Beléndez et al. [26].

All nonlinear applications intrinsically require specific formulations<sup>4</sup> of the nonlinear terms, especially the vector of the nonlinear internal forces  $\mathbf{g}(\mathbf{u})$ . In order to avoid being too specific, the following development of the Harmonic Balance Method, which demonstrates the course of action taken by Liu and Kalmár-Nagy [139], is limited to a linear system. Should the extension to nonlinear systems become necessary e.g. the alternating time/frequency approach by Cameron and Griffin [50] provides a possible way of accounting nonlinearities.

Assuming a linear system as e.g.

$$\mathbf{M}\ddot{\mathbf{u}} + \mathbf{C}\dot{\mathbf{u}} + \mathbf{K}\mathbf{u} = \mathbf{f}_E(t), \quad (3.21)$$

---

<sup>4</sup>Refer to section 3.2.3 for the identification of the requirement of such an autonomous formulation

### 3.1. SELECTING A REDUCTION APPROACH

---

as an approximation of equation (2.82), and

$$u_i(t) = \bar{u}_0^{(i)} + \sum_{j=1}^r \hat{s}_j^{(i)} \sin(j\omega t) + \hat{c}_j^{(i)} \cos(j\omega t) \quad (3.22)$$

as the formulation of the displacements as a truncated Fourier series, suitable equations can be found for finding the parameters  $\hat{s}_j^{(i)}$  and  $\hat{c}_j^{(i)}$  with  $1 \leq i \leq n$ . To this end equation (3.22) is derived with respect to time, giving

$$\dot{u}_i(t) = \sum_{j=1}^r j\omega \hat{s}_j^{(i)} \cos(j\omega t) - j\omega \hat{c}_j^{(i)} \sin(j\omega t) \quad (3.23)$$

$$\ddot{u}_i(t) = \sum_{j=1}^r -j^2\omega^2 \hat{s}_j^{(i)} \sin(j\omega t) - j^2\omega^2 \hat{c}_j^{(i)} \cos(j\omega t) \quad (3.24)$$

for the velocities and the accelerations respectively. “[C]ollecting terms associated with each harmonic” (Liu and Kalmár-Nagy [139]) ultimately leads to a formulation of the linear system in equation (3.21) in the form of

$$(\omega^2 \mathbf{M} \mathbf{J}^2 + \omega \mathbf{C} \mathbf{J} + \mathbf{K}) \mathbf{Q} = \mathbf{F}_E, \quad (3.25)$$

where the matrix  $\mathbf{J}$  accounts for the factors  $j$ , resulting from the derivatives in equations (3.23) and (3.24), the matrix  $\mathbf{Q}$  regroups the parameters  $\hat{s}_j^{(i)}$  and  $\hat{c}_j^{(i)}$ , that are being determined by solving equation (3.25), and the matrix  $\mathbf{F}_E$  is obtained by projecting the vector of external forces on the sine- and cosine terms

$$f_0^{(i)} = \frac{1}{T} \int_0^t f_{E,i}(t) dt \quad (3.26)$$

$$f_{j,s}^{(i)} = \frac{1}{T} \int_0^t f_{E,i}(t) \sin(jt) dt \quad (3.27)$$

$$f_{j,c}^{(i)} = \frac{1}{T} \int_0^t f_{E,i}(t) \cos(jt) dt. \quad (3.28)$$

A problem that remains to be solved is the fact that the period  $T$  is not known a priori. It is however linked to the basic frequency  $\omega$ , introduced in passing in equation (3.22), by  $T = \frac{2\pi}{\omega}$ . This can be exploited by normalising the time  $t$  with the factor  $\omega$  and performing the integrations in equations (3.26) to (3.28) from 0 to  $2\pi$ . This leaves only the angular frequency  $\omega$  as an additional unknown.

The Harmonic Balance Method differs in several ways from the other methods. In total there are  $n \times (2r + 1) + 1$  unknowns, these are the terms  $\hat{s}_j^{(i)}$  and  $\hat{c}_j^{(i)}$  associated with the sines and cosines, respectively, and the static factors  $\bar{u}_0^{(i)}$  for all  $n$  degrees of freedom and the basic angular frequency  $\omega$ . However, the system (3.25) does only offer  $n \times (2r + 1)$  equations. The necessary additional equation can be constructed from the so-called phase-fixing conditions, which forces e.g.  $\hat{s}_1^{(1)} = 0$ .

This requirement of  $n \times (2r + 1) + 1$  equations with an equal number of unknowns highlights one of the major shortcomings of the Truncated Harmonic Balance method. It does not alter the number of degrees of freedom of the system to be solved and the only true reduction lies in the fact that only the finite number of the first  $r$  harmonics is included in equation (3.22) and not an infinite number as required by the original

### 3.1. SELECTING A REDUCTION APPROACH

---

formulation of a Fourier-series.

Furthermore, both Liu and Kalmár-Nagy [139] and Peng et al. [172] stress that the inclusion of nonlinear terms, a feature that has been deliberately excluded from the developments above, would require analytic expressions of the nonlinear forces in terms of the variables  $\bar{u}_0^{(i)}$ ,  $\hat{s}_j^{(i)}$  and  $\hat{c}_j^{(i)}$ . This requirement puts the Truncated Harmonic Balance approach out of reach for almost all but the most basic nonlinearities. Also, the initial assumptions of this work provide the nonlinear internal forces as a vector.

Finally, the result of the Harmonic Balance approach is the steady state solution. A solution that can only imperfectly be reached with the transient solution techniques presented in section 3.2. The singular suitability of the HBM for obtaining steady state solutions of harmonically excited system is exploited by Grolet and Thouverez [85]. They use the Harmonic Balance Method in conjunction with the Proper Generalised Decomposition, which is described in the section 3.1.2.5 below, to create frequency-dependent amplitude response curves of geometrically nonlinear beams. However, the focus of the present work is transient solutions and the preference of the Harmonic Balance approach for steady solutions does not respond to this requirement.

#### 3.1.2.4 Nonlinear Normal Modes

The Nonlinear Normal Modes (NNM) might appear, due to their denomination, as a conceptual extension of the well known Linear Normal Modes (LNM), as they were introduced in section 3.3.1. Yet the construction of NNM is based on an entirely different concept. They describe the dependency of all the system's degrees of freedom on a set of master coordinates, which have to be chosen among the system's degrees of freedom. In this way, Nonlinear Normal Modes reduce complex systems to a single or low-order multiple degree of freedom system without a projection on a reduced basis  $\Phi$ .

NNMs strive to find explicit relations between the  $u_i$  and the  $q_k$ , such that the  $q_k$  remain physical displacements  $u_k$  that do not coincide with other  $u_i$  and  $i \neq k$ . Instead of using a projection as in equation (3.1) the relation between the displacements of the high-fidelity system and the displacements of the reduced order system now reads

$$u_i = u_i(u_k). \quad (3.29)$$

As opposed to equation (3.12), where the  $q_k$  are modal coordinates, during the course of a nonlinear normal mode reduction the  $u_k$  remain physical displacements and are denominated master coordinates because of their seed function in the reduction.

From the historic perspective it is noteworthy that Rosenberg [192] described NNMs for conservative systems as a "vibration in unison" of the degrees of freedom of the system. This first, graphic description of NNMs was later expanded into the so-called invariant manifold approach by Shaw and Pierre [204], which will be expanded later in this section.

If a discretised system has  $n$  degrees of freedom in displacement  $u_i$  together with the  $n$  corresponding velocities  $\dot{u}_i$ , the phase space of the system is of the dimension  $2n$ . Among these  $n$  degrees of freedom one displacement-velocity-pair  $\{u_k, \dot{u}_k\}$  can be chosen as master coordinates. The NNM is now the  $2n - 2$ -dimensional manifold in the  $2n$ -dimensional phase space of the system that expresses all slave coordinates  $\{u_i, \dot{u}_i\}$  with  $1 \leq i \leq n$  and  $i \neq k$  as a function of the master coordinates  $\{u_k, \dot{u}_k\}$ , which effectively reduces the system to a single degree of freedom system. This nonlinear manifold is called invariant because every motion of the system initiated in the manifold remains inside the manifold. This is a property that is shared by both linear and nonlinear normal modes. Kerschen et al. [117] point out that the connection between the nonlinear normal modes and the classic, linear normal modes consists in the fact that the LNMs, which represent flat surfaces in the phase-space, are tangent to the curved manifolds of the NNMs in the equilibrium point of the system. Opposed to their linear counterparts, nonlinear normal modes display two

### 3.1. SELECTING A REDUCTION APPROACH

---

decisive differences:

- NNMs cannot be superposed
- NNMs lack a stringent orthogonality relation - which means that they are not linearly independent.

Within the scope of this section the review of solution techniques is limited to the requirements of discretised systems. For an exhaustive review of direct analytical techniques for the construction of nonlinear normal modes of continuous systems one may refer to Nayfeh [159] and, for another example, to Rand [184] or to Bellizzi and Bouc [33]. The entire theory and numerical formulation of NNM, as it was used for numerical experimentations, is laid out in the annex section D.

The concept of Nonlinear Normal modes initially originates in the research works of Rosenberg [190, 191, 192]. He supposed that the following four conditions are met by the system:

- for all  $n$  degrees of freedom  $u_i$  there exists a single constant period  $T$  so that the equation

$$u_i(t) = u_i(t + T) \quad \forall i \in \{1 \dots n\} \quad (3.30)$$

renders all  $n$  degrees of freedom equiperiodic.

- for an arbitrary instant  $t_r$ , there exists one and only one instant  $t_0$  with  $t_r \leq t_0 \leq t_r + \frac{T}{2}$  so that the equation

$$u_i(t_0) = 0 \quad \forall i \in \{1 \dots n\} \quad (3.31)$$

requires that all degrees of freedom pass precisely once per half period through an equilibrium configuration.

- for a single  $t_1 \neq t_0$  with  $t_r \leq t_1 \leq t_r + \frac{T}{2}$  the equation

$$\dot{u}_i(t_1) = 0 \quad \forall i \in \{1 \dots n\} \quad (3.32)$$

indicates that all degrees of freedom attain their maximum displacement simultaneously once and only once per half period

- for an arbitrary but fixed  $k$  with  $1 \leq k \leq n$  the remaining  $n - 1$  degrees of freedom  $u_i$  with  $i \neq k$  can be expressed as a single valued function of  $u_k$ , which is expressed in the equation

$$u_i = u_i(u_k) \quad \forall i \neq k \quad (3.33)$$

and represents the very heart of the modal formulation.

Rosenberg [190, 191, 192] then begins his development of NNMs by introducing the normalisation of each degree of freedom with its associated mass<sup>5</sup>

$$x_i = \sqrt{m_i} u_i(u_k) \quad (3.34)$$

and the potential

$$\bar{U} = \bar{U}(x_1, \dots, x_n) \quad (3.35)$$

---

<sup>5</sup>This normalisation somewhat limits this original approach for determining NNM because in complex finite element systems there are off-diagonal terms in the mass-matrix. But it is performed here to follow closely the procedure established by Rosenberg [190, 191, 192].

### 3.1. SELECTING A REDUCTION APPROACH

---

so that the energy balance of the system can be written as

$$\frac{1}{2} \sum_{i=1}^n \dot{x}_i^2 = \bar{U}(x_1, \dots, x_n) + h + \sum_{i=1}^n F_i(x_i, X_i) \quad (3.36)$$

where the integration constant  $h$  already anticipates the energy-dependence of the mode shape, which is discussed in detail later, and the term  $F_i(x_i, X_i)$  accounts for the work done by the external forces  $f_i$  on the corresponding degree of freedom, through

$$F_i(x_i, X_i) = \int_{X_i}^{x_i} f_i(t(x_i)) dx_i. \quad (3.37)$$

Subjecting equation (3.33) to the normalisation in equation (3.34) and establishing the first and second time derivatives at the same time, yields

$$x_i = x_i(x_k) \quad (3.38)$$

$$\dot{x}_i = \frac{\partial x_i}{\partial x_k} \dot{x}_k \quad (3.39)$$

$$\ddot{x}_i = \frac{\partial x_i}{\partial x_k} \ddot{x}_k + \frac{\partial^2 x_i}{\partial x_k^2} \dot{x}_k^2. \quad (3.40)$$

Injecting equations (3.38), (3.39) and (3.40) into the energy balance, formulated with equation (3.36), allows for the elimination of the time  $t$  in the latter and yields:

$$\begin{aligned} & 2 \left[ \bar{U}(x_1, \dots, x_n) + h + \sum_{l=1}^n F_l(x_l, X_l) \right] \frac{\partial^2 x_i}{\partial x_k^2} \\ & + \sum_{l=1}^n \left( \frac{x_l}{x_k} \right)^2 \left[ \frac{\partial x_i}{\partial x_k} \left( \frac{\partial \bar{U}}{\partial x_k} + f_k(t(x_k)) \right) - \left( \frac{\partial \bar{U}}{\partial x_i} + f_i(t(x_i)) \right) \right] = 0 \end{aligned} \quad (3.41)$$

with  $i \neq k$ . These  $n - 1$  equations for all  $x_i$  yield the mode based on the degree of freedom  $x_k$ , or the mode for the  $u_i$  depending on  $u_k$  if the normalisation in equation (3.34) is reversed. It is only in later literature that  $u_k$  is designated a master coordinate and the  $u_i$  became the slave coordinates. Even later, multiple  $u_k$  were enabled as master coordinates as a basis of a nonlinear normal mode to allow for internal resonance. Already at this stage Rosenberg introduced the concept of similar nonlinear modes, whose shape does not depend on their amplitude and thus omits the integration constant  $h$ .

With the separation of displacements in master and slave coordinates the NNM have a conceptual commonality with the Guyan-reduction from section 3.1.2.2. Furthermore, the space spanned by the Linear Normal Modes of the structure, one of the common reduced bases, is tangent to the curved spaces described by the NNM at the point of the linearisation. These and other features of the NNM are described in the annex section D alongside a detailed numerical procedure for the creation of NNM.

#### 3.1.2.5 Proper Generalised Decomposition

The following brief expansion of the Proper Generalized Decomposition (PGD) follows the work of Ammar et al. [7] and Ammar et al. [9], who, in their extensive layout of the PGD method, give a very comprehensive overview. The scope of the overview below is however limited in detail because, in the following section, the main focus of interest lies on the discrete formulation.

The PGD is an approach that reduces the full order system by a projection on a curved subspace. While e.g. the projection on a reduced basis in section 3.1.2.1 uses a single matrix to represent a flat subspace on which the full order system is projected, the PGD uses tensors and separated variables to represent a curved subspace. To this effect the PGD separates the variables of a problem and seeks isolated solutions for each variable while imposing conditions so that the different solutions in their totality satisfy the initial problem. As such, this approach of separated variables is applicable to almost every problem and it is not limited to the field of structural dynamics. It has however a very close equivalent in classic structural dynamics, where e.g. the theories of plates and shells provide an illustration of this approach. The contraction of the shell's or the plate's properties on the description of the neutral fibre is such a reduction. It illustrates the separation of the three space variables into a part orthogonal to the neutral plane and in the plane of the neutral fibre itself. These parts are solved separately and the conditions are given to connect these parts so that their totality describes the behaviour of the shell or plate.

Leygue and Verron [135] use the PGD in the context of optimisation. Their reasoning is similar to the arguments for indirect approaches made by Mignolet et al. [149]. They stress the explicit availability of a cost-function as an advantage unlike Bui-Thanh et al. [43] who prefer to reduced directly to the cost-function.

Taking a linearised variation of the form

$$\begin{aligned} & \int_{\Theta} \delta u \rho \ddot{u} d\Theta + \int_{\Theta} \delta u c \dot{u} d\Theta + \int_{\Theta} \delta u g(u) d\Theta \\ &= \int_{\Theta} \delta u \rho \frac{\partial^2 u}{\partial t^2} d\Theta + \int_{\Theta} \delta u c \frac{\partial u}{\partial t} d\Theta + \int_{\Theta} \delta u g(u) d\Theta = \int_{\Omega} \delta u f_E d\Omega. \end{aligned} \quad (3.42)$$

the very initial Principle of Virtual Work (2.8) yields a possible starting point for the formulation of a PGD for an application in structural dynamics. The entire space-time-domain of the problem is denoted by  $\Theta = \Omega \times (t_0, t_e]$  and consists of the volume  $V$  of the system and the time interval  $T$ , on which the solution is to be calculated.

The basic idea of the PGD is to express the sought-after quantity  $u$  as a product of independent, mono-dimensional nucleus functions of its variables. As the dynamic displacements of a three-dimensional structure  $u = u(x_1, x_2, x_3, t)$  depend on the three space coordinates  $x_1$ ,  $x_2$  and  $x_3$  and the time  $t$  they can be expressed in the sense of a PGD as

$$u \approx \sum_{k=1}^r \alpha_k F_{1,k}(x_1) F_{2,k}(x_2) F_{3,k}(x_3) F_{t,k}(t), \quad (3.43)$$

if an equal number  $r$  of reduction functions for the three dimensions of space is used. The same notion of assembling a function from nucleus functions is also applied to the virtual displacements

$$\delta u \approx \sum_{k=1}^r \delta \alpha_k F_{1,k}(x_1) F_{2,k}(x_2) F_{3,k}(x_3) F_{t,k}(t). \quad (3.44)$$

### 3.1. SELECTING A REDUCTION APPROACH

The power of this approach of separated variables lies in the fact that equation (3.43) can be expanded as required. Should e.g. the displacements also depend on an external parameter  $\mu$ , it would pose no problem to expand equation (3.43) with additional nucleus functions  $F_{\mu,k}(\mu)$  to take the dependence of the solution on the parameter into account. If there are several parameters, an additional nucleus function for each parameter can be included without complexifying the problem.

Introducing the two equations (3.43) and (3.44) into the Principle of Virtual Work (3.42) yields

$$\begin{aligned}
& \int_{\Theta} \left( \sum_{k=1}^r \delta\alpha_k \prod_{j=1}^3 F_{j,k}(x_j) F_{t,k}(t) \right) \rho & \frac{\partial^2}{\partial t^2} \left( \sum_{k=1}^r \alpha_k \prod_{j=1}^3 F_{j,k}(x_j) F_{t,k}(t) \right) d\Theta \\
& + \int_{\Theta} \left( \sum_{k=1}^r \delta\alpha_k \prod_{j=1}^3 F_{j,k}(x_j) F_{t,k}(t) \right) c & \frac{\partial}{\partial t} \left( \sum_{k=1}^r \alpha_k \prod_{j=1}^3 F_{j,k}(x_j) F_{t,k}(t) \right) d\Theta \\
& + \int_{\Theta} \left( \sum_{k=1}^r \delta\alpha_k \prod_{j=1}^3 F_{j,k}(x_j) F_{t,k}(t) \right) g & \left( \sum_{k=1}^r \alpha_k \prod_{j=1}^3 F_{j,k}(x_j) F_{t,k}(t) \right) d\Theta \\
& = \int_{\Theta} \left( \sum_{k=1}^r \delta\alpha_k \prod_{j=1}^3 F_{j,k}(x_j) F_{t,k}(t) \right) f_E d\Theta & .
\end{aligned} \tag{3.45}$$

In this equation the integrals can be split along the different dimensions and time, giving e.g.

$$\begin{aligned}
\int_{\Theta} \left( \sum_{k=1}^r \alpha_k \prod_{j=1}^3 F_{j,k}(x_j) F_{t,k}(t) \right) d\Theta &= \sum_{k=1}^r \alpha_k \left( \int_{x_{1,min}}^{x_{1,max}} F_{1,k}(x_1) dx_1 \right. \\
& \int_{x_{2,min}}^{x_{2,max}} F_{2,k}(x_2) dx_2 \\
& \int_{x_{3,min}}^{x_{3,max}} F_{3,k}(x_3) dx_3 \\
& \left. \int_{t_0}^{t_{max}} F_{t,k}(t) dt \right), \tag{3.46}
\end{aligned}$$

which greatly eases the computational burden and complexity.

Supposing that the functions  $F_{1,k}(x_1)$ ,  $F_{2,k}(x_2)$ ,  $F_{3,k}(x_3)$  and  $F_{t,k}(t)$  are known for all  $k \in \{1 \dots r\}$  and assuming that they all comply with the initial and the boundary conditions, equation (3.45) can be used to compute the coefficients  $\alpha_k$ . Their virtual counterparts  $\delta\alpha_k$  are arbitrary and can be discarded.

The iterative calculation of the nucleus functions  $F_{j,k}$  starts at  $r = 1$ . From equation (3.45) a residual can be build, which indicates if the reduction of order  $r$  is sufficient. If this is the case, corresponding to the chosen formulation of the residual, the Proper Generalized Decomposition reaches its objective and the obtained functions  $F$  can be used as an approximation to the solution as defined in equation (3.43).

But if the chosen threshold for the residual objects a successful convergence, the algorithm has to be continued beyond the  $r$  existing function by the introduction of an additional term, raising the order of the approximation to  $r + 1$  :

### 3.1. SELECTING A REDUCTION APPROACH

---

$$\begin{aligned}
 u \approx & \sum_{k=1}^r \alpha_k F_{1,k}(x_1) F_{2,k}(x_2) F_{3,k}(x_3) F_{t,k}(t) \\
 & \times \alpha_{r+1} F_{1,r+1}(x_1) F_{2,r+1}(x_2) F_{3,r+1}(x_3) F_{t,r+1}(t)
 \end{aligned} \tag{3.47}$$

From this the function of the virtual displacements  $\delta u$  is formulated as

$$\begin{aligned}
 \delta u = & \delta F_{1,r+1}(x_1) F_{2,r+1}(x_2) F_{3,r+1}(x_3) F_{t,r+1}(t) \\
 & F_{1,r+1}(x_1) \delta F_{2,r+1}(x_2) F_{3,r+1}(x_3) F_{t,r+1}(t) \\
 & F_{1,r+1}(x_1) F_{2,r+1}(x_2) \delta F_{3,r+1}(x_3) F_{t,r+1}(t) \\
 & F_{1,r+1}(x_1) F_{2,r+1}(x_2) F_{3,r+1}(x_3) \delta F_{t,r+1}(t)
 \end{aligned} \tag{3.48}$$

with the new additions to equation (3.47) acting, in turn, as test functions.

Introducing this into equation (3.42) yields a system of equations whose results are the different additional functions. To this end the added functions  $F_{j,r+1}$  and  $F_{t,r+1}$  are discretised and eventually normalised to be used in the next iteration step, beginning with the calculation of the respective multiplicative factors  $\alpha$  as per equation (3.45) which now comprises  $r + 1$  equations.

Even though a discretisation remains necessary, the merit of the Proper Generalised Decomposition lies in the considerable reduction of the computational effort of this discretisation and its numerical solution. This is due to the fact that it is no longer the physical system that is discretised but its abstract, reduced representation.

#### 3.1.3 Choosing the reduction approach

The choice of an appropriate reduction approach is difficult. The approaches evaluated above are developed with different purposes and respond to different requirements.

Within the scope of this study the reduction approaches have to answer to the requirement of providing a computational tool, which has to recreate the full order transient solution of a geometrically nonlinear, non-conservative system as faithfully as possible while considerably reducing the computational cost. This imperative is stated in section 3.1.1.

It is against this requirement that the reduction approaches are judged. However, most of them do also offer additional specific characteristics that are included in the evaluation.

The projection on a reduced basis from section 3.1.2.1 is the standard approach for the reduction of problems in the context structural dynamics. This is understandable, as some reduced bases do have a physical meaning and contribute thus not only to the solution, but also to the interpretation of the problem. It is a modular approach with a clear separation of the reduction, by projection on a reduced basis, and the solution of the reduced system. This implies that, first, a suitable integration scheme can probably be found for any given problem and, if formulated correctly, this integration scheme does not distinguish between the reduced and the full order system. Following the definition of Mignolet et al. [149] this makes the projection on a reduced basis an indirect approach, because it is non-intrusive with respect to e.g. available commercial finite element software. Furthermore, and second, a reduced basis can be chosen, which provides an optimal performance for the problem at hand, and which can be readily adapted in size. The modular character of the reduction by projection approach also allows focusing the necessary adaptations either on the reduced basis or on the algorithm for obtaining the transient solution.

The Guyan reduction, presented in section 3.1.2.2, is a monolithic technique. It offers few starting points for extensions. Furthermore, it is conceived for linear problems and has undergone no significant devel-

## 3.2. OBTAINING TRANSIENT SOLUTIONS OF FULL ORDER AND REDUCED ORDER SYSTEMS

---

opments since its inception. It can hence be considered as a well developed, and stable, method and a conversion for the solution of nonlinear systems does not seem to show much promise.

The truncated harmonic balance method, section 3.1.2.3, is also a monolithic approach. It is conceived for stationary solutions. Here, again, the necessary modifications for obtaining transient solutions are judged as not too promising. These would be further complicated by the fact that the reduction and the solution are not clearly separable within the approach of the truncated harmonic balance method.

The nonlinear normal modes, section 3.1.2.4, were conceived as an analysis tool to study the stationary orbits of already low-dimensional, simple systems. It is only recently that their application has been extended to model reduction. However, for the reduction of large, structural dynamic systems they still seem limited by the original intention of their inception. Their properties, in particular the impossibility to superpose modes, and thus to readily change the order of the reduced system if needed, are strong arguments against their application on a problem as extensive as the transient solution of the dynamic equilibrium of a geometrically nonlinear structure discretised in space, as it is described in equation (2.82). Finally, the NNMs are already a monolithic approach, in which reduction and solution are intimately amalgamated, which renders all possible extensions difficult.

The Proper Generalised Decomposition, section 3.1.2.5, is the most recently developed one of the surveyed approaches. It has hence the advantage of still being an open approach which would be easily extensible as needed. On the other hand it is certainly still battling teething troubles and does hence not offer a well-proven platform for further extensions, which could draw on its inherent robustness. Finally, the PDG starts on the level of a continuous description of the problem, and this is contradictory to the stated aims of this study, which assumes the underlying problem as already discretised.

Against the given requirement and with a strong emphasis on the anticipated needs for adapting the most modular reduction approach of the projection on a reduced basis is chosen.

Besselink et al. [37] point out that the reduction by projection approach is by far the approach requiring the most intervention, knowledge and experience from its user. Exaggerating their assessment, it can be stated that the targeted and successful application of the reduction by projection on a reduced basis borders on an art-form. This becomes obvious in the following.

The first of the two following sections is dedicated to the introduction of the Newmark scheme, a time integration scheme for the transient solution of full order and reduced order systems alike. In the second section a selection of common reduced basis is presented, which will ultimately be tested for their suitability in reducing a geometrically nonlinear system.

### **3.2 Obtaining transient solutions of full order and reduced order systems**

The choice of the reduced basis as the solution method in section 3.1 is, among the other cited arguments, based on its strong interdependence with the nonlinear Newmark scheme. This allows to formulate a reduced system and to have its transient solution established with basically the same algorithm as the one used for the full order system. This section aims at presenting the full order nonlinear Newmark scheme and then introduces the reduced basis in a consistent manner. This allows demonstrating the high degree of similarity between the full order and the reduced order algorithm. Additionally, some variants of the Newmark algorithm are presented. On the full order side the HHT- $\alpha$ -method is prepared for a use with the finite element test-cases.

The transient solution is based on the Newmark scheme (Newmark [160]) because this algorithm is the mainstay for transient solutions in structural dynamics. It proved itself as being robust, flexible and extensible. Furthermore, it provides a simple frame on which the entire problematic of reduction, and the solutions that are to be found, can be attached. Therefore, more complex integration schemes, such as

## 3.2. OBTAINING TRANSIENT SOLUTIONS OF FULL ORDER AND REDUCED ORDER SYSTEMS

---

nonlinear Jacobian methods, which iteratively solve the required Newton-Raphson iterations as a set of uncoupled nonlinear equations, the Broyden-Fletcher-Goldfarb-Shanno (BFGS) method, that includes an evolution of the system's Jacobian (presented by e.g. Dennis and Schnabel [66]), or the Runge-Kutta and Rosenbrock classes of methods, that are of higher order in the time integration (both compared by John and Rang [111]), are not considered. Once the superstructure of a reduced solution is described consistently, it should be no problem to return to the underlying integration scheme and insert an appropriate one.

Har and Tamma [93] consider the Newmark family of algorithms as the "perhaps the most widely used family of [...] integration methods". While the Newmark scheme and its variants are the most dominating techniques for obtaining transient solutions of dynamic systems in structural dynamics, and are the ones exclusively used in the course of the present study, there exist other approaches. For comparison, three of these approaches from literature are mentioned below without striving neither for a complete survey of available solution methods nor for an in detail description of the different methods.

A first method is based on the variation of the incremental displacements. It is described by Batoz and Dhatt [23] and relies on prescribing a component of the displacement vector, eliminating the corresponding row and column from the matrices and solving the thus reduced system. At the same time a factor called the load level is introduced for the external load, which is used to balance the internal and external forces and serves as an additional variable, replacing the prescribed deformation.

Another method is proposed by Felippa and Park [80], who take a very broad approach in their report, which encompasses implicit and explicit integrations and they focus strongly on stability concerns related to algorithmic properties and step-size control. The Newmark scheme being a much specialised variant in the class of explicit integrations.

Finally Houbolt [101] can be cited as an example of the application of classic difference formulations to a real-world problem. Again this is yet a generic case, but as the publication Houbolt [101] precedes the two other publications discussed in this section by almost thirty years, it can serve as an illustration of the roots of the constant evolution of solution algorithm, which eventually lead to the highly refined and efficient Newmark scheme.

### 3.2.1 Obtaining a transient solution of full order nonlinear systems

The solutions for linear systems have evolved to significant performance and culminated in the Newmark scheme, whose main ideas are briefly sketched in this section. The Newmark scheme is a direct time integration algorithm which calculates the time history of the displacements  $\mathbf{u}$  starting from initial conditions  $\mathbf{u}_0$  and  $\dot{\mathbf{u}}_0$ .

For the solution, the system to be solved is considered discretised. The dynamic behaviour of the system can simply be described by an equilibrium formulation as it is expressed in matrices by equation (2.82).

The solution of a full order nonlinear system differs significantly from the solution of a linear system as it requires constant updating of the system's stiffness properties as the displacements evolve. To account for this need the tangent stiffness matrix is defined as the derivation of the nonlinear function  $\mathbf{g}$  with respect to the displacements in the course of the nonlinear solution process.

#### 3.2.1.1 Nonlinear Newmark scheme

The nonlinear Newmark scheme for the time resolution of nonlinear systems, as it can be found in a number of standard volumes on structural dynamics, as for example Krenk [123], consists of two distinct loops: the outer loop advances in time while the inner loop converges a residual towards zero for each time-step. It can be easily adapted to operate on reduced displacements  $\mathbf{q}$ , as is shown later in section 3.2.2.1. For now, the algorithm is set up to operate on the physical displacements  $\mathbf{u}$ .

The nonlinear Newmark scheme uses a prediction-correction-time-integration for establishing the time

### 3.2. OBTAINING TRANSIENT SOLUTIONS OF FULL ORDER AND REDUCED ORDER SYSTEMS

---

history of the displacements under the varying external forces. Hence, an important prerequisite to the following course of action is the supposition that the external forces  $\mathbf{f}_E(t)$  are known at all times and do not depend on the displacements of  $\mathbf{u}$ . This excludes e.g. contact problems between multiple bodies, for whose treatment special procedures would have to be introduced.

Being given the mass matrix  $\mathbf{M}$  and the damping matrix  $\mathbf{C}$  of the system, the vector of external forces  $\mathbf{f}_E^{(0)}$ , which provides the external forces at the instant  $t = t^{(0)}$ , and the initial conditions for the displacements and the velocities

$$\mathbf{u}^{(0)} = \mathbf{u}(t = t_0) \quad (3.49)$$

$$\dot{\mathbf{u}}^{(0)} = \dot{\mathbf{u}}(t = t_0) \quad (3.50)$$

the initial accelerations  $\ddot{\mathbf{u}}^{(0)} = \ddot{\mathbf{u}}(t = t_0)$  are calculated as

$$\ddot{\mathbf{u}}^{(0)} = \mathbf{M}^{-1} \left( \mathbf{f}_E^{(0)} - \mathbf{C}\dot{\mathbf{u}}^{(0)} - \mathbf{g}(\mathbf{u}^{(0)}) \right). \quad (3.51)$$

Thus a complete state of the system, containing the displacements  $\mathbf{u}^{(t)}$ , the velocities  $\dot{\mathbf{u}}^{(t)}$  and the accelerations  $\ddot{\mathbf{u}}^{(t)}$ , is established. The availability of these three quantities distinguishes this state as being the numerical state of the system. In a purely theoretical setting the use of the denomination state is limited to the displacements and the velocities. From now on, these three calculated quantities bear the superscript  $(t)$  instead of the superscript  $(0)$ , as they can stand for every completely calculated state  $t$  between  $t_0$  and  $t_e$ . Once such a complete state is established at the instant  $t$  the next complete state at  $t + \Delta t$  is calculated with Newton-Raphson iterations.

An iterative process<sup>6</sup> is used at every instant  $t$  to achieve convergence on the quantities of motion at the next instant  $(t + \Delta t)$ . To this end the current time is augmented by the time-step  $\Delta t$  to give the next instant,

$$t \rightarrow t + \Delta t. \quad (3.52)$$

At this instant the entire state of the system, i.e. the values of  $\mathbf{u}^{(t+\Delta t)}$ ,  $\dot{\mathbf{u}}^{(t+\Delta t)}$  and  $\ddot{\mathbf{u}}^{(t+\Delta t)}$ , is yet unknown.

Finding them engages the outer loop of the nonlinear Newmark scheme. This outer loop initialises the inner, iterative loop with predictive values. The first iterative, predictive values for the new instant are calculated with the values from the preceding instant at the time  $(t)$  with an extrapolation

$$\ddot{\mathbf{u}}_{(i=1)}^{(t+\Delta t)} = \ddot{\mathbf{u}}^{(t)} \quad (3.53)$$

$$\dot{\mathbf{u}}_{(i=1)}^{(t+\Delta t)} = \dot{\mathbf{u}}^{(t)} + \Delta t \ddot{\mathbf{u}}^{(t)} \quad (3.54)$$

$$\mathbf{u}_{(i=1)}^{(t+\Delta t)} = \mathbf{u}^{(t)} + \Delta t \dot{\mathbf{u}}^{(t)} + \frac{1}{2} \Delta t^2 \ddot{\mathbf{u}}^{(t)}. \quad (3.55)$$

From here on the quantities of motion at the new instant  $(t + \Delta t)$  are determined by pursuing the disappearance of a residual force in an iteration over the index  $i$ . This approach is a Newton-Raphson iteration on the residual force.

The formulation of the dynamic equilibrium at the instant  $(t + \Delta t)$  with equation (2.82) would require knowledge of the velocities  $\dot{\mathbf{u}}^{(t+\Delta t)}$  and the accelerations  $\ddot{\mathbf{u}}^{(t+\Delta t)}$ . As the dynamic equilibrium at the current instant  $(t + \Delta t)$  is not yet achieved, the residual force  $\mathbf{r}_{(i)}^{(t+\Delta t)}$  is calculated with the predictive

<sup>6</sup>The linear Newmark scheme would only use a simple prediction-correction step at this point.

### 3.2. OBTAINING TRANSIENT SOLUTIONS OF FULL ORDER AND REDUCED ORDER SYSTEMS

---

values from equations (3.53) to (3.55). It is defined as the difference between the current internal forces resulting from the displacements, velocities, accelerations and the actually applied external forces at the current instant

$$\mathbf{r}_{(i)}^{(t+\Delta t)} = \mathbf{f}_E(t + \Delta t) - \mathbf{M}\ddot{\mathbf{u}}_{(i)}^{(t+\Delta t)} - \mathbf{C}\dot{\mathbf{u}}_{(i)}^{(t+\Delta t)} - \mathbf{g}\left(\mathbf{u}_{(i)}^{(t+\Delta t)}\right). \quad (3.56)$$

Here it becomes crucial that the external forces at the instant  $(t + \Delta t)$  are known and that they do not depend on the deformation of the system.

The overarching aim of the inner iterative loop over the index  $i$  is to drive the residual force  $\mathbf{r}_{(i)}^{(t+\Delta t)}$  to zero by determining the corresponding displacements  $\mathbf{u}^{(t+\Delta t)}$  that solve equation (3.56). The adaptation of the displacements is done by the calculation of the incremental displacement  $\Delta\mathbf{u}_{(i)}^{(t+\Delta t)}$ , which in turn requires the calculation of the tangent stiffness matrix,

$$\bar{\mathbf{K}}_{(i)} = \left. \frac{\partial \mathbf{g}(\mathbf{u})}{\partial \mathbf{u}} \right|_{\mathbf{u}_{(i)}^{(t+\Delta t)}}. \quad (3.57)$$

At this point the underlying assumption is that the nonlinear internal forces can be expressed with a first-order approximation

$$\begin{aligned} \mathbf{g}\left(\mathbf{u}_{(i+1)}^{(t+\Delta t)}\right) &\approx \mathbf{g}\left(\mathbf{u}_{(i)}^{(t+\Delta t)}\right) + \left. \frac{\partial \mathbf{g}(\mathbf{u})}{\partial \mathbf{u}} \right|_{\mathbf{u}_{(i)}^{(t+\Delta t)}} \Delta\mathbf{u}_{(i)}^{(t+\Delta t)} \\ &= \mathbf{g}\left(\mathbf{u}_{(i)}^{(t+\Delta t)}\right) + \bar{\mathbf{K}}_{(i)} \Delta\mathbf{u}_{(i)}^{(t+\Delta t)}, \end{aligned} \quad (3.58)$$

where  $\bar{\mathbf{K}}_{(i)} = \left. \frac{\partial \mathbf{g}(\mathbf{u})}{\partial \mathbf{u}} \right|_{\mathbf{u}_{(i)}^{(t+\Delta t)}}$  designates the tangent stiffness matrix and  $\Delta\mathbf{u}_{(i)}^{(t+\Delta t)}$  the incremental displacements. The preparation for this assumption go back to equation (2.34), where the discrete formulation of the problem is prepared specifically for this type of time-marching solution algorithm.

This tangent stiffness matrix is the major component in the system's Jacobian  $\mathbf{S}_{(i)}$  at the central point of the Newton-Raphson iterations

$$\mathbf{S}_{(i)} = \bar{\mathbf{K}}_{(i)} + \frac{\gamma}{\beta \Delta t} \mathbf{C} + \frac{1}{\beta \Delta t^2} \mathbf{M}. \quad (3.59)$$

The parameters  $\gamma$  and  $\beta$  are introduced to allow for differently weighted integration schemes of the terms  $\mathbf{u}$ ,  $\dot{\mathbf{u}}$  and  $\ddot{\mathbf{u}}$  between  $t$  and  $t + \Delta t$ . Their values are determined in section 3.2.2.3.

The Jacobian matrix  $\mathbf{S}$  allows the calculation of the incremental displacement  $\Delta\mathbf{u}_{(i)}^{(t+\Delta t)}$  from the residual force  $\mathbf{r}_{(i)}^{(t+\Delta t)}$ ,

$$\Delta\mathbf{u}_{(i)}^{(t+\Delta t)} = \mathbf{S}_{(i)}^{-1} \mathbf{r}_{(i)}^{(t+\Delta t)}. \quad (3.60)$$

The next iterative values of the quantities of motion are initialised with their preceding values and the incremental displacement

### 3.2. OBTAINING TRANSIENT SOLUTIONS OF FULL ORDER AND REDUCED ORDER SYSTEMS

---

$$\mathbf{u}_{(i+1)}^{(t+\Delta t)} = \mathbf{u}_{(i)}^{(t+\Delta t)} + \Delta \mathbf{u}_{(i)}^{(t+\Delta t)} \quad (3.61)$$

$$\dot{\mathbf{u}}_{(i+1)}^{(t+\Delta t)} = \dot{\mathbf{u}}_{(i)}^{(t+\Delta t)} + \frac{\gamma}{\beta \Delta t} \Delta \mathbf{u}_{(i)}^{(t+\Delta t)} \quad (3.62)$$

$$\ddot{\mathbf{u}}_{(i+1)}^{(t+\Delta t)} = \ddot{\mathbf{u}}_{(i)}^{(t+\Delta t)} + \frac{1}{\beta \Delta t^2} \Delta \mathbf{u}_{(i)}^{(t+\Delta t)}, \quad (3.63)$$

This concludes one cycle of the inner, iterative loop.

At this point a decision has to be made whether the iteration is to be continued or not. The iterations are halted if the iterated solution  $\mathbf{u}_{(i+1)}^{(t+\Delta t)}$  is close enough to the assumed exact solution  $\mathbf{u}^{(t+\Delta t)}$ . This can be determined by comparing the norm of the most recent value of the norm of residual  $\|\mathbf{r}_{(i+1)}^{(t+\Delta t)}\|$  with an appropriate upper limit derived from the norm of the initial residual

$$\|\mathbf{r}_{(i+1)}^{(t+\Delta t)}\| \leq \epsilon \|\mathbf{r}_{(i=1)}^{(t+\Delta t)}\|, \quad (3.64)$$

with  $\epsilon \ll 1$ .

Other criteria can be based on the incremental displacement  $\Delta \mathbf{u}_{(i)}^{(t+\Delta t)}$  or a combination of the incremental displacement and the residual for considerations involving energy.

If the results fall short of the selected convergence criterion the next iteration loop over  $i$  is launched with the calculation of a new residual force (3.56), without changing the time but with augmenting the index  $i$  by one,

$$i \rightarrow i + 1. \quad (3.65)$$

If the convergence criterion is met the iterated solution  $\mathbf{u}_{(i+1)}^{(t+\Delta t)}$  is set to be the assumed exact solution  $\mathbf{u}^{(t+\Delta t)}$  and the next series of iterations towards the next time-step can be launched by returning to equation (3.52). The values of  $\mathbf{u}^{(t+\Delta t)}$ ,  $\dot{\mathbf{u}}^{(t+\Delta t)}$  and  $\ddot{\mathbf{u}}^{(t+\Delta t)}$  are used to initialise the values for the next inner, iterative loop towards the next instant in time.

This concludes the solution of the full order nonlinear system. The next subsection introduces the concept of HHT- $\alpha$ -methods, which alters the nonlinear Newmark scheme, as it is presented above, in order to render it more stable. This variant will be largely used for the finite element test-cases. The following section 3.2.2.1 is dedicated to the introduction of the reduction into the nonlinear Newmark scheme.

#### 3.2.1.2 HHT- $\alpha$ -method

The  $\alpha$ -methods are a generalisation of the Newmark algorithm. The Newmark scheme, as it is presented above, can be obtained as a special case of an  $\alpha$ -method.

The  $\alpha$ -methods provide certain advantages concerning the stability of the solution. They are required for the finite element test-cases that will be treated later on. But first of all, the inclusion of the HHT- $\alpha$ -methods proves that all techniques and procedures that are developed in the following are applicable to a wider variety of solution procedures than just the classic nonlinear Newmark scheme. In fact, apart from the nonlinear Newmark scheme and the HHT- $\alpha$ -methods, a wide variety of numerical algorithms for obtaining transient solutions of structural dynamic systems can be used as a backbone for the reduced transient solution of geometrically nonlinear systems. All techniques that are developed in the following chapters are integrated into this backbone of the solution algorithm.

### 3.2. OBTAINING TRANSIENT SOLUTIONS OF FULL ORDER AND REDUCED ORDER SYSTEMS

---

The central feature of the  $\alpha$ -methods is that the equilibrium in equation (3.56) is obtained not directly at the instant  $t + \Delta t$  but at the intermediate instant  $t + \alpha\Delta t$ , with  $\alpha < 1$ . The matrices of the system, i.e. the damping matrix  $\mathbf{C}$  and the tangent stiffness matrix  $\bar{\mathbf{K}}$ , are weighted accordingly and, once convergence on a zero residual at  $t + \alpha\Delta t$  is achieved, the state of the system at  $t + \Delta t$  is calculated.

Compared to the standard Newmark scheme, the  $\alpha$ -methods provide an increased algorithmic damping of the high-frequency oscillations which stabilises the solution. This is the main reason for its application because the stabilisation of the solution proves advantageous for the transient solutions of the finite element test-cases which are built from the elements in section 2.2.

There are two variants within the class of  $\alpha$ -methods:

- the Hilber-Hughes-Taylor- $\alpha$ -method, or HHT- $\alpha$ -method, going back to Hilber et al. [97], that weighs the displacements and the velocities at  $t + \alpha\Delta t$  and calculates the accelerations at  $t + \Delta t$ , and
- the Generalised- $\alpha$ -method by Chung and Hulbert [63], which comprises a second parameter  $\alpha_M$  to weigh the mass matrix and to calculate the accelerations at an instant  $t + \alpha_M\Delta t$ .

The HHT- $\alpha$ -method is the generalised  $\alpha$ -method with  $\alpha_M = 1$ . Detailed explorations for the two methods' stability in the context of structural dynamics are given in the original references by Hilber et al. [97] and Chung and Hulbert [63]. Additional, and more recent, developments for the application of the methods to nonlinear problems have been achieved by e.g. Kuhl and Ramm [124], including the necessary approximations for the differences of the nonlinear forces, and Wood et al. [242]. Extensions for their use in fluid dynamics are also available, e.g. Jansen et al. [107]. Preliminary numerical experiments allow the conclusion that the HHT- $\alpha$ -method is sufficient for stabilising the transient solutions of the finite element test-cases in chapter 6. Hence only this variant is presented in detail.

Equation (3.56) defines the residual in the inner, iterative loop of the classic nonlinear Newmark scheme. The dynamic equilibrium of the structure can be shifted to an intermediate instant between  $t$  and  $\Delta t$  by introducing the weighting parameter  $\alpha$ . This leads to the residual

$$\mathbf{r}_{(i)}^{(t+\Delta t)} = \mathbf{f}_E(t + \Delta t) - \mathbf{M}\ddot{\mathbf{u}}_{(i)}^{(t+\Delta t)} - \mathbf{C}\dot{\mathbf{u}}_{(i)}^{(t+\alpha\Delta t)} - \mathbf{g}\left(\mathbf{u}_{(i)}^{(t+\alpha\Delta t)}\right). \quad (3.66)$$

The tangent stiffness matrix, as it is necessary for the system's Jacobian matrix  $\mathcal{S}_{(i)}$  in equation (3.59), is also defined at the intermediate displacements. This turns equation (3.57) into

$$\bar{\mathbf{K}}_{(i)} = \left. \frac{\partial \mathbf{g}(\mathbf{u})}{\partial \mathbf{u}} \right|_{\mathbf{u}_{(i)}^{(t+\alpha\Delta t)}}. \quad (3.67)$$

The necessary expressions for the displacements and the velocities are obtained by a sum of the preceding iterative values and the values of the preceding time-step. The parts of this sum are weighted with  $\alpha$  in order to adapt it to the definitions of the residual and the Jacobian

$$\mathbf{u}_{(i)}^{(t+\alpha\Delta t)} = (1 - \alpha)\mathbf{u}_{(i)}^{(t)} + \alpha\mathbf{u}_{(i-1)}^{(t+\Delta t)} \quad (3.68)$$

$$\dot{\mathbf{u}}_{(i)}^{(t+\alpha\Delta t)} = (1 - \alpha)\dot{\mathbf{u}}_{(i)}^{(t)} + \alpha\dot{\mathbf{u}}_{(i-1)}^{(t+\Delta t)}. \quad (3.69)$$

These values allow obtaining an increment  $\Delta\mathbf{u}_{(i)}^{(t+\Delta t)}$  that is used in equations (3.61), (3.62) and (3.63). These three and all other equations of the Newmark scheme, as it is presented in section 3.2.1.1, are left unchanged.

### 3.2.2 Obtaining a transient solution of reduced order nonlinear systems

Section 3.1.2.1 demonstrates that the equation for describing the dynamic equilibrium of the reduced system in equation (3.11) has the exact same structure as its equivalent of the full order system in equation (2.82). It is hence natural to subject it to the very same procedure in order to obtain a transient solution. This is done in order to stress the property of non-intrusiveness of the projection on a reduced basis as it is demonstrated by Mignolet et al. [149]. An approach that is much more slanted towards the actual implementation of a code for solving reduced models can be found in Aquino [16].

The adaptation of the full order nonlinear Newmark scheme to treat a reduced system as (3.11) forms the first part of this section. The second part of this section sees the demonstration of the introduction of the reduction into the HHT- $\alpha$ -method. This adaptation of the HHT- $\alpha$ -method follows the same lines as the adaptation of the nonlinear Newmark scheme and requires no additional conceptual effort. The third part concludes this section with considerations of the determination of the parameters  $\beta$ ,  $\gamma$  and  $\alpha$ . The next section addresses the validity of the assumption of the availability of a reduced expression  $\tilde{\mathbf{g}}(\mathbf{q})$  as it is stipulated in equation (3.10) and supposed to be available throughout the first two parts of this section.

#### 3.2.2.1 Introducing the reduced basis into the nonlinear Newmark scheme

It is possible to find a formulation of a nonlinear reduced system that enables a solution with a nonlinear Newmark scheme. This possibility is one of the great advantages of the reduction approach of the projection on a reduced basis and greatly facilitates its implementation and its application. In addition to the correct transformation of the initial conditions to the generalised coordinates, the reduced nonlinear Newmark scheme will crucially hinge on an effective reduction of the nonlinear forces vector  $\mathbf{g}(\mathbf{u})$ , which is by no means given. The transformation of the HHT- $\alpha$ -method is analogous to the following approach. Their adaptation for reduced systems is hence detailed very briefly.

The reduced nonlinear Newmark scheme is based on equation (3.11). It reads

$$\tilde{\mathbf{M}}\ddot{\mathbf{q}} + \tilde{\mathbf{C}}\dot{\mathbf{q}} + \tilde{\mathbf{g}}(\mathbf{q}) = \tilde{\mathbf{f}}_E \quad (3.70)$$

and provides the reduced mass matrix  $\tilde{\mathbf{M}}$ , the reduced damping matrix  $\tilde{\mathbf{C}}$  and the reduced vector of the external forces  $\tilde{\mathbf{f}}_E^{(0)} = \mathbf{\Phi}^T \mathbf{f}_E^{(0)}$ . In equation (3.70) it is also implied that a reduced formulation of the nonlinear internal forces is available. The availability of this expression  $\tilde{\mathbf{g}}(\mathbf{q})$  is of central importance to the reduced solution algorithm and discussed further in section 3.2.3.

In order to obtain a complete state of the reduced system the generalised initial conditions

$$\mathbf{q}^{(0)} = \mathbf{q}(t = t_0) \quad (3.71)$$

$$\dot{\mathbf{q}}^{(0)} = \dot{\mathbf{q}}(t = t_0) \quad (3.72)$$

and the external forces at  $t = t_0$  are required. If the generalised initial conditions are to be derived from the full order initial conditions in equations (3.49) and (3.50), a consistent reduction has to be ensured. This can be done by determining the reduced initial conditions from the full order initial conditions in the least-squares sense

### 3.2. OBTAINING TRANSIENT SOLUTIONS OF FULL ORDER AND REDUCED ORDER SYSTEMS

---

$$\mathbf{q}^{(t_0)} = (\mathbf{\Phi}^T \mathbf{\Phi})^{-1} \mathbf{\Phi}^T \mathbf{u}_0 \quad (3.73)$$

$$\dot{\mathbf{q}}^{(t_0)} = (\mathbf{\Phi}^T \mathbf{\Phi})^{-1} \mathbf{\Phi}^T \dot{\mathbf{u}}_0 \quad (3.74)$$

$$\ddot{\mathbf{q}}^{(t_0)} = \tilde{\mathbf{M}}^{-1} \left( \mathbf{\Psi}^T \mathbf{f}_E(t_0) - \tilde{\mathbf{C}} \dot{\mathbf{q}}^{(t_0)} - \mathbf{\Psi}^T \mathbf{g} \left( \mathbf{\Phi} \mathbf{q}^{(t_0)} \right) \right). \quad (3.75)$$

The initial generalised accelerations  $\ddot{\mathbf{q}}^{(0)}$  are calculated with the reduced equivalent of equation (3.51) as

$$\ddot{\mathbf{q}}^{(0)} = \tilde{\mathbf{M}}^{-1} \left( \tilde{\mathbf{f}}_E^{(0)} - \tilde{\mathbf{C}} \dot{\mathbf{q}}^{(0)} - \tilde{\mathbf{g}} \left( \mathbf{q}^{(0)} \right) \right). \quad (3.76)$$

Following the exact same path of action as with the full order Newmark scheme, a complete state at every time-step is required. From there on the yet unknown state at the next instant  $t + \Delta t$  after the time-step<sup>7</sup> is found with an iteration.

The predictive values of the next generalised state are obtained with the reduced equivalents of equations (3.53) to (3.55). The inner, iterative loop over the index ( $i$ ) is initialised with

$$\ddot{\mathbf{q}}_{(i=1)}^{(t+\Delta t)} = \ddot{\mathbf{q}}^{(t)} \quad (3.77)$$

$$\dot{\mathbf{q}}_{(i=1)}^{(t+\Delta t)} = \dot{\mathbf{q}}^{(t)} + \Delta t \ddot{\mathbf{q}}^{(t)} \quad (3.78)$$

$$\mathbf{q}_{(i=1)}^{(t+\Delta t)} = \mathbf{q}^{(t)} + \Delta t \dot{\mathbf{q}}^{(t)} + \frac{1}{2} \Delta t^2 \ddot{\mathbf{q}}^{(t)}. \quad (3.79)$$

The increment in generalised coordinates  $\Delta \mathbf{q}_{(i)}^{(t+\Delta t)}$  is calculated to continue the iterations from these initial values towards the presumed converged values of the reduced system's state at  $t + \Delta t$ . The increment is calculated as

$$\Delta \mathbf{q}_{(i)}^{(t+\Delta t)} = \tilde{\mathbf{S}}_{(i)}^{-1} \tilde{\mathbf{r}}_{(i)}^{(t+\Delta t)}. \quad (3.80)$$

It requires the generalised residual

$$\tilde{\mathbf{r}}_{(i)}^{(t+\Delta t)} = \tilde{\mathbf{f}}_E(t + \Delta t) - \tilde{\mathbf{M}} \ddot{\mathbf{q}}_{(i)}^{(t+\Delta t)} - \tilde{\mathbf{C}} \dot{\mathbf{q}}_{(i)}^{(t+\Delta t)} - \tilde{\mathbf{g}} \left( \mathbf{q}_{(i)}^{(t+\Delta t)} \right). \quad (3.81)$$

The inner Newton-Raphson iteration operates on this residual  $\tilde{\mathbf{r}}_{(i)}^{(t+\Delta t)}$ , with the aim of driving it towards zero. Equation (3.80) also required is the generalised Jacobian

$$\tilde{\mathbf{S}}_{(i)} = \tilde{\mathbf{K}}_{(i)} + \frac{\gamma}{\beta \Delta t} \tilde{\mathbf{C}} + \frac{1}{\beta \Delta t^2} \tilde{\mathbf{M}}. \quad (3.82)$$

This Jacobian matrix  $\tilde{\mathbf{S}}$  requires, in addition to the already known matrices  $\tilde{\mathbf{M}}$  and  $\tilde{\mathbf{C}}$ , the generalised

---

<sup>7</sup>At this point no stipulation regarding the time-step  $\Delta t$  of the reduced order Newmark scheme is made. For ease of comparing the reconstructed reduced solution with the full order solution it is advisable to have the same time-step for the two solutions. This practice of an equal time-step is kept throughout this work but it is by no means necessary.

tangent stiffness matrix

$$\tilde{\mathbf{K}}_{(i)} = \left. \frac{\partial \tilde{\mathbf{g}}(\mathbf{q})}{\partial \mathbf{q}} \right|_{\mathbf{q}_{(i)}^{(t+\Delta t)}}. \quad (3.83)$$

Here it is supposed that the expressions for  $\tilde{\mathbf{K}}$  and also for  $\tilde{\mathbf{g}}(\mathbf{q})$ , as the two nonlinear terms, are available, in order to stress the similarity with the full order nonlinear Newmark scheme. This is supposed in equation (3.10). However, making these two expressions available requires considerable effort and ultimately leads to the notion of autonomy of the reduced system. This is discussed in detail in section 3.2.3.

The equations above are the reduced order equivalents of equations (3.56) to (3.60). Here, the reduced system is required to comply with the same condition, i.e. that the reduced external force at  $t + \Delta t$  has to be known. Also the parameters  $\gamma$  and  $\beta$  are the exact same ones as they are introduced for the full order Newmark scheme.

With the generalised increment  $\Delta \mathbf{q}_{(i)}^{(t+\Delta t)}$  determined by equation (3.80), the next, iterative values of the generalised state at  $t + \Delta t$  are calculated with

$$\mathbf{q}_{(i+1)}^{(t+\Delta t)} = \mathbf{q}_{(i)}^{(t+\Delta t)} + \Delta \mathbf{q}_{(i)}^{(t+\Delta t)} \quad (3.84)$$

$$\dot{\mathbf{q}}_{(i+1)}^{(t+\Delta t)} = \dot{\mathbf{q}}_{(i)}^{(t+\Delta t)} + \frac{\gamma}{\beta \Delta t} \Delta \mathbf{q}_{(i)}^{(t+\Delta t)} \quad (3.85)$$

$$\ddot{\mathbf{q}}_{(i+1)}^{(t+\Delta t)} = \ddot{\mathbf{q}}_{(i)}^{(t+\Delta t)} + \frac{1}{\beta \Delta t^2} \Delta \mathbf{q}_{(i)}^{(t+\Delta t)}. \quad (3.86)$$

This concludes one cycle of the inner, iterative loop. The iterations over  $(i)$  are repeated as necessary to obtain satisfactory results for the generalised coordinates at  $(t + \Delta t)$  and the Newton-Raphson iterations are then launched again after advancing in time. For decision of the quality of the convergence, equation (3.64), formulated in reduced quantities, is used.

The bottom line of the demonstration of the reduction of the nonlinear Newmark scheme above is that there is absolutely no difference between the reduced and the full order variant of this algorithm for obtaining transient solutions. This is not surprising because the equations (3.11) and (2.82) to be solved by this type of algorithm have the exact same structure. Furthermore, this is highly advantageous because the two variants share the common parameters  $\gamma$  and  $\beta$  and also the time-step  $\Delta t$  can be shared, allowing for ideal conditions for comparing the obtained full order and reduced solutions.

Once the time histories of the  $\mathbf{q}$ ,  $\dot{\mathbf{q}}$  and  $\ddot{\mathbf{q}}$  are obtained, the full order, physical solution can be obtained simply by applying equation (3.1).

### 3.2.2.2 Introducing the reduced basis into the HHT- $\alpha$ -method

The introduction of the reduced basis into the HHT- $\alpha$ -method, which is presented in section 3.2.1.2, requires no additional conceptual effort, beyond the assumptions that are already made for introduction of the reduction into the classic nonlinear Newmark scheme. The most notable assumption is the availability of a reduced vector  $\tilde{\mathbf{g}}(\mathbf{q})$  of the nonlinear internal forces as it is stipulated in equation (3.10).

The full order HHT- $\alpha$ -method is introduced into the full order nonlinear Newmark scheme by means of equations (3.66) to (3.69). These equations can be formulated on reduced order level

### 3.2. OBTAINING TRANSIENT SOLUTIONS OF FULL ORDER AND REDUCED ORDER SYSTEMS

---

$$\tilde{\mathbf{r}}_{(i)}^{(t+\Delta t)} = \tilde{\mathbf{f}}_E(t + \Delta t) - \tilde{\mathbf{M}}\tilde{\mathbf{q}}_{(i)}^{(t+\Delta t)} - \tilde{\mathbf{C}}\dot{\tilde{\mathbf{q}}}_{(i)}^{(t+\alpha\Delta t)} - \tilde{\mathbf{g}}\left(\mathbf{q}_{(i)}^{(t+\alpha\Delta t)}\right), \quad (3.87)$$

$$\tilde{\tilde{\mathbf{K}}}_{(i)} = \left. \frac{\partial \tilde{\mathbf{g}}(\mathbf{q})}{\partial \mathbf{q}} \right|_{\mathbf{q}_{(i)}^{(t+\alpha\Delta t)}}, \quad (3.88)$$

$$\mathbf{q}_{(i)}^{(t+\alpha\Delta t)} = (1 - \alpha)\mathbf{q}^{(t)} + \alpha\mathbf{q}_{(i-1)}^{(t+\Delta t)}, \quad (3.89)$$

$$\dot{\mathbf{q}}_{(i)}^{(t+\alpha\Delta t)} = (1 - \alpha)\dot{\mathbf{q}}^{(t)} + \alpha\dot{\mathbf{q}}_{(i-1)}^{(t+\Delta t)}. \quad (3.90)$$

These reduced equations are introduced into the reduced order non-linear Newmark scheme in section 3.2.2.1 above in exactly the same way as done with their full order equivalents. All other equations of the reduced non-linear Newmark scheme remain valid and are used unaltered.

#### 3.2.2.3 Determining the parameters $\gamma$ , $\beta$ and $\alpha$

The concerns for the stability of solutions have always given rise to an abundant variety of considerations of theoretical, practical and numerical nature. Naturally it should be required for a reduced system to reflect the same properties of stability, defined in whichever sense (Amabili [6]), of the full order system. Recently Amsallem et al. [15] opened a new line of inquiry by proposing a method for stabilising linear reduced order models which are obtained by a projection of the full order equations on a reduced basis. The method operates only on the reduced matrices, but alters them.

In the following, the stability of the solution is of no concern because it lies outside of the scope of this research. A major effort to avoid instabilities is undertaken by choosing the parameters of the numerical algorithm as restrictively as possible to avoid unnecessary instabilities. This includes various parameters of the algorithms, see e.g. section 3.2.2.3 below, the thresholds for convergence, and such obvious parameters as e.g. the time-step  $\Delta t$ , to minimise the chances of the occurrence of numerical instabilities. Also the used test-cases are chosen to be well-behaved, without any explicit or non-physical tendency to diverge.

**3.2.2.3.1 Newmark scheme** The nature of the integration, which is performed during a Newmark solution, is determined by the two parameters  $\beta$  and  $\gamma$ , which appear several times throughout the process. Possible choices for these parameters are given in table 3.1 along with the stability conditions resulting from them. Their influence on the algorithmic dissipation is explored in the annex section A.2.2.

method	$\gamma$	$\beta$	stability
linear acceleration	$\frac{1}{2}$	$\frac{1}{6}$	$\Delta t \leq 0.551 \max(T_i)$
constant average acceleration	$\frac{1}{2}$	$\frac{1}{4}$	unconditional
Bathe [22]	$\geq \frac{1}{2}$	$\geq \frac{1}{4}(\frac{1}{2} + \gamma)^2$	-
verification of energy fluctuation	$\frac{3}{5}$	$\frac{2}{5}$	$\Delta t \leq \frac{2\pi}{\omega_{max}}$

Table 3.1: The integration parameters for the nonlinear Newmark scheme

The common choice for the parameters is

- $\gamma = \frac{1}{2}$  and
- $\beta = \frac{1}{4}$ ,

in order to achieve a conditional stability, which is not given by using e.g. a linear acceleration formulation (Tacioglu [219]). This does not exclude all sources of divergence but at least eliminates the ones

### 3.2. OBTAINING TRANSIENT SOLUTIONS OF FULL ORDER AND REDUCED ORDER SYSTEMS

---

linked directly to the time integration scheme.

In Har and Tamma [93] the value  $\gamma = \frac{1}{2}$  is directly linked to the fact that this choice does not introduce a numerical damping. For  $\gamma < \frac{1}{2}$  the algorithm introduces a negative algorithmic damping and destabilises the solution. If  $\gamma > \frac{1}{2}$  is chosen, the algorithmic damping becomes positive and a transient response would be annihilated. Additional conditions can be put on the time-step in order to achieve stability of the algorithm. These conditions are closely linked to the highest frequencies present in the system. In the course of this work, the time-step  $\Delta t$  is simply set to an appropriate value in order to avoid numerical divergence without dwelling on the theoretical background of the employed algorithms.

**3.2.2.3.2 HHT- $\alpha$ -method** For the HHT- $\alpha$ -method, the two parameters  $\gamma$  and  $\beta$  of the surrounding Newmark scheme can be expressed depending on  $\alpha$  for unconditional stability, if the parameter  $\alpha$  is determined first. In Hilber et al. [97] the respective values of

$$\beta = \frac{(2 - \alpha)^2}{4} \quad (3.91)$$

and

$$\gamma = \frac{3}{2} - \alpha, \quad (3.92)$$

are suggested. This is the corresponding adaptation for the use of  $\alpha$  in the current framework with respect to the formulation in the original publication Hilber et al. [97], where the parameter  $1 - \alpha$  is used.

### 3.2.3 Identifying of the requirement for an autonomous formulation of the nonlinear terms

In equation (3.10) it is postulated that a simple transformation of the type

$$\mathbf{g}(\mathbf{u}) \xrightarrow{\Phi} \tilde{\mathbf{g}}(\mathbf{q}) \quad (3.93)$$

is possible. The reduced vector of the nonlinear internal forces  $\tilde{\mathbf{g}}(\mathbf{q})$  as a function of the generalised coordinates has been used ever since, especially in the reduced nonlinear Newmark scheme in section 3.2.2.1. The reduced nonlinear Newmark scheme hinges on the fact that the matrix equations (2.82) and (3.11) have the exact same structure. This equality is enabled mainly due to the introduction of  $\tilde{\mathbf{g}}(\mathbf{q})$ .

Such an expression of the nonlinear internal forces, which solely depends on the generalised coordinates  $\mathbf{q}$  and is completely independent from the full order formulation  $\mathbf{g}(\mathbf{u})$ , is designated an autonomous formulation.

For the reduced vector of nonlinear forces this course of action is not directly feasible and hence an inflation type formulation  $\tilde{\mathbf{g}}(\mathbf{q}) = \Psi^T \mathbf{g}(\Phi \mathbf{q})$  is retained for now. This leaves the actual reduction somewhat incomplete. Possible formulations for autonomous reduced nonlinear forces vectors are being investigated in section 5.2.

The inflation is the least promising approach for the introduction of the reduction of the nonlinear forces vector  $\mathbf{g}(\mathbf{u})$ . It is included here as reference for the more sophisticated approaches that are to be developed in response to the identified requirement for an autonomous formulation in section 5.2 of chapter 5. Also, the inflation formulation is consequently used when it comes to measuring the effectiveness of projection-based reduction with the intention to rule out any possible bias introduced by the use of one of the approaches for an autonomous formulation from section 5.2.

The inflation type reduction takes its name from the fact that within  $\mathbf{g}$  the generalised coordinates  $\mathbf{q}$  are always inflated to full order displacements  $\mathbf{u}$ , which ultimately results in a semi-reduced equation. Beginning with equation (2.82)

$$M\ddot{\mathbf{u}} + C\dot{\mathbf{u}} + \mathbf{g}(\mathbf{u}) = \mathbf{f}_E \quad (3.94)$$

an inflation type reduction would transform it into a semi-reduced equation

$$\tilde{M}\ddot{\mathbf{q}} + \tilde{C}\dot{\mathbf{q}} + \Phi^T \mathbf{g}(\Phi \mathbf{q}) = \tilde{\mathbf{f}}_E \quad (3.95)$$

where the reduced terms for the inertia and the external forces are defined as in equations (3.7) and (3.93), respectively. The inflation formulations for the reduced vector of the nonlinear internal forces and the reduced tangent stiffness matrix read

$$\tilde{\mathbf{g}}(\mathbf{q}) = \Phi^T \mathbf{g}(\Phi \mathbf{q}) \quad (3.96)$$

and

$$\tilde{\mathbf{K}}_{(i)} = \Phi^T \left. \frac{\partial \mathbf{g}(\Phi \mathbf{q})}{\partial \Phi \mathbf{q}} \right|_{\mathbf{q}_{(i)}^{(t+\Delta t)}} \Phi, \quad (3.97)$$

respectively.

The shortcoming of this inflation formulation for the reduced tangential stiffness matrix, required for the reduced system's Jacobian in equation (3.83), is blatant. Albeit it permits to use the original formulation of the nonlinear forces vector  $\mathbf{g}$ , it requires its in- and deflation<sup>8</sup> for every step of a solution algorithm. Furthermore, this renders the reduced system dependent on the full order formulation of the vector of nonlinear internal forces  $\mathbf{g}$ , while it is definitely the aspiration of every reduction approach to rely on an entirely autonomous and self-contained reduced system. It is obvious that such an approach is not feasible for a successful application.

The next chapter 4 deals with a survey of the reduced bases, which are presented in the section 3.3 directly below. To avoid a bias of the performance of the reduced basis by an autonomous formulation of the nonlinear internal forces and to isolate the error due to the introduction of the reduced basis the inflation formulation is used for this limited purpose. Thereafter, in section 5.2, major efforts are directed at obtaining a truly autonomous formulation of the reduced system.

## 3.3 Creating some common reduced bases

For establishing the reduced basis  $\Phi$ , that is used in equation (3.1) for the reduction, there is a considerable number of procedures and algorithms documented in literature. All of these approaches yield the projection matrix that spans the trial space.

In the following sections different approaches for creating the reduced basis  $\Phi$  are summarised. These are

- Linear Normal Modes (e.g. Bathe [22]),
- Ritz-vectors (Wilson et al. [241]),

---

<sup>8</sup>Here, the expression of deflation is used for consistency. Naturally the deflation is another denomination for reduction.

### 3.3. CREATING SOME COMMON REDUCED BASES

---

- Proper Orthogonal Decomposition (Han and Feeny [91]),
- A Priori Reduction (Ryckelynck et al. [196]),
- Centroidal Voronoi Tessellation (Du et al. [71]),
- Local Equivalent Linear Stiffness Method (AL-Shudeifat and Butcher [2]).

This list represents only the major families of approaches for the creation of a reduced basis  $\Phi$ , yet it has to be understood that it cannot be exhaustive, especially not with the various sub-methods present for every major method. All the projection based techniques presented above, their historical development, their state-of-the-art and major sub-branches are presented along general lines in the following.

Additionally, Rhee [188] gives a very high level overview over reduction techniques, based on a projection, and nonlinear normal modes. For further information one may refer to practically every item listed in the bibliography because basically each and every publication related to model reduction techniques commences with a general overview.

The constitution of the reduced bases is discussed in the closing section of this chapter. The constitution regroups the normalisation, the sign and the alignment of the reduced bases. Harmonising these properties between the different bases ensures the highest possible comparability.

#### 3.3.1 Linear Normal Modes

The Modal Decomposition, also Modal Superposition, technique is a method for decoupling coupled linear differential equations (Bathe [22]). For discrete systems the modes are the eigenvectors of the system's matrix equation. If only a limited number of these eigenvectors are used for a projection, this method allows for a very efficient reduction and is commonly denominated Linear Normal Modes (LNM) (e.g. Feeny and Liang [79]). The first application of LNM to non-linear systems is most probably from Nickell [161].

For linear or linearised dynamic systems such as

$$M\ddot{\mathbf{u}} + C\dot{\mathbf{u}} + K\mathbf{u} = \mathbf{f}_E(t) \quad (3.98)$$

the Linear Normal Modes (LNM) can decouple the equations of motion by diagonalising its symmetric matrices  $M$  and  $K$ . Here the stiffness matrix can be either a stiffness matrix of the linear system or any tangent stiffness matrix  $\bar{K} = \frac{\partial g(\mathbf{u})}{\partial \mathbf{u}}$  of a nonlinear system. The damping matrix  $C$  can also be diagonalised if it is formulated as a fraction of the tangent stiffness matrix. This the case for all systems used in this work, as prescribed by equation (2.81).

For now the aim of the LNM approach is to decouple the system's equations and to this effect the system is projected on a basis of its own, suitably normalised eigenvectors  $\phi$ . By considering a conservative variation of the system in a first approach reduces the basic equation (3.98) to

$$M\ddot{\mathbf{u}} + K\mathbf{u} = \mathbf{f}_E(t). \quad (3.99)$$

This equation can be transformed into the so-called modal space, which corresponds to the space of the generalised coordinates  $q$ , where the different modes are decoupled and the associated differential equation can be easily solved each at a time. The decoupled modes are then recombined to allow for a representation of the solved system in physical displacements.

Supposing a solution for the displacements of the type  $\mathbf{u} = \hat{\mathbf{u}} e^{i\omega t}$ , which also relies on the homogeneous

### 3.3. CREATING SOME COMMON REDUCED BASES

---

system, i.e.  $\mathbf{f}_E = 0$ , leads to the eigenproblem

$$\mathbf{K}\phi_i = -\omega_i^2 \mathbf{M}\phi_i. \quad (3.100)$$

Its eigenfrequencies are calculated using the characteristic polynomial

$$\det(\omega^2 \mathbf{M} + \mathbf{K}) = 0. \quad (3.101)$$

As the discrete system has  $n$  degrees of freedom, there is a corresponding number of eigenfrequencies  $\omega_1^2, \omega_2^2, \dots, \omega_n^2$ . The related eigenvectors  $\phi_i$  are to be found by solving

$$(\omega_i^2 \mathbf{M} + \mathbf{K}) \phi_i = 0, \quad (3.102)$$

for non-trivial solutions  $\phi_i \neq \mathbf{0}$ . The matrix

$$\Phi = [\phi_1, \dots, \phi_n], \quad (3.103)$$

assembled from the eigenvectors  $\phi_i$ , is then used as a basis of projection for the mass matrix  $\mathbf{M}$  as per equations (3.7) and for the stiffness matrix  $\mathbf{K}$  in a similar way. Using an adequate normalisation of the eigenvectors, this yields e.g.

$$\tilde{\mathbf{M}} = \Phi^T \mathbf{M} \Phi = \mathbf{I} \quad (3.104)$$

$$\tilde{\mathbf{K}} = \Phi^T \mathbf{K} \Phi = \text{diag}(\omega_i^2). \quad (3.105)$$

$n \times n$

Setting  $\tilde{\mathbf{M}} = \mathbf{I}$  forces the ortho-normalisation of the columns of  $\Phi$  with respect to the mass matrix. This normalisation has the advantages of giving the physical meaning of the squares of the eigenfrequencies to the elements of  $\tilde{\mathbf{K}}$  and it prepares the academic test-cases that are applied later. However, any other normalisation of the LNM is theoretically possible.

Now the modes are decoupled and each one is governed by its own, independent differential equation in its distinct generalised coordinate  $q_i$

$$\ddot{q}_i + \omega_i^2 q_i = 0 \quad (3.106)$$

due to the diagonalisation of the mass and the stiffness matrix. The mass ortho-normalisation of the columns of  $\Phi$  allows obtaining the differential equations for each generalised coordinate directly as it is shown in equation (3.106). These decoupled modal differential equations are solved e.g. by supposing a harmonic solution.

The re-transformation into the state space of these harmonic solutions for a homogeneous system is then done by combining the modes:

$$\mathbf{u}(t) = \sum_{i=1}^r \phi_i \left( q_{ic} \cos\left(\sqrt{\omega_i^2} t\right) + q_{is} \sin\left(\sqrt{\omega_i^2} t\right) \right) \quad (3.107)$$

### 3.3. CREATING SOME COMMON REDUCED BASES

---

where the amplitude factors  $q_{ic}$  and  $q_{is}$  are derived from the initial conditions of displacement  $\mathbf{u}_0 = \mathbf{u}(t = t_0)$  and velocity  $\dot{\mathbf{u}}_0 = \dot{\mathbf{u}}(t = t_0)$ :

$$q_{ic} = \phi_i^T \mathbf{M} \mathbf{u}_0 \cos\left(\sqrt{\omega_i^2} t_0\right) - \frac{1}{\sqrt{\omega_i^2}} \phi_i^T \mathbf{M} \dot{\mathbf{u}}_0 \sin\left(\sqrt{\omega_i^2} t_0\right) \quad (3.108)$$

$$q_{is} = \phi_i^T \mathbf{M} \mathbf{u}_0 \sin\left(\sqrt{\omega_i^2} t_0\right) + \frac{1}{\sqrt{\omega_i^2}} \phi_i^T \mathbf{M} \dot{\mathbf{u}}_0 \cos\left(\sqrt{\omega_i^2} t_0\right), \quad (3.109)$$

as the free vibration response of the unforced system. If the system is non-homogeneous and the excitation can be approximated by a harmonic function of the form

$$\mathbf{f}_E(t) = \mathbf{f}_E e^{i\Omega t} \quad (3.110)$$

the re-transformation from the modal into the state-space, which is the particular solution to the non-homogeneous system, becomes

$$\mathbf{u}(t) = \left( \sum_{i=1}^r \phi_i \phi_i^T \frac{1}{\omega_i^2 - \Omega^2} \right) \mathbf{f}_E e^{i\Omega t}. \quad (3.111)$$

In addition to solutions for unforced and forced systems, there also exist approaches for the inclusion of damping effects that use a linear combination of the mass matrix  $\mathbf{M}$  and the stiffness matrix  $\mathbf{K}$  to render the damping matrix  $\mathbf{C} = \epsilon \bar{\mathbf{K}}$  from equation (2.81) diagonalisable. Still other approaches introduce a diagonal damping matrix directly into the decoupled equations in equation (3.106), where a damping term acts on every single modal degree of freedom independently but is deprived of actual physical meaning.

Beyond simply decoupling the linear or linearised equations of motion the LNM approach can also present a very effective reduction technique, if only a lesser number  $r$  than  $n$  of significant eigenvectors is introduced into the basis  $\Phi$  in equation (3.103):

$$\Phi = [\phi_1, \dots, \phi_r]. \quad (3.112)$$

It is obvious that in this case the full eigenproblem of equation (3.100), which yields the complete set of eigenvectors of equation (3.102), is replaced by adapted techniques to extract only a limited number of eigenvectors. For the most meaningful information to be contained in the reduced system the reduced basis consists of the first  $r$  eigenvectors, corresponding to the eigenfrequencies arranged in increasing order  $0 < \omega_1^2 < \dots < \omega_r^2 < \dots < \omega_n^2$ .

Thus, in the context of a linear analysis, the modal decomposition is limited in the treatment of damping but, as an evening-up, it allows direct access to the governing modes of an oscillation and can offer a starting point for model reduction by using a truncated basis.

Furthermore it offers direct access to the natural frequencies of the systems, whose squares  $\omega_i^2$  are just the eigenvalues of equation (3.100). These natural frequencies point to external forcing that may lead to resonance and as such the linear modal decomposition lends itself naturally to systems with harmonic or close to harmonic excitation. Also the frequencies can be used as starting point for the construction of nonlinear normal modes, as they are described in section 3.1.2.4.

#### 3.3.1.1 Classic formulation of the LNM for nonlinear systems

The Linear Normal Modes define the tangent stiffness matrix  $\mathbf{K} = \left. \frac{\partial \mathbf{g}(\mathbf{u})}{\partial \mathbf{u}} \right|_{\mathbf{u}_0}$  as the partial derivative of the nonlinear forces vector with respect to the displacements  $\mathbf{u}$  at the equilibrium configuration  $\mathbf{u}_0$ , which yields the properties of the underlying linear system. The projection basis  $\Phi$  is defined as the first  $r$  eigenvectors of the eigenproblem

$$\mathbf{K} \phi_i = \omega_i^2 \mathbf{M} \phi_i, \quad (3.113)$$

as

$$\Phi = [\phi_1, \dots, \phi_r], \quad (3.114)$$

if the corresponding eigenfrequencies  $\omega_i^2$  are sorted in increasing order  $0 < \omega_1^2 < \dots < \omega_r^2 < \dots < \omega_n^2$  and if the damping for equation (3.113) is neglected.

#### 3.3.1.2 Formulating the LNM at a given displacement

Linear Normal Modes at a given displacement use the stiffness matrix built at a given displacement  $\hat{\mathbf{u}}$  as

$$\mathbf{K} = \left. \frac{\partial \mathbf{g}(\mathbf{u})}{\partial \mathbf{u}} \right|_{\hat{\mathbf{u}}} \quad (3.115)$$

for the eigenproblem (3.113).

Common choices for the given displacement are the maximum displacements of the reference solution  $\hat{\mathbf{u}} = \mathbf{u}_{\max}$ . This is supposed to take into account the nonlinear nature of the system. Other possibilities are to obtain the given displacement from a static solution  $\hat{\mathbf{u}} = \mathbf{K}^{-1} \hat{\mathbf{f}}_E$  or from the initial displacements  $\hat{\mathbf{u}} = \mathbf{u}_0 \neq \mathbf{0}$ . The latter case, when the initial conditions are not all zeros, may occur if the system is prestressed.

If the modes are constantly or periodically updated during the solution, i.e. the system is reduced with a projection basis evolving during the solution as a function of the generalised coordinates, the LNM are denominated tangent modes in literature (e.g. Idelsohn and Cardona [102]). In this case the given displacement is chosen to be the current displacement of the solution  $\hat{\mathbf{u}} = \mathbf{u}^{(t)}$  and the LNM are established continuously.

#### 3.3.1.3 Formulating the LNM with Second Order Terms

Slaats et al. [210] summarise several approaches to expand the use of LNM to nonlinear systems. These include the use of LNMs as tangent modes on the tangent stiffness matrix of a nonlinear Newmark scheme and the addition of modal derivations to form new basis vectors. These derivations  $\check{\phi}_i$  of the eigenvectors with respect to the modal coordinates are defined as<sup>9</sup>

$$\check{\phi}_{i,k} = \left( \frac{\partial \phi_k}{\partial q_i} + \frac{\partial \phi_i}{\partial q_k} \right). \quad (3.116)$$

---

<sup>9</sup>the index  $_{,k}$  does not imply a partial derivation with respect to  $k$ . Neither do the repeated indices  $i$  and  $k$  in equation (3.116) imply a summation as stipulated by the Einstein notation.

### 3.3. CREATING SOME COMMON REDUCED BASES

These SOT are the sum of partial derivatives of the LNM  $\Phi_i$  and  $\Phi_k$  with respect to generalised coordinates  $q_k$  and  $q_i$ , respectively. They are added to the already existing base  $\Phi$  from equation (3.114) to form the expanded base  $\check{\Phi}$ , which is now of  $n \times 2r$ -dimension:

$$\check{\Phi} = [\phi_1, \dots, \phi_r, \check{\phi}_{i_1, k_1}, \dots, \check{\phi}_{i_r, k_r}]. \quad (3.117)$$

Following Slaats et al. [210] the LNM basis can be enriched with SOT. A certain number  $r_{\text{SOT}}$  of Second Order Terms  $\check{\phi}_{i,k}$  is added as columns to the basis, which already contains  $r_{\text{LNM}}$  classic LNM. This yields a reduced model of the overall order  $r = r_{\text{LNM}} + r_{\text{SOT}}$  under the assumption of  $i = k$ . The proper selection of  $r_{\text{SOT}}$  and of the values for  $i$  and  $k$  would certainly justify a dedicated study in its own right. Within the limits of the present study equal numbers for the contributing Second Order Terms are chosen. The number of Second Order Terms  $r_{\text{SOT}}$  is limited to be not more than half the overall size  $r$  of the reduced system, i.e.  $r_{\text{SOT}} \leq \frac{r}{2}$ . This choice seems justified because Slaats et al. [210] compare several combinations of LNM and Second Order Terms and find only barely noticeable differences for different combinations of  $i$  and  $k$ . They also investigate the inclusion of static modes, i.e. characteristic displacements, an approach which is pursued in this study for the Enhanced Proper Orthogonal Decomposition below.

The numerical approach for obtaining the Second Order Terms modifies the generalised coordinate  $q_k$  by a  $\Delta q_k$ , introduces this into the displacements  $\mathbf{u}_k = \Phi \mathbf{q}_0 + \phi_k \Delta q_k$  and uses this new displacement for a new tangent stiffness matrix  $\mathbf{K}_k = \frac{\partial \mathbf{g}(\mathbf{u})}{\partial \mathbf{u}} \Big|_{\mathbf{u}_k}$ , in order to obtain a new set of eigenvectors  $\phi_k$  from the eigenproblem in equation (3.100). The  $i$ -th column of  $\Phi_k$  is then used with the  $i$ -th column of the original LNM basis  $\Phi$  in a finite difference divided by  $\Delta q_k$  to obtain the second order term  $\check{\phi}_{i,k}$  numerically.

Slaats et al. [210] also present several methods how to compute the derivations in equation (3.116) with and without mass-consideration. Among them they give the direct numerical approach:

$$\frac{\partial \phi_i}{\partial q_k} \approx \frac{\phi_i(\mathbf{u}_0 + \phi_k \Delta q_k) - \phi_i(\mathbf{u}_0)}{\Delta q_k}, \quad (3.118)$$

which is based on the finite difference  $\Delta q_k$  of the modal coordinate under consideration. The results of equation (3.118) for different  $i$  and  $k$  are eventually assembled in SOT in equation (3.116).

An alternative approach for constructing the Second Order Terms  $\check{\phi}_{i,k}$  relies on deriving equation (3.100) with respect to the generalised coordinate  $q_k$  and is presented for the Second Order Terms of Ritz-vectors below.

#### 3.3.2 Ritz-vectors

An alternative to the eigenvectors of the Linear Normal Modes as a basis for a projection are the Ritz-vectors. They were proposed by Wilson et al. [241] as an extension of the Lanczos [130] algorithm for the estimate of eigenvectors. The use of the Lanczos algorithm classes this approach among the Krylov subspace methods. Kapania and Byun [113] performed a comparative analysis of Ritz-vectors and Linear Normal Modes with respect to their suitability for correctly and effectively reducing systems in a transient analysis. In their results they stress that Ritz-vectors are much more suited to reflect a given spatial load distribution than Linear Normal Modes. This property of the Ritz-vectors also renders them well suited for damage detection, when load paths change as the most stressed ones of the structural elements fail one after another. This suitability is due to the fact that the algorithm for computing the Ritz-vectors is initialised with the static response of the system under the external loads. Furthermore it is pointed out by the cited authors that the computational cost for establishing the Ritz-vectors is much smaller because of their iterative approach, than the establishment of Linear Normal Modes, which require the treatment of complete matrices.

The work of Kapania and Byun [113] was pushed further by Rhee [188], who, in his dissertation and the related article Burton and Rhee [47], compares a Ritz-vector dependent linear based reduction of nonlinear systems to Nonlinear Normal Modes (see section 3.1.2.4) and obtains reasonable results.

This approach was later extended to an enhanced order reduction method for forced nonlinear systems by AL-Shudeifat et al. [3], who used Ritz-vectors to enhance a POD-based<sup>10</sup> reduced basis.

#### 3.3.2.1 Classic formulation of the Ritz-vectors

Following the approach taken by Kapania and Byun [113], the algorithm for the establishment of Ritz-vectors begins with the initialisation of the first Ritz-vector as the system's static response to the external load:

$$\check{\phi}_1 = \bar{\mathbf{K}}^{-1} \mathbf{f}_E, \quad (3.119)$$

where the matrix  $\bar{\mathbf{K}}$  is a tangent stiffness matrix to the system, that is solved with a nonlinear Newmark scheme, as it is introduced in equation (3.57). This predictive vector  $\check{\phi}_1$  is now normalised with respect to the mass matrix  $\mathbf{M}$  via

$$\phi_1 = \frac{\check{\phi}_1}{\left(\check{\phi}_1^T \mathbf{M} \check{\phi}_1\right)^{\frac{1}{2}}}, \quad (3.120)$$

to become the first Ritz-vector  $\phi_1$ . The following Ritz-vectors, for  $2 \leq k \leq r$  are calculated by using the two predictive vectors

$$\phi_{k+1}^* = \mathbf{K}^{-1} \mathbf{M} \phi_k \quad (3.121)$$

and (see Kapania and Byun [113, (9)])

$$\check{\phi}_{k+1} = \phi_{k+1}^* - \sum_{j=1}^{k-1} c_j \phi_j. \quad (3.122)$$

Where

$$c_j = \phi_j^T \mathbf{M} \phi_{k+1}^* \quad (3.123)$$

in the second vector amounts to a Gram-Schmidt ortho-normalisation (e.g. Strang [218]) with respect to the mass matrix. The second predictive vector gives the  $k + 1$ -th Ritz-vector by normalising it with respect to the mass-matrix in the same way as in equation (3.120):

$$\phi_{k+1} = \frac{\check{\phi}_{k+1}}{\left(\check{\phi}_{k+1}^T \mathbf{M} \check{\phi}_{k+1}\right)^{\frac{1}{2}}}. \quad (3.124)$$

---

<sup>10</sup>Refer to section 3.3.3.

### 3.3. CREATING SOME COMMON REDUCED BASES

---

This procedure is repeated, until a number  $r$ , which is smaller than the number of the system's degrees of freedom  $n$ , of Ritz-vectors is established. A careful choice of the number  $r$  should allow for a reduction of the system, which is at the same time sufficiently small to effectively reduce the computational effort and large enough to closely reflect the system's behaviour. To this end, the  $r$  Ritz-vectors are assembled in a matrix  $\Phi$ , as it was done with the LNM-vectors in equation (3.114). The resulting basis

$$\Phi = [\phi_1, \dots, \phi_r], \quad (3.125)$$

can now be used as a basis for a projection of the system.

#### 3.3.2.2 Formulating the Ritz-vectors with Second Order Terms

The basic practice for establishing Ritz-vectors, presented above, can be enhanced by including ortho-normal derivations of the initial vectors from equation (3.124) with respect to the displacements  $\mathbf{q}$  in the basis  $\Phi$ , in a way much similar to the SOT of LNM, discussed in section 3.3.1.3. The use of Second Order Terms of Ritz-vectors is proposed by Idelsohn and Cardona [102] and Chang and Engblom [57], who both, together with Kapania and Byun [113], use the advantages of the load-dependence of the Ritz-vectors for studying the transient response of a system following an impulsively applied load.

Another possible enhancement of Ritz-vectors is proposed by Sohn and Law [212], who calculate Ritz-vectors from experimental test data. Unlike Cao and Zimmerman [52], who proposed a Ritz-vector generation algorithm which reflects the actual load from the experiment only, their algorithm is also capable of generating Ritz-vectors for presumed, arbitrary loads. The general dependence of the algorithms on the time history of the displacements may spawn a development for Ritz-vectors similar to the proper orthogonal decomposition, as it will be discussed in the next section, once the transition from experimental to numerical results as the basis for the construction of Ritz-vectors is carried out.

The basic practice for establishing Ritz-vectors can be enhanced by including ortho-normal derivatives of the initial vectors from equation (3.124) with respect to the displacements  $\mathbf{u}$  in the basis  $\Phi$

Finding the derivatives of a Ritz-vector for the SOT  $\check{\phi}_{i,k}$  as per equation (3.116) could be achieved by applying the direct numerical way via a finite difference  $\Delta q_k$ , as it was done for the LNM in equation (3.118). However, an alternative approach yields better results during preliminary numerical tests. It relies on deriving equation (3.100) directly with respect to the generalised coordinate  $q_k$ , which is implicitly contained in the stiffness matrix  $\mathbf{K}$ , and neglecting the inertial terms

$$\frac{\partial \phi_i}{\partial q_k} = -\mathbf{K}^{-1} \frac{\Delta \mathbf{K}}{\Delta q_k} \phi_i. \quad (3.126)$$

This equation can be readily applied to the already established Ritz-vectors, albeit it was originally conceived for LNM and applied successfully to several simple systems by e.g. Idelsohn and Cardona [102] and Chang and Engblom [57].

#### 3.3.3 Orthogonal Decomposition

The orthogonal decomposition methods included in the following paragraphs comprise the classic Proper Orthogonal Decomposition (POD), an enhanced variation of it and the Smooth Orthogonal Decomposition (SOD). Orthogonal decomposition methods are the prototypical data-based methods, as opposed to model-based methods, because they rely solely on some kind of data that is disconnected from the actual model and its physic.

The Proper Orthogonal Decomposition is one of the great classics of reduction. Aubry [17] even at-

tributes even a “hidden beauty” to the method. While this method was initially used for experimental data, Sirovich [207] is credited with introducing the concept of snapshots and making the POD procedure computationally tractable. Despite its relative age this method still spawns considerable research activity, with, as two of the most recent examples, Amsallem [12] using it for the very sophisticated Least-Squares Petrov-Galerkin approach for the solution of nonlinear systems and Bellizzi and Sampaio [30] creating the Smooth Orthogonal Decomposition by including the field of the derivations.

#### 3.3.3.1 Classic Proper Orthogonal Decomposition

The Proper Orthogonal Decomposition (POD) relies on a full order result to establish a basis of projection with the aim to reduce the system. These full order results may come from the simulation of the high-fidelity system<sup>11</sup> and are organised in so-called snapshots, arranged in an appropriate mean-value and then searched for their main components, which will eventually form the basis of a projection.

An overview on POD, its origins and its use are given by e.g. Placzek [181], Verdon [235] and many others.. To locate the specific origins of POD is however difficult because its underlying principles have found use in a vast variety of applications, where they are grouped under the denomination of Karhunen-Loève decomposition.

Han and Feeny [91] show very explicitly, how this generic technique can be applied in a directed way to structural vibration analysis. Their analysis is still based on experimentally measured responses, as it was the original idea of the POD, which regrouped experimentally obtained data. But the POD method soon found its way into numerical simulation, again triggered by the advances in the field of fluid dynamics. Lenaerts et al. [132] give an overview over the POD method in its application to structural dynamics and compare it to an experimental set-up. So the POD is no longer executed on the basis of experimental snapshots but on snapshots generated by the high-fidelity formulation which they are designated to reduce. Sirovich [207] commonly is credited with introducing the concept of snapshots and making the POD procedure computationally tractable.

Valuable aid for the interpretation of POD-modes is given by Feeny and Kappagantu [78], Feeny and Liang [79] and Kerschen and Golinval [116]. Even though the authors limit their studies to linear-systems, they point out the very important fact that the modes, identified during the application of POD, converge on the Linear Normal Modes of the linear system, as the number of snapshots taken of the system increases.

The most decisive property of this reduction technique is, that it is based on the result of the simulation, rather than on its properties, as its origins lie in the analysis of statistical data. This can also be considered as their major short-fall, as shown by e.g. Amsallem [12], who uses the dependence on the Mach-number of a reduced CFD-model, in order to show the lack of robustness of the POD, respectively of reduced order models in general, with respect to the change of external parameters. This spawned several ameliorations of the POD method like the Smooth Orthogonal Decomposition by Bellizzi and Sampaio [30], described below and justifies the discussion of possible remedies to this lack of robustness in the dedicated section 5.3.

In addition to the overview over the POD-technique, reproduced in the next section, Amsallem [12] points also out that POD can equally well be executed in the frequency domain, which can be useful for some applications. Amabili et al. [5] concludes his study of the vibrations of a water-filled cylinder with a very insightful reflection as to the usefulness of the POD method, opposed to projections on different projection basis.

The reproduction of the course of action necessary for the conduction of a POD is taken from Amsallem [12], who used this approach for the reduction of a fluid-dynamical problem involving transonic flow.

The basic idea of this approach, here limited to the field of structural dynamics, is to take a series of snapshots  $\tilde{\mathbf{u}}(t_j)$  of the displacements of the system at  $m$  different times  $t_j$ , within the period under con-

---

<sup>11</sup>If the full order results are not available the A Priori Reduction, that is introduced in section 3.3.4.1, can be used to overcome this requirement.

### 3.3. CREATING SOME COMMON REDUCED BASES

---

sideration  $t_j \in \{t_1, \dots, t_2\}$  with  $t_1 \geq t_0$ ,  $t_2 \leq t_e$  and  $j \in \{1, \dots, m\}$ , develop a mean of this series of snapshots with an appropriate operation and search the result for its main components. A selection of these main components is then used as a reduced basis for projection.

The formulation of the dynamic equilibrium in the nonlinear equation (2.82) forms the basic equation for the POD. It is supposed that this equation

$$\mathbf{M}\dot{\mathbf{u}} + \mathbf{C}\dot{\mathbf{u}} + \mathbf{g}(\mathbf{u}) = \mathbf{f}_E(t) \quad (3.127)$$

has been solved at full order for a given time period. The time histories of the physical degrees of freedom, as the result of the full order transient solution, are supposed to be stored and readily available.

Let  $\check{\mathbf{u}}(t_j)$  be the snapshots of the system's solution at instants of time which lie in the interval under consideration  $t_j \in [t_1, \dots, t_2]$  and  $1 \leq j \leq m$ , where  $m$  is the number of snapshots taken<sup>12</sup>. From this the matrix  $\check{\mathbf{U}}$  can be constructed by

$$\check{\mathbf{U}} = \sum_{j=1}^m \delta_j \check{\mathbf{u}}(t_j) \check{\mathbf{u}}^T(t_j) \quad (3.128)$$

with the  $\delta_j$  as weights, reflecting the averaging over the period  $t_1 \leq t \leq t_2$ . If the mean values of the  $\check{\mathbf{u}}(t_j)$  are zero, which can be easily arranged for, as done by e.g. Rathinam and Petzold [186], this matrix is the covariance matrix, a parameter well known in statistics.

This snapshot-matrix  $\check{\mathbf{U}}$  is still an  $n \times n$ -matrix, with  $n$  as the number of degrees of freedom of the system. Prior to its eventual truncation it is now subjected to an eigenvalue procedure:

$$\check{\mathbf{U}}\phi_i = \lambda_i\phi_i \quad (3.129)$$

which yields the  $n$  eigenvectors and eigenvalues

$$\boldsymbol{\lambda} = [\lambda_1, \dots, \lambda_n] \quad (3.130)$$

$$\boldsymbol{\Phi} = [\phi_1, \dots, \phi_n] \quad (3.131)$$

where the matrix  $\boldsymbol{\Phi}$  contains the  $n$  eigenvectors  $\phi_i$  as columns.

The decisive difference between this basis for projection and e.g. the basis used in equation (3.114) for the linear modal decomposition, is that here  $\boldsymbol{\Phi}$  does solely depend on the results or the output of the system and not on its properties. Their commonality is however that they are both of dimension  $n \times n$  and have to be truncated in order to allow for a reduction of the system.

To this end, any number  $r \ll n$  can be chosen, to reduce the size of the system in the course of a reduction. Other and more elegant truncations are however provided by e.g. the balanced truncation, as expanded in Moore [150] or by yet another approach, which is presented by Amsallem [12], who uses the ratio of the total energy contained in the truncated subspace to the total energy in the full state-space  $E_r$  as criterion for choosing  $r$ . By grouping the spectrum  $\boldsymbol{\lambda}$  of  $\check{\mathbf{U}}$  in a descending manner

$$\lambda_1 > \lambda_2 > \dots > \lambda_n \quad (3.132)$$

---

<sup>12</sup>The annex section A.1.1 investigates briefly have many snapshots  $m$  from which period between  $t_1$  and  $t_2$  are advisable to take into account.

the energy ratio is defined as

$$E_r = \frac{\sum_{i=1}^r \lambda_i}{\sum_{j=1}^n \lambda_j} \quad (3.133)$$

as the ratio between the energy contained in the first  $r$  modes  $\sum_{i=1}^r \lambda_i$  and the total energy of the full order system. The residual energy  $\sum_{j=r+1}^n \lambda_j$ , as it is defined by Vigo [238], is not embodied in the reduced system.

By aiming for an energy ratio close to one, the dimension  $r$  of the truncated subspace can be defined and the basis from equation (3.131) becomes

$$\Phi = [\phi_1, \dots, \phi_r], \quad (3.134)$$

which can now be used as a basis for projection the overall system from equation (3.127).

This above course of action is the classic approach, which aims at a descriptive representation. For real applications the presented procedure and the calculation of the eigenvectors in equation (3.129) in particular are heavily modified, depending on the case whether there are

- $m \gg n$ , significantly more snapshots than degrees of freedom,
- $m \ll n$ , significantly less snapshots than degrees of freedom or
- $m \approx n$ , about the same number of snapshots as degrees of freedom

available. For each of the three cases, specially adapted algorithms exist and are applied with great efficiency, see e.g. Kirby et al. [120].

#### 3.3.3.2 Discussing a limitation of the applicability of the POD for nonlinear systems

Above, the Proper Orthogonal Decomposition is presented in an already discrete form, operating only on vectors and matrices. As shown by Liberge and Hamdouni [137], the fact of directly introducing the POD on matrix level obscures an important limitation of the applicability of the POD to nonlinear problems with finite deformations.

By returning to the continuous formulation, the space correlation in equation (3.128) is written as

$$\check{U}_{ij} = \int_{t_0}^{t_e} u(x_i, t) u(x_j, t) dt. \quad (3.135)$$

For geometrically nonlinear problems, with finite deformations, the question to be asked at this point, is whether the space points  $x_i$  and  $x_j$  are defined in the same configuration. This could determine, if they can be used in the same integral.

To highlight this problem equation (3.135) can be transformed to represent a time correlation instead of the space correlation. This is already done by Sirovich [207], using the ergodic hypothesis. Deane et al. [65] describes the ergodic hypothesis in a very intuitive manner by stating that it stipulates "that time averages represent ensemble [i.e. space] averages". Supposing that this ergodic hypothesis is met, allows writing

equation (3.135) as a time correlation. This yields

$$\check{U}_{ij} = \int_V u(x, t_i) u(x, t_j) dV, \quad (3.136)$$

and makes it obvious that this integral cannot be evaluated properly if the volumes  $V(t_i)$  and  $V(t_j)$  are different due to finite displacements. This problem is somewhat hidden in the discrete formulation of equation (3.128). This difficulty has to be kept in mind when applying the POD method to nonlinear systems.

To solve this difficulty e.g. Liberge and Hamdouni [137] uses the immersed boundary method, based on initial works by Peskin [177], in order to disconnect the movement of a body, immersed in a fluid, from the grid that is used to describe the quantities of the fluid's behaviour. Placzek [181] proposes the introduction of a relative grid, which follows the rigid body movements of the immersed body, but does not allow a deformation of the body.

For the current studies this difficulty can be circumvented by the introduction of the Total Lagrangian formulation in section 2.2. Especially the vector of the nodal displacements in equation (2.26) does not contain the displacements as absolute positions in space, but as incremental displacements between the reference configuration of the system and the current, deformed configuration. It is specific for the total Lagrangian-formulation that the reference configuration is the same for all instants  $t \in (t_0, t_e]$ . This particularity allows applying the POD method, as it is formulated in equation (3.128), without further adaptation to the geometrically nonlinear systems that are used in this work.

#### 3.3.3.3 Enhanced Proper Orthogonal Decomposition

While the original POD basis relies solely on the main components of the autocorrelation matrix of the displacements, additional vectors can be included in the reduction matrix  $\Phi$ . One of these approaches leads to the Enhanced Proper Orthogonal Decomposition and is used by e.g. Chinesta et al. [61]. The origins of the Enhanced Proper Orthogonal Decomposition probably lie in the so-called shift modes, or non-equilibrium modes, devised by Noack et al. [162] and Bergmann and Cordier [36], among others. These shift modes are added vectors that point from one configuration to another to the POD basis. This is promising if e.g. two excitations have different means.

Still aiming for a reduction of order  $r$  only the first  $r - 1$  eigenvectors are taken from the POD procedure and the basis  $\Phi$  is topped up with a significant displacements vector  $\tilde{u}$  such as the maximum displacements. Choosing  $\tilde{u} = \mathbf{u}_{\max}$  turns equation (3.134) into

$$\Phi = [\mathbf{u}_{\max}, \phi_1, \dots, \phi_{r-1}]. \quad (3.137)$$

The motivation behind this approach is to include additional information in an attempt to compensate for the information cut off with the modes beyond  $r - 1$ , i.e. the fraction  $1 - E_{r-1}$  from equation (3.133) of energy that is not represented in the system.

#### 3.3.3.4 Additional Proper Orthogonal Decompositions variants

In literature a variety of POD variants exist, which, being based on the classic POD approach described above, aim at augmenting the performance of a simple POD basis by adding additional fields to the procedure. The majority of these approaches have been pioneered and explored in the field of fluid dynamics.

These additional POD variants are classed as the so-called Taylor subspace method. Peterson [178] and Keane and Nair [114] give ample insight into this subject. By adding information on the velocities  $\dot{\mathbf{u}}$  and

### 3.3. CREATING SOME COMMON REDUCED BASES

---

sometimes even the accelerations  $\ddot{\mathbf{u}}$  to the process of obtaining a POD basis it is hoped that this additional information helps in better resolving the full order model and allows to weigh initial information along steep gradients, as pointed out by Amsallem [12] in his extensive literature survey in his thesis.

Another approach, proposed by Hay et al. [95], relies on the sensitivities of the projection basis with respect to the external parameters. A method of interleaved snapshots is proposed by Vigo [238] but limited to Orthogonal Decomposition methods. The specific origins of this approach can be found in the so-called Lagrange subspace method or the Global Proper Orthogonal Decomposition (GPOD) for fluid mechanics, e.g. Keane and Nair [114], Ito and Ravindran [105] and Taylor and Glauser [220], Schmit and Glauser [201], respectively. The GPOD approach is used by Kumar and Burton [125] on differently parameterised systems. They also add a form of Ritz-vectors to adapt the reduced basis and obtain good results at the expense of a more complex reduced basis. Some of these approaches, combining different fields from different simulations, are discussed further in section 5.3.4 with the aim of adapting POD bases to different operating points of a dynamic system.

#### 3.3.3.5 Smooth Orthogonal Decomposition

For the time being the different fields are limited as originating all from the same simulation, but more fields can be used in addition to the displacements. In the domain of structural dynamics Bellizzi and Sampaio [30] propose an approach to this extent, based on the work of Chelidze and Zhou [59] and Farooq and Feeny [76], who added the presence of an external excitation to the concept, which is commonly denominated as Smooth Orthogonal Decomposition (SOD) and which takes into account snapshots not only of the displacements  $\check{\mathbf{u}}(t_j)$  but also of the velocities  $\dot{\check{\mathbf{u}}}(t_j)$ . The idea for this stems most probably from the author's history in experimental model identification e.g. Capiez-Lernout and Soize [53].

Their motivation is to perform certain calculations on the obtained modes without knowledge of the actual mass-matrix involved, which is a requirement if these calculations are carried out with the modes obtained from the POD. Thus, until now, the SOD-modes have not been used to project and to reduce the system's equation (2.82). This makes the following approach a first.

For the SOD, in addition to the displacement based matrix  $\check{\mathbf{U}}$  from equation (3.128), a second covariance matrix  $\dot{\check{\mathbf{U}}}$  is constructed from velocity-snapshots

$$\dot{\check{\mathbf{U}}} = \sum_{j=1}^m \delta_j \dot{\check{\mathbf{u}}}(t_j) \dot{\check{\mathbf{u}}}^T(t_j). \quad (3.138)$$

The velocity-snapshots can come directly from a full order simulation, or they can be obtained as finite differences of the displacements divided by the time-step of the time-marching solution algorithm.

The two covariance matrices are then subjected to a combined eigenproblem, which is a variation of equation (3.129)

$$\check{\mathbf{U}} \hat{\phi}_i = \lambda_i \dot{\check{\mathbf{U}}} \hat{\phi}_i. \quad (3.139)$$

With the so obtained eigenvectors  $\hat{\phi}_i$  the construction of a reduction basis is pursued by

$$\check{\mathbf{\Phi}} = \left[ \hat{\phi}_1, \dots, \hat{\phi}_n \right]^{-T}, \quad (3.140)$$

### 3.3. CREATING SOME COMMON REDUCED BASES

---

and finally

$$\Phi = [\check{\phi}_1, \dots, \check{\phi}_r], \quad (3.141)$$

from the first  $r$  columns of the intermediate matrix in equation (3.140).

Proceeding like this, i.e. inverting and transposing the intermediate matrix (3.140), requires all eigenvectors of the original eigenproblem in equation (3.139) to be calculated. This is a must which is prohibitive for the successful application of SOD modes. However, this can be circumvented by normalising the eigenvectors  $\hat{\phi}$  with respect to a matrix  $N$ , forcing

$$[\hat{\phi}_1, \dots, \hat{\phi}_n]^T N [\hat{\phi}_1, \dots, \hat{\phi}_n] = \mathbf{I} \quad (3.142)$$

and, in consequence, obtaining directly

$$\Phi = N [\hat{\phi}_1, \dots, \hat{\phi}_n] \quad (3.143)$$

by premultiplying equation (3.142) with  $[\hat{\phi}_1, \dots, \hat{\phi}_n]^{-T}$ , which is just the reduction matrix  $\Phi$ . For obvious reasons it is sensible to choose the normalisation matrix  $N$  in equation (3.142) as either  $\check{U}$  or  $\check{U}^T$ , in order to maintain a relation with the problem at hand. Numerically, this procedure can be refined further, so that not all  $n$  column vectors have to be included.

Although this relatively recent development is, until now, limited to linear-systems, Chelidze and Zhou [59] estimate that the SOD approach offers veritable advantages such as the elimination of a necessary mass normalisation and elevated sampling times, which will certainly drive its future development. A first step in that direction was taken by Bellizzi and Sampaio [31], who compare different families of modes obtained by the application of the Karhunen-Loève method.

#### 3.3.3.6 Investigating the equivalence of Proper and Smooth Orthogonal Decomposition

Concerning the equivalence of POD and SOD reduced basis it is suspected that, depending on the conditions, the POD and the SOD vectors might become identical. Chelidze and Zhou [59] show that the SOD vectors obtained from equation (3.143) give the LNM for an conservative, linear and unforced case. This mirrors the findings by Feeny and Kappagantu [78], Feeny and Liang [79] for the POD. If both, the SOD and the POD, vectors give the LNM under certain assumptions, it might not be too farfetched to suggest that such equality might also appear under different assumptions, notably the nonlinearity of the system under consideration.

For the nonlinear case this strict theoretical foundation does not yet exist, but it can be observed that the column vectors of the obtained SOD reduced basis are very similar to the POD-vectors.

#### 3.3.4 A Priori Reduction

An enhancement of the course of action followed during a Proper Orthogonal Decomposition is the A Priori Reduction (APR), which uses an iterative way for constructing a reduced basis from the reduced system, to circumvent the need for a series of snapshots of solutions to the full order high-fidelity system. The A Priori Reduction tries to overcome the integral shortcoming of the Proper Orthogonal Decomposition by,

### 3.3. CREATING SOME COMMON REDUCED BASES

---

as indicated by its name, constructing a reduced basis prior to the execution of any simulation, rather than drawing on the results of a high-fidelity simulation.

There are two variants of the APR. The first variant is used to create a reduced basis  $\Phi$ . The second variant also delivers a reduced transient solution by exploiting the availability of solutions. Both variants are discussed below.

#### 3.3.4.1 A Priori Reduction for creating a reduced basis

Following its first application in thermo-mechanics, by Ryckelynck [197], the APR was soon adapted to more general problems and eventually applied to structural dynamics by Ryckelynck et al. [196]. They describe the APR as reduction of the problem's basis by "using the Krylov subspaces generated by the governing equation residuum for enriching the approximation basis, [while] at the same time [...] a proper orthogonal decomposition extracts relevant information in order to maintain the low order of the approximation basis." Further, decisive input for the application of APR for structural problems was made by Ryckelynck and Benziane [195], albeit the authors do not consider finite element based problems. However, this principle is still largely and effectively applied to fluid dynamics, as e.g. by Ammar et al. [8], more specifically the micro-simulations of molecular behaviour within the kinetic theory framework with the aim of simulating polymer flow. Even the example reproduced below, was prepared and intended for fluid dynamics by its author Verdon [235]. It is however such a generic solution technique that it can be equally well applied to structural dynamics, simply by changing the underlying equation.

The APR consecutively solves reduced systems of increasing order and uses the information and errors gained from the preceding step to augment and to enhance an evolving reduced basis until the desired order of reduction is reached.

To this end the basis  $\Phi_{(k)}$ , with its evolving size  $r_{(k)}$ , is initialised at  $r_{(1)} = 1$  with e.g. the maximum displacements of the reference solution

$$\Phi_{(1)} = \mathbf{u}_{max}. \quad (3.144)$$

This basis is used for a first solution of the reduced system, as a single degree of freedom system, yielding a time history of the single generalised coordinate  $q(t_j)$ , a scalar. As this initial basis is far from being optimal the residual

$$\mathbf{r}(t_j) = \mathbf{f}_E(t_j) - \mathbf{M}\Phi_{(1)}\ddot{q}(t_j) - \mathbf{C}\Phi_{(1)}\dot{q}(t_j) - \mathbf{g}(\Phi_{(1)}q(t_j)), \quad (3.145)$$

which is reconstructed from the reduced solution, rises quickly. Usually this residual rises quickly, because the single degree of freedom approximation of the full order system is completely insufficient. The first residual whose norm exceeds a deliberately chosen limit  $\|\mathbf{r}(t)\| = \epsilon$  is designated as  $\mathbf{r}^+$  and will be used for the expansion of the basis  $\Phi_{(k)}$  with  $k > 1$ .

The creation of the subsequent basis  $\Phi_{(k+1)}$  takes the two distinct steps of first ameliorating the preceding basis and second enhancing it with the residual  $\mathbf{r}^+$ . For the amelioration of the basis, which is basically a realignment, the generalised coordinates  $\mathbf{q}(t_j)$ , now written as vectors for  $r_k = k > 1$ , obtained during the preceding solution with  $t_0 \leq t_j \leq t^+$ , are subjected to a POD procedure (see section 3.3.3). The column vectors  $\check{\phi}$  of the ameliorated basis  $\check{\Phi}_{(k)}$  are obtained by projecting the existing basis  $\Phi_{(k)}$  on the eigenvectors  $\hat{\phi}$  from the POD procedure, which finally yields

$$\check{\Phi}_{(k)} = [\check{\phi}_1, \dots, \check{\phi}_{r_{(k)}}], \quad (3.146)$$

### 3.3. CREATING SOME COMMON REDUCED BASES

---

for the realigned reduced basis.

For the expansion of the basis the residual designated as  $\mathbf{r}^+$  is added to the realigned basis. This yields

$$\Phi_{(k+1)} = [\check{\phi}_1, \dots, \check{\phi}_{r(k)}, \mathbf{r}^+]. \quad (3.147)$$

At this point the enriched basis is subjected to a Gram-Schmidt procedure, in order to ensure its orthormality (Verdon et al. [236]).

For completeness it has to mentioned that, in a purely theoretical setting, the residual  $\mathbf{r}^+$  may be used to define an  $l$ -dimensional Krylov-subspace with  $l > 1$ . Its definition then replaces the equation (3.147) with

$$\mathcal{K}^{(l)} = [\mathbf{r}^+, \mathbf{S}\mathbf{r}^+, \mathbf{S}^2\mathbf{r}^+, \dots, \mathbf{S}^{l-1}\mathbf{r}^+] \quad (3.148)$$

$$\Phi_{(k+l)} = [\check{\phi}_1, \dots, \check{\phi}_{r(k)}, \mathcal{K}^{(l)}], \quad (3.149)$$

where  $\mathbf{S}$  is the Jacobian-matrix of equation (2.82) and the dimension  $l$  has to be adequately chosen. This leads to faster increase in the order  $r_k$  of the reduced systems that is now no longer increased by one per iterative step but by  $l$ . In the case of Ryckelynck et al. [196] this number of dimensions can reach three. Yet, beyond the scope of the theoretical definition of an A Priori Reduction and especially in the numerical context the dimension  $l$  of the Krylov-subspace  $\mathcal{K}$  is set to  $l = 1$  to avoid the complex and costly numerical computation of the Jacobian-matrix  $\mathbf{S}$  in equation (3.59). This consideration has been made by Verdon [235] and Placzek [181] alike. A decision that ultimately leads to an enrichment of the basis' dimension by one.

With this new basis  $\Phi_{(k+1)}$  the system is again solved in time at its new size of  $r_{k+1} = r_k + 1$ . The obtained time history of the reduced displacements  $\mathbf{q}(t_j)$  is used in a post-treatment to establish a new evolution of the residual  $\mathbf{r}(t_j) = \mathbf{f}_E(t_j) - \mathbf{M}\Phi_{(k+1)}\dot{\mathbf{q}}(t_j) - \mathbf{C}\Phi_{(k+1)}\dot{\mathbf{q}}(t_j) - \mathbf{g}(\Phi_{(k+1)}\mathbf{q}(t_j))$ .

These three steps, of the solution of a reduced system, the amelioration of the basis and its expansion, are repeated until the size  $r_{(k)}$  of the obtained reduction matrix  $\Phi_{(k)}$  equals the desired order  $r$  or all residuals  $\mathbf{r}(t_j)$  lie below the threshold.

#### 3.3.4.2 A Priori Reduction for establishing a reduced solution

The APR is based on repeated solutions of reduced systems of increasing order. In fact, in order to obtain a reduced basis of order  $r_k$  the reduced solutions with the orders 1 to  $r_k - 1$  are already available. If the aim of the application of the APR is not to obtain a reduced basis with a given order  $r$ , as it is the case here, but simply to obtain a reduced transient solution with a given quality, the APR can be applied to deliver such a solution.

At a certain  $r_k$  a reduced solution is obtained. The APR provides a new basis of order  $r_{k+1}$  and with this new basis, a second reduced solution is obtained. By keeping the first of order  $r_k$  and comparing it with the following solution of order  $r_{k+1}$ , either in generalised coordinates or in physical displacements, an abortion criterion can be established. This criterion halts the APR iterations regardless of the current order  $r$  of the reduced system, as it is only based on the quality of the reduced solution.

This approach is not pursued further because the aim of the following study is to compare different reduced bases at a given order  $r$ .

### 3.3.5 Centroidal Voronoi Tessellation

The Centroidal Voronoi Tessellation (CVT) is a data extraction and reduction technique, which aims at finding significant data in a set. In this it resembles to Orthogonal Decomposition, discussed in section 3.3.3, but its approach is different. The CVT is well referenced by Du et al. [71] and compared to the POD method by Burkardt et al. [46] for fluid dynamics. An illustrative overview is made available by Allen et al. [4].

The idea of the CVT is to regroup data in  $r$  regions  $V_k$  with  $k \in \{1, \dots, r\}$  around  $r$  significant points, called generators  $\phi_k$ , and then to approximate the data inside that region by the value of the region's generator. These regions are called Voronoi regions if the points inside  $\mathbf{u}(t_j) \in V_k$  fulfil the condition

$$|\mathbf{u}(t_j) - \phi_k| \leq |\mathbf{u}(t_j) - \phi_i| \quad \forall k \neq i \quad (3.150)$$

and  $\{k, i\} \in \{1, \dots, r\}$ . The closest generator to a point inside a Voronoi region  $\mathbf{u}(t_j) \in V_k$  is the generator  $\phi_k$  of the region  $V_k$  to which the point  $\mathbf{u}(t_j)$  belongs. A Voronoi region becomes centroidal, when the centroid of the region coincides with the generator, i.e.

$$\phi_k = \frac{\int_{V_k} \mathbf{u} \rho(\mathbf{u}) dV}{\int_{V_k} \rho(\mathbf{u}) dV} \quad (3.151)$$

where  $\rho(\mathbf{u})$  is a density function, which weighs the different  $\mathbf{u} \in V_k$ . This density function  $\rho(\mathbf{u})$  is set to one in order to allow for an easy computation and to weigh all snapshots the same.

The idea of the application of the CVT is to apply its procedure to the same snapshots  $\tilde{\mathbf{u}}(t_j)$ , that are already used for the POD in section 3.3.3.1, and use the obtained generators  $\phi_k$  as vectors of a reduced basis  $\Phi$ . Being given  $\tilde{\mathbf{u}}(t_j)$  as the snapshots of the system's solution, with  $t_j \in \{t_1, \dots, t_m\}$  and  $1 \leq j \leq m$ , the task of the CVT algorithm is to find the generators  $\phi_k$ , with  $k \in \{1, \dots, r\}$  that tessellate the ensemble of the snapshots  $\tilde{\mathbf{u}}(t_j)$  in a centroidal Voronoi sense.

The computation of the generators  $\phi_k$  done with the Sequential Sampling algorithm. This requires an initial set of generators

$$\Phi^{(0)} = [\phi_1^{(0)}, \phi_2^{(0)}, \dots, \phi_r^{(0)}], \quad (3.152)$$

which will be refined iteratively. The initial set of generators has to come from another method providing a reduced basis. Usually the LNM from section 3.3.1 provide a good starting point. The corresponding regions  $V_k^{(0)}$  with  $k \in \{1, \dots, r\}$  are defined with equation (3.150).

For each element of the set of the snapshots  $[\tilde{\mathbf{u}}(t_1), \dots, \tilde{\mathbf{u}}(t_j), \dots, \tilde{\mathbf{u}}(t_m)]$  the following three-step procedure is repeated, in order to find the  $\Phi_0$ , which takes into account all snapshots and should represent their optimal centroidal Voronoi tessellation.

1. For a given  $\tilde{\mathbf{u}}(t_j)$  the closest generator  $\phi_k^{(j-1)}$  is sought.
2. The  $\tilde{\mathbf{u}}(t_j)$  is assigned to the corresponding region  $V_k^{(j)} = V_k^{(j-1)} \cup \tilde{\mathbf{u}}(t_j)$ .
3. The new generator  $\phi_k^{(j)}$  is calculated as the mean of the region  $V_k^{(j)}$ , defined in the preceding step.

In the basis only the column vector of the newly found generator is updated

$$\Phi^{(j)} = [\phi_1^{(j-1)}, \phi_2^{(j-1)}, \dots, \phi_k^{(j)}, \dots, \phi_r^{(j-1)}] \quad (3.153)$$

and the next iteration for  $j + 1$  is launched until all  $m$  snapshots are assigned to a set  $V_k^{(m)}$ . The obtained basis  $\Phi^{(m)}$  is subjected to a Gram-Schmidt procedure, with the aim of ensuring ortho-normality and then used to project equation (2.82).

The work of Du et al. [71] is an example for the approach that the distance of the vectors  $\check{\mathbf{u}}(t_j)$  and  $\phi_k^{(j-1)}$  in the first step of the algorithm is determined in the Euclidian sense. However, during preliminary numerical experiments, it has been proven that the use of the modal assurance criterion (MAC) is highly beneficial. This is an original contribution to the formulation of the CVT.

In order to determine the affiliation of a snapshot  $\check{\mathbf{u}}(t_j)$  to a region  $V_k$  equation (3.150) requires a measure of the distances between the snapshot and the generator  $\phi_k$ . This defined as the Euclidian norm of the resulting vector  $\check{\mathbf{u}}(t_j) - \phi_k$  in equation (3.150). Using the MAC requires the reformulation of equation (3.150) as

$$\frac{|\check{\mathbf{u}}(t_j)^T \phi_k|}{|\check{\mathbf{u}}(t_j)^T \check{\mathbf{u}}(t_j)| |\phi_k^T \phi_k|} \geq \frac{|\check{\mathbf{u}}(t_j)^T \phi_l|}{|\check{\mathbf{u}}(t_j)^T \check{\mathbf{u}}(t_j)| |\phi_l^T \phi_l|}. \quad (3.154)$$

The  $\leq$ -sign turns into a  $\geq$ -sign, due to the MAC being a measure of closeness and not of distance. The MAC is evaluated for all  $k \neq l$  and  $\{k, l\} \in \{1, \dots, r\}$ .

The three-step procedure for constructing the CVT-basis is applied with equation (3.154) instead of equation (3.150) as a measure of the distance for the snapshots within each region  $V_k$  from now on. The differences between the two possible measures are documented in the annex section C.2.

### 3.3.6 Local Equivalent Linear Stiffness Method

The Local Equivalent Linear Stiffness Method (LESLM) is, as its name suggests, a method specifically designed to include localised nonlinearities. It employs an iterative approximation process for creating an equivalent linear stiffness matrix and then builds upon this equivalent stiffness matrix to create a special breed of LNMs, the so-called LELSM modes. While the LELSM was conceived initially only for nonlinearities that connect a degree of freedom to an inertial point in space it is expanded to nonlinearities that connect two degrees of freedom within the same system and even entirely nonlinear systems.

Laid out in its basic shape by AL-Shudeifat and Butcher [2] it was soon extended by Butcher and AL-Shudeifat [49] to include the iterative process for creating the updated LELSM. Butcher and AL-Shudeifat [49] also claim a near equivalence between the updated LELSM modes and the POD-vectors. The approach for generating the equivalent linear stiffness depends on the type of the nonlinearity and Butcher and Lu [48] provide an overview for a wide variety of nonlinearities.

Butcher and AL-Shudeifat [49] argue that a conservative and unforced system, whose displacements are initialised with a specific mode, will oscillate in that specific mode alone without any excitation of other modes. This is to be reflected in the orthogonality of the LELSM modes. The updated LELSM relies hence on finding specific modes that comply with this condition. However, this is not done on the underlying linear system, but on an equivalent linear system that takes into account the nonlinearity via a specific linear stiffness term.

### 3.3.6.1 LELSM for a grounded cubic nonlinearity

For a grounded cubic stiffness the equivalent linear stiffness term is obtained by isolating the nonlinear degree of freedom and then dismissing its dampening term. This allows the equation of motion for this single degree of freedom system to be written as

$$\ddot{u}_j + \omega_j^2 \left( u_j + \frac{k_{NL}}{\omega_j^2} u_j^3 \right) = 0, \quad (3.155)$$

supposing that this degree of freedom is not forced and with the introduction of the linear oscillation frequency  $\omega_j^2 = \frac{k_j + k_{j+1}}{m_j}$ . The harmonic balance method allows approximating the nonlinear oscillation frequency of this system. Beléndez et al. [25] suggests

$$\omega_{j,NL}^2 = \frac{\omega_j^2}{144} \left( 80 + 62 \frac{k_{NL}}{\omega_j^2} \hat{u}_j^2 + \sqrt{4096 + 5888 \frac{k_{NL}}{\omega_j^2} \hat{u}_j^2 + 1684 \left( \frac{k_{NL}}{\omega_j^2} \right)^2 \hat{u}_j^4} \right), \quad (3.156)$$

while Butcher and AL-Shudeifat [49] propose

$$\omega_{j,NL}^2 = 1 + \frac{3}{4} k_{NL} \omega_j^2 - \frac{3}{128} k_{NL}^2 \omega_j^4, \quad (3.157)$$

as a somewhat leaner formulation, yet under the considerable limitation of  $k_j = k_{j+1} = m_j = 1$ . The formulation (3.156) for the equivalent nonlinear oscillation frequency depends on the modal amplitude  $\hat{u}_j$  of the degree of freedom subjected to the nonlinearity. As this quantity is not known an iterative process is used, based on the stipulation of the existence of specific modes with reoccurring patterns of displacements that are orthogonal to each other.

The following iteration is repeated for all  $k$  LELSM modes up to the desired size  $r$  of the reduced model. The process of finding the right modal amplitude for a given mode is started by initialising  $\hat{u}_j$  with the  $j$ -th value in the corresponding LNM. To this end the tangent stiffness matrix of the underlying linear system is created with a variation of equation (3.102),

$$\left( \omega_k^2 \mathbf{I} + \tilde{\mathbf{K}} \right) \phi_k^{(1)} = 0, \quad (3.158)$$

in which the stiffness matrix is normalised with respect to the mass matrix

$$\tilde{\mathbf{K}} = \mathbf{M}^{-\frac{1}{2}} \left. \frac{\partial \mathbf{g}(\mathbf{u})}{\partial (\mathbf{u})} \right|_{\mathbf{u}_0} \mathbf{M}^{-\frac{1}{2}}. \quad (3.159)$$

The initial modal amplitude is thus set to the  $j$ -th component of the current LNM

$$\hat{u}_j^{(l)} = \phi_{jk}^{(l)}, \quad (3.160)$$

where the current iteration is indexed with the superscript  $(l)$ . This value of the modal amplitude  $\hat{u}_j$  is used with equation (3.156) or equation (3.157) in order to obtain the corresponding nonlinear oscillation

### 3.3. CREATING SOME COMMON REDUCED BASES

frequency  $(\omega_{j,NL}^{(l)})^2$ . This, in turn, is used to define the equivalent stiffness of the single degree of freedom system of the  $j$ -th degree of freedom from equation (3.155), by simple multiplication with the mass

$$k_{j,eq}^{(l)} = m_j (\omega_{j,NL}^{(l)})^2. \quad (3.161)$$

This equivalent linear stiffness  $k_{j,eq}^{(l)}$ , which is at the origin of the LELSM's name, is introduced into a specific equivalent stiffness matrix  $\mathbf{K}_{eq}^{(l)}$ , where it replaces the terms at  $j$ -th column in the  $j$ -th row. This amounts to

$$\mathbf{K}_{eq}^{(l)} = \begin{bmatrix} 2 & -1 & & & & \\ -1 & 2 & -1 & & & \mathbf{0} \\ & \ddots & \ddots & \ddots & & \\ & -1 & k_{eq}^{(l)} & -1 & & \\ & & \ddots & \ddots & \ddots & \\ \mathbf{0} & & & -1 & 2 & -1 \\ & & & & -1 & 1 \end{bmatrix}, \quad (3.162)$$

if the example of a locally nonlinear system is used, which will be introduced in section 4.1.3.1. Obviously this equivalent stiffness matrix is subjected to normalisation of equation (3.159) before being processed further.

The so normalised equivalent linear stiffness matrix  $\mathbf{K}_{eq}^{(l)}$  is then used in equation (3.158) in order to obtain the next LELSM-mode  $\phi_k^{(l+1)}$  and a new value for the modal amplitude

$$\hat{u}_j^{(l+1)} = \frac{1}{2} (\hat{u}_j^{(l)} + \phi_{jk}^{(l+1)}), \quad (3.163)$$

as the arithmetic mean of its preceding value  $\hat{u}_j^{(l)}$  and the current modal amplitude  $\phi_{jk}^{(l+1)}$  resulting from the current linear stiffness.

An error metric, for example the modal assurance criterion (refer to equation (3.154)), can be used to determine the similarity between the two iterations of the current LELSM-mode  $\phi_k^{(l)}$  and  $\phi_k^{(l+1)}$ , and lead to a decision whether the iteration is continued by returning to equation (3.161) or to hold the iterations and consider the current LELSM-mode to have converged. In the latter case the current LELSM-mode  $\phi_k^{(l+1)}$  is integrated as the  $k$ -th column-vector into the reduced basis  $\Phi$  and the process repeated until all  $r$  LELSM-modes have been treated and successfully converged.

To ensure the orthogonality of the LELSM-basis it is eventually treated with a Gram-Schmidt procedure (e.g. Strang [218]).

#### 3.3.6.2 LELSM for a coupling cubic nonlinearity

The work of AL-Shudeifat and Butcher [2] provides also an approach for isolated coupling cubic nonlinearities. Its main features are that the modal amplitude  $\hat{u}$  is built from the difference of the modal amplitudes of the degrees of freedom connected by the coupling nonlinearity and that the equivalent linear stiffness  $k_{j,eq}$  is obtained from the equivalence of the equations of motion of a nonlinear equivalent system with two degrees of freedom and an exclusively linear equivalent sub-system. In the process, this two degree of



### 3.3. CREATING SOME COMMON REDUCED BASES

---

If there are several neighbouring coupling nonlinearities, the corresponding equivalent linear stiffnesses add up along the diagonal of the equivalent linear stiffness matrix. This equivalent linear stiffness matrix is used in repeatedly in the iterative approximation of the LELSM-vector in exactly the same way as for the grounded nonlinearities.

In the presence of additional grounded nonlinearities, which e.g. connect the end DOFs of a system to inertial points in space, these can be included in the process by simply adding their equivalent linear stiffnesses to the system's equivalent linear stiffness matrix at the corresponding position.

#### 3.3.6.3 LELSM with Sh-B-vectors

AL-Shudeifat and Butcher [2] propose to augment the LELSM basis with to additional vectors that are a type of new Ritz-vectors and called Sh-B-vectors. Sh-B vectors are static solutions for distinctive forces. These vectors account for the localised application of the excitation and also for the presence of this nonlinearity, if such a nonlinearity is present in the system.

Two distinctive force vectors are defined as

$$\mathbf{f}_1 = [0, \dots, -k_p, k_p + k_{p+1}, -k_{p+1}, \dots, 0]^T, \quad (3.168)$$

for the point of application of the external forcing and, if applicable,

$$\mathbf{f}_2 = [0, \dots, -k_j, k_{j,eq}, -k_{j+1}, \dots, 0]^T, \quad (3.169)$$

for the localised nonlinearity, by simply multiplying the corresponding columns of the stiffness matrices with a unit length. The normalisation with respect to the mass matrix is maintained. The equivalent stiffness  $k_{j,eq}$  is taken from the LELSM procedure.

The two Sh-B-vectors are computed with the equivalent stiffness matrix  $\mathbf{K}_{eq}$  from the regular LELSM procedure.

$$\Phi_1 = \mathbf{K}_{eq}^{-1} \mathbf{f}_1 \quad (3.170)$$

$$\Phi_2 = \mathbf{K}_{eq}^{-1} \mathbf{f}_2 \quad (3.171)$$

They are then included in the existing LELSM reduced basis  $\Phi$ , where they replace the two least significant vectors.

### 3.3.7 Homogenising the constitution of the reduced bases

This section regroups several necessary considerations, which affect the definition of the different methods for obtaining the reduced bases beyond the scope of their purely theoretic definition in the current section. These deal mainly with the specific set-ups of the methods and prepare the conduction of the following studies.

The constitution of a basis describes its normalisation, the algebraic sign of its vectors and its alignment. This concerns primarily the methods which are based on eigenproblems, i.e. the LNM and the orthogonal decomposition bases and their respective variants. These considerations do not apply to the Ritz-vectors and the basis formed by the APR reduction because these approaches possess inherent normalisation mechanisms.

From the point of view of the solution algorithm the constitution of a basis cannot influence the quality

### 3.3. CREATING SOME COMMON REDUCED BASES

of the solution. The central equation (3.60) of the applied Newmark scheme implicitly contains a linear development of the non-linear forces vector

$$\begin{aligned} \mathbf{g} \left( \Phi \mathbf{q}_{(i+1)}^{(t+\Delta t)} \right) = & \mathbf{g} \left( \Phi \mathbf{q}_{(i)}^{(t+\Delta t)} \right) \\ & + \left. \frac{\partial \mathbf{g}(\Phi \mathbf{q})}{\partial (\Phi \mathbf{q})} \right|_{\Phi \mathbf{q}_{(i)}^{(t+\Delta t)}} \left( \Phi \mathbf{q}_{(i+1)}^{(t+\Delta t)} - \Phi \mathbf{q}_{(i)}^{(t+\Delta t)} \right) + \dots, \end{aligned} \quad (3.172)$$

which neglects higher order terms. As a result of this linearisation and by forcing the physical meaning of every reconstituted generalised coordinate  $\mathbf{u} = \Phi \mathbf{q} = \check{\Phi} \check{\mathbf{q}}$ , where  $\check{\Phi} = \Phi \mathbf{D}$  is supposed to be a differently constituted variant of  $\Phi$ , which has its constitution changed by the multiplicative, diagonal matrix  $\mathbf{D}$ . It follows that  $\check{\mathbf{q}} = \mathbf{D}^{-1} \mathbf{q}$ , which effectively cancels out the different constitution of the basis. The two differently reduced systems simply operate on different generalised coordinates and give the same result in physical displacements.

The systems used for the following studies in chapter 4 do contain exclusively odd nonlinearities, which are ensuring the stability of the systems. The non-linear forces vectors  $\mathbf{g}$  is hence symmetric with respect to the algebraic sign of the displacements. To ensure that this particularity is not a contributing factor for the independence of the results from the constitution of the basis and the results are indeed applicable to generic nonlinearities, a series of tests has been executed on specifically conceived systems containing additional quadratic nonlinearities. These tests show no indication for an influence of the normalisation, the sign or the alignment of the basis.

- The normalisation of the reduced basis determines the normalisation of the column vectors of the reduced basis. For testing purposes the obtained eigenvectors are normalised in the Euclidian sense,  $\Phi_i = \Phi_i / \sqrt{\Phi_i^T \Phi_i}$ , in the engineering sense,  $\Phi_i = \Phi_i / \max(\Phi_i)$ , and with respect to the initial stiffness matrix of the respective system,  $\Phi_i = \Phi_i / \sqrt{\Phi_i^T \mathbf{K}(\mathbf{u}_0) \Phi_i}$ . All three normalisations yield the exact same results.
- The sign of the reduced basis determines to which side the column vectors are flipped<sup>13</sup>. Tests executed in which the concerned original bases  $\Phi$  are pitched against their negative counterparts  $-\Phi$  yield the exact same results.
- The alignment of the reduced basis determines if its column vectors are all flipped to the same side or not. The results obtained from the original bases  $\Phi$  were compared with the ones obtained from a variant of  $\Phi$  which deliberately breaks any existent alignment by replacing every second vector  $\Phi$  with its negative counterpart, i.e.  $\Phi_i = -\Phi_i \quad \forall i \in \{1 \dots r\}$  and  $i$  odd and  $\Phi_i = \Phi_i \quad \forall i \in \{1 \dots r\}$  and  $i$  even. The exact same results were obtained for both cases.

Tests with extremely large bases show that the available numerical precision has to be equally distributed between the two components of the product  $\Phi \mathbf{q}$ , in order to avoid meaningless results. However, this problem is disconnected from the non-linear nature of the test-cases.

It can thus be established that the discussed properties of the bases' vectors have no measurable influence on the solution of the reduced systems. The obtained errors in the following studies are hence to be ascribed exclusively to the quality of the used basis. Differences in quality of the different solutions are exclusively linked to basis and the reduction itself.

This result has been carefully and extensively validated for the present test-cases and the used solution procedure. Yet, it does not allow for a generalisation, stipulating that comparable tests prior to every other reduction of a non-linear system have to be executed.

Following these results, the constitution of the eigenvector bases is strictly homogenised among the dif-

<sup>13</sup>The somewhat colloquial notion of flipping the column vectors can be understood best by looking at the figures 4.3 to 4.6. There the column vectors of the reduced bases are traced and flipping would mean mirroring them along the horizontal axis of the plot.

### 3.3. CREATING SOME COMMON REDUCED BASES

---

ferent methods, by normalising their vectors to unit length and aligning them in such a way that their first value is negative.

## Chapter 4

# Comparing the reduced bases and testing their robustness

---

The preparation of the methods required for describing, solving and reducing a geometrically nonlinear system is finished. The methods that have been chosen are the nonlinear Newmark scheme with inflation for the transient solution and the projection on reduced bases for the reduction. Numerical experiments are now conducted in order to determine whether there is a reduced basis that is particularly well suited for the reduction of a nonlinear system and if a basis is particularly robust with respect to changing parameters. This double-objective defines the main structure of the current chapter.

The chapter starts with preparing the necessary elements of the numerical experiments. The first of these elements is a detailed description of the studies' aims and scope with respect to the two-fold aspiration to compare the suitability of the reduced bases and to explore their robustness. As an additional element of the preparation of the study the four test-cases are defined as combinations of two different nonlinear systems and two different transient excitations together with their parameters. Finally, the development of criteria that allow judging the performance of a reduced basis with respect to the defined aims of the study is detailed.

In its major parts, this chapter contains two comprehensive studies. The first study compares the different reduced bases among each other as they are applied to the four test-cases. The second study takes the projection bases obtained during the first study and explores how well they are applicable if the excitation of the system changes. These studies demonstrate that the decision for the selection of a reduced basis should primarily be based on the type of excitation to which the nonlinear system is subjected.

Furthermore, the results show that no reduced basis is capable of reproducing the full order solution with the required accuracy. Also, none of the tested reduced bases exhibits a sufficient robustness under the applied criteria.

These two central findings give raise to the need to embrace a broader approach that goes beyond the selection of a reduced basis. This approach should possibly enclose the solution algorithm and also modify the reduced bases in a suitable manner. It leads to the following chapter 5, where these two points are addressed.

### 4.1 Preparing the studies

The preparation of the studies covers the aspects of defining its aims, and setting up the test-cases and criteria in accordance with these aims.

The definition of the studies' aims distinguishes clearly the two aspects of the comparison of the reduced bases and the investigation of their robustness. This distinction is continued in the definition of the criteria. There, several commonly used criteria are presented and they are congregated into two single error metrics: the score for the comparison and the relative performance for the robustness. Finally, the test-cases are defined. Again in accordance with the studies' aims, they are set up to cover different scenarios of transient solutions of nonlinear systems.

Compared to already published works the originality of the present study resides in the fact that it investigates rigorously the applications to be preferred for the most commonly used reduced bases, while limiting itself to generic types of nonlinear systems. This broad approach is an expansion of existing literature, where never more than three reduced basis seem to be compared at the same time. This study is aimed at consolidating the comprehensive understanding of the areas of application of the different reduced bases.

#### 4.1.1 Defining the studies' aims and scope

For establishing a reduced basis all of the methods for creating a reduced basis  $\Phi$  that are listed in the section 3.3, the Linear Normal Modes, the Ritz-vectors, the various orthogonal decompositions, the A Priori Reduction, the Centroidal Voronoi Tessellation and the Local Equivalent Linear Stiffness Method, have very distinctive ways of using information from the system, from the excitation, and for some cases also from the solution. The different methods give different results depending on types of nonlinearities and excitations. The first part of the study to be undertaken investigates precisely this suitability of the different bases for different test-cases. This first part is termed the comparison because it compares the reduced bases among each other.

The aim of the comparative study is double in the sense that, first, it allows to gain insight into how well a certain reduction method performs on a certain combination of non-linearity and excitation and that, second, this overview allows comparing the different reduction methods among each other.

The second part of the study investigates the inherent robustness of the different reduced bases. All of the methods for creating reduced bases rely on the properties and parameters of the distinct combination of nonlinear system and excitation under consideration. These are contained in the matrices and vectors describing the discrete system. The fact that the Linear Normal Modes, the Ritz-vectors, the A Priori Reduction and the Local Equivalent Linear Stiffness Method do not require information from the solution of the full order system, allows them to be categorized as a priori methods. Opposite to them are the so-called a posteriori methods, the Proper Orthogonal Decomposition, the Smooth Orthogonal Decomposition and the Centroidal Voronoi Tessellation, which require information from an actual, albeit maybe only partial, full order solution. Neither of these two categories of bases can be simply applied to other test-cases as the ones they were designed for. This second part of the study is termed the robustness investigation.

This study of the robustness determines the robustness of the different reduction methods if they are applied to a differently parameterised test-case. It takes the reduced bases that are established during the comparative study and uses them to reduce the same test-cases with differently parameterised excitations. The result of this second study is an overview of which method is to be expected to be particularly robust if applied to a system under an excitation that was not used to create it. A desirable aim is certainly a procedure using optimal bases, to build a robust framework for the simulations of different and differently parameterised reduced nonlinear structures.

Within the limits of the selection of solution methods and methods for generating the reduced bases that is made in the preceding chapter 3, the present study is comprehensive as it covers all selected methods. The

## 4.1. PREPARING THE STUDIES

---

reduced bases are constructed from Linear Normal Modes, Ritz-vectors, Proper and Smooth Orthogonal Decomposition, A Priori Reduction, Centroidal Voronoi Tessellation and Local Equivalent Linear Stiffness Method, as well as from several variants.

These two aims are in accordance of the requirement of exploring the application of reduced bases to geometrically nonlinear systems and to explore their behaviour under different parameterisations as they are stated in the introduction. Further tests with additional or other objectives are not conducted.

### 4.1.2 Defining the criteria for judging the capabilities of the reduced bases

“... a proper selection of basis vectors is of great importance. The ideal set of basis vectors is one which maximizes the quality of the results and minimises both the computation times for the reduced system integration and the efforts to obtain these modes.” This quote from Slaats et al. [210] contains exactly what has to be expected from a reduced basis.

To ensure a correct decision on a selected reduced basis and procedure, its performance has to be evaluated against well-founded criteria. These criteria are established with respect to the methods ability to recreate most closely the transient solution of the full order system and its capability to do so in the least computational time possible. This spawns two sets of criterion, which do focus on the quality and on the speed of the solution respectively.

The first set of criteria comprises an error formulation which gives an integral impression of the 'distance' between the solutions obtained through the use of the full order model and the solution of the reduced model.

The second set of criteria uses a notion of computational time, usually normalised with the time required for the solution of the full order system, or the number of required operations, which scale with multiples of the dimensions of the involved matrices.

Because a reduction method can be considered useful only if it balances the two basically contrarious requirements of accuracy and speed, several approaches to measure a method's performance with respect to these two demands a reviewed in the following subsections. Also studied are ways to combine the measurements of these two requirements into single value, which reflects the overall performance of the method.

In much the same way as the improper selection of a test-case might favour a specific reduced basis a single, unique criterion would most probably do the same<sup>1</sup>. While the influence of the test-case should be mostly ruled out by testing four different cases, testing a multitude of error metrics becomes impractical. This is due to the fact that there is already a number of reduced bases that are presented in section 3.3 and that will be used four times for the four different test-cases. Multiplying this number further by a number of different error metrics for the two different studies - comparison and robustness - will most certainly yield an unwieldy amount of results that will become impossible to treat.

To counter this effect and to have a single, meaningful result for each basis that does not prefer any of them, a number of error metrics is presented in the following and then congregated into a single error metric for each of the two studies. For the comparison of the reduced bases this will results in the basis' performance and for the study of the bases' robustness the relative performance is developed.

#### 4.1.2.1 Presenting a selection of common error metrics

With the aim of judging the performance of the reduced bases a selection of common error metrics is presented in the following and their congregation into the unique error metrics is described. Ross et al. [193] suggest a classification of the quality of the predictive accuracy of a simulation in variability, which accounts for the random character of a variable or a real world item and uncertainty. Uncertainty accounts for all errors introduced into the process of simulation by scarce or misleading data, unknown biases and,

---

<sup>1</sup>For the POD basis its optimality in the R2MSE sense is even proven. This will be mentioned specifically later on.

## 4.1. PREPARING THE STUDIES

---

most important, assumptions injected into the process. The main difference between the two sources of predictable inaccuracy is that uncertainties can be reduced, while variabilities can only be quantified. As no real-world testing is used, variability is not present as a possible source for predictive inaccuracies. The focus has thus to be set on gauging and reducing the uncertainty in the process of a reduction.

An obvious approach to measure the accuracy of a reduction in terms of uncertainty is to compare physical displacements obtained from the full order system to displacements reconstituted from the reduced order system. Certain quantities of the solution of the full order model (FOM) can be used directly in order to gain an impression of the quality of the reduction, as the solution of the reduced order model (ROM) is reconstructed from the generalised coordinates  $\mathbf{u}^{(\text{ROM})}(t_j) = \Phi \mathbf{q}(t_j)$ . These are required to be verifiable by the naked eye in the case of basic curve comparison and they are supposed to be accessible by engineering judgement.

These quantities would e.g. be

- the mean value, which has to be preserved and that is needed to retain the equilibrium configuration,
- the amplitudes, defined as the maximum positive and negative deviations from the mean value,
- the governing frequencies that have to be resolved and can be correlated to their respective amplitudes via a Fourier transform and,
- the damping which ultimately indicates the stability of the solution

These are the points to be verified by the naked eye in the case of basic curve comparison and they are supposed to be accessible by engineering judgement. More quantitative metrics are established in the following paragraphs.

Yet, such an approach becomes unfeasible if facing the several thousand simulations that are required to cover all combinations of reduced bases, test-cases and configurations. The performance of a reduced basis is hence abstracted by means of score and a relative performance, both carefully constructed and diligently verified against the naked eye impression of the time histories.

Elements of stationary solutions, such as attractors and bifurcation characteristics, are not considered because they are commonly associated with stabilised, periodic solutions and the exclusive focus in this study is on the recreation of the transient solution.

Also not included is the investigation of the gradual stabilisation or attenuation of the transient solution due to damping effects. The main reason for this, is that the available tools as e.g. the spectrum method and, even more so, the time history method, which are both presented in the annex section A.2.2, are by far too imprecise to allow for meaningful contributions to the judgement of the performance of the reduced bases if compared to other error metrics. Furthermore, the damping was introduced in the dynamic equilibrium in equation (2.82) foremost as an artificial measure to ensure the numerical stability of the system by means of equation (2.81). It is therefore limited in its impact on the transient solution, which contributes to the meaninglessness of the numerical tools for gauging damping from a transient solution.

The criteria that are used are:

**4.1.2.1.1 the relative mean deviation** is an indication of how much the means of the full order solution (FOM) and the reconstructed reduced order solution (ROM) differ. It is a single value for given transient solution. It is obtained by the difference of the temporal means of the full order and the reconstructed reduced order solution over the simulated period  $(t_0, t_e]$  that is normalised with the oscillation of the full order solution for each degree of freedom. Then, the square mean is applied to condense the  $n$  values, which

#### 4.1. PREPARING THE STUDIES

---

can be positive or negative, into a single value.

$$e_m = \sqrt{\frac{1}{n} \sum_{i=1}^n \left( \frac{\frac{1}{t_e - t_0} \sum_j u_i^{(\text{FOM})}(t_j) - \frac{1}{t_e - t_0} \sum_j u_i^{(\text{ROM})}(t_j)}{\max(u_i^{(\text{FOM})}) - \min(u_i^{(\text{FOM})})} \right)^2}. \quad (4.1)$$

**4.1.2.1.2 the relative oscillation deviation** for each of the  $n$  physical degrees of freedom is defined as

$$o_i = \max(u_i) - \min(u_i). \quad (4.2)$$

It is already introduced implicitly in equation (4.1) above. In order to obtain a single value for the comparison of the reconstructed reduced solution with the full order solution the square mean of the differences of the oscillations of the two solutions over all  $n$  degrees of freedom is taken

$$e_d = \sqrt{\frac{1}{n} \sum_{i=1}^n \left( \frac{o_i^{(\text{ROM})} - o_i^{(\text{FOM})}}{o_i^{(\text{FOM})}} \right)^2}. \quad (4.3)$$

**4.1.2.1.3 the relative root mean square error (R2MSE)** is defined as

$$e_{r,i} = \frac{\sqrt{\sum_j \left( u_i^{(\text{ROM})}(t_j) - u_i^{(\text{FOM})}(t_j) \right)^2}}{\sqrt{\sum_j \left( u_i^{(\text{FOM})}(t_j) \right)^2}} \quad (4.4)$$

for the displacements of the  $i$ -th degree of freedom. Included in the set of criteria are the mean of the R2MSE over all degrees of freedom

$$e_r = \frac{1}{n} \sum_{i=1}^n e_{r,i} \quad (4.5)$$

and its variance

$$v_r = \frac{1}{n-1} \sum_{i=1}^n (e_{r,i} - e_r)^2 \quad (4.6)$$

Here, the arithmetic mean of the R2MSE is sufficient because this error metric is always positive.

**4.1.2.1.4 the energy difference** is the difference of the combined kinetic and potential energies of the two solutions at the instant  $t_j$

$$\begin{aligned} \Delta E(t_j) = & \left( \left( \mathbf{u}^{(\text{ROM})}(t_j) \right)^T \mathbf{K} \mathbf{u}^{(\text{ROM})}(t_j) + \left( \dot{\mathbf{u}}^{(\text{ROM})}(t_j) \right)^T \mathbf{M} \dot{\mathbf{u}}^{(\text{ROM})}(t_j) \right) \\ & - \left( \left( \mathbf{u}^{(\text{FOM})}(t_j) \right)^T \mathbf{K} \mathbf{u}^{(\text{FOM})}(t_j) + \left( \dot{\mathbf{u}}^{(\text{FOM})}(t_j) \right)^T \mathbf{M} \dot{\mathbf{u}}^{(\text{FOM})}(t_j) \right). \end{aligned} \quad (4.7)$$

To be exploitable as a single value the mean of the energy difference is established as

$$\Delta E = \sqrt{\frac{1}{n_t} \sum_{j=1}^{n_t} (\Delta E(t_j))^2}, \quad (4.8)$$

where it has to be noted that this mean is taken over the simulated time period between  $t_0$  and  $t_e$ , split up in  $m$  time-steps. This also applies to the variance of the energy difference

$$v_{\Delta E} = \frac{1}{n_t - 1} \sum_{j=1}^{n_t} (\Delta E(t_j) - \Delta E)^2. \quad (4.9)$$

Here, the same quadratic mean as for the relative oscillation deviation in equation (4.3) is chosen because the energy difference can become positive or negative. Under stability considerations, it is noteworthy that the energy difference only becomes positive, if the reduced order model contains more energy than the full order model.

**4.1.2.1.5 the modal assurance criterion** (MAC) relates the shapes for certain column vectors of two different reduced bases. While the error metrics above are applicable to the time history of the different solutions it is also possible to introduce this criterion based on the modal properties of the full order and the reduced order system, respectively. The MAC is used previously in equation (3.154) for the Centroidal Voronoi Tessellation. Peeters [171] uses the modal assurance criterion to determine the quality of a reduced order model by comparing the mode shapes of the full order model  $\phi_i^{(\text{FOM})}$  with the ones derived from the reduced order model  $\phi_i^{(\text{ROM})}$  by

$$e_a = \frac{\left| \left( \phi_i^{(\text{FOM})} \right)^T \phi_i^{(\text{ROM})} \right|^2}{\left| \left( \phi_i^{(\text{FOM})} \right)^T \phi_i^{(\text{FOM})} \right| \left| \left( \phi_i^{(\text{ROM})} \right)^T \phi_i^{(\text{ROM})} \right|}. \quad (4.10)$$

The MAC attains one if the two mode shapes  $\phi_i^{(\text{FOM})}$  and  $\phi_i^{(\text{ROM})}$  match and tends towards zero as the reduced order model fails to reproduce the same mode shape after it has been inflated to full order. It is worth noting that here the  $\phi_i$  are not used as generic vectors of the reduction matrix but in fact corresponding to their initial definition in linear normal modes, where the eigenvectors describe the mode's shape directly and have actually a physical significance. This means that also the shapes of time histories can be compared regardless of their amplitude, if the time histories  $([u_i(t_0), u_i(t_0 + \Delta t), \dots, u_i(t_0 + n_t \Delta t)])^T$  are introduced at the place of the  $\phi_i$ . It is self-evident that only corresponding mode-shapes can be compared.

At this point the MAC is listed for the sake of completeness only. Later, it is used to compare the time histories of displacements and the shapes of the reduced expressions  $\tilde{\mathbf{g}}(\mathbf{q})$  of the vector of the nonlinear internal forces.

#### 4.1.2.2 Performance assessment for comparison by defining the score

The aim of the relative scoring system is to gain access to a comprehensive classification of the reduced bases. It uses a maximum of abstraction for the inclusion of different criteria and allows assessing the reduced bases' performance with a maximum of conceptual distance from the actual time histories of the transient solutions.

To cope with the considerable number of reduced solutions the performance of the reduced bases is assessed by applying a weighted sum model for multi-criteria decision analysis. Drawing on this inspiration from the multi-criteria decision analysis techniques allows combining a set of criteria as e.g. means, the relative root mean square error, the energy difference and others.

The theory of the multi-criteria decision analysis introduces the notion of alternatives, which correspond to possible choices that can be made. Here, the alternatives are pairs of a reduced basis and an order  $r$  of the reduced system, e.g. the LNM at  $r = 4$  or the POD vectors at  $r = 8$ . Including the order of the reduced system in the alternatives allows e.g. that one reduced basis at a given  $r$  may perform better than another one at a higher  $r$ . For each criterion a ranking is established in which the pairs are given a rank  $\mathcal{R}_e^{(\text{basis}, r)}$ .

For each pair of a reduced basis approach and an order of the reduced system  $r$  the required values for the parameters are extracted. Being given a test-case the pairs are now rated independently for each criterion, i.e. a 1 is assigned to the worst performing pair of approach and  $r$ , a 2 is assigned to the second worst performing one and the process is repeated until the best performing pair receives the highest score. The rankings are then united in a weighted sum that yields a score for each pair

$$\text{score}^{(\text{basis}, r)} = \sum_i w_i \mathcal{R}_{e_i}^{(\text{basis}, r)}. \quad (4.11)$$

The actual application of the relative scoring system uses the criteria and associated weights in table 4.1.

designation		equation	weight $w_i$
overall reduction time			0.1
relative deviations of the solution's means	$e_m$	(4.1)	5
relative oscillation deviation	$e_d$	(4.3)	5
arithmetic mean of the relative root mean square error	$e_r$	(4.5)	10
variance of the relative root mean square error	$v_r$	(4.6)	1
quadratic mean of the energy difference	$\Delta E$	(4.8)	10
variance of the energy difference	$v_{\Delta E}$	(4.9)	1

Table 4.1: The criteria selected for the score and their associated weights

A smaller value for any of these criteria gives a better ranking because all these criteria have to be minimised. For each pair the scores for the different error metrics are then weighted corresponding to the importance that is assigned to the individual error metric and a single integrated score can be assigned to every pair consisting of a method for creating the reduced basis and an order of the reduced system  $r$ .

The weighting favours mean values of the criteria over their variances. These scores are then plotted against the order of the reduced model for every reduced basis to allow an assessment of the bases' performance. The score is also used to assess the suitability of second order terms in the annex section B. A higher score<sup>(basis, r)</sup> indicates a better performing pair.

The overall reduction time, i.e. the overall CPU time for establishing the reduced basis, solving the reduced system and returning to a full order solution, which is a measure for the total effort needed to obtain the time history of the displacements by means of a reduction procedure, is included only with a very

## 4.1. PREPARING THE STUDIES

---

small weight. This is due to numerical reasons that do not allow a precise exploitation of this criterion. It is the subject of a dedicated study in the annex section A.2.1. The MAC from equation (4.10) is not included in the score because it is defined for comparing the column vectors of the reduced basis and not the time histories of the solutions.

The score<sup>(basis,r)</sup> is then plotted over against the order  $r$  of the reduced system. The methods for creating the reduced basis add an additional dimension to the plot and are treated by different symbols and colours. This allows an assessment of the bases' performances at one go. Also, by treating the classifications for the distinct criteria as columns of a database, additional observations can be derived, e.g. the variance of classifications for a specific pair or the pair's maximum classification.

### 4.1.2.3 Performance assessment for the robustness by defining the relative performance

Vigo [238] defines in his dissertation robustness in the context of fluid dynamics as “the capacity of the POD [method] to correctly recreate a flow similar to but distinct from the initial flow, used for the creation of the basis.”<sup>2</sup> This definition is based on a POD reduction method but as the underlying full order system is the dominant factor in the determination of the different bases  $\Phi$  with the different methods of creating them, discussed in the section 3.3, the criterion from Vigo [238] can be expanded to all reduced bases alike, if the necessary adaptation for structural dynamics are made as well.

In the context of this study robustness of a projection based reduction method is defined as the method's capacity to correctly recreate a transient solution of a system similar to but distinct from the initial system, used for the creation of the base. Such similarity could mean differences in external parameters<sup>3</sup>  $\mu$ . As such the robustness of a method, or the lack thereof, will be a criterion for the quality of the reduced basis. A robust reduced basis is considered positive because it can be used to reduce systems with different values for the external parameters. Applying a less robust method to systems with different sets of external parameters  $\{\mu_1, \dots, \mu_m\}$  would lead to a reduced transient solution with unacceptably high levels of error. In such a case a new reduced basis is required to be build specifically for the current set of external parameters or the existing reduced basis has to be adapted to function properly with the current set of parameters<sup>4</sup>.

Another major approach in judging a method's robustness is its capacity to handle perturbations. The robustness of a method indicates its ability to handle perturbations of physical and numeric origin that may have an influence on the correctness or even on the stability of the solution. Following this reasoning it may become necessary to sacrifice speed for robustness in a trade-off in order to obtain a method which is stable.

For evaluating the robustness of the basis their performance has to be assessed in comparison to a reference configuration. The relative performance is introduced as the inverse of the weighted sum of the relative mean deviation, the relative oscillation deviation, the mean of the relative root mean square error and the variance of the relative root mean square error of the reduced solution at hand, all normalised with the respective values of the reference configuration. It covers several aspects of the solution's behaviour with the aim of capturing improvements in qualitative behaviour that is not captured by the R2MSE alone.

$$\text{relative performance}^{(\text{basis},r)} = \frac{1}{\sum_i w_i \frac{e_i^{\text{actual configuration}}}{e_i^{\text{reference configuration}}}} \quad (4.12)$$

The relative performance uses the same weights as the score and it is written as the inverse of the weighted sum in order to have the same orientation as the score. For a relative performance equal to one the reduced basis performs as well for the actual, differently parameterised configuration as for the reference

---

<sup>2</sup>The original passage from Vigo [238, p.147] reads: “On entend par robustesse : la capacité de la POD à bien reconstruire un écoulement proche mais distinct de l'écoulement initial ayant servi à créer la base.”

<sup>3</sup>The concept of external parameters is introduced in great detail in section 5.3.1.

<sup>4</sup>The techniques for the adaptation of the basis are introduced in section 5.3.

## 4.1. PREPARING THE STUDIES

---

configuration. A relative performance greater than one indicates a better performance for the differently parameterised configuration. Values smaller than one show a decrease in performance.

### 4.1.2.4 Reflecting on measuring computational speed

To measure the speed of a calculation it is common to start a stop-watch type asset at the beginning of a calculation and to stop it at the calculation's ending. The elapsed time gives an indication of the method's speed. By applying this technique to the full order system and to the reduced system the gain in speed can be calculated as the quotient of the two elapsed times. But this only holds, if the full order model and the reduced order model are solved in the same computational framework and on the same hardware. In times of shared and distributed computing, neither can be guaranteed and one can't even be sure to have the entire processor allocated to the solution of the problem. Thus these means of judging the method's gains in computational effort and speed are not viable and other means have to be found.

Browne et al. [41] oppose the comparison of different algorithm by performing executions test and define the collection of performance data as having been "an imprecise art". They propose a comparison based on counting the necessary basic floating point operations and provide adapted software. Aquino [16] demonstrates that the computational performance of a reduced order simulation hinges crucially on the actual implementation of the code and proposes an object-oriented framework for maximum performance. This passes the question for an optimal implementation on to the domain of pure informatics. This implies a type of knowledge that is not pursued within the scope of this work. Furthermore, the prototype character and the limited projected reuse of all code that is implemented during this work prohibits a significant effort for elaborate implementations. All this blurs the comparability of the computational performances of the different models and methods.

It is tautological to stress that every gain in the result's accuracy leads to a corresponding increase in the computational cost of that solution. The question to be answered in the determination of the overall performance of a reduction method is whether the gain in computation speed justifies the decrease of accuracy. And, should this question be given a positive answer, to which extend one is willing to trade accuracy for speed.

For now, the delicate nature of the measurements of the computational speeds and the limited trust that is put in them, are reflected by the very low weight  $w_i$  that is attributed to the overall reduction time in the score in equation (4.11).

A meaningful analysis of computational performance becomes feasible later with the introduction of the finite element test-cases and by augmenting considerably the size of the academic test-cases. The latter is done in the annex section A.2.1 with the expressed intention of gaining insight into the computational performance of the different methods for creating the reduced bases.

### 4.1.3 Setting up the test-cases

This section introduces and defines the test-cases that are used to test the reduced bases, for a comparison among each other and with respect to their robustness. A test-case consists of a nonlinear dynamic system and an excitation. To cover several possible applications and to ensure that the judgement of the reduced bases' performances is not biased by the selection of a single, specific test-case, different test-cases are developed. They cover a system with a localised nonlinearity and a system that is entirely nonlinear. These two are subjected to a harmonic and an impulse excitation. The combinations of these four elements allows for four different test-cases:

- the locally nonlinear system under the harmonic excitation,
- the locally nonlinear system under the impulse excitation,
- the entirely nonlinear system under the harmonic excitation, and,

- the entirely nonlinear system under the impulse excitation.

The central and most important criterion for the choice of the systems is that they are representative for the nonlinear formulations that are introduced in chapter 2. Thus, each of these test-cases has its justification with respect to a multitude of imaginable engineering applications. Especially the entirely nonlinear system subjected to the harmonic excitation is most representative for geometric nonlinearities because of their non-localised, distributed character. Also the harmonic excitation as a first approximation of an excitation, other than an impulse load, that can be considered as a precursor of a larger class of loads that are distributed and varying in time.

### 4.1.3.1 Defining the systems

The prerequisites to the study are the definitions of several distinct test-cases, consisting of possible combinations of two different nonlinear systems and two different excitations that are applied to these systems.

Among all initially considered and reviewed possible systems every single one displays distinct advantages and shortcomings. The decision to choose the two systems presented below is based on several considerations that deal mostly with the numerical solvability of the defined system, for example the frequencies present in the solution and the resulting minimal time-step. The fact that the two selected systems are not conservative can be regarded as an advantage. The comparison of the different reduction methods can be based on the initial transient phase.

Furthermore, for the first, locally nonlinear system its authors, AL-Shudeifat et al. [3], publish all critical values for parameters alongside a reference solution for one degree of freedom. This degree of freedom is connected to the localised nonlinearity and, with its two well distinguishable frequencies, it allows a direct assessment of the reduction's performance. The published values for the parameters are also later used again for defining the more generic, entirely nonlinear systems. With their dominant cubic nonlinearities the systems are certainly based on the Duffing-oscillator, which as a standard test-case for nonlinear dynamics of any flavour and described by e.g. Novak and Frehlich [164] for an electric circuit. While the strong localisation of the nonlinearity to a single degree of freedom in the locally nonlinear system is not necessarily representative for physical system's that will be encountered in real world applications, it offers a controllable environment for testing different parameter set-ups.

So, for the following studies, a system, proposed and used by AL-Shudeifat et al. [3], represents the system with the localised nonlinearity. And a system having been used by Rosenberg [192] is the basis for the remaining, completely nonlinear one. These are also using the same basic parameters as the first system. Together they are the cornerstones of the effort to determine the performance of the different reduced bases.

The nonlinear systems to be used for the test-cases for the different reduction methods are selected to be most simple, so that they can easily be implemented and verified and the system's reaction to external forcing remains accessible to engineering instinct for a fast and direct interpretation of observations. The two systems are

1. a basically linear system with a localised cubic nonlinearity, with all neighbouring degrees of freedom connected to each other, resulting in a tri-diagonal, largely constant stiffness matrix,
2. an entirely nonlinear system, where all degrees of freedom are connected to their direct neighbours with cubically nonlinear stiffnesses, in order to achieve an all nonlinear, tridiagonal tangent stiffness matrix.

Both systems are based on a common underlying linear system. None of the systems is strictly conservative. A certain damping is introduced for the reason of numerical stability, see section 2.3.

The two systems comply with the conditions that are most probably to be encountered in real world applications. Worden and Tomlinson [244] require them to have banded matrices and no negative damping.

#### 4.1. PREPARING THE STUDIES

---

The former is ensured by connecting only degrees of freedom neighbours<sup>5</sup> to each other through stiffnesses and damping elements and the latter comes naturally by employing a positive definite damping matrix  $C$ . In addition exclusively nonlinearities of odd order with positive coefficients are used.

The rationale for having two different systems as the basis of the test-cases is to ensure that the used reduced bases are applied to different types of nonlinear systems with different characteristics. One system is defined with a localised nonlinearity only and one system is completely nonlinear. It will hence be an important point to assess if some methods perform differently on the different systems.

The two selected systems comply with the exigencies for admissible systems by Rosenberg [192]. These state that the system is to be able to perform periodic movements with the period  $T$  so that

$$\mathbf{u}(t) = \mathbf{u}(t + T) \quad (4.13)$$

as it was stated in equation (3.30). This condition has to hold for  $t \rightarrow \infty$  and indicates a stationary, not diverging solution that is established over time. Furthermore these periodic movements have to occur around a static equilibrium position with

$$\frac{1}{T} \int_t^{t+T} \mathbf{u}(t) dt = 0, \quad (4.14)$$

again for a period  $T$  towards  $t \rightarrow \infty$ . This notion of a stable equilibrium position is essential for the projection based reduction methods. This equilibrium may be used as the state on which the algorithm for the establishment of the projection basis is based for the necessary linearisations.

The systems also comply with the criteria for a weakly nonlinear system as they allow to focus on the physical meaning of the simulation's results without being hampered by general questions concerning the "existence, uniqueness, boundedness and stability of solutions." (Rosenberg [192])

The overall structure of the systems

$$M\ddot{\mathbf{u}} + C_h\dot{\mathbf{u}} + \mathbf{g}_h(\mathbf{u}) = \mathbf{f}_{E,k}(t) \quad (4.15)$$

is modelled after equation (2.82). The nonlinear part is defined by the vector of nonlinear forces  $\mathbf{g}_h$ . The indices  $k$  and  $h$  indicate the type of nonlinearity and the type of the excitation. The index  $h$  indicates if the system is locally or entirely nonlinear. The excitation of the systems is defined by the term  $\mathbf{f}_{E,k}(t)$ . The index  $k$  indicates if the excitation is either harmonic or of impulse type. The components of the four test-cases corresponding to the indices  $k$  and  $h$  are defined in the following.

---

<sup>5</sup>In real world application the bandedness of the matrices would be assured by the use of an optimizer for the bandwidth of the matrices, which orders the nodes to this effect.

**4.1.3.1.1 Locally nonlinear system** The first system depicted in figure 4.1, comprises only a localised nonlinearity

$$\mathbf{g}_{\text{loc}}(\mathbf{u}) = \begin{bmatrix} g_1(\mathbf{u}) \\ \vdots \\ g_i(\mathbf{u}) \\ g_j(\mathbf{u}) \\ \vdots \\ g_n(\mathbf{u}) \end{bmatrix} = \begin{bmatrix} ku_1 + k(u_1 - u_2) \\ \vdots \\ k(u_i - u_{i-1}) - k(u_{i+1} - u_i) \\ k(u_j - u_{j-1}) - k(u_{j+1} - u_j) + k_{NL}u_j^3 \\ \vdots \\ k(u_n - u_{n-1}) \end{bmatrix}. \quad (4.16)$$

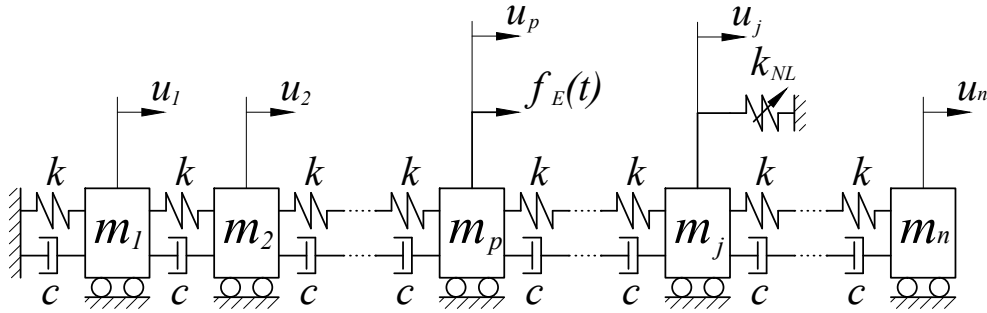


Figure 4.1: The locally nonlinear system

**4.1.3.1.2 Entirely nonlinear system** The second system, shown in figure 4.2, is entirely nonlinear

$$\mathbf{g}_{\text{ent}}(\mathbf{u}) = \begin{bmatrix} g_1(\mathbf{u}) \\ \vdots \\ g_i(\mathbf{u}) \\ \vdots \\ g_n(\mathbf{u}) \end{bmatrix} = \begin{bmatrix} ku_1 + k(u_1 - u_2) + k_{NL}u_1^3 + k_{NL}(u_1 - u_2)^3 \\ \vdots \\ k(u_i - u_{i-1}) - k(u_{i+1} - u_i) + k_{NL}(u_i - u_{i-1})^3 - k_{NL}(u_{i+1} - u_i)^3 \\ \vdots \\ k(u_n - u_{n-1}) + ku_n + k_{NL}(u_n - u_{n-1})^3 + k_{NL}u_n^3 \end{bmatrix}. \quad (4.17)$$

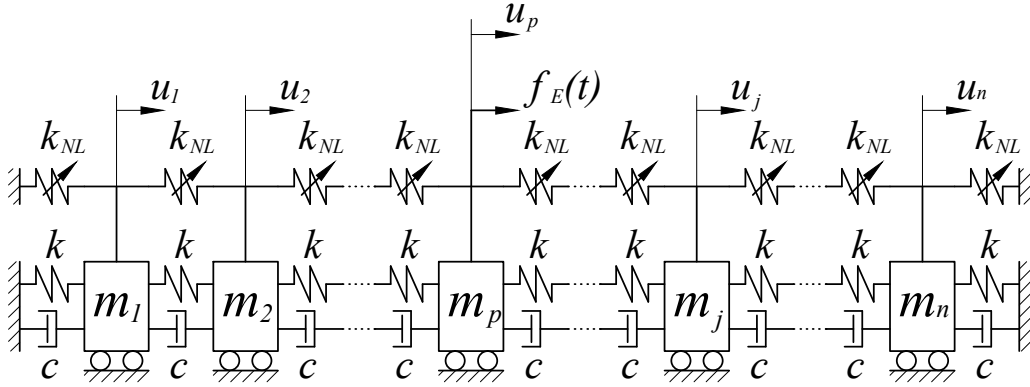


Figure 4.2: The entirely nonlinear system

**4.1.3.1.3 Defining the mass matrix and the damping matrix** For both systems the mass matrix is set to the unity matrix to avoid inertial coupling  $M = I$ :

$$M = \begin{bmatrix} 1 & & & & \\ & 1 & & & \\ & & 1 & & \\ & & & \ddots & \\ & 0 & & & 1 \\ & & & & & 1 \end{bmatrix}. \quad (4.18)$$

The absence of inertial coupling is a prevailing and defining feature that allows concentrating the ongoing study on geometric nonlinearities.

The damping matrix  $C$  is constructed as a fraction of the stiffness matrix of the underlying linear system

$$C_h = \epsilon \bar{K}_h = \epsilon \left. \frac{\partial g_h(\mathbf{u})}{\partial \mathbf{u}} \right|_{\mathbf{u}_0}. \quad (4.19)$$

For the locally nonlinear system, whose nonlinear internal forces are defined in equation (4.16), this results in

$$C_{loc} = \epsilon \begin{bmatrix} 2 & -1 & & & \\ -1 & 2 & -1 & & \mathbf{0} \\ & -1 & 2 & -1 & \\ & & \ddots & \ddots & \ddots \\ \mathbf{0} & & & -1 & 2 & -1 \\ & & & & -1 & 1 \end{bmatrix}. \quad (4.20)$$

The distinctive feature of  $C_{extloc}$  is the 1 in the last element of the diagonal, which indicates the unclamped right-hand side of the locally nonlinear system in figure 4.1.

For the entirely nonlinear system, with its in nonlinear internal forces defined in equation (4.17), the



## 4.1. PREPARING THE STUDIES

---

**4.1.3.3.1 Harmonic excitation** The first, harmonic excitation introduces a sinusoidal force and applies it to the  $p$ -th degree of freedom. It reads

$$\mathbf{f}_{E,\text{har}} = \begin{bmatrix} f_{E,1} \\ \vdots \\ f_{E,p} \\ \vdots \\ f_{E,n} \end{bmatrix} = \begin{bmatrix} 0 \\ \vdots \\ \hat{f}_E \sin(\Omega t) \\ \vdots \\ 0 \end{bmatrix}, \quad (4.22)$$

where the amplitude is defined by  $\hat{f}_E$  and the frequency by  $\Omega$ . The numeration of the components  $1 \dots n$  corresponds to the numeration of the degrees of freedom of the full order system. A phase shift or a cosine-part are not included because the simulations are started from a static equilibrium configuration and the smooth raise of the sine as a function of the progressing time assures the absence of numerical problems.

**4.1.3.3.2 Impulse excitation** The Dirac  $\delta$ -function is an impulse excitation and in addition to the harmonic excitation the most typical test-case for many applications.

It is defined for an instant in time  $t_\delta$  as

$$\delta(t_\delta) = \begin{cases} 1 & \forall t = t_\delta \\ 0 & \forall t \neq t_\delta \end{cases}, \quad (4.23)$$

and can be found in every textbook on mathematics, such as Bartsch [21]. In its application as the external forcing this theoretical definition is used as

$$\mathbf{f}_{E,\text{imp}} = \begin{bmatrix} f_{E,1} \\ \vdots \\ f_{E,p} \\ \vdots \\ f_{E,n} \end{bmatrix} = \begin{bmatrix} 0 \\ \vdots \\ \hat{f}_E \delta(t_\delta) \\ \vdots \\ 0 \end{bmatrix}. \quad (4.24)$$

To be numerical feasible, the Dirac impulse, which is in theory infinite in amplitude and infinitesimal in duration, is modelled as a look-up table for the external forces, which in turn is based on a formulation that expresses the amplitude  $\hat{f}_E$  as a non-uniform rational B-spline dependent on the time  $t$ . This approach, based on the work of Yassouridis [246], allows for meticulous control over the slopes and transitions of an impulse of finite duration and finite amplitude that is used to model the Dirac- $\delta$  impulse.

In this study the impulse has the prescribed amplitude  $\hat{f}_E$  and a duration of just about<sup>6</sup> 0.22. The latter value is set in an arbitrary way to this value which is negligible with respect to the overall simulated period of time  $T$  and the period of the of the harmonic excitation. To initiate the systems' displacements from the all-zero initial conditions at  $t = 0$  without numerical problems, the precise instant  $t_\delta$  at which the Dirac- $\delta$  impulse is set to occur is defined as half its duration, i.e.  $t_\delta = 0.11$ . This bypasses all numerical problems associated with a non-zero initial forcing and a zero external forcing, which do not induce any displacements and lead to convergence problems within the nonlinear Newmark solution scheme, alike.

Repeating Dirac impulses at a certain frequency is known as Dirac comb. A Dirac comb is not treated

---

<sup>6</sup>There are no units assigned to the parameters of the test-cases. This is expanded further in section 4.1.3.4

during this study because it resembles, in general lines, a degenerate harmonic excitation.

### 4.1.3.4 Setting the values of the parameters of the test-cases

For the different reduction techniques different studies are to be performed. This is due to the fact that the parameters that define each reduction method can be divided in global and it local ones. A global parameter is a parameter that describes the system to be solved and which is not proprietary for a specific reduction method or a specific method for creating a reduced basis. An example for a global parameter would e.g. be the size of the reduced system  $r$ , which can equally well defined for all reduction techniques. In contrast, local parameters are distinct for a specific reduction method, a specific method for creating a reduced basis or the specific method for obtaining a transient solution and thus limited to within the scope of the overall process to the particular reduction method.

Only global parameters will be changed in the subsequent studies. The local parameters for the different reduction methods are defined hereunder and remain, once determined, unchanged throughout the studies to ensure comparability. For the proper determination of the local parameters preliminary studies are conducted.

- global parameters: The paramount global parameter of a reduction process is the size  $r$  of the reduced order model. It determines the gain in computational speed and the loss of correctness compared to full order model of dimension  $n$ . The size of the reduced order model will be the discriminating variable against which the different error metrics will be plotted.

Other global parameters that are not set on the level of a single reduction method are the parameters linked to the excitation of the system, which are determining e.g. its type, its amplitude and its point of application. These global parameters are varied for the following studies to determine their impact on the performance of the different methods and the robustness of the different methods with respect to changing global parameters.

- local parameters are defined individually for each reduction method. Unlike the global parameters the local parameters are not changed during the upcoming studies to ensure comparability between the different studies. They are set beforehand to obtain most reliable results from the different reduction methods.

The local parameters are mainly convergence criteria within the nonlinear Newmark algorithm or within the algorithms from section 3.3, which establish the reduced basis. These local parameters determine e.g. whether the obtained precision is sufficient<sup>7</sup>. As always in numerical simulations it is a very delicate choice that has to balance the quality of the result with the necessary computational effort.

The equations above, which define the different systems and the two excitations, depend on several parameters. They are considered as global parameters and some of them will thus be used as variables in the studies to follow. These parameters and the values assigned to them by AL-Shudeifat et al. [3] are

- $n$ , the order of the overall system. The order of the overall system is to be chosen as a compromise between a sufficiently large system and a sufficiently small computation time. Like the entirety of the parameters' values too, it is set to the values proposed by AL-Shudeifat et al. [3], who selected in this case  $n = 20$ ,
- $j$ , the degree of freedom where the nonlinearity is localised is set to  $j = 16$ ,
- $p$ , the degree of freedom subjected to the external forcing. The selection of  $j$  and  $p$  introduces the notion of a 'distance' between the nonlinearity and the point of application of the external forcing. As the used nonlinear Newmark scheme yields a temporal solution this 'distance' determines how fast the external forcing's influence impacts the nonlinearity. AL-Shudeifat et al. [3] proposes  $p = 4$ ,

---

<sup>7</sup>Some local parameters of the POD method require special attention and their determination is pursued in the dedicated annex section A.1.1.

- $\epsilon$ , the damping parameter which defines the linear damping matrix  $C_L$  in equation (4.15). The damping matrix is obtained by scaling the underlying linear stiffness matrix with the parameter  $\epsilon = 0.04$ . Its impact on the system's dynamic is rather small and the implied, small damping ratio places all simulations to be conducted in the transient phase. This is contradictory to the initial intention, stated above, of judging the reductions' performance based on the stationary response of the system. But as a concession to solution time and due to the fact that a very characteristic response is established very quickly this consideration of the transient phase has been judged admissible,
- $\hat{f}_E$ , the amplitude of the external forcing in equations (4.22) and (4.24) is set to  $\hat{f}_E = 3$  and
- $\Omega$ , the frequency of the external forcing to  $\Omega = 0.2289$ , as the average value of the first three lowest eigenfrequencies of the underlying linear system of the generic description of the systems in equation (4.15).

## 4.2 Conducting the studies and analysing the results

The conduction of the studies follows the aims of comparing the reduced bases among each other and investigating their robustness, as are defined in section 4.1.1.

In a first step, the comparison of the reduced bases is accomplished. It covers an inspection of the shapes of the reduced bases' column vectors, which carry the information of the system's displacements, an overview over the actual physical displacements coming from reconstructed reduced order solutions and, ultimately, the application of the score, which was created as a dedicated criterion for the comparison.

In a second step the investigation of the reduced bases' robustness is carried out. It starts with the description of the configurations of parameters that are used to alter the excitation and then surveys the relative performance of the different reduced bases.

While the survey's basic data is strictly deterministic because the simulated physical effects and employed mathematical treatments always deliver the same result, the survey's character becomes somewhat heuristic. This is because the enormous amount of data and combinations of possibilities requires efficient and abstracting data mining techniques. This is still not comparable to classic heuristic surveys with probabilities, as they are common in e.g. social sciences, yet an ultimately pervasive analysis of all acquired data cannot be performed.

### 4.2.1 Comparison of the reduced bases

The comparison of the different reduced bases is targeted at identifying the most suited reduced basis for a given test-case. To this end all bases are applied to the four different test-cases and the quality of the reconstructed solution obtained from the different reduced bases is compared for each test-case. The order  $r$  of the reduced system is a parameter.

In line with the aim of this study, which is formulated above, the following steps are taken.

- The test-case is defined as a combination of the systems and the excitations presented in sections 4.1.3.1 and 4.1.3.3, respectively, and it is parameterised with the values presented in 4.1.3.4.
- The reference solution for the test-case at hand is established with a full order nonlinear Newmark scheme, as described in section 3.2.1.1. This solution is stored and serves as the reference for assessing the quality of the reduced solutions.
- The procedures described in section 3.3 are used to establish the different reduced bases at different orders  $r$ . The Second Order Terms of the LNM and the Ritz-vector are not included due to their specific construction and varying size. Their scores are discussed in the dedicated annex section B.
- These bases are used to create a reduced system, as in equation (3.11), which is then solved in time

with a reduced nonlinear Newmark scheme (section 3.2.2.1). The inflation formulation of the nonlinear forces vector is retained, equation (3.96), in order to ensure that all appearing errors are solely due to the reduced basis.

- Finally, the full order solution, reconstructed from the just obtained reduced order solution by means of equation (3.1), is compared with the reference solution at hand, using the error metrics from section 4.1.2.1.

### 4.2.1.1 Inspecting the shapes of the column vector of the reduced bases

The shapes of the column vectors of the reduced bases offer a basic, yet highly insightful, instrument in comparing the different methods. The figure 4.3 shows the first and the second column vector of the different reduced bases for the locally nonlinear system under harmonic excitation. The first vector is traced with markers and the second vector is traced without markers. The vectors' constitutions are in accordance with the section 3.3.7 to ensure comparability.

The LNM are oblivious to the presence of the nonlinearity and the excitation. If they are obtained at maximum displacements this changes. They show a pronounced bend in the first vector at  $j = 16$ , where the nonlinearity is located. Most of the remaining methods' vectors, Ritz-vectors, POD, SOD, and LELSM, also show this distinctive feature and even add a slight bend at  $p = 4$ , the point of application of the excitation. It is remarkable how similar the first vectors of the different methods look. The second vector of the CVT also shares these distinctive features. The LELSM with Sh-B-vectors have a single entry at the degrees of freedom where the nonlinearity and the external forcing are localised.

Taking the POD-vectors, whose order depends by definition on the energy they are capturing, as gauge it can be stated nearly all discussed methods allow to capture the largest portions of the energy in the displacements rather well.

All APR vectors depend on the order of the reduced system due to the updating. In this point the APR approach differs from all other methods, where the first vectors remain untouched while other vectors are added to the basis if the order of the reduced system is increased. The example in figure 4.3 shows the first two vectors for  $r = 2$ . They demonstrate well the impact of the localised force application and the localised nonlinearity. If  $r$  is increased, the updating process smears these features and the vectors show a barely coherent behaviour.

While the first column vectors are largely comparable the second vectors show a larger variety, yet again with distinctive features at the degrees of freedom 4 and 16. These on-setting differences between the vectors increase for higher vectors and determine whether the reduced basis is capable of correctly resolving the details of the solution and capturing its characteristics.

For the three remaining test-cases the first two column vectors of the different reduced bases are shown in figures 4.4 to 4.6. The two figures 4.5 and 4.6 for the entirely nonlinear system display common shapes of the column vectors. These are distinct for the entirely nonlinear system, which is held by two grounded nonlinearities at both extremities.

Also, the difference of the APR vectors between the test-cases under harmonic excitation and the ones under impulse excitation is notable. The point of application of the impulse excitation is very prominent in figures 4.4 and 4.6. This may come from the nature of the APR method, which solves transient solutions of increasing order. In the case of an impulse solution the obtained residual rises so fast that the displacement is still localised, when the algorithm stops.

### 4.2.1.2 Surveying the time histories of reconstructed physical quantities

Reconstructed physical quantities are quantities with a physical signification that are obtained by inflating the reduced transient solution that has been obtained in generalised coordinates. The survey of their time

#### 4.2. CONDUCTING THE STUDIES AND ANALYSING THE RESULTS

histories is the next step in assessing the quality of a reduced solution. Surveying the time histories allows to gauge the expressiveness the more abstracting error metrics, e.g. the score. The most important physical quantities whose time histories have to be surveyed are naturally the displacement. The displacements

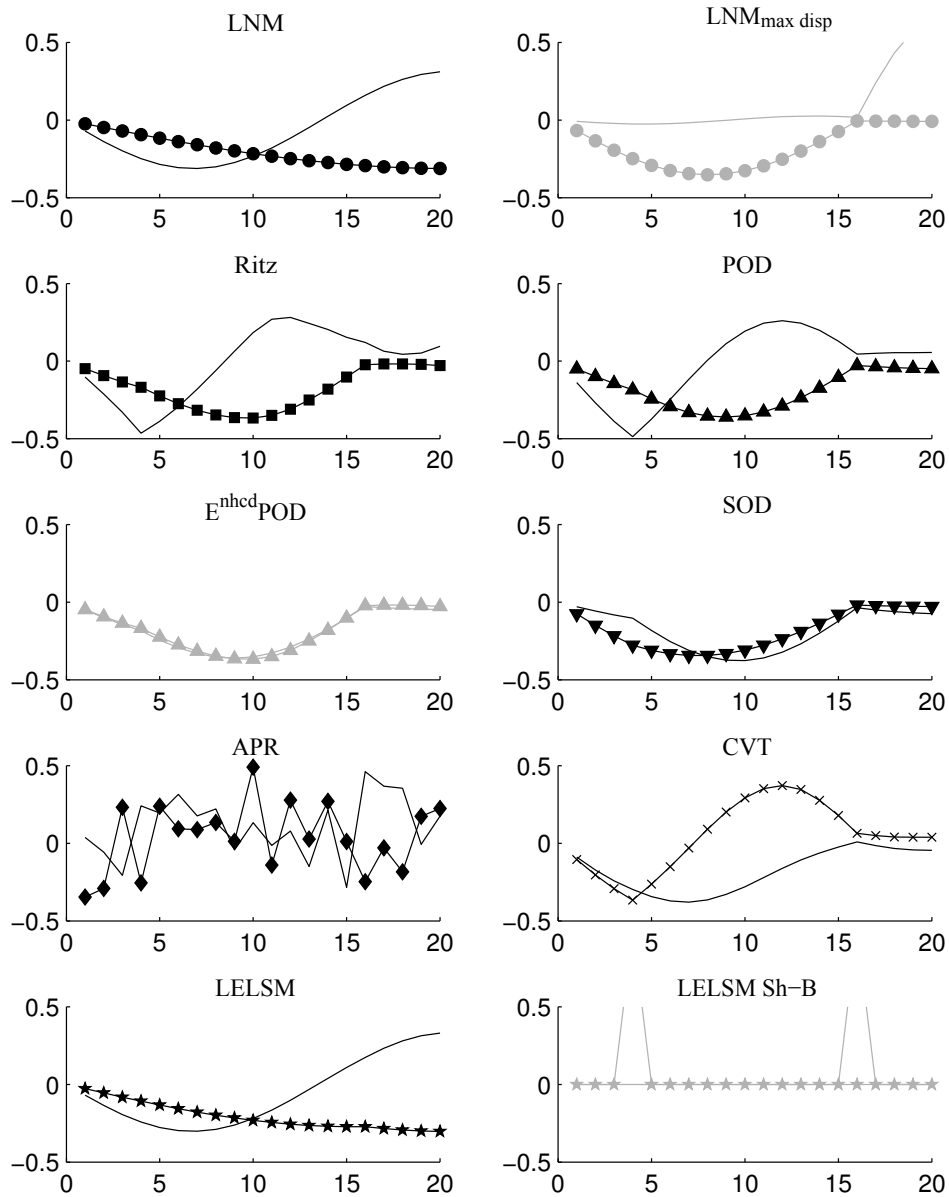


Figure 4.3: The first two column vectors of the different reduced bases for the locally nonlinear system under harmonic excitation

## 4.2. CONDUCTING THE STUDIES AND ANALYSING THE RESULTS

are given for all four test-cases and all applied reduced bases. The survey of the displacements of the entirely nonlinear system under harmonic excitation is augmented by combining the displacements with the velocities and plotting them over the phase plane. The combination of displacements and velocities

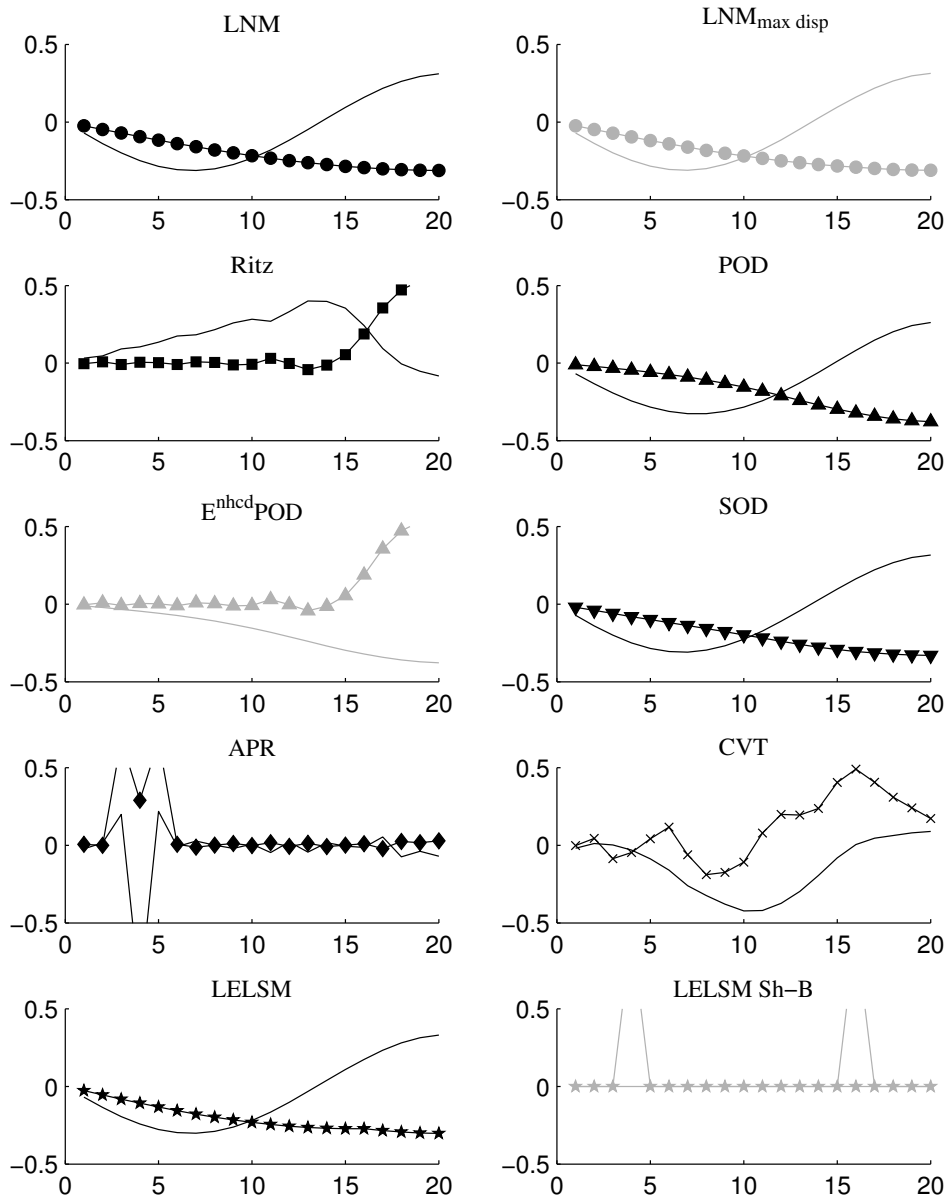


Figure 4.4: The first two column vectors of the different reduced bases for the locally nonlinear system under impulse excitation

#### 4.2. CONDUCTING THE STUDIES AND ANALYSING THE RESULTS

is eventually continued by obtaining information on the energy content of the reduced system from the displacements and velocities. The survey of all these quantities illustrates the qualities of the transient solutions that are obtained with the different reduced bases and prepares the application of the abstracting

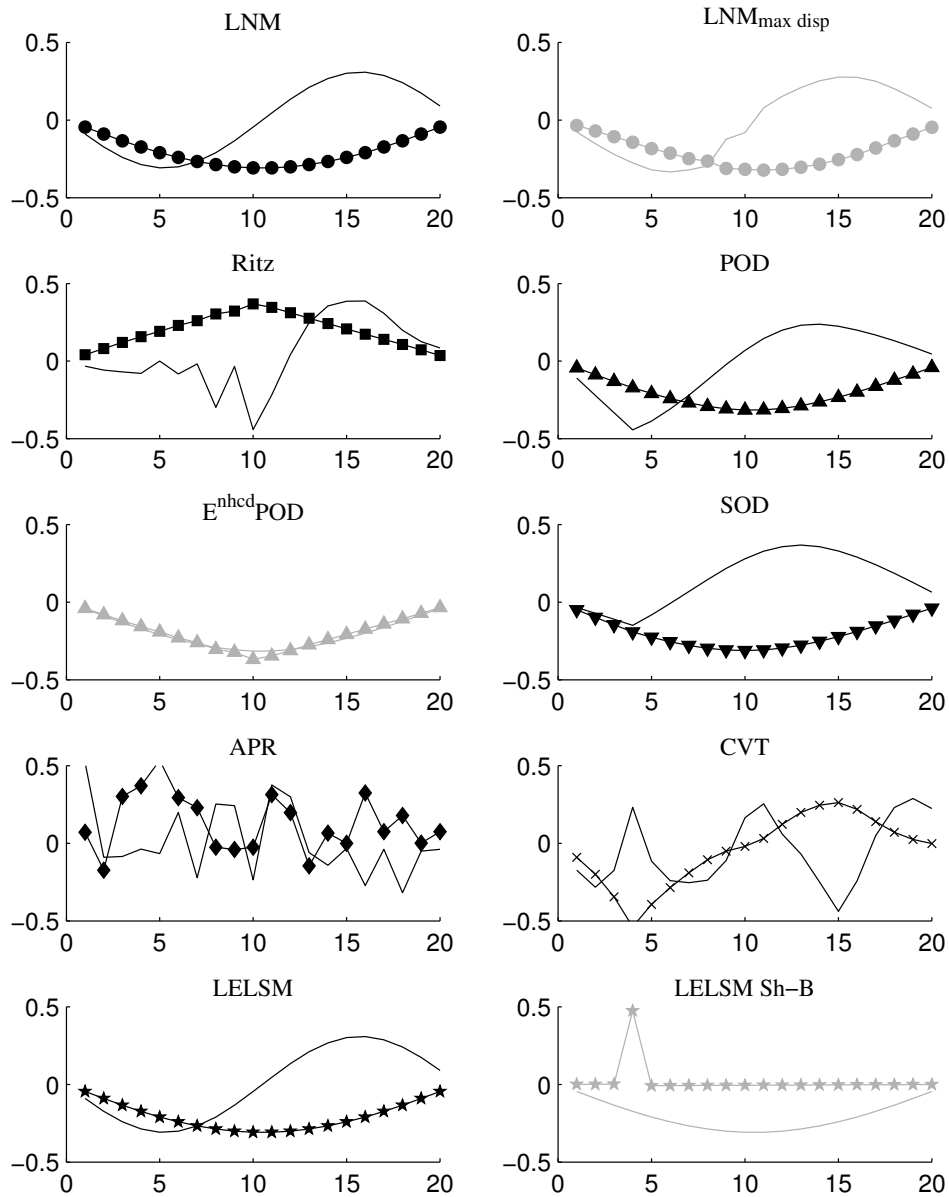


Figure 4.5: The first two column vectors of the different reduced bases for the entirely nonlinear system under harmonic excitation

## 4.2. CONDUCTING THE STUDIES AND ANALYSING THE RESULTS

error metric of the score in the following section.

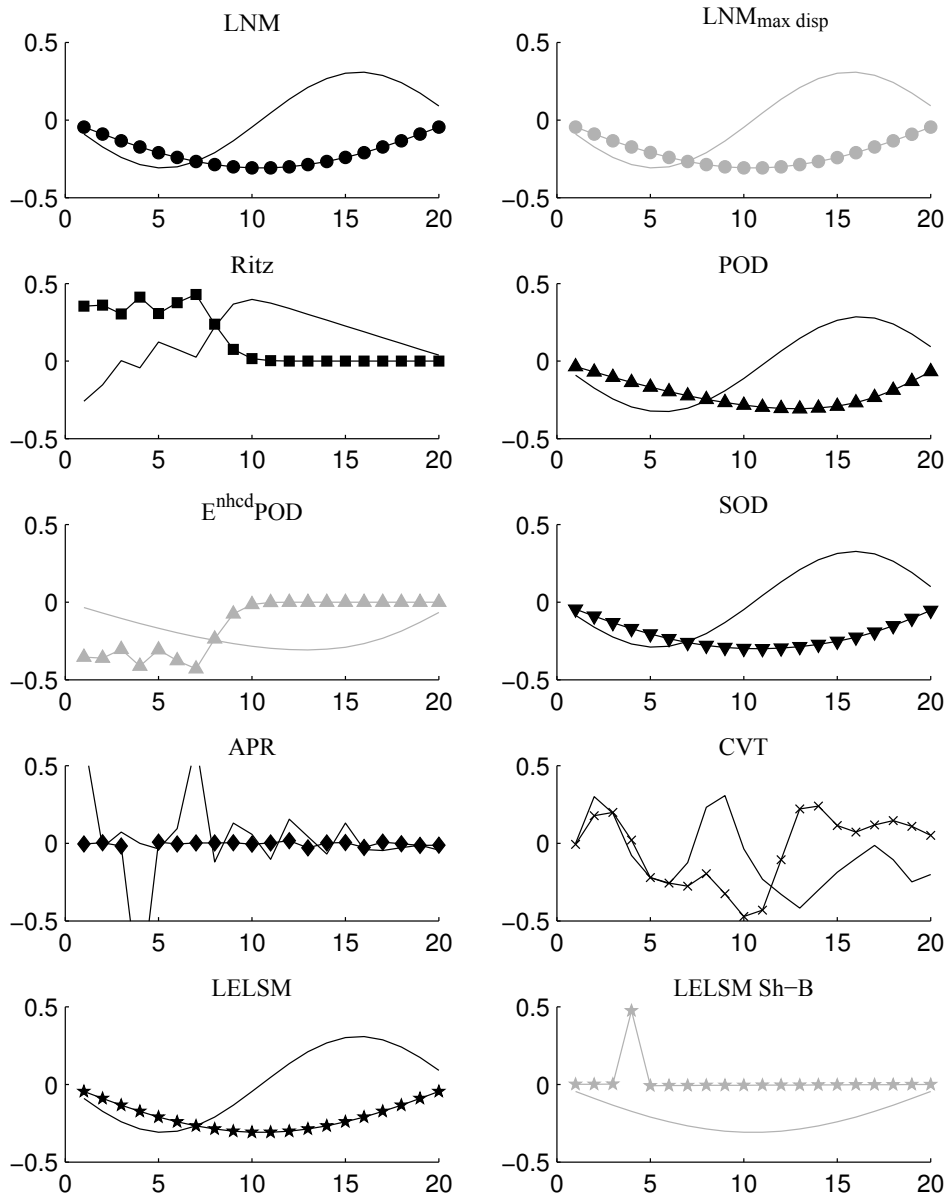


Figure 4.6: The first two column vectors of the different reduced bases for the entirely nonlinear system under impulse excitation

**4.2.1.2.1 Displacements** The physical displacements of the transient solutions are the central touch-stone for the determination of the quality of the reduced model. The displacements have to be recreated faithfully because they provide the vital information of the position of the part at a given time. Such information is crucial in e.g. a situation where clearances with respect to adjacent structures are required. The quality of the recreation of the physical displacement forms hence a major part of the score as it is introduced in section 4.1.2.2.

The figure 4.7 shows the physical displacements of the locally nonlinear system under harmonic excitation obtained with different reduced bases for the degree of freedom where the nonlinearity is localised and  $r = 4$  as the order of the reduced model. The reference solution is shown in dark grey in each plot.

The figure shows that most methods can recreate the overall response rather well. The LNM, the CVT and the LELSM basis also tend to resolve the fine ripples, but with a too low frequency and a too large relative amplitude. Only the Ritz-vectors tend to resolve this feature of the reference solution correctly.

The figure 4.7 does only partially reflect the findings of the analysis of the shapes of the column vectors of the reduced bases in figure 4.3 because higher modes contribute in general significantly to the bases' ability to recreate the reference solution. In order to take into account the quality of the reduced solution for all degrees of freedom the results are concentrated with the score.

## 4.2. CONDUCTING THE STUDIES AND ANALYSING THE RESULTS

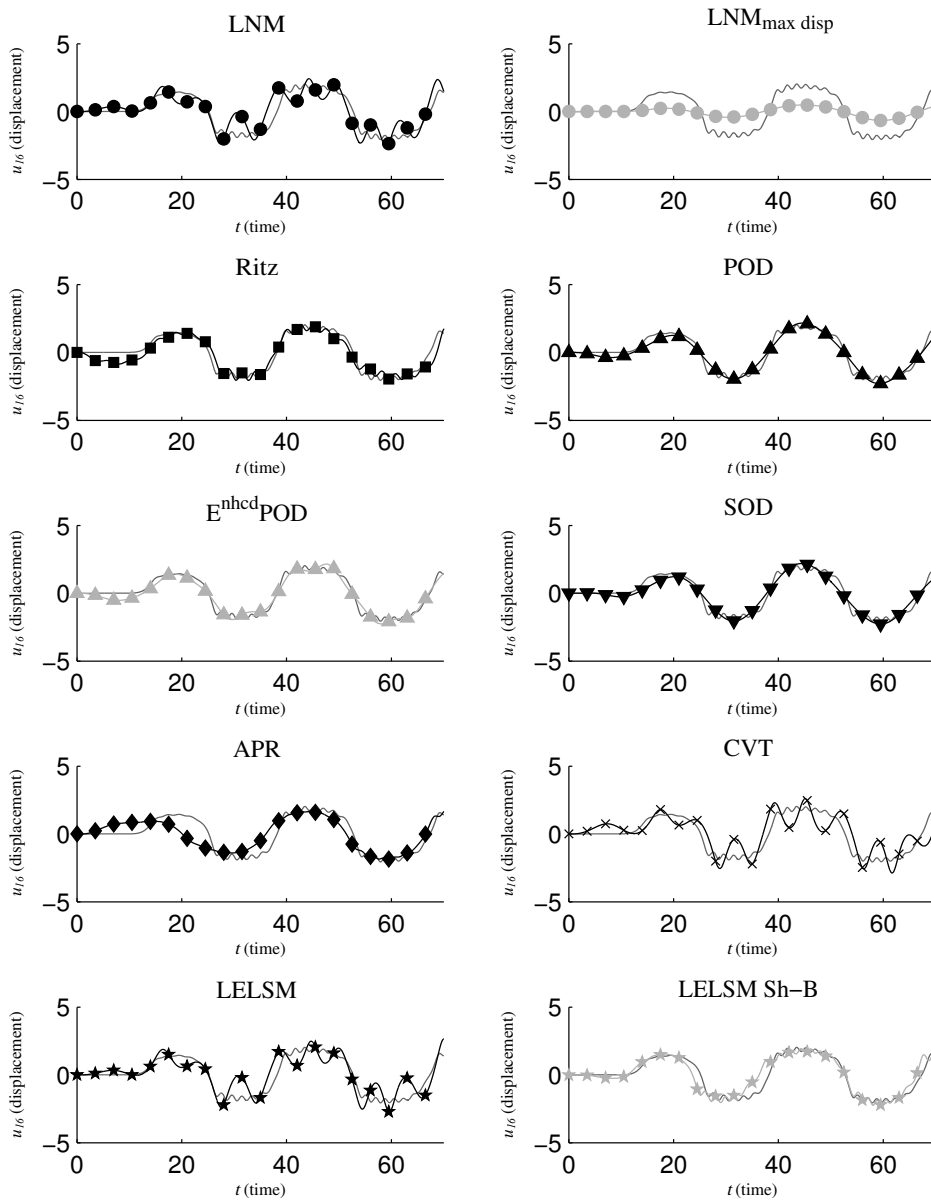


Figure 4.7: The time histories of the 16<sup>th</sup> degree of freedom of the locally nonlinear system under harmonic excitation obtained with different reduced bases at  $r = 4$

## 4.2. CONDUCTING THE STUDIES AND ANALYSING THE RESULTS

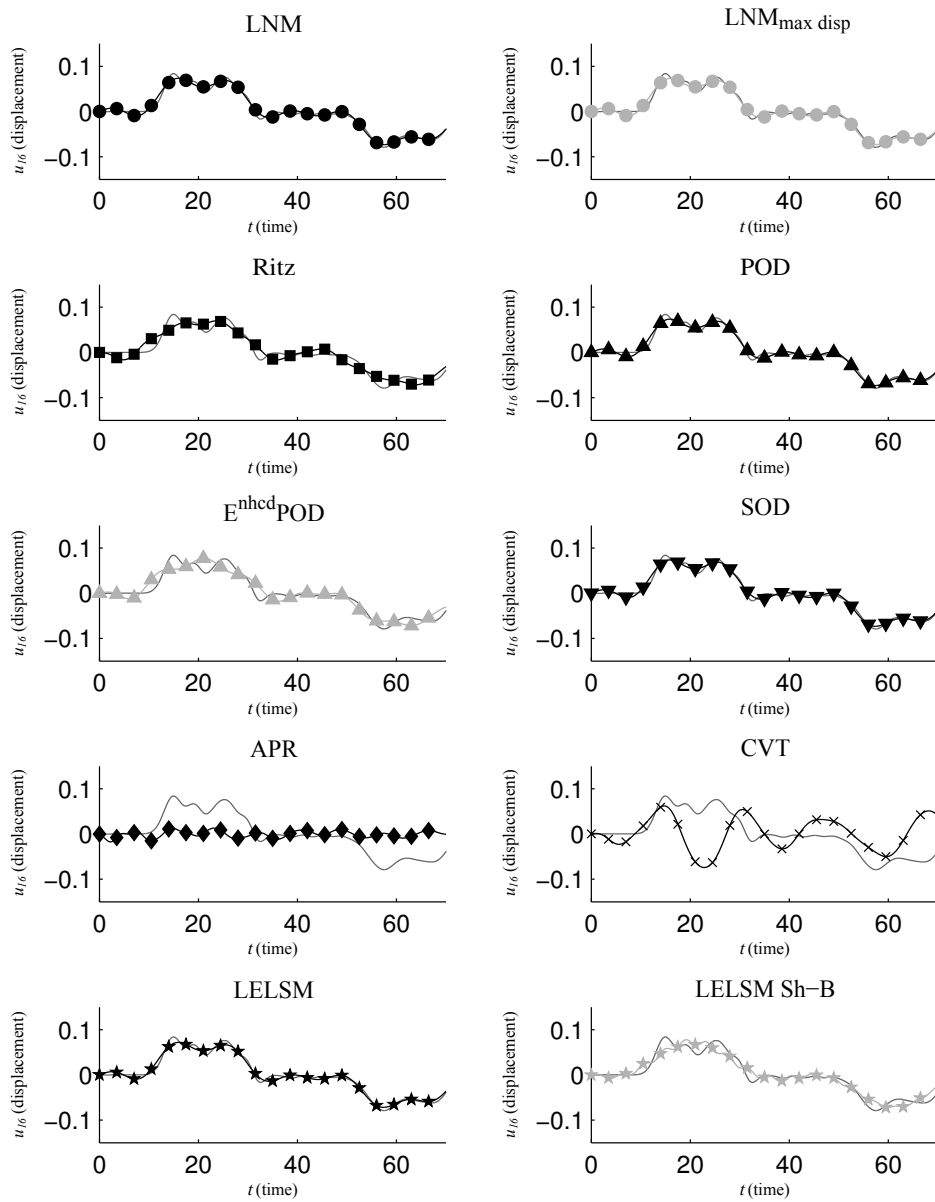


Figure 4.8: The time histories of the 16<sup>th</sup> degree of freedom of the locally nonlinear system under impulse excitation obtained with different reduced bases at  $r = 4$

## 4.2. CONDUCTING THE STUDIES AND ANALYSING THE RESULTS

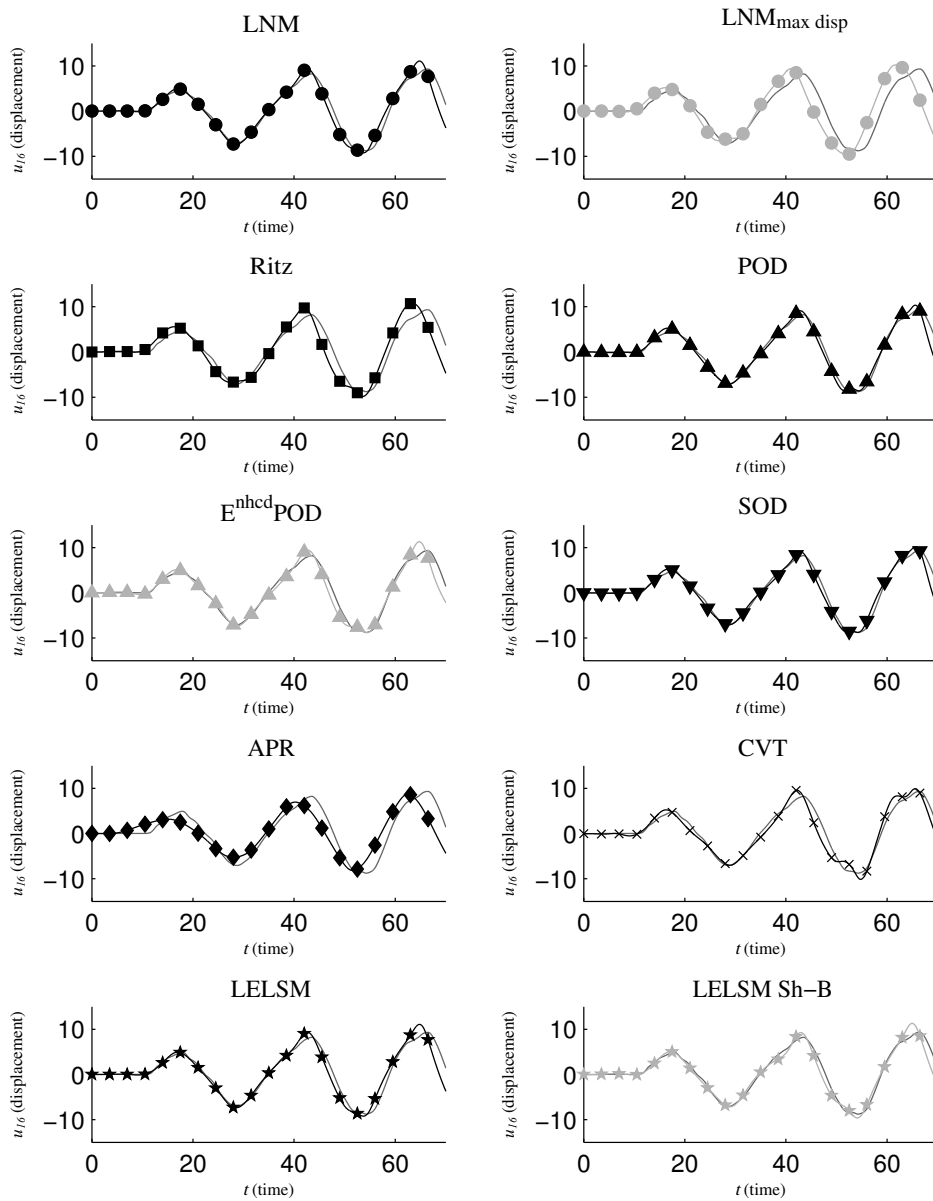


Figure 4.9: The time histories of the 16<sup>th</sup> degree of freedom of the entirely nonlinear system under harmonic excitation obtained with different reduced bases at  $r = 4$

## 4.2. CONDUCTING THE STUDIES AND ANALYSING THE RESULTS

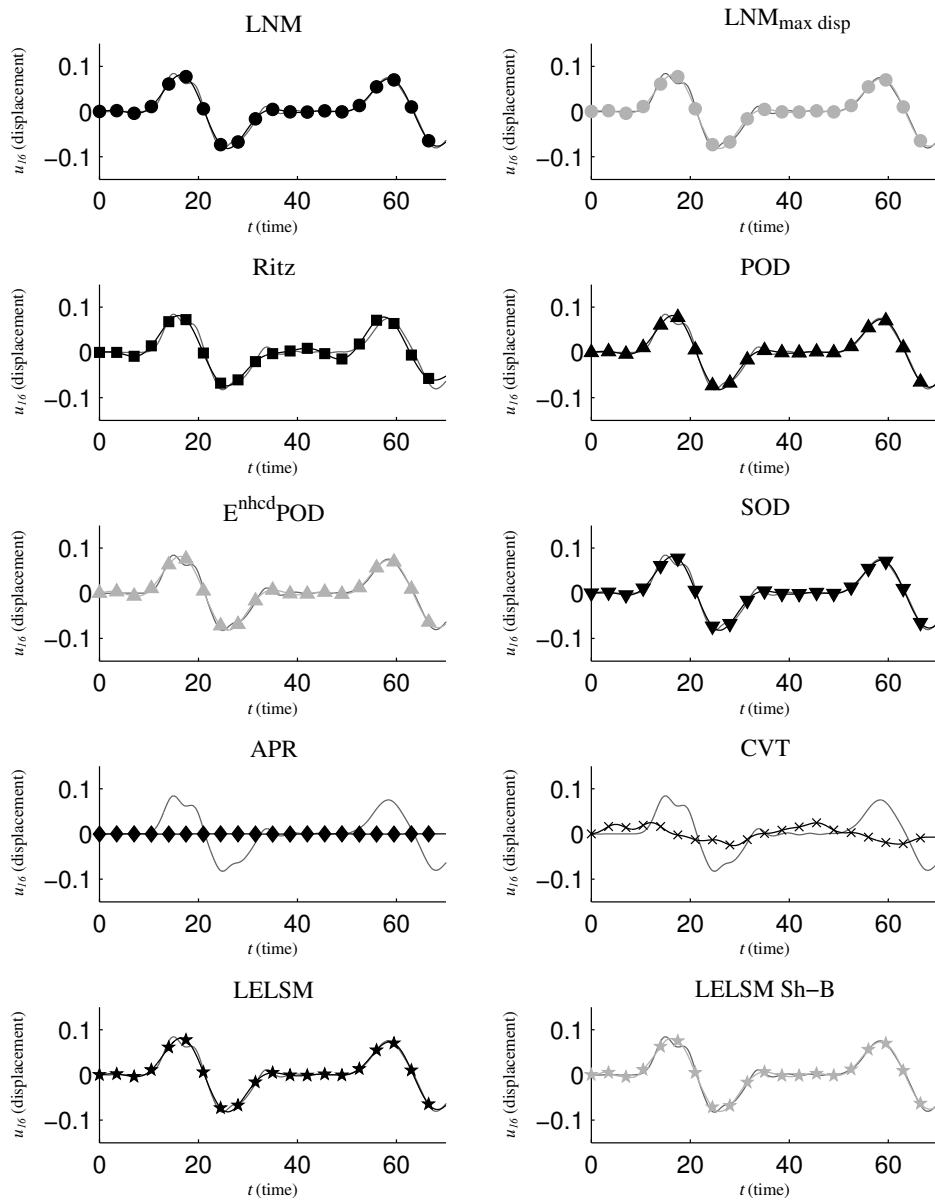


Figure 4.10: The time histories of the 16<sup>th</sup> degree of freedom of the entirely nonlinear system under impulse excitation obtained with different reduced bases at  $r = 4$

The same displacements for the remaining test-cases are shown in figures 4.8 to 4.10. Together, the four figures allow to gain an impression, how the shapes of the column vectors from figures 4.3 to 4.6 translate to the quality of the transient solutions. Furthermore, the four figures in this section prepare the application of the score in the following section. There, the reconstructed reduced solutions are ranked with different criteria and then compared among each other. This is done for all degrees of freedom and much more orders of the reduced system than just  $r = 4$ .

**4.2.1.2.2 Phase space** The phase space representation of a displacement and a velocity is commonly used for determining the attractors and bifurcation characteristics of the stationary solution of a dynamic system. For transient solution the phase diagram illustrates how the solution stabilises.

Figure 4.11 plots the displacement  $u_{16}$  and the velocity  $\dot{u}_{16}$  of the entirely nonlinear system under harmonic excitation. The time history of this displacement is already plotted in figure 4.9, above. Again the reduced systems are obtained at  $r = 4$ . The LNM and the POD vectors are used as reduced bases.

The entire figure 4.11 has to be read clockwise. The solutions start at  $u_{16}^{(0)} = 0$  and  $\dot{u}_{16}^{(0)} = 0$  in the centre of the figure and begin to evolve in the positive direction for the displacement  $u_{16}(t)$  and in positive direction for the velocity  $\dot{u}_{16}(t)$ . The markers on the line are equidistant in time and show an increasing velocity towards the end of the simulated period.

The phase diagram highlights the problems that reduced models have with the resolution of fine structures in the transient solution. This becomes evident while observing the first decreasing period of the displacement between  $5 \geq u_{16} \geq -5$  at  $\dot{u}_{16} \approx -1.5$ . The first order solution displays a prominently oscillating velocity  $\dot{u}_{16}$  during this period. The velocities that are reconstructed from the reduced solutions are basically constant during the same period.

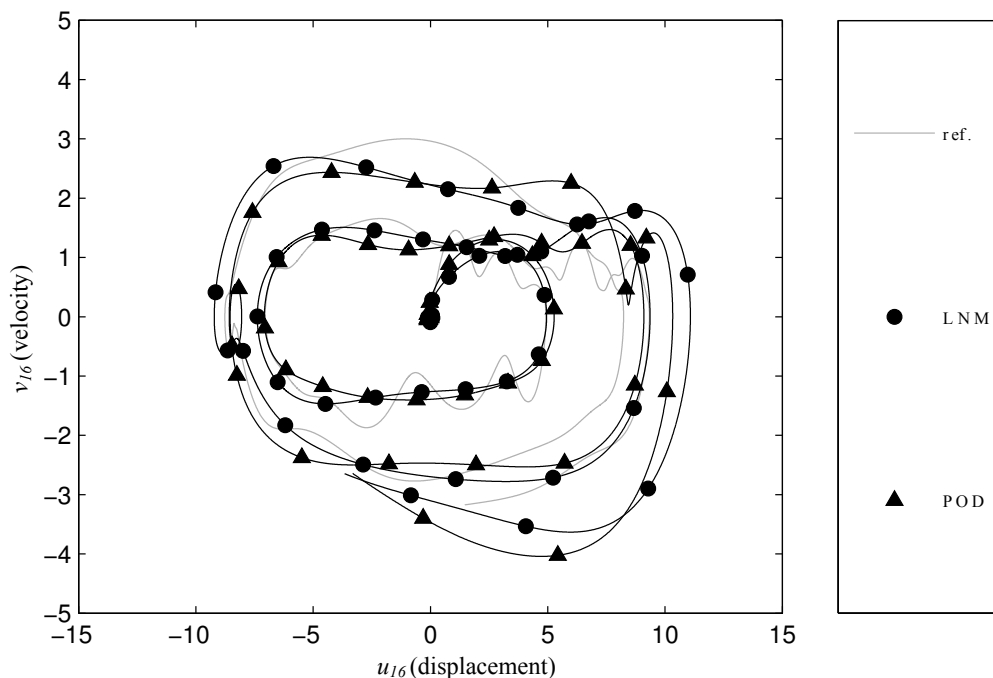


Figure 4.11: The phase space representation of the 16<sup>th</sup> degree of freedom of the entirely nonlinear system under harmonic excitation obtained with different reduced bases at  $r = 4$

As such, the phase plot highlights the possible shortcomings of reduced solutions. The most characteristic

shortcoming lies in their difficulty to resolve fine structures in the reference solution. These fine structures are flattened out with the truncation of the reduced basis. However, on a general level, it can be observed that the displacements are reconstructed rather well and even approximated in a conservative fashion. This confirms the results that are obtained from figure 4.9.

**4.2.1.2.3 Energy** The energy that is present in the system at a given time  $t_j$  and the evolution of this energy are a good indicator for the stability of the solution. The energy is injected into the system by the work done by the external forcing. As the locally nonlinear system is barely damped it can be expected that the energy contained in the system increases during the transient solution. It is not dissipated at the same rate with which is injected into the system.

The energy in the system is the sum of the potential energy and the kinetic energy<sup>8</sup>. The energy of the actual solution of the system at the instant  $t_j$  is defined as

$$E^{(\text{actual solution})}(t_j) = (\Phi \mathbf{q}(t_j))^T \mathbf{K} \Phi \mathbf{q}(t_j) + (\Phi \dot{\mathbf{q}}(t_j))^T \mathbf{M} \Phi \dot{\mathbf{q}}(t_j) \quad (4.25)$$

The relative energy that is plotted in figure 4.12 is defined as

$$E(t_j) = \frac{E^{(\text{actual solution})}(t_j)}{\max(E^{(\text{reference solution})}(t_j))} \quad (4.26)$$

It is normalised with the maximum of the energy of the reference solution in order to stress the most important result of the figure.

The most important result to be drawn from figure 4.12, is that there may be more energy in the reduced system than in the full order system. This can happen if mode that contribute to inter-degree-of-freedom damping are not included in the truncated reduced basis. Here, the reduced systems remain stable, even though they contain more energy than the full order system. Should the reduced model become unstable a verification of the development of the total energy could explain why this instability occurs.

Placzek [181] works on this aspect under the denomination of calibration in his dissertation. The calibration of the reduced model is conceived to make up for the loss of damping during the reduction. However, this loss of damping is predominantly due to neglecting several highly nonlinear operators for e.g. boundary layers. This is not the case for the current problem. Here all operators from the full order system are accounted for in the reduced model. Here, the loss of damping comes solely from the introduction of the reduced basis.

Amsallem and Farhat [14] propose a method that conserves the property of the stability of the full order system in the reduced order model. Their approach is however not applied, because the reduced models of the used test-cases do not show a particularly unstable behaviour even while containing more energy than the full order system.

---

<sup>8</sup>This is already used in equation (4.7) for the criterion of the energy difference.

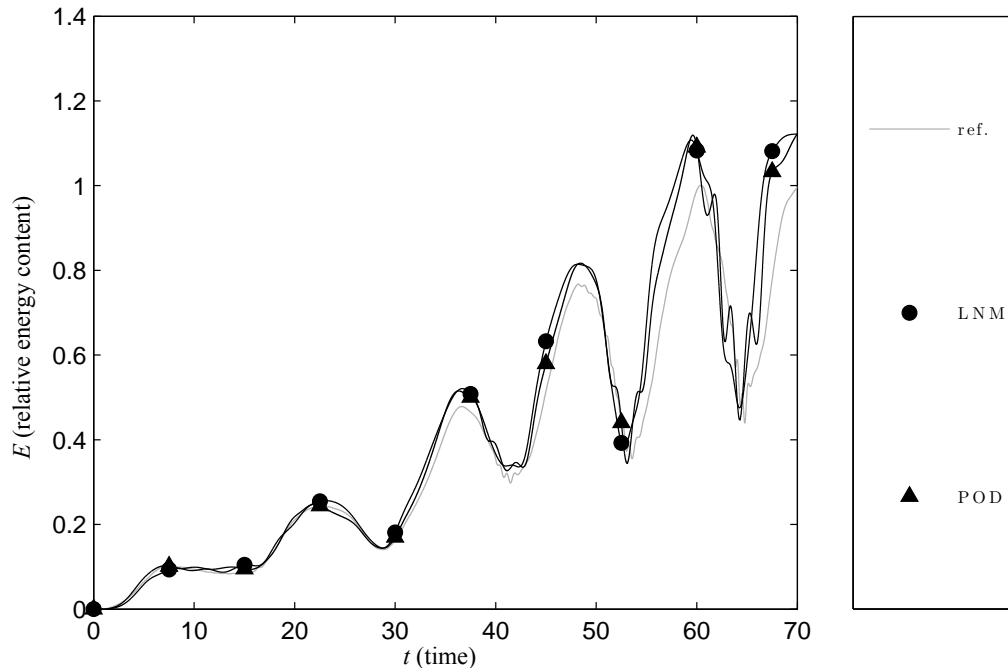


Figure 4.12: The relative energy of the entirely nonlinear system under harmonic excitation obtained with different reduced bases at  $r = 4$

#### 4.2.1.3 Studying the scores

The score, which is developed in section 4.1.2.2, allows an abstraction of an enormous number of transient solutions, obtained with different reduced bases at different orders  $r$ , and the condensation of the results in a single diagram per test-case. The scores for the different reduced bases are shown in the figures 4.13 to 4.16 for each test-case. To gain a qualitative impression of the genesis of the scores at  $r = 4$ , it is referred to the figures 4.7 to 4.10, which plot physical displacements of  $u_{16}$ .

In the following, the main observations for scores of the different reduced bases are discussed briefly. The observations are concentrated on the range  $4 \leq r \leq 8$  that represents an interesting and plausible relative size of the reduced system. Reduced orders beyond  $r = 8$  are mainly included for illustrative purposes and to show tendencies. The core of the study's results are obtained from the limited range of  $4 \leq r \leq 8$ .

The reduced bases of the LNM are consistently among the best performing ones, except for the locally nonlinear system under harmonic excitation (see fig. 4.13). This combination of nonlinearity and excitation is also the only configuration under which the establishment of the LNM at maximum displacement has a considerable positive impact in the considered range  $4 \leq r \leq 8$ . This influence is reversed for the entirely nonlinear system under harmonic excitation, whose scores are plotted in figure 4.15. There, establishing the LNM at maximum displacements deteriorates the LNM's performance. For the two systems under impulse excitations in figures 4.14 and 4.16 there is no notable difference between the two LNM variants. Their performance is similar to the performance of the POD variants.

The Ritz-vectors deliver good scores for the locally nonlinear system under harmonic excitation, where the LNM perform less well. Otherwise their results tend to lower scores, especially for the impulse excitation. This seems contradictory to the works of Idelsohn and Cardona [102] and Chang and Engblom [57], who both, together with Kapania and Byun [113], use the advantages of the load-dependence of the Ritz-vectors for studying the transient response of a system following an impulsively applied load and observe a

particular suitability of Ritz-vectors for this kind of excitation.

The most important feature of the POD variants is that they require the solution, or at least a part of the solution, of the full order system to be available beforehand. In return for this considerable effort, the POD methods yield overall results that are universally good and maybe even the best. Thus, a clear preference for the system and for the excitation on which these methods should be used cannot be identified. It is however certain that the process of enriching the POD basis with the maximum displacements does seem to deteriorate the reduction's performance marginally in the case of a harmonic excitation (figs. 4.13 and 4.15) and considerably in the case of an impulse excitation (figs. 4.14 and 4.16). The intention to account for the cut off modes by adding information to the basis through the inclusion of the maximum displacements does obviously not have the desired effect. The verdict on the SOD modes is that they are largely comparable to the POD modes. A dedicated study in the annex section A.1.1 shows that the difference in order of magnitude between the mass and the stiffness matrix does not influence the performance of the SOD. Also a different mass distribution does not influence the similar performance of the POD and SOD bases. The high scores for the orthogonal decomposition methods are also based on the fact that they offer by definition the smallest error in the root mean square sense, on which the score depends heavily.

While the APR yields already mediocre results for the systems under harmonic excitation, it fails completely for the two systems if they are subjected to the impulse excitation (figures 4.14 and 4.16). This is most certainly due to the fact that the iterative manner of constructing the APR basis does not yield enough modes fast enough to resolve the initial peak in displacements correctly.

The CVT is initialised with the LNM. It yields good to reasonable results for the test-cases with harmonic excitation. For impulse excitations it is less suited.

The LELSM reduced bases show low scores for the locally nonlinear system under harmonic excitation, where they are on par with the LNM. For the locally nonlinear system under impulse excitation they yield high scores. Including the Sh-B-vectors in the LELSM bases has a positive effect only for locally nonlinear system under harmonic excitation. For the entirely nonlinear system under harmonic excitation they have no significant influence and for the two systems under impulse excitation, they even decrease the performance of the LELSM bases.

## 4.2. CONDUCTING THE STUDIES AND ANALYSING THE RESULTS

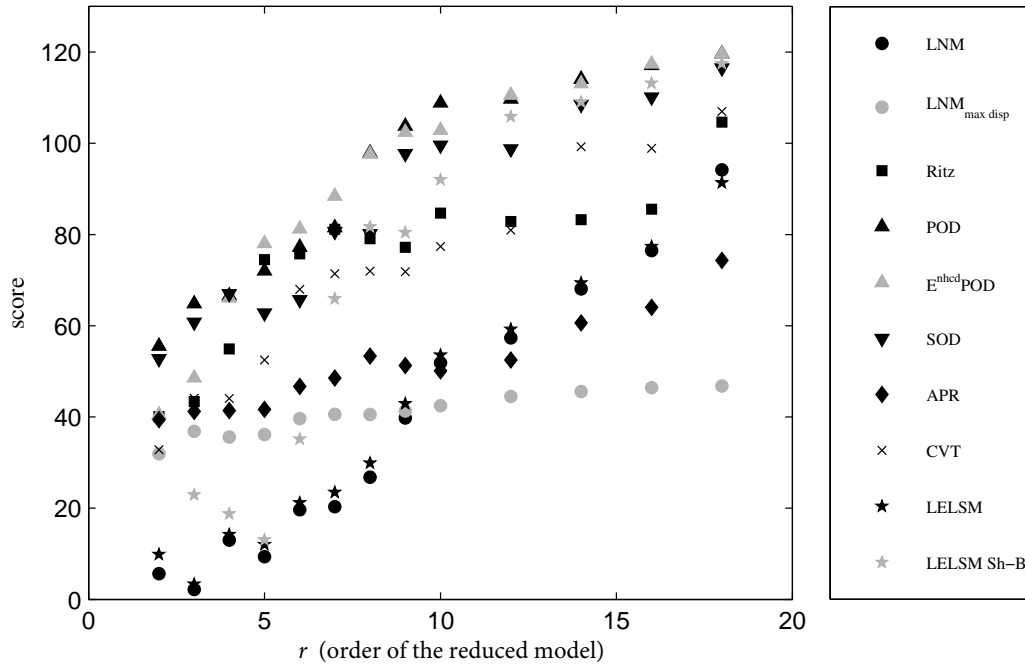


Figure 4.13: The score for different reduced basis for the locally nonlinear system under harmonic excitation

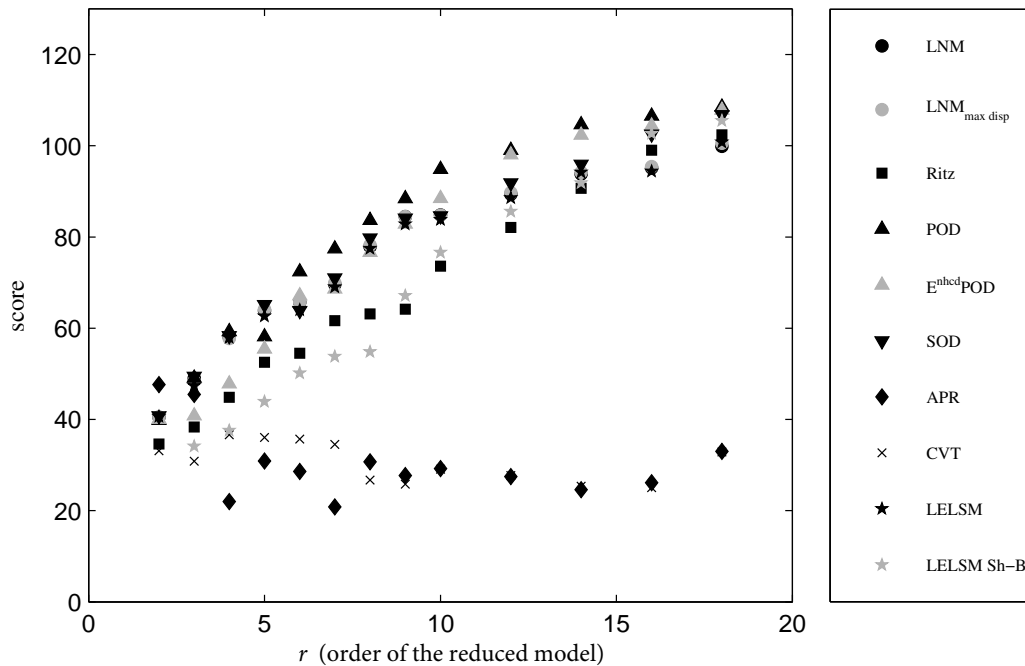


Figure 4.14: The score for different reduced basis for the locally nonlinear system under impulse excitation

#### 4.2. CONDUCTING THE STUDIES AND ANALYSING THE RESULTS

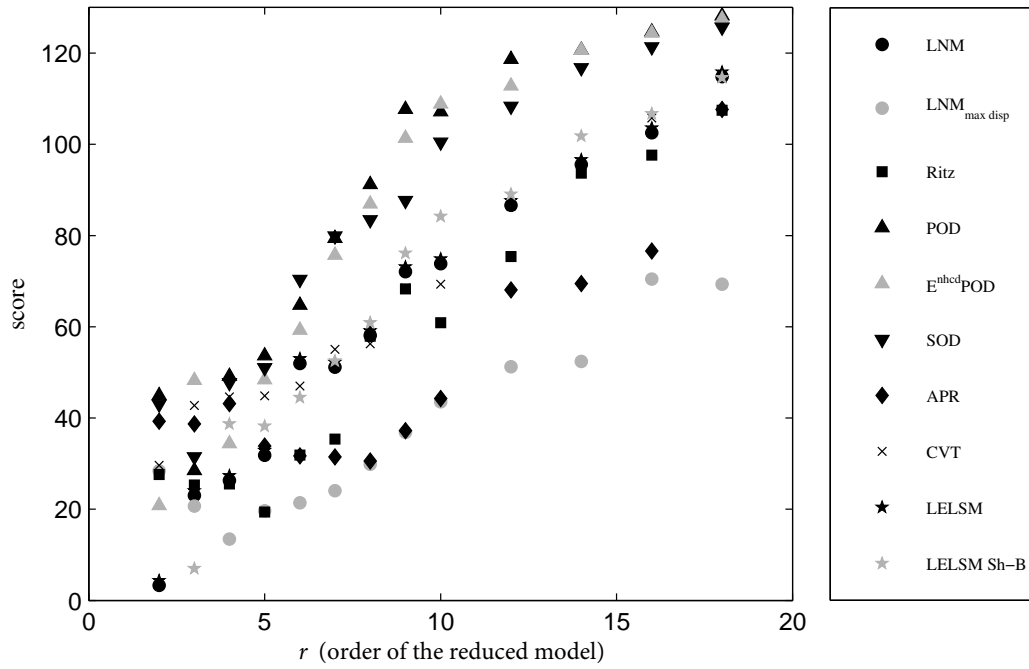


Figure 4.15: The score for different reduced basis for the entirely nonlinear system under harmonic excitation

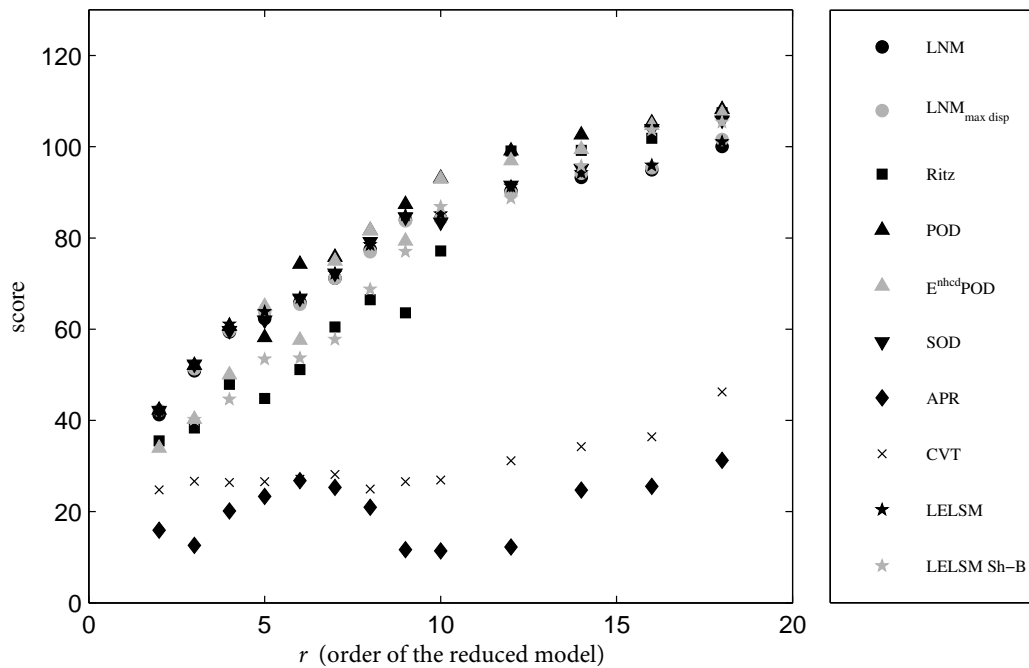


Figure 4.16: The score for different reduced basis for the entirely nonlinear system under impulse excitation

### 4.2.1.4 Observations for the comparative study

In addition to the respective advantages and shortcomings of each method and its possible variants, it seems that the most important results to be drawn from this study are that the appropriateness of a reduction method is mainly determined by the excitation of the system and the properties of the displacement history resulting from it. The nature of the nonlinearity present in the system seems to influence the appropriateness only to a lesser extent. Especially with regard to the rather smooth and regular response of both systems under harmonic excitation, these seem to be the properties that allow for a successful reduction if any appropriate reduced basis is selected. All bases are less suited for impulse excitations, where even the POD bases are not performing better than the LNM bases. However, for both methods, this happens at a higher error level than for the test-cases with harmonic excitation. The overall similar performance of LNM and POD bases supports the findings of Sampaio and Soize [198], who state that the LNM bases are as efficient as the POD bases for their specific applications. The findings are confirmed to be independent from the size of the reduced system in the annex section A.2.1.4.

Among the investigated methods, the quality of the recreated solution varies greatly depending on the test-case. The general conclusions to be drawn from the inspection of the scores in figures 4.13 to 4.16 are:

- the Linear Normal Modes are among the best performing reduction methods for the locally and the entirely nonlinear system under impulse excitation and remain applicable despite the nonlinearities present in the system. If a harmonic excitation is applied, their performance degrades. Their establishment at maximum displacement has a positive influence only for the locally nonlinear system under harmonic excitation.
- the Ritz-vectors excel for the locally nonlinear system under harmonic excitation, where they show a great advantage over the LNM variants.
- the classic Proper Orthogonal Decomposition basis is constantly among the best performing bases regardless of the system or the excitation. Its enrichment with the maximum displacements however slightly deteriorates the excellent performance and is thus objectionable, for a fixed order  $r$  of the reduced system. On the downside the POD bases require knowledge of the full order solution.
- the Smooth Orthogonal Decomposition can be considered as useful reduction method, being on par with the classic POD, yet requiring considerably more effort for creating the reduced bases.
- the A Priori Reduction performs not as well as other methods and especially if related to the effort necessary to compute its basis. If its application should become necessary, it is better suited for harmonic excitations on locally and entirely nonlinear systems. Its application to systems under an impulse excitation should be avoided because this method does not cope well with the rapidly changing displacements resulting from the impulse.
- the Centroidal Voronoi Tessellation allows for reasonable results, especially for the locally nonlinear system under harmonic excitation. For impulse excitations it is not performing very well and comparable to the APR.
- the Local Equivalent Linear Stiffness Method approach yields reduced bases that perform similar to the LNM, albeit with a slight improvement for the locally nonlinear system under harmonic excitation.

The entire evaluation of the bases' performance is condensed in table 4.2. It shows the relative preference of the bases for a given combination of nonlinearity and excitation. The absolute error levels of the test-cases are not included.

### 4.2.2 Robustness of the reduced bases

The robustness of the several possible reduced bases can be investigated in two different directions. The first one limits itself to an alteration of the external forcing, as it is defined in equations (4.22) and (4.24). This does not include changes to the systems itself. The second direction with the actual application of changes

	$f_{E,har}$		$f_{E,imp}$	
	$g_{loc}$	$g_{ent}$	$g_{loc}$	$g_{ent}$
LNМ	--	+	++	++
LNМ <sub>max dsp</sub>	-	-	++	++
Ritz	+	+	+	-
POD	++	++	++	++
E <sup>nhcd</sup> POD	++	+	+	+
SOD	++	++	++	++
APR	-	-	--	--
CVT	+	-	--	--
LELSM	--	+	++	++
LELSM Sh-B	-	-	+	+

Table 4.2: The comparison of the reduced bases

to the system itself would include e.g. different material properties, minor changes in geometry and changes in boundary conditions, which are more than easily recreated with a purely academic system, like the one used for testing. This second direction is, for the moment, not pursued because it would require the use of interpolation of different bases, as e.g. the techniques discussed in section 5.3. So the scope of this section is limited to altering the external forcing, which can be easily changed without major interference in the system. It is the first touchstone for testing the robustness of the system.

For harmonic excitation in equation (4.22) the amplitude and the frequency present themselves in a natural way to parameter variations. But also their point of application can be changed, so that the system is subjected to an excitation that is different from the one used for establishing the basis. For the impulse excitation in equation (4.24) only the amplitude and the point of application will be changed. The point of application of the excitation is crucial, because this feature is present in the column vectors of the reduced basis, as the inspection of figures 4.3 to 4.6 shows.

The study of the robustness of the reduced bases requires, in a first step, the definition of the arrangement of the study. The arrangement introduces the notion of configurations that allow different parameterisations of the excitations. Then, for the different configurations, transient solutions are generated that are reduced with bases that have already been established for the comparison. The results are treated with the relative performance and are extensively studied for each of the methods that is used to create reduced bases.

#### 4.2.2.1 Defining the arrangement of the study

The exact arrangement of the present study is to a certain degree complicated and requires hence an amount of abstraction, in order to have a direct access to the major results.

The excitations are described by a set of parameters which are global parameters in the sense of section 4.1.3.4. Equation (4.27), below, lists these parameters as the amplitude  $f_e$ , the frequency  $\Omega$  and the point of application  $p$ . Every set of values for these three parameters  $\mu$  is called a configuration; or an operating point.

The configuration that is used to create the bases for the different methods in the preceding, comparative study in section 4.2.1 is called the reference configuration  $\mu_k$ . The bases from the preceding study remain unaltered during the present study. For each test-case there is one specific basis for every order of the associated reduced model. They have in common that they are constructed on the basis of the respective system subjected to either of the two excitations, described by a set of parameters taken from the reference configuration, defined in equation (4.28), below.

If now the parameters of the external forcing are changed as per table 4.4, the additional configurations

emerge, each one describing a certain set of parameters used in turn to alter the excitation to which a system can be subjected. From these test-cases, whose excitations are parameterised by means of configurations, reference solutions are created by using the full order system. Per test-case there is a specific reference solution for each configuration  $\mu_i$ . The error metrics in the following sections, each one dedicated to a specific reduction method, are obtained by comparing the re-established solution, produced by reducing the test-case at hand with the respective basis constructed from the same test-case under the reference configuration of the external forcing, with the reference solution, distinct and unique for the current configuration and produced by a full order simulation.

By vigorous application of this course of action it is ensured that, in a first step, only the robustness of basis under scrutiny as a function of the external forcing's properties is investigated and that no other influences act upon the solution. The different test-cases and configurations are then used as additional parameters to determine if, under certain circumstances, certain combinations of different nonlinearities with different types of excitation are susceptible of enhancing or deteriorating a basis' robustness.

**4.2.2.1.1 Defining the configurations** The configurations designate the different excitations that are used to test the robustness of the reduction methods under a changing in external forcing. The parameters of the reference configurations<sup>9</sup>  $\mu_k$ , with which the bases are established, for the four test-cases are summarised in sections 4.1.3.1 and 4.1.3.3 along with the constitutions of the four test-cases as combinations from the two different systems with the two different excitations. The parameters therein are in turn coming from section 4.1.3.4.

All three parameters for the external forcing listed in section 4.1.3.4 are altered in the following study. This defines the vector of parameters, which describe<sup>10</sup> the system as

$$\boldsymbol{\mu} = [\Omega, \hat{f}_E, p]. \quad (4.27)$$

where it is obvious that the frequency of the external forcing  $\Omega$ , defined in equation (4.22), can only be altered in the case of a harmonic excitation, as it is simply not defined for an impulse excitation. If the vector above describes the reference configuration, it contains the following values

$$\boldsymbol{\mu}_k = [\Omega, \hat{f}_E, p] = [0.2289, 3, 20]. \quad (4.28)$$

The different configurations for the following studies are defined in equation (4.27) by bisecting and doubling the parameters of the external forcing and altering its point of application.

Albeit the fact that the entirely nonlinear system (4.17) is stiffer than the locally nonlinear system (4.16) and would require thus a more powerful forcing to yield the same amplitude, the same variations to the external forcing are applied in amplitude and frequency to all systems alike in order to ensure comparability. It is important to note that only one parameter is changed at a time, while the two others remain at their respective reference value. With the respective numerical values inserted, table 4.3 reads

These five different configurations  $\mu_i$  of the external forcing are used on all four test-cases. The notable exceptions are the configurations 1 and 2, which alter the frequency of the excitations, and are only applicable if the system at hand is subjected to an harmonic excitation. The configuration 5 places the excitation at the free end of the locally nonlinear system. For the entirely system the parameter  $p = 20$  implies an excitation at the extremity, which is connected with an fixed point in space.

<sup>9</sup>In order to comply already with the notation that is introduced later, the index  $k$  is chosen for the original, reference configuration instead of the more common index  $0$ . In section 5.3.2 the index  $k$  denotes the origin of an interpolation.

<sup>10</sup>The entire and unified description of the parameters is introduced in section 5.3. For now, the preliminary description of the parameters in equation (4.27) is sufficient.

## 4.2. CONDUCTING THE STUDIES AND ANALYSING THE RESULTS

configuration	frequency $\Omega$	amplitude $\hat{f}_E$	point of application $p$
1	$\frac{1}{2}\Omega_0$	$\hat{f}_E$	$p_0$
2	$2\Omega_0$	$\hat{f}_E$	$p_0$
3	$\Omega_0$	$\frac{1}{2}\hat{f}_E$	$p_0$
4	$\Omega_0$	$2\hat{f}_E$	$p_0$
5	$\Omega_0$	$\hat{f}_E$	$p_l$

Table 4.3: The different configurations for the study of the robustness of the methods

configuration	frequency $\Omega$	amplitude $\hat{f}_E$	point of application $p$
1	0.114 Hz	3	4
2	0.456 Hz	3	4
3	0.228 Hz	1.5	4
4	0.228 Hz	6	4
5	0.228 Hz	3	20

Table 4.4: The numerical values of the different configurations for the study of the robustness of the methods

**4.2.2.1.2 Listing the reduced bases included in the study of robustness** The reduced bases used for the solution of the test-cases with a different configuration are not generated explicitly for this purpose. Instead the bases created for the reference excitation  $\mu_k$  in equation (4.28). These are used during the comparative study of the different methods in section 4.2.1 and are used unaltered.

In total there are ten different reduced bases, established with the different methods from section 3.3 for each test-case and each order  $r$  of the reduced system. In detail the reduced bases  $\Phi$  are obtained from

- the Linear Normal Modes, as they are obtained from the underlying linear system, i.e. the nonlinear system in its equilibrium state with all-zero initial configuration variables,
- the Linear Normal Modes, as they are obtained from the system in a configuration corresponding to the maximum dynamic deflection  $\mathbf{u}_{max}$  during the reference solution. These maximum displacements are used to construct the tangent stiffness matrix  $\bar{\mathbf{K}}$  which is in turn used in the eigenproblem for the Linear Normal Modes as per equation (3.102),
- the established procedure for the construction of Ritz-vectors, as described in section 3.3.2.1,
- the classic Proper Orthogonal Decomposition procedure,
- the Proper Orthogonal Decomposition enriched with the maximum displacements  $\mathbf{u}_{max}$  as defined in equation (3.137),
- the Smooth Orthogonal Decomposition whose velocity snapshots are taken directly from the reference solution,
- the unaltered A Priori Reduction as it is defined in section 3.3.4.1,
- the Centroidal Voronoi Tessellation from section 3.3.5 with the MAC from equation 4.10 as a measure of closeness,
- the classic Local Equivalent Linear Stiffness Method in section 3.3.6, and,
- the Local Equivalent Linear Stiffness Method with additional Sh-B-vectors.

The shapes of the first two column vectors of all these bases are presented as they are applied in this study

of the robustness in the figures 4.3 to 4.6.

### 4.2.2.2 Studying the relative performance

This study of the relative performance determines the robustness of the different reduction methods. It takes the reduced bases which are established during the comparative study and uses them to reduce the same test-cases with differently parameterised excitations. The result of this second study is an overview of which method is to be expected to be particularly robust if applied to a system under an excitation that was not used to create it. Concerning the necessary abstraction it has been decided not to work on the actual plots of the results, but to work exclusively on an the abstraction layer of the relative performance, as it is introduced in section 4.1.2.3. This allows grasping the qualitative behaviour of the different bases.

The possible combinations of different types of harmonic or impulse excitation, different systems and the variety of reduction methods presents an overwhelming amount of information. Thus, the results of this study are ultimately condensed in tables 4.5 to 4.6. They contain the two different systems under the two types of excitation and the five differently parameterised variants thereof. Symbols are used to indicate if the quality of the solution improves or degrades depending on changes in the parameters that define the excitation. In order to illustrate the genesis of these two tables, the plots of the relative performances of the LNM and the POD for all four test-cases are shown and discussed below.

The original LNM and POD reduced bases are taken as a representative example. The corresponding plots of the relative performances are shown in figures 4.17 to 4.24. These give an impression of the transition from the plots of the relative performance to the condensation of the observations in the tables in the section 4.2.2.3.

**4.2.2.2.1 Linear Normal Modes** First, it is recalled that basic LNM, unlike their variant that is established at maximum displacements, are not influenced by the excitation or the time history of the solutions. The basis  $\Phi$ , composed of the Linear Normal Modes of the respective underlying linear system, i.e. the tangential system of the nonlinear system at its initial conditions, does depend exclusively on the properties of that system and its initial conditions. So, strictly speaking, applying the established Linear Normal Modes to a different system, where only the external forcing has been altered, does not reveal any information on the method's robustness in the sense it is defined within this study. The investigation into the performance of the Linear Normal Mode-basis is included nonetheless because it contributes to providing insight into how well this method work under different excitations and where possible shortcomings might be expected. Also, the LNM set a pattern which is reflected by almost all reduced bases that follow.

The simulations for the harmonic excitation, conducted with the Linear Normal Modes, gain significantly in quality if the frequency and the amplitude of the external forcing are reduced. For the reverse case, increasing the frequency and the amplitude, the quality seems to degrade as well for the change in the point of application.

The LNM bases perform significantly worse if they are applied to the entirely nonlinear system with a shifted point of application of the external force. For the locally nonlinear system this deterioration is however well controlled for both excitations. This is understandable because, in this particular case, the basic mode shapes of the LNM do favour an excitation at an extremity of the entirely nonlinear system.

Under impulse excitation and for all systems the changing amplitude has no impact, while the change of point of application produces only degradations in the solution's quality. That is, except for the locally nonlinear, where the presence of the localised nonlinearity makes the smallest difference between the nonlinear and the underlying linear system and the positioning of the excitation at one extremity of the system is most likely to excite the lower eigenmodes of the system.

#### 4.2. CONDUCTING THE STUDIES AND ANALYSING THE RESULTS

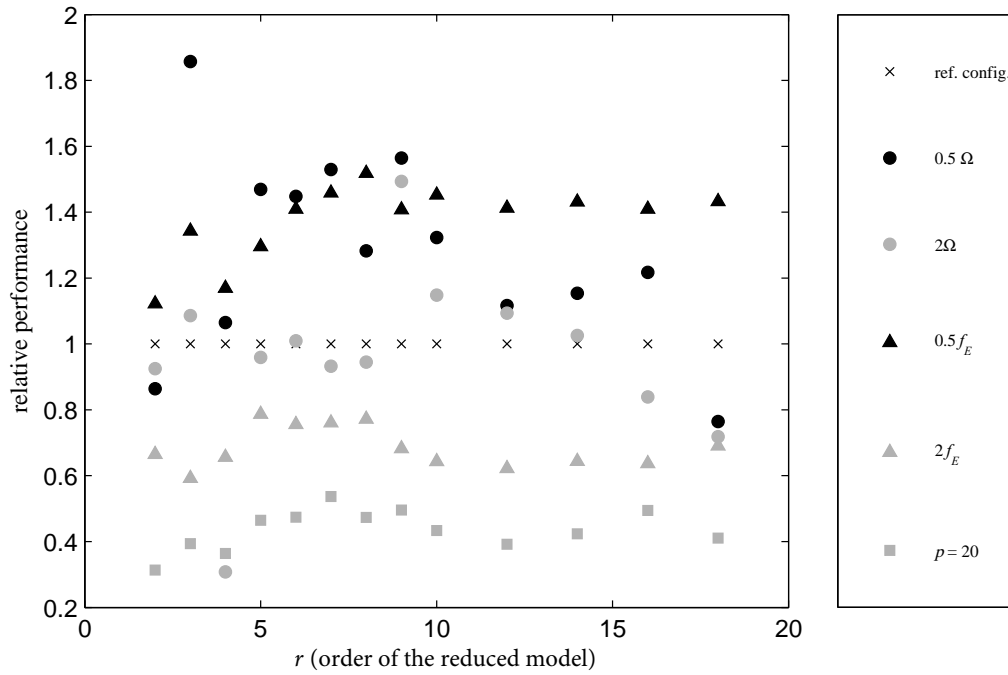


Figure 4.17: The relative performance for studying the robustness of LNM bases for the locally nonlinear system under harmonic excitation

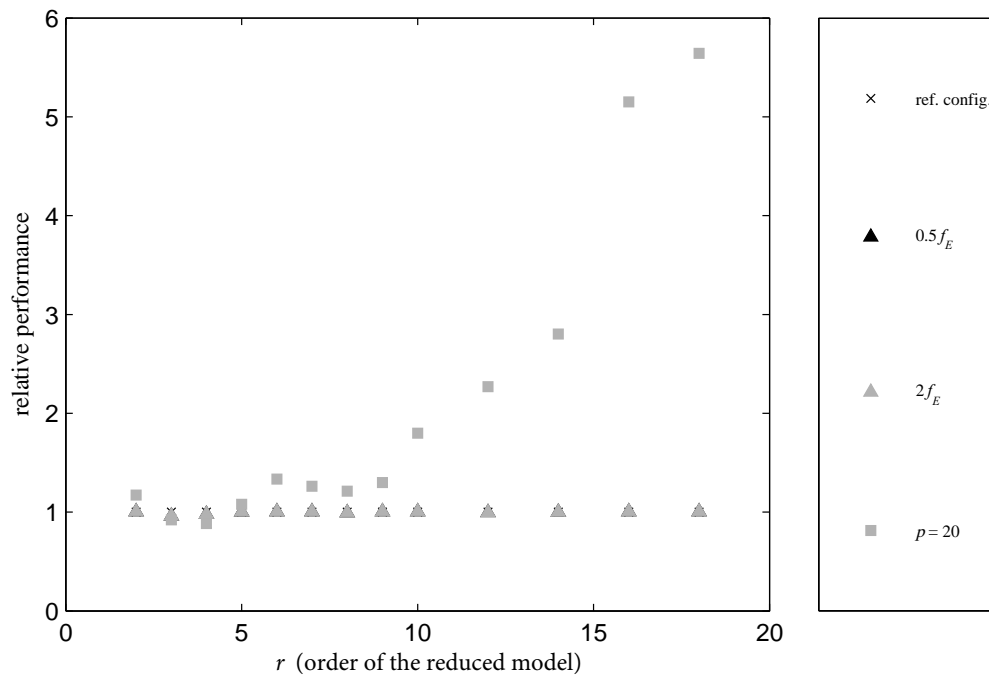


Figure 4.18: The relative performance for studying the robustness of LNM bases for the locally nonlinear system under impulse excitation

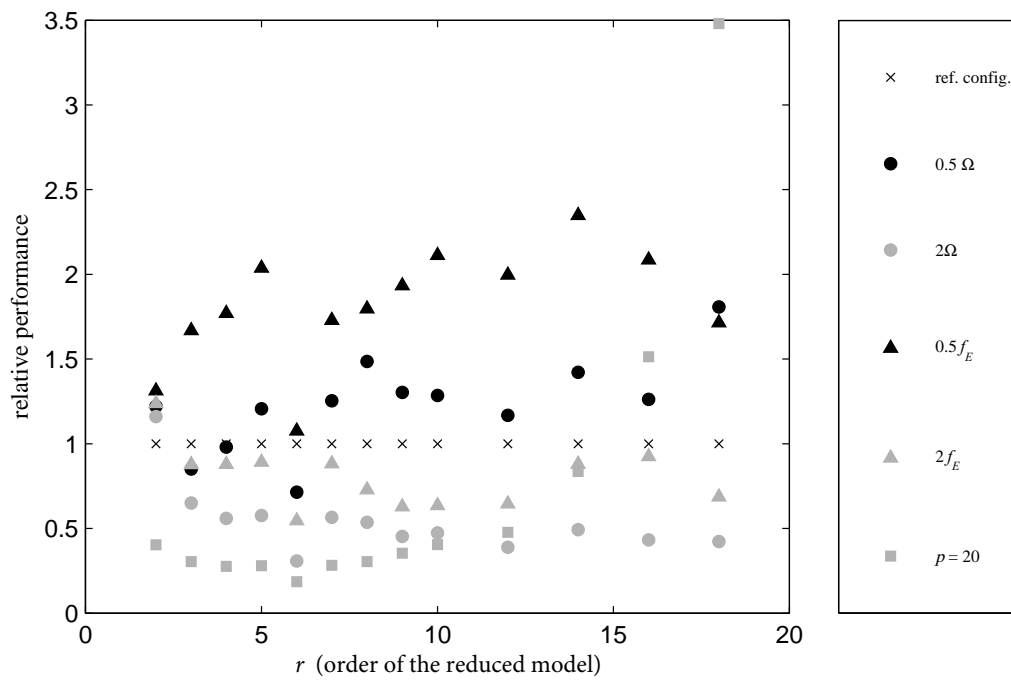


Figure 4.19: The relative performance for studying the robustness of LNM bases for the entirely nonlinear system under harmonic excitation

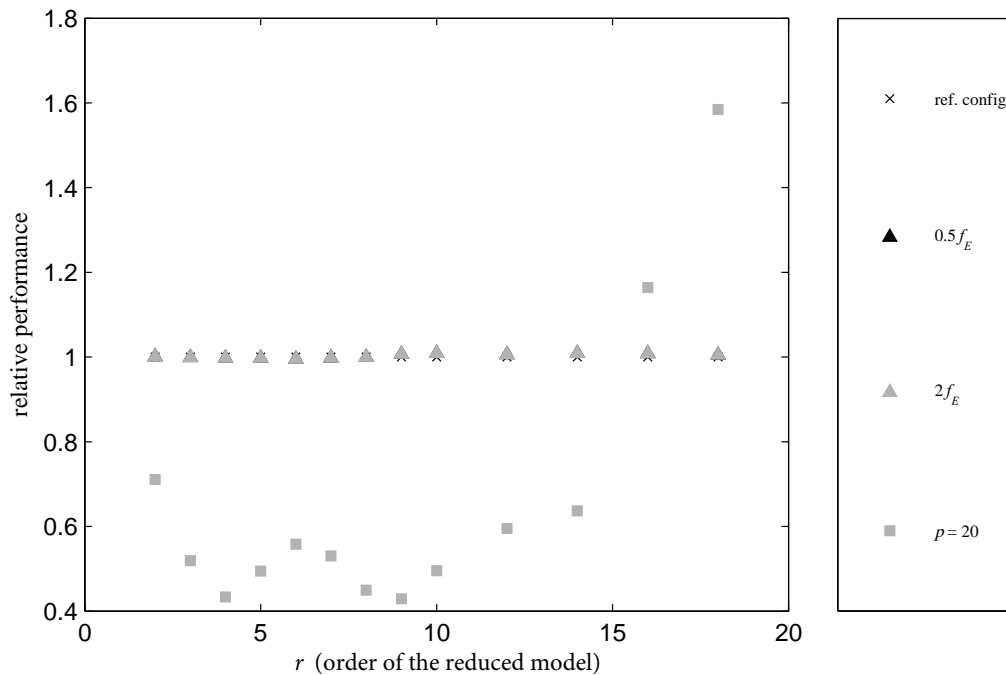


Figure 4.20: The relative performance for studying the robustness of LNM bases for the entirely nonlinear system under impulse excitation

**4.2.2.2.2 Linear Normal Modes at maximum displacement** The Linear Normal Modes obtained at maximum displacement do represent a real interest in the course of this study because they do depend on the external forcing through the intermediate step of the reference solution. Even though not too strongly, as they are still mostly influenced by the system's properties. As such they are specific for defined excitation and have to prove a certain robustness if they should be applied to a system that is subjected to an excitation different from the one used for establishing the Linear Normal Modes at maximum displacement.

In general the Linear Normal Modes at maximum displacement have to be considered as extremely sensitive to a changing point of application of the external forcing, which results in a degradation of the solution's quality. Also the error in oscillation seems to scale with the amplitude of the respective configuration. Greater amplitude tends to produce an overestimation while smaller amplitude leads to an underestimation of the oscillation.

The differences in behaviour between the two LNM variants are marginal. The most influential parameters are the point of application and the frequency and, second to that, the amplitude.

**4.2.2.2.3 Ritz vectors** The Ritz-vectors show basically the same behaviour as the LNM. Like the LNM at maximum displacements, the Ritz-vectors depend on the excitation of the system, too. The algorithm for their establishment is initialised with the maximum static displacements occurring during the solution and that the same maximum displacements are used to create the tangent stiffness matrix, which is used during that algorithm. Only for the locally nonlinear system under harmonic excitation, where the Ritz-vectors already performed well in the first comparative study, they appear much more robust with respect to changes in the frequency of the excitation.

For the test-cases under the harmonic excitation the basis built from Ritz-vectors shows to be prone to variations in the excitation's frequency  $\Omega$ . Especially the doubling of the frequency leads to a considerable overestimation of the amplitude for the locally nonlinear system and an underestimation of a comparable

magnitude for the entirely nonlinear system. In both cases this is especially pronounced for small orders of the reduced systems.

Changing the point of application to the extremity of the systems has the inverse effect, i.e. an underestimation of the amplitude for the locally nonlinear system under harmonic excitation and an overestimation for the entirely nonlinear system under harmonic excitation, but resulting in a degradation of the solution's quality all the same.

Rather good is the performance of the Ritz-vectors when the configuration with half the reference amplitude is applied to the entirely nonlinear system. However, these are the only cases in which a configuration actually yields better results than the reference configuration and this only for orders of the reduced system that are greater than 5.

For the test-cases with an impulse excitation the changing amplitudes of the external forcing lead to amplitudes in displacements that are mostly comparable to the results obtained with the reference solution. Only the change of the point of application of the excitation alters the performance of the Ritz-vector basis considerably. The performance seems to improve for the locally nonlinear system, while it undergoes a serious degradation, resulting from an underestimation of the oscillation, for all remaining systems.

In summary the bases built from Ritz-vectors are particularly suitable for changing amplitudes while they are sensitive to changing points of application. In this regard they resemble closely the two LNM variants.

**4.2.2.2.4 Proper Orthogonal Decomposition** The Proper Orthogonal Decomposition is the archetype of a reduction method that exclusively depends on the solution of a system. Its robustness with respect to changes in the solution has been widely studied. Yet, there seems to be a lack of a definite conclusion in literature as to if and when reduced bases originating from POD procedures can be applied to systems and configurations different from the ones that were used to establish the basis. It is thus of particular interest to investigate the suitability of POD most closely and to contribute to the search for a set of criteria that might be able to define possible applicability of the POD reduced bases beyond the case that was used to create it with.

Within the margins of the applied configurations and the accompanying changes in parameters of the external forcing, the original POD-bases, established for the different test-cases under the reference configuration, yield mixed results. For all test-cases the shift in the point of application deteriorates the bases' performance, except for the combination of the locally nonlinear system with an impulse excitation, which is already observed for the classic Linear Normal Modes above. The same deterioration applies for the locally nonlinear system and changes in the frequency of the harmonic excitation. This effect seems however less pronounced if the frequency is bisected and unfolds to full effect while it doubles and it even reverses into a gain of quality for the entirely nonlinear system. Changes in the amplitude return more favourable results, which are close to the ones from the reference solution and for the entirely nonlinear system under harmonic excitation. At the same time, the configuration with half the reference amplitude, gives even better results than the reference configuration for which the basis is established and for which it is thought to be optimal.

These POD bases appear to be especially sensitive to changes in the frequency of the harmonic excitation. Changes in the amplitude of the forcing provoke some deterioration for the harmonic excitations for both systems alike. For an impulse excitation, this effect is less pronounced for the locally nonlinear system and does practically not exist for the entirely nonlinear system. For the entirely nonlinear system under either excitation, the POD modes are very sensitive with respect to changes in the point of application of the external forcing, which is obvious if seen in relation with the characteristics present in the shapes of the vectors. At the same time their performance is virtually invariant if the amplitude of the forcing is changed. For the locally nonlinear systems under both excitations, it is foremost the point of application but also an increase in frequency which degrades the performance of the POD bases.

#### 4.2. CONDUCTING THE STUDIES AND ANALYSING THE RESULTS

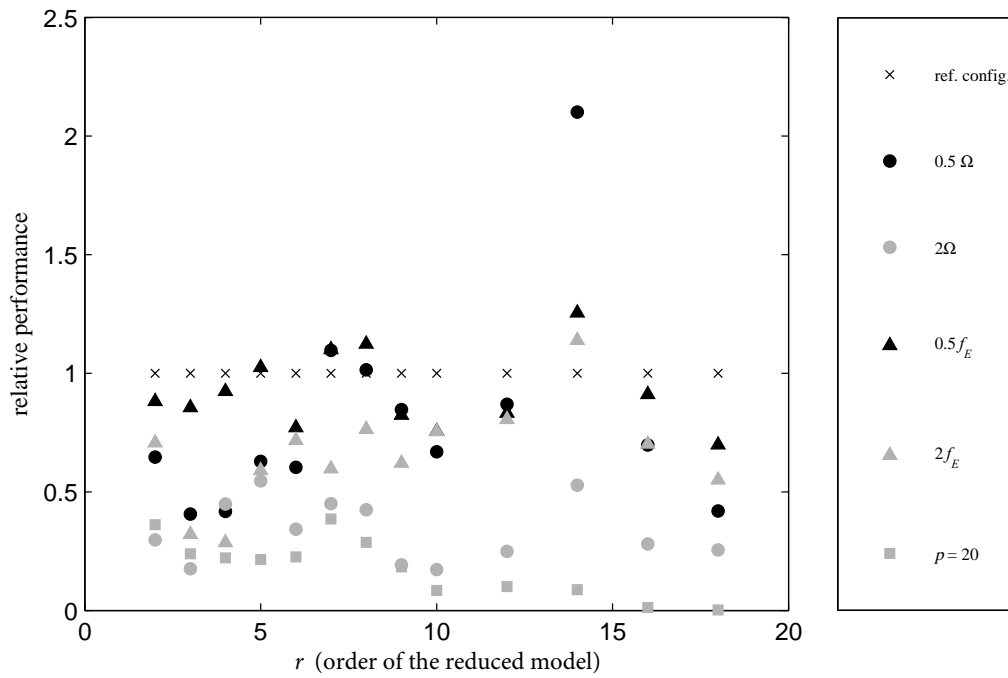


Figure 4.21: The relative performance for studying the robustness of POD bases for the locally nonlinear system under harmonic excitation

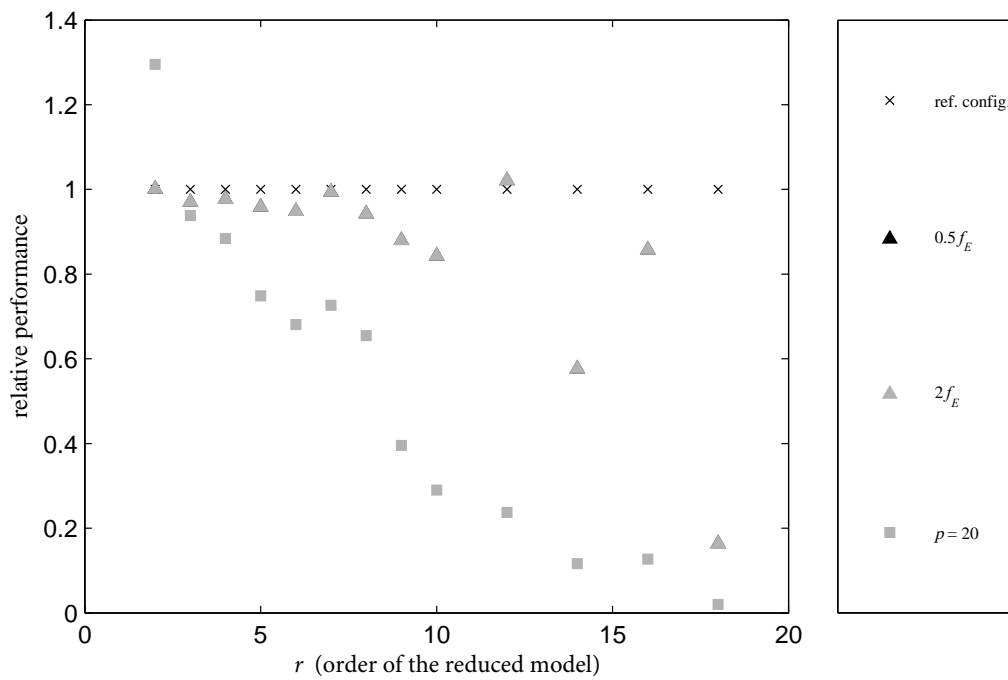


Figure 4.22: The relative performance for studying the robustness of POD bases for the locally nonlinear system under impulse excitation

## 4.2. CONDUCTING THE STUDIES AND ANALYSING THE RESULTS

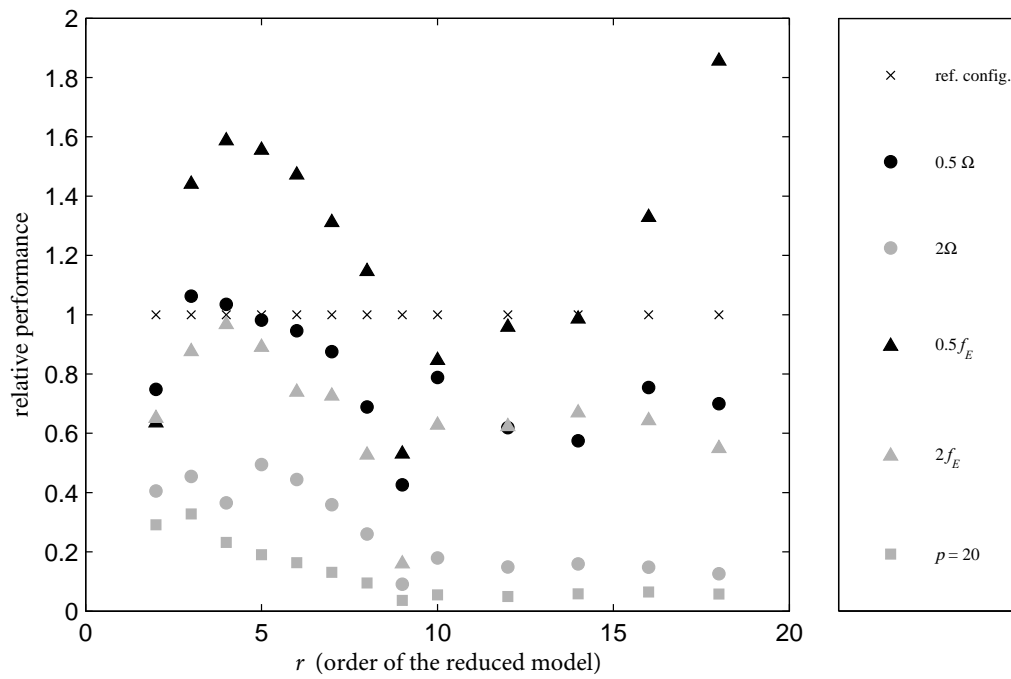


Figure 4.23: The relative performance for studying the robustness of POD bases for the entirely nonlinear system under harmonic excitation

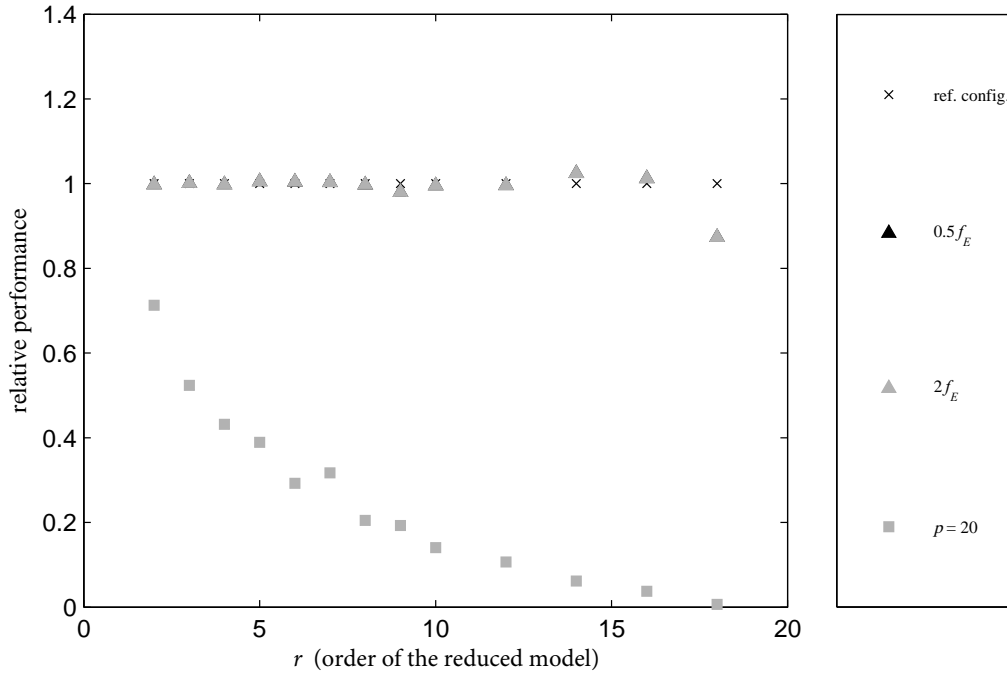


Figure 4.24: The relative performance for studying the robustness of POD bases for the entirely nonlinear system under impulse excitation

**4.2.2.2.5 Enriched Proper Orthogonal Decomposition** The Enriched Proper Orthogonal Decomposition’s results are virtually identical in shape to the results of the original Proper Orthogonal Decomposition albeit they are situated on a slightly inferior level, as it may be identified by a direct comparison of the two POD variants.

**4.2.2.2.6 Smooth Orthogonal Decomposition variants** The Smooth Orthogonal Decomposition bases produce nearly the same solutions as the POD. The additional effort from the combined eigenproblem in equation (3.139) and the following normalisation in equation (3.141) is hence difficult to justify.

**4.2.2.2.7 A Priori Reduction** The APR bases already produce considerable errors for either system subjected to the impulse excitation in the reference configuration. These errors are not reduced by the application of a differently parameterised excitation. The APR bases seem to be especially prone to reduce in performance if the frequency of the harmonic excitation is changed for both systems. If the frequency is doubled in the entirely nonlinear case, the resulting errors are even greater than the errors induced by changing the point of application of the excitation, which is the worst possible deterioration for least for all other methods.

During the comparative study in section 4.2.1 the A Priori Reduction’s results are remarkable for the broad spread of the error metrics for the different systems under harmonic excitation. While the error metrics of configurations with half and twice the reference amplitude of the excitation are only slightly worse or even on par with the results from the reference configuration, the remaining configurations, which change the frequency and the point of application, are spread widely and considerably worse than the reference configuration, in both the Relative Oscillation Deviation and the Relative Root Mean Square Error alike.

For all systems excited by an impulse excitation, already the reference configuration yields rather poor

results, as it is stated in section 4.2.1.4. These are not improved by altering the amplitude of the excitation. Only the excitation configuration with a changed point of application, applied to the locally nonlinear system, returns a small amplitude. Yet it is still far below levels that are useful.

**4.2.2.2.8 Centroidal Voronoi Tessellation** The Centroidal Voronoi Tessellation, described in section 3.3.5, is applied in this study with the LNM as initialising vectors. The CVT bases offer considerable robustness for a large range of configurations. Yet, if they are influenced by changes in the parameterisation of the excitation, they tend to a decrease in performance. Beyond the large range of configurations the CVT bases are prone to a decrease in performance under changes in the parameterisation of the excitation.

**4.2.2.2.9 Local Equivalent Linear Stiffness Method** The bases of the Local Equivalent Linear Stiffness Method from section 3.3.6 increase in performance if the amplitude and the frequency of the excitation are reduced. On the other hand, their performance deteriorates if the values of these parameters are increased. In this they resemble the LNM. Adding the Sh-B-vectors lessens the increases in performance of the original LELSM bases.

### 4.2.2.3 Observations for the study of robustness

The results detailed above certainly allow the conclusion that none of the investigated methods is persistently robust with respect to changes in the external forcing. And this conclusion heralds the investigation into and the use of the adaptation techniques that are discussed in section 5.3. But a careful consideration of the results of this study allows deciding which parameters are when to be used in the course of such an adaptation.

Among the shortcomings of all the methods the most reoccurring one for all methods is the extreme sensitivity with respect to changes of the point of application of the excitation for the entirely nonlinear system subjected to an impulse excitation. If the amplitude of the forcing is changed, all reduced bases reproduce approximately the levels of error that they yield during the preceding study for this combination of system constitution and excitation under the reference configuration. Changing the point of application severely deteriorates the bases' performances. Even the APR, which does not succeed in recreating the reference solution for the reference configuration of the test-cases with impulse excitation in the first place, deteriorates further in performance. For the tests cases under harmonic excitation doubling the frequency poses major problems to all methods, yet the configuration 5, which shifts the point of application, deteriorates the methods' performances the most.

These observations are concentrated in tables 4.5 and 4.6, where the mathematical signs indicate different degrees of alteration in the relative performance of the reduced bases depending on the change in the parameterisation of the excitation and the test-case (+ + the quality of the reduced solution increases significantly, + the quality improves, o the quality does not change, - the quality decreases, - - the quality decreases significantly, n.a. parameter not applicable, × the solution fails to converge, \* the solution in reference configuration already has a considerably decreased quality or it does not converge. These cases are identified during the comparative study in section 4.2.1.).

#### 4.2. CONDUCTING THE STUDIES AND ANALYSING THE RESULTS

---

		LNM				
configuration		$1/2\Omega$	$2\Omega$	$1/2\hat{f}_E$	$2\hat{f}_E$	$p = 20$
$f_{E,\text{har}}$	$g_{\text{loc}}$	+	-	+	-	--
	$g_{\text{ent}}$	+	-	+	-	-
$f_{E,\text{imp}}$	$g_{\text{loc}}$	n.a.	n.a.	o	o	+
	$g_{\text{ent}}$	n.a.	n.a.	o	o	-

		LNM <sub>max disp</sub>				
configuration		$1/2\Omega$	$2\Omega$	$1/2\hat{f}_E$	$2\hat{f}_E$	$p = 20$
$f_{E,\text{har}}$	$g_{\text{loc}}$	-	o	-	+	-
	$g_{\text{ent}}$	+	-	+	o	-
$f_{E,\text{imp}}$	$g_{\text{loc}}$	n.a.	n.a.	o	o	+
	$g_{\text{ent}}$	n.a.	n.a.	o	o	-

		Ritz-vectors				
configuration		$1/2\Omega$	$2\Omega$	$1/2\hat{f}_E$	$2\hat{f}_E$	$p = 20$
$f_{E,\text{har}}$	$g_{\text{loc}}$	-	-	o	o	-
	$g_{\text{ent}}$	o	-	+	-	-
$f_{E,\text{imp}}$	$g_{\text{loc}}$	n.a.	n.a.	o	o	+
	$g_{\text{ent}}$	n.a.	n.a.	o	o	-

		POD				
configuration		$1/2\Omega$	$2\Omega$	$1/2\hat{f}_E$	$2\hat{f}_E$	$p = 20$
$f_{E,\text{har}}$	$g_{\text{loc}}$	o	-	o	-	-
	$g_{\text{ent}}$	-	o	-	-	-
$f_{E,\text{imp}}$	$g_{\text{loc}}$	n.a.	n.a.	o	o	+
	$g_{\text{ent}}$	n.a.	n.a.	o	o	-

		E <sup>nhed</sup> POD				
configuration		$1/2\Omega$	$2\Omega$	$1/2\hat{f}_E$	$2\hat{f}_E$	$p = 20$
$f_{E,\text{har}}$	$g_{\text{loc}}$	o	×	o	-	-
	$g_{\text{ent}}$	o	-	o	-	-
$f_{E,\text{imp}}$	$g_{\text{loc}}$	n.a.	n.a.	o	o	+
	$g_{\text{ent}}$	n.a.	n.a.	o	o	-

Table 4.5: The robustness of the reduced bases - table one

## 4.2. CONDUCTING THE STUDIES AND ANALYSING THE RESULTS

---

		SOD				
configuration		$1/2\Omega$	$2\Omega$	$1/2\hat{f}_E$	$2\hat{f}_E$	$p = 20$
$f_{E,\text{har}}$	$g_{\text{loc}}$	○	—	○	—	—
	$g_{\text{ent}}$	○	—	○	—	—
$f_{E,\text{imp}}$	$g_{\text{loc}}$	n.a.	n.a.	○	○	+
	$g_{\text{ent}}$	n.a.	n.a.	○	○	—

		APR				
configuration		$1/2\Omega$	$2\Omega$	$1/2\hat{f}_E$	$2\hat{f}_E$	$p = 20$
$f_{E,\text{har}}$	$g_{\text{loc}}$	+	—	○	—	—
	$g_{\text{ent}}$	+	—	○	—	—
$f_{E,\text{imp}}$	$g_{\text{loc}}$	n.a.	n.a.	○*	○*	—*
	$g_{\text{ent}}$	n.a.	n.a.	○*	○*	+*

		CVT				
configuration		$1/2\Omega$	$2\Omega$	$1/2\hat{f}_E$	$2\hat{f}_E$	$p = 20$
$f_{E,\text{har}}$	$g_{\text{loc}}$	+	—	+	—	—
	$g_{\text{ent}}$	—	—	○	—	—
$f_{E,\text{imp}}$	$g_{\text{loc}}$	n.a.	n.a.	○*	○*	+*
	$g_{\text{ent}}$	n.a.	n.a.	○*	○*	+*

		LELSM				
configuration		$1/2\Omega$	$2\Omega$	$1/2\hat{f}_E$	$2\hat{f}_E$	$p = 20$
$f_{E,\text{har}}$	$g_{\text{loc}}$	++	—	+	--	--
	$g_{\text{ent}}$	+	--	++	—	--
$f_{E,\text{imp}}$	$g_{\text{loc}}$	n.a.	n.a.	○	○	+
	$g_{\text{ent}}$	n.a.	n.a.	○	○	--

		LELSM Sh-B				
configuration		$1/2\Omega$	$2\Omega$	$1/2\hat{f}_E$	$2\hat{f}_E$	$p = 20$
$f_{E,\text{har}}$	$g_{\text{loc}}$	+	○	+	—	--
	$g_{\text{ent}}$	○	—	+	—	--
$f_{E,\text{imp}}$	$g_{\text{loc}}$	n.a.	n.a.	○	○	--
	$g_{\text{ent}}$	n.a.	n.a.	○	○	--

Table 4.6: The robustness of the reduced bases - table two

In conclusion it can be stated that, like in the comparative study, the methods' performances with respect to the chosen criterion depend crucially on the nature of the forcing and only to a lesser extend of the system. The study reveals an extreme sensitivity with respect to changes of the point of application  $p$  for nearly all methods. It provokes the most severe deterioration in performance. Second to that is the doubling of the frequency, which poses major problems to all methods on all test-cases.

There are less problems appearing for almost all methods if the amplitude of the harmonic excitation is changed. The same observation can be made for both systems if the amplitude of the impulse excitation is doubled.

If a change in one of the two parameters of the excitation, amplitude  $\hat{f}_E$  or frequency  $\Omega$ , causes the performance of a method to deteriorate, this deterioration may be less pronounced if the respective parameter is scaled down, i.e. if the system is forced to oscillate with a smaller amplitude or more slowly, due to a decreased excitation frequency. If improvements in the performance of an already existing base can be expected, they are most likely to occur if the basis is applied to a case where the values of these two parameters are scaled down. The recommendation from this observation is to establish the bases at the most critical values for the external forcing before reusing them on less demanding excitations.

Except for certain configurations, no reduced basis presents enough robustness to circumvent adaptation techniques. The point of application of any excitation and the frequency of a harmonic forcing are inevitably to prioritize among the parameters that are treated by an adaptation technique.

The three main conclusions to be drawn from this study of the bases' robustness are:

- changes in amplitude have much less, and sometimes virtually no impact, than changes in frequency and especially changing the point of application because it does not change the pattern of the displacements, which is abstracted in the bases' vectors.
- the performance of a basis applied to a system different from the one it was constructed with drops much less if the original system operates at a more critical value of the respective parameter.
- every single method lacks robustness and will thus require the use of adaptation techniques if they are to be applied to different systems. The differences in performance are more pronounced between the test-cases than between the methods themselves.

As one possible remedy to the established lack of robustness, Amsallem et al. [11] propose a much evolved approach for the interpolation between reduced bases, which relies on an interpolation in a projected space, tangent to the one of the reduced bases. Another approach, proposed by Hay et al. [95], relies on the sensitivities of the projection basis with respect to the external parameters. A method of interleaved snapshots from differently parameterised models is available but limited to orthogonal decomposition methods. These approaches can be found among the Lagrange subspace methods or the composite Proper Orthogonal Decomposition for fluid mechanics, e.g. Ito and Ravindran [105] and Taylor and Glauser [220], respectively. Another approach linked to POD are the so-called shift modes, or non-equilibrium modes, proposed for instance by Noack et al. [162] and Bergmann and Cordier [36], which add a vector pointing from one configuration to another to the POD basis, which should become promising if the two excitations have different means. Through simply adding a vector, this approach has a certain commonality with the Enhanced POD technique, discussed in section 3.3.3.3.

## 4.3 Discussing the outcome of the numerical study

Using four different combinations of nonlinear systems and excitations a comparative study and a study into the robustness of several common reduced bases is undertaken<sup>11</sup>. The results of the comparative study allow identifying the preferred application in terms of type of nonlinearity and type of excitation for each reduced

---

<sup>11</sup>A more targeted study on large systems in the annex section A.2.1.2 confirms the obtained results and highlights the possible gains through the application of a reduction

### 4.3. DISCUSSING THE OUTCOME OF THE NUMERICAL STUDY

---

basis. They showcase that the choice of a specific reduction basis for a nonlinear system should primarily be based on the type of excitation to which the system is subjected. The constitution of the nonlinearity is only an additional criterion. The most suited basis has to be carefully chosen amongst the presented ones on a case by case basis and following the established guidelines. Specially constructed POD bases are constantly the best performing ones, explaining their widespread use. Yet it is surprising to see that the Linear Normal Modes are, in general, performing as good as the Proper Orthogonal Decomposition bases or only slightly worse.

The results of the study of the robustness allows to judge the robustness of the reduced bases if they are applied to a differently parameterised test-case and to identify the parameters of the excitation that have the most impact on the performance of a reduced basis. The point of application of any excitation and the frequency of a harmonic forcing are inevitably to prioritize among the parameters that are treated. Also, the investigation shows clearly that, should the use of a single basis on a system under differently parameterised excitations become necessary, this basis has to be established with the most critical values for the parameters.

The results also reveal a number of shortcomings. With respect to the initially formulated expectation of identifying a single basis, which is especially well suited for treating nonlinear structures, it has to be stated that, in fact, no basis is broadly suited for all types of nonlinearities and for each specific case. Concerning the inherent robustness of the different bases it can be stated that none of the studied bases possesses this particular property in a desirably sufficient measure.

No basis is good enough before the applied criteria. This result is somewhat sobering because a large number of common reduced basis has been studied under near optimal conditions. This includes e.g. the POD, which could use all available snapshots<sup>12</sup>. And also the modifications that were specifically added to some reduced bases did, despite some improvements, not contribute substantially to the quality of the solution. Examples for such modifications are e.g. the use of the MAC for the CVT in section 3.3.5, or the extension of the LELSM to entirely nonlinear systems in section 3.3.6.2.

Further efforts are hence not directed at proposing yet another reduced basis. Instead, research must be concentrated on other elements of the process for solving reduced systems.

In particular, the requirements that are identified from this study and that remain<sup>13</sup> are

- adapting the time-marching solution process so that it takes into account the non-linear evolution of the solution,
- rendering the reduced system autonomous again, and
- adding a method that allows the parameterisation of the reduced solution process.

These requirements have to be met while the keeping the overall algorithm applicable to industrial sized structures.

---

<sup>12</sup>Refer to the annex section A.1.1 for the choice of the snapshots.

<sup>13</sup>The requirement of an autonomous reduced system is already identified in section 3.2.3. The fact that it is not yet met has proven advantageous for the presented studies because it limits the origin of the introduced error to the reduced basis. However, the inflation of the nonlinear terms has to be replaced.

## Chapter 5

# Addressing the identified requirements of an adapted solution algorithm, of the autonomy of the nonlinear terms and of parameterisation

---

This chapter is the response to the results of the numerical studies. The results of the previous chapter 4 seem to indicate that none of the examined reduced bases responds entirely to the stated requirements of quality and robustness. Keeping in mind the considerable work performed to develop the often complex methods for creating the different reduced bases it is sobering to see these bases fall short. Therefore proposing yet another reduced basis seems not a promising way of progressing in the creation and solution of reduced nonlinear systems. Instead the work is directed towards adapting the solution algorithm, providing the autonomy of the reduced systems and adapting the reduced bases to external parameters.

The major part of the presented methods will be illustrated by and tested independently from each other with applications to the test-case from the numerical study in the preceding chapter 4. It is chosen to present a selection of common methods for each requirement in order to have a tool box available. From this selection of different methods the choice can then be made as required, depending on the actual problem at hand. The main result of this chapter is the choice of one method in response to each of the three identified requirements.

For adapting the solution algorithm an approach that updates and augments the reduced basis is developed and chosen. Additional approaches that are also tested are the quasistatic correction and the Least-Squares Petrov-Galerkin method.

The autonomy of the nonlinear terms is assured with the selection of the polynomial formulation. The distinguishing feature of the polynomial formulation is that it can be rendered independent from the reduced basis. This crucial requirement emerges from the choice of the update and augmentation approach.

For the adaptation of the reduced bases to parameters an elegant interpolation in tangent spaces approach is chosen from literature.

These three elements are the three-fold response that addresses the entirety of the requirements that have

---

been identified to be key for the successful reduction of a geometrically nonlinear, parameterised system in the context of a transient solution. In the next step in chapter 6 the three methods are combined and applied to finite element test-cases.

## 5.1 Adapting the solution algorithm

The results of the comparative study in section 4.2.1.4 show that introducing a reduced basis alone is not sufficient to successfully reduce a non-linear system. Furthermore it seems to have been proven that this holds for all applied reduced bases and that most possibly there is no reduced basis that is adapted to nonlinear systems in a satisfactory manner. Therefore, in section 4.3, the decision has been made to direct further efforts with the aim of reducing a nonlinear system at the adaptation of the solution algorithm rather than at the reduced basis. This section explores how the solution algorithms can be adapted to solve reduced nonlinear systems with a lesser error than obtained with the introduction of the reduced basis alone.

The adaptation of the solution algorithm has to succeed in relatively tight boundaries. It has to be compatible with the reduced nonlinear Newmark scheme (section 3.2.2) and the HHT- $\alpha$ -method because these solution algorithms have been chosen in section 3.1.3 to function with the approach of reduced bases. Furthermore, a minimal intrusive adaptation of the existing schemes is desirable for practical reasons such as coding and verification.

Luckily, there are already a number of approaches available in literature that allow adapting the nonlinear Newmark scheme to reduced solutions of nonlinear systems. Once the reduced equivalent of the reduced nonlinear Newmark scheme is adapted to successfully solve reduced nonlinear systems, this adaptation can simply be carried over to the HHT- $\alpha$ -method.

The common approaches that are selected to be tested and that are presented in the following are

- the quasi-static correction, as it is expanded by e.g. Hansteen and Bell [92],
- the Least-Squares Petrov-Galerkin method, as it is proposed by Carlberg et al. [55], and
- the update of the reduced basis, which is perceived as a common idea.

The quasi-static correction and Least-Squares Petrov-Galerkin have in common that they built on the nonlinear Newmark scheme and are specially conceived for the transient solution of reduced systems. The update of the reduced basis is rather an extension of the reduced nonlinear Newmark scheme and aims at making the reduced basis follow the nonlinear evolution of the reduced solution. All three approaches are compared with the standard nonlinear reduced Newmark scheme with inflation as a benchmark in order to determine if they yield any benefits for the quality of the solution.

### 5.1.1 Describing and testing the quasi-static correction

The quasi-static correction is a possible improvement of the reduced nonlinear Newmark scheme. It aims at re-including the displacements due to the part of the external forces, which is cut-off by the projection, i.e. which is perpendicular to the basis. The usual projection of the external forces vector<sup>1</sup>  $\mathbf{f}_E$  is simply

$$\tilde{\mathbf{f}}_E = \Phi^T \mathbf{f}_E, \quad (5.1)$$

as it is indicated as early as in equation (3.93). But this simple projection of the external forces vector comes at a price, which is very well expanded by Hansteen and Bell [92], together with a possible remedy. The use of the quasi-static correction has recently risen in interest again by the work of Thomas et al. [224].

In equation (5.1) the reduced external forces vector  $\tilde{\mathbf{f}}_E$  no longer contains terms of  $\mathbf{f}_E$ , which are normal to  $\Phi$ . This is of course in the nature of a projection, which has as purpose the generation of the  $r$ -dimensional vector  $\tilde{\mathbf{f}}_E$  for the reduced external forces. Yet, from the mechanical point of view it is questionable, whether the components of  $\mathbf{f}_E$  that are normal to  $\Phi$ , can be neglected without endangering a correct result. And this

<sup>1</sup>The explicit dependence of the external forces  $\mathbf{f}_E(t)$  on time is assumed throughout this section. The necessary notation is however adapted to increase the readability of the equations.

is where the quasi-static correction plugs in by finding the components of  $\mathbf{f}_E$ , which are normal to  $\Phi$ , and constructing a static correction term from them. The aim is thus to decompose the full order external forces vector  $\mathbf{f}_E$  in a part  $\mathbf{f}_E^{\parallel}$ , which is within the span of  $\Phi$ , and a complementary part  $\mathbf{f}_E^{\perp}$ , which is orthogonal to the span of  $\Phi$ . The complementary part  $\mathbf{f}_E^{\perp}$  is used for the static correction.

### 5.1.1.1 Describing the quasi-static correction

To find the static correction term  $\mathbf{f}_E^{\perp}$  it is supposed that the full order external forces vector  $\mathbf{f}_E$  can be expressed as

$$\mathbf{f}_E = \mathbf{f}_E^{\parallel} + \mathbf{f}_E^{\perp}. \quad (5.2)$$

where the vector  $\mathbf{f}_E^{\parallel}$  is of size  $n \times 1$  and holds only the components of  $\mathbf{f}_E$ , that are in the span of  $\Phi$ . Using a generic set of generalised multipliers  $\mathbf{q}_E$  this translates to

$$\mathbf{f}_E^{\parallel} = \Phi \mathbf{q}_E. \quad (5.3)$$

The generalised multipliers  $\mathbf{q}_E$  are only introduced as an illustrative aid to the construction of  $\mathbf{f}_E^{\parallel}$ . They are eliminated in an instant by using the definition of the vector  $\mathbf{f}_E^{\perp}$ .

The vector  $\mathbf{f}_E^{\perp}$  is required for the quasistatic correction and most efforts below are directed to render it accessible. It is defined as being perpendicular to the span of  $\Phi$ . This is enforced by

$$\Phi^T \mathbf{f}_E^{\perp} = \mathbf{0}. \quad (5.4)$$

Reducing equation (5.2) by premultiplying  $\Phi^T$ , as required by equation (3.93), yields the reduced vector of the external forces

$$\tilde{\mathbf{f}}_E = \Phi^T \mathbf{f}_E, \quad (5.5)$$

$$= \Phi^T (\mathbf{f}_E^{\parallel} + \mathbf{f}_E^{\perp}). \quad (5.6)$$

Exploiting equations (5.3) to replace the  $\mathbf{f}_E^{\parallel}$  and (5.4) to eliminate  $\mathbf{f}_E^{\perp}$ , this yields

$$\tilde{\mathbf{f}}_E = \Phi^T (\Phi \mathbf{q}_E + \mathbf{f}_E^{\perp}), \quad (5.7)$$

$$= \Phi^T \Phi \mathbf{q}_E. \quad (5.8)$$

Recalling that  $\tilde{\mathbf{f}}_E = \Phi^T \mathbf{f}_E$  from equation (5.5) equation (5.8) can be used to determine the of generalised multipliers

$$\mathbf{q}_E = (\Phi^T \Phi)^{-1} \Phi^T \mathbf{f}_E. \quad (5.9)$$

They can hence be eliminated from equation (5.3) and  $\mathbf{f}_E^{\parallel}$  is expressed exclusively with the reduced basis

$$\mathbf{f}_E^\parallel = \Phi(\Phi^T\Phi)^{-1}\Phi^T\mathbf{f}_E, \quad (5.10)$$

$$= \Phi(\Phi^T\Phi)^{-1}\tilde{\mathbf{f}}_E, \quad (5.11)$$

Feeding this result back into equation (5.2) allows to extract the vector of the external forces that is not in the span of the reduced basis

$$\mathbf{f}_E^\perp = \mathbf{f}_E - \mathbf{f}_E^\parallel, \quad (5.12)$$

$$= \mathbf{f}_E - \Phi(\Phi^T\Phi)^{-1}\Phi^T\mathbf{f}_E. \quad (5.13)$$

The quasistatic correction term  $\mathbf{f}_E^\perp$  of the external forces orthogonal to the span of  $\Phi$  is ultimately obtained as

$$\mathbf{f}_E^\perp = \left( \mathbf{I} - \Phi(\Phi^T\Phi)^{-1}\Phi^T \right) \mathbf{f}_E \quad (5.14)$$

If the reduced basis  $\Phi$  is constant throughout the solution process the entire matrix in brackets  $\mathbf{I} - \Phi(\Phi^T\Phi)^{-1}\Phi^T$  in equation (5.14) can be calculated once and stored.

The component  $\mathbf{f}_E^\perp$  of the external forces from equation (5.14), which is orthogonal to the projection basis  $\Phi$  and as such ignored in the solution process, can be used as a quasi-static correction at the end of each time-step. Once the inner iteration of the reduced nonlinear Newmark scheme for reduced model has converged on the generalised coordinates  $\mathbf{q}_{i+1}^{(t+\Delta t)}$  the quasi-static correction can be applied without or with feedback. This property of the quasi-static correction of being applied without or with feedback determines whether the static displacements due to  $\mathbf{f}_E^\perp$  are fed back into the dynamic solution.

**5.1.1.1.1 Quasi-static correction without feedback** The quasi-static displacements  $\bar{\mathbf{K}}^{-1}\mathbf{f}_E^\perp$  are simply added to the reconstructed displacements

$$\begin{aligned} \mathbf{u}^{(t+\Delta t)} &= \Phi\mathbf{q}^{(t+\Delta t)} + (\bar{\mathbf{K}})^{-1}\mathbf{f}_E^\perp(t+\Delta t) \\ &= \Phi\mathbf{q}^{(t+\Delta t)} + (\bar{\mathbf{K}})^{-1}\left(\mathbf{I} - \Phi(\Phi^T\Phi)^{-1}\Phi^T\right)\mathbf{f}_E(t+\Delta t). \end{aligned} \quad (5.15)$$

The reduced order model, which otherwise runs independently, is not aware of the correction. As the following generalised coordinates  $\mathbf{q}_{(1)}^{(t+2\Delta t)}$  are still defined directly within the Newmark scheme, they are oblivious to the quasi-static correction. In fact, the correction is only applied directly before storing the current displacement in the memory of the computer that runs the algorithm. The reduced order model is solved independently of the quasi-static correction and the latter is simply introduced as an additive layer between the reconstructed solution and the final solution from the reduced system.

**5.1.1.1.2 Quasi-static correction with feedback** Dickens et al. [69] expand the quasi-static correction by using the static displacements of the quasi-static correction as additional vectors in the reduced basis. This makes the quasi-static correction participate in the dynamic solution. This approach is used as an inspiration to feed the displacements of the quasi-static correction back into the solution process.

With feedback the final solution at  $t+\Delta t$ , including the quasi-static correction is fed back into the reduced model. This is done by determining the next reduced displacements  $\mathbf{q}_{(i=1)}^{(t+2\Delta t)}$  in the least squares sense from

the final solution  $\mathbf{u}_{(i+1)}^{(t+\Delta t)}$ .

For the application of the quasi-static solution with feedback the final displacements  $\mathbf{u}^{(t)}$  at time  $t$  are obtained by equation (5.15), as the sum of the final value of the inner iteration  $\Phi \mathbf{q}_{(i+1)}^{(t)}$  and the quasi-static correction  $\bar{\mathbf{K}}^{-1} \mathbf{f}_E^\perp$ . The initial values for the next time-step  $t+2\Delta t$ , as they are required in equation (3.55), are now defined as the least squares approximation of the reduced final displacements, giving

$$\begin{aligned} \check{\mathbf{q}}^{(t+\Delta t)} &= (\Phi^T \Phi)^{-1} \Phi^T \mathbf{u}^{(t+\Delta t)} \\ &= (\Phi^T \Phi)^{-1} \Phi^T \left( \Phi \mathbf{q}^{(t+\Delta t)} + (\bar{\mathbf{K}})^{-1} \mathbf{f}_E^\perp(t + \Delta t) \right) \\ &= (\Phi^T \Phi)^{-1} \Phi^T \left( \Phi \mathbf{q}^{(t+\Delta t)} + (\bar{\mathbf{K}})^{-1} \left( \mathbf{I} - \Phi (\Phi^T \Phi)^{-1} \Phi^T \right) \mathbf{f}_E(t + \Delta t) \right), \end{aligned} \quad (5.16)$$

where the  $\mathbf{u}^{(t+\Delta t)}$  comes from equation (5.15). The predictive values for the inner, iterative loop are then based upon the definition (5.16), giving

$$\mathbf{q}_{(i=1)}^{(t+\Delta t)} = \check{\mathbf{q}}^{(t+\Delta t)} + \Delta t \dot{\mathbf{q}}^{(t)} + \frac{1}{2} \Delta t^2 \ddot{\mathbf{q}}^{(t)}, \quad (5.17)$$

as a replacement for equation (3.79). In this way the reduced order model becomes aware of the quasi-static correction, which took place in the preceding time-step, and the quasi-static correction is fed back into the reduced system via the displacements. The velocities and the accelerations of the solution are not affected by neither of the two variants of the quasi-static correction. This is determined by the nature of the correction terms, which are defined as the solution of an exclusively static problem.

### 5.1.1.2 Testing the quasi-static correction numerically and evaluating the results

The results of the quasi-static correction, applied to the solutions of the LNM and the Ritz-vector reduced test-cases, are shown in the following. The test-cases' set-up is the same as for the comparative study in section 4.2.1. The results are presented for the quasi-static correction without and with feedback. The figures 5.1 to 5.4 show the overall reduction time for the different test-cases. The figures 5.5 to 5.8 show the mean of the R2MSE. The results obtained with the quasi-static correction are marked with the subscript QSC in all figures. The results obtained without feedback bear no further identification. Solutions obtained with feedback are marked with the additional letters FB.

## 5.1. ADAPTING THE SOLUTION ALGORITHM

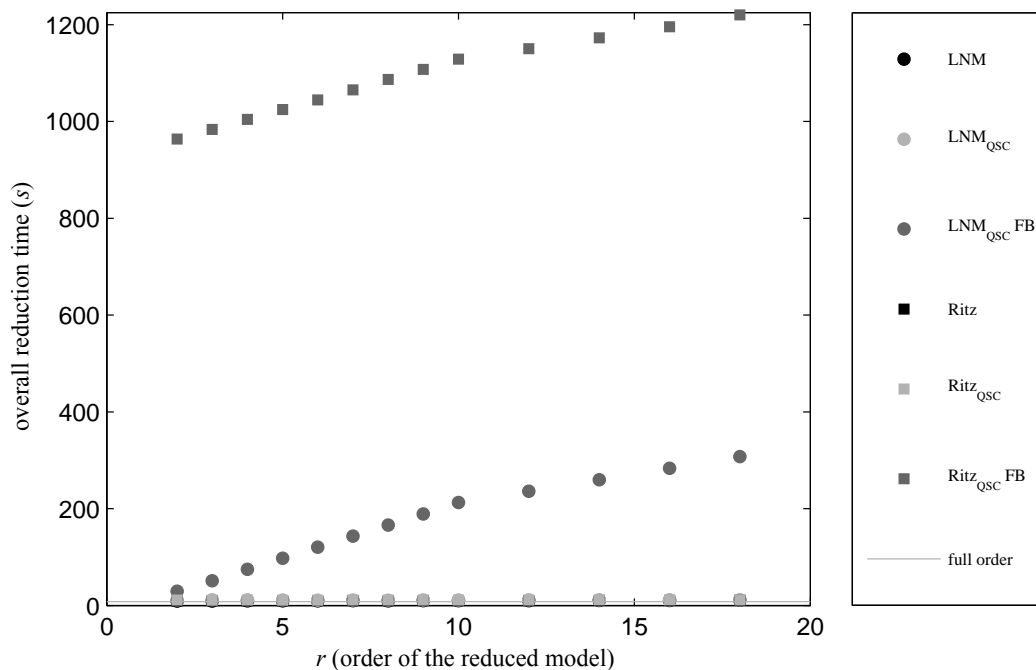


Figure 5.1: The overall reduction time for the locally non-linear system under harmonic excitation solved with the quasi-static correction

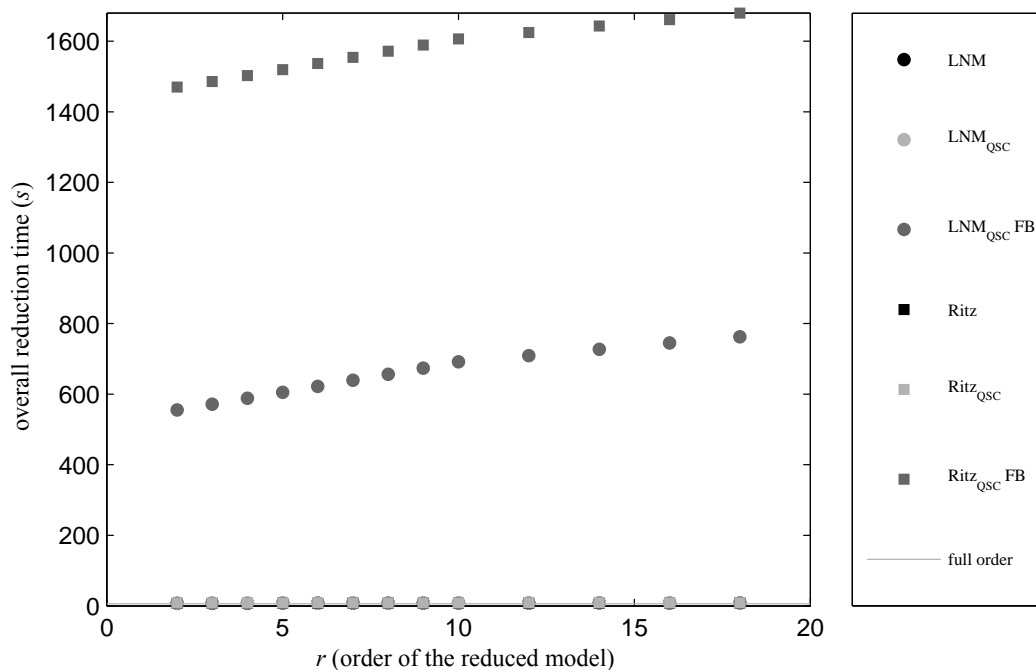


Figure 5.2: The overall reduction time for the entirely non-linear system under harmonic excitation solved with the quasi-static correction

## 5.1. ADAPTING THE SOLUTION ALGORITHM

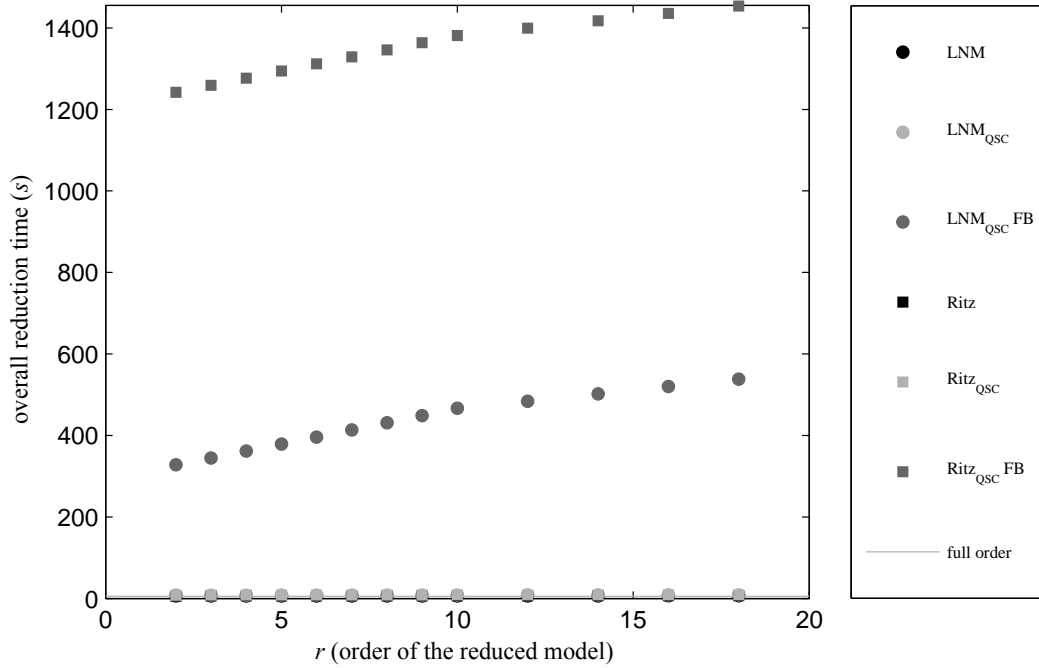


Figure 5.3: The overall reduction time for the locally non-linear system under impulse excitation solved with the quasi-static correction

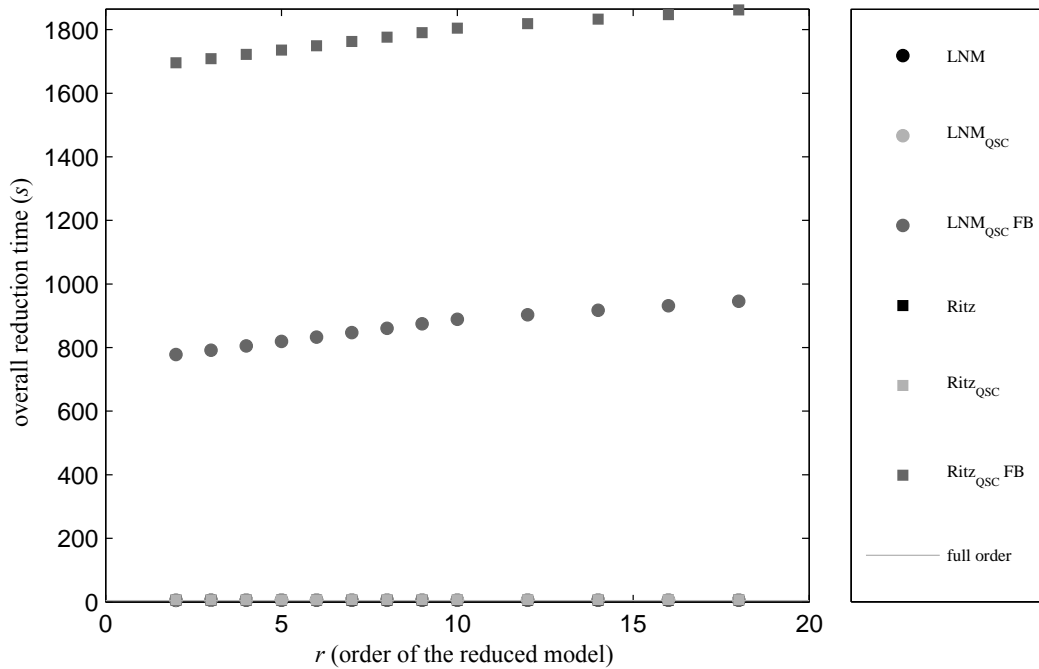


Figure 5.4: The overall reduction time for the entirely non-linear system under impulse excitation solved with the quasi-static correction

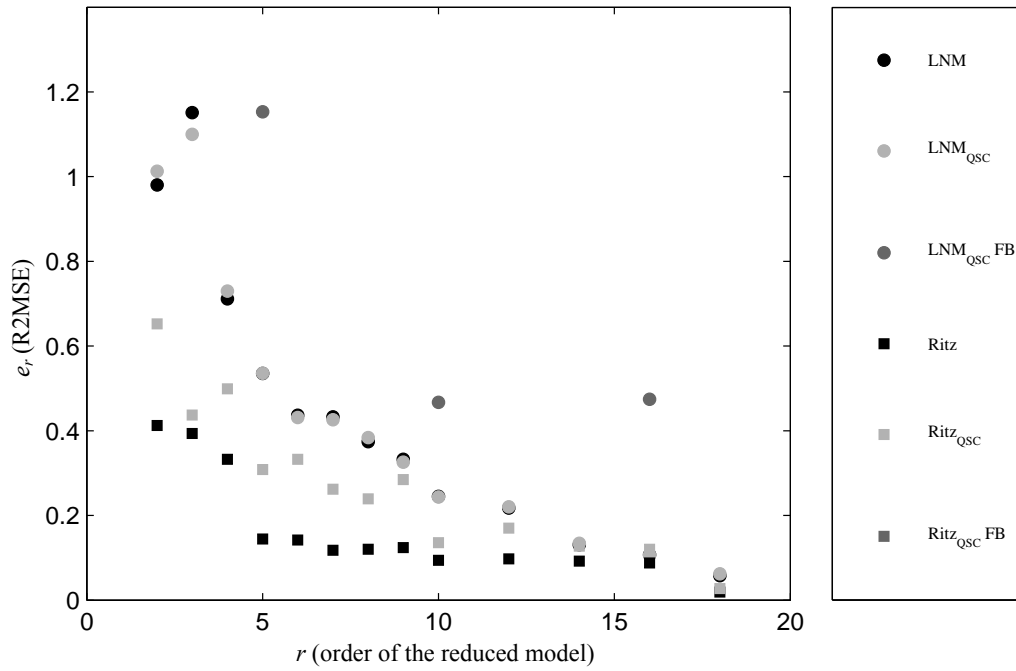


Figure 5.5: The R2MSE for the locally non-linear system under harmonic excitation solved with the quasi-static correction

## 5.1. ADAPTING THE SOLUTION ALGORITHM

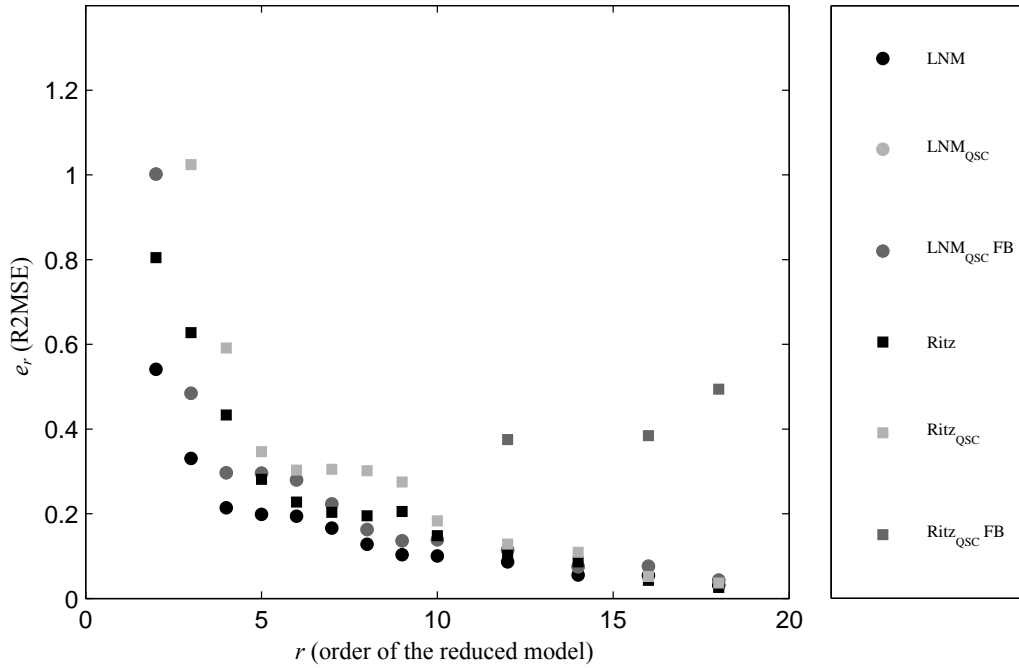


Figure 5.6: The R2MSE for the locally non-linear system under impulse excitation solved with the quasi-static correction

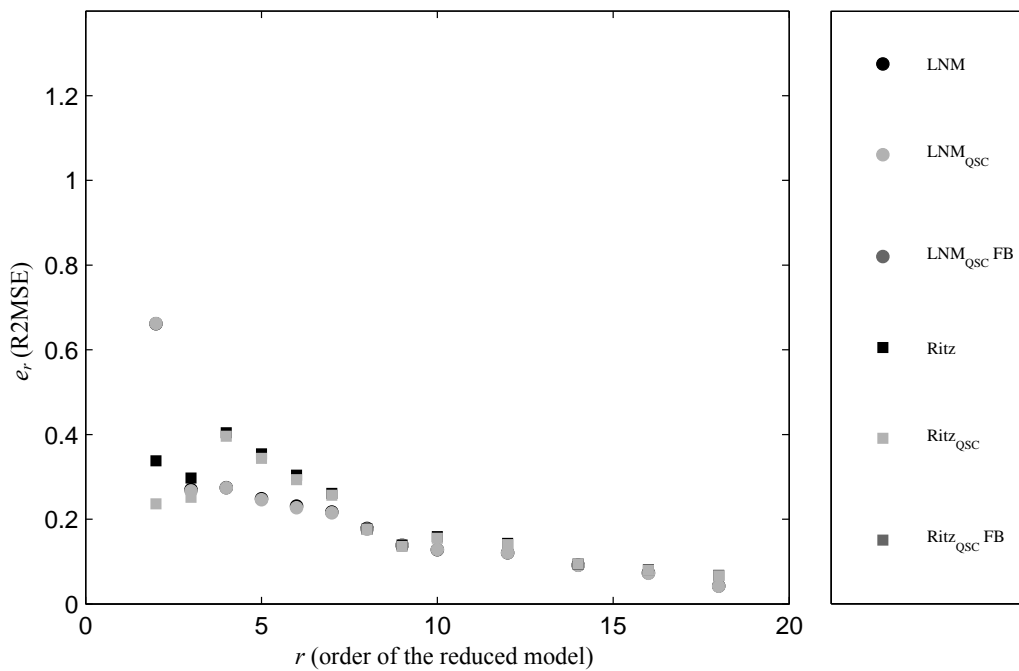


Figure 5.7: The R2MSE for the entirely non-linear system under harmonic excitation solved with the quasi-static correction

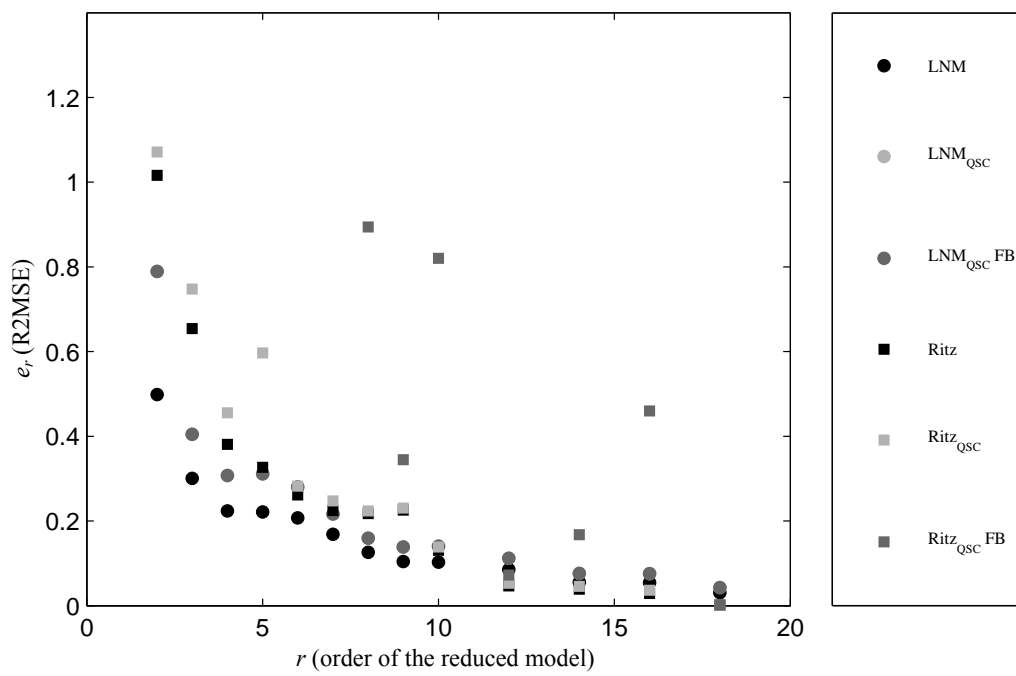


Figure 5.8: The R2MSE for the entirely non-linear system under impulse excitation solved with the quasi-static correction

**5.1.1.2.1 Evaluating the quasi-static correction without feedback** The figures 5.1, 5.2, 5.3 and 5.4 show the overall reduction time for the four test-cases, compared to the solution time of the reference solution and to the overall reduction time of the respectively reduced system without quasi-static correction. The inclusion of the quasi-static correction increases the overall solution time considerably. This is somewhat evident, as the quasi-static solution adds a full order static problem to be solved for each time-step to the solution effort. It has to be remembered that the evaluation of equation (5.15) takes place at full order and at every time-step. In fact, this equation is more than a static problem because it includes the construction of the orthogonal components of the external forces vector and the construction of the tangent stiffness matrix  $\bar{K}$  at every time-step. The latter is not readily available because the Jacobian of the system in equation (3.57) is constructed at reduced level and the full order stiffness matrix of the system has thus to be constructed explicitly<sup>2</sup> from the nonlinear forces vector at full order  $g(u)$ . All these are considerable additional efforts that reflected in the overall reduction time.

The remaining figures in 5.5 to 5.8 show the R2MSE  $e_r$  from equation (4.5) for the different test-cases, again compared to the errors obtained from the reduced systems without corrections. Only for the entirely nonlinear system under harmonic excitation, in figure 5.7, and its rather smooth solution, the application of the quasi-static correction without feedback improves the result. For the remaining test-cases there is a, sometimes even significant, degradation of the solution's quality observable. Together with the considerable additional computational efforts, this somewhat limits the applicability of the quasi-static correction.

**5.1.1.2.2 Evaluating the quasi-static correction with feedback** The figures 5.1 to 5.8 are summing up the results for the quasi-static correction with feedback. They show the same augmentation of the overall reduction time, as already discussed for the approach without feedback above. The R2MSE  $e_r$  is however up to five times larger as for the reference reconstructed solutions, obtained from the systems reduced with the LNM or the Ritz-vectors alone. A fact which voids including a feedback loop of all interest.

### 5.1.2 Introducing and discussing the Least-Squares Petrov-Galerkin method

The Least-Squares Petrov-Galerkin (LSPG) method is a variation of the original nonlinear Newmark scheme and replaces the inner Newton-Raphson iteration, represented by equations (3.80) to (3.83). The main idea of the Least-Squares Petrov-Galerkin reduction technique, is to apply a projection on the basis  $\Psi$  to the residual  $r$  of a dynamic system's solution and to adapt this projection basis as the displacements evolve. To this effect the  $\Psi = \Phi$ , as it is originally used in section 3.2.2.1, is replaced by the product of the original reduced basis and the system's Jacobian  $\Psi = S\Phi$ . With this approach the LSPG technique hooks into the nonlinear Newmark Scheme and alters the way, the residual  $r$  in equation (3.81) is driven towards zero. Because the LSPG approach requires the evaluation of the residual  $r$  and the Jacobian  $S$ , i.e. namely the nonlinear tangent stiffness matrix  $\bar{K}$ , at full order, Carlberg et al. [55] devised approximations for these two terms. In Carlberg et al. [56] this is denominated hyper reduction, as it introduces a second layer of reduction into the process.

The notion of Galerkin- and Petrov-Galerkin-projection was briefly touched in section 3.1.2.1. Following the introduction of the trial and the test-space the exclusive use of Galerkin-projection with  $\Psi = \Phi$  is quickly accepted for the present scope within an application in structural dynamics throughout this work. Petrov-Galerkin-projections with  $\Psi \neq \Phi$  have their legit application mainly for certain first-order differential equations. The LSPG approach may offer a possibility to derive benefit from the application of a Petrov-Galerkin-projection for the transient solution of a reduced structural system.

The LSPG method is introduced by Carlberg et al. [55], whose approach is sketched hereunder. Their approach is based partially on the work of Bui-Thanh et al. [44], who uses a simple Least-Squares approach

---

<sup>2</sup>This remains true for the actual implementation of the current test-cases. Even though the solutions are obtained with the reduced nonlinear Newmark scheme with inflation, the full order nonlinear tangent stiffness matrices that become available during the evaluation of equation (3.83) are not reused in the quasi-static correction. Thus, it is ensured that the additional numerical effort due to the introduction of the quasi-static correction becomes visible.

with an emphasis on the adaptation of the reduction for different external parameters. A general presentation of the Least Squares technique is omitted in the scope of this section. Kim and Langley [119] give a brief overview and show that successful applications of this generic technique can range as far as the resolution of ambiguities in GPS-signals. Most recently, Carlberg et al. [56] developed the LSPG method further into the Gauss-Newton with Approximated Tensors (GNAT) method. The second layer of reduction for the full order quantities is formalised as hyper-reduction and the method is extended to finite volume computations for applications in CFD. However, the hyper-reduction is not applied here because these additional approximations might introduce additional errors. This argument is similar to the one made for justifying the use of the inflation formulation for the numerical studies of the reduced bases in chapter 4.

Carlberg et al. [55] write about the Least-Squares Petrov-Galerkin projection that this approach “can capture in principle the nonlinear effects but is practical primarily when the nonlinear model reduction is performed at the fully discrete level.” This claim is to be verified in the following, by applying it to the same test-cases as used for the numerical studies in chapter 4.

In the following a different look is taken at the introduction of the right-hand reduced basis  $\Psi$  the nonlinear Newmark scheme in order to introduce the LSPG and to explain the motivation for this introduction. The developed LSPG method is then applied in numerical tests.

### 5.1.2.1 Taking a different look at reduced nonlinear Newmark scheme

In order to begin with the introduction of the LSPG method a step back is made and a different look at the Newton-Raphson iterations of the nonlinear Newmark scheme is taken. Equation (3.60), for determine the incremental displacement  $\Delta \mathbf{u}$  is considered. It reads

$$\mathbf{S}\Delta \mathbf{u} = \mathbf{r}, \quad (5.18)$$

if all super- and subscripts are omitted for the sake of simplicity. It is also arranged in its original state, prior to the inversion of system’s Jacobian  $\mathbf{S}$ . If now the reduction of the physical displacements  $\mathbf{u}$  is introduced by means of a reduced basis  $\Phi$  via equation (3.1), equation (5.18) becomes

$$\mathbf{S}\Phi\Delta \mathbf{q} = \mathbf{r}, \quad (5.19)$$

for the reduced incremental displacements  $\Delta \mathbf{q}$ .

It is obvious that equation (5.19) cannot be solved exactly for the  $r$  unknowns in the vector  $\Delta \mathbf{q}$  because it represents an over determined system with  $n$  equations. This requires some kind of approximation and leads to the introduction of the left-hand reduced basis  $\Psi$ , which transforms equation (5.19) into

$$\Psi^T \mathbf{S}\Phi\Delta \mathbf{q} = \Psi^T \mathbf{r}. \quad (5.20)$$

This is no different from the actions taken until now, only the interpretation of the introduction of  $\Psi$  as an instrument to approximate the solution for the reduced incremental displacements  $\Delta \mathbf{q}$  is new. Because what equation (5.20) effectively does, is to reduce the number of equations that define  $\Delta \mathbf{q}$  from  $n$  to  $r$ , so that an exact solution for the approximation of  $\Delta \mathbf{q}$  can be found.

This is exactly what is done in section 3.2.2.1 with the introduction of the reduction for the nonlinear Newmark scheme. However, the reduction there is much less obvious. First because the left-hand reduced basis  $\Psi$  is set equal to  $\Phi$  and, second, it is applied to all components of  $\mathbf{S}$  and  $\mathbf{r}$  individually, and sometimes, especially for the reduced matrices  $\tilde{\mathbf{M}}$  and  $\tilde{\mathbf{C}}$ , even permanently for numerical efficiency. This approach somewhat hides the meaning and intention of the introduction of  $\Psi$ , as it is spread from its core

application in equation (5.20) over the entire algorithm. Furthermore the equality  $\Psi = \Phi$  is pervasively assumed outside of the current section, so that equation (5.20) becomes a Galerkin projection which offers an approximated solution for  $\Delta q$  which is optimal for computational exploitation because the residual is minimised with respect to  $\Phi$ . However, this has not to be the case.

Equation (5.20) is solved such for  $\Delta q$  such that the approximation

$$\Psi^T (r - S\Phi\Delta q) = 0 \quad (5.21)$$

holds. It states that the resulting difference from the approximation ( $r - S\Phi\Delta q$ ) is orthogonal on the space which is spanned by  $\Psi$ . In the case of  $\Psi = \Phi$  this approximation is not optimal in the least-squares sense (Strang [218]) because  $\Phi$  is not related<sup>3</sup> to  $S$ . In fact, any  $n \times r$  matrix could be used as  $\Psi$ .

The LSPG approach sets  $\Psi = S\Phi$ , with the intention of making the optimality of the approximation follow the evolution of the system's solution, by including the system's Jacobian  $S$ . This renders the solution of equation (5.21) optimal in the least-squares sense (Strang [218]). Yet, the optimality is not exclusively limited neither to the system's Jacobian nor to the actual reduced basis  $\Phi$ . It is not the aim to discuss the optimality of different  $\Psi$  in a theoretical setting, and only  $\Psi = S\Phi$  is used in the following, explorational study.

Before continuing with the discussion of the numerical results of an explorational study, the concept LSPG approach is first introduced on algorithmic level into the nonlinear Newmark scheme.

### 5.1.2.2 Introducing the LSPG method on algorithmic level

This section does not describe the entire LSPG approach, as it is proposed by Carlberg et al. [55]. Their original method features two layers of reduction. The first layer is the projection on a reduced basis. It is kept and adapted for providing a high accuracy during the solution of a nonlinear system by setting  $\Psi = S\Phi$ . The second layer of reduction is intended to significantly speed up the computation by means of a hyper-reduction. Only the first layer of reduction is treated here, in order to avoid the introduction of additional errors through the approximations of the full order-residual  $r$  and the full order Jacobian  $S$ . Both full order quantities are required for the LSPG approach.

During a LSPG solution the residual is calculated at full order level, much like in equation (3.56),

$$r_{(i)}^{(t+\Delta t)} = f_E(t + \Delta t) - M\Phi\ddot{q}_{(i)}^{(t+\Delta t)} - C\Phi\dot{q}_{(i)}^{(t+\Delta t)} - g\left(\Phi q_{(i)}^{(t+\Delta t)}\right), \quad (5.22)$$

and the Jacobian of the system alike

$$S_{(i)} = \left. \frac{\partial g(\Phi q)}{\partial(\Phi q)} \right|_{\Phi q_{(i)}^{(t+\Delta t)}} + \frac{\gamma}{\beta \Delta t} C + \frac{1}{\beta \Delta t^2} M. \quad (5.23)$$

The increment's direction is optimised by putting  $\Psi_{(i)} = S_{(i)}\Phi$  and thus obtaining

$$\Phi^T S_{(i)}^T S_{(i)} \Phi \Delta q_{(i)}^{(t+\Delta t)} = \Phi^T S_{(i)}^T r_{(i)}^{(t+\Delta t)}. \quad (5.24)$$

---

<sup>3</sup>However, in the case of a linear system with modal damping, the matrix  $\Phi^T S \Phi$  becomes diagonal if  $\Phi$  is created with the LNM. This is expressed by equations (3.104) and (3.105) and leads to a tremendous alleviation of the computational burden required for solving the equation.

## 5.1. ADAPTING THE SOLUTION ALGORITHM

---

as replacement of equation (3.60). With a  $QR$ -decomposition of  $S_{(i)}\Phi$  the equation above can be computationally optimised, giving

$$\Delta q_{(i)}^{(t+\Delta t)} = R_{(i)}^{-1} Q_{(i)}^T r_{(i)}^{(t+\Delta t)}. \quad (5.25)$$

The outer loop of the nonlinear Newmark scheme, advancing in the time, is not affected by the LSPG-approach. With this new algorithm, containing the LSPG nested inside the time marching part of the reduced nonlinear Newmark scheme from section 3.2.2.1, some explorative numerical studies can be performed.

### 5.1.2.3 Discussing the results of the explorative numerical study of the LSPG method

The explorative numerical study of the LSPG method mirrors the two studies from section 4.2. In a first step the LSPG method is applied on the test-case without alteration in order to compare the reduced solutions. In a second step the possible application of the LSPG method for increasing the robustness of the reduced basis is explored.

**5.1.2.3.1 Applying the LSPG method for a comparison of different reduced bases** The explorative numerical study of the LSPG method draws on the test-cases, criteria and algorithms that are developed for the comparative study of the reduced bases in section 4.2.1. Because of the fact that the same numerical tools and examples are used, the results of the comparative study serve as a benchmark for judging the possible improvements that might be obtained with the application of the LSPG method.

The results are listed for the two systems under harmonic excitation only because the impulse excitation solution's fail to converge with the newly introduced convergence criterion. This criterion is required to be reformulated because it has to work on a full order residual of a reduced system.

The course of action consists in consequently reducing the entire system and to use full order values for the Jacobian  $S$  and the residual  $r$  only as stipulated in section 5.1.2. The full order Jacobian matrix  $S$  is then used together with the reduced basis  $\Phi$  for optimising the search direction within the inner loop of the nonlinear Newmark scheme, by building the left-hand reduction basis as  $\Psi = S\Phi$ . This procedure corresponds to the method introduced by Carlberg et al. [55], yet it does not feature the underlying approximations for the Jacobian  $S$  and the residual  $r$ . This is important because these approximations might introduce additional errors, which are undesirable while investigating the performance of the reduced bases. Furthermore the main question to be asked is, if the optimisation of the search direction yields any gains in quality of the reduced solution. This question comes before any possible gains in computational performance.

In fact, especially the question for computational performance is difficult to answer. Obviously the calculation of the Jacobian and the residual at full order requires more computational effort than reduced operations. This effort should even be significant because for matrix operations the effort scales with higher orders of the matrix' size. Another problem arising from switching between a completely reduced system in the outer loop of the nonlinear Newmark scheme to a partially full order system in the inner loop is the definition on the convergence criterion. If using a norm of the residual of the reduced system of the outer loop, scaled with a factor, it cannot be applied directly as a threshold for verifying the convergence of the full order residual of the inner loop. To render the two residual comparable, an additional step is required, in which the full order residual is projected on  $\Psi = S^T\Phi$ , in order to make it comparable with the reduced order residual of the inner loop.

The figures 5.9 and 5.10 show the overall reduction time of LSPG solutions for the two systems under harmonic excitation as examples. They reveal a noticeable increase of the overall reduction time while switching from the reduced Newmark scheme with inflation to the LSPG method.

However, as with the previous section 4.1.2.4 no definite answer can be given for the questions related to the computational performance on the small academic test-cases. It is highly doubtful that the possible

## 5.1. ADAPTING THE SOLUTION ALGORITHM

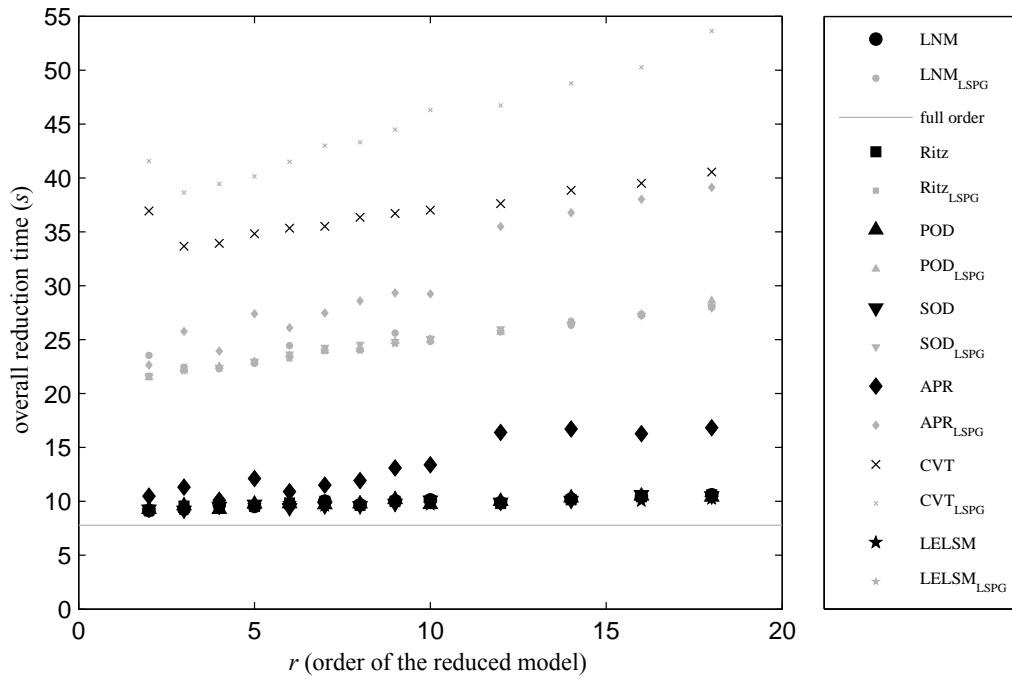


Figure 5.9: The overall reduction time for the large variant of the locally non-linear system under harmonic excitation solved with the LSPG method

decrease of the number of required inner iterations due to the optimisation of the search direction, can offset the full order calculations from a performance point of view.

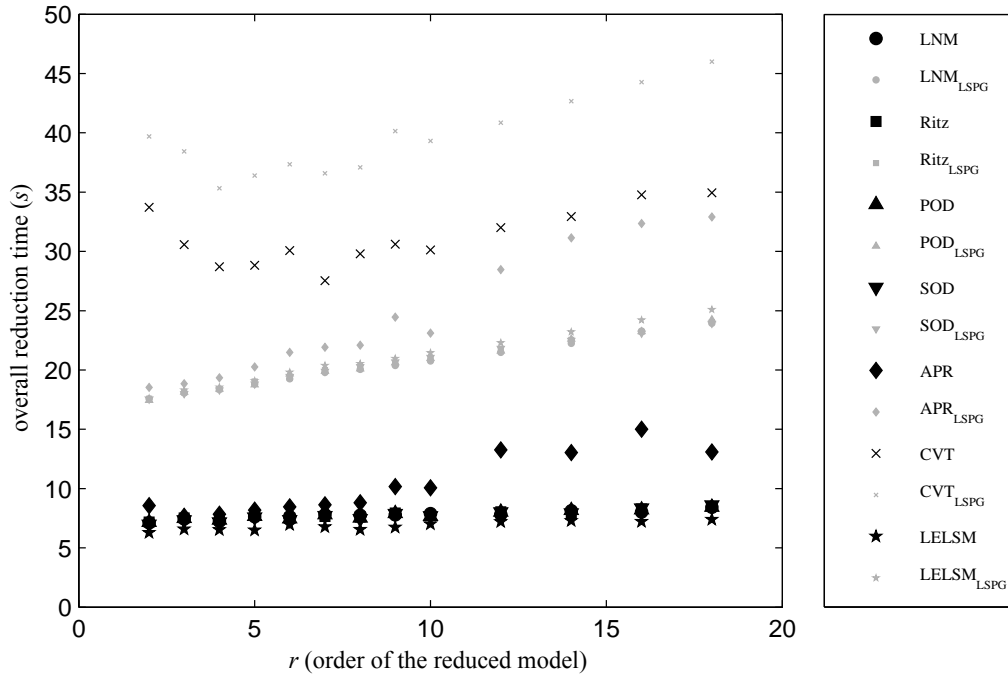


Figure 5.10: The overall reduction time for the large variant of the entirely non-linear system under harmonic excitation solved with the LSPG method

The figures 5.11 to 5.12 contain the results of the simulations with the LSPG procedure in terms of the mean of the R2MSE  $e_r$  from equation (4.5). The R2MSE is chosen as a single error-metric because it allows a more direct comparison of the two types of solutions than the score from section 4.1.2.2. The R2MSE of the two types of solution are identical.

This observation also applies to the time histories of the solutions. If time histories of degrees of freedom are superposed, the ones that are obtained with the classic reduced nonlinear Newmark scheme from section 3.2.2.1 and the ones obtained with the LSPG are indistinguishable. They are identical. After thorough inspection of the implementation an erroneous realisation of the concept of the LSPG in the code can be ruled out with near certainty. Obviously, with this possibility ruled out, the LSPG method does not provide an edge over the classic reduced nonlinear Newmark scheme with inflation in terms of quality of the solution. The solutions are in fact identical for the most part. This is a somewhat sobering result. Especially if seen in conjunction with the considerably longer overall simulation times.

A possible cause for this behaviour might be identified in the very strict convergence criterion  $\epsilon$  applied to the reduced counterpart of equation (3.64) of the classic reduced nonlinear Newmark scheme and the exaggeratedly small time-step. Both are introduced in the numerical studies in chapter 4 with the aim of elimination every other possible source of error other than the introduction of the reduced basis. Should this be the case, the LSPG might regain its merit if it allows to relax these criteria considerably.

## 5.1. ADAPTING THE SOLUTION ALGORITHM

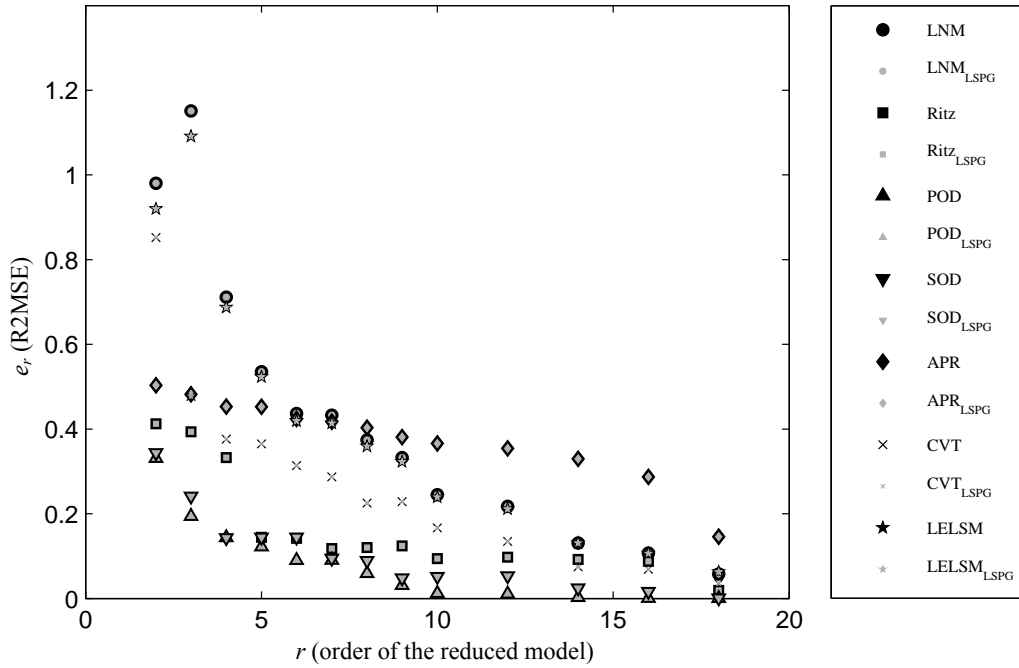


Figure 5.11: The R2MSE for the large variant of the locally non-linear system under harmonic excitation solved with the LSPG method

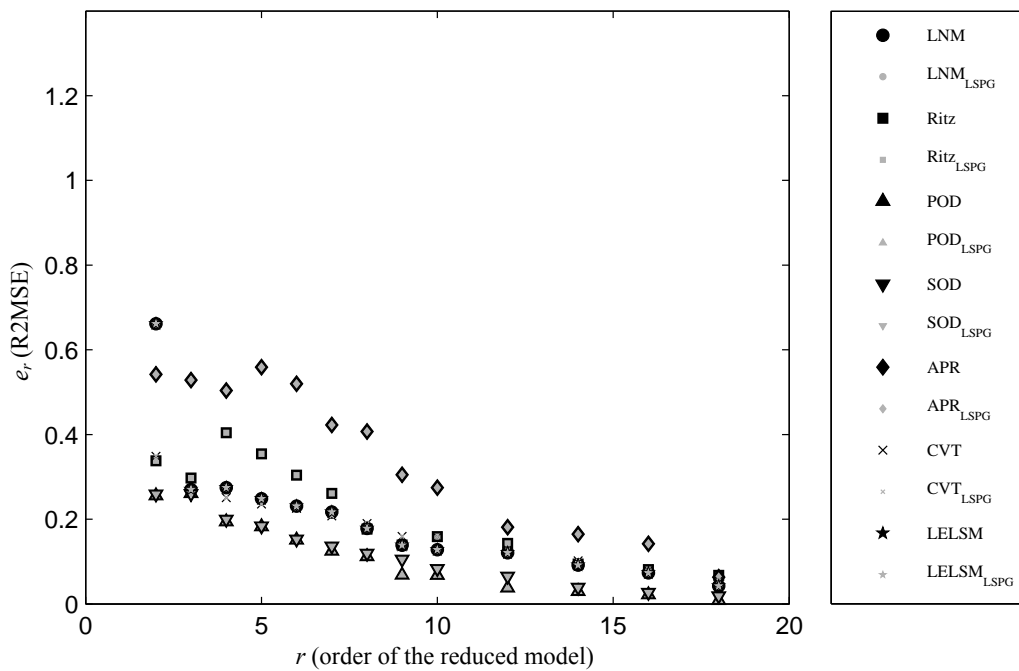


Figure 5.12: The R2MSE for the large variant of the entirely non-linear system under harmonic excitation solved with the LSPG method

## 5.1. ADAPTING THE SOLUTION ALGORITHM

---

Still, the LSPG method offers to introduce approximations for the full order nonlinear terms, which might offer a way to performance improvements. This is especially interesting because the full order approximations could be obtained with full order static solutions and they are certainly independent of the reduced basis.

For the two systems under impulse excitation the convergence can still be achieved by forcing only one iteration of the inner loop, regardless of the norm of the residual. In this case the bases perform slightly worse in terms of R2MSE than the nonlinear reduced Newmark scheme with inflation.

**5.1.2.3.2 Applying the LSPG method for a study of the robustness of the reduced basis** The results above are obtained with the same nonlinear Newmark scheme for a reduced system with an inflation type formulation of the nonlinear forces vector  $\mathbf{g}$  as it is described in section 3.2.3 and used for the reference configurations. Following the sobering results coming from the Least-Squares Petrov-Galerkin method, it is only natural to verify whether the LSPG solution procedure might at least improve the reduced solutions of the differently parameterised configurations in section 4.2.2.1.1.

For a rapid execution of this study, the applied bases are limited to the LNM and the classic POD vectors, as they are defined in section 4.2.2.1.2. With these bases the same investigation into their robustness is undertaken as described in section 4.2.2.1.1. The actual reduced bases are not adapted for the current configuration but carried over from the reference configuration. The only difference is that the nonlinear Newmark scheme is replaced by a LSPG procedure.

The results show that the introduction of the LSPG procedure does not eliminate the influence of all of the differently parameterised excitations from table 4.3 and for all bases on both systems. In most cases, there is no distinguishable difference between the solution obtained with the reduced non-linear Newmark scheme and the solution obtained with the LSPG method. This confirms the limited prospect of the LSPG as a solution technique for reduced nonlinear systems.

### 5.1.2.4 Improving on the LSPG method

In order to improve upon the sobering results of the explorative numerical study, several directions for improving on the LSPG method are investigated before making a definitive decision concerning the application of the LSPG method. These directions are different  $\Psi$ , a study on the large variants for gaining insight into the real increase in computational effort and a relaxation of the convergence criterion.

Different left-hand reduction bases  $\Psi$  are applied in the fashion of a regular LSPG approach, on the locally nonlinear academic test-case from section 4.1.3.1.1, subjected to the harmonic excitation and reduced by the LNM and POD with a variety of orders  $r$  of the reduced model. The Newton-Raphson iterations of the LSPG method fail to converge with all alternative  $\Psi$ . This result is surprising because the Newton-Raphson method is considered to be rather robust. Here it fails to cope with the newly introduced left-hand reduced bases  $\Psi$ . This underlines the particularity of the LSPG approach and stresses why it is important to use the current full order Jacobian of the system.

The large variants of the test-cases, introduced in the annex section A.2.1 to allow an assessment of the performance of the reduced solutions while limiting the computational overhead, are used for an explorative study into the performance of the LSPG. Only the LNM and POD reduced bases are applied to these large variants of both systems under harmonic excitation. The results show that, by applying the LSPG, the overall reduction time can increase by up to one order of magnitude. Concerning the R2MSE, there is a slight improvement observable for the large variant of the locally nonlinear system. However, this behaviour is slightly erratic and comes with an equal number of deteriorations. No improvement is detectable for the large variant of the entirely nonlinear system.

A final effort is undertaken to demonstrate an effect of the application of the LSPG. The threshold  $\epsilon$ , to which the norm of residual is compared during the inner Newton-Raphson iterations, was, up to now, set to

## 5.1. ADAPTING THE SOLUTION ALGORITHM

---

0.1 times the norm of the initial residual  $\tilde{\mathbf{r}}_{(i=1)}^{(t+\Delta t)}$  from equation (3.81). This can be considered as not very severe. However, should it force a very exact solution with a classic reduced nonlinear Newmark scheme it could equalise any advantage of the LSPG. To test this, the threshold is further relaxed to  $0.5 \|\tilde{\mathbf{r}}_{(i=1)}^{(t+\Delta t)}\|$  and the solution is obtained with the classic reduced nonlinear Newark and the LSPG. Again, the result is that the two solutions are identical. A relaxed threshold for convergence does not favour the LSPG.

### 5.1.3 Updating the reduced basis

The update of the reduced basis is a procedure which makes the reduced basis follow the nonlinear evolution of the transient solution. Such an approach seems in order because the results of the comparative study in section 4.2.1 show that no constant reduced basis is satisfactory for a successful reduction of a nonlinear system for a transient solution.

For the update procedure a mechanism has to be devised which determines the necessity of updating the basis on the grounds of an error metric measuring the quality of the reduced solution and the update itself has to be defined. The variable frequency of the update is defined with the parameter of the update rate  $m$ . Another important property of the update that has to be determined is the position within the Newmark scheme, where the update algorithm taps into the full order displacements  $\mathbf{u}^{(t)}$  to create the new basis. The update of the reduced basis is less intrusive on the reduced nonlinear Newmark scheme, than the quasi-static correction and the LSPG method. These two methods deliver rather discouraging results in their respective sections 5.1.1 and 5.1.2, above.

If the reduced basis, which is updated, is composed of the LNM the resulting approach is commonly denominated as tangent modes, as done by e.g. Idelsohn and Cardona [102]. This is because the LNM are formed with the current full order tangent stiffness matrix  $\bar{\mathbf{K}}$  of the nonlinear Newmark scheme. Such an approach is comparable to the creation of the LNM at the current displacement  $\mathbf{u}(t)$  and uses the technique described in section 3.3.1.2, but with the current displacement instead of the maximum displacement. But beyond the LNM any reduced bases can be updated during the transient solution. The update of the reduced basis is not to be confused with the update of the entire model, which is a common, problematic challenge in the domain of the resolution of inverse problems (e.g. Hemez and Doebling [96] and Galbally et al. [81]).

In the following it will be explored how and where the update of the reduced basis is introduced in the reduced nonlinear Newmark scheme from section 3.2.1.1. The update of the reduced basis is easily accommodated by the reduced nonlinear Newmark scheme. An original feature of the proposed update method is the augmentation of the updated basis with physical quantities to even out appearing jumps in the displacements, velocities and accelerations. Once the update is introduced, a novel criterion is proposed that triggers the update based on an error metric of the reduced solution with a variable rate of update.

#### 5.1.3.1 Describing the basis update

A pseudo algorithm that performs the update of the reduced basis is described in the following. It forms a self-contained block that can be inserted into the nonlinear Newmark algorithm at any time. The algorithm consists of three distinct steps. The first step covers the provision of full order quantities, i.e. a return from the reduced system to the full order system that can also be termed an inflation. The second step is the provision of the new reduced basis. The third step is the return to the reduced system with the new, updated reduced basis.

A reduced solution is considered to have been established at the instant  $t$  as  $\mathbf{q}^{(t)}$ ,  $\dot{\mathbf{q}}^{(t)}$  and  $\ddot{\mathbf{q}}^{(t)}$ . The external forcing  $\mathbf{f}_E(t)$  is supposed to be known as well as the time histories of the generalised coordinates, the generalised velocities and the generalised accelerations up to the instant of the current update. These assumptions allow to safely consider that all information required for the update of the reduced basis are available.

Also, the current reduced basis  $\Phi^{(t-m\Delta t)}$  is known. It is noteworthy that now also the reduced basis

bears a superscript in the form of  $t - m\Delta t$ , to indicate that it evolves during the solution. The parameter  $m$  indicates that the last update of the reduced basis took place at an instant at  $m\Delta t$  prior to the current instant  $t$ . It effectively counts the number of time-steps  $\Delta t$  that have passed since the last update and does not have to have a fixed value. If required by the procedure that provides the new reduced basis, also the history of all reduced basis between  $t_0$  and  $t$  can be considered as known.

For illustration purposes the algorithm below is detailed with the LNM at the current displacements as the reduced basis. All numerical tests in this section are executed with this reduced basis. However, any reduced basis that depends on the current displacements of the system can be used.

The following pseudo algorithm can be inserted at any position in the reduced nonlinear Newmark scheme described in section 3.2.2.1. If an update is required at the instant  $t$  the three following steps take place

1. The solution is inflated to full order with  $\mathbf{u}^{(t)} = \Phi^{(t-m\Delta t)} \mathbf{q}^{(t)}$  and all other required full order entities are generated from their reduced counterparts.
2. The reduced basis is updated and the new basis  $\Phi^{(t)}$  becomes available, which is slated to replace the preceding reduced basis  $\Phi^{(t-m\Delta t)}$ 
  - With the full order solution  $\mathbf{u}^{(t)}$  the full order tangent stiffness matrix is established as  $\mathbf{K}^{(t)} = \left. \frac{\partial \mathbf{g}(\mathbf{u})}{\partial \mathbf{u}} \right|_{\mathbf{u}^{(t)}}$
  - The tangential stiffness matrix is then used for a LNM procedure which is to yield the new basis  $\Phi^{(t)}$  with equations (3.113) and (3.114). The left-hand reduced basis is set as  $\Psi = (\Phi^{(t)})^T$ .
3. The new generalised coordinates are established as

$$\mathbf{q}^{(t)} = \left( (\Phi^{(t)})^T \Phi^{(t)} \right)^{-1} (\Phi^{(t)})^T \mathbf{u}^{(t)}, \quad (5.26)$$

according to equation (3.73). The same goes for all other required reduced entities

$$\dot{\mathbf{q}}^{(t)} = \left( (\Phi^{(t)})^T \Phi^{(t)} \right)^{-1} (\Phi^{(t)})^T \dot{\mathbf{u}}^{(t)}, \quad (5.27)$$

and

$$\ddot{\mathbf{q}}^{(t)} = \left( (\Phi^{(t)})^T \Phi^{(t)} \right)^{-1} (\Phi^{(t)})^T \ddot{\mathbf{u}}^{(t)}, \quad (5.28)$$

and especially for the static matrices  $\mathbf{M}$  for the mass and  $\mathbf{C}$  for the damping, according to equations (3.7) and (3.8), respectively.

Once the update is completed, the reduced nonlinear Newmark scheme continues until the basis is updated again or the limit of the simulated period  $t_e$  is reached.

### 5.1.3.2 Deciding on the position of the basis update within the reduced nonlinear Newmark scheme

To decide upon the position of the basis update within the reduced nonlinear Newmark scheme a small numerical test is executed. The position indicates the point of insertion of the three step algorithm above in relation to the inner and outer loops in the nonlinear Newmark scheme.

The three step basis update block can be placed within the reduced nonlinear Newmark scheme, as it is described in section 3.2.1.1, at least four positions. The update can take place

## 5.1. ADAPTING THE SOLUTION ALGORITHM

1. preceding the predictions in equations (3.77) to (3.79) with a possible update per time-step. This position leads to the execution of the predictions in a reduced basis that is trailing the actual solution as it is adapted to the solution at the preceding time-step.
2. after the predictions in equations (3.77) to (3.79) with a possible update per time-step. This position leads to the execution of the iterations in a reduced basis that is adapted as a function of the predictions.
3. preceding the calculation of the residual in equation (3.56) with a possible update at each iteration. This position lets all calculations in the inner loop take place in the new basis and especially the incremental displacement  $\Delta q_{(i)}^{(t+\Delta t)}$  is already established in the new basis.
4. after the updates of the solution variables with the incremental displacements in equations (3.61) to (3.63) with a possible update at each iteration. This position leads to the most up-to-date basis in the whole process.

The figure 5.13 shows the four positions.

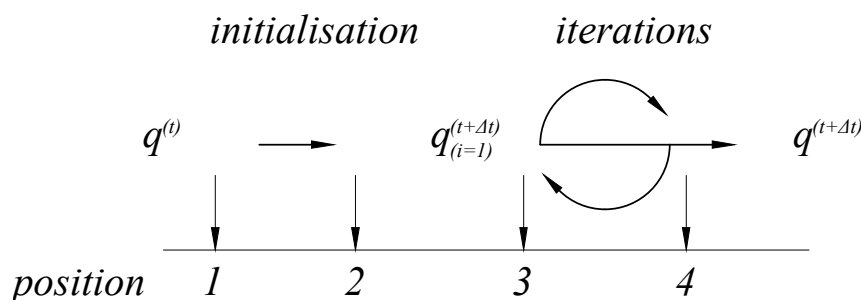


Figure 5.13: The four possible positions of the basis update in the nonlinear Newmark scheme

The study for finding the optimal position of the update is based on the techniques and test-cases used in the numerical studies in chapter 4. It uses the LNM at the current displacement and updates them at least every time-step, which translates to  $m \leq 1$ .

As an example, the figure 5.14 shows the results for these four positions for the entirely nonlinear system under harmonic excitation. The 16<sup>th</sup> degree of freedom is chosen for his exemplary behaviour.

Testing the different proposed positions of the basis update reveals that updates within the inner loop of iteration destabilise and deteriorate the solution. The position two, which leads to the execution of the iterations in a reduced basis that is adapted as a function of the predictions, also leads to less than optimal solutions. With the continuous update of the reduced basis, all four position fare rather bad. In fact, setting  $m \leq 1$  produces solutions that are worse than the solution with a constant reduced basis. Especially the updates at positions three and four lead to severe high-frequency oscillations of the solution within the inner and outer loops for every time-step. The result of figure 5.14 is inconclusive. All positions perform equally poor.

Updating the basis at the beginning of each time-step  $t$ , based on the solution at the preceding instant  $t - \Delta t$ , and letting all operations, from the predictions, over the iterations to the updates, taking place in this new, updated reduced basis presents the natural choice and is expected to yield the most benefit for the solution. Corresponding to its character an update at the position one is termed a trailing update. It is used for the remainder of this work.

The conclusion for the rate of the basis update  $m$  show that an update at the rate of  $m = 1$ , i.e. once per

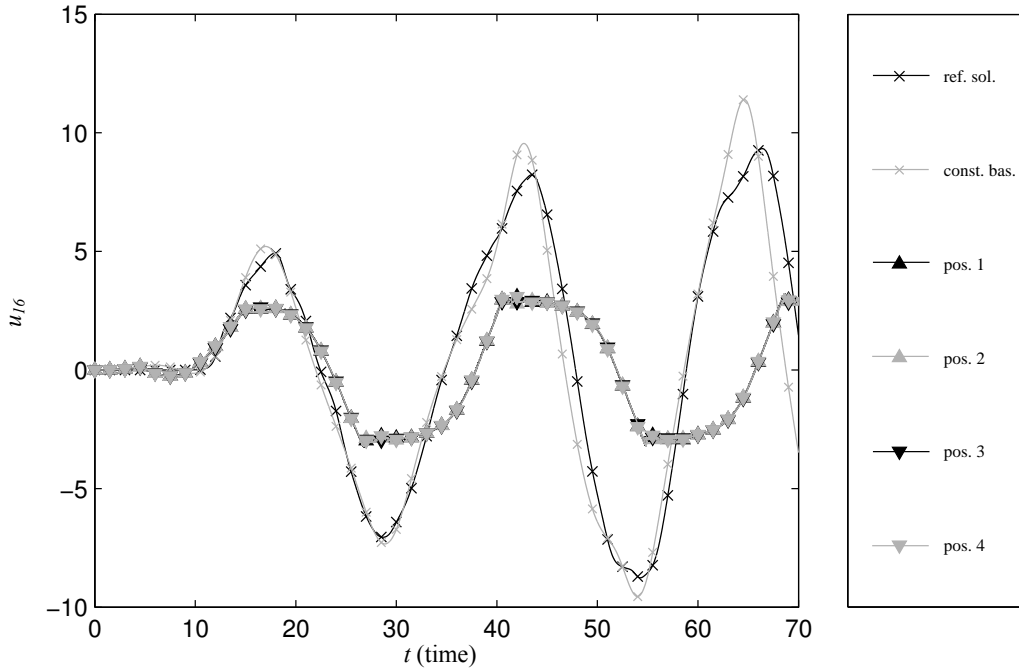


Figure 5.14: The time histories of the 16<sup>th</sup> degree of freedom of the entirely nonlinear system for different positions of the basis update (LNM with  $r = 3$ )

time-step, is by no means satisfactory. This is addressed by determining the rate of the basis update.

### 5.1.3.3 Determining the rate $m$ of the basis update

As shown above, an update rate of  $m = 1$ , which means an update of the reduced basis at every time-step, may render the solution useless. A rate of  $m \gg 1$  for triggering the update is thus desirable. With  $m$  of  $\mathcal{O}(10^2)$  or  $\mathcal{O}(10^3)$ , the update might actually contribute to the quality of the solution, for the test-cases from section 4.1.3.1. At the same time a fixed rate is not worthwhile because the solution and its development are not known a priori. A method has to be devised which determines the instant of a basis update if the update is executed as trailing update, without prescribing a fixed rate.

Especially for the LNM at the actual displacement, a trigger of the update as a function of the displacements seems to make sense because the current displacements describe the actual state of the structure. This deformation, in turn, governs the characteristics of the reduced basis. At the same time, a trigger based on the similarity of the current nonlinear forces vector  $\mathbf{g}(\mathbf{u}(t))$  with some reference seems also possible. This is because the internal stress situation of the structure may indicate an appropriate criterion for the selection of the reduced basis. For such an approach not the similarity between the actual displacements and the displacements at which the reduced basis was established beforehand is used, but the similarity between the actual nonlinear internal forces and the nonlinear internal forces that result from the displacement at which the reduced basis was established beforehand. This approach seems possible from an algorithmic point of view but neglects inertial effects in the dynamic simulation that will certainly influence the nonlinear internal forces and render a comparison meaningless.

For determining the trigger for the update of the reduced basis some considerations are made, while reasoning on the example of the entirely nonlinear system under harmonic excitation. As a first shot, it is explored if the MAC (4.10) could be used as the criterion at the basis of the method that triggers the update

## 5.1. ADAPTING THE SOLUTION ALGORITHM

of the reduced basis. A MAC equal to one identifies two vectors as collinear. The figure 5.15 plots the evolutions of two error metrics for the entirely nonlinear system under harmonic solution, reduced with a constant LNM basis at  $r = 3$ , against time:

- the evolution of the R2MSE  $e_r$  from equation (4.5) between the current  $\mathbf{u}^{(t)}$  of the reference solution and the current reconstructed physical displacements  $\Phi \mathbf{q}^{(t)}$  from a reduced solution with a constant classic LNM basis and
- the MAC of the current reconstructed physical displacements  $\Phi \mathbf{q}^{(t)}$  and the first column vector  $\phi_1$  of the constant LNM basis.

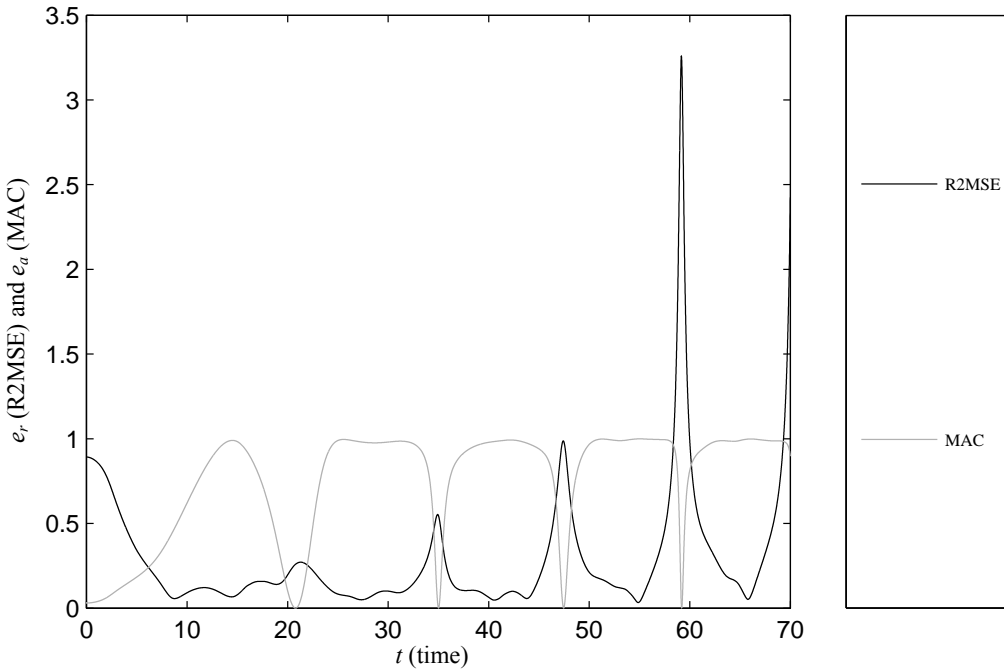


Figure 5.15: The R2MSE and the MAC of the entirely nonlinear system under harmonic excitation reduced with the LNM at  $r = 3$

It is easily recognisable, that the two evolve with a consistent behaviour. Whenever the R2MSE raises the MAC decreases. This indicates that, whenever the error increases, the solution is poorly represented by one of the major components of the reduced basis. One might thus ponder a trigger based on the MAC. But, while the MAC is a possible criterion, it is not well suited. It compares only the shapes of the vectors, not if they are anti-parallel or if they differ in amplitude. In fact, the MAC, as it used here, only compares the actual displacements to the first vector of the reduced basis. Even though a clear link between the MAC and the R2MSE error between the actual displacements and the reference solution has been established, the use of the MAC in this fashion is objectionable. In conclusion, neither the MAC nor the R2MSE are considered well suited for triggering the update because these two quantities require an inflation of the current generalised coordinates  $\Phi \mathbf{q}^{(t)}$  because they operate on full order entities. at the same time applying these two error metrics to the generalised coordinates  $\mathbf{q}^{(t)}$  directly is not possible. The generalised coordinates, their evolution and their shape are not known a priori and thus no quantities can be defined to which they can be compared. To remedy this problem a different criterion is required that works exclusively on reduced entities to trigger the update of the reduced basis.

The initial generalised residual  $\tilde{\mathbf{r}}_{(1)}$  presents itself naturally. The residual is termed initial because it is the residual at the beginning of each time-step, which corresponds to the choice of the position one within the

## 5.1. ADAPTING THE SOLUTION ALGORITHM

reduced nonlinear Newmark scheme as the place where the update takes place. It is obtained by evaluating equation (3.81) at  $i = 1$ . But the norm of the reduced initial residual  $\|\tilde{\mathbf{r}}_{(1)}\|$  cannot be used directly because a threshold of magnitude cannot be determined prior to the execution of the solution itself. The criterion of choice is hence the rate of change of the norm of the initial generalised residual. Whenever

$$\left| \frac{d \|\tilde{\mathbf{r}}\|}{dt} \right| > \epsilon_r \quad (5.29)$$

an update is initiated. This translates to the fact that no fixed rate of the basis update  $m$  is prescribed. Computationally the derivative is approximated as a backward finite difference across the time steps of the nonlinear Newmark scheme. This gives

$$\left| \frac{d \|\tilde{\mathbf{r}}\|}{dt} \right| \approx \left| \frac{\|\tilde{\mathbf{r}}^{(t)}\| - \|\tilde{\mathbf{r}}^{(t-\Delta t)}\|}{\Delta t} \right|. \quad (5.30)$$

To verify that this approach is indeed feasible and meaningful with respect to the comparability of the full order and the reduced order solution some investigations are necessary. In a first step it is verified that the evolution of the derivation of the reduced order system follows the evolution of this metric of the full order system. The figure 5.16 contains these two evolutions. It shows that the  $\left| \frac{d\|\mathbf{r}\|}{dt} \right|$  and the  $\left| \frac{d\|\tilde{\mathbf{r}}\|}{dt} \right|$  evolve in perfect accordance. This is also the case for all other test-cases that are investigated. However, this remains only an indication of the equivalence of  $\left| \frac{d\|\mathbf{r}\|}{dt} \right|$  and  $\left| \frac{d\|\tilde{\mathbf{r}}\|}{dt} \right|$ . A strict prove remains outside the scope of the performed work.

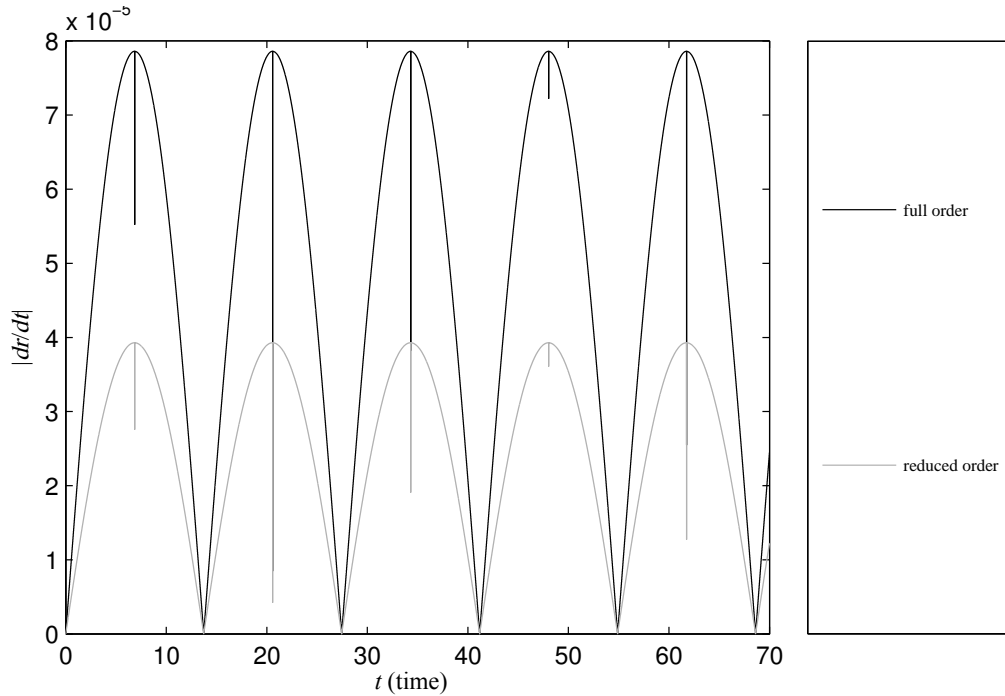


Figure 5.16: The evolution of the norm of the derivation of the initial residual for the locally nonlinear system

The figure 5.16 also reveals that the evolution of  $\left| \frac{d\|\tilde{\mathbf{r}}\|}{dt} \right|$  is in perfect tune with the excitation. In accordance with the values from section 4.1.3.4 the frequency of the harmonic excitation is set to  $\Omega =$

## 5.1. ADAPTING THE SOLUTION ALGORITHM

0.2289. Adding units to this value results in a period for the oscillation of roughly  $T = 27.4$ . This is clearly visible in the figure. Only the derivation of the residual seems to oscillate with twice that frequency because it is treated as absolute value.

Should the derivation of the reduced initial residual only depend on the frequency of the excitation, it would be not fit to serve as a trigger for the update of the reduced basis. This is however only partially true.

The figure 5.17 plots the evolution of the R2MSE and the MAC between the current full order displacements  $\mathbf{u}^{(t)}$  and the displacements reconstructed from the generalised coordinates  $\Phi \mathbf{q}^{(t)}$ . The use of these two error metrics at the same time assures that departures of the reduced solution from the reference solution are detected in amplitude and shape of the displacement vectors. The plot of the error metrics reveals that these two departures coincide and that they become more and more severe as the solution progresses. Also, they are rather limited to certain time intervals and this time intervals correspond to maxima of the  $|\frac{d\|\tilde{\mathbf{r}}\|}{dt}|$  in figure 5.16. the derivation of the generalised initial residual is thus the metric that is used to trigger the update.

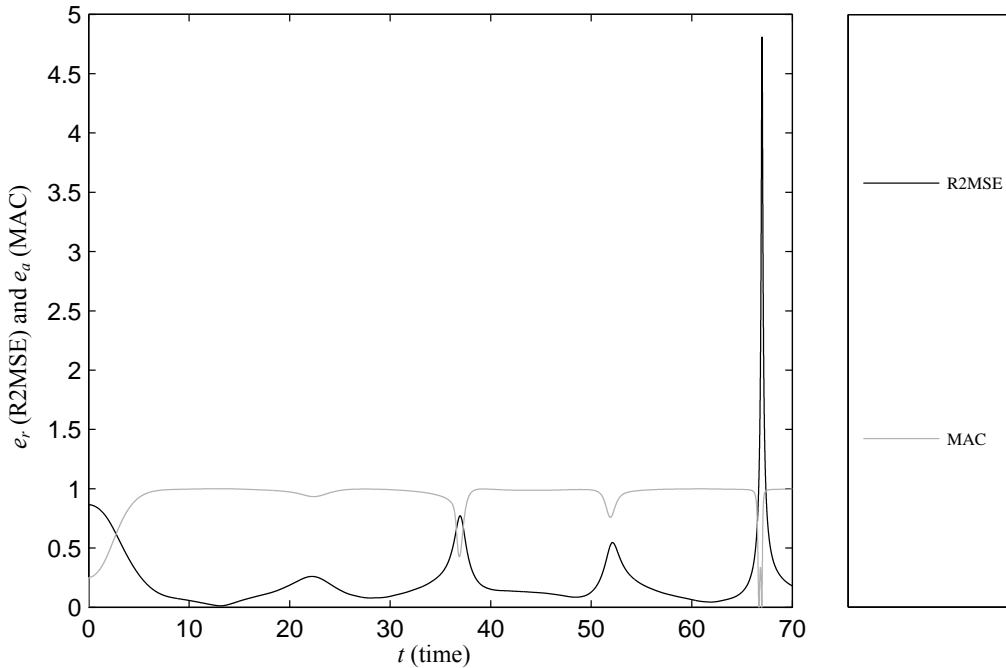


Figure 5.17: The evolution of error metrics for the reduced solution for the locally nonlinear system

The determination of the threshold  $\epsilon_r$  that is required for equation (5.29) and that has to be surpassed by the actual absolute value of the derivation of the generalised initial residual to trigger the update remains as a minor issue. Defining this threshold requires either good engineering judgement or a limited time reduced solution until at  $t \ll t_e$ , in order to gain insight into the order of magnitude and the behaviour of the derivation.

A criterion like the one expressed in equation (5.30) might seem difficult to grasp from a theoretical point of view. The derivative of converged residual should be constantly zero, because, at the end of each time-step, the dynamical equilibrium is fulfilled and the equation (3.81), respectively is equivalence (3.87) for the HHT- $\alpha$ -method, is bound to give zero. In an ideal setting this perfect dynamic equilibrium is to prevail once a complete convergence at the instant  $t + \Delta t$  is achieved.

However, in a real, numerical setting such a perfect convergence can never be achieved. Furthermore,

## 5.1. ADAPTING THE SOLUTION ALGORITHM

---

it has to be observed that the residual, that is considered to have converged at the end of a time step, is proportional to the initial residual at the beginning of the time step via the threshold of convergence in equation (3.64). As such, even the imperfectly converged residual reflects the quality of the solution and can be used to trigger the update.

A final thought might be given to another use of observing the quality of the solution. Criteria in the form of equation (5.30) are commonly used to adapt the time step if the solution deteriorates. This might lead to the question why, in this case, the reduced basis is updated and not the time step reduced in order to maintain the quality of the solution. An adaptation of the time step is not desirable for two reasons. First, the reduction of the time step would lead to more numerical efforts, which is contradictory to the aim of a fast-executing reduced order model. Naturally it cannot be determined if the additional numerical effort due to smaller time steps outweighs the additional numerical effort of the update of the reduced basis, but against the background of the results obtained with the numerical studies in chapter 4, updating and augmenting the reduced basis is much more promising than just reducing the time step. The second argument against an adaptation of the time step comes from an anticipated application of the reduced order model. If the reduced order model of the structure is used in conjunction with a code simulating another physic, the coupling becomes much easier if a constant and known time step is used in both codes.

### 5.1.3.4 Refining the triggering of the update with a retainer

A major component for stabilising the solution with the updated reduced basis is the retainer. The retainer mechanism limits the frequency of the update of the reduced basis and imposes a minimum time interval of  $m_r \Delta t$  between two consecutive updates. Supposing a basis update has taken place at instant  $t - m \Delta t$  with  $m = 1$ , i.e. at the preceding time-step. Now, the numerical approximation of the derivation of the generalised residual would read

$$\left| \frac{d \|\tilde{\mathbf{r}}\|}{dt} \right| \approx \left| \frac{\|\tilde{\mathbf{r}}_{(\Phi(t-\Delta t))}^{(t)}\| - \|\tilde{\mathbf{r}}_{(\Phi(t-\Delta t))}^{(t)}\|}{\Delta t} \right|. \quad (5.31)$$

The value of  $\left| \frac{d \|\tilde{\mathbf{r}}\|}{dt} \right|$  would be well beyond the threshold  $\epsilon_r$ , as it is used in equation (5.29) because of the fact that the residuals  $\tilde{\mathbf{r}}^{(t+\Delta t)}$  and  $\tilde{\mathbf{r}}^{(t)}$  are defined in different reduced bases. This would immediately trigger another update, which is not desirable because, first,  $m$  is supposed to be of  $\mathcal{O}(10^3)$  for the given test-case and, second, the figure 5.17 shows that updates are only required with a relatively low frequency.

To address this problem the retainer is introduced. It is a mechanism that prohibits a new basis update for a given time once the basis is updated. This can be expressed by adding the condition

$$m \geq m_r \quad (5.32)$$

to the threshold condition in equation (5.29). Both conditions have to be met before the next update can be triggered. Again, the determination of  $m_r$  requires some kind of knowledge about the evolution of the reduced solution.

### 5.1.3.5 Augmenting the updated basis

With the numerical tools available a reduced transient solution can be run. The observation of the results reveals immediately large jumps, or discontinuities, in the solution whenever the basis is updated. This can be seen in figure 5.18. Similar jumps are present in all other degrees of freedom as well as in the velocities and the accelerations.

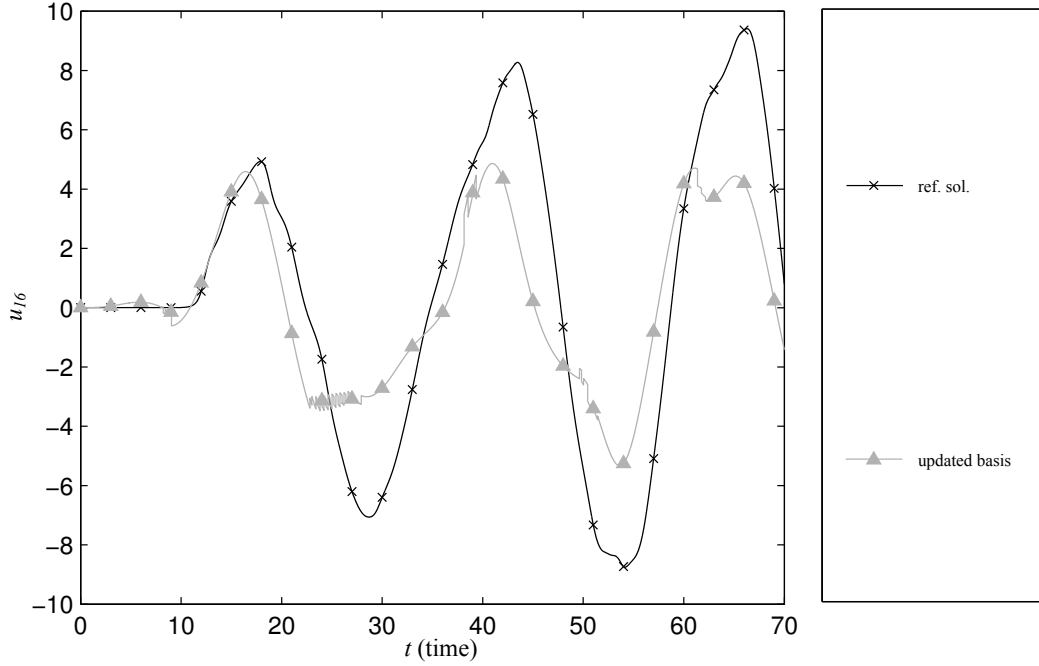


Figure 5.18: The time histories of the 16<sup>th</sup> degree of freedom of the entirely nonlinear system with the basis update triggered by the rate of change of the generalised initial residual and showing characteristic jumps

**5.1.3.5.1 Determination of the provenance of the jumps** To understand the nature and provenance of these jumps the notion of a  $\mathbf{q}_{\text{before}}^{(t)}$  and a  $\mathbf{q}_{\text{after}}^{(t)}$  is introduced. These two quantities coexist at the same instant  $t$  and describe the generalised coordinates before and after the update of the reduced basis at that instant. Their coexistence is introduced by the three-step algorithm for conducting the update from section 5.1.3.1. The  $\mathbf{q}_{\text{before}}^{(t)}$  is the result of the transient solution between  $t - m\Delta t$  and  $t$ , while the  $\mathbf{q}_{\text{after}}^{(t)}$  comes from the least-squares reduction of the unique physical displacements  $\mathbf{u}^{(t)}$  with the new basis  $\Phi^{(t)}$ .

It is important to note that the jumps only appear at update rates  $m > 1$ . If the reduced basis would be reduced at every time-step, the continuity of the jumps would most probably let the solution appear continuous and smooth. It is only the abrupt change of the reduced basis after a time interval  $m\Delta t$  that leads to the jumps.

So, simply updating the basis at a given time  $t$  leads to the problem that

$$\mathbf{u}^{(t)} = \Phi^{(t-m\Delta t)} \mathbf{q}_{\text{before}}^{(t)} \neq \Phi^{(t)} \mathbf{q}_{\text{after}}^{(t)} \quad (5.33)$$

The same goes for the velocities  $\dot{\mathbf{u}}^{(t)}$ , with  $\Phi^{(t-m\Delta t)} \dot{\mathbf{q}}_{\text{before}}^{(t)} \neq \Phi^{(t)} \dot{\mathbf{q}}_{\text{after}}^{(t)}$ , and for the accelerations  $\ddot{\mathbf{u}}^{(t)}$  with  $\Phi^{(t-m\Delta t)} \ddot{\mathbf{q}}_{\text{before}}^{(t)} \neq \Phi^{(t)} \ddot{\mathbf{q}}_{\text{after}}^{(t)}$ . They all show jumps and discontinuities in their physical equivalents  $\mathbf{u}$ ,  $\dot{\mathbf{u}}$  and  $\ddot{\mathbf{u}}$ .

Before the basis update the physical displacements are described in the basis  $\Phi^{(t-m\Delta t)}$  as

$$\mathbf{u}^{(t)} = \Phi^{(t-m\Delta t)} \mathbf{q}_{\text{before}}^{(t)}, \quad (5.34)$$

## 5.1. ADAPTING THE SOLUTION ALGORITHM

---

After the basis update the generalised coordinates are reinitialised as

$$\mathbf{q}_{\text{after}}^{(t)} = \left( \left( \Phi^{(t)} \right)^T \Phi^{(t)} \right)^{-1} \left( \Phi^{(t)} \right)^T \mathbf{u}^{(t)} \quad (5.35)$$

where the unique physical displacements  $\mathbf{u}^{(t)}$  are used again because these physical displacements do not change during basis updates.

The problem appearing at this point is that the difference<sup>4</sup>

$$\Delta \mathbf{u} = \Phi^{(t)} \mathbf{q}_{\text{before}}^{(t-m\Delta t)} - \Phi^{(t)} \mathbf{q}_{\text{after}}^{(t)} \quad (5.36)$$

is orthogonal to the updated basis  $\Phi^{(t)}$

$$\left( \Phi^{(t)} \right)^T \left( \Phi^{(t)} \mathbf{q}_{\text{after}}^{(t)} - \Phi^{(t-m\Delta t)} \mathbf{q}_{\text{before}}^{(t)} \right) = \mathbf{0} \quad (5.37)$$

and can hence not be captured correctly in the ongoing solution. The physical displacements  $\mathbf{u}^{(t)}$  from equation (5.34) are a linear combination of the columns of the reduced basis before the update  $\Phi^{(t-m\Delta t)}$  and are thus in the space spanned by this matrix. If the same displacement  $\mathbf{u}^{(t)}$  is now reduced in the least squares sense by the reduced basis after the update  $\Phi^{(t)}$ , as done in equation (5.35), it is certain that some components of  $\mathbf{u}^{(t)}$  are not captured as they are orthogonal on  $\Phi^{(t)}$ . The difference between the original  $\mathbf{u}^{(t)} = \Phi^{(t-m\Delta t)} \mathbf{q}_{\text{before}}^{(t)}$  and their approximation by  $\Phi^{(t)} \mathbf{q}_{\text{after}}^{(t)}$  is necessarily also orthogonal on  $\Phi^{(t)}$ . This is expressed by equation (5.37). The remedy to this problem is the inclusion of the jumps in an augmented updated basis.

In order to enhance the understanding of the provenance of the jumps it has to be observed that, strictly speaking, the return to the new generalised coordinates by means of the least-squares solutions in equations (5.26) to (5.28) are not feasible, because the space of the physical displacements does not possess the properties required for the application of Euclidian geometry (Strang [218]). However, with treating only translational degrees of freedom and for the sake of simplicity this approach is retained. This simplification might aggravate the occurrence of the jumps.

**5.1.3.5.2 Augmenting the updated basis by including the jumps** In order to augment the updated reduced basis the jumps in the displacements  $\Delta \mathbf{u}$ , velocities  $\Delta \dot{\mathbf{u}}$  and accelerations  $\Delta \ddot{\mathbf{u}}$  are extracted from equation (5.36), and the equivalents for the velocities and accelerations, and then used to augment the reduced basis. This augmentation is done systematically for every update and with the ultimate aim of smoothing the solution.

Whenever the reduced basis is updated and augmented, the three additional vectors  $\Delta \mathbf{u}$ ,  $\Delta \dot{\mathbf{u}}$  and  $\Delta \ddot{\mathbf{u}}$  are used to bridge the jumps in the physical displacements and to smooth the solution. To this effect the procedure for a basis update from section 5.1.3.1 is slightly adapted. All entities at the end of the third step of the update pseudo algorithm are considered as intermediate values and a fourth step for bridging the jumps is added.

At the end of the third step the new reduced basis  $\check{\Phi}^{(t)}$  as well as the new generalised coordinates  $\check{\mathbf{q}}^{(t)} = \left( \left( \check{\Phi}^{(t)} \right)^T \check{\Phi}^{(t)} \right)^{-1} \left( \check{\Phi}^{(t)} \right)^T \mathbf{u}^{(t)}$  are available. The check accent signals their character as intermediate values. The  $\check{\mathbf{q}}^{(t)}$  is the  $\mathbf{q}_{\text{after}}^{(t)}$  that is used in the previous paragraph to explore the provenance of the jumps.

---

<sup>4</sup>Not to be confused with the incremental displacements  $\Delta \mathbf{u}$ , defined in equation (3.60), from the nonlinear Newmark scheme in section 3.2.1.1.

## 5.1. ADAPTING THE SOLUTION ALGORITHM

---

The new intermediate reduced basis  $\check{\Phi}^{(t)}$  is still a  $n \times r$  matrix and the generalised coordinates  $\check{q}^{(t)}$  remain consequently a  $n \times 1$  vector.

It is of central importance to understand that the parameter  $r$ , which determines the order of the reduced system and which was defined prior to the reduced transient solution, does not change in the following and that all reduced bases that are established in the third step of the pseudo algorithm are always established with this value of  $r$ . It is only in the fourth step, which is expanded now, that the reduced basis of order  $r$  is augmented. Furthermore, constantly increasing the order of the reduced basis would be limited by the practical consideration that, after a given number of augmentations, the order of the reduced system  $r$  would actually become greater than  $n$ , the number of degrees of freedom of the full order system.

After the third step of the update all required information is available and the jumps are calculated

$$\Delta \mathbf{u}^{(t)} = \Phi^{(t-m\Delta t)} \mathbf{q}_{\text{before}}^{(t)} - \check{\Phi}^{(t)} \check{\mathbf{q}}^{(t)}, \quad (5.38)$$

$$\Delta \dot{\mathbf{u}}^{(t)} = \Phi^{(t-m\Delta t)} \dot{\mathbf{q}}_{\text{before}}^{(t)} - \check{\Phi}^{(t)} \dot{\check{\mathbf{q}}}^{(t)}, \quad (5.39)$$

$$\Delta \ddot{\mathbf{u}}^{(t)} = \Phi^{(t-m\Delta t)} \ddot{\mathbf{q}}_{\text{before}}^{(t)} - \check{\Phi}^{(t)} \ddot{\check{\mathbf{q}}}^{(t)}. \quad (5.40)$$

The intermediate reduced basis  $\check{\Phi}^{(t)}$  is then augmented with three  $n \times 1$ -vectors  $\Delta \mathbf{u}$ ,  $\Delta \dot{\mathbf{u}}$  and  $\Delta \ddot{\mathbf{u}}$ , to become the augmented updated reduced basis

$$\Phi^{(t)} = [\check{\Phi}^{(t)}, \Delta \mathbf{u}, \Delta \dot{\mathbf{u}}, \Delta \ddot{\mathbf{u}}]. \quad (5.41)$$

The generalised coordinates from equation (5.26) are augmented accordingly to become

$$\mathbf{q}^{(t)} = \begin{bmatrix} \check{\mathbf{q}}^{(t)} \\ 1 \\ 0 \\ 0 \end{bmatrix} \quad (5.42)$$

$$\dot{\mathbf{q}}^{(t)} = \begin{bmatrix} \dot{\check{\mathbf{q}}}^{(t)} \\ 0 \\ 1 \\ 0 \end{bmatrix} \quad (5.43)$$

$$\ddot{\mathbf{q}}^{(t)} = \begin{bmatrix} \ddot{\check{\mathbf{q}}}^{(t)} \\ 0 \\ 0 \\ 1 \end{bmatrix}. \quad (5.44)$$

Adding a unit displacement assigned to their respective additional vector bridges effectively the jump that results from updating the basis. Augmenting the reduced basis with the jumps bears a certain resemblance to the work of Dickens et al. [69]. There, different types of reduced basis vectors are used, leading to two different types of generalised coordinates. The first type of generalised coordinates acts on the column vector of the reduced basis. The second type of generalised coordinates acts as quasi-static corrections that are used as additional vectors to augment the reduced basis.

These operations increase the effective order of the reduced system to  $r^{(t)} = r + 3$ . This increase occurs only once for the very first update. For all following updates the order remains constant at  $r + 3$  because the new, updated bases  $\check{\Phi}^{(t)}$  are always established at the order  $r$  and only afterwards the three additional vectors are added. The initial reduced basis  $\Phi^{(t_0)}$  is established with any reduction method prior to the

## 5.1. ADAPTING THE SOLUTION ALGORITHM

beginning of the solution at a given order  $r^{(t_0)}$  of the reduced system. The corresponding reduced initial conditions are established as given in equations (3.73) to (3.75).

The result of the application of this method is a smooth solution without jumps in displacements and velocities. The accelerations may still exhibit some minor jumps but appear largely smooth. This shown in figure 5.19.

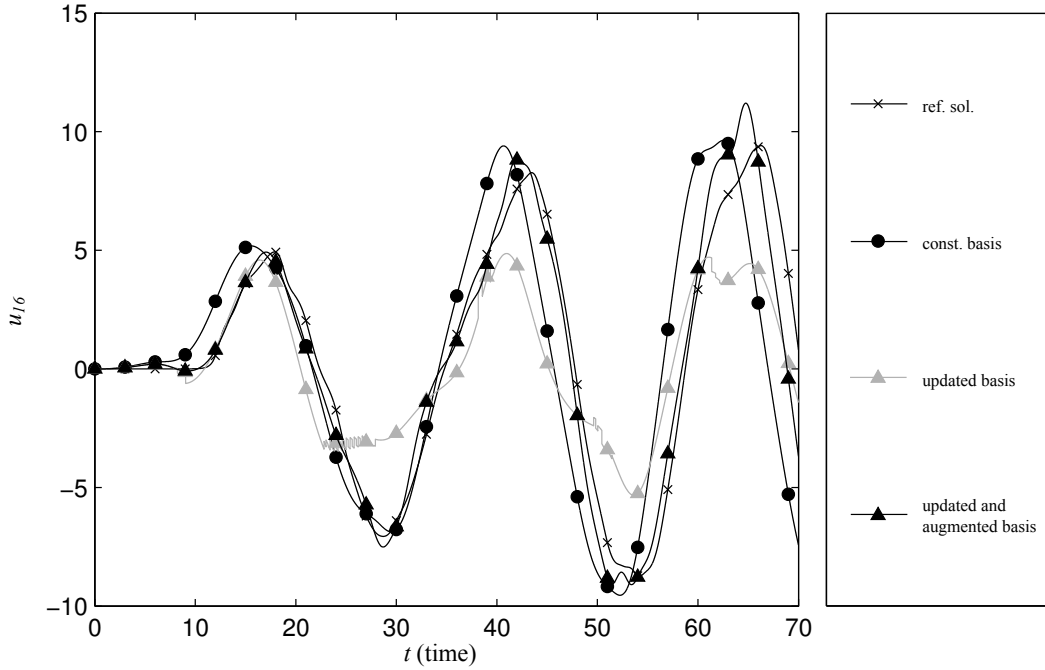


Figure 5.19: The time histories of the 16<sup>th</sup> degree of freedom of the entirely nonlinear system obtained with a constant reduced basis and with an updated and augmented reduced basis

Compared to the reduced solution with a constant basis differences become evident. However, only the error metrics allow a judgement because the two reduced solutions oscillate around the reference solution. Table 5.1 shows that the inclusion of the updating and augmentation mechanisms reduces the R2MSE between the reduced solution and the reference solution to one third if compared with the reduced solution obtained with a constant reduced basis. This division by three of the mean value is attained while maintaining a comparable variance. Comparing the solution obtained with an updated but not augmented basis in figure 5.18 with the solution obtained with the update and augmentation of the reduced basis reveals a considerable improvement of the quality.

		constant basis	updated and augmented basis
R2MSE mean	$e_r$	0.6602	0.2517
R2MSE var.	$v_r$	0.0346	0.0495

Table 5.1: The error metrics for the solutions of the entirely nonlinear system obtained with a constant reduced basis and with an updated and augmented reduced basis

The generalised coordinates associated with the three additional vectors evolve during the solution and attain values within one additional order of magnitude. This shows their participation in the solution process. The three additional vectors  $\Delta \mathbf{u}^{(t)}$ ,  $\Delta \dot{\mathbf{u}}^{(t)}$  and  $\Delta \ddot{\mathbf{u}}^{(t)}$  are all three orthogonal to the basis, as described in

equation (5.33). They are, however, not necessarily orthogonal among each other, so that transfers between these three modes do most certainly take place.

### 5.1.3.6 Testing the update of the reduced basis

The simple proposition of just updating the reduced basis evolved considerably due to the required tools, as e.g. the determination of the criterion that triggers the update, and identified shortcomings, most notably the jumps that appeared in the physical solution. All these issues are addressed in satisfactory manner and an original update method, consisting of the elements of the update itself, the time derivation of the generalised initial residual as triggering criterion, the retainer as numerical tool for stabilising the solution and the augmentation of the reduced basis to smooth the solution, is proposed.

The introduced elements are of predominantly of numerical nature. In order to verify their applicability some numerical test are conducted. The questions to be answered by this study concern mainly the augmentation of the basis. The augmentation presents a major intervention in the solution process. The update triggering and the retainer are merely numerical problems and can be solved by aptly choosing the values for the associated parameters  $\epsilon_r$  and  $m_r$ . The questions to be asked regarding the augmentation of the reduced basis do concentrate on the addition of the three vectors.

- Is it necessary to augment the intermediate reduced basis with the jumps, or could the jumps only replace the three least significant vectors in  $\check{\Phi}^{(t)}$ , thus keeping the initial order of the reduced system at  $r = r^{(t_0)}$  instead of  $r^{(t_0)} + 3$  after the first update?
- Do the updated and augmented reduced bases indeed deliver a better result than a constant basis at the same order  $r + 3$  ?

**5.1.3.6.1 Augmenting the reduced basis or replacing the three least significant vectors ?** To answer this question the number of jumps, which result from the update of the basis, are used as a measure for the quality of four different variants of the update of the reduced basis. The variants of the update are different combinations of the inclusion of the jumps in the updated reduced basis  $\Phi^{(t)}$  and if all jumps or only the jumps of the displacements are included. The variants are

- augmenting the basis by appending  $\Delta \mathbf{u}$ ,  $\Delta \dot{\mathbf{u}}$  and  $\Delta \ddot{\mathbf{u}}$  to the updated basis  $\check{\Phi}^{(t)}$  as it is described in equation (5.41). The updated reduced basis  $\check{\Phi}^{(t)}$  is obtained at  $r$  and the updated and augmented basis  $\Phi^{(t)}$  is of order  $r + 3$ .
- augmenting the basis by appending only  $\Delta \mathbf{u}$  to the updated basis  $\check{\Phi}^{(t)}$ . This means that the updated and augmented reduced basis  $\Phi^{(t)}$  is of order  $r + 1$ .
- updating the basis and replacing  $\Delta \mathbf{u}$ ,  $\Delta \dot{\mathbf{u}}$  and  $\Delta \ddot{\mathbf{u}}$  in the updated basis  $\check{\Phi}^{(t)}$ . For this variant the updated basis  $\check{\Phi}^{(t)}$  is of order  $r - 3$ . The jumps  $\Delta \mathbf{u}$ ,  $\Delta \dot{\mathbf{u}}$  and  $\Delta \ddot{\mathbf{u}}$  are calculated with this basis in equation (5.36). The basis  $\Phi^{(t)}$  in equation (5.41) continues to be of order  $r$ .
- updating the basis by replacing only  $\Delta \mathbf{u}$  in the updated basis  $\check{\Phi}^{(t)}$ . This makes the updated basis  $\check{\Phi}^{(t)}$  a basis of order  $r - 1$ .

The solution with the constant reduced basis is also included as a reference.

To count the actual number of jumps in the time histories of the different displacements  $u_i(t)$  and their time derivations the different solutions are subjected to a post-processing procedure that is designed to detect any sudden changes in the displacement that can be qualified as a jump. The procedure is centred around the displacement  $u_i^{(t)}$  at the instant  $t$ , at which a jump in  $u_i(t)$  is supposed to occur. In order to have a predictive value  $\bar{u}_i^{(t+\Delta t)}$  for the following instant available the current displacement is extrapolated with

## 5.1. ADAPTING THE SOLUTION ALGORITHM

the finite difference of its time derivation

$$\bar{u}_i^{(t+\Delta t)} = u_i^{(t)} + \frac{u_i^{(t)} - u_i^{(t-\Delta t)}}{\Delta t}. \quad (5.45)$$

The same two instants are used to define a tolerance value

$$\Delta \bar{u} = \max \left\{ \epsilon \mid u_i^{(t)} - u_i^{(t-\Delta t)} \mid, \epsilon_0 \right\}, \quad (5.46)$$

where the tuning threshold  $\epsilon$  is greater than 1. This is necessary to distinguish some rapid changes from actual jumps. The alternative threshold  $\epsilon_0$  is provided in case the  $u_i$  evolves without a pronounced gradient. In this case the alternative threshold limits false positives from numerical inaccuracy.

A jump is recorded, whenever the actual value of  $u_i$  at  $t + \Delta t$  departs from the predictive value  $\bar{u}_i^{(t+\Delta t)}$  by more than the tolerance value  $\Delta \bar{u}$ , giving

$$\left| u_i^{(t+\Delta t)} - \bar{u}_i^{(t+\Delta t)} \right| > \Delta \bar{u} \quad (5.47)$$

as the condition for a jump. Naturally this approach can be equally well applied to the velocities  $\dot{u}_i$  and the accelerations  $\ddot{u}_i$ .

The simple counting of jumps in the displacements  $u_i$ , the velocities  $\dot{u}_i$  and the accelerations  $\ddot{u}_i$  is an indicator of quality for each update method. A further, deeper investigation is not considered necessary at this time because the results in tables 5.2 and 5.3 are meaningful.

Tables 5.2 and 5.3 contain the combined counts for the jumps in the displacements, the velocities and the accelerations for the locally and the entirely nonlinear system, respectively. The calculations are performed with a LNM reduced basis at  $r = 11$  to provide enough margin for update methods which replace vectors in the basis. The excitation is the harmonic forcing from section 4.1.3.3. The tables also contain the mean  $e_r$  and the variance  $v_r$  over the  $n$  displacements of the R2MSE, as they are described in equations (4.5) and (4.6), respectively, as additional rows. In order to put these values into perspective the solution with a constant reduced basis is included as the first column.

		const. basis	appending $\Delta \mathbf{u}, \Delta \dot{\mathbf{u}}$ and $\Delta \ddot{\mathbf{u}}$	appending only $\Delta \mathbf{u}$	replacing $\Delta \mathbf{u}, \Delta \dot{\mathbf{u}}$ and $\Delta \ddot{\mathbf{u}}$	replacing only $\Delta \mathbf{u}$
R2MSE mean	$e_r$	0.5135	0.0115	0.0165	0.0283	0.0358
R2MSE var.	$v_r$	0.6298	0.0002	0.0005	0.0005	0.0036
jumps in $u$		0	0	0	0	0
jumps in $\dot{u}$		0	0	69	0	99
jumps in $\ddot{u}$		0	81	106	45	101

Table 5.2: The error metrics and the combined numbers of jumps for the locally nonlinear system under harmonic excitation reduced with  $r = 11$  LNM at given displacements

The seemingly high values for the combined jumps in the two tables 5.2 and 5.3 has to seen in relation to 100000 time-steps and 20 degrees of freedom.

For the two systems the update by appending  $\Delta \mathbf{u}$ ,  $\Delta \dot{\mathbf{u}}$  and  $\Delta \ddot{\mathbf{u}}$  to the reduced basis leads to a massive drop in the mean of the R2MSE in the order of ten. If only  $\Delta \mathbf{u}$  is appended, the drop in the mean of R2MSE is of the same order of magnitude, yet slightly less pronounced, if compared to a solution with a

## 5.1. ADAPTING THE SOLUTION ALGORITHM

		const. basis	appending $\Delta \mathbf{u}$ , $\Delta \dot{\mathbf{u}}$ and $\Delta \ddot{\mathbf{u}}$	appending only $\Delta \mathbf{u}$	replacing $\Delta \mathbf{u}$ , $\Delta \dot{\mathbf{u}}$ and $\Delta \ddot{\mathbf{u}}$	replacing only $\Delta \mathbf{u}$
R2MSE mean	$e_r$	0.3333	0.0661	0.1013	0.1155	0.1125
R2MSE var.	$v_r$	0.0022	0.0009	0.0011	0.0012	0.0013
jumps in $u$		0	0	0	0	0
jumps in $\dot{u}$		0	0	185	2	205
jumps in $\ddot{u}$		0	239	198	238	219

Table 5.3: The error metrics and the combined numbers of jumps for the entirely nonlinear system under harmonic excitation reduced with  $r = 11$  LNM at given displacements

constant basis. If the  $\Delta \mathbf{u}$ ,  $\Delta \dot{\mathbf{u}}$  and  $\Delta \ddot{\mathbf{u}}$  are used to replace vectors in the reduced basis, the error decreases to a comparable level. These findings are also present, albeit to a lesser extent, if only  $\Delta \mathbf{u}$  is replaced.

These behaviours are mirrored in the number of jumps, which are reported as sums over the displacements, the velocities and the accelerations for all degrees of freedom. Only appending all three jumps to the reduced basis or replacing all three jumps in the basis ensures a solution, which is smooth in displacements and velocities. Appending or replacing only  $\Delta \mathbf{u}$  results in a solution which is only smooth in displacements.

In conclusion it can be stated that augmenting the reduced basis by appending all three vectors is the most promising path to follow if looking at the resulting drop in error and at the solution which is smooth in displacements and velocities. The extra cost of adding two additional vectors over the alternative of appending only  $\Delta \mathbf{u}$  is considered limited against the actual size of reduced order models, which should be in the order of several hundred degrees of freedom. Replacing vectors in the updated reduced basis leads to a higher error and has thus to be avoided.

The introduction of the update of the reduced basis imposes the requirement for the autonomous formulation to be independent from the reduced basis. This requirement is taken into account in section 5.2 and allows to update the reduced basis without compromising the autonomous formulation.

**5.1.3.6.2 Using a higher order reduced solution at  $r + 3$  from the beginning ?** The order of the reduced system is prescribed by the value of  $r$ . In the case of a constant reduced basis, the value of  $r$  does not change and remains constant for the entire duration of the solution. However, in section 5.1.3.1, which covers the update of the basis, a method is introduced for which it is necessary to add the three vectors  $\Delta \mathbf{u}$ ,  $\Delta \dot{\mathbf{u}}$ , and  $\Delta \ddot{\mathbf{u}}$  to the reduced basis. This is termed augmenting the reduced basis and performed during the first update. This means that, after the first update until the end of the simulated time, the order of the reduced system is indeed  $r + 3$ .

The question to be asked is, if the update of the reduced basis is really necessary. Or, more precisely, does the additional effort invested into the update is justified based on the quality of the obtained solution if compared to a solution obtained with a constant reduced basis with an equivalent order?

The answer to this question is found in a straightforward manner. It requires the comparison of three solutions

- a solution with a constant reduced basis and an initial and constant order of  $r^{(t_0)} = 4$ ,
- a solution with a constant reduced basis and an initial and constant order of  $r^{(t_0)} = 7$ , and
- a solution during which the reduced basis is updated as described in section 5.1.3.1, and an initial order of  $r^{(t_0)} = 4$  that increases to  $r^{(t_0+m\Delta t)} = r^{(t_0)} + 3 = 7$  during the first update of the reduced basis due to augmenting the reduced basis. The order of the augmented basis  $r^{(t_0+m\Delta t)}$  then remains constant for all remaining updates.

## 5.1. ADAPTING THE SOLUTION ALGORITHM

The resulting time histories are shown in the figure 5.20 for the 16<sup>th</sup> degree of freedom. The entirely nonlinear system under harmonic excitation is used as an illustrative example. The initial order of the reduced system is set to  $r^{(t_0)} = 4$ , the same value that is used previously in this study.

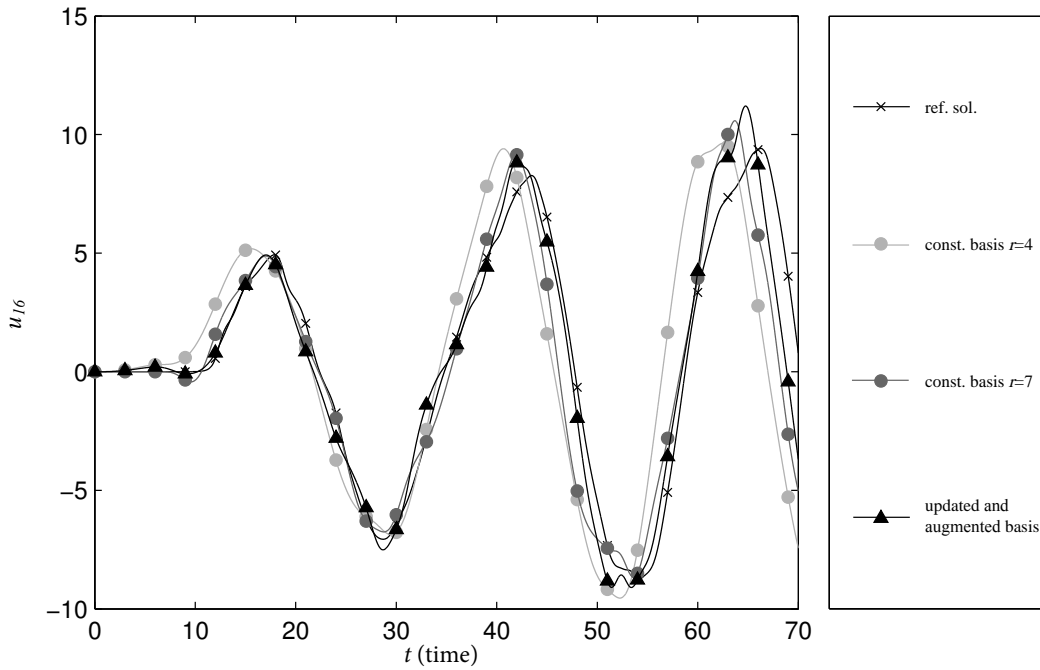


Figure 5.20: The time histories of the 16<sup>th</sup> degree of freedom of the entirely nonlinear system obtained with a constant reduced basis and with an updated and augmented reduced basis

The investigation into the R2MSE of the three solutions is shown in table 5.4. The middle column for the reduced solution is added, if compared to table 5.1. From these R2MSE it becomes evident that the simple increase of the order of the reduced solution from  $r^{(t_0)} = 4$  to  $r^{(t_0)} = 7$  does not reduce the error to the same extend as it is done by the application of the update and augmentation mechanism. This result demonstrates the interest in applying this approach of updating and augmenting the reduced bases in order to achieve a superior quality of the reduced solution.

		constant basis with $r^{(t_0)} = 4$	constant basis with $r^{(t_0)} = 7$	updated and augmented basis with $r^{(t_0)} = 4$
R2MSE mean	$e_r$	0.6602	0.3814	0.2517
R2MSE var.	$v_r$	0.0346	0.0495	0.0495

Table 5.4: The error metrics for the solutions of the entirely nonlinear system obtained with different constant reduced basis and with an updated and augmented reduced basis

Again, this example is not a proof of the superiority of the update and augmentation mechanisms. However, this case is representative for all test-cases that are used and therefore strong confidence is placed in these mechanisms.

### 5.1.4 Outcome of the adaptation of the solution algorithm

The choice for an adaptation of the solution algorithm, with the aim of improving the quality of the reduced solution, is mainly based on the numerical results that have been obtained with the three methods of quasi-static correction, Least-Squares Petrov-Galerkin method and the update and augmentation of the reduced basis. The remaining limitation of this study that is there is no direct comparison between the three methods' solutions remains. This is a deliberate choice because the different methods are conceptually very different on the algorithmic level and there is no common reference solution except the full order solution. Different reduced order reference solutions have been chosen because they are needed to demonstrate the different aspects of the three methods as clearly as possible. By indirectly comparing the methods among each other by means of comparisons with their respective full order reference solutions enough information is available to decide for one adaptation method that is pursued further.

The quasi-static correction, especially its variant without feedback, does offer some potential for an improvement. However, it requires the solution of full order static problems and is hence disadvantaged on the performance level. The LSPG does not yield any improvement. Furthermore, it would require an additional hyper-reduction to remedy its performance shortcomings. Also, the LSPG approach is highly intrusive in the reduced nonlinear Newmark scheme. The update and augmentation method presents a complex construct of several sub-methods, but it is also self-contained and can be introduced at any point in the reduced nonlinear Newmark algorithm. It delivers reasonable improvements for a reasonable effort.

The update and augmentation method is chosen to be pursued and developed further, for an application to the finite element test-cases in the next chapter.

## 5.2 Replacing the inflation of the nonlinear terms with an autonomous formulation

The requirement for an autonomous formulation of the nonlinear terms is identified in the section 3.2.3. This requirement results from the inspection of the proposed nonlinear Newmark-type solution procedures in section 3.2.2 and is not identified from any form of numerical results. It is hence a requirement that is driven by the process of obtaining reduced nonlinear transient solutions rather than by the quality of the outcomes. During the comparative study and the study of robustness, in sections 4.2.1 and 4.2.2, respectively, the formulation of the reduced order solution algorithm without an autonomous formulation proves advantageous. There, it allows limiting the source of error exclusively to the introduction of the reduced bases. However, to have a truly reduced system, an autonomous formulation for the nonlinear terms have to be found.

The generic equation of a nonlinear system (2.82) contains the function  $g(\mathbf{u})$ , which regroups all nonlinearities present in the system. The intrinsic property of this function is that it may not be reduced easily to a form  $\tilde{g}(\mathbf{q})$ . The same goes for the reduced tangent stiffness matrix  $\tilde{\mathbf{K}}$ . However, to have a truly reduced system, all links with the full order formulation have to be severed during the transient solution phase<sup>5</sup>. Furthermore, the calculations are in dire need for such a reduction of the nonlinear terms because the inflation type formulation of the nonlinear forces vector appears computationally far too costly. Also, having a truly reduced system addresses the issues of portability, which is the possibility to embark it, and to run it without connection to possibly licensed software. The autonomous formulations of the nonlinear terms have to respond to these requirements and render the reduced system autonomous from any full order entities outside the creation of the reduced basis.

An additional requirement that has to be imposed is that the autonomous formulations have to accom-

---

<sup>5</sup>The transient solution phase is confined to the time-marching solution algorithm. During the update of the reduced basis, as it is described in the section 5.1.3, an access to the full order system might still be required. This access is however limited to the requirements for the update of the reduced basis and does not concern the transient solution itself.

modate any of the reduced bases that are proposed in section 3.3. This additional requirement is imposed because the results of the comparative study in section 4.2.1 show that the proper selection of the most promising reduced basis for a given test-case is very important for a successful reduction. Furthermore, the update of the reduced basis, which is chosen as the adaptation of the solution algorithm in section 5.1, requires an independence of the autonomous formulations from a specific reduced basis.

This section is dedicated to explore different approaches to achieve a reduced formulation of the nonlinear forces vector and the nonlinear tangent stiffness matrix and thus to circumvent an inflation formulation. These comprise the common approaches of linear interpolation, direct linearisation and a polynomial approximation that are available in literature. For the polynomial approximation a novel formulation is proposed that renders this approach independent from the reduced basis and draws heavily on the algorithmic implementation to achieve a maximum of numerical performance.

### 5.2.1 Presenting the linear interpolation and the direct linearisation

The linear interpolation is possibly the most crude approach to expressing the nonlinear forces vectors  $\mathbf{g}(\mathbf{u})$ . It decomposes the current displacement  $\mathbf{u}$  in a sum of predetermined displacements  $\tilde{\mathbf{u}}_j$ , each multiplied by a factor  $\alpha_j$ . The factors are then used to assemble the sought-for nonlinear forces vector by summing the nonlinear forces corresponding to the predetermined displacements. The direct linearisation is the reduced equivalent of the linear interpolation. It uses the same approach for expressing the reduced nonlinear forces vector  $\tilde{\mathbf{g}}(\mathbf{q})$ .

Both approaches are briefly presented. The linear interpolation is presented first because the direct linearisation builds on it.

#### 5.2.1.1 Linear interpolation

This linear interpolation requires, as a first preparation, a set of displacements  $\tilde{\mathbf{u}}_j$  with  $j \in \{1, \dots, m\}$ . These displacements have to be representative for the behaviour of the system. They can either be physical displacements, as e.g. the snapshots of the POD method (see section 3.3.3.1), or modes of a reduced basis. In the latter case this method leads to the direct linearisation that is expanded below. The displacements  $\tilde{\mathbf{u}}_j$  are regrouped in the matrix  $\tilde{\mathbf{U}} = [\tilde{\mathbf{u}}_1, \dots, \tilde{\mathbf{u}}_m]$

In a second preparation step the nonlinear forces  $\mathbf{g}_j = \mathbf{g}(\tilde{\mathbf{u}}_j)$  are calculated for each displacement  $\tilde{\mathbf{u}}_j$ . These nonlinear forces vectors are regrouped as  $\tilde{\mathbf{G}} = [\tilde{\mathbf{g}}_1, \dots, \tilde{\mathbf{g}}_m]$ .

The current displacement is supposed to be approximated as

$$\mathbf{u} \approx \sum_{j=1}^m \alpha_j \tilde{\mathbf{u}}_j, \quad (5.48)$$

in order to identify the factors  $\alpha_j$  and to apply them for the approximation of the nonlinear forces vector

$$\mathbf{g}(\mathbf{u}) \approx \sum_{j=1}^m \alpha_j \mathbf{g}_j. \quad (5.49)$$

To identify the  $\alpha_j$  numerically equation (5.48) is reformulated in matrix form

$$\tilde{\mathbf{U}} \boldsymbol{\alpha} = \mathbf{u}, \quad (5.50)$$

## 5.2. REPLACING THE INFLATION OF THE NONLINEAR TERMS WITH AN AUTONOMOUS FORMULATION

---

where the  $\alpha_j$  are regrouped in the column vector  $\alpha$ . Equation (5.50) is solved in the least-squares sense (Strang [218]) to yield

$$\alpha = (\check{U}^T \check{U})^{-1} \check{U}^T \mathbf{u}, \quad (5.51)$$

because usually the matrix  $\check{U}$  is not square as the number  $m$  for the displacements is not equal to the number  $n$  of degrees of freedom in the system.

The sought-for nonlinear forces vector  $\mathbf{g}(\mathbf{u})$  is then approximated by

$$\mathbf{g}(\mathbf{u}) \approx \check{G}\alpha. \quad (5.52)$$

The same process can also be applied for the nonlinear tangent stiffness matrix, which is approximated as

$$\bar{K}(\mathbf{u}) \approx \sum_{j=1}^m \alpha_j \bar{K}_j, \quad (5.53)$$

supposing that the nonlinear stiffness matrices  $\bar{K}_j = \left. \frac{\partial \mathbf{g}(\mathbf{u})}{\partial \mathbf{u}} \right|_{\mathbf{u}_j}$  have been calculated beforehand.

### 5.2.1.2 Direct linearisation

The direct linearisation of the reduced nonlinear forces vector is a variation of the linear interpolation. It builds on pre-calculating the nonlinear forces vector  $\mathbf{g}$  with the columns of the reduction matrix  $\Phi$ . This allows to obtain a reduced matrix that contains the reduced nonlinear forces as columns. This matrix can then be multiplied directly with the vector of generalised coordinates  $\mathbf{q}$ . This method is applied by e.g. Tran et al. [229] who provides further references. The direct linearisation provides the advantage of a simple matrix multiplication for expressing the reduced nonlinear forces vector, which makes its computational effort comparable to a linear approximation with a constant reduced tangent stiffness matrix.

Regarding the reduced basis  $\Phi$ , which can be obtained with any method, as being composed of its columns  $[\phi_1, \dots, \phi_r]$ , allows to establish the  $n \times r$  matrix

$$\mathbf{G} = [\mathbf{g}(\phi_1), \dots, \mathbf{g}(\phi_r)], \quad (5.54)$$

whose columns are the nonlinear forces vectors corresponding to columns of the basis. These are obtained by static solutions of the full order system while imposing the columns of the reduced basis as displacements. As  $\mathbf{G}$  is neither depending on time, nor on displacements, it can be further reduced to a  $r \times r$  matrix, by premultiplying it with the left-hand reduced basis, giving

$$\check{G} = \Phi^T \mathbf{G} = \Phi^T [\mathbf{g}(\phi_1), \dots, \mathbf{g}(\phi_r)]. \quad (5.55)$$

From this constant matrix the reduced formulation of the nonlinear forces vector can be specified as

$$\tilde{\mathbf{g}}(\mathbf{q}) \approx \check{G}\mathbf{q}, \quad (5.56)$$

## 5.2. REPLACING THE INFLATION OF THE NONLINEAR TERMS WITH AN AUTONOMOUS FORMULATION

---

which is the product of the reduced direct linearisation matrix  $\tilde{\mathbf{G}}$  from equation (5.55) with the generalised coordinates  $\mathbf{q}$ . This requires a suitable normalisation of the generalised coordinates. Such a normalisation can be achieved with the constitution of the reduced basis as demonstrated in section 3.3.7.

The direct linearisation can be extended to approximate the reduced nonlinear tangent stiffness matrix by

$$\tilde{\mathbf{K}}(\mathbf{q}) \approx \sum_{k=1}^r \left( \Phi^T \frac{\partial \mathbf{g}(\mathbf{u})}{\partial \mathbf{u}} \Big|_{\phi_{(k)}} \Phi \right) q_k. \quad (5.57)$$

The terms  $\Phi^T \frac{\partial \mathbf{g}(\mathbf{u})}{\partial \mathbf{u}} \Big|_{\phi_{(k)}} \Phi$  for the  $r$  columns of the reduced basis are to be calculated beforehand and then stored for an efficient numerical process. Except the multiplications with  $\Phi^T$  and  $\Phi$ , equation (5.57) is the exact reduced equivalent of full order approximation in equation (5.53).

### 5.2.2 Developing the polynomial formulation of the reduced nonlinear forces vector

The presentation of the polynomial formulation and especially of the identification-algorithm are following the lines proposed by Muravyov and Rizzi [155], with some refinements by Chang et al. [58], who proposed a shift of the identification's origin. The reduction of the tensors follows the developments of Phillips [179].

The use of the polynomial formulation for reconstructing the nonlinear tangent stiffness matrix is an original contribution of this work. However, preceding works in this direction include the application of the method to clamped beams by Hollkamp et al. [99] and Spottswood and Allemang [214] for the prediction of sonic fatigue responses. A novel approach is also the attempt to apply an indirect identification technique to the full order solutions with an added reduction of the tensors.

The polynomial formulation of the nonlinear forces vector  $\mathbf{g}(\mathbf{u})$  simply supposes it to be of the form of a polynomial of order  $d$  in terms of the displacements

$$\begin{aligned} \mathbf{g}(\mathbf{u}) &= \sum_{h=1}^d \mathbf{A}^{(h)} \mathbf{u}^h \\ &= \mathbf{A}^{(1)} \mathbf{u} + \mathbf{A}^{(2)} (\mathbf{u} \otimes \mathbf{u}) + \mathbf{A}^{(3)} (\mathbf{u} \otimes \mathbf{u} \otimes \mathbf{u}) + \dots, \end{aligned} \quad (5.58)$$

where the  $\mathbf{A}^{(h)}$  are tensors of order  $\mathbb{R}^{n \times n^h}$ . The second line of equation (5.58) is a lean, symbolic notation of the connection between the tensors  $\mathbf{A}^{(h)}$  and the vectors  $\mathbf{u}$ . This connection will be detailed later. For each component  $i \in \{1, \dots, n\}$  this can be written as

$$g_i(\mathbf{u}) = A_{ij}^{(1)} u_j + A_{ijl}^{(2)} u_j u_l + A_{ijlm}^{(3)} u_j u_l u_m + \dots \quad (5.59)$$

in indexed notation. This does not necessarily imply the Einstein notation with full summations over equal indices. The ranges of the dummy indices  $j$ ,  $l$  and  $m$  are defined later.

On a conceptual level, the formulation in equation (5.58) can be linked to a Taylor development of the components of the vector of the nonlinear internal forces  $\mathbf{g}(\mathbf{u})$  (Bartsch [21]). A Taylor series approaches

## 5.2. REPLACING THE INFLATION OF THE NONLINEAR TERMS WITH AN AUTONOMOUS FORMULATION

---

a function as a sum of its derivatives in a given point  $\hat{\mathbf{u}}$ . For the nonlinear forces this would give

$$\mathbf{g}(\mathbf{u}) \approx \mathbf{g}(\hat{\mathbf{u}}) + \sum_{h=1}^d \frac{1}{h!} \frac{\partial^h \mathbf{g}(\mathbf{u})}{\partial \mathbf{u}^{(h)}} \Big|_{\hat{\mathbf{u}}} (\mathbf{u} - \hat{\mathbf{u}})^h \quad (5.60)$$

in an illustrative notation. In the Taylor series the elements  $A_{ij}^{(1)}$ ,  $A_{ijl}^{(2)}$  and  $A_{ijlm}^{(3)}$  of the tensors are defined as

$$A_{ij}^{(1)} = \frac{\partial g_i(\mathbf{u})}{\partial u_j} \Big|_{\hat{\mathbf{u}}}, \quad (5.61)$$

$$A_{ijl}^{(2)} = \frac{1}{2} \frac{\partial^2 g_i(\mathbf{u})}{\partial u_j \partial u_l} \Big|_{\hat{\mathbf{u}}}, \quad (5.62)$$

$$A_{ijlm}^{(3)} = \frac{1}{6} \frac{\partial^3 g_i(\mathbf{u})}{\partial u_j \partial u_l \partial u_m} \Big|_{\hat{\mathbf{u}}}, \quad (5.63)$$

and so on. As one example in literature Hollkamp et al. [99] discusses a Taylor development of the nonlinear forces.

But before engaging in the actual definition of the tensors  $\mathbf{A}$  and how they can be used for rendering the reduced system autonomous, the polynomial formulation is explored on a conceptual level. The representation of  $\mathbf{g}(\mathbf{u})$  as a polynomial is very powerful for at least three reasons.

First, it seems to be commonly accepted in literature (Mignolet and Soize [148], Muravyov and Rizzi [155], Thomas [223], Touzé et al. [225]) that a limitation of the degree of the polynomial to  $d = 3$  is sufficient for geometrically nonlinear structures. Notably Mignolet and Soize [148] claim in their work that the nonlinear internal forces of “an arbitrary linearly elastic [...] structure undergoing large deformations”, which applies without restrictions to the finite elements used in the context of this work, can be expressed analytically as a polynomial of third order in the derivations of the basic functions with respect to the spatial coordinates. The development hinges on a general Total-Lagrangian formulation of the problem and is not limited to a specific type of nonlinear finite element. The same argument is made by Grolet and Thouverez [85], who also use the polynomial expression. They claim that a degree of  $d = 3$  corresponds to a geometrically nonlinear structure. Perret et al. [173] conduct a reduction of turbulent flows and replace the Navier-Stokes equations with a polynomial expression. They also find  $d = 3$  sufficient.

Second, there are several approaches available to identify the components of the tensors  $\mathbf{A}^{(1)}$ ,  $\mathbf{A}^{(2)}$  and  $\mathbf{A}^{(3)}$  on discrete level without actually doing the derivations that are the definition of the tensors in equations (5.61) to (5.63). Mignolet and Soize [148] distinguishes between direct and indirect approaches. Direct approaches draw on the finite element formulations and obtain the tensors  $\mathbf{A}^{(h)}$  by integration. They are developed by Touzé et al. [225], Thomas [223] and Sénéchal [203]. The drawback of direct approaches is that they require access to the formulations of the finite elements and are thus specific for a given type of nonlinear finite element. Indirect approaches identify the tensors  $\mathbf{A}^{(h)}$  by means of combining different static evaluations of  $\mathbf{g}(\mathbf{u})$  with imposed displacements. An indirect approach is proposed by Muravyov and Rizzi [155] and developed further by Chang et al. [58]. The advantage of an indirect approach is that it does not require knowledge on the elements and can be used with any, even a proprietary, finite element code. However, it requires a considerable number of static evaluations of the nonlinear internal forces vector.

Third, while the definition of the polynomial formulation of the nonlinear internal forces in equation (5.58) is written on full order level, it can be easily reduced. The polynomial formulation for the reduced vector of the nonlinear internal forces can equally well be written in generalised coordinates

## 5.2. REPLACING THE INFLATION OF THE NONLINEAR TERMS WITH AN AUTONOMOUS FORMULATION

---

$$\begin{aligned}\tilde{\mathbf{g}}(\mathbf{q}) &= \sum_{h=1}^3 \tilde{\mathbf{A}}^{(h)} \mathbf{q}^h \\ &= \tilde{\mathbf{A}}^{(1)} \mathbf{q} + \tilde{\mathbf{A}}^{(2)} (\mathbf{q} \otimes \mathbf{q}) + \tilde{\mathbf{A}}^{(3)} (\mathbf{q} \otimes \mathbf{q} \otimes \mathbf{q}),\end{aligned}\tag{5.64}$$

where the  $\tilde{\mathbf{A}}^{(h)}$  are tensors of order  $\mathbb{R}^{r \times r^h}$ . In fact, all direct and indirect approaches, which have been proposed until now, only treat the identification of the reduced tensors  $\tilde{\mathbf{A}}^{(h)}$ . This is because the current computer technology does not even allow to store all of the full order tensors  $\mathbf{A}^{(h)}$ . However, it is shown in the following that, when the full order tensors  $\mathbf{A}^{(h)}$  are known, they can be reduced easily by any reduced basis with an approach proposed by Phillips [179].

### 5.2.2.1 Sketching the reduced direct approach for identifying the components of the tensors

As pointed out by S en echal [203], the reduced direct approach consists in introducing the reduction by projection on a reduced basis into the system's description prior to the discretisation. This limits already the applicability of the reduced direct approach for identifying the components of the tensors because the system under consideration is supposed to be fully discretised in section 2.3 and to be written as stipulated in equation (2.82).

Mignolet and Soize [148] present a direct approach that relies directly on the finite element formulation, as it is developed in section 2.2.3. This approach allows to establish the full order tensors  $\mathbf{A}^{(1)}$ ,  $\mathbf{A}^{(2)}$  and  $\mathbf{A}^{(3)}$  directly, by integrating combinations of the derivations of the displacements with respect to the spatial coordinates.

While the full order direct approach in its entirety is of no concern, it allows to make the important observation that the linear tensor  $\mathbf{A}^{(1)}$  is actually the linear stiffness matrix  $\bar{\mathbf{K}}_0 = \frac{\partial \mathbf{g}(\mathbf{u})}{\partial \mathbf{u}}$ . If the hinging point is set to  $\hat{\mathbf{u}} = \mathbf{0}$  the resulting MacLaurin series (Bartsch [21]) greatly simplifies the calculations and the notation. The development around  $\hat{\mathbf{u}} = \mathbf{0}$  is continued without loss of generality. The hinging point  $\hat{\mathbf{u}}$  will be considered again briefly prior to the actual numerical implementation

Mignolet and Soize [148] write

$$A_{op}^{(1)} = \int_{V^{(0)}} \frac{\partial u_i^{(o)}}{\partial x_j} C_{ijlm} \frac{\partial u_l^{(p)}}{\partial x_m} dV^{(0)},\tag{5.65}$$

for a single element, which is the exact equivalence of equation (2.77) if the displacements are set to  $u_0$ . It therefore is viable to set

$$A_{ij}^{(1)} = \frac{\partial g_i(\mathbf{u})}{\partial u_j},\tag{5.66}$$

and

$$\tilde{A}_{ko}^{(1)} = \Phi_{ki}^T \frac{\partial g_i(\mathbf{u})}{\partial u_j} \Phi_{jo},\tag{5.67}$$

## 5.2. REPLACING THE INFLATION OF THE NONLINEAR TERMS WITH AN AUTONOMOUS FORMULATION

---

which uses the Einstein summation convention to express

$$\tilde{\mathbf{A}}^{(1)} = \Phi^T \bar{\mathbf{K}}_0 \Phi. \quad (5.68)$$

This equality (5.68) is universal for all approaches for identifying the components of the tensors. It remains basically unaltered because the linear stiffness matrix  $\bar{\mathbf{K}}_0$  is always readily available.

The quadratic  $\tilde{\mathbf{A}}^{(2)}$  and cubic  $\tilde{\mathbf{A}}^{(3)}$  tensors that remain to be identified, require some more attention. Following the propositions of S en echal [203] they can be written element wise as

$$\tilde{\mathbf{A}}_{kop}^{(2)} = \phi_{e,k}^T \left( \int_{V_e^{(0)}} (\mathbf{B}_e^{(1)})^T \mathbf{C} \mathbf{B}_e^{(2)} \Phi_{e,o} + (\mathbf{B}_e)^T \phi_{e,o} \mathbf{B}_e^{(1)} dV_e \right) \phi_{e,p}, \quad (5.69)$$

and

$$\tilde{\mathbf{A}}_{kops}^{(3)} = \phi_{e,k}^T \left( \int_{V_e^{(0)}} (\mathbf{B}_e)^T \phi_{e,o} \mathbf{C} \mathbf{B}_e^{(2)} \phi_{e,s} dV_e \right) \phi_{e,p}. \quad (5.70)$$

The integrations are expected to be performed numerically, as described in section 2.2.3.4, for each element. The reduced basis  $\Phi$  are modified so that only their elements that are connected to the element under consideration are retained. For the actual calculation of  $\tilde{\mathbf{A}}_{kop}^{(2)}$  and  $\tilde{\mathbf{A}}_{kops}^{(3)}$  only the columns  $\phi_{e,k}$ ,  $\phi_{e,o}$ ,  $\phi_{e,s}$  and  $\phi_{e,p}$  that are indicated by the second indices are used. The matrix expression  $\mathbf{C}$  for the stress-strain-relation can be directly ported over from the finite element formulation. If the material is supposed to isotropic and ideally elastic, equation (2.59) can be used. The matrices  $\mathbf{B}_e^{(1)}$  and  $\mathbf{B}_e^{(2)}$  are variants of the building blocks of the linear strain displacement transformation matrix. Being based on equation (2.69) the matrix  $\mathbf{B}_e^{(1)}$  is an adaptation to represent a single element. The same goes for the matrix  $\mathbf{B}_e^{(2)}$ , which is based on equation (2.71). The matrix  $\mathbf{B}_e$  assembles the remaining terms that are required to describe the nonlinear behaviour of the element. It has no direct equivalent in section 2.2.3.3.3 because S en echal [203] uses a different description of the nonlinear element. In his work he also stresses that, even though the matrices and column vectors of the reduced bases are altered so that they are connected to only one element at a time, there is no assembly operation required to obtain the tensors  $\tilde{\mathbf{A}}^{(2)}$  and  $\tilde{\mathbf{A}}^{(3)}$ . They become available by applying a simple summation over elements.

The reduced direct approach for identifying the components of the tensors is not pursued further beyond this point. It is helpful for demonstrating that the reduced linear tensor  $\tilde{\mathbf{A}}^{(1)}$  is indeed the reduced linear stiffness matrix. However, this approach requires knowledge of the finite element formulation of the full order system, notably the interpolation function within each element. This knowledge is, per definition, not available in the context of this work, see section 2.3. Another disadvantage of this approach, that weighs much more heavily, is the fact that the reduced basis can no longer be changed, once the tensors  $\tilde{\mathbf{A}}^{(2)}$  and  $\tilde{\mathbf{A}}^{(3)}$  are obtained because the reduced basis' column vectors form an central part of the integrals in equations (5.69) and (5.70). This is incompatible with the requirement of the independence of the autonomous formulation from the reduced basis, as it has been formulated to allow the continued application of the update and augmentation of the reduced basis<sup>6</sup>.

---

<sup>6</sup>A loop hole exists however because the tensors  $\mathbf{A}^{(2)}$  and  $\mathbf{A}^{(3)}$  could still be identified directly on the full order system by setting the reduced basis as  $\Phi = \mathbf{I}$ . Once the full order tensors are obtained, they can be reduced with a procedure from Phillips [179]. This is expanded in equations (5.100) to (5.102) below.

### 5.2.2.2 Applying the reduced indirect approach for identifying the components of the tensors

The identification of a polynomial formulation is the determination of the tensors  $\tilde{\mathbf{A}}^{(h)}$  with the aim of establishing the forces vector  $\tilde{\mathbf{g}}(\mathbf{q})$  as per equation (5.64). To this end Muravyov and Rizzi [155] propose a direct identification technique for the case  $d = 3$ , which aims at identifying the elements of  $\tilde{\mathbf{A}}^{(2)}$  and  $\tilde{\mathbf{A}}^{(3)}$  directly from repeated static solutions. It is refined by Chang et al. [58], who propose to explicitly include a reference configuration  $\hat{\mathbf{u}}$ . Detailed insight into the actual implementation in the commercial FEM code NASTRAN is given by Rizzi and Muravyov [189].

To stress the strong focus on the numerical implementation, a different formulation of equation (5.64) is introduced. It treats the tensors  $\tilde{\mathbf{A}}^{(h)}$  as sets of vectors. This cuts one dimension for the numerical implementation. In this vector form, the polynomial formulation of the reduced nonlinear internal forces reads

$$\tilde{\mathbf{g}}(\mathbf{q}) = \sum_{o=1}^r [\tilde{\mathbf{A}}_o^{(1)}] q_o + \sum_{o=1}^r \sum_{p=o}^r [\tilde{\mathbf{A}}_{op}^{(2)}] q_o q_p + \sum_{o=1}^r \sum_{p=o}^r \sum_{s=p}^r [\tilde{\mathbf{A}}_{ops}^{(3)}] q_o q_p q_s, \quad (5.71)$$

where staggered sums are used.

The tensor  $\tilde{\mathbf{A}}^{(1)}$  is defined in  $\mathbb{R}^{r^2}$ . It has been shown in equations (5.65) to (5.68) that it corresponds to the reduced tangent stiffness matrix  $\tilde{\mathbf{K}}$ . This fact will be exploited in the following identification of the tensors  $\tilde{\mathbf{A}}^{(2)}$  and  $\tilde{\mathbf{A}}^{(3)}$ . In fact, the linear tensor can easily be established via equation (3.57) as

$$\tilde{\mathbf{A}}^{(1)} = \Phi^T \bar{\mathbf{K}} \Phi. \quad (5.72)$$

where

$$\bar{\mathbf{K}} = \frac{\partial \mathbf{g}(\mathbf{u})}{\partial \mathbf{u}}, \quad (5.73)$$

might be established at a convenient reference deformation  $\hat{\mathbf{u}}$ . The reference deformation  $\hat{\mathbf{u}}$  provides the hinging point of the identification process. It is introduced by Chang et al. [58], who demonstrates that its application can be highly advantageous. The remaining development for the identification of the tensors supposes  $\hat{\mathbf{u}} = \mathbf{0}$  because it prepares the actual numerical implementation.

This settles the linear part of the identification and allows to concentrate on the tensors  $\mathbf{A}^{(2)}$  and  $\mathbf{A}^{(3)}$ .

For the quadratic and the cubic part of equation (5.71), the vectors  $[\tilde{\mathbf{A}}_{op}^{(2)}]$  and  $[\tilde{\mathbf{A}}_{ops}^{(3)}]$ , both of dimension  $r$ , are now obtained from repeated static solutions as follows. By defining the finite displacement  $\Delta q_o$  of the  $o$ -th generalised coordinate the  $2r$  equations

$$\Phi^T \mathbf{g}(+\phi_o \Delta q_o) - \Phi^T \mathbf{K}(+\phi_o \Delta q_o) = [\tilde{\mathbf{A}}_{oo}^{(2)}] \Delta q_o \Delta q_o + [\tilde{\mathbf{A}}_{ooo}^{(3)}] \Delta q_o \Delta q_o \Delta q_o \quad (5.74)$$

$$\Phi^T \mathbf{g}(-\phi_o \Delta q_o) - \Phi^T \mathbf{K}(-\phi_o \Delta q_o) = [\tilde{\mathbf{A}}_{oo}^{(2)}] \Delta q_o \Delta q_o - [\tilde{\mathbf{A}}_{ooo}^{(3)}] \Delta q_o \Delta q_o \Delta q_o \quad (5.75)$$

are established. They can be solved for the  $2r$  unknown  $r \times 1$  vectors  $[\tilde{\mathbf{A}}_{oo}^{(2)}]$  and  $[\tilde{\mathbf{A}}_{ooo}^{(3)}]$ .

The left-hand sides of equations (5.74) and (5.75) can be interpreted as some kind of pure nonlinear force. It is obtained by subtracting the linear part, introduced in equation (5.71), from the original, full order nonlinear forces vector, leaving only the reduced nonlinear part. To calculate these left-hand sides

## 5.2. REPLACING THE INFLATION OF THE NONLINEAR TERMS WITH AN AUTONOMOUS FORMULATION

---

it is necessary to obtain static, nonlinear evaluation of the nonlinear forces vector  $\mathbf{g}(\mathbf{u})$  for varied finite displacements  $\Delta q_o$ , which are inflated to  $\Delta u_i$  by the appropriate column  $\phi_o$  of the reduced matrix  $\Phi$ , as per equation (3.1).

The procedure of first adding equation (5.74) to equation (5.75) to eliminate the  $[\tilde{A}_{ooo}^{(3)}]$  and to solve for the  $[\tilde{A}_{oo}^{(2)}]$  and then substituting the obtained result into either equation to solve for the  $[\tilde{A}_{ooo}^{(3)}]$  can be applied for all  $o \in \{1, \dots, r\}$ , using the appropriate  $\Delta q_o$  and  $\phi_o$ . While operating on the corresponding vectors this is done by adding equation (5.74) to equation (5.75), allowing for the vector of  $[\tilde{A}_{oo}^{(2)}]$  to be obtained as

$$[\tilde{A}_{oo}^{(2)}] = \frac{1}{2(\Delta q_o \Delta q_o)} (\Phi^T \mathbf{g} (+\phi_o \Delta q_o) + \Phi^T \mathbf{g} (-\phi_o \Delta q_o)), \quad (5.76)$$

for all  $o \in \{1, \dots, r\}$ . The term  $\Phi^T \mathbf{K} \phi_o \Delta q_o$  from equations (5.74) and (5.75) cancel each other out, as the multiplication with the partially reduced stiffness matrix  $\Phi^T \mathbf{K}$  is a linear operation. Introducing the result from equation (5.76) into equation (5.74), the coefficients for the terms of third order are obtained as

$$[\tilde{A}_{ooo}^{(3)}] = \frac{1}{\Delta q_o \Delta q_o \Delta q_o} (\Phi^T \mathbf{g} (+\phi_o \Delta q_o) - \Phi^T \mathbf{K} (+\phi_o \Delta q_o) - [\tilde{A}_{oo}^{(2)}] \Delta q_o \Delta q_o), \quad (5.77)$$

again for all  $o \in \{1, \dots, r\}$ . This approach, successful for terms of equal indices, can be generalised to terms with different indices.

For the components  $[\tilde{A}_{opp}^{(2)}]$ ,  $[\tilde{A}_{oop}^{(3)}]$  and  $[\tilde{A}_{opp}^{(3)}]$  with two different indices  $o \neq p$ , a total of three equations is necessary. These equations are defined by combining the finite displacements  $\Delta q_o$  and  $\Delta q_p$  to obtain

$$\begin{aligned} \Phi^T \mathbf{g} (+\phi_o \Delta q_o + \phi_p \Delta q_p) - \Phi^T \mathbf{K} (+\phi_o \Delta q_o + \phi_p \Delta q_p) = \\ [\tilde{A}_{oo}^{(2)}] \Delta q_o \Delta q_o + [\tilde{A}_{pp}^{(2)}] \Delta q_p \Delta q_p + [\tilde{A}_{op}^{(2)}] \Delta q_o \Delta q_p \end{aligned} \quad (5.78)$$

$$\begin{aligned} + [\tilde{A}_{ooo}^{(3)}] \Delta q_o \Delta q_o \Delta q_o + [\tilde{A}_{ppp}^{(3)}] \Delta q_p \Delta q_p \Delta q_p + [\tilde{A}_{oop}^{(3)}] \Delta q_o \Delta q_o \Delta q_p + [\tilde{A}_{opp}^{(3)}] \Delta q_o \Delta q_p \Delta q_p \\ \Phi^T \mathbf{g} (-\phi_o \Delta q_o - \phi_p \Delta q_p) - \Phi^T \mathbf{K} (-\phi_o \Delta q_o - \phi_p \Delta q_p) = \end{aligned} \quad (5.79)$$

$$\begin{aligned} [\tilde{A}_{oo}^{(2)}] \Delta q_o \Delta q_o + [\tilde{A}_{pp}^{(2)}] \Delta q_p \Delta q_p + [\tilde{A}_{op}^{(2)}] \Delta q_o \Delta q_p \\ - [\tilde{A}_{ooo}^{(3)}] \Delta q_o \Delta q_o \Delta q_o - [\tilde{A}_{ppp}^{(3)}] \Delta q_p \Delta q_p \Delta q_p - [\tilde{A}_{oop}^{(3)}] \Delta q_o \Delta q_o \Delta q_p - [\tilde{A}_{opp}^{(3)}] \Delta q_o \Delta q_p \Delta q_p \end{aligned}$$

$$\begin{aligned} \Phi^T \mathbf{g} (+\phi_o \Delta q_o - \phi_k \Delta q_k) - \Phi^T \mathbf{K} (+\phi_o \Delta q_o - \phi_k \Delta q_k) = \\ [\tilde{A}_{oo}^{(2)}] \Delta q_o \Delta q_o + [\tilde{A}_{pp}^{(2)}] \Delta q_p \Delta q_p - [\tilde{A}_{op}^{(2)}] \Delta q_o \Delta q_p \\ + [\tilde{A}_{ooo}^{(3)}] \Delta q_o \Delta q_o \Delta q_o - [\tilde{A}_{ppp}^{(3)}] \Delta q_p \Delta q_p \Delta q_p - [\tilde{A}_{oop}^{(3)}] \Delta q_o \Delta q_o \Delta q_p + [\tilde{A}_{opp}^{(3)}] \Delta q_o \Delta q_p \Delta q_p. \end{aligned} \quad (5.80)$$

The quadratic coefficients with non-equal indices  $[\tilde{A}_{op}^{(2)}]$  are obtained by adding equation (5.78) to equation (5.79), which yields

## 5.2. REPLACING THE INFLATION OF THE NONLINEAR TERMS WITH AN AUTONOMOUS FORMULATION

---

$$\begin{aligned} \left[ \tilde{A}_{op}^{(2)} \right] = \frac{1}{2(\Delta q_o \Delta q_p)} & \left( \Phi^T \mathbf{g} (+\phi_o \Delta q_o + \phi_p \Delta q_p) + \Phi^T \mathbf{g} (-\phi_o \Delta q_o - \phi_p \Delta q_p) \right. \\ & \left. - 2 \left[ \tilde{A}_{oo}^{(2)} \right] \Delta q_o \Delta q_o - 2 \left[ \tilde{A}_{pp}^{(2)} \right] \Delta q_p \Delta q_p \right) \end{aligned} \quad (5.81)$$

for  $o < p$  within the ranges of  $\{o\} \in \{1, \dots, r\}$  and  $\{p\} \in \{o+1, \dots, r\}$ . It is important at this point to notice that the tensor  $\tilde{A}^{(2)}$  contains the symmetry  $\left[ \tilde{A}_{op}^{(2)} \right] = \left[ \tilde{A}_{po}^{(2)} \right]$ . This has to be exploited for the computational implementation.

The coefficients  $\left[ \tilde{A}_{oop}^{(3)} \right]$  are obtained by subtracting equation (5.80) from equation (5.78)

$$\begin{aligned} \left[ \tilde{A}_{oop}^{(3)} \right] = \frac{1}{2(\Delta q_o \Delta q_o \Delta q_p)} & \left( (\Phi^T \mathbf{g} (+\phi_o \Delta q_o + \phi_p \Delta q_p) - \Phi^T \mathbf{K} (+\phi_o \Delta q_o + \phi_p \Delta q_p)) \right. \\ & - (\Phi^T \mathbf{g} (+\phi_o \Delta q_o - \phi_p \Delta q_p) - \Phi^T \mathbf{K} (+\phi_o \Delta q_o - \phi_p \Delta q_p)) \\ & \left. - 2 \left[ \tilde{A}_{ppp}^{(3)} \right] \Delta q_p \Delta q_p \Delta q_p - 2 \left[ \tilde{A}_{op}^{(2)} \right] \Delta q_o \Delta q_p \right). \end{aligned} \quad (5.82)$$

The coefficients  $\left[ \tilde{A}_{opp}^{(3)} \right]$  are eventually obtained by simple application of equation (5.78), into which all beforehand established terms are injected

$$\begin{aligned} \left[ \tilde{A}_{opp}^{(3)} \right] = \frac{1}{\Delta q_o \Delta q_p \Delta q_p} & \left( \Phi^T \mathbf{g} (+\phi_o \Delta q_o + \phi_p \Delta q_p) - \Phi^T \mathbf{K} (+\phi_o \Delta q_o + \phi_p \Delta q_p) \right. \\ & - \left[ \tilde{A}_{oo}^{(2)} \right] \Delta q_o \Delta q_o - \left[ \tilde{A}_{pp}^{(2)} \right] \Delta q_p \Delta q_p - \left[ \tilde{A}_{op}^{(2)} \right] \Delta q_o \Delta q_p \\ & \left. - \left[ \tilde{A}_{ooo}^{(3)} \right] \Delta q_o \Delta q_o \Delta q_o - \left[ \tilde{A}_{ppp}^{(3)} \right] \Delta q_p \Delta q_p \Delta q_p - \left[ \tilde{A}_{oop}^{(3)} \right] \Delta q_o \Delta q_o \Delta q_p \right). \end{aligned} \quad (5.83)$$

The coefficients  $\left[ \tilde{A}_{ops}^{(3)} \right]$ , with all different indices, are obtained from a single equation, formulated with the three finite displacements  $\Delta q_o$ ,  $\Delta q_p$  and  $\Delta q_s$ , giving:

$$\begin{aligned} \Phi^T \mathbf{g} (+\phi_o \Delta q_o + \phi_p \Delta q_p + \phi_s \Delta q_s) - \Phi^T \mathbf{K} (+\phi_o \Delta q_o + \phi_p \Delta q_p + \phi_s \Delta q_s) = & \quad (5.84) \\ \left[ \tilde{A}_{oo}^{(2)} \right] \Delta q_o \Delta q_o + \left[ \tilde{A}_{pp}^{(2)} \right] \Delta q_p \Delta q_p + \left[ \tilde{A}_{ss}^{(2)} \right] \Delta q_s \Delta q_s & \\ + \left[ \tilde{A}_{op}^{(2)} \right] \Delta q_o \Delta q_p + \left[ \tilde{A}_{os}^{(2)} \right] \Delta q_o \Delta q_s + \left[ \tilde{A}_{ps}^{(2)} \right] \Delta q_p \Delta q_s & \\ + \left[ \tilde{A}_{ooo}^{(3)} \right] \Delta q_o \Delta q_o \Delta q_o + \left[ \tilde{A}_{ppp}^{(3)} \right] \Delta q_p \Delta q_p \Delta q_p + \left[ \tilde{A}_{sss}^{(3)} \right] \Delta q_s \Delta q_s \Delta q_s & \\ + \left[ \tilde{A}_{oop}^{(3)} \right] \Delta q_o \Delta q_o \Delta q_p + \left[ \tilde{A}_{opp}^{(3)} \right] \Delta q_o \Delta q_p \Delta q_p + \left[ \tilde{A}_{oos}^{(3)} \right] \Delta q_o \Delta q_o \Delta q_s & \\ + \left[ \tilde{A}_{oss}^{(3)} \right] \Delta q_o \Delta q_s \Delta q_s + \left[ \tilde{A}_{pps}^{(3)} \right] \Delta q_p \Delta q_p \Delta q_s + \left[ \tilde{A}_{pss}^{(3)} \right] \Delta q_p \Delta q_s \Delta q_s & \\ + \left[ \tilde{A}_{ops}^{(3)} \right] \Delta q_o \Delta q_p \Delta q_s & \end{aligned}$$

Despite the rather monstrous aspect to this equation, it can be verified that the only unknown in it is the vector  $\left[ \tilde{A}_{ops}^{(3)} \right]$ , which allows for a direct solution

## 5.2. REPLACING THE INFLATION OF THE NONLINEAR TERMS WITH AN AUTONOMOUS FORMULATION

---

$$\begin{aligned}
\left[ \tilde{A}_{ops}^{(3)} \right] = & \frac{1}{\Delta q_o \Delta q_p \Delta q_s} \left( \Phi^T \mathbf{g} (+\phi_o \Delta q_o + \phi_p \Delta q_p + \phi_s \Delta q_s) \right. \\
& - \Phi^T \mathbf{K} (+\phi_o \Delta q_o + \phi_p \Delta q_p + \phi_s \Delta q_s) \\
& - \left[ \tilde{A}_{oo}^{(2)} \right] \Delta q_o \Delta q_o - \left[ \tilde{A}_{pp}^{(2)} \right] \Delta q_p \Delta q_p - \left[ \tilde{A}_{ss}^{(2)} \right] \Delta q_s \Delta q_s \\
& - \left[ \tilde{A}_{op}^{(2)} \right] \Delta q_o \Delta q_p - \left[ \tilde{A}_{os}^{(2)} \right] \Delta q_o \Delta q_s - \left[ \tilde{A}_{ps}^{(2)} \right] \Delta q_p \Delta q_s \\
& - \left[ \tilde{A}_{ooo}^{(3)} \right] \Delta q_o \Delta q_o \Delta q_o - \left[ \tilde{A}_{ppp}^{(3)} \right] \Delta q_p \Delta q_p \Delta q_p - \left[ \tilde{A}_{sss}^{(3)} \right] \Delta q_s \Delta q_s \Delta q_s \\
& - \left[ \tilde{A}_{oop}^{(3)} \right] \Delta q_o \Delta q_o \Delta q_p - \left[ \tilde{A}_{opp}^{(3)} \right] \Delta q_o \Delta q_p \Delta q_p - \left[ \tilde{A}_{oos}^{(3)} \right] \Delta q_o \Delta q_o \Delta q_s \\
& - \left[ \tilde{A}_{oss}^{(3)} \right] \Delta q_o \Delta q_s \Delta q_s - \left[ \tilde{A}_{pps}^{(3)} \right] \Delta q_p \Delta q_p \Delta q_s - \left[ \tilde{A}_{pss}^{(3)} \right] \Delta q_p \Delta q_s \Delta q_s \left. \right)
\end{aligned} \tag{5.85}$$

with  $o < p < s$  within the ranges of  $\{o\} \in \{1, \dots, r\}$ ,  $\{p\} \in \{o+1, \dots, r\}$  and  $\{s\} \in \{p+1, \dots, r\}$ . This concludes the identification of all parameters necessary to describe the reduced nonlinear forces vector. The identified tensors  $\tilde{A}^{(1)}$ ,  $\tilde{A}^{(2)}$  and  $\tilde{A}^{(3)}$  can now be used in equation (5.71).

The direct identification method requires  $\frac{1}{6} (r^3 + 6r^2 + 5r)$  evaluations of the full order vector of the nonlinear internal forces  $\mathbf{g}(\mathbf{u})$  and two parameters to be specified. These parameters are

- the vector  $\Delta \mathbf{q}$ , which contains all the finite displacements  $\Delta q_o$ , because of the nonlinearity of  $\mathbf{g}(\mathbf{u})$  it has to be ensured that the  $\Delta q_o$  are representative for the generalised coordinates that are expected during the actual solution, and,
- should it be chosen, the reference deformation  $\hat{\mathbf{u}} \neq \mathbf{0}$ , on which the procedure resides and which defines not only the origin of the algorithm, from where the finite displacements  $\Delta q_o$  are applied, but also the definition of the tangent matrix  $\mathbf{K}$  in equation (5.73), which is used throughout the process,

to ensure a successful identification of the tensors in the polynomial formulation of the reduced vector of the expression of the reduced nonlinear internal forces  $\tilde{\mathbf{g}}(\mathbf{q})$  in equation (5.71).

A major drawback of this approach is that it is specific for a chosen reduced basis  $\Phi$ . This choice has to be made prior to the identification of the parameters and the selected basis then becomes an integral part of the tensors  $\tilde{A}^{(1)}$ ,  $\tilde{A}^{(2)}$  and  $\tilde{A}^{(3)}$ . Such a formulation of the reduced nonlinear forces vector may become impractical, if the reduced basis is altered during the solution process, as it is intended by the update of the reduced basis in section 5.1.3.

At the same time, numerical experiments and results from other authors (Muravyov and Rizzi [155], Chang et al. [58]) show that this identification technique works rather well and that a full order variant of it might be just the element necessary to render the reduced system autonomous if it coupled with a high-performance tensor reduction procedure. Obtaining the full order tensors  $\mathbf{A}^{(h)}$  would be done by applying the procedure above with the reduced matrix set to the square unity matrix  $\Phi = \mathbf{I}$ . Yet, it is almost certain that such an approach would be severely hindered by the tremendous number of necessary evaluations of the nonlinear internal forces, which scales over-proportionally with the number of degrees of freedom  $n$ .

### 5.2.2.3 Reconstructing the nonlinear tangent stiffness matrix

Until now, only the polynomial formulation of the reduced nonlinear forces vector  $\tilde{\mathbf{g}}(\mathbf{q})$  is considered in equation (5.64). However, all reduced nonlinear solution procedures in section 3.2.2 also require constantly

## 5.2. REPLACING THE INFLATION OF THE NONLINEAR TERMS WITH AN AUTONOMOUS FORMULATION

---

the evaluation of a tangent stiffness matrix, defined as

$$\tilde{\mathbf{K}} = \left. \frac{\partial \tilde{\mathbf{g}}(\mathbf{q})}{\partial \mathbf{q}} \right|_{\mathbf{q}^{(t)}}. \quad (5.86)$$

Naturally it is out of the question to perform these derivations numerically at every iteration of a nonlinear Newmark scheme, even if operating on the reduced system. To alleviate this computational burden, the polynomial formulation from equation (5.64) can be used to reconstruct the reduced tangent stiffness matrix. The reduced tangent stiffness matrix  $\tilde{\mathbf{K}}$  is required for the time-marching solution algorithm in section 3.2.2. It is obtained by introducing an analytic derivation of equation (5.64) which can be quickly evaluated numerically. The general development hereunder is taken from Hollkamp et al. [99], who tweaks the aspect of the sums that are used in the equation (5.71).

To begin it is recalled that the  $k$ -th component in the  $r \times 1$  column vector of the reduced nonlinear forces  $\tilde{\mathbf{g}}(\mathbf{q})$  is written as

$$\tilde{g}_k(\mathbf{q}) = \sum_{o=1}^r \tilde{A}_{ko}^{(1)} q_o + \sum_{o=1}^r \sum_{p=o}^r \tilde{A}_{kop}^{(2)} q_o q_p + \sum_{o=1}^r \sum_{p=o}^r \sum_{s=p}^r \tilde{A}_{kops}^{(3)} q_o q_p q_s, \quad (5.87)$$

in its polynomial formulation. This is the complete equivalent of equation (5.71) without the vectors that were used for the numerical implementation.

The components of the nonlinear tangent stiffness matrix  $\tilde{K}_{kl}$  in equation (5.86) are defined as the derivation of the  $k$ -th component of the vector nonlinear forces with respect to the  $l$ -th generalised coordinate

$$\tilde{K}_{kl} = \frac{\partial \tilde{g}_k(\mathbf{q})}{\partial q_l} \quad (5.88)$$

with  $1 \leq k \leq r$  and  $1 \leq l \leq r$ . Applying this definition to equation (5.87) yields

$$\begin{aligned} \tilde{K}_{kl} = & \sum_{o=1}^r \tilde{A}_{ko}^{(1)} \delta_{lo} + \sum_{o=1}^r \sum_{p=o}^r \tilde{A}_{kop}^{(2)} (\delta_{lo} q_p + \delta_{lp} q_o) \\ & + \sum_{o=1}^r \sum_{p=o}^r \sum_{s=p}^r \tilde{A}_{kops}^{(3)} (\delta_{lo} q_p q_s + \delta_{lp} q_o q_s + \delta_{ls} q_o q_p). \end{aligned} \quad (5.89)$$

The linear tensor  $\tilde{\mathbf{A}}^{(1)}$  is directly integrated in  $\tilde{\mathbf{K}}$  because it presents the reduced linear tangent stiffness matrix as shown in equations (5.65) to (5.68). The Kronecker terms  $\delta_{lo}$ ,  $\delta_{lp}$  and  $\delta_{ls}$  account for the derivations of quadratic and cubic terms with equal indices with respect to a single generalised coordinate.

The lean symbolic formulation of equation (5.89) reads

$$\tilde{\mathbf{K}} = \tilde{\mathbf{A}}^{(1)} + \tilde{\mathbf{A}}^{(2)} \delta \mathbf{q} + \tilde{\mathbf{A}}^{(3)} \delta(\mathbf{q} \otimes \mathbf{q}). \quad (5.90)$$

For computational performance, the tangent stiffness matrix is obtained vector by vector. To this effect the equation (5.89) is cast in vector format by dropping the index  $k$ . This yields

## 5.2. REPLACING THE INFLATION OF THE NONLINEAR TERMS WITH AN AUTONOMOUS FORMULATION

---

$$\begin{aligned} \left[ \tilde{\mathbf{K}}_l \right] &= \left[ \tilde{\mathbf{A}}_l^{(1)} \right] + \sum_{o=1}^r \sum_{p=o}^r \left[ \tilde{\mathbf{A}}_{op}^{(2)} \right] (\delta_{lo} q_p + \delta_{lp} q_o) \\ &+ \sum_{o=1}^r \sum_{p=o}^r \sum_{s=p}^r \left[ \tilde{\mathbf{A}}_{ops}^{(3)} \right] (\delta_{lo} q_p q_s + \delta_{lp} q_o q_s + \delta_{ls} q_o q_p). \end{aligned} \quad (5.91)$$

The actual tangent stiffness matrix is obtained by assembling the resulting vectors  $\left[ \tilde{\mathbf{K}}_l \right]$ , with  $l \in \{1, \dots, r\}$ , to give the  $r \times r$  matrix  $\tilde{\mathbf{K}}$ .

### 5.2.2.4 Reversing the order of reduction and identification

The identification approaches that are presented until now, the direct and the indirect one, have in common that they work on the reduced system and that they result in reduced tensors  $\tilde{\mathbf{A}}^{(h)}$ . The reduced basis  $\Phi$ , which was chosen prior to the identification of the reduced tensors, is inextricably embedded in these reduced tensors. This is unacceptable with respect to the requirement of the autonomous formulation to be independent from the reduced basis. This independence is required to enable the application of the update and augmentation mechanism, which is selected in section 5.1.4 as the adaptation of the solution algorithm, and it will be required when the reduced basis is adapted as a function of parameters in the following section 5.3.

To solve this problem the order of reduction and identification has to be reversed. Until now the system is reduced by projection on a reduced basis  $\Phi$  and then the reduced tensors are identified. These reduced tensors cannot be changed readily as the reduced basis changes. The solution would be to first identify the full order tensors  $\mathbf{A}^{(h)}$  and only then reduced the entire system, including the tensors, by projection on any reduced basis  $\Phi$ .

To allow this approach to be successful two central points have to be addressed. While the principle of the indirect identification process, which is presented above, can simply applied to a full order identification by setting  $\Phi = \mathbf{I}$ , it requires considerable work on the actual implementation to render it numerically feasible. This point is termed enabling an indirect identification for a full order system. The second point has to provide a high-performance reduction of the full order tensors. These two points are explored below.

**5.2.2.4.1 Enabling the indirect identification for a full order system** Returning to the initial equation (5.58) of the polynomial formulation in its symbolic notation

$$\mathbf{g}(\mathbf{u}) = \mathbf{A}^{(1)} \mathbf{u} + \mathbf{A}^{(2)} (\mathbf{u} \otimes \mathbf{u}) + \mathbf{A}^{(3)} (\mathbf{u} \otimes \mathbf{u} \otimes \mathbf{u}), \quad (5.92)$$

it is recalled that also the full order vector of the nonlinear internal forces  $\mathbf{g}(\mathbf{u})$  can be written as a polynomial expression of the physical displacements  $\mathbf{u}$ . This formulation of the nonlinear forces vector  $\mathbf{g}$  allows for a reconstitution of the entire nonlinear forces vector  $\mathbf{g}(\mathbf{u})$  as well as the nonlinear tangent stiffness matrix  $\tilde{\mathbf{K}}$  at full order.

As stated in the opening of the paragraph above the application of the direct identification to a full order system would be possible by simply selecting  $\Phi = \mathbf{I}$  and letting all indices running from 1 to  $n$ . The required number of  $\frac{1}{6} (n^3 + 6n^2 + 5n)$  evaluations of the full order nonlinear forces expression  $\mathbf{g}(\mathbf{u})$  would render such an approach unfeasible. Not to mention the requirement to actually store the  $n^4$  elements of the tensors  $\mathbf{A}^{(3)}$  alone.

However, there is a way to circumvent this problem. The following two-pronged approach for reducing the number of necessary operations relies first on limiting the number of evaluations of the vector of non-

## 5.2. REPLACING THE INFLATION OF THE NONLINEAR TERMS WITH AN AUTONOMOUS FORMULATION

---

linear internal forces by exploiting the constitution of the FEM-model of the full order system and second on the numerical structure of the indirect identification process.

**5.2.2.4.1.1 Limiting the number of evaluations of the full order vector of nonlinear internal forces by analysing the linear stiffness matrix** Should the identification technique discussed above be applied to a full order system, the required number of  $(n^2 + 1)n$  evaluations of the nonlinear forces vector  $\mathbf{g}$  for identifying the  $[A_{jl}^{(2)}]$  and the  $[A_{jlm}^{(3)}]$  would quickly become prohibitive. This computational burden can be alleviated to a certain extend by exploiting the structure of the  $[A_j^{(1)}]$ , which are the columns of the tangent stiffness matrix of the underlying linear system. This matrix is sparse for common structures, indicating that only a small number of elements meet at given node. The stiffness matrix  $\mathbf{K}$  of any system states which elements are joined at which nodes. This is expressed by the sparsity of the matrix.

The rationale to be exploited here is the fact that there are no additional connections between the elements in the higher order terms for a purely geometrically nonlinear formulation of the problem. This results in supposing that the higher order terms are of the same sparse structure as  $[A_j^{(1)}]$ .

For the numerical exploitation of the structure index-sets  $\hat{\sigma}_i$  are constructed that reflect the sparse structure of  $[A_j^{(1)}]$ . This yields

$$\hat{\sigma}_i = \left\{ j \in \{1, \dots, n\} \mid A_{ij}^{(1)} \neq 0 \right\}, \quad (5.93)$$

with  $i \in \{1, \dots, n\}$  and becomes prominently evident if one regards the reconstitution of the nonlinear forces vector. The use of index sets turns equation (5.87) into

$$g_i(\mathbf{u}) = \sum_{j \in \hat{\sigma}_i} A_{ij}^{(1)} u_j + \sum_{\substack{j \in \hat{\sigma}_i \\ l \geq j}} \sum_{l \in \hat{\sigma}_i} A_{ijl}^{(2)} u_j u_l + \sum_{\substack{j \in \hat{\sigma}_i \\ l \geq j}} \sum_{\substack{l \in \hat{\sigma}_i \\ m \geq l}} \sum_{m \in \hat{\sigma}_i} A_{ijlm}^{(3)} u_j u_l u_m. \quad (5.94)$$

By restricting the operations to these index-sets the number of required operations is significantly reduced and the process sped up. While this holds for the reconstitution of the component  $g_i(\mathbf{u})$  of the nonlinear forces vector, this is even more the case for the reconstitution for the nonlinear stiffness matrix  $\bar{\mathbf{K}}$  in equation (5.89). When index sets are used, the element  $\bar{K}_{io} = \frac{\partial g_i(\mathbf{u})}{\partial u_o}$  becomes

$$\begin{aligned} \bar{K}_{io} &= \sum_{j \in \hat{\sigma}_i} A_{ij}^{(1)} \delta_{oj} + \sum_{\substack{j \in \hat{\sigma}_i \\ l \geq j}} \sum_{l \in \hat{\sigma}_i} A_{ijl}^{(2)} (\delta_{oj} u_l + \delta_{ol} u_j) \\ &+ \sum_{\substack{j \in \hat{\sigma}_i \\ l \geq j}} \sum_{\substack{l \in \hat{\sigma}_i \\ m \geq l}} \sum_{m \in \hat{\sigma}_i} A_{ijlm}^{(3)} (\delta_{oj} u_l u_m + \delta_{ol} u_j u_m + \delta_{om} u_j u_l). \end{aligned} \quad (5.95)$$

The possible ranges of the indices of  $\bar{K}_{io}$  are  $1 \leq i \leq n$  and  $1 \leq o \leq n$ . Using the index sets, they are practically limited to  $i \in \hat{\sigma}_i$  and  $o \in \hat{\sigma}_i$ . The symbolic notation of equation (5.95) is identical to equation (5.90), yet with full order quantities. It reads

$$\mathbf{K} = \mathbf{A}^{(1)} + \mathbf{A}^{(2)} \delta \mathbf{u} + \mathbf{A}^{(3)} \delta(\mathbf{u} \otimes \mathbf{u}). \quad (5.96)$$

However, the introduction of index sets  $\hat{\sigma}_i$  unfolds to full effect for the identification stage of the poly-

## 5.2. REPLACING THE INFLATION OF THE NONLINEAR TERMS WITH AN AUTONOMOUS FORMULATION

---

nomial expression approach for the full order system because the logic is that only the indices which are actually used in equations (5.94) and (5.95) have to be identified. Such an approach is easily feasible because the components of the stiffness matrix of the underlying linear system  $A_{ij}^{(1)}$  are known prior to the identification of the higher order terms  $A_{ijl}^{(2)}$  and  $A_{ijlm}^{(3)}$  and the index-sets can be obtained beforehand. The number of the necessary evaluations of the nonlinear forces vector  $\mathbf{g}(\mathbf{u})$  can then be greatly reduced depending on the sparsity of  $A_{ij}^{(1)}$  and the overall process can be efficiently streamlined.

With the typical stiffness matrices<sup>7</sup> at hand, the simple fact of limiting the ranges of the indices corresponding to the sparsity of the matrix might allow a gain of a factor of nearly 5 in terms of necessary evaluations of the nonlinear forces vector. For  $n = 72$ , introducing the index sets leads to only 13781 evaluations, instead of the  $\frac{1}{6}(n^3 + 6n^2 + 5n) = 67452$  evaluations that would be required if the the sparsity of the stiffness matrix is ignored.

While the introduction of index-sets greatly improves the efficiency of the identification and the reconstruction for the full order nonlinear system, its application to the reduced order system is less promising. This is due to the fact that the reduced stiffness linear matrix  $\tilde{\mathbf{K}} = \tilde{\mathbf{A}}^{(1)}$  is of compact and highly dense form and requires all  $\frac{1}{6}(r^3 + 6r^2 + 5r)$  terms to be identified.

**5.2.2.4.1.2 Optimising the computations for the indirect identification procedure** Additional computational effort can be saved if the numerical aspects of the process are closely monitored. The equations that determine the values of the  $[A_{op}^{(2)}]$  and the  $[A_{ops}^{(3)}]$ , such as (5.76) and (5.77) as typical examples, are divided by terms  $\mathcal{O}(\Delta q^2)$  or even  $\mathcal{O}(\Delta q^3)$ . For avoiding numerical problems it is imperative to monitor these terms closely because, especially for the full order system, its components are  $\Delta q \ll 1$ , with a corresponding impact on the numerical stability. By excluding the combinations of indices where the products  $\Delta q_o \Delta q_p$  and  $\Delta q_o \Delta q_p \Delta q_s$  are below a given threshold the direct identification method can be numerically stabilised and freed from many unnecessary operations. This eventually adds an additional factor of 2 to 2.5 to its efficiency. Together these two measures are capable of speeding up the identification process on a full order system up to tenfold.

For reduced identifications a computationally optimised indirect identification procedure is less feasible because the reduced stiffness matrix  $\tilde{\mathbf{K}} = \tilde{\mathbf{A}}^{(1)}$  is usually densely packed and also for the LNM, which diagonalise the linear tangent stiffness matrix  $\mathbf{A}^{(1)}$  in equation (3.105), it cannot be assured that the tensors  $\tilde{\mathbf{A}}^{(2)}$  and  $\tilde{\mathbf{A}}^{(3)}$  have the property of uncoupling the generalised coordinates.

**5.2.2.4.2 Reduction of the full order tensors** This paragraph discusses how the full order tensors  $\mathbf{A}^{(h)}$  of the polynomial formulation from equation (5.92) can be reduced at any time. The reduction of the polynomial formulation (5.92) is achieved by separating the reduction matrix  $\Phi$  and the vector of generalised coordinates  $\mathbf{q}$ . Such an approach was demonstrated successfully by Phillips [179] for an electrical system of first order. Because his approach concerns only the nonlinear part it can be easily integrated into the second order systems that are common in structural dynamics.

Applying the reduction of equation (3.1) and a Galerkin projection as in equation (3.3) to equation (5.92) yields

$$\begin{aligned} \tilde{\mathbf{g}}(\mathbf{q}) &= \Phi^T \mathbf{g}(\Phi \mathbf{q}) \\ &= \Phi^T \mathbf{A}_1 \Phi \mathbf{q} + \Phi^T \mathbf{A}_2 (\Phi \mathbf{q} \otimes \Phi \mathbf{q}) + \Phi^T \mathbf{A}_3 (\Phi \mathbf{q} \otimes \Phi \mathbf{q} \otimes \Phi \mathbf{q}) \end{aligned} \quad (5.97)$$

for the reduced nonlinear forces vector. Breaking this down to indicial notation and recalling that the

---

<sup>7</sup>Refer to the finite element test-case with volume elements in section 6.3.1.

## 5.2. REPLACING THE INFLATION OF THE NONLINEAR TERMS WITH AN AUTONOMOUS FORMULATION

---

projection can be written as  $u_i = \Phi_{ik}q_k$  as per equation (3.12) gives

$$\tilde{g}_k(\mathbf{u}) = \Phi_{ki}^T A_{ij}^{(1)} \Phi_{jo} q_o + \Phi_{ki}^T A_{ijl}^{(2)} \Phi_{jo} q_o \Phi_{lp} q_p + \Phi_{ki}^T A_{ijlm}^{(3)} \Phi_{jo} q_o \Phi_{lp} q_p \Phi_{ms} q_s, \quad (5.98)$$

where the indices  $k, o, p$  and  $s$  range from 1 to  $r$  as the size of the reduced system, while the indices  $i, j, l$  and  $m$  cover the range of the full order system from 1 to  $n$ . The staggered sums over the latter indices are omitted for better readability. Rearranging the terms brings forward

$$\tilde{g}_k(\mathbf{u}) = \Phi_{ki}^T A_{ij}^{(1)} \Phi_{jo} q_o + \Phi_{ki}^T A_{ijl}^{(2)} \Phi_{jo} \Phi_{lp} q_p q_p + \Phi_{ki}^T A_{ijlm}^{(3)} \Phi_{jo} \Phi_{lp} \Phi_{ms} q_o q_p q_s, \quad (5.99)$$

and allows to define the reduced tensors

$$\tilde{A}_{kp}^{(1)} = \Phi_{ki}^T A_{ij}^{(1)} \Phi_{jo} \quad (5.100)$$

$$\tilde{A}_{kop}^{(2)} = \Phi_{ki}^T A_{ijl}^{(2)} \Phi_{jo} \Phi_{lp} \quad (5.101)$$

$$\tilde{A}_{kops}^{(3)} = \Phi_{ki}^T A_{ijlm}^{(3)} \Phi_{jo} \Phi_{lp} \Phi_{ms} \quad (5.102)$$

Returning to matrix notation leads to

$$\begin{aligned} \Phi^T \mathbf{g}(\Phi \mathbf{q}) &= \Phi^T \mathbf{A}^{(1)} \Phi \mathbf{q} \\ &+ \Phi^T \mathbf{A}^{(2)} (\Phi \otimes \Phi) (\mathbf{q} \otimes \mathbf{q}) \\ &+ \Phi^T \mathbf{A}^{(3)} (\Phi \otimes \Phi \otimes \Phi) (\mathbf{q} \otimes \mathbf{q} \otimes \mathbf{q}). \end{aligned} \quad (5.103)$$

As such the reduced tensors  $\tilde{\mathbf{A}}^{(h)}$  can be introduced as

$$\tilde{\mathbf{A}}^{(h)} = \Phi^T \mathbf{A}^{(h)} \Phi^h. \quad (5.104)$$

This is for three tensors

$$\tilde{\mathbf{A}}^{(1)} = \Phi^T \mathbf{A}^{(1)} \Phi, \quad (5.105)$$

$$\tilde{\mathbf{A}}^{(2)} = \Phi^T \mathbf{A}^{(2)} (\Phi \otimes \Phi) \quad (5.106)$$

and

$$\tilde{\mathbf{A}}^{(3)} = \Phi^T \mathbf{A}^{(3)} (\Phi \otimes \Phi \otimes \Phi). \quad (5.107)$$

The reduced tensors are now in  $\mathbb{R}^{r \times r^h}$  with  $r$  as number of degrees of freedom of the reduced order system. With this definition in place, the vector of nonlinear forces  $\mathbf{g}$  can be reduced to

$$\tilde{\mathbf{g}}(\mathbf{q}) = \tilde{\mathbf{A}}^{(1)} \mathbf{q} + \tilde{\mathbf{A}}^{(2)} (\mathbf{q} \otimes \mathbf{q}) + \tilde{\mathbf{A}}^{(3)} (\mathbf{q} \otimes \mathbf{q} \otimes \mathbf{q}) \quad (5.108)$$

Following this procedure every polynomial formulation of the nonlinear forces vector of the type (5.58) can be transformed into its reduced equivalent (5.108).

### 5.2.2.5 Correctly identifying the tensors

An important point that has to be included in the discussion of the polynomial formulation is the fact that the  $\tilde{\mathbf{A}}^{(h)}$  and the  $\mathbf{A}^{(h)}$  are not unique, and probably neither optimal. Due to the nonlinear nature of the internal forces  $\mathbf{g}(\mathbf{u})$  the elements of the tensors do not scale linearly with the amplitude of the  $\Delta q$  that are used during the indirect identification and they depend also on the normalisation of the column vectors of the reduced basis, which is, taking the prominent example of the LNM, arbitrary.

The section 3.3.7 shows that the choice of the  $\Delta q$  is also closely connected to the normalisation and constitution of the reduced basis  $\Phi$  as supposed in the initial equation 3.1 during the introduction of the reduced basis. The only condition that has to hold is  $\mathbf{u} = \Phi \mathbf{q}$ . Due to this linear relation the contributions to the physical displacements  $\mathbf{u}$  can be shifted arbitrarily between  $\Phi$  and  $\mathbf{q}$ . The choice of one component determines the other one.

The  $\Delta q$ , which are used in equations (5.76) to (5.85), among others, for the indirect identification. These incremental displacements are either given directly, as proposed by Muravyov and Rizzi [155], or as variations of a shifted origin of the identification  $\Delta \mathbf{q} \rightarrow \hat{\mathbf{u}} + \Delta \mathbf{q}$ , as proposed by Chang et al. [58]. In either case the choice of the  $\Delta q$  is at the discretion of the user and has to be adapted to the problem at hand. The elements of the tensors depend on the choice of the  $\Delta q$  because the static evaluation of  $\mathbf{g}(\hat{\mathbf{u}} + \phi_o \Delta q_o)$ , that is at the heart of the indirect identification procedures, is nonlinear and the effect of increasing or decreasing the value of  $\Delta q_o$  is not cancelled out by the divisions by  $\frac{1}{\Delta q_o}$ .

So, if the elements of  $\tilde{\mathbf{A}}^{(h)}$  do depend on the choice of the  $\Delta q_o$  the question that has to be asked is if there are certain  $\Delta q_o$  that lead to optimal  $\tilde{\mathbf{A}}^{(h)}$ . The answer to this question is not pursued in the limits of this work because it entails first the question in which sense the  $\tilde{\mathbf{A}}^{(h)}$  could be optimal. The definition of the optimality would certainly include a relation on the basis of the transient solution of the system and lead to overwhelming numerical efforts.

Instead, the values of the  $\Delta q_o$  are chosen such that they are representative for the range of the generalised coordinates  $\mathbf{q}(t)$  that is expected to appear during the transient solution. Enforcing this property of the  $\Delta q_o$  ensures that the evaluation of the  $\tilde{\mathbf{g}}(\mathbf{q})$  take place at meaningful levels of their nonlinear behaviour. Naturally, this range is difficult to determine prior to the actual solution. As a remedy a representative  $\Delta q_o$  can be obtained from a static nonlinear solution with the maximum of the external forcing, whose time history is known prior to the actual solution. This makes the tensors  $\tilde{\mathbf{A}}^{(h)}$  specific for a given external excitation, but the introduction of the basis update and augmentation in the previous section 5.1, heralds that the reduced tensors will be subjected to other adaptations as well.

Muravyov and Rizzi [155] give two additional conditions that are required to be fulfilled by the system. The constitutive properties of the material are supposed to be linear and the deformation has to depend only on the applied excitation, i.e. it is independent from the load path. The properties are fulfilled by all systems that are used in this work.

Another point that has to be discussed is the inclusion of the second order tensor  $\tilde{\mathbf{A}}^{(2)}$  for the quadratic terms  $(\mathbf{q} \otimes \mathbf{q})$ . Theoretic considerations in e.g. Bathe [22] define a force as the derivative of a symmetric energy potential. Such a derivative should not have quadratic terms and the tensor should be  $\tilde{\mathbf{A}}^{(2)} = \mathbf{0}$ . However, numerical results indicate that the elements of  $\tilde{\mathbf{A}}^{(2)}$  are by no means zero and contribute significantly to the reduced nonlinear force  $\tilde{\mathbf{g}}(\mathbf{q})$ . The implication that the second tensor  $\tilde{\mathbf{A}}^{(2)}$  has to be identified too, that comes from these numerical results, is backed by the fact that the second tensor is duly identified in the original approach proposed by Muravyov and Rizzi [155]. Furthermore, the definition of  $\tilde{\mathbf{A}}^{(2)}$  as the term of a Taylor development in equation (5.62) give no hint whether  $\tilde{\mathbf{A}}^{(2)} = \mathbf{0}$  holds, is required, or altogether wrong. As the present study is a numerical one, the emphasis is put on the numerical results. These numerical results clearly show that the elements of  $\tilde{\mathbf{A}}^{(2)}$  are required for a successful polynomial approximation of the reduced nonlinear internal forces  $\tilde{\mathbf{g}}(\mathbf{q})$ . A theoretical discussion of the properties of  $\tilde{\mathbf{A}}^{(2)}$  is seen to be outside the scope of this work, where the polynomial formulation is only applied as one proven method from literature among others.

### 5.2.2.6 Summarising the polynomial formulation of the reduced nonlinear forces vector

Figure 5.21 sketches an overview of the different possibilities of the polynomial formulation. These different elements of this figure will be discussed in the remainder of this section. They are

- the general constitution of the polynomial formulation,
- the indirect identification procedure for the reduced tensors  $\tilde{\mathbf{A}}^{(j)}$  and its possible extension to a full order system,
- two reductions of the polynomial formulation, and,
- the reconstitution of the nonlinear forces vector and of the nonlinear tangent stiffness matrix.

The two outer columns of figure 5.21 represent the two levels of systems, the full order and the reduced one. The initial point of identifying the tensors  $\mathbf{A}^{(h)}$  or  $\tilde{\mathbf{A}}^{(h)}$ , respectively, can be achieved on both levels. Two reduction procedures for the tensors in the central column allow at any point to reduce the tensors and to continue the operations on the level of the reduced system.

Once the identification of the tensors is completed they can be used in the two applications that are presented in the lower rows: reconstructing the nonlinear forces vector and reconstructing the nonlinear tangent stiffness matrix. It states that, following an identification of the  $\mathbf{A}^{(h)}$ , or the  $\tilde{\mathbf{A}}^{(h)}$  respectively, a polynomial formulation like equation (5.58) can be used to

- reconstruct the nonlinear forces vector itself with the computationally optimised equation (5.94) and to
- reconstruct the nonlinear tangent stiffness matrix  $\tilde{\mathbf{K}}$  by applying equation (5.95).

Again these applications of the polynomial formulation are available on both levels, the full order and the reduced order. If the reduced vector of nonlinear forces  $\tilde{\mathbf{g}}$  is expressed as a polynomial, it can equally easily be expressed by use of equation (5.108). In the reduced case the tangent stiffness matrix is expressed by equation (5.90).

The algorithm proposed by Muravyov and Rizzi [155] provides for an indirect determination of the reduced tensors  $\tilde{\mathbf{A}}^{(h)}$  and could be also applied to a full order identification in case of need. If the full order tensors  $\mathbf{A}^{(h)}$  are known, switching to the reduced system is possible at any time by applying equation (5.104), as proposed by Phillips [179]

For obtaining the reduced terms of the internal nonlinear forces  $\tilde{\mathbf{g}}$  and of the tangential stiffness matrix  $\tilde{\mathbf{K}}$  there are three variants of the polynomial approximation present in figure 5.21. They differ with respect to whether the identification takes place on full order or on reduced level, and, in the former case, when the reduction takes place. In detail the variants are:

1. the full order identification with trailing reduction:
  - the tensors  $\mathbf{A}^{(1)}$ ,  $\mathbf{A}^{(2)}$  and  $\mathbf{A}^{(3)}$  are identified for the full order system
  - the nonlinear terms are approximated at full order with equations (5.92) and (5.95)
  - the so obtained terms are reduced with  $\tilde{\mathbf{g}} = \Phi^T \mathbf{g}$  (see equation (5.103)) and  $\tilde{\mathbf{K}} = \Phi^T \mathbf{K} \Phi$ , respectively.
2. the full order identification with included reduction:
  - the tensors  $\mathbf{A}^{(1)}$ ,  $\mathbf{A}^{(2)}$  and  $\mathbf{A}^{(3)}$  are identified for the full order system
  - the tensors are reduced with equation (5.104) in order to obtain  $\tilde{\mathbf{A}}^{(1)}$ ,  $\tilde{\mathbf{A}}^{(2)}$  and  $\tilde{\mathbf{A}}^{(3)}$
  - the nonlinear terms are approximated at reduced order with equations 5.108 and 5.90
3. the reduced order identification:
  - the tensors  $\tilde{\mathbf{A}}^{(1)}$ ,  $\tilde{\mathbf{A}}^{(2)}$  and  $\tilde{\mathbf{A}}^{(3)}$  are identified for the reduced order system

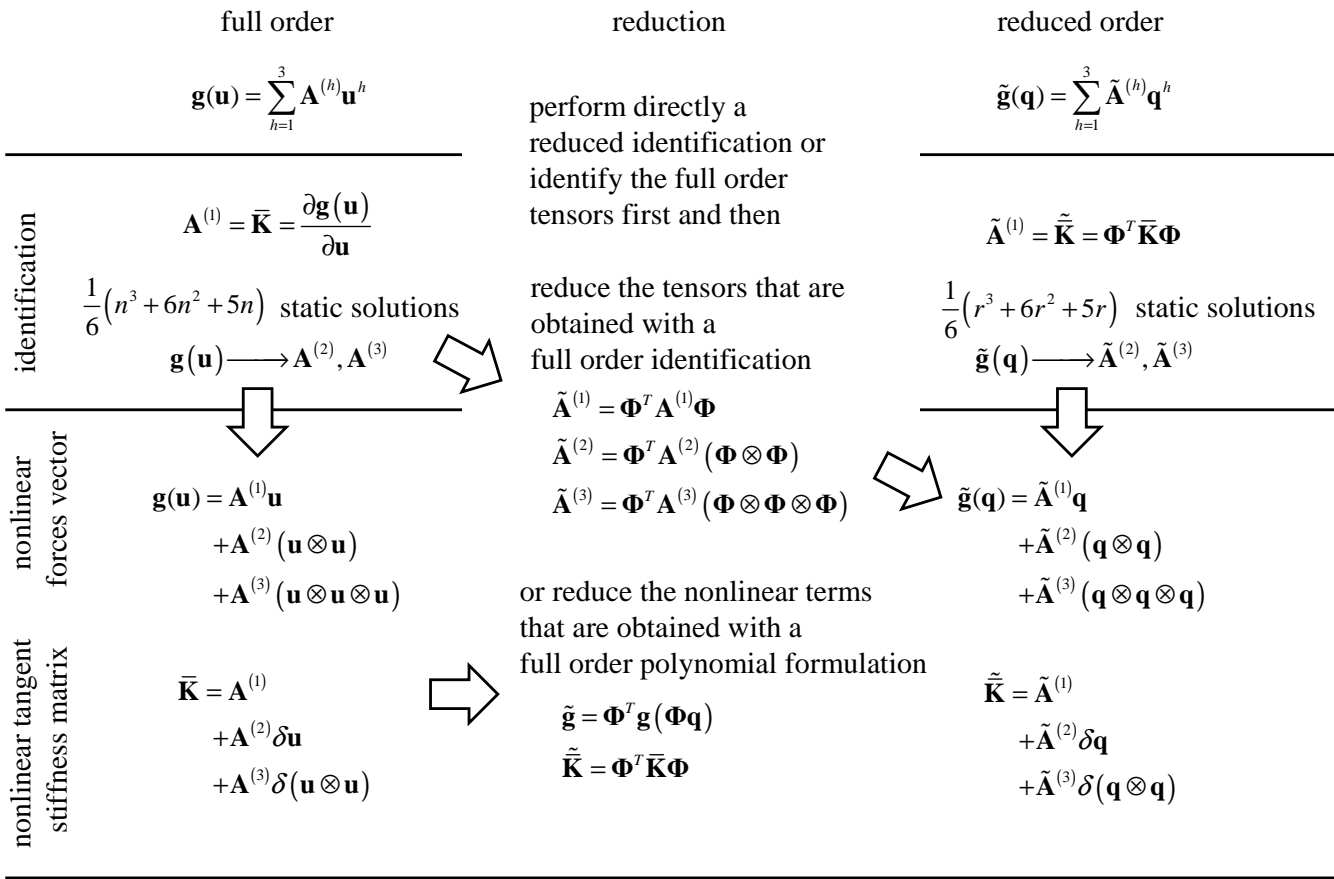


Figure 5.21: The overview of the possible operations based on the polynomial formulation of the nonlinear terms

## 5.2. REPLACING THE INFLATION OF THE NONLINEAR TERMS WITH AN AUTONOMOUS FORMULATION

---

- the nonlinear terms are approximated at reduced order with equations 5.108 and 5.90.

The first variant presents no conceptual advantage with respect to an inflation formulation of the nonlinear terms because it replaces the nonlinear terms on full order and not on reduced order. It is hence dropped from further investigations.

The third variant corresponds to the original formulation by Muravyov and Rizzi [155]. It presents the disadvantage of being specific for a given reduced basis. This is not the case for the first and the second variant, which are both independent from any reduced basis. The second variant requires a considerable effort for the initial identification of the tensors at full order. This considerable effort to be invested to identify the elements of the  $\mathbf{A}^{(h)}$  presents the major inconvenience of this approach, even though it has been considerably alleviated by exploiting the sparsity of the full order linear stiffness matrix. At the price of no longer having a separation between the tensors  $\mathbf{A}^{(h)}$  and the reduced basis  $\Phi$ , this effort can be circumvented if the corresponding reduced terms  $\tilde{\mathbf{A}}^{(h)}$  are indirectly identified.

### 5.2.3 Considering neuronal networks as an additional approach

There are many more possible approaches for approximating the nonlinear terms, be they reduced or not. A major class among these, which generated much research in the recent past are soft computing and machine learning techniques. Most notably among these are neural networks, as presented by e.g. Palau et al. [168]. Kirby and Miranda [122] notice the fact that optimal descriptions of systems with neural networks can be linked with the Karhunen-Loève procedure, which is the basis of the POD method in section 3.3.3.1 (see also Kirby et al. [120] and Kirby [121]). Even though these approaches may yield promising results, their requirements for specific knowledge are supposed to be beyond the scope of this work (Beale et al. [24]). Furthermore, there is no theory known to the author that would allow a reduction of a neural network with a reduced basis. This would mean that the introduction of the neural network as a replacement for the nonlinear internal forces would only replace one full order formulation with another one, which is not as easily reduced as the first one. Neural networks are hence not included but only mentioned here as an additional approach.

### 5.2.4 Selecting an autonomous formulation by performing a numerical study

The techniques that are presented as possible candidates to replace the inflation formulation of the nonlinear terms are put to a brief numerical test. This numerical test is aimed at contributing information to the decision on which of these techniques is to be selected. Additional input for this decision will be drawn from inspecting the respective properties, especially with respect to the requirement of being independent of the reduced basis, of each one of the techniques.

The tests are performed with the set-up that has been developed in section 4.1 for the numerical comparative study and the study of robustness. The same test-cases, solution algorithm and error metrics are used here.

Included in the study are the inflation formulation, as reference, the interpolation, the direct linearisation and the second and third variant of the polynomial formulation. In order to test whether the choice of the reduced basis may have an influence on the tendencies of the criteria reduced bases coming from the LNM and the POD procedure are included. For now, the reduced bases are kept constant during the transient solutions to limit the appearing error to the autonomous formulation. The four test-cases from section 4.1.3 are tested. Only the entirely nonlinear system under harmonic excitation is shown below as an example, typical for the setting that is to be expected from a finite element test-case. The results that are observed are the overall reduction time, the solution time and the mean of R2MSE of the transient solution with respect to the reference solution obtained at full order.

Tracing the overall reduction time, i.e. the wall-time from preparing the reduced basis and the autonomous formulation to the completion of the transient solution, in figure 5.22 presents some real interest.

## 5.2. REPLACING THE INFLATION OF THE NONLINEAR TERMS WITH AN AUTONOMOUS FORMULATION

Until now, this is not the case because the small test-cases do not present enough variation in overall reduction time. On the scale of the overall reduction time it becomes evident that every autonomous formulation is an element that requires a considerable amount of computational time, mostly for the preparation of the database or the identification of the tensors. The slight increase of the overall reduction time for the direct linearisation with increasing  $r$  comes from the increase in the number of configurations. The most striking feature is the enormous increase of the overall reduction time for the polynomial formulation.

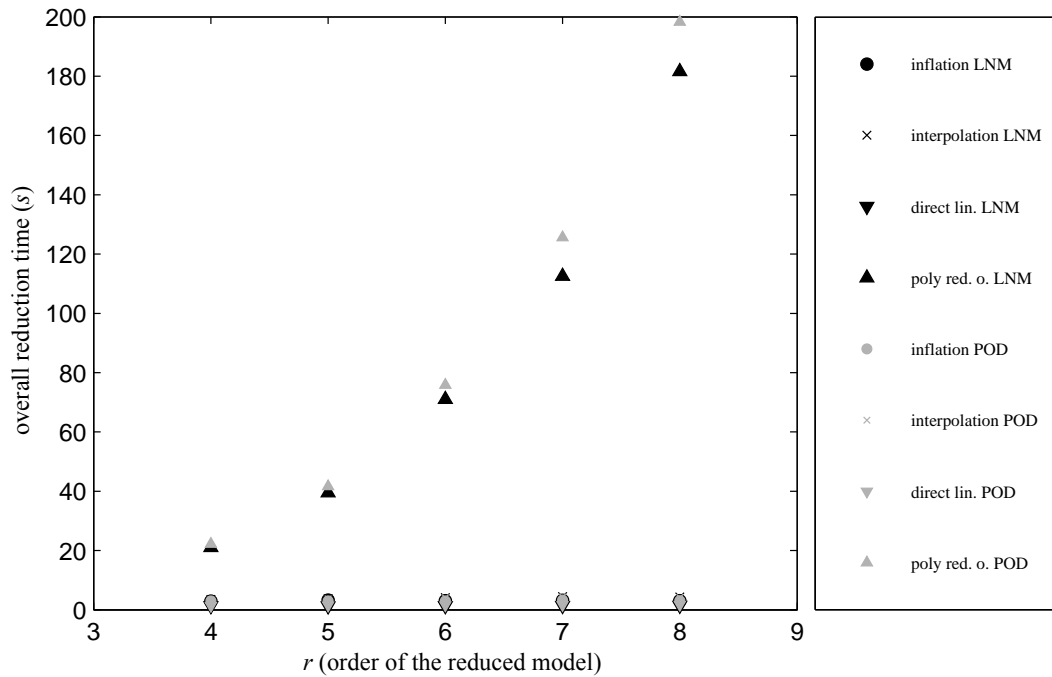


Figure 5.22: The overall reduction time for the autonomous solutions of the entirely nonlinear system under harmonic excitation

The analysis of the overall reduction time is accompanied by an analysis of the solution time. The solution time comprises only the wall time that is required for completing the transient solution. All preparations are excluded.

An inspection of the two times allows to localise the increase in the overall reduction time for the polynomial formulation at the level of the actual transient solution. In fact, there is a considerable increase in the solution time, which is more than linear, for an increase in the order  $r$  of the reduced system. This result seems plausible because the number of required vector operations, that is identified during the presentation of the polynomial formulation, for the evaluation of the reduced nonlinear forces vector and the reduced nonlinear stiffness matrix scales with the summation factorial of  $r$ . At the same time it becomes obvious that the number of evaluations of the full order nonlinear forces vector, that are required to identify the reduced tensors during the preparation of the transient solution, which scales with  $r^3$ , does not add excessively to the overall required time of the polynomial formulation. At the same time, the solution times of the transient solutions that are obtained with the interpolation and the direct linearisation do barely evolve with  $r$  and remain practically instantaneous. This is also plausible because these two methods only require linear matrix operations.

Including the inflation in this comparison is misleading because, for the academic test-cases, the inflation formulation relies on analytic expressions which can be evaluated very quickly. So it cannot be determined if the application of the polynomial formulation actually slows the solution down considerably, as it appears

## 5.2. REPLACING THE INFLATION OF THE NONLINEAR TERMS WITH AN AUTONOMOUS FORMULATION

to be the case, or if a more complex inflation formulation would instead require longer solution times than the polynomial formulation.

To analyse the quality of the autonomous solutions the values of the mean of the R2MSE with respect to a full order reference solution are plotted in figure 5.23.

The interpolation and the direct interpolation yield solutions with an elevated level of R2MSE. With the experiences from the comparative study in section 4.2.1 a solution at such a level of error has to be considered useless.

The polynomial formulation always yields errors that are equal to those of the inflation formulation. This had to be expected because the used nonlinear systems from equations (4.16) and (4.17) use exclusively linear and cubic nonlinearities. For these, the polynomial formulation provides an exact replacement and the error is reduced to the error due to the introduction of the reduced basis.

In fact, the most intriguing feature of using the academic test-cases from section 4.1.3 for testing the different variants of the polynomial formulation is that the resulting full order tensors can be verified by hand. If the indirect full order identification procedure is implemented correctly this can be easily verified on the locally nonlinear system. The correct implementation is confirmed because equation (4.16) results in to  $A^{(2)} = 0$  and  $A^{(3)} = 0$  for all components except  $A_{16,16,16,16}^{(3)} = 1$  for the locally nonlinear system. A similar test is possible for the entirely nonlinear system from equation (4.17). Once this is verified, the procedure can be applied with confidence.

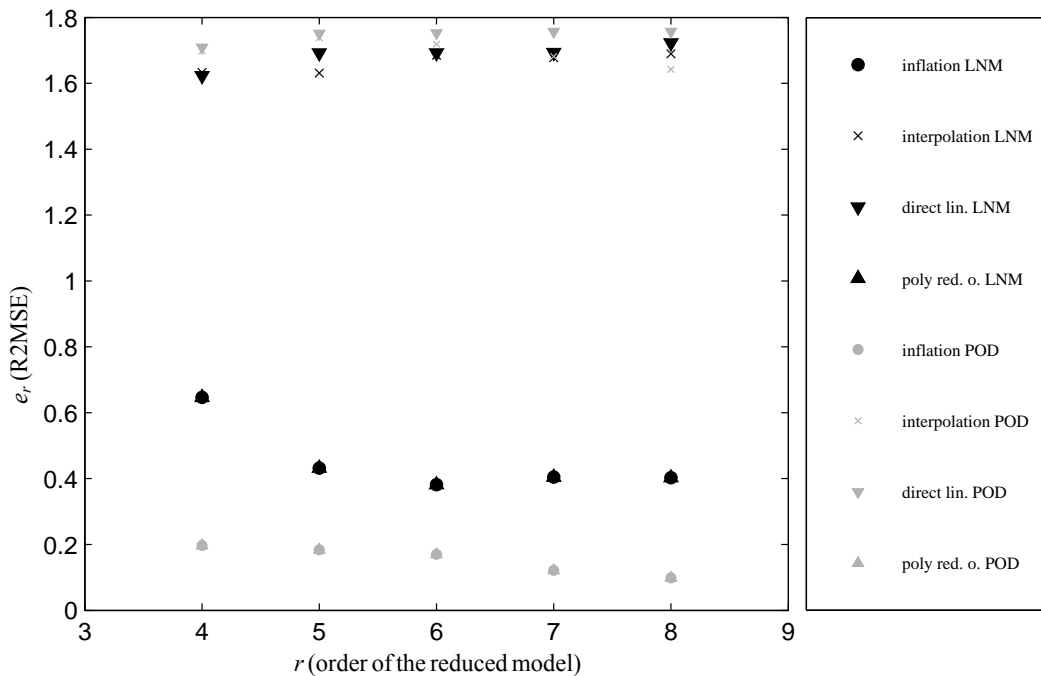


Figure 5.23: The mean of the R2MSE for the autonomous solutions of the entirely nonlinear system under harmonic excitation

This concludes the numeric study of the autonomous formulations. They have been tested for their computational performance and the error they produce. In the next step, one of the formulations has to be chosen to replace the inflation of the nonlinear terms.

#### 5.2.5 Outcome of the requirement to replace the inflation of the nonlinear terms with an autonomous formulation

The presented work takes a new look at the solution of reduced order systems in the setting of non-linear structural transient dynamics and highlights at which points in the solution procedure the formulations of the non-linear terms appear. It demonstrates that these points are hinging points for the successful solution of the reduced model and require thus special attention. A number of candidates for such an autonomous formulation are passed in review. A first application of these formulations on an academic system leads to the concentration on the polynomial approximation. In the following extension of the application of this particular formulation to a finite element test-case, the polynomial approximation is applied to the full order and to the reduced non-linear system. The so obtained solutions prove to be acceptably correct if compared to a full order solution with finite elements. Furthermore, a considerable gain in computational time is proved to take place if the solution is obtained with the reduced polynomial formulation.

However, the specific requirement of the polynomial approximation for a considerable number of static solutions is revealed. This possibly may be a major obstacle in the application of this method on full order systems. In response the numerical shortcut of index sub-setting is developed to enable a successful application. With the index sub-setting approach a novel numerical shortcut is presented, that might enable the application of the polynomial approximation from Muravyov and Rizzi [155], and therein especially the identification, to full order systems. This is an important step towards an autonomous formulation of the non-linear terms that is independent from the reduced basis. Such a formulation is required for reduced systems which reduced basis changes during the solution. Such a non-constant reduced basis is necessary if external parameters change, such as the operating point which appears in the form of the prestressing in the used finite element test-case, or if during the solution process the reduced basis is updated in response to the non-linear evolution of the solution.

The polynomial formulation is chosen to be pursued and developed further for an application to the finite element test-cases in the next chapter 6.

### 5.3 Adapting reduced basis to external parameters

The fact that no explicit declaration as to the dependency of the dynamical system's quantities,  $M$ ,  $C$ ,  $\mathbf{g}(\mathbf{u})$  and  $\mathbf{f}_E$ , from external parameters has been made until now, does not mean that this dependence does not exist. The dependency on external parameters is initially required in the introduction in chapter 1. It has since been neglected in order to focus on the reduction without obscuring important developments. The external parameters are briefly introduced in a preliminary manner during the study of the bases robustness in section 4.2.2. The external parameters  $\mu$  are defined as not directly related to the system, but having an impact on the system. They can be of physical nature, defining e.g. an operating point by a temperature, which affects the constitutional equation of the material, or a rotational speed for a stationary rotating system, which induces different prestressings. They can also be related to an optimisation problem, e.g. different materials with different densities or changing geometries or implicitly impacting the modelling process, e.g. a change in the parameters of the solution algorithms. The objective of this section is to survey possible approaches to include this dependency in the analysis.

The results of the study of the robustness of the reduced bases in section 4.2.2 seem to show that such an approach is essential for a successful reduced solution. In the study of the robustness the parameterisations were limited to the properties of the external forcing. For the finite element test-cases that follow in the next chapter the prestressing will be chosen as parameter. While conducting the following survey of methods that allow to adapt the reduced basis and the systems static matrices to external parameters properties of practical importance like the prestressing are to be kept in mind as possible applications.

As one possible candidate, Amsallem et al. [11], Amsallem and Farhat [10] propose a very evolved approach for the interpolation between reduced order systems, which relies on an interpolation in a projected

space, tangent to the reduced order model. Another approach, proposed by Hay et al. [95], relies on the sensitivities of the projection basis with respect to the external parameters. A method of interlaced snapshots is proposed by Vigo [238] but limited to Proper and Smooth Orthogonal Decompositions.

Some of these proposed methods are compared by Vetrano et al. [237] in an aeroelastic setting. Their study shows that the methods are rather capable of interpolation between reduced bases if the underlying behaviour of the bases is linear with respect to changes in the parameters. However, the performance of all methods degrades if this dependence becomes nonlinear. Furthermore, it is stated that most methods only allow the interpolation for a single parameter, and not for a set of different parameters.

A topic a bit apart from external parameters are the initial conditions of the simulation. These can be directly linked to external parameters through e.g. prestressing or set in a completely independent manner. The topic is studied with great attention to detail by Amsallem et al. [15] and will not be pursued further in the context of the present work.

### 5.3.1 Defining the problem of the adaptation of the reduced basis to external parameters

The external parameters mentioned above are supposed to be regrouped in the vector  $\boldsymbol{\mu}$  which completely describes the physical and modelling environment of the operating point, in which a high fidelity nonlinear system is established. The system from equation (2.82) can thus be written as

$$M_{\boldsymbol{\mu}}\ddot{\boldsymbol{u}} + C_{\boldsymbol{\mu}}\dot{\boldsymbol{u}} + \boldsymbol{g}_{\boldsymbol{\mu}}(\boldsymbol{u}) = \boldsymbol{f}_E(t, \boldsymbol{\mu}). \quad (5.109)$$

Such a dependence on external parameters is already introduced in passing for testing the robustness of the reduced basis in section 4.2.2. Now, the introduction of external parameters and the treatment of such dependencies is formalised. All external parameters are considered to be global parameters in the sense of section 4.1.3.4 because they do not affect a specific method for creating a reduced basis but the whole test-case. It is self evident that, whichever reduced basis from section 3.3 is chosen for the reduction, the selected projection basis  $\boldsymbol{\Phi}$  also depends on  $\boldsymbol{\mu}$ .

Several studies, like e.g. Hay et al. [95, 94] with their very insightful POD sensitivity analysis, have shown that reduced order models are rather sensitive to changes in external parameters and are prone to produce rapidly deteriorating results, as they are applied to reduced systems that have external parameters further away from the initial parameterisation. Their findings are confirmed by the results of study of the robustness in section 4.2.2. The necessity to solve reduced order models at different operating points arises e.g. when systems are studied that have a wide range of operating points as an intrinsic property, e.g. turbomachines or whole planes, or when specific systems are subjected to optimisation studies, in which external parameters can be varied as a part of the optimisation. A logical remedy to this problem is to establish several reduced bases  $\boldsymbol{\Phi}_i$  at different operating points  $\boldsymbol{\mu}_i$ , with  $i \in \{1, \dots, m\}$ , and use some kind of interpolation between these different operating points, in order to obtain the reduced basis  $\boldsymbol{\Phi}_0$  at the actual operating point  $\boldsymbol{\mu}_0$ .

However, multi-parameter interpolation between subspaces based on matrices is not likely to be straightforward and fairly evolved procedures have had to be developed to this effect. Their common aim is, being given an operating point  $\boldsymbol{\mu}_0$ , which is not part of the operating points  $\{\boldsymbol{\mu}_1, \dots, \boldsymbol{\mu}_m\}$ , for which bases have been established, to find a suitable approach to express the required basis  $\boldsymbol{\Phi}_0 = \boldsymbol{\Phi}(\boldsymbol{\mu}_0)$  by using the already established reduced bases  $\{\boldsymbol{\Phi}_1, \dots, \boldsymbol{\Phi}_m\}$  so that  $\boldsymbol{\Phi}_0 \notin \{\boldsymbol{\Phi}_1, \dots, \boldsymbol{\Phi}_m\}$ . Such an approach might be extended to directly obtained the static matrices  $M_{\boldsymbol{\mu}_0}$  and  $C_{\boldsymbol{\mu}_0}$  of the system.

The first of the procedures that are presented hereunder uses an interpolation approach, while the second procedure relies on the sensitivities of the bases with respect to the external parameters. A third method, which is restricted to Proper Orthogonal Decomposition approaches, uses snapshots from differently pa-

parameterised simulations.

### 5.3.2 Presenting the interpolation method

Despite the fact that a linear interpolation between two bases  $\Phi_1$  and  $\Phi_2$  for the special case of a single, scalar external parameter  $\mu$ , might seem feasible, it is in fact not because the interpolation does not conserve the orthogonality condition for the interpolated base  $\Phi_0$ . Being aware of this, Lieu and Lesoinne [138] propose an approach by interpolating not the vectors of the bases but the angles between them. This approach was later generalised by Amsallem [12], who selected one of the precomputed bases  $\Phi_k$  as origin of a Grassmann manifold and executed the interpolation in a space tangent to that manifold, which yields the endpoint of a geodesic as the sought after new basis  $\Phi_0$ . As of Amsallem and Farhat [13] the proper selection of the origin is still an open question. The entire method is sketched along its central equations below.

Albeit this procedure requires a considerable amount of transformations, it is still deemed less costly by its authors, than reconstructing a dedicated reduced order model on the operating point  $\mu_0$  from a high fidelity model. However it requires to establish and to handle a database of reduced order models for different operating points prior to the initialisation of an approach that requires different operating points. But once this database is established over a wide range of operating conditions. The interpolation method allows the construction of dedicated reduced order models in the same range of values for the parameters.

The interpolation approach proposed by Amsallem [12], described in this section, takes the four steps of

1. the selection of an origin of interpolation,
2. the transformation into the tangent space,
3. the interpolation proper,
4. the reverse transformation into the original manifold.

While this approach and the interpolation itself are universal, the necessary transformations are specific to the type of matrix which is to be interpolated. Amsallem [12] contains a comprehensive list of possible transformations for a multitude of matrix types. Limited to the scope of the present work there are two types of matrices, which are of interest:

- symmetric positive definite (SPD) matrices, e.g.  $M$ ,  $C$  and  $K$ , and
- the reduced bases  $\Phi$ .

Each of these two types of matrices requires a specific transformation and corresponding reverse transformation in order to switch between the original manifold and the tangent space.

Amsallem and Farhat [13] introduce an additional rotation stage prior the interpolation. In this rotation stage the reduced operators of linear systems for different parameter sets  $\mu$  are aligned to operate on consistent generalised coordinates. This becomes interesting of the change of bases is to be performed smoothly. In the following the two transformation procedures specific to the two types of encountered matrices are expanded. The interpolation itself, which they have in common, is detailed in a dedicated section.

#### 5.3.2.1 Interpolating symmetric positive definite matrices

For the sake of generality the symmetric positive definite (SPD) matrix is called  $A$ , which may stand for any of the SPD-matrices  $M$ ,  $C$  and  $K$  that are encountered in structural dynamics.

Let  $\{A_1, \dots, A_m\}$  be the available SPD-matrices corresponding to the known working points  $\{\mu_1, \dots, \mu_m\}$ . Then the SPD-matrix  $A_0$ , corresponding to a new operating point  $\mu_0$ , with  $\mu_0 \notin \{\mu_1, \dots, \mu_m\}$ , can be found by the four-step algorithm:

1. The origin of the interpolation  $\mathbf{A}_k$  is chosen among the  $\{\mathbf{A}_1, \dots, \mathbf{A}_m\}$ . The primary criterion for its selection is the distance of the operating point  $\boldsymbol{\mu}_k$  from the operating point  $\boldsymbol{\mu}_0$ .
2. A number of matrices  $\mathbf{A}_i$  is chosen among the  $\{\mathbf{A}_1, \dots, \mathbf{A}_m\}$  with  $i \neq k$ . The subset of the  $\mathbf{A}_i$  contains the matrices corresponding to the operating points  $\boldsymbol{\mu}_i$  from the vicinity to the operating point  $\boldsymbol{\mu}_k$ . The matrices  $\mathbf{A}_i$  are to partake in the interpolation around the origin  $\mathbf{A}_i$ .

The transformation into the tangent space is performed by the logarithm map ( Amsallem [12] eq. 5.9)

$$\check{\mathbf{A}}_i = \text{logm} \left( \mathbf{A}_k^{-\frac{1}{2}} \mathbf{A}_i \mathbf{A}_k^{-\frac{1}{2}} \right) \quad \forall i, \quad (5.110)$$

where the function  $\text{logm}$  denotes the matrix logarithm.

3. The interpolated matrix in the tangent space  $\check{\mathbf{A}}_0$ , corresponding to the operating point  $\boldsymbol{\mu}_0$ , is then obtained by the interpolation between the  $\check{\mathbf{A}}_i$  from equation (5.110) with the procedure described in section 5.3.2.3.
4. The reverse transformation of the interpolated matrix  $\check{\mathbf{A}}_0$  is done by reversing equation (5.110):

$$\mathbf{A}_0 = \mathbf{A}_k^{\frac{1}{2}} \text{expm} \left( \check{\mathbf{A}}_0 \right) \mathbf{A}_k^{\frac{1}{2}}, \quad (5.111)$$

where the function  $\text{expm}$  denotes the matrix exponential. Like the transformation, the reverse transformation hinges on the selected origin  $\mathbf{A}_k$ , which highlights the importance of an adequate selection of this quantity.

These four steps allow the interpolation of SPD-matrices, like  $\mathbf{M}$ ,  $\mathbf{C}$  and  $\mathbf{K}$ .

### 5.3.2.2 Interpolating reduced bases

The most important difference between the interpolation of reduced bases  $\Phi$  and the interpolation of SPD-matrices is that for the interpolation of the rectangular reduced bases the interpolations are done separately for each column vector. Additionally the transformation and the reverse transformations, i.e. the equivalences to equations (5.110) and (5.111), are different.

The reduced basis  $\Phi$  contains  $r$  column vectors so that it can be represented as  $[\phi_1, \phi_2, \dots, \phi_r]$ . In order to interpolate a reduced basis the procedure below has to be repeated for all  $r$  column vectors. This requires that the column vectors are ordered in the same fashion among all  $m$  reduced bases  $\Phi$ , which are pre-computed for the  $m$  operation points. To avoid confusion the bases' vectors do not bear any additional indices, beyond the one designating their associated operating point.

Let  $\{\phi_1, \dots, \phi_m\}$  be the available, precomputed column vectors of the reduced bases corresponding to the known working points  $\{\boldsymbol{\mu}_1, \dots, \boldsymbol{\mu}_m\}$ . If system has to be reduced at a new operating point  $\boldsymbol{\mu}_0$ , with  $\boldsymbol{\mu}_0 \notin \{\boldsymbol{\mu}_1, \dots, \boldsymbol{\mu}_m\}$  the associated basis vector  $\phi_0$  can be found by the following four-step algorithm:

1. Among the precomputed bases' vectors  $\{\phi_1, \dots, \phi_m\}$ , one  $\phi_k$  is chosen as the origin of the transformation. Its selection depends on various considerations, but obviously it should belong to the operating point  $\boldsymbol{\mu}_k$  in the vicinity of  $\boldsymbol{\mu}_0$ .
2. In the vicinity of the selected origin  $\phi_k$  a number of vectors  $\phi_i$  is selected  $\phi_i \in \{\phi_1, \dots, \phi_m\}$  with  $i \neq k$ , which are designated to partake in the following interpolation. The criterion of the selection of the  $\Phi_i$  is obviously their capability to contribute to the interpolation of the associated  $\boldsymbol{\mu}_i$  to obtain  $\boldsymbol{\mu}_0$ .

The transformation into the tangent space, is done by a singular value decomposition (SVD)

$$(\mathbf{I} - \phi_k \phi_k^T) \phi_i (\phi_k^T \phi_i)^{-1} \rightarrow \mathbf{U}_i \Sigma_i \mathbf{V}_i^T \quad \forall i, \quad (5.112)$$

with  $\mathbf{I}$  as the  $n \times n$  identity matrix, and the establishment of the transformed vectors  $\check{\phi}_i$  in the tangent space

$$\check{\phi}_i = \mathbf{U}_i \arctan(\Sigma_i) \mathbf{V}_i^T \quad \forall i. \quad (5.113)$$

3. The interpolation proper is now performed with each of the transformed column vectors  $\check{\phi}_i$ . As each of them is associated to an operating point  $\mu_i$  appropriate interpolation procedures can be applied to reach  $\mu_0$ . The used interpolation procedure is explained in section 5.3.2.3. It yields the interpolated column vector  $\check{\phi}_0$  in the tangent space.
4. The reverse transformation from the tangent space into original manifold, follows equations (5.112) and (5.113) in reverse order, beginning with a singular value decomposition of the interpolated vector

$$\check{\phi}_0 \rightarrow \mathbf{U}_0 \Sigma_0 \mathbf{V}_0^T \quad (5.114)$$

and finally the vector under consideration  $\phi_0$

$$\phi_0 = \phi_k \mathbf{V}_0 \cos(\Sigma_0) + \mathbf{U}_0 \sin(\Sigma_0), \quad (5.115)$$

is obtained. The vector  $\phi_0$  can be inserted as the appropriate column vector in the reduced basis  $\Phi_0$  associated with the operating point  $\mu_0$

Due to the algorithm, which prescribes to treat one column of the reduced bases at a time, the  $\Sigma_i$  and  $\Sigma_0$  are actually scalar values. The final interpolated reduced basis  $\Phi_0$  is obtained by assembling all  $r$  interpolated column vectors  $\phi_0$ .

Once this is done the matrix  $\Phi_0$  is subjected to a Gram-Schmidt procedure (e.g. Strang [218]) to ensure its orthogonality.

### 5.3.2.3 Presenting multiparameter interpolation

For the actual interpolation Amsallem [12] lists two dimensional spline interpolation, as proposed by Späth [213], or polynomial interpolation, as proposed by De Boor and Ron [64], as possibilities. The used multivariate interpolation algorithm uses a smooth interpolation function hinging on radial basis functions.

Being given a set of items  $\{\mathbf{A}_1, \dots, \mathbf{A}_m\}$ , which may represent SPD-matrices,  $\mathbf{M}$ ,  $\mathbf{C}$  and  $\mathbf{K}$ , as well as vectors of reduced bases  $\phi$ , of which each element corresponds to an operating point  $\{\mu_1, \dots, \mu_m\}$  the challenge is to find a continuous interpolation function of the form

$$\mathbf{H}(\mu) = \sum_{j=1}^m \hat{\mathbf{A}}_j h_j(\mu), \quad (5.116)$$

where the  $h_j(\boldsymbol{\mu})$  are basis functions and the parameter  $\hat{\mathbf{A}}_j$  are determined by the constraint relations

$$\mathbf{H}(\boldsymbol{\mu}_i) = \sum_{j=1}^m \hat{\mathbf{A}}_j h_j(\boldsymbol{\mu}_i) = \mathbf{A}_i \quad \forall i. \quad (5.117)$$

Choosing the interpolation functions  $h_j(\boldsymbol{\mu})$  as Hardy's multiquadrics radial basis functions they become

$$h_j(\boldsymbol{\mu}) = \left( (r_j(\boldsymbol{\mu}))^2 + R_j^2 \right)^{\frac{1}{4}}, \quad (5.118)$$

where the multidimensional radius  $r(\boldsymbol{\mu})$  is defined as

$$r_j(\boldsymbol{\mu}) = \sqrt{\sum_l \left( \mu_l - \mu_l^{(j)} \right)^2}, \quad (5.119)$$

with the  $\mu_l$  as the components of the vector  $\boldsymbol{\mu}$  describing the operating point. Also, Späth [213] suggests to choose

$$R_j = \sqrt{\frac{1}{10} \max_l \left( \left| \mu_l - \mu_l^{(j)} \right| \right)}. \quad (5.120)$$

Inserting these two choices into equation (5.116), allows to determine the coefficients  $\hat{\mathbf{A}}_j$  from the constraints (5.117), which concludes the construction of the interpolation function. The sought-for value  $\mathbf{A}_0$  is then easily obtained by evaluating the interpolation function at the corresponding operating point  $\boldsymbol{\mu}_0$ :

$$\mathbf{A}_0 = \mathbf{H}(\boldsymbol{\mu}_0). \quad (5.121)$$

#### 5.3.2.4 Rotating symmetric positive definite matrices

The section 5.3.2.1 describes the interpolation of SPD-matrices. For the described four-step algorithm it is required to establish a data-base of matrices  $\{\mathbf{A}_1, \dots, \mathbf{A}_m\}$  that correspond to the known working points  $\{\boldsymbol{\mu}_1, \dots, \boldsymbol{\mu}_m\}$ . Naturally, the SPD-matrices can already be reduced with the reduced basis for each operating point. This would yield

$$\left\{ \tilde{\mathbf{A}}_1, \dots, \tilde{\mathbf{A}}_m \right\} = \left\{ \boldsymbol{\Phi}_1^T \mathbf{A}_1 \boldsymbol{\Phi}_1, \dots, \boldsymbol{\Phi}_m^T \mathbf{A}_m \boldsymbol{\Phi}_m \right\}. \quad (5.122)$$

If this is the case it is obvious that the reduced matrices  $\tilde{\mathbf{A}}$  do not operate on the same generalised coordinates  $\mathbf{q}$ . In order to transform them into a consistent set of generalised coordinates Amsallem and Farhat [13] propose the following approach.

If the reduced SPD-matrices for the different operating points are reduced by different bases they do not operate on the same generalised coordinates. This feature depends on equation (3.1), which forces the equality of the physical displacements  $\mathbf{u}$  for all reduced bases, and is explored in great detail in the section 3.3.7, albeit in the context of the solution algorithm.

Because the reduced SPD-matrices from equation 5.122 are not made for a single, consistent set of

generalised coordinates, the procedure to follow would be

1. interpolate between the full order  $\{\mathbf{A}_1, \dots, \mathbf{A}_m\}$  to obtain  $\mathbf{A}_0$  at  $\boldsymbol{\mu}_0$  with  $\mathbf{A}_k$  at  $\boldsymbol{\mu}_k$  as origin with the algorithm from section 5.3.2.1,
2. interpolate between the  $\{\boldsymbol{\Phi}_1, \dots, \boldsymbol{\Phi}_m\}$  to obtain  $\boldsymbol{\Phi}_0$  at  $\boldsymbol{\mu}_0$  with  $\boldsymbol{\Phi}_k$  at  $\boldsymbol{\mu}_k$  as origin with the algorithm from section 5.3.2.2, and
3. reduce  $\mathbf{A}_0$  to obtain  $\tilde{\mathbf{A}}_0 = \boldsymbol{\Phi}_0^T \mathbf{A}_0 \boldsymbol{\Phi}_0$ .

Such an approach is not really efficient because it requires manipulations on full order matrices. A direct interpolation between the reduced matrices  $\{\tilde{\mathbf{A}}_1, \dots, \tilde{\mathbf{A}}_m\}$  would be much more efficient. To this effect these reduced matrices have to be defined in a consistent set of reduced bases.

Amsallem and Farhat [13] observe that the reduced matrices can be rotated to ensure their definition in a consistent set of generalised coordinates. For all  $j \in \{1, \dots, m\}$  the operation

$$\boldsymbol{\Phi}_j^T \boldsymbol{\Phi}_k = \mathbf{U} \boldsymbol{\Sigma} \mathbf{V}^T \quad (5.123)$$

is performed. It is a singular value decomposition of the correlation of the current reduced basis  $\boldsymbol{\Phi}_j$  with the reduced basis  $\boldsymbol{\Phi}_k$  at the origin  $\boldsymbol{\mu}_k$ . The SVD is then stripped of its scaling component  $\boldsymbol{\Sigma}$  and reassembled into a pure rotation with

$$\mathbf{Q}_j = \mathbf{U} \mathbf{V}^T. \quad (5.124)$$

This pure rotation matrix is used to align all  $m$  reduced SPD-matrices  $\tilde{\mathbf{A}}_j$  by

$$\tilde{\mathbf{A}}_j \xrightarrow{\mathbf{Q}_j} \mathbf{Q}_j^T \tilde{\mathbf{A}}_j \mathbf{Q}_j. \quad (5.125)$$

Now the interpolation algorithm of section 5.3.2.1 can be applied directly on the reduced SPD-matrices, which are all aligned to operate on the generalised coordinate set of the origin.

### 5.3.3 Presenting the sensitivity analysis method

The sensitivity analysis method, introduced by Hay et al. [95] as a remedy for encountered problems with the operating point dependence of reduced order models, circumvents the establishment of a large database. This limits this approach however to the close proximity of an already established reduced order basis  $\boldsymbol{\Phi}_k$ . Hay et al. [95] propose two different approaches, the extrapolated basis and the expanded basis. Both are briefly sketched hereunder.

#### 5.3.3.1 Extrapolated Basis

The extrapolated basis is simply a first order expansion including the negligence of higher order terms. Being given the operating point  $\boldsymbol{\mu}_k$  with the associated basis  $\boldsymbol{\Phi}_k$  the new basis  $\boldsymbol{\Phi}_0$ , associated with the operating point  $\boldsymbol{\mu}_0$  is calculated as

$$\boldsymbol{\Phi}_0 \approx \boldsymbol{\Phi}_k + (\boldsymbol{\mu}_0 - \boldsymbol{\mu}_k) \frac{\partial \boldsymbol{\Phi}_k}{\partial \boldsymbol{\mu}}. \quad (5.126)$$

This straight-forward approach is valid, as long as the difference  $(\boldsymbol{\mu}_0 - \boldsymbol{\mu}_k)$  between the operating points does not become too big, and very practical, if a formulation of the gradient of the basis with respect to the operating conditions is available.

### 5.3.3.2 Expanded Basis

For the method of the expanded base, also proposed by Hay et al. [95], it is first recalled that, knowing a reduced basis  $\Phi$ , the displacements can be expressed by the sum over the columns  $\phi_k$  of this basis

$$\mathbf{u}(\mathbf{x}, t) = \sum_{k=1}^r q_k(t) \phi_k(\mathbf{x}). \quad (5.127)$$

The idea of the expanded basis approach is now to expand the basis with the sensibilities of shape functions with respect to the operating conditions. This yields:

$$\mathbf{u}(\mathbf{x}, t) = \sum_{k=1}^r q_k(t) \phi_k(\mathbf{x}) + \sum_{k=r+1}^{2r} q_k(t) \frac{\partial \phi_{k-r}(\mathbf{x})}{\partial \mu}. \quad (5.128)$$

Again, this does not require the establishment of an extensive database and seems to give satisfactory results for an operating point  $\mu_0$  in the vicinity of  $\mu_k$ . However, this approach does only work for a single scalar parameter  $\mu$  or would require the inclusion of sensibilities for all the components of the vector  $\boldsymbol{\mu}$  of parameters.

## 5.3.4 Presenting the interlaced snapshot method

The interlaced snapshot method is only applicable for the Proper and the Smooth Orthogonal Decomposition. It is used by e.g. Vigo [238] for the reduction of a pulsed jet at different frequencies and ejection velocities. The origins of this method, also designated Lagrange subspace method or Global Proper Orthogonal Decomposition (GPOD), according to literature as Keane and Nair [114], Ito and Ravindran [105] and Taylor and Glauser [220], Schmit and Glauser [201] respectively, lie again in the research dealing with fluid mechanics. One of the few known application of the GPOD method to differently parameterised reduced order systems is made by Kumar and Burton [125]. However, they need to add additional Ritz-vectors in order to obtain satisfactory results. The representation below describes its application to structural dynamics.

The POD and the SOD method rely both on the decomposition of matrices that represent e.g. the covariance of the displacements in  $\check{U}$  or the velocities in  $\check{\dot{U}}$ . Both types of matrices are build from snap-shots of the full order system, as defined in equation (3.128) for the POD and in equation (3.138) for the SOD. While the basic Orthogonal Decomposition methods rely on a single system's snapshots to construct the matrices  $\check{U}$  and  $\check{\dot{U}}$ , the interlaced snapshot method combines snapshots from several systems at different operating points  $\{\boldsymbol{\mu}_1, \dots, \boldsymbol{\mu}_l\}$ , which are designated  $\{\check{\mathbf{u}}_{\boldsymbol{\mu}_1}(t_j), \dots, \check{\mathbf{u}}_{\boldsymbol{\mu}_l}(t_j)\}$  and  $\{\check{\dot{\mathbf{u}}}_{\boldsymbol{\mu}_1}(t_j), \dots, \check{\dot{\mathbf{u}}}_{\boldsymbol{\mu}_l}(t_j)\}$  for a specific instant  $t_j$  and the displacements and the velocities, respectively.

With these equation (3.128) for the original Proper Orthogonal Decomposition becomes

$$\check{U} = \sum_{j=1}^m \sum_{i=1}^l \delta_j \check{\mathbf{u}}_{\boldsymbol{\mu}_i}(t_j) \check{\mathbf{u}}_{\boldsymbol{\mu}_i}^T(t_j) \quad (5.129)$$

and equation (3.138) from the Smooth Orthogonal Decomposition reads

$$\dot{\tilde{U}} = \sum_{j=1}^m \sum_{i=1}^l \delta_j \dot{\tilde{u}}_{\mu_i}(t_j) \dot{\tilde{u}}_{\mu_i}^T(t_j). \quad (5.130)$$

In both equations (5.129) and (5.130) the  $\delta_j$  are suitable averaging operators. Following these new definitions the two methods follow their normal development with equations (3.129) and (3.139), respectively.

A variation of this method, being treated under the names of Hermite subspace method or Compact Proper Orthogonal Decomposition, depending on if and how the snapshots are weighted, adds the derivations of the snapshots  $\dot{\tilde{u}}_{\mu_i}$  with respect to the parameter  $\mu$  to the database of this method. In this, it somewhat resembles the tangent modes, discussed in section 3.3.1. Applied to the equations above, this yields

$$\tilde{U} = \sum_{j=1}^m \sum_{i=1}^l \delta_j \tilde{u}_{\mu_i}(t_j) \tilde{u}_{\mu_i}^T(t_j) + \sum_{j=1}^m \sum_{i=1}^l \delta_j \frac{\partial \tilde{u}_{\mu_i}(t_j)}{\partial \mu_i} \frac{\partial \tilde{u}_{\mu_i}^T(t_j)}{\partial \mu_i}. \quad (5.131)$$

This method is detailed, among others, by Keane and Nair [114] and Carlberg and Farhat [54].

### 5.3.5 Evaluating the adaptation methods by means of a numerical study

The identification of a lacking robustness for all types of reduced bases in the preceding chapter clearly shows that an adaptation of the reduced bases as a function of the different parameters is necessary. In the current section 5.3 several methods for the adaptation of reduced bases are discussed. Their suitability is tested in the following. Because the methods are basically presented as they are described in literature and no extensive modifications are applied, they can be compared in a unified study. The study uses POD bases on the entirely non-linear system under harmonic excitation.

To facilitate the present study a novel presentation of the errors over the two-dimensional parameter space is used. The relative error metric that is defined to this purpose compares the reconstructed physical solutions that have been obtained with different reduced bases. A comparison of the bases does not take place because the only interest lies on the faithful recreation of the physical displacements.

The amplitude and the frequency define the two dimensions of the parameter space. The vector of the parameters  $\boldsymbol{\mu}$  is hence an  $2 \times 1$  vector. The hinging point of the methods is defined as

$$\boldsymbol{\mu}_k = \begin{bmatrix} \hat{f}_{E,k} \\ \Omega_k \end{bmatrix} = \begin{bmatrix} 3 \\ 0.2289 \end{bmatrix}, \quad (5.132)$$

with the reference values from section 4.1.3.4. Around this point the different methods from the current section 5.3 are tested. These include

- the interpolation method (section 5.3.2, Amsallem [12]),
- the extrapolation method, coming from the sensitivity analysis of the bases (section 5.3.3, Hay et al. [95]), and
- the two variants of the interlaced snapshots method (section 5.3.4, Vigo [238]), which is only available in the specific context of POD bases.

The adaptation methods require a certain set of  $m$  precomputed reduced basis. These precomputed bases are established at operating points that are grouped in a stencil around the hinging point  $\boldsymbol{\mu}_k$ . The stencil is set to be symmetric. It includes a square of values in the two directions of the parameters space  $\hat{f}_E$  and  $\Omega$ .

The total number of predefined operating points of  $m = 9$ . They are listed in table 5.5.

i	$\hat{f}_E$	$\Omega$	position
1	$\hat{f}_{E,k}$	$\Omega_k$	centre
2	$\frac{1}{2}\hat{f}_{E,k}$	$\Omega_k$	edge
3	$\frac{3}{2}\hat{f}_{E,k}$	$\Omega_k$	edge
4	$\hat{f}_{E,k}$	$\frac{1}{2}\Omega_k$	edge
5	$\hat{f}_{E,k}$	$\frac{3}{2}\Omega_k$	edge
6	$\frac{1}{2}\hat{f}_{E,k}$	$\frac{1}{2}\Omega_k$	corner
7	$\frac{3}{2}\hat{f}_{E,k}$	$\frac{1}{2}\Omega_k$	corner
8	$\frac{1}{2}\hat{f}_{E,k}$	$\frac{3}{2}\Omega_k$	corner
9	$\frac{3}{2}\hat{f}_{E,k}$	$\frac{3}{2}\Omega_k$	corner

Table 5.5: The nine points of the stencil for testing the reduced basis adaptation methods

The operating points  $\mu_0$  on which the adaptation methods are to be tested are organised in a grid over the space of parameters. This grid spans all combinations that are available with

$$0.2\hat{f}_{E,k} \leq \hat{f}_{E,0} \leq 2\hat{f}_{E,k}, \quad (5.133)$$

with  $\Delta\hat{f}_E = 0.2\hat{f}_{E,k}$ , and

$$0.2\Omega_k \leq \Omega_0 \leq 2\Omega_k, \quad (5.134)$$

with  $\Delta\Omega = 0.2\Omega_k$ . No operating point from the stencil in table 5.5, except the hinging point  $\mu_k$ , corresponds to a point on the grid.

Every point on the grid is defined as the current operating point  $\mu_0$ . For each  $\mu_0$  the appropriate reduced basis  $\Phi_0$  is established with the different methods and a reduced transient solution is obtained during which the reduced basis  $\Phi_0$  is kept constant. This reduced solution is inflated to physical displacements and compared to its equivalent that has been obtained with a constant  $\Phi_0^{(\text{ref})}$ . The reduced basis  $\Phi_0^{(\text{ref})}$  is the reference reduced basis that is obtained directly with the parameters' values at  $\mu_0$ . The comparison takes place in a relative manner, so that only the gain that is obtained by applying the method that adapts the reduced basis as a function of the parameters is considered. In this way, two reduced solutions are compared among each other. The full order solution at  $\mu_0$  only serves to establish the reference reduced basis  $\Phi_0^{(\text{ref})}$ .

The relative error metric  $\bar{e}_r$  is introduced to describe the relative gain in the quality of the reduced solution by using an adapted basis  $\Phi_0$  at  $\mu_0$  instead of the fixed basis  $\Phi_k$  in the centre of the stencil  $\mu_k$ . It is normalised with the error obtained with the gain due to the application of a reference basis  $\Phi_0^{(\text{ref})}$  at the respective operating point. The adapted basis  $\Phi_0$  is build specifically for the given operating point  $\mu_0$  by means of an adaptation method. This is done for every adaptation method.

For each point of the grid, i.e. every  $\mu_0$ , there are four solutions that are established:

- a full order reference solution.
- a reduced order reference solution, which is obtained with the reference reduced basis  $\Phi_0^{(\text{ref})}$ . This reference reduced basis is obtained from the full order reference solution.
- a reduced order solution with the unaltered reduced basis  $\Phi_k$  from the hinging point of the stencil  $\mu_k$ .

### 5.3. ADAPTING REDUCED BASIS TO EXTERNAL PARAMETERS

---

- a reduced order solution with the adapted reduced basis  $\Phi_0$ , which is obtained by the different adaptation methods at the current point of the grid  $\mu_0$ .

From these four solutions three errors can be derived. These are obtained by comparing the three reduced solutions with the full order solution by means of the mean of the R2MSE  $e_r$  from equation (4.5). In particular these errors are

- $e_r^{(\text{ref})}$  that comes from the reduced solution that is obtained with  $\Phi_0^{(\text{ref})}$ ,
- $e_r^{(k)}$  that comes from the reduced solution that is obtained with  $\Phi_k$ , and,
- $e_r^{(0)}$  that comes from the reduced solution that is obtained with  $\Phi_0$ .

These three errors can be combined to define the relative error metric for the adaptation method

$$\bar{e}_r = \frac{e_r^{(k)} - e_r^{(0)}}{e_r^{(\text{ref})}}. \quad (5.135)$$

It expresses the difference in the error on the level of the physical displacements that are obtained with the specifically adapted reduced basis  $\Phi_0$  and the physical displacements obtained without adapting the basis, using the unaltered reduced basis  $\Phi_k$  instead, normalised with the absolute error that can be obtained with a reference basis  $\Phi_0^{(\text{ref})}$ . This relative error metric measures the improvement (or the deterioration) in the quality of the reduced solution that is obtained if an adapted reduced basis is used at the operating point  $\mu_0$ , instead of the fixed reduced basis, which was obtained at the origin  $\mu_k$ . The relative error metric increases when the adapted reduced basis performs better than the basis from the hinging point. Using only the R2MSE should not favour a particular method for the adaptation of the reduced bases to external parameters. There are no known optimality considerations for such methods available in literature.

The testing takes place on the entirely nonlinear system under harmonic excitation. The harmonic excitation allows to have two parameters that can be varied continuously. The reduced basis that is applied comes from the classic POD procedure in section 3.3.3.1. This procedure allows to use all adaptation techniques, including the interlaced snapshots method, and the resulting reduced bases have been proven to be the most sensitive ones with respect to changing parameters during the study of the bases' robustness in section 4.2.2. The order of the reduced system is set to  $r = 3$ .

In the following some considerations are made for the practical application of the adaptation methods in a numerical setting. Then, in order to put the following study of the relative error metric into perspective, the absolute error  $e_r^{(\text{ref})}$  is studied. Finally, the relative error metric from equation (5.135) is explored for all adaptation methods.

#### 5.3.5.1 Considerations for the practical application of the adaptation methods

The adaptation methods are introduced in sections 5.3.2 to 5.3.4 in a rather theoretical manner. To apply them practically in the context of the current study requires some additional considerations. These are listed below to give a complete picture of the approach of this study.

**5.3.5.1.1 Interpolation method** The interpolation method for the creation of the reduced basis  $\Phi_0$ , corresponding to the operating point  $\mu_0$ , is applied in a straight-forward manner, as it is described in section 5.3.2. The operating points  $\mu_i$  of the bases  $\Phi_i$ , which are used for the interpolation, defined as the nine point stencil from table 5.5. The origin of the interpolation  $\Phi_k$  is corresponding to the centre point of the stencil, i.e.  $\mu_1$ .

**5.3.5.1.2 Sensitivity analysis' extrapolated basis** The extrapolated reduced basis, which is obtained by the sensitivity analysis, is obtained from a linear extrapolation. The derivatives are taken along the axes of the parameter space,  $\hat{f}_E$  and  $\Omega$  in this case. As such only the operating points at the centre and along the edges the nine point stencil in table 5.5 are used for the finite differences that are to approximate the local derivations of the reduced bases with respect to the operating point's parameters. The use of combined derivatives is precluded by the linear nature of this approach, as stipulated in equation 5.126. To finalise the construction of the matrix  $\Phi_0$ , the extrapolated basis is subjected to a Gram-Schmid procedure (Strang [218]).

**5.3.5.1.3 Interlaced snapshot methods** For the interlaced snapshot there are two possible variants. Being given a set of  $m$  sets of snapshots  $\tilde{u}_{\mu_i}$ , corresponding to the operating points  $\mu_i$  of the nine point stencil one can

- first construct the corresponding matrix  $\tilde{U}_{\mu_i}$  for each  $\tilde{u}_{\mu_i}$  as per equation (5.129) and then proceed to define a single matrix  $\tilde{U}$  as the mean of all  $\tilde{U}_{\mu_i}$ , or,
- first construct a single displacement snapshot matrix  $\tilde{u}$  by taking the mean of all  $\tilde{u}_{\mu_i}$  and then define a single matrix  $\tilde{U}$  from the interlaced snapshots  $\tilde{u}$  as per equation (5.131).

These two variants are used.

### 5.3.5.2 Studying the absolute error

The absolute error  $e_r^{(\text{ref})}$  is obtained with the reduced basis  $\Phi_0^{(\text{ref})}$ . This reduced basis is the POD basis obtained from the full order reference solution at the current operating point  $\mu_0$ . It is considered to be optimal in an energy sense (Feeny and Kappagantu [78], Feeny and Liang [79]). The resulting absolute error  $e_r^{(\text{ref})}$  is thus expected to be the lowest one that is achievable. It forms the reference for the relative error metric in equation (5.135). In the following it is briefly studied because this allows a finer judgement of the relative error metrics obtained with the different adaptation methods.

The figure 5.24 plots the error metric of the R2MSE  $e_r^{(\text{ref})}$ , colour-coded over the values of  $\hat{f}_E$  and  $\Omega$ . The range for these two dimensions of the parameter space is much enlarged compared to the initial definitions (5.133) and (5.134), to include some interesting features of the behaviour of the absolute error. The following study of the reduced error will return to the initial range of parameters.

A directly obvious feature of the plot of the absolute error  $e_r^{(\text{ref})}$  in figure 5.24 is the emergence of patterns, which span ridges of high error values along the first diagonal.

The different values of the error metric represent directly the ability of the reduced basis to capture the behaviour of the system at that operating point because every reduced basis is specifically adapted to the operating point and, following the theory on POD bases, optimal in an energy sense. Hence, the level of error to be obtained reflects upon the basis and its capabilities and a property of the reduced basis has to exist, which links its structure to its ability to correctly reduce the test-case at the given operating point.

In this context it is useful to recall that the column vectors of the POD basis represent the main components of the solution. In order to identify the peculiarities of the simulations at the operating points, which result in larger values for the error, it is hence necessary to closely inspect these column vectors.

The natural candidate for comparing the column vectors  $\phi$  of a basis is the modal assurance criterion from equation (4.10). Unfortunately this very sensitive criterion only delivers numeric noise near zero.

The application of the R2MSE  $e_{r,\Phi}$ , that is defined in equation (4.4), to the first two column vectors  $\phi_1$  and  $\phi_2$  of the reduced basis reveals however an insightful correlation. It shows clearly that the regions where the similarity between the two first column vectors  $\phi_1$  and  $\phi_2$ , expressed by low values for  $e_{e,\Phi}$ , correspond well with the regions of high error on the level of the results in figure 5.24. A high similarity of

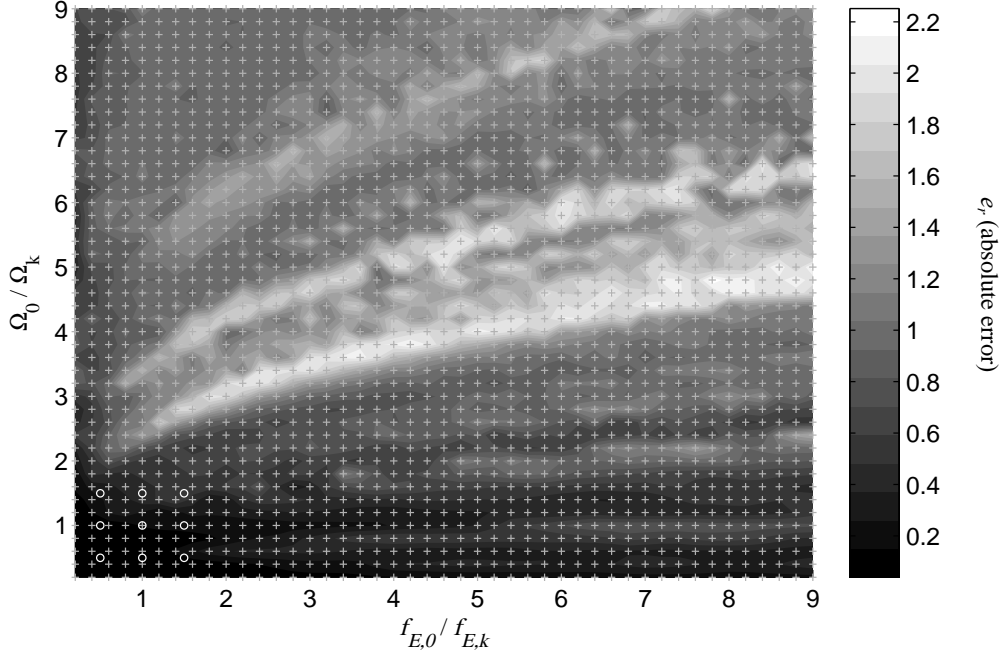


Figure 5.24: The absolute error of the solutions obtained with the reference bases as a function of  $\hat{f}_E$  and  $\Omega$

the first two modes of the POD basis corresponds to a high error in the solution obtained from the reduced system.

To verify that there are no other influences the energy ratio  $E_r$  from equation 3.133 also studied. It does not exhibit the characteristic patterns and is mainly very homogenous. It is interesting to observe that the frontier, where the  $E_r$  drops below 0.95 corresponds to first ridge of error in figure 5.24. This behaviour stresses the importance of a representation of a high fraction of energy in the reduced basis  $\Phi$ , in order to ensure a successful reduction.

Having thus confirmed that a high similarity between the first two modes of the reduced basis corresponds to a high level of error in the reduced simulation allows the conclusion that most certainly the two major characteristics of the solution correspond to two nearly confounded modes. This observation applies to all three ridges of higher error level on figure 5.24. All three are mirrored in valleys of high similarity between the first two modes.

The fact that the presence of confounded modes is in fact a property of the solution of the system at that operating point, which is only identified by the established POD basis, and not a property of the POD basis itself, can be shown by keeping the reduced basis constant. Taking the POD basis, which is established at the centre of the stencil  $\mu_k$  in equation (5.132), and using it to reduce all other operating points yields the mapping of the corresponding error metric  $e_r$ . This indicates that the level of error, with which a non-linear system can be reduced, may more depend on the characteristics of the solution than on the basis itself. These findings confirm the results of the comparative study in section 4.2.1.

### 5.3.5.3 Studying the relative error metric

The study of the relative error metric  $\bar{e}_r$  from equation (5.135) allows a comparison of the adaptation methods. This comparison is centred on their capability to contribute to a faithful reconstruction of the physical displacements. The actual reduced basis that is created by the adaptation method at the current

operating point  $\mu_0$  is not considered. In the following the plots of the relative error metrics for the different adaptation methods are shown in figures 5.25 to 5.28 and each one is discussed briefly. To gauge the information that is available through the relative error metric, these plots are compared with the plot of the absolute reference error  $e_r^{(\text{ref})}$ . For this study the ranges for the parameters  $\mu_0$  are again as defined in equations (5.133) and (5.134). To allow an easy comparison of the relative error metrics of the different methods, they colour-coding is harmonised among the figures 5.25 to 5.28.

**5.3.5.3.1 Interpolation method** The interpolation method interpolates all bases from the operating points in the nine-point stencil from table 5.5. The obtained relative error is shown in figure 5.25. It is interesting to observe that there is no improvement within the stencil. Further improvements below the first ridge of error, counted in positive  $\Omega$  direction, in figure 5.24 are rather sparse in appearance. Within the ridge the improvements are very pronounced and by far the best that can be obtained with any method.

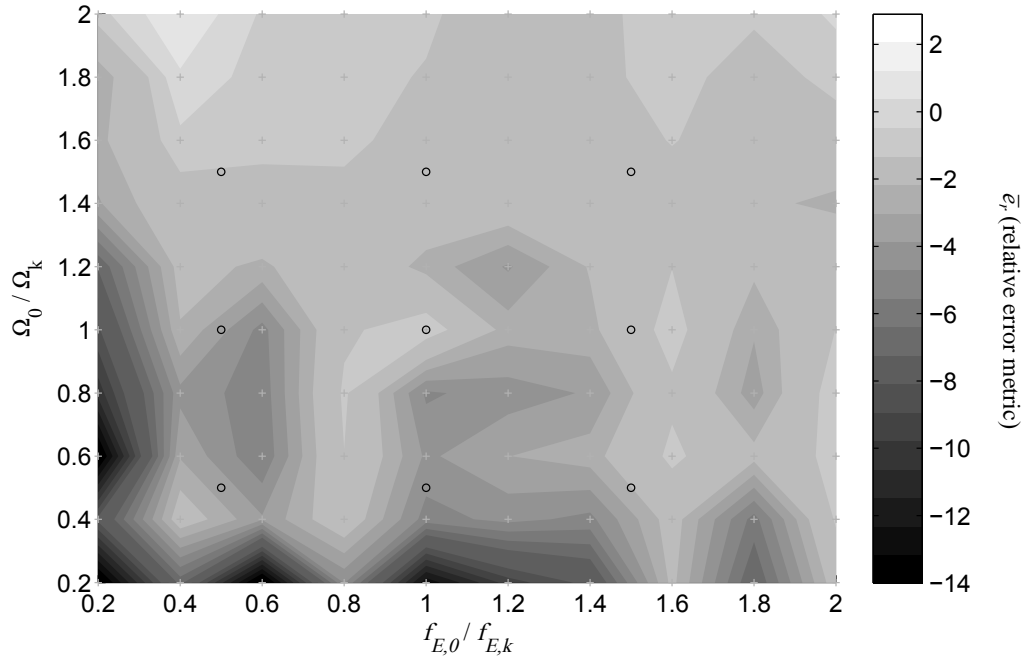


Figure 5.25: The relative error obtained with the interpolation method

**5.3.5.3.2 Sensitivity analysis method** For the sensitivity analysis method the edge operating points of the nine point stencil from table 5.5 are used. Finite differences are calculated in the amplitude  $\hat{f}_E$  and in the frequency  $\Omega$  direction. All reduced bases for operating points on the grid are extrapolated with the sensitivities applied from the centre of the stencil. The relative error obtained with the sensitivity analysis method is plotted in figure 5.26. It is widespread but not too pronounced along the first ridge of error.

**5.3.5.3.3 Interlaced snapshot** The two variants of the interlaced snapshots method take snapshots from all nine operating points in the stencil from table 5.5 and construct a unified reduced basis, albeit with a slight difference between the two variants.

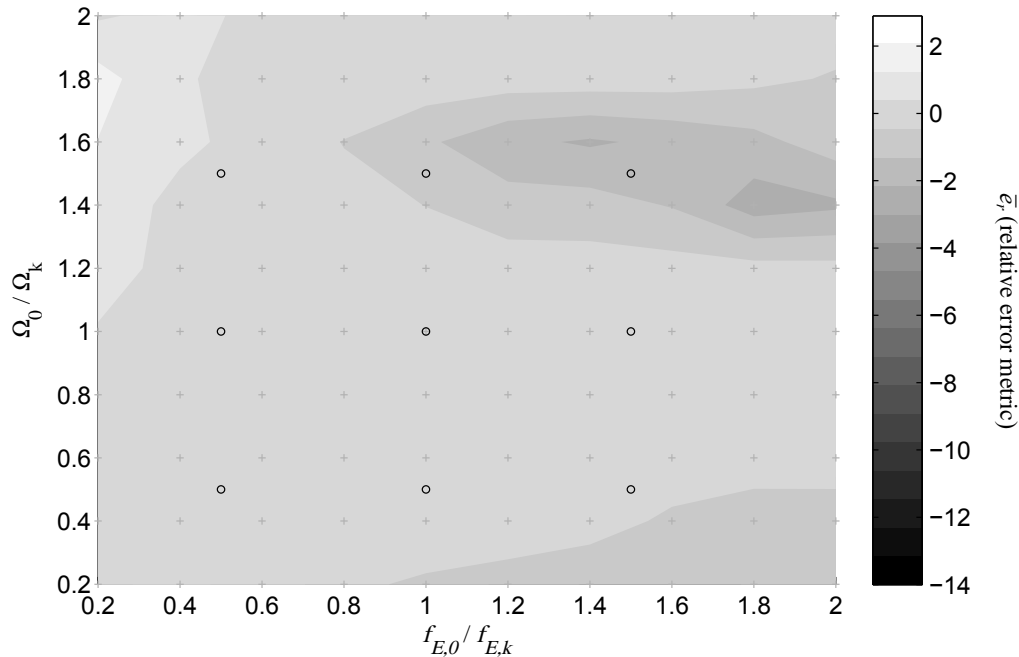


Figure 5.26: The relative error obtained with the sensitivity analysis method

**5.3.5.3.3.1 First variant** In the first variant of the interlaced snapshot method there is at first a specific correlation matrix constructed for each simulation at every operating point of the stencil. It is only then that the correlation matrix are summed and treated further in order to obtain a unified POD basis. This is then used to reduce all other operating points. The resulting relative error is plotted in figure 5.27. The first variant shows some improvement for the low frequency range, around  $\Omega_0$ , for all amplitudes. The most improvements are along the first ridge of error from figure 5.24, just before the energy ratio  $E_r$  drops below 0.95.

**5.3.5.3.3.2 Second variant** In the second variant of the interlaced snapshots methods the solutions of the simulation of the operating points in the stencil are summed for each time-step. Only then this unified snapshot collection is subjected to a POD procedure to create a unified reduced basis. This basis is then used to reduce all other operating points. The resulting relative error metric is plotted in figure 5.28. The second variant of the interlaced snapshots method delivers improvements which follow the general pattern of the first variant. However, the resulting improvements are more pronounced and more widespread this time. This becomes directly evident when comparing figures 5.28 and 5.27. Following this result the second variant of the interlaced snapshot method is to be preferred over the first variant.

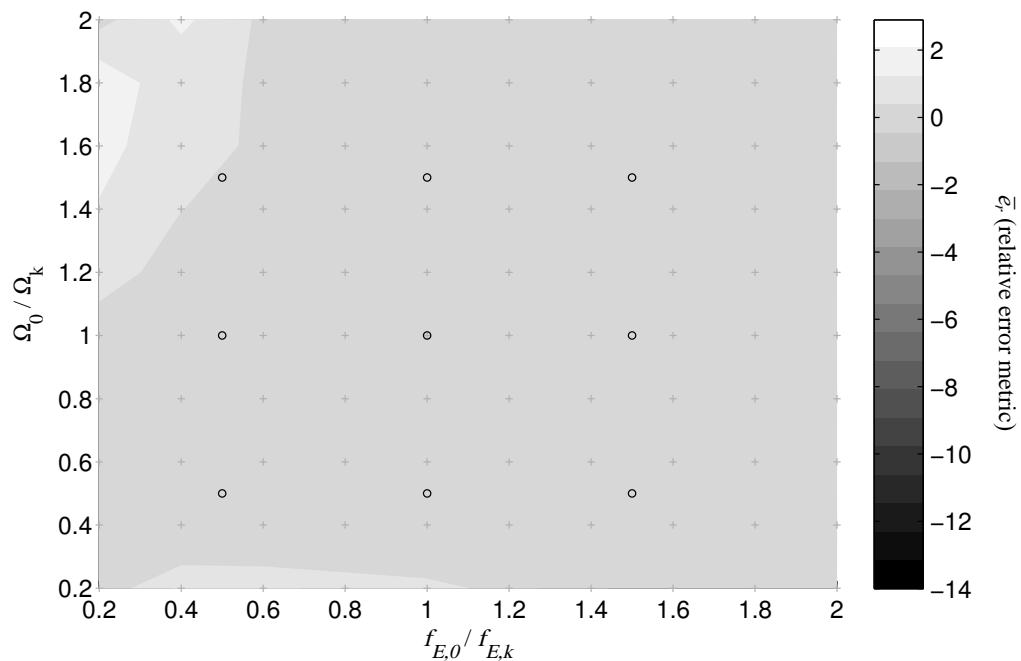


Figure 5.27: The relative error obtained with the interlaced snapshots method's first option

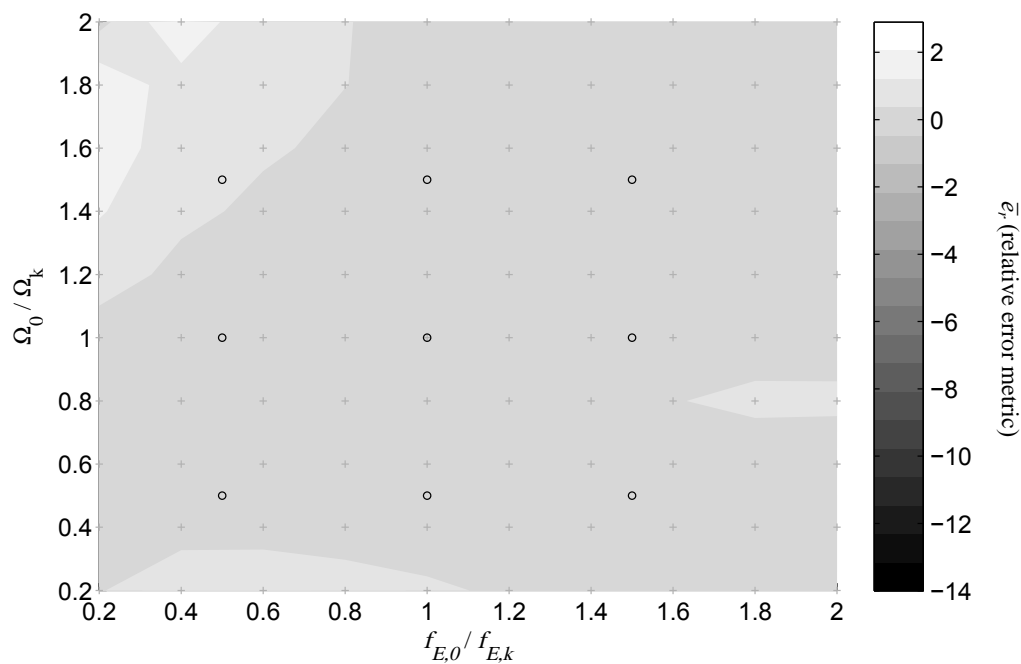


Figure 5.28: The relative error obtained with the interlaced snapshots method's second option

### 5.3.6 Outcome for the requirement of parameterising the reduced system

For the selection of the method that is to adapt the reduced system as a function of the external parameters  $\mu$ , a numerical study is performed that employs a relative error metric as major criterion. However, the results of this study are only of a very limited importance to the decision on the selection of an adaptation method. The selection of the update as the major improvement of the solution algorithm in section 5.1 leads to the situation that only the initial reduced basis  $\Phi^{(t=t_0)}$  can be subjected to a parameterisation. Beyond that, it is the update and augmentation method and the actual procedure for creating the reduced basis itself that are charged with updating the reduced basis. Naturally they are required to take into account any form of parameterisation. This reduces the parameterisation of the reduced system to a minor problem.

Any of the three methods that are presented in this section is theoretically capable of working with an autonomous system that is solved with a reduced nonlinear Newmark scheme with updating and augmenting the reduced basis. However, only the interpolation in tangent spaces allows also to treat the static matrices of the system. It is hence this approach that is selected to be pursued further. This choice will be justified extensively with the finite element test-cases in the chapter 6.

As possible directions of future research it might be possible to introduce an interpolation method inside the update method. In such a configuration the updated reduced basis  $\Phi^{(t)}$  would not be generated from scratch with the actual procedure for creating the reduced basis, but as the result of an interpolation of previously generated bases.

Another possible abuse of the interpolation in tangent spaces approach would be to use it as an approximation for the internal nonlinear forces and to thus render the reduced system autonomous. This would work especially well for the interpolation tangent stiffness matrix  $\bar{K}$  that is an SPD-matrix and for which only very few autonomous formulations are available. The two major obstacles are the performance and the fact that the characteristics of the generalised coordinates  $q$  are not known prior to the actual reduced solution. It would hence difficult to establish a database on which the interpolation could be performed. Nevertheless, the approach is briefly sketched below.

### 5.3.7 Abusing the interpolation approaches in tangent spaces as an autonomous formulation

Another approach for expressing the tangent stiffness matrix  $\bar{K}$  and the vector of the nonlinear internal forces  $g$ , both for the full order and the reduced order system, is the interpolation. It consists in abusing in a way the interpolation approach presented in section 5.3.2 by interpreting the displacements  $u$ , or the generalised coordinates  $q$  for the reduced system, as operating points and interpreting the vector  $g$  as a reduced basis  $\Phi$  with a single column. From there on the application is straightforward. All theory is given in section 5.3.2.

#### 5.3.7.1 Using direct interpolation on the full order system

The direct interpolation on the full order system treats all nodal displacements  $u$  as parameters. It is the most straightforward application of the interpolation approach to the vector of nonlinear forces and the tangent stiffness matrix.

Prior to the beginning of a solution, a number of  $m$  significant displacements  $\{\tilde{u}_1, \dots, \tilde{u}_m\}$  is selected. These are treated as the  $m$  operating points  $\{\mu_1, \dots, \mu_m\}$ , each defined by the  $n$  nodal displacements, which stand in for the parameters.

A first database is established for tangent stiffness matrices  $\{\bar{K}(\mu_1), \dots, \bar{K}(\mu_m)\}$  corresponding to the operating points. The notation  $\bar{K}(\mu_i) = \left. \frac{\partial g(u)}{\partial u} \right|_{\mu_i}$  is used. A second database is established with the

corresponding internal forces  $\{\mathbf{g}(\boldsymbol{\mu}_1), \dots, \mathbf{g}(\boldsymbol{\mu}_m)\}$ , that are regarded as the single column vectors of a degenerated reduced basis  $\{\boldsymbol{\phi}(\boldsymbol{\mu}_1), \dots, \boldsymbol{\phi}(\boldsymbol{\mu}_m)\}$ .

All three elements, the set of significant displacements and the two databases, are used in the interpolation approximation of the tangent stiffness matrix and the nonlinear forces vector. The current displacement  $\mathbf{u}_{(i)}^{(t+\Delta t)}$  in the nonlinear Newmark scheme is treated as the current operating point  $\boldsymbol{\mu}_0$ . The required tangent stiffness matrix is obtained by applying the interpolation procedure for SPD matrices and the required internal forces vector is obtained by applying the method for the interpolation for reduced bases with a single column vector.

This direct approach has the advantage of being well-arranged, which makes its application straightforward. Its main disadvantage is that the number of parameters for each predetermined operating point  $\boldsymbol{\mu}$ , which is defined by the overall number of degrees of freedom in the full order system  $n$ , may be very large. This leads to considerable computational efforts for executing the interpolations and typically negates applicability of the direct approach.

### 5.3.7.2 Using modal interpolation on the full order system

To remedy the identified disadvantage of too many parameters per predetermined operating point of the direct approach, the interpolation of the full order system can also be executed on generalised coordinates. This requires a given and constant reduced basis  $\bar{\Phi}$ .

The predetermined operating points  $\{\boldsymbol{\mu}_1, \dots, \boldsymbol{\mu}_m\}$  are now defined as the generalised coordinates of the significant displacements, where each significant displacement is reduced as  $\boldsymbol{\mu}_i = (\Phi^T \Phi)^{-1} \Phi^T \tilde{\mathbf{u}}_i$ . Naturally, at this point, it is advantageous to choose the  $\tilde{\mathbf{u}}$  in a way that they give pertinent generalised coordinates. The databases are constructed accordingly as

$$\{\bar{\mathbf{K}}(\Phi \boldsymbol{\mu}_1), \dots, \bar{\mathbf{K}}(\Phi \boldsymbol{\mu}_m)\} \quad (5.136)$$

and

$$\{\mathbf{g}(\Phi \boldsymbol{\mu}_1), \dots, \mathbf{g}(\Phi \boldsymbol{\mu}_m)\}. \quad (5.137)$$

If the tangent stiffness matrix or the nonlinear forces vector are required in the course of the solution, the corresponding operating point is retrieved as the generalised coordinates of the current displacement  $\boldsymbol{\mu}_0 = (\Phi^T \Phi)^{-1} \Phi^T \mathbf{u}_{(i)}^{(t+\Delta t)}$ .

The modal interpolation for obtaining the full order tangent stiffness matrix and the nonlinear forces vector operates entirely on generalised coordinates and reduces the number of involved parameters from the number of degrees of freedom of the full order system  $n$  to a considerably smaller number  $r$ . The additional computations for expressing the current displacements in generalised coordinates is typically more than offset by the gain due to the reduced number of parameters.

### 5.3.7.3 Using interpolation on the reduced order system

From the modal interpolation of the full order system, the conversion of the process to the reduced order system is direct by simply left multiplying the whole process by  $\Phi^T$ .

This gives for the databases

$$\{\tilde{\bar{\mathbf{K}}}(\boldsymbol{\mu}_1), \dots, \tilde{\bar{\mathbf{K}}}(\boldsymbol{\mu}_m)\} = \{\Phi^T \bar{\mathbf{K}}_{\boldsymbol{\mu}_1} \Phi, \dots, \Phi^T \bar{\mathbf{K}}_{\boldsymbol{\mu}_m} \Phi\} \quad (5.138)$$

and

$$\{\tilde{\mathbf{g}}(\boldsymbol{\mu}_1), \dots, \tilde{\mathbf{g}}(\boldsymbol{\mu}_m)\} = \{\boldsymbol{\Phi}^T \mathbf{g}(\boldsymbol{\Phi} \boldsymbol{\mu}_1), \dots, \boldsymbol{\Phi}^T \mathbf{g}(\boldsymbol{\Phi} \boldsymbol{\mu}_m)\} \quad (5.139)$$

and the current operating point  $\boldsymbol{\mu}_0$  is directly the current vector of generalised coordinates  $\mathbf{q}_{(i)}^{(t+\Delta t)}$ . The main disadvantage of this approach is that it requires a constant reduced basis or the significant displacements have to be kept in physical coordinates and the databases have to be updated whenever the basis changes.

All three approaches for abusing the interpolation that are sketched above are merely hypothetical thought experiments. An actual application would require much more efforts to render the methods more robust in order to enable their application outside the well controlled environment of the reduced bases and SPD matrices depending on only a handful of external parameters. The large number of  $r$  of generalised coordinates that would have to be interpolated would certainly pose a bottle-neck for the interpolation, not to mention the full order interpolation with  $n$  degrees of freedom. However, first, brief ventures into a numerical implementation seem to indicate that such an abuse of the interpolation approaches for obtaining an autonomous formulation of the nonlinear terms might actually be feasible.

## Chapter 6

# Creating the integrated method from the approaches addressing the identified requirements and applying it to nonlinear finite element test-cases

---

The update of the reduced basis, the polynomial formulation of the nonlinear terms and the interpolation as a function of external parameters are the approaches that are selected to address the previously identified shortcomings of the initial procedures for obtaining the transient solutions of reduced nonlinear systems. In the preceding chapter 5 these three approaches have been thoroughly tested on academic test-cases and adapted where necessary. They are now united in an integrated method and applied to finite element test-cases. The finite element test-cases are built with the finite elements that are developed in the chapter 2.

In a first step the integrated method is assembled by uniting the methods of the introduction of a reduced basis, the replacement of the finite element expressions of the nonlinear terms with a polynomial formulation, the update and augmentation of the reduced basis and of interpolating the reduced basis as a function of the external parameters. This integrated method is formalised and tested on the academic test-cases.

In a second step the integrated method is applied to two finite element test-cases. The first finite element test-case is constructed with nonlinear bar elements and the second one is constructed with nonlinear volume elements. Great effort is spent on defining, characterising and exploring the finite element test-cases because their nonlinear behaviour and the resulting transient solutions set the limits of confirmed validity for the application of the integrated method.

## 6.1 Uniting the three elements and applying the integrated method

The integration of the three elements of adapting the solution algorithm by updating the reduced basis, rendering the reduced system autonomous with the polynomial formulation of the nonlinear terms and adapting the initial reduced basis as a function of the external parameters with the interpolation method marks the central aspect of the performed research. All three methods are tested isolated in their respective section 5.1, 5.2 and 5.3. Each one of them addresses a specific requirement that has been identified during the introduction of the reduced basis into the solution algorithm in section 3.2.3 or during the comprehensive numerical studies in chapter 4. The integration of these three methods allows treating reduced systems of geometrically nonlinear and parameterised structures.

The interpolation of the reduced bases as a function of external parameters  $\mu$  is treated as being slightly apart and not directly integrated with the two other methods because it provides only the initial reduced basis  $\Phi_0$  at  $t_0$  of the transient solutions. Subsequent bases are adapted by the update and augmentation algorithm that takes the parameterisation into account. Furthermore, the adaptation of the reduced basis for the finite element test-cases is already studied during the introduction of the prestress in section 6.3.2. There it is proven that the prestress can be introduced into a nonlinear structure by adding a static component to the external forcing and choosing corresponding initial conditions.

The most critical task is hence the integration of the autonomous formulation with the update and augmentation method. These two elements are integrated into the HHT- $\alpha$ -method as the overall backbone of the integrated method in an explicit manner. The integration on the reduced nonlinear Newmark scheme is also performed and considered to be equivalent.

The autonomous formulation and the update and augmentation method are first integrated and applied on the academic test-case from section 4.1.3. This cautious approach is necessary because the polynomial expression from section 5.2.2, which constitutes the autonomous formulation of the nonlinear terms, provides several variants that can be combined with the update and augmentation method. All of these variants provided good results in the numerical testing of the autonomous formulation alone in section 5.2.4 but at this point it is not yet known which variant integrates best with the update and augmentation method. The variant to be used for the finite element test-cases is determined by the application of the integrated method to the academic test-cases. So, in a second step, only the most promising variant of the polynomial expression is used for rendering the finite element test-cases autonomous.

### 6.1.1 Describing the integrated method

The integrated solution approach is the central result of the performed work. It is a novel combination of existing and original methods that are combined to obtain the transient solution of the reduced model of a parameterised and geometrically nonlinear structure.

For the finite element test-case the basic underlying structure of the approach is provided by the HHT- $\alpha$ -method that is described in section 3.2.2.2. This solution method is chosen to demonstrate that the approach can be build on top of all Newmark-type solution schemes and that it is not limited to the classic nonlinear Newmark scheme from section 3.2.2.1.

The reduction of the full order system is achieved by the projection on a reduced basis. The main advantages of this approach are its modularity and the possibility to use a common basic solution scheme for reduced and full order problems. This is discussed in detail in section 3.1.

The reduced solution is rendered autonomous by the introduction of the polynomial expression for the nonlinear terms. This requirement is identified from the inspection of the underlying solution algorithm in section 3.2.3. Again, the use of the HHT- $\alpha$ -method instead of the classic reduced nonlinear Newmark scheme, shows that this requirement is universal to the members of the Newmark-type solution algorithms and also that the chosen response in form of the polynomial formulation is universal and portable. The poly-

nomial formulation is discussed in great detail and adapted to the specific requirements of computational feasibility and the independence from a specific reduced basis in section 5.2.2.

The parameterisation of the initial reduced basis is assured by the interpolation approach from section 5.3.2. This is a method taken from literature without adaptation because it performs well on the given problems. Its introduction is identified as necessary after the inspection of the results of the test of the robustness of some reduced bases in section 4.2.2.

The main ingredient of the integrated solution approach is the updating and augmentation of the reduced basis from section 5.1.3. This method allows making the reduced basis follow the evolution of the nonlinear transient solution and considerably boosts the quality over a solution that has been obtained with a constant reduced basis. The necessity to update the reduced basis is identified with the numerical studies for the comparison of reduced bases in section 4.2.1 and the appearance of jumps is successfully countered by the inclusion of the augmentation of the updated reduced basis. The updating and augmentation approach draws on the modularity of the concept of the reduction by projection on a reduced basis and can thus be integrated easily in the Newmark scheme as well as in the HHT- $\alpha$ -method. It is independent of the particular choice of the method that actually provides the reduced basis. Several common methods are presented in section 3.3. The update and augmentation approach is compatible with the polynomial expression of the nonlinear terms, after the latter has been rendered independent from a specific reduced basis.

The integrated solution approach with these three ingredients is presented below along general lines. The sections that are referenced in this introduction serve as source for detailed information. The particular choices that have to be made in the specific case of a finite element system with respect to the actual variant of each method are explored in the following sections. The description of the integrated solution approach is presented below in three steps. In the first step the solution is prepared by providing the necessary databases, e.g. for the interpolation of the initial reduced basis. In a second step, the reduced transient solution is initialised and continued until the reduced basis is augmented for the first time. The third step covers the update and augmentation of the reduced basis and the continuation of the reduced transient solution with repeated basis updates and augmentations until the end of the simulated period  $t_e$ .

### 6.1.1.1 Preparing the reduced transient solution and interpolating the initial reduced basis

The preparation of the reduced transient solution takes place foremost in the classic domain of pre-processing. The mass and the damping matrix  $M$  and  $C$  are required as well as an expression for  $g(\mathbf{u})$ . Also the time history of the external forces  $\mathbf{f}_E(t)$  has to be defined. It is recalled at this point that the definition of the geometric nonlinearity as it is used in this work excludes the appearing of contact forces, so that the entire time history of the external forces is known prior to the solution. All these pre-processing tasks take place at full order and can be obtained from a commercial finite element solver.

If the variant of the polynomial expression of full order identification with included reduction is chosen, the necessary tensors  $\mathbf{A}^{(1)}$ ,  $\mathbf{A}^{(2)}$  and  $\mathbf{A}^{(3)}$  are required to be identified now by using the expression for  $g(\mathbf{u})$  and the identification procedure from section 5.2.2.4.

For the parameterisation a number of representative operating points  $\{\boldsymbol{\mu}_1, \dots, \boldsymbol{\mu}_m\}$  have to be stored in or retrieved from a database to become available at the beginning of the transient solution. The actual operating point  $\boldsymbol{\mu}_0$ , at which the reduced transient solution is supposed to take place, has also to be defined. It is supposed that  $\boldsymbol{\mu}_0 \notin \{\boldsymbol{\mu}_1, \dots, \boldsymbol{\mu}_m\}$ . Also it is supposed that the operating point only influences the reduced basis and maybe the initial conditions, too, in order to streamline the presentation. All other quantities that are describing the system, notably  $M$ ,  $C$  and  $\mathbf{f}_E(t)$ , are supposed to be independent from the operating point. Should the SPD matrices among these quantities depend on external parameters a dedicated interpolation approach is available in section 5.3.2.1. If the initial conditions  $\mathbf{u}_0 = \mathbf{u}(t_0)$  and  $\dot{\mathbf{u}}_0 = \dot{\mathbf{u}}(t_0)$  are not depending on the operating point they are also given at this stage.

Finally, the order of the reduced model  $r$  has to be determined along with a choice for the method of generating the reduced basis. These decisions are difficult to make because, first, they require knowledge

of the behaviour of the structure and, second, they are not independent from each other. For example, if a structure is subjected to an external loading that provokes foremost torsion and this structure is to be reduced with the LNM, the  $r$  has to be chosen in such a way that also torsion modes are included in the reduced basis. Other approaches from section 3.3 for creating the basis, such as e.g. the POD, do provide decision criteria, e.g. the energy ratio that are somewhat more targeted. In any case, these difficult decisions remain with the engineer and his or her experience.

A decision of comparable difficulty is the choice of the values for the parameters of the solution procedure, especially the time-step  $\Delta t$ , the parameters  $\alpha$  and the threshold for convergence  $\epsilon$ , as well as the parameters for the updating and augmentation, notably the threshold for triggering the update  $\epsilon_r$  and the retainer  $m_r$ .

### 6.1.1.2 Initialising and computing the reduced transient solution with basis update and augmentation

The time-marching solution algorithm is the backbone of the solution process. It is initialised with the interpolated reduced basis and all other variables, which are prepared in the section above. In the following the reduced HHT- $\alpha$ -method from section 3.2.2.2 is developed in its full extension. This includes the introduction of the polynomial formulation from section 5.2.2 to ensure the autonomy of the reduced nonlinear terms and the introduction of the two metrics of the derivation of the initial reduced residual  $|\frac{d\|\tilde{r}_{(i=1)}\|}{dt}|$  and of the retainer  $m$ , which govern the update process, into the reduced HHT- $\alpha$ -method. The update and augmentation itself is, for now, only mentioned as a self-contained block, which is introduced in the time-marching algorithm at a given position and only called when the two metrics allow its execution. This is possible because the update and augmentation algorithm in section 5.1.3 is constructed explicitly as such a self-contained block and the reduced HHT- $\alpha$ -method that surrounds this self-contained block is oblivious to its presence. Everything that happens inside the block of the actual update and augmentation is described in the section 6.1.1.3 below.

The first step towards reducing the system and to use the resulting reduced model for a transient solution is to provide the reduced basis  $\Phi_0$ . This initial reduced basis is to serve until the first update and augmentation. It is obtained at the actual operating point  $\mu_0$  with the interpolation method from section 5.3.2.

To prepare the interpolation a database of reduced bases  $\{\Phi_1, \dots, \Phi_m\}$  at the given operating points  $\{\mu_1, \dots, \mu_m\}$  is established. The initial basis  $\Phi_0$  is established by following the four-step approach from Amsellem [12], as it is presented in section 5.3.2.2. An origin of the interpolation  $\mu_k$  is chosen among the given operating points in the database. The database of the reduced basis is transformed in the tangent space with equations (5.112) and (5.113). The interpolation takes place with the multiparameter interpolation from section 5.3.2.3. The interpolated basis is retransformed by equations (5.114) and (5.114).

With the initial reduced basis  $\Phi_0$  available, the reduced matrices  $\tilde{M} = \Phi_0^T M \Phi_0$  and  $\tilde{C} = \Phi_0^T C \Phi_0$  can be established with equations (3.7) and (3.8), respectively. If a suitable database is available, these matrices can also be established with the interpolation of SPD-matrices in section 5.3.2.1 as a function of the actual operating point  $\mu_0$ .

The initial conditions of the reduced system can be obtained in the least-squares sense from the initial conditions of the full order system. by simply putting

$$q_0 = (\Phi_0^T \Phi_0)^{-1} \Phi_0^T \mathbf{u}(t_0), \quad (6.1)$$

$$\dot{q}_0 = (\Phi_0^T \Phi_0)^{-1} \Phi_0^T \dot{\mathbf{u}}(t_0). \quad (6.2)$$

If the initial conditions  $\mathbf{u}(t_0)$  depend on the operating point  $\mu_0$ , as this is e.g. the case with prestressing, a more sophisticated approach, e.g. a reduced static solution under the prestressing force, might be necessary

at this point to obtain the generalised initial conditions<sup>1</sup>. The initial external forces are known because they are supposed to depend only on the time  $t$ . They are reduced to the vector of the reduced external forces as

$$\tilde{\mathbf{f}}_E(t_0) = \Phi_0^T \mathbf{f}_E^{(0)}. \quad (6.3)$$

The counter for the retainer is also initialised to  $m = 1$ .

In order to prepare the polynomial expression, providing that the variant of the reduced order identification is chosen, the reduced tensors  $\tilde{\mathbf{A}}^{(1)}$ ,  $\tilde{\mathbf{A}}^{(2)}$  and  $\tilde{\mathbf{A}}^{(3)}$  are identified. This requires the initial reduced basis  $\Phi_0$ , the expression of the full order nonlinear internal forces  $\mathbf{g}(\mathbf{u})$  from the pre-processing and the identification procedure from Muravyov and Rizzi [155] as it is described in section 5.2.2.2. If, on the other hand, the variant of full order identification with included reduction is chosen and the full order tensors  $\mathbf{A}^{(1)}$ ,  $\mathbf{A}^{(2)}$  and  $\mathbf{A}^{(3)}$  are already available, they have to be reduced with  $\Phi_0$  and the procedure proposed by Phillips [179] and described in section 5.2.2.4.

With all these preparations provided for, the reduced transient solution itself can be launched. It is based on the reduced nonlinear Newmark scheme from section 3.2.2.1 with the adaptation for the HHT- $\alpha$ -method from section 3.2.2.2. This algorithm contains the monitoring of the derivation  $|\frac{d\|\tilde{\mathbf{r}}\|}{dt}|$  from equation (5.30) that is responsible for triggering the update and augmentation of the reduced basis. The polynomial expressions from section 5.2.2 replace the reduced nonlinear terms in order to render the reduced system autonomous.

The state of the system at  $t_0$  is completed by applying equation (3.76) in order to obtain the generalised accelerations

$$\begin{aligned} \ddot{\mathbf{q}}^{(0)} = & \tilde{\mathbf{M}}^{-1} \left( \tilde{\mathbf{f}}_E(t_0) - \tilde{\mathbf{C}}\dot{\mathbf{q}}^{(0)} \right. \\ & \left. - \left( \tilde{\mathbf{A}}^{(1)}\mathbf{q}^{(0)} + \tilde{\mathbf{A}}^{(2)}\left(\mathbf{q}^{(0)} \otimes \mathbf{q}^{(0)}\right) + \tilde{\mathbf{A}}^{(3)}\left(\mathbf{q}^{(0)} \otimes \mathbf{q}^{(0)} \otimes \mathbf{q}^{(0)}\right) \right) \right). \end{aligned} \quad (6.4)$$

Together with the initial conditions from equations (6.1) and (6.2), these generalised accelerations describe the entire state of the system at  $t_0$ . Here the polynomial formulation of the generalised nonlinear internal forces  $\tilde{\mathbf{g}}(\mathbf{q})$  from equation (5.64) is used. The following course of action is valid for advancing from any completely defined state  $t$  to the next instant  $t + \Delta t$ .

First and foremost the need for an update of the reduced basis is determined. Introducing the update and augmentation of the reduced basis at this point corresponds to the position one, with an update at the beginning of each time-step, based on the solution of the previous time-step. This decision is made in section 5.1.3.2 and verified numerically.

The update and augmentation of the reduced basis is triggered with the derivation of the residual with respect to time. This requires the current reduced residual, which is calculated as

$$\begin{aligned} \tilde{\mathbf{r}}^{(t)} = & \tilde{\mathbf{f}}_E(t) - \tilde{\mathbf{M}}\ddot{\mathbf{q}}^{(t)} - \tilde{\mathbf{C}}\dot{\mathbf{q}}^{(t)} \\ & - \left( \tilde{\mathbf{A}}^{(1)}\mathbf{q}^{(t)} + \tilde{\mathbf{A}}^{(2)}\left(\mathbf{q}^{(t)} \otimes \mathbf{q}^{(t)}\right) + \tilde{\mathbf{A}}^{(3)}\left(\mathbf{q}^{(t)} \otimes \mathbf{q}^{(t)} \otimes \mathbf{q}^{(t)}\right) \right). \end{aligned} \quad (6.5)$$

Actually, this residual is carried over from the preceding converged inner iterations of the preceding time-step. The equation above is placed here only for illustrative purposes. This residual is used to approximate

<sup>1</sup>The inclusion of the prestressing force  $\mathbf{f}_{E,a}$  is given by equation (6.44). Using this definition, equation (6.3) would become  $\tilde{\mathbf{f}}_E(t_0) = \Phi_0^T \mathbf{f}_E^{(0)} + \Phi_0^T \mathbf{f}_{E,a}$  if prestressing is included. Notably prestressing might also require the addition of a static component to the external forces  $\mathbf{f}_E(t)$ , as detailed in section 6.3.2.

the derivation of the initial residual as backward finite difference

$$\left| \frac{d \|\tilde{\mathbf{r}}\|}{dt} \right| \approx \left| \frac{\|\tilde{\mathbf{r}}^{(t)}\| - \|\tilde{\mathbf{r}}^{(t-\Delta t)}\|}{\Delta t} \right| \quad (6.6)$$

as done in equation (5.30). If the current time is  $t = t_0$  the  $\|\tilde{\mathbf{r}}^{(t_0-\Delta t)}\|$  is set to 0. Alongside the determination of the  $\left| \frac{d\|\tilde{\mathbf{r}}\|}{dt} \right|$  the counter for the retainer is augmented with

$$m \rightarrow m + 1. \quad (6.7)$$

If the two conditions  $\left| \frac{d\|\tilde{\mathbf{r}}_{(i=1)}\|}{dt} \right| \geq \epsilon_r$  and  $m \geq m_r$  are met the transient solution is paused at this point and a new basis is introduced. This is discussed in the section 6.1.1.3, below. Regardless of whether an update has taken place or not, the transient solution is continued with establishing the dynamic equilibrium at the instant  $t + \alpha\Delta t$ .

The inner, iterative loop over the index ( $i$ ) is initialised with

$$\ddot{\mathbf{q}}_{(i=1)}^{(t+\Delta t)} = \ddot{\mathbf{q}}^{(t)} \quad (6.8)$$

$$\dot{\mathbf{q}}_{(i=1)}^{(t+\Delta t)} = \dot{\mathbf{q}}^{(t)} + \Delta t \ddot{\mathbf{q}}^{(t)} \quad (6.9)$$

$$\mathbf{q}_{(i=1)}^{(t+\Delta t)} = \mathbf{q}^{(t)} + \Delta t \dot{\mathbf{q}}^{(t)} + \frac{1}{2} \Delta t^2 \ddot{\mathbf{q}}^{(t)}. \quad (6.10)$$

While the index  $i$  is still in its first loop, the initial generalised residual is extracted

$$\begin{aligned} \tilde{\mathbf{r}}_{(i=1)}^{(t+\Delta t)} &= \tilde{\mathbf{f}}_E(t + \Delta t) - \tilde{\mathbf{M}}\ddot{\mathbf{q}}_{(i=1)}^{(t+\Delta t)} - \tilde{\mathbf{C}}\dot{\mathbf{q}}_{(i=1)}^{(t+\Delta t)} \\ &\quad - \left( \tilde{\mathbf{A}}^{(1)}\mathbf{q}_{(i=1)}^{(t+\Delta t)} + \tilde{\mathbf{A}}^{(2)}\left(\mathbf{q}_{(i=1)}^{(t+\Delta t)} \otimes \mathbf{q}_{(i=1)}^{(t+\Delta t)}\right) + \tilde{\mathbf{A}}^{(3)}\left(\mathbf{q}_{(i=1)}^{(t+\Delta t)} \otimes \mathbf{q}_{(i=1)}^{(t+\Delta t)} \otimes \mathbf{q}_{(i=1)}^{(t+\Delta t)}\right) \right). \end{aligned} \quad (6.11)$$

The initial values for the generalised velocities and the generalised coordinates are established with equations (6.9) and (6.10). The predictive values are

$$\mathbf{q}_{(i)}^{(t+\alpha\Delta t)} = (1 - \alpha)\mathbf{q}^{(t)} + \alpha\mathbf{q}_{(i-1)}^{(t+\Delta t)}, \quad (6.12)$$

and

$$\dot{\mathbf{q}}_{(i)}^{(t+\alpha\Delta t)} = (1 - \alpha)\dot{\mathbf{q}}^{(t)} + \alpha\dot{\mathbf{q}}_{(i-1)}^{(t+\Delta t)}. \quad (6.13)$$

The current residual is calculated as

$$\begin{aligned} \tilde{\mathbf{r}}_{(i)} &= \tilde{\mathbf{f}}_E(t + \Delta t) - \tilde{\mathbf{M}}\ddot{\mathbf{q}}_{(i)}^{(t+\Delta t)} - \tilde{\mathbf{C}}\dot{\mathbf{q}}_{(i)}^{(t+\alpha\Delta t)} \\ &\quad - \left( \tilde{\mathbf{A}}^{(1)}\mathbf{q}_{(i)}^{(t+\alpha\Delta t)} + \tilde{\mathbf{A}}^{(2)}\left(\mathbf{q}_{(i)}^{(t+\alpha\Delta t)} \otimes \mathbf{q}_{(i)}^{(t+\alpha\Delta t)}\right) + \tilde{\mathbf{A}}^{(3)}\left(\mathbf{q}_{(i)}^{(t+\alpha\Delta t)} \otimes \mathbf{q}_{(i)}^{(t+\alpha\Delta t)} \otimes \mathbf{q}_{(i)}^{(t+\alpha\Delta t)}\right) \right). \end{aligned} \quad (6.14)$$

The Jacobian of the reduced model is obtained as

$$\tilde{\mathbf{S}}_{(i)} = \tilde{\mathbf{A}}^{(1)} + \tilde{\mathbf{A}}^{(2)} \delta \mathbf{q}_{(i)}^{(t+\alpha\Delta t)} + \tilde{\mathbf{A}}^{(3)} \delta \left( \mathbf{q}_{(i)}^{(t+\alpha\Delta t)} \otimes \mathbf{q}_{(i)}^{(t+\alpha\Delta t)} \right) + \frac{\gamma}{\beta \Delta t} \tilde{\mathbf{C}} + \frac{1}{\beta \Delta t^2} \tilde{\mathbf{M}}, \quad (6.15)$$

where the current tangent stiffness  $\tilde{\mathbf{K}}_{(i)}$  matrix is calculated by injecting  $\mathbf{q}_{(i)}^{(t+\alpha\Delta t)}$  into equation (5.90). The Jacobian is used together with the residual from equation (6.14) to calculate the increment of the generalised coordinates

$$\Delta \mathbf{q}_{(i)}^{(t+\Delta t)} = \tilde{\mathbf{S}}_{(i)}^{-1} \tilde{\mathbf{r}}_{(i)}. \quad (6.16)$$

With this increment available, the next values for the generalised coordinates, velocities and accelerations can be obtained as

$$\mathbf{q}_{(i+1)}^{(t+\Delta t)} = \mathbf{q}_{(i)}^{(t+\Delta t)} + \Delta \mathbf{q}_{(i)}^{(t+\Delta t)} \quad (6.17)$$

$$\dot{\mathbf{q}}_{(i+1)}^{(t+\Delta t)} = \dot{\mathbf{q}}_{(i)}^{(t+\Delta t)} + \frac{\gamma}{\beta \Delta t} \Delta \mathbf{q}_{(i)}^{(t+\Delta t)} \quad (6.18)$$

and

$$\ddot{\mathbf{q}}_{(i+1)}^{(t+\Delta t)} = \ddot{\mathbf{q}}_{(i)}^{(t+\Delta t)} + \frac{1}{\beta \Delta t^2} \Delta \mathbf{q}_{(i)}^{(t+\Delta t)}. \quad (6.19)$$

These values are used for determining the convergence of the inner Newton-Raphson iterations over the index  $i$ . The convergence criterion is to multiply the norm of the initial residual from equation (6.11) with a factor  $\epsilon \ll 1$  and to verify if the norm of the current residual in equation (6.14) is above or below this threshold value. If the convergence criterion is not met, the iteration index is augmented

$$i \rightarrow i + 1. \quad (6.20)$$

and the next iteration is launched by returning to equation (6.12). By cautiously choosing the value of  $\epsilon$ , the initial residual  $\tilde{\mathbf{r}}_{(i=1)}^{(t)}$  from equation (6.11) can be used to define the threshold of the residual  $\tilde{\mathbf{r}}_{(i)}$  from equation (6.14) that is defined partially at  $t + \alpha\Delta t$ .

If, on the other hand, the convergence is given, the time is increased

$$t \rightarrow t + \Delta t. \quad (6.21)$$

and the HHT- $\alpha$ -method returns to equation (6.8) to launch the next iteration towards the next instant in time. This is repeated until the end  $t_e$  of the simulated time period is reached.

This short sketch of the autonomous reduced HHT- $\alpha$ -methods demonstrates how easy it is in fact to integrate the polynomial formulation of the nonlinear terms in the solution procedure. However, it should not be forgotten that this requires the considerable amount of preparation that is developed in section 5.2.2.

Also the integration of the measures  $\left| \frac{d\|\tilde{\mathbf{r}}_{(i=1)}^{(t)}\|}{dt} \right|$  in equation (6.6) and  $m$  in equation (6.7), that govern the updating and augmentation of the reduced basis, pose no particular problem. Due to the monolithic

structure of the basis update and augmentation method developed in section 5.1.3, this adaptation of the solution algorithm also integrates flawlessly.

### 6.1.1.3 Performing the basis update and augmentation and continuing the reduced transient solution

The thresholds  $\epsilon_r$  and  $m_r$ , that govern the triggering of the updating and augmentation of the reduced basis, are integrated into the autonomous reduced HHT- $\alpha$ -method with the equations (6.6) and (6.7) that provide the two metrics  $\left| \frac{d\|\tilde{\mathbf{r}}_{(i=1)}\|}{dt} \right|$  and  $m$ , respectively. If these metrics trigger an update the approach that is developed in section 5.1.3 can be inserted as a self-contained block at the position one, between equation (6.11) and (6.12) of the autonomous reduced HHT- $\alpha$ -method above, at the beginning of the current time-step and based on the solution of the previous time-step, as it is determined in section 5.1.3.2. The sequence of the autonomous reduced HHT- $\alpha$ -method remains oblivious to the introduction of the new basis.

In detail the update and augmentation process takes the following ten steps

1. At the instant of the update the solution is inflated to full order with the current reduced basis. For the displacements the inflation reads  $\mathbf{u}^{(t)} = \Phi^{(t-m\Delta t)} \mathbf{q}^{(t)}$  and it is performed in an analogous manner for the velocities and the accelerations.
2. The current generalised state is stored as  $\mathbf{q}_{\text{before}}^{(t)}$ ,  $\dot{\mathbf{q}}_{\text{before}}^{(t)}$  and  $\ddot{\mathbf{q}}_{\text{before}}^{(t)}$ .
3. The preliminary new basis  $\check{\Phi}^{(t)}$  becomes available through application of the method for creating the reduced basis that is chosen prior to the solution. For the example of the LNM at a given displacement from section 3.3.1.2 this becomes

- the full order tangent stiffness matrix  $\mathbf{K}^{(t)} = \left. \frac{\partial \mathbf{g}(\mathbf{u})}{\partial \mathbf{u}} \right|_{\mathbf{u}^{(t)}}$  is established with the inflated full order solution
- it is then used in equations (3.113) and (3.114) to obtain the updated reduced basis  $\check{\Phi}^{(t)}$
- this preliminary reduced basis  $\check{\Phi}^{(t)}$  is of order  $r$

4. The preliminary generalised coordinates are established as

$$\check{\mathbf{q}}^{(t)} = \left( \left( \check{\Phi}^{(t)} \right)^T \check{\Phi}^{(t)} \right)^{-1} \left( \check{\Phi}^{(t)} \right)^T \mathbf{u}^{(t)}, \quad (6.22)$$

The same is done to obtain the preliminary generalised velocities  $\dot{\check{\mathbf{q}}}^{(t)}$  and accelerations  $\ddot{\check{\mathbf{q}}}^{(t)}$ .

5. The jumps are calculated by applying equation (5.38) for the generalised coordinates

$$\Delta \mathbf{u}^{(t)} = \Phi^{(t-m\Delta t)} \mathbf{q}_{\text{before}}^{(t)} - \check{\Phi}^{(t)} \check{\mathbf{q}}^{(t)} \quad (6.23)$$

and equations (5.39) and (5.40) for the velocities and accelerations, respectively.

6. The updated and augmented reduced basis is provided by equation (5.41) as

$$\Phi^{(t)} = \left[ \check{\Phi}^{(t)}, \Delta \mathbf{u}, \Delta \dot{\mathbf{u}}, \Delta \ddot{\mathbf{u}} \right]. \quad (6.24)$$

This basis is now of order  $r + 3$ , where  $r$  is the order that is chosen initially prior to the solution. The order of  $\Phi^{(t)}$  in equation (6.24) does not change with the number of updates that have already taken place since the beginning of the reduced solution at  $t_0$ .

7. The new generalised coordinates are augmented, too, by applying equations (5.42) to (5.44). For the

generalised coordinates this reads

$$\mathbf{q}^{(t)} = \begin{bmatrix} \tilde{\mathbf{q}}^{(t)} \\ 1 \\ 0 \\ 0 \end{bmatrix}. \quad (6.25)$$

The same augmentation is applied to the velocities

$$\dot{\mathbf{q}}^{(t)} = \begin{bmatrix} \dot{\tilde{\mathbf{q}}}^{(t)} \\ 0 \\ 1 \\ 0 \end{bmatrix}, \quad (6.26)$$

and to the accelerations

$$\ddot{\mathbf{q}}^{(t)} = \begin{bmatrix} \ddot{\tilde{\mathbf{q}}}^{(t)} \\ 0 \\ 0 \\ 1 \end{bmatrix}. \quad (6.27)$$

These three vectors are augmented to link them with the jumps of the augmented reduced basis from equation (6.24).

8. The left-hand reduced basis is set as  $\Psi = (\Phi^{(t)})^T$ .
9. The two static matrices  $M$  and  $C$  are reduced with the updated and augmented reduced basis  $\Phi^{(t)}$  in order to correspond to the new generalised coordinates.
10. The counter for the retainer is reset to  $m = 0$  in order to indicate that an update took place and to block the update for the following  $m_r$  time-steps.

Once the new reduced basis  $\Phi^{(t)}$  is available, the tensors  $\tilde{\mathbf{A}}^{(1)}$ ,  $\tilde{\mathbf{A}}^{(2)}$  and  $\tilde{\mathbf{A}}^{(3)}$  have to be identified again with the updated and augmented basis from equation (6.24). Corresponding to the chosen variant of the identification algorithm this is done either by the renewed reduction of the full order tensors or by a renewed direct identification of the reduced tensors. This step promises to become the computationally most costly part of the update of the reduced basis, and a dedicated study is performed to decide on the variant of the polynomial formulation that is most suited. Once the ten steps plus the additional adaptation of the tensors have been performed, the HHT- $\alpha$ -method can continue without becoming aware of the updated and augmented basis.

### 6.1.2 Integrating the autonomous formulation and the update and augmentation on the academic test-cases

This section takes the numerical experiments on the academic test-cases from the section 5.2.4, where the polynomial expression is explored, and adds the updating method for the reduced basis that is developed in section 5.1.3.1. The aim is to understand how these two major aspects of a successful reduction interact. The result is a first validation of the integrated solution method with a polynomial expression of the nonlinear terms and update and augmentation of the reduced basis as it is described in the previous section 6.1.1.

### 6.1.2.1 Presenting an exemplary result and determining the variant of the indirect identification of the polynomial formulation

In particular it is to be studied which variant of the polynomial expression for the reduced nonlinear terms is compatible with the update and augmentation method for the reduced basis. The listing on page 187 contains the variants of full order identification with trailing reduction, full order identification with included reduction and reduced order identification. The full order identification with trailing reduction is not included because evaluating constantly the initial equation (5.58) just for the internal nonlinear forces is deemed too costly. Furthermore, only the variants full order identification with included reduction and reduced order identification offer a real interest in the context of an already reduced system. These two variants are included in the current study.

As a first demonstration the entirely nonlinear system under harmonic excitation is subjected to the integrated solution procedure. The applied solution procedure takes the classic reduced nonlinear Newmark scheme as backbone. This is identified as the algorithm to be preferred for the academic test-cases in chapter 4 and presented in detail in section 3.2.2.1. The solution procedure is thus not entirely the one described in the section 6.1.1, because the HHT- $\alpha$ -method is replaced by the nonlinear Newmark scheme. The reduction takes place with LNM at the current displacement with  $r = 8$  as the order of the reduced system. All parameters are taken from the definition of the academic test-cases in section 4.1.3.4.

As variants of the polynomial formulation of the nonlinear terms the full order identification with included reduction and the reduced order identification are included. They are described in detail in the listing in section 5.2.2.6.

Table 6.1 shows error metrics for the different solutions. Two solutions are obtained with the full order identification variant of the polynomial formulation, one with a constant basis and one with an updated and augmented basis. While the solution with the constant basis delivers error metrics that indicate a largely useless reconstructed solution, the solution with the basis update fails completely. This is most probably due to the fact that the update of the reduced basis introduces small perturbations in the time histories of the displacements and that the tensor reduction process does not deliver accurate reductions. These two effects combine and make the solution fail to converge.

On the other hand, the tensors that are identified on the reduced level deliver good results with the constant basis. The addition of the update and augmentation still improves this good solution by a factor of nearly four in the mean of the R2MSE. The increase in the mean of the MAC between the physical deformations corroborates this tendency and shows that also the shape of the time histories of the solutions approach the reference solution.

identification		full order	full order	reduced order	reduced order
reduced basis		constant	updated	constant	updated
R2MSE mean	$e_r$	120.3726	—	0.4030	0.1110
R2MSE var.	$v_r$	68.2303	—	0.0534	0.0387
MAC mean	$e_a$	0.0017	—	0.9205	0.9939

Table 6.1: The error metrics for the different solutions of the entirely nonlinear test-case under harmonic excitation

The time histories of the 16<sup>th</sup> degree of freedom are traced for the different solutions in figure 6.1. The solutions with the full order identification variant of the polynomial formulation are included as far as they converge numerically. After it is cut off, the solution with the constant reduced basis does not yield non-numerical values but behaves completely erratic. In both cases, without and with update, the solutions with the full order identification variant of the polynomial expressions are already largely departed from the reference solution by the time they cease to converge, thus nullifying the interest in their application even

## 6.1. UNITING THE THREE ELEMENTS AND APPLYING THE INTEGRATED METHOD

for initial calculations.

The two solutions with the reduced order identification variant of the polynomial formulation confirm their good recreation of the reference solution that is already indicated by the error metrics in the table 6.1. The solution with the constant reduced basis follows the development of the reference solution already very well. Both, the reduced solution with the constant basis and the reduced solution with the updated and augmented basis, deliver comparable oscillations. The reduced solution with a constant basis could be considered as slightly more conservative, but this effect remains marginal. Including the update and augmentation block makes the resulting solution adapt even closer to the time history of the displacement. The reduced solution and the reference solution remain distinguishable, so no direct match is given. The inclusion of the updating and augmentation block unfolds to its full effect later in the solution, when the solution with the reduced basis starts to lead the reference solution. Here, beyond  $t = 35$ , the update and augmentation of the reduced basis prevents a phase shift between the reconstructed solution and the reference solution.

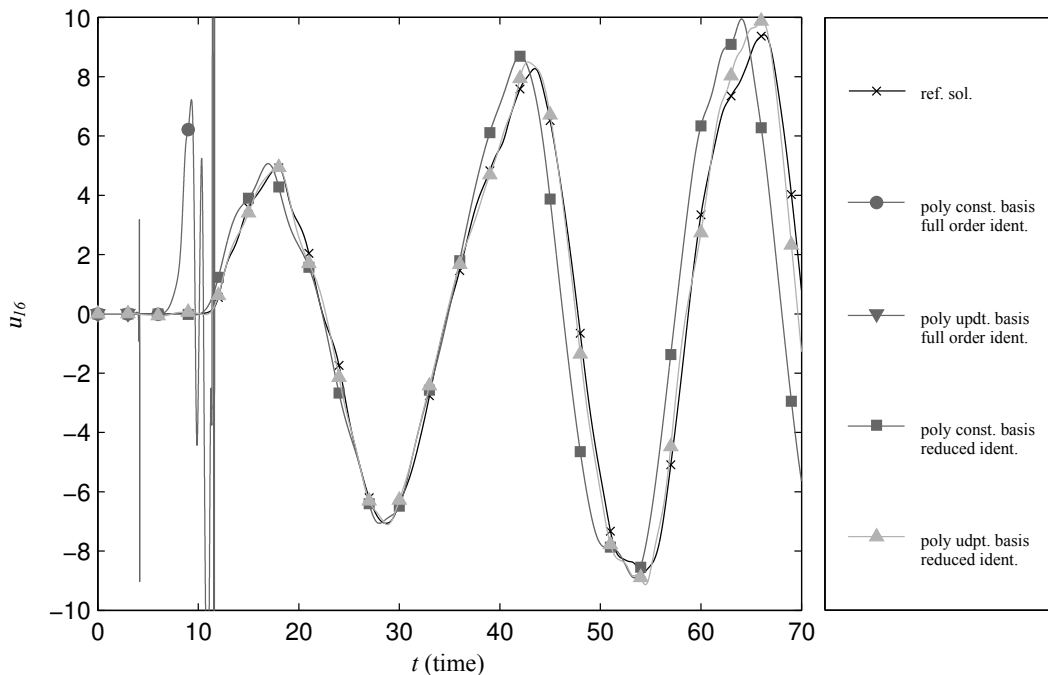


Figure 6.1: The time histories of the 16<sup>th</sup> degree of freedom of the entirely nonlinear system under harmonic excitation obtained with different reduced solutions with LNM at  $r = 8$

As outcome of this first, explorative application of the update and augmentation of the reduced basis, it can be noted that this application is very beneficial for the reduced transient solution of the studied case. The update of the reduced basis seems to correct the lag or lead of the reduced solution with respect to the reference solution. For a successful application of the integrated solution procedure, the tensors of the polynomial formulation of the nonlinear terms have to be identified directly at the reduced level. This corresponds to the original approach by Muravyov and Rizzi [155] as it is described in section 5.2.2.2. The reversal of the order of reduction and identification, which is introduced in section 5.2.2.4, can thus likely be considered as not useful for the type of nonlinearities that are treated in this study.

### 6.1.2.2 Observing the dynamic disequilibrium directly after the update and augmentation and proposing a possible remedy

If it is observed very closely, the time-history obtained with the integrated method in figure 6.1 displays a tiny flicker directly after the update and augmentation. An example of such a flicker is shown in figure 6.2. It is an echo of the update and augmentation block that is executed immediately before. The update and augmentation take place at  $t = 34.6130$ . The origin of the flicker is the struggle of the non-linear Newmark-scheme to preserve the convergence of the solution directly subsequent to the update and augmentation. While the augmentation of the reduced basis ensures the continuity of the physical quantities of displacements, velocities and accelerations it does so at the price of injecting a major dynamic disequilibrium into the course of the transient solution. The flicker only occurs for the integrated method with its combination of update and augmentation with the polynomial formulation of the nonlinear terms. The inflation formulation of the nonlinear terms is apparently robust enough to suppress the flicker. The approximation of the nonlinear forces with the polynomial formulation introduces an error that becomes manifest in the flicker.

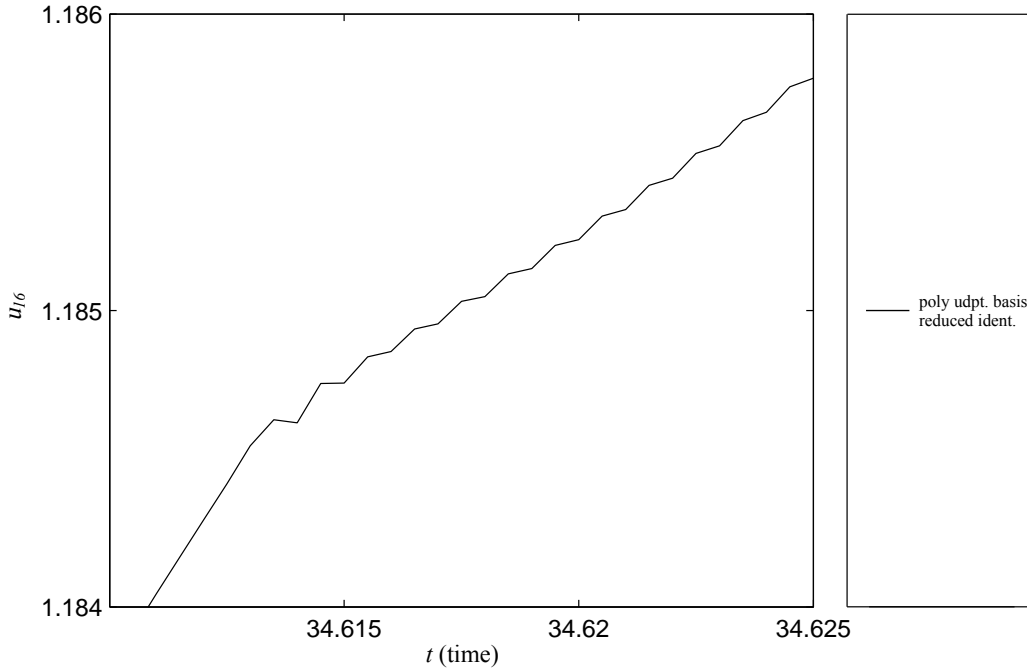


Figure 6.2: The time history of the 16<sup>th</sup> degree of freedom of the entirely nonlinear system under harmonic excitation obtained with the integrated method with LNM at  $r = 8$

The augmented generalised coordinates from equations (6.25) to (6.27) do not fulfil the dynamic equilibrium. While the dynamic equilibrium at the current  $t$  holds in generalised coordinates in  $\Phi^{(t-m\Delta t)}$  and in physical displacements, this is no longer the case after the update. In particular, it can be stated that

$$\left(\Phi^{(t)}\right)^T M \Phi^{(t)} \begin{bmatrix} \ddot{\tilde{q}} \\ 0 \\ 0 \\ 1 \end{bmatrix} + \left(\Phi^{(t)}\right)^T C \Phi^{(t)} \begin{bmatrix} \dot{\tilde{q}} \\ 0 \\ 1 \\ 0 \end{bmatrix} + \left(\Phi^{(t)}\right)^T g \left( \Phi^{(t)} \begin{bmatrix} \tilde{q} \\ 1 \\ 0 \\ 0 \end{bmatrix} \right) \neq \left(\Phi^{(t)}\right)^T f_e(t), \quad (6.28)$$

even if the inflation formulation for the nonlinear forces is used.

This condition has no direct influence on the physical solution, because the physical displacements at the instant  $t$  are obtained with the generalised coordinates prior to the update in the basis  $\Phi^{(t-m\Delta t)}$ , where convergence is achieved. Furthermore, the new, augmented reduced quantities  $[\tilde{\mathbf{q}}; 1; 0; 0]$ ,  $[\dot{\tilde{\mathbf{q}}}; 0; 1; 0]$  and  $[\ddot{\tilde{\mathbf{q}}}; 0; 0; 1]$  serve only as basis points for the predictive values in equations (6.12) and (6.13) for the next inner iterations of the solution algorithm towards the instant  $t + \Delta t$ .

However, the condition of disequilibrium, that is expressed in equation (6.28), might impede the ability of the inner convergence loop of the solution algorithm if its values for the reduced quantities are used as basis for the predictive values. Should this become the case, it might be advisable to accept jumps in the accelerations while allowing for the dynamic equilibrium at the instant  $t$  after the update. This leads to a new, updated and augmented reduced basis

$$\Phi^{(t)} = [\check{\Phi}^{(t)}, \Delta \mathbf{u}, \Delta \dot{\mathbf{u}}], \quad (6.29)$$

which is an adaptation of equation (6.24). The generalised coordinates and velocities are adapted accordingly. The equations (6.25) and (6.26) now read

$$\mathbf{q}^{(t)} = \begin{bmatrix} \tilde{\mathbf{q}}^{(t)} \\ 1 \\ 0 \end{bmatrix} \quad (6.30)$$

and

$$\dot{\mathbf{q}}^{(t)} = \begin{bmatrix} \dot{\tilde{\mathbf{q}}}^{(t)} \\ 0 \\ 1 \end{bmatrix}, \quad (6.31)$$

respectively.

The equation (6.27) is replaced with the determination of the generalised accelerations from the dynamic equilibrium

$$\begin{aligned} \ddot{\mathbf{q}}^{(t)} = & \tilde{\mathbf{M}}^{-1} \left( \left( \Phi^{(t)} \right)^T \mathbf{f}_e(t) - \tilde{\mathbf{C}} \dot{\mathbf{q}}^{(t)} \right. \\ & - \left( \tilde{\mathbf{A}}^{(1)} \mathbf{q}^{(t)} + \tilde{\mathbf{A}}^{(2)} \left( \mathbf{q}^{(t)} \otimes \mathbf{q}^{(t)} \right) \right. \\ & \left. \left. + \tilde{\mathbf{A}}^{(3)} \left( \mathbf{q}^{(t)} \otimes \mathbf{q}^{(t)} \otimes \mathbf{q}^{(t)} \right) \right) \right). \end{aligned} \quad (6.32)$$

The reduced matrices and tensors are already built with the updated and augmented basis from equation (6.29).

This variation of the integrated method allows to conserve a converged solution. It also allows to solve the reduced system with an order of only  $r + 2$ . On the downside it leads to jumps in the accelerations. Furthermore it is required that the inner iterative loop of the solution algorithm is parameterised to handle the accelerations resulting from equation (6.32). Depending on the degree of disequilibrium their values may become substantial. If this is the case and the discontinuous accelerations are acceptable, this variation of the integrated method can improve the convergence of the reduced solution directly after the update. It also displays potential to do so at a lesser computational cost.

In severe cases of disequilibrium, with accelerations that become too large to recover the equilibrium

and to ensure the convergence, it might even be considered to project an extension of the treatment of the generalised accelerations to the generalised velocities. This would require an approach to repartition the necessary adaptations for the dynamic equilibrium between the augmented accelerations and the augmented velocities while ensuring the continuity of the physical displacements. Fortunately, this is not necessary for the test-cases that are treated in the context of this work.

### 6.1.2.3 Extending the application to other reduced bases

The results above are obtained exclusively with reduced bases obtained by applying the approach of the LNM at a given displacement from section 3.3.1.2. This approach is the natural choice for a basis that has to be updated. However, theoretically any of the approaches from presentation of the common reduced bases in section 3.3 can be used for creating the reduced basis during the update and augmentation. Given the limited performances of the reduced bases during the numerical studies in chapter 4 not all approaches are earmarked to be tested.

Below, the POD reduced bases are compared to the LNM bases. The astonishing result is that they perform worse than the LNM. This is most probably because the POD bases look back across the time history of the already established solution while the LNM use the current state of the system.

Another method whose application requires verification is the rotation of the reduced matrices that is introduced in section 5.3.2.4. The rotation is used to align the quantities of the reduced system on a common set of generalised coordinates. It is treated in the second paragraph of this section.

**6.1.2.3.1 Comparing the results obtained with the LNM and the POD reduced bases** The figures 6.3 to 6.6 trace the R2MSE  $e_r$  for the two academic systems under harmonic excitation. There are two figures for each system, one for the LNM reduced bases and one for the POD reduced bases. The results whose errors are shown in black are obtained with constant bases. These solutions with constant bases are obtained during the numerical study in section 4.2.1 and serve as a reference. The newly generated results from the integrated method with update and augmentation of the reduced basis and the polynomial expression for the nonlinear terms are shown in grey.

The most important result is that the two aspects of basis update and autonomy do not interfere with each other in the sense that they reverse already identified effects, such as e.g. the lower values for the error from the POD bases. All behaviours of the autonomous approximations identified in the previous section are still present in the solutions with the updated bases. Especially the results still highlight the tendency that the updated LNM tend to lead to an improvement in the quality of the reduced solution, while the update of the POD-bases tends to lead to a decreasing quality.

However, a major problem is the convergence of the autonomous solutions with basis update. Sometimes it is simply non-existent. This is especially the case for the entirely non-linear system in figures 6.5 and 6.6, where only the inflation solution exists. Here the two methods of autonomy and update undergo a major interaction.

The figures 6.3 to 6.6 indicate that the integration of an autonomous systems with basis update leads to considerable instabilities which prevent convergence. To counter this, the study is repeated with a considerably smaller time-step and relaxed convergence criteria. The smaller time-step leads to more numerical effort and so only a very small variety of alternatives are included in the current study. The most promising ingredients are selected.

These are the reduced bases formed by the Linear Normal Modes at  $r = 4$  for the reduction. As tangent modes they follow the evolution of the solution better for each update as e.g. the POD reduced bases. For the autonomy several variants of the polynomial approximation from the enumeration in section 5.2.2.6 are included.

## 6.1. UNITING THE THREE ELEMENTS AND APPLYING THE INTEGRATED METHOD

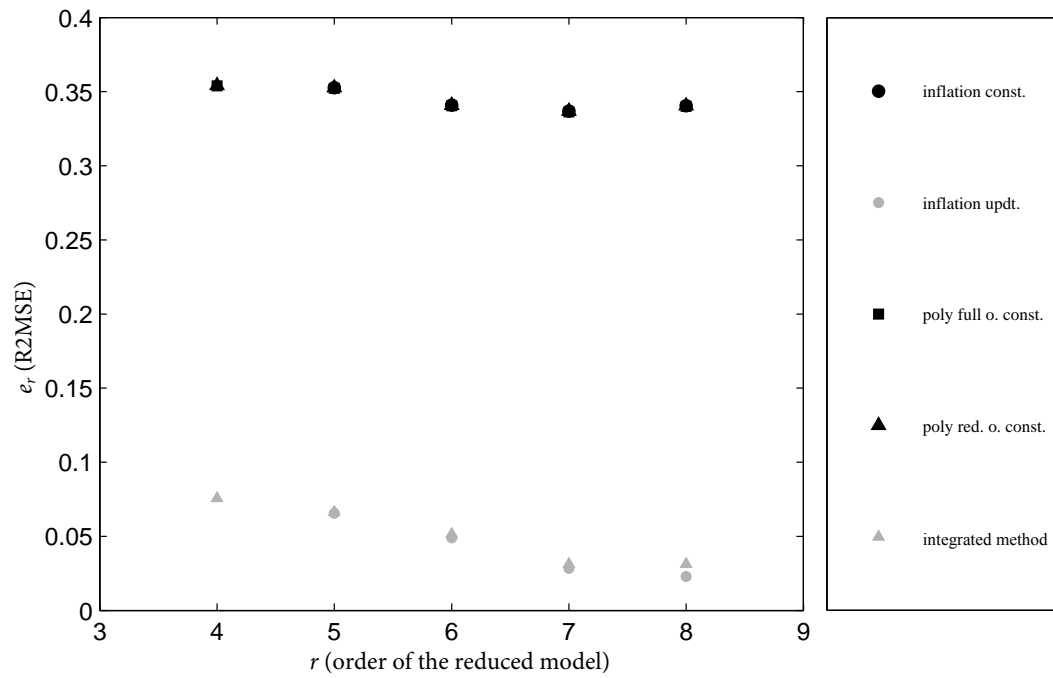


Figure 6.3: The R2MSE for the locally non-linear system under harmonic excitation for different autonomous approximations with constant and updated LNM bases

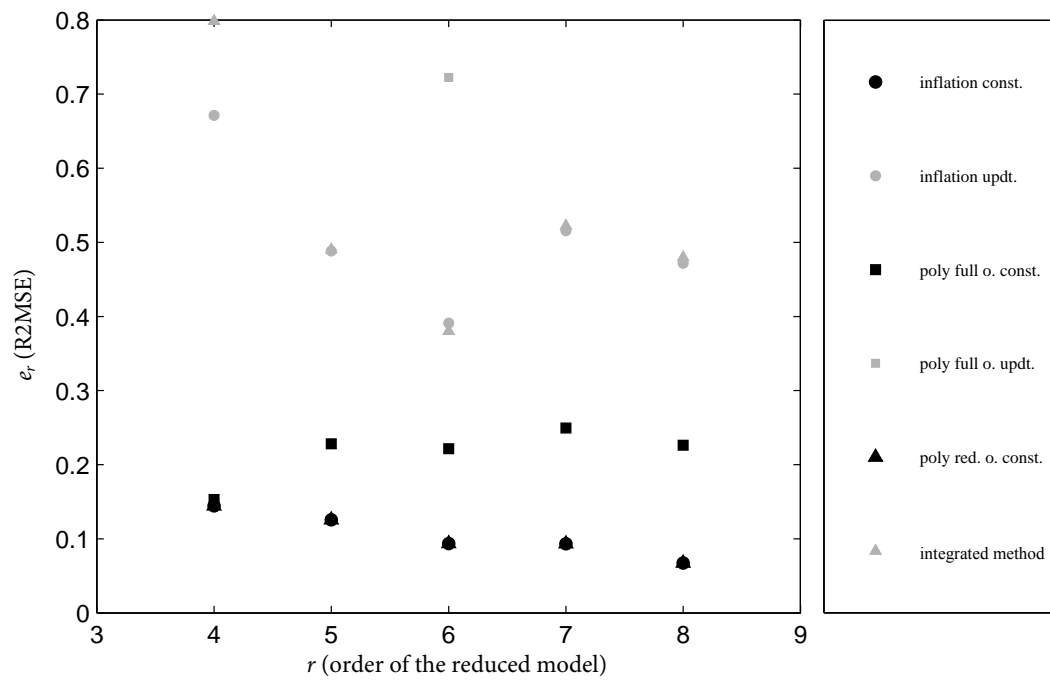


Figure 6.4: The R2MSE for the locally non-linear system under harmonic excitation for different autonomous approximations with static and updated POD bases

6.1. UNITING THE THREE ELEMENTS AND APPLYING THE INTEGRATED METHOD

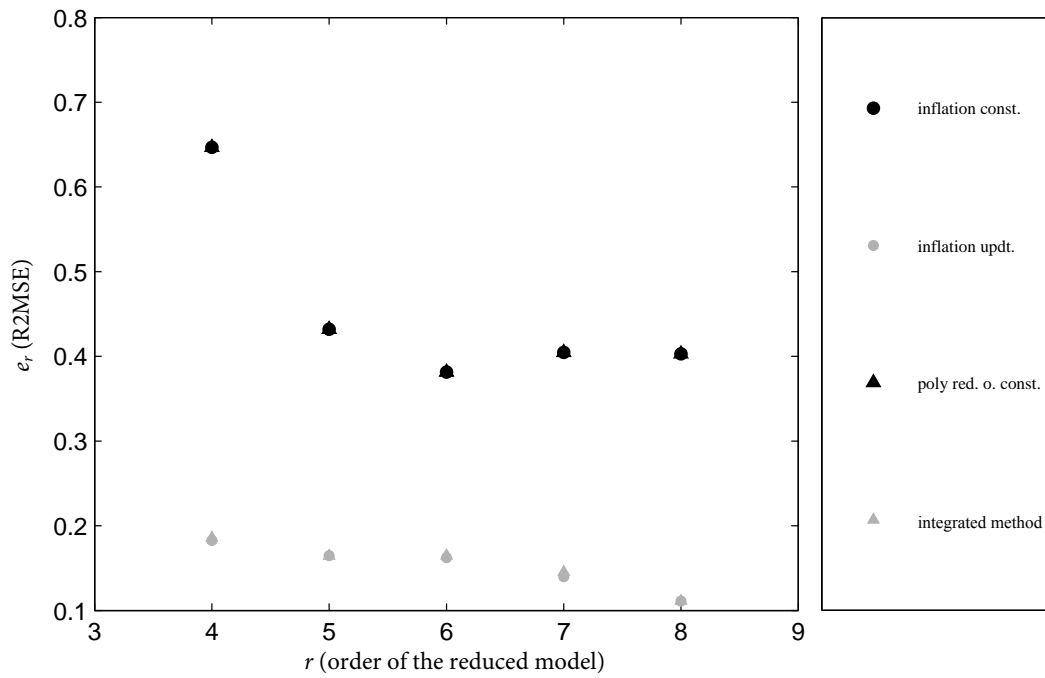


Figure 6.5: The R2MSE for the entirely non-linear system under harmonic excitation for different autonomous approximations with constant and updated LNM bases

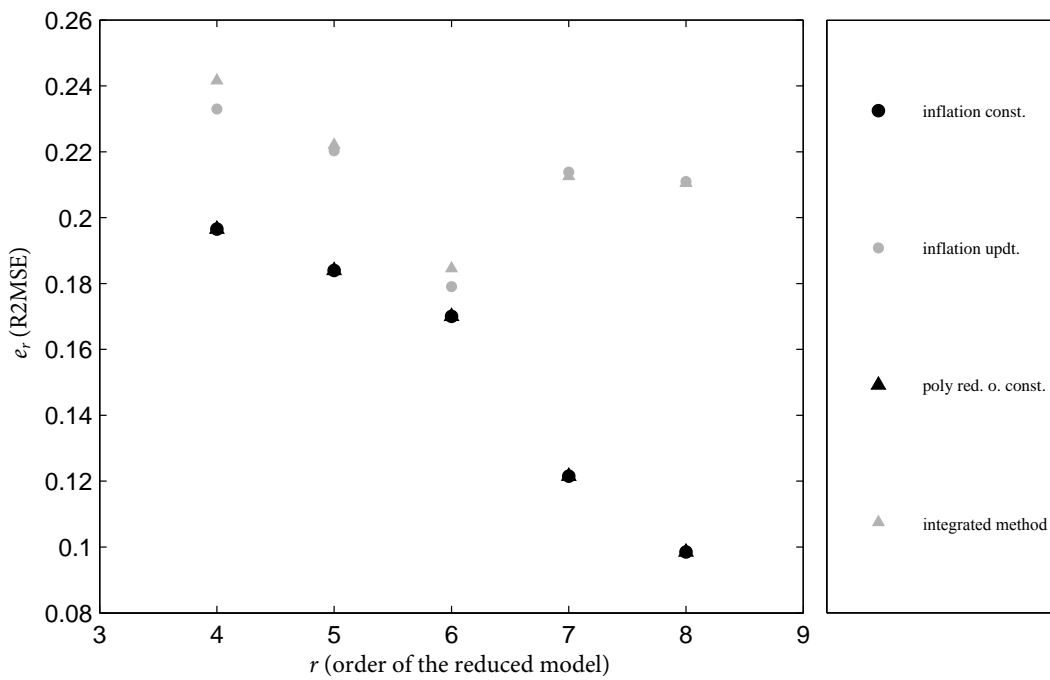


Figure 6.6: The R2MSE for the entirely non-linear system under harmonic excitation for different autonomous approximations with constant and updated POD bases

**6.1.2.3.2 Applying the rotation of the reduced matrices** The rotation algorithm is used to align the tensors of the polynomial approximation to the current basis after each update instead of identifying or reducing them again. It is detailed in section 5.3.2.4. Here it is applied to the locally and the entirely nonlinear systems under harmonic excitation and compared to other solution approaches. The results of this refined study are shown in table 6.2. It contains the error metrics of the mean  $e_r$  and the variance  $v_r$  of the R2MSE between the actual time history of the reconstructed displacements and the reference displacements that have been obtained at full order for the different solutions.

The locally non-linear system yields the results in the upper half of table 6.2 if solved with the different combinations of methods. The R2MSE values are with respect to the full order reference solution. For the autonomous reduced solution without update the identification of the tensors does only slightly influence the solution. This is no longer the case when the reduced basis is updated. The introduction of the rotation of the tensors shows to be very promising because the identical results indicate that the rotation of the tensors can in fact replace a renewed identification of the tensors. This renewed identification after an update takes place at reduced order but is costly all the same. Rather sobering are the results for the polynomial approximation with included reduction combined with an update. Here an additional mechanism has to be found to enhance the solution. An inspection of the time histories reveals that this method offers the best recreation of the amplitude, but often with an oscillation in the phase opposite to the one of the reference solution.

The results of the application of the methods to the entirely non-linear system are shown in the lower half of table 6.2. They demonstrate the advantage of the polynomial approximation with identification at reduced order over the polynomial approximation with included reduction. The solutions for the polynomial approximation with full order identification and included reduction fail to converge independently whether they are operating on a constant reduced basis or on an updated reduced basis. At the same time the polynomial approximation with reduced order identification gives a rather faithful recreation of the reference solution which is enhanced even more by including the update of the reduced basis. These two solutions distinguish themselves by a rather low variance of the R2MSE. If inspecting the physical displacements the polynomial approximation with reduced order identification offers a conservative recreation of the amplitude, i.e. the recreated amplitudes are slightly too large and not slightly as small as for the polynomial approximation with full order identification and included reduction. This has to be considered as rather advantageous from the practical point of view.

The fact that the two solutions with the polynomial approximation identified at reduced order and with update are identical seems to indicate that in these cases the update of the reduced basis is not triggered. This update is required to take place at least once in order to have the correct size of  $r + 3$  for the reduced system. After this initial update took place the rotation can replace the renewed identification. Because of this the approach of rotation is not pursued further.

solution of the locally non-linear system under harmonic excitation	R2MSE mean	R2MSE variance
	$e_r$	$v_r$
reduced, polynomial approximation (full order identification with included reduction), constant basis	0.2580	0.0617
reduced, polynomial approximation (reduced order identification), constant basis	0.2583	0.0617
reduced, polynomial approximation (full order identification with included reduction), update	0.8469	0.5230
reduced, polynomial approximation (reduced order identification), update	0.5475	0.2299
reduced, polynomial approximation (full order identification with included reduction), update, rotation	0.5475	0.2299
solution of the entirely non-linear system under harmonic excitation	R2MSE mean	R2MSE variance
	$e_r$	$v_r$
reduced, polynomial approximation (full order identification with included reduction), constant basis	not converged	
reduced, polynomial approximation (reduced order identification), constant basis	0.6472	0.0019
reduced, polynomial approximation (full order identification with included reduction), update	not converged	
reduced, polynomial approximation (reduced order identification), update	0.2637	0.0066
reduced, polynomial approximation (full order identification with included reduction), update, rotation	0.2637	0.0066

Table 6.2: The error metrics for the transient solutions of the academic systems obtained with different combinations of methods

## 6.2 Applying the integrated method to geometrically nonlinear bar elements

The application on a nonlinear finite element test-case is important because most research is conducted on linear finite element test-cases with artificial nonlinearities, e.g. Siller [206].

The geometric nonlinearities are weak and well-behaved. The nonlinearities are not strong in the sense that they produce some easily observable features in the time history of the displacements which identifies the problem as nonlinear. In fact, the nonlinearities are weak and make themselves felt only in the amplitude of the resulting motion. This renders the problem of a reduced system overly complex because the distinction between different solutions can only be made on quantitative grounds and not on the quality with which some characteristics of the transient solution are recreated.

The characterisation of the nonlinearity of the volume element might seem to be a self-evident necessity for assuring the quality of the implementation of the equations developed in section 2.2.3. However, in the present case an exact characterisation of the nonlinearity is important because it describes the context of the application of the developed methods and procedures. It becomes hence an important and central part of the study, as it may give indications on the extent and limitations of the applicability of the developed methods. Predicting the extent of the applicability is only possible on the grounds of a study with a correctly characterised nonlinearity.

### 6.2.1 Describing and characterising the test-case with nonlinear bar elements

The finite element test-case with bar elements is a precursor to the three-dimensional finite element test-case with volume elements. The bar elements are much more easily implemented, yet they allow gaining an impression of the types of consequences to be expected to result from the use of nonlinear finite elements. These should not be considerably different from the behaviour observed until now on the academic systems from section 4.1.3.1. If this is indeed the case can be easily verified due to the simple interpretation of the physical displacements of the bar elements.

In the following, the finite element test-case with bar elements is first described and then tested for different aspects of convergence. These aspects include the number of elements  $n$ , the physical property of the Young's modulus  $E$  and the different order  $r$  of a reduced model. All these tests are performed to demonstrate and to characterise the nonlinear behaviour of the test-case with bar elements. In a last step the thus characterised test-case with bar elements is used to demonstrate the superiority of an updated reduced basis over an equivalently sized constant reduced basis. The question leading to this test first arose in section 5.1.3.6.2. There, it is asked if using a constant basis of order  $r + 3$  could match the gains in quality of updating and augmenting a reduced basis of order  $r$ . The ensuing test is now repeated and confirms the initial result.

#### 6.2.1.1 Describing the test-case with bar elements

The elementary nonlinear bar is shown in figure 2.1 in the section 2.2.2 that introduces the nonlinear bar element and its discrete formulation. For the finite element test-case with bar elements a number  $n$  of these elementary bars is assembled. The resulting bar is clamped at one end and subjected to a harmonic external forcing at the other end. The whole bar is supposed to be supported laterally, so that no buckling can occur. This assembly is shown in figure 6.7.

Its physical properties are

- $L = 4$  m for the overall length,
- $A = 0.02$  m<sup>2</sup> for the constant section area,

## 6.2. APPLYING THE INTEGRATED METHOD TO GEOMETRICALLY NONLINEAR BAR ELEMENTS

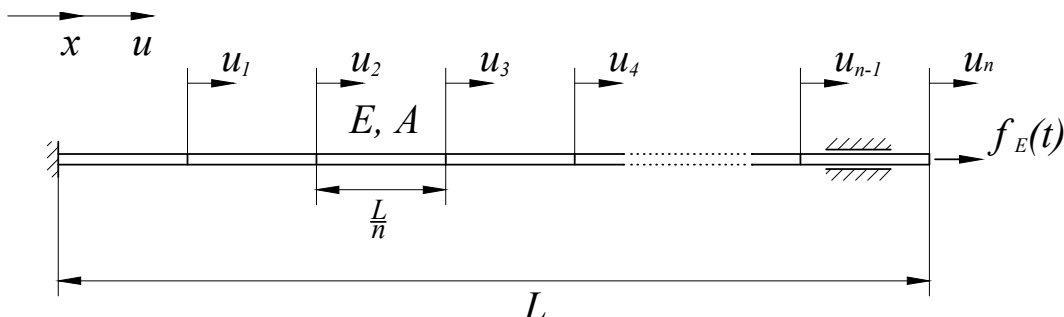


Figure 6.7: The finite element test-case with nonlinear bar elements

- $E = 20 \cdot 10^3 \frac{\text{N}}{\text{m}^2}$  as constant Young's modulus,
- $\rho = 2700 \frac{\text{kg}}{\text{m}^3}$  as constant density, and,
- $\epsilon = 0.04$  as the constant numerical damping coefficient.

The number  $n$  of nonlinear bar elements, that constitute the test-case will be determined later. Also the Young's modulus  $E$  is not fixed but will be used for a convergence study.

The parameters of the harmonic external force are  $\hat{f}_E = 30 \text{ N}$  for the amplitude and  $\Omega = \frac{1}{15} \frac{1}{\text{s}}$  for the frequency. The transient solutions are obtained between  $t_0 = 0 \text{ s}$  and  $t_e = 30 \text{ s}$  with a time-step of  $\Delta t = 0.0001 \text{ s}$ .

### 6.2.1.2 Characterising the test-case with bar elements by testing its convergence properties

The discussion of the convergence covers, in a first step, the coarseness of the discretisation. That is, the number of elements  $n$  used in the discretisation of the bar. This study is required to determine the number of elements that is to be used for the test-case with bar elements. In a second step the Young's modulus is investigated and its effects on the nonlinear behaviour of the bar are studied. This study serves to justify the choice of a non-physical  $E$  to accentuate the nonlinear behaviour of the bar. In a third and final step the convergence behaviour of the reduced system of the finite element test-case with bar elements is investigated.

**6.2.1.2.1 Discretisation** In order to ensure a numerically consistent behaviour of the test-case with bar elements, the solution has to converge with an increasing number of elements. In table 6.3 the number of elements is listed and for each number  $n_i$  the R2MSE  $e_r$  relative to the preceding number of elements  $n_{i-1}$ .

It can easily be verified that the solution converges with an increasing number of elements. To ensure a consistent behaviour it is decided to take a step beyond table 6.3 and to discretise the test-case with bar elements with  $n = 100$  elementary nonlinear bar elements. This overly large number of degrees of freedom may also give leverage for the study of the computational performances.

**6.2.1.2.2 Young's modulus** In the listing at the beginning of the current section the value of the physical property of the Young's modulus  $E$  is set to  $20000 \frac{\text{N}}{\text{m}^2}$ . This value has no physical justification and, in particular, it does not correspond to the common material that might be suggested by setting the material's density to  $\rho = 2700 \frac{\text{kg}}{\text{m}^3}$ . In fact, the value of the Young's modulus has only been chosen to tune the relation

## 6.2. APPLYING THE INTEGRATED METHOD TO GEOMETRICALLY NONLINEAR BAR ELEMENTS

---

number of elements	relative error
1	—
5	0.29153
10	0.02259
15	0.00421
20	0.00147
25	0.00068
30	0.00037
35	0.00022
40	0.00015
45	$9.9418 \cdot 10^{-5}$
50	$7.1115 \cdot 10^{-5}$

Table 6.3: The convergence of nonlinear transient solutions of the finite element test-case with bar elements for different discretisations

between elastic and inertial forces during the transient solution so that geometrically nonlinear behaviour is accentuated.

The test of the influence of the Young's modulus  $E$  is undertaken by applying the maximum amplitude  $\hat{f}_E$  in a static manner and comparing the resulting displacements at the free end of the bar. The tests are conducted with  $n = 50$  elements. Table 6.4 lists various values for  $E$  and the corresponding displacements at the free end of the bar for three different approaches for obtaining static solutions. The direct linear solution is obtained with the linear equation for the displacement of a bar under traction

$$u = \frac{\hat{f}_E}{EA} L, \quad (6.33)$$

which is taken from Schnell et al. [202]. To verify a correct implementation of the finite elements, this direct result is also obtained with linear elements. In a final step, the static displacements are also obtained with nonlinear bar elements.

Young's modulus in $\frac{N}{m^2}$	direct solution in $m$	linear FEM solution in $m$	nonlinear FEM solution in $m$
200	30.000	30.000	12.000
2000	3.000	3.000	2.325
20000	0.300	0.300	0.289
200000	0.030	0.030	0.029
2000000	0.003	0.003	0.003

Table 6.4: The linear and nonlinear static displacements at the free end of the finite element test-case with bar elements for different values of Young's modulus

Table 6.4 shows that the direct linear solution and the solution with linear finite elements are in perfect accordance. This allows putting a lot of confidence in the numerical procedure. Also, it can be seen that, for the nonlinear solution, the relation between the Young's modulus and the displacement is in fact nonlinear. This confirms the nonlinearity of the test-case in which the bar is to be used. The choice of  $E = 20000 \frac{N}{m^2}$  is now obvious because it leads to a reasonable strain of  $\mathcal{O}(10^{-1})$  of compared to the overall length  $L$  of the entire bar.

**6.2.1.2.3 Reduction** Following the investigation of the properties of the full order model, it has also to be demonstrated that reduced order models converge on the full order solution if the order  $r$  of the reduced model increases. To this effect a number of reduced models with increasing order  $r$  are solved consecutively. Each generates a transient solution. The error between their respective solution and the full order solution, as a reference, is recorded and traced as a function of the order of the reduced model  $r$ . The reduction is performed with the LNM from section 3.3.1 in their classic formulation. The reduced basis is not updated. The inflation formulation of the nonlinear terms is kept in order to limit the error to the introduction of the reduced basis.

The figure 6.8 traces the mean of the R2MSE  $e_r$  from equation (4.4). The mean is obtained among the  $n = 100$  degrees of freedom between the full order reference solution and the current reduced order solution. The variance  $v_r$  of R2MSE is also included in the figure.

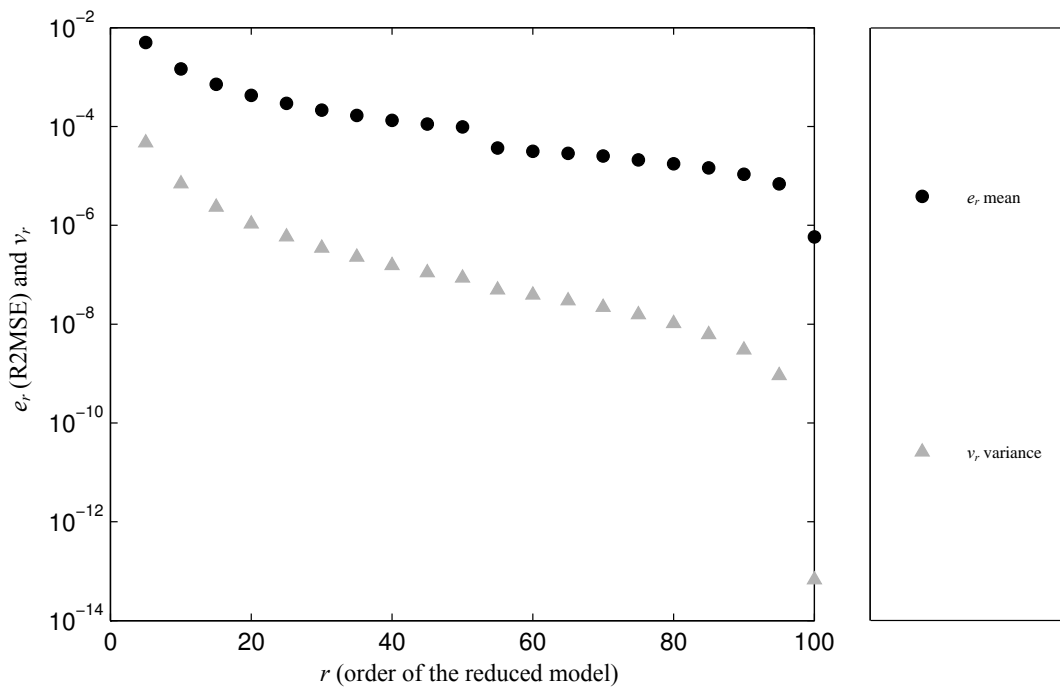


Figure 6.8: The mean and the variance of the R2MSE as a function of the order  $r$  of the reduced model of the finite element test-case with bar elements

Both metrics, the mean and the variance, decrease with an increasing order of the reduced model  $r$ . For  $r \rightarrow n$  the errors attain machine level. This demonstrates the convergence of the reduced transient solutions towards the full order solution for an increasing order of the reduced model. This result is consistent with the expectations and the theory.

A particular feature of figure 6.8 are the discontinuities of the error metrics at a given  $r$ . There it becomes obvious how certain modes, that are included in the reduced basis successively, resolve the transient behaviour of the test-case especially well and boost the decrease of the error metrics. For more complex structures, that exhibit e.g. additional torsion behaviour, such discontinuities are important because they allow to determine if modes for all significant behaviours are included or not. For this simple test-case with bar elements the overall smooth, decreasing evolution of the error metrics shows that, at any order  $r$ , only significant modes are included in the reduced basis. This behaviour is to be expected because this simple test-case does only exhibit compression deformations.

This concludes the testing of the convergence of the full order system with the number of elements  $n =$

100. Also studied are the behaviour of the full order system with different stiffnesses and the convergence of the solutions obtained with the reduced order model to the solution obtained with the full order system as a function of the order  $r$  of the reduced model. The test-case with bar elements can be used without limitations for applying all previously developed methods to this finite element test-case.

## 6.2.2 Applying the integrated method to the finite element test-case with bar elements

The application of the integrated method to the finite element test-case with bar elements spans three aspects. At first, the adaptation of the reduced basis by interpolation is tested. This preparatory step is necessary to initialise the integrated method with its first reduced basis. To this effect, the test-case is parameterised with prestress. The prestress is not applied in theoretically stringent fashion, but serves only as a mean to introduce parameters that allow evaluating the initialisation of the first reduced basis, as it is discussed during the preparation of the integrated method in section 6.1.1.1. The second aspect covers the application of the integrated method itself and demonstrates that the integrated method can be applied successfully to a more complex test-case. This confirms that the integrated method is also applicable to a finite element test-case and that the results, which are obtained, until now, with the academic test-cases, remain valid. The third aspect repeats another study that is already performed for the academic test-case. In section 5.1.3.6.2 the question, if using a higher order reduced solution at  $r + 3$  from the beginning would yield better results than the update, is posed and clearly answered in favour of the update. This result is confirmed with the finite element test-case with bar elements.

### 6.2.2.1 Testing the basis adaptation by prestressing the finite element test-case with bar elements

The prestressing is used as a mean of introducing external parameters in the finite-element test-case with bar elements as it is described in section 6.2.1.1. The introduction of the prestress is governed by this requirement and it is hence performed in a phenomenological manner without any theoretical rigour. The prestressing is modelled by means of a rotation of the entire test-case around an axis that is perpendicular to the axis of the bar, which allows introducing two variables. The radius  $r_a$ , that describes the distance between the clamping point of the bar and the axis of rotation, can be considered as a design parameter. The frequency of the rotation  $\Omega_a$  can be considered as a parameter describing the operating point of the structure. With these two variables these two categories of parameters are covered. However, no further distinction between the two parameters is made.

The aim of the prestressing is the introduction of parameters and not a faithful simulation of all the effects and phenomena resulting from the rotation of the entire system. The simple one-dimensionality of the test-case with bar elements is hence continued and no off-axis effects like Coriolis forces are treated.

The prestressing force is built on the centrifugal accelerations that are determined for each node as

$$a_N = (x_i + r_a) \Omega_a^2. \quad (6.34)$$

The set-up for the prestressing is shown in figure 6.9. This one-dimensional problem is considerably simpler than the three-dimensional formulation, which would be required for a test-case with volume elements<sup>2</sup>. The nodal accelerations from equation (6.34) are assembled in the accelerations vector  $\mathbf{a}_N = [a_1; \dots; a_n]$ . The prestressing force is then obtained as  $\mathbf{f}_{E,a} = \mathbf{M}\mathbf{a}_N$  and applied as an additional external force in a static

---

<sup>2</sup>The entire process of prestressing is detailed in the section 6.3.2 for the test-case with volume elements. Due to its three-dimensionality and the resulting geometric and specific considerations, the prestressing of the test-case with volume elements deserves higher attention than the prestress of the one-dimensional test-case with bar elements. However, the process of prestressing that is developed for the test-case with volume elements can be used without required an adaptation to the test-case with bar elements. Here, its application is anticipated.

## 6.2. APPLYING THE INTEGRATED METHOD TO GEOMETRICALLY NONLINEAR BAR ELEMENTS

manner. The nonlinear static solution for this external force yields the displacements  $\mathbf{u}_a$ , resulting from the prestress.

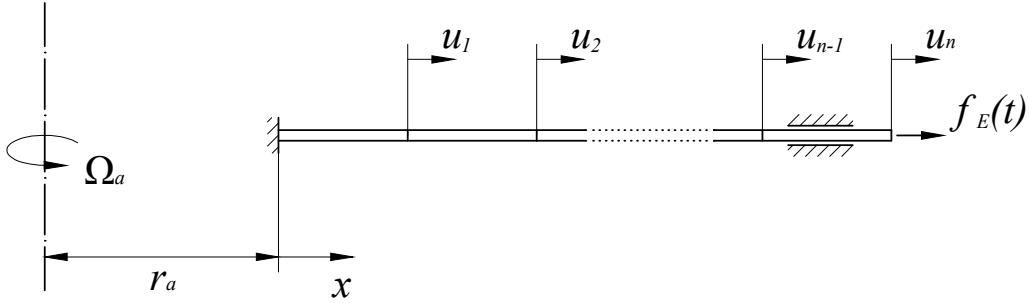


Figure 6.9: The set-up for prestressing the finite element test-case with nonlinear bar elements

The test-case with bar elements offers the advantage of having easily observable modes. Thus the first application of the interpolation of the reduced basis for different parameters  $\boldsymbol{\mu} = [\Omega_a, r_a]$  will be judged by comparing the modes of the reduced basis created with the LNM at the initial displacement  $\mathbf{u}_a$ .

The operating point with  $\boldsymbol{\mu}_0 = [\Omega_{a,0}, r_{a,0}]$ , at which the reduced basis is to be interpolated, is defined at  $\boldsymbol{\mu}_0 = [0.5 \frac{1}{s}, 3 m]$ . The origin of the interpolation is set at the operating point  $\boldsymbol{\mu}_k = [0.43 \frac{1}{s}, 2.7 m]$ . This operating point is the closest one on the grid spanning  $\{0.05 \frac{1}{s} \leq \Omega_a \leq 0.81 \frac{1}{s}\}$  and  $\{1.5 m \leq r_a \leq 3.9 m\}$  with five points in each direction of the parameter space. This grid is used to generate the precomputed operating points, between which the interpolation takes place.

The figures 6.10 and 6.11 show the interpolations of the first and the 15<sup>th</sup> mode, respectively. The number is assigned to the mode in function of their ranking with increasing eigenfrequencies. All modes are normalised with  $\|\boldsymbol{\phi}_k\| = 1$ .

From the figure 6.10 the advantage of producing smooth and easily observable modes of the test-case with bar elements becomes obvious. Given this smoothness it is not surprising that the interpolation method performs well and achieves a successful recreation of the first mode.

If the mode shape becomes more oscillating the interpolation method still achieves a reasonably correct recreation of the mode at the operating point  $\boldsymbol{\mu}_0$ . This can be seen in figure 6.11 for the 15<sup>th</sup> mode.

The numerical results of the study are given in table 6.5. It contains the R2MSE  $e_r$  and the MAC  $e_a$  between the first fifteen modes  $\boldsymbol{\phi}_0$  at the operating point that are obtained with the interpolation methods and the modes  $\boldsymbol{\phi}_{0,\text{ref}}$  that have been obtained directly from the linear tangent stiffness matrix at  $\boldsymbol{\mu}_0$  as a reference. The values confirm a gradual decrease in the quality of the modes that have been recreated with interpolation with an increasing number of the mode. Even for the 15<sup>th</sup> mode the values of the error metrics are still very good. This, together with the visual inspection of the modes' shapes in figure 6.11, show that the interpolation method can successfully recreate a reduced basis.

## 6.2. APPLYING THE INTEGRATED METHOD TO GEOMETRICALLY NONLINEAR BAR ELEMENTS

---

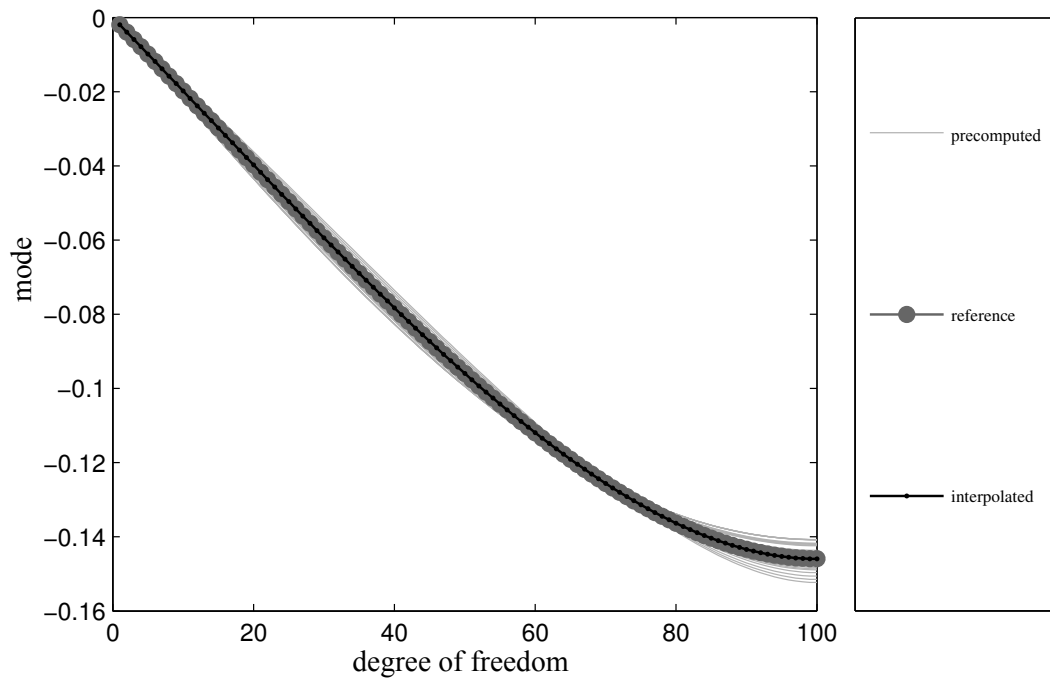


Figure 6.10: The interpolation of the first mode of the finite element test-case with bar elements

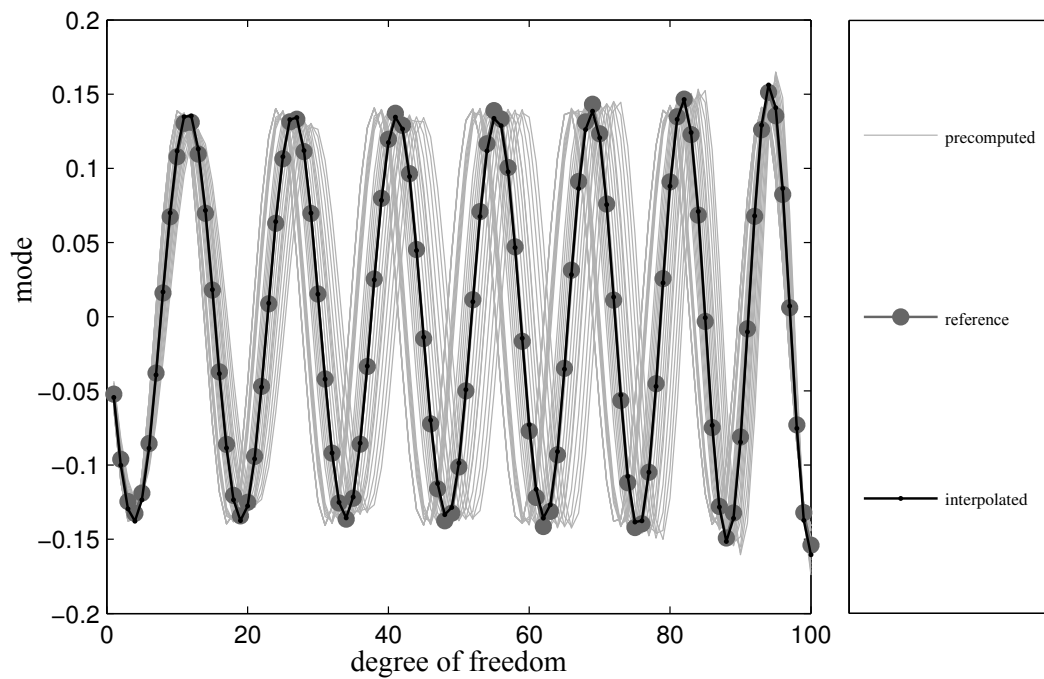


Figure 6.11: The interpolation of the 15<sup>th</sup> mode of the finite element test-case bar volume elements

6.2. APPLYING THE INTEGRATED METHOD TO GEOMETRICALLY NONLINEAR BAR ELEMENTS

---

mode	R2MSE	MAC
	$e_r$	$e_a$
1	0.000177	1.0000
2	0.000685	1.0000
3	0.001344	1.0000
4	0.002142	1.0000
5	0.003108	1.0000
6	0.004275	1.0000
7	0.005674	1.0000
8	0.007337	0.9999
9	0.009296	0.9999
10	0.011587	0.9999
11	0.014252	0.9998
12	0.017338	0.9997
13	0.020902	0.9996
14	0.025012	0.9994
15	0.029749	0.9991

Table 6.5: The comparison of the interpolated modes with the reference modes for the finite element test-case with bar elements

### 6.2.2.2 Applying the integrated method for obtaining a transient solution of the finite element test-case with geometrically nonlinear bar elements

The integrated method for obtaining a transient solution is applied to the finite element test-case with nonlinear bar elements. The test-case is described in section 6.2.1.1, prestressed as in section 6.2.2.1 and solved with the integrated method from section 6.1.1. The integrated method combines the polynomial formulation for the autonomy and the basis update and augmentation for making the reduced basis follow the nonlinear evolution of the transient solution. It is applied with the HHT- $\alpha$ -method as backbone because this solution scheme proved advantageous for finite element test-cases. Furthermore this application proves that the autonomous formulation and the basis update and augmentation can be integrated on a given time-marching solution procedure.

The reduction is performed with the LNM at the current displacement. The LNM are hence initialised at the prestressing displacement  $\mathbf{u}_a$ . However, this is not done directly but with the application of the interpolation from section 5.3.2 with the external parameters  $\boldsymbol{\mu}_0 = [\Omega_{a,0}, r_{a,0}]$  that describe the prestressing. This is described in detail in section 6.2.2.1. Once the first update takes place, the LNM are determined with the current displacements  $\mathbf{u}^{(t)}$ . Other types of reduced bases are not included because the results of the application of the integrated method on the academic test-cases in section 6.1.2.3 shows that even the POD does perform poorly while being updated. The LNM are retained as the best option.

In the following the correct identification of the tensors of the polynomial formulation of the reduced nonlinear terms is finalised. Then the time histories of different solutions are inspected in the ultimate aim of applying the score, which is developed in section 4.1.2.2, as a mean to demonstrate the benefits of the application of the integrated method.

**6.2.2.2.1 Correctly identifying the tensors by dynamically adapting the indirect identification** The identification of the tensors  $\tilde{\mathbf{A}}^{(h)}$  in the context of the update and augmentation of the reduced basis has only been treated briefly during the description of the integrated process in section 6.1.1.3. This is mainly because the actual variant of the identification is only chosen later. In section 6.1.2.1 numerical results show that the indirect identification of the reduced tensors  $\tilde{\mathbf{A}}^{(h)}$  is the most promising variant. This variant is described in detail in section 5.2.2.2 and can be applied as a self-contained block within of the integrated method. During the current preparation of the application of the integrated method to the finite element test-case with bar elements it can be demonstrated that the indirect identification of the reduced tensors requires a well balanced approach and does not stand isolated. Especially the work of Feeny [77] shows that generalised coordinates have to be monitored closely. This is also the case during the identification of the reduced tensors  $\tilde{\mathbf{A}}^{(h)}$ .

The figure 6.12 shows the evolution of the generalised coordinates  $q_1$  and  $q_{r+1}$  for the reduced test-case with bar elements at  $r = 10$ . The generalised coordinate  $q_1$  acts on the first column vector  $\phi_1$  of the reduced basis and the generalised coordinate  $q_{r+1}$  acts on the jump in the displacements  $\Delta \mathbf{u}$ . The large amplitudes of  $q_{r+1}$  show that the jumps participate in the definition of the physical displacements. The discontinuities in the jagged time history of  $q_{r+1}$  is an indication of the updates that are taking place. Their frequency is mainly determined by the value of the retainer  $m_r$ .

The most striking feature is that the order of magnitude of  $q_{r+1}$  is greater by a factor of about 100 than the order of magnitude of  $q_1$ . The same goes for the jumps in the velocities  $\Delta \dot{\mathbf{u}}$  and in the accelerations  $\Delta \ddot{\mathbf{u}}$ . Because of the fact that the generalised coordinate  $q_1$  acts upon the first column  $\phi_1$  of the reduced basis, which is the column that is supposed to contribute the most characteristic deformation to the actual physical displacements  $\mathbf{u}$ , the difference in the order of magnitude between  $q_{r+1}$  and the  $q_k$  with  $2 \leq k \leq r$  is even greater. It is safe to suppose

$$\mathcal{O}(q_k)_{(1 \leq k \leq r)} \neq \mathcal{O}(q_k)_{(r+1 \leq k \leq r+3)}. \quad (6.35)$$

## 6.2. APPLYING THE INTEGRATED METHOD TO GEOMETRICALLY NONLINEAR BAR ELEMENTS

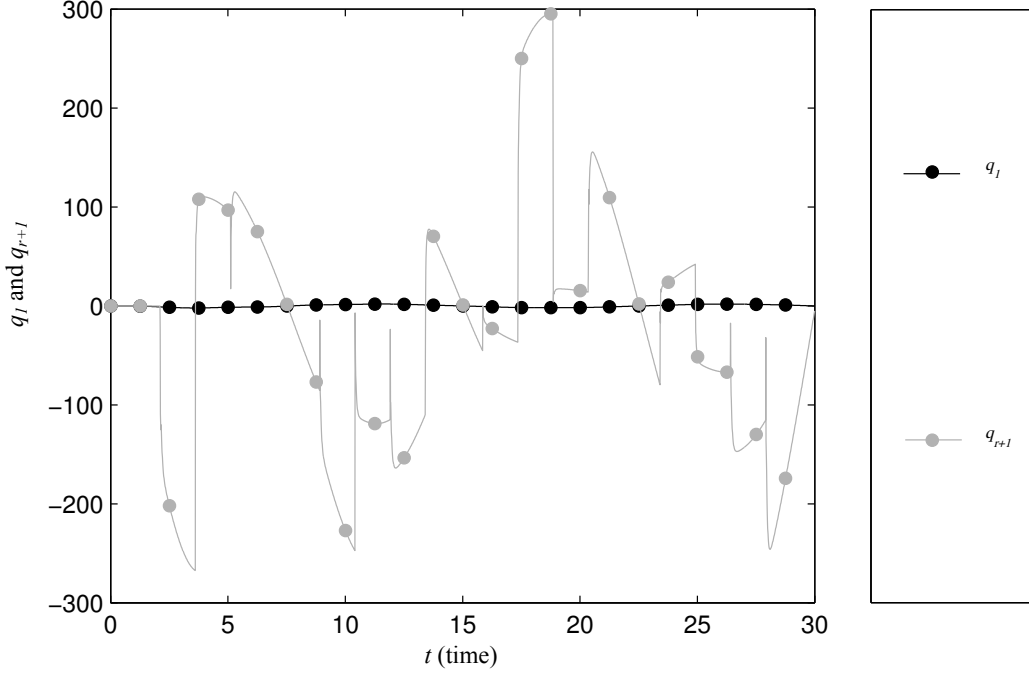


Figure 6.12: The time histories of the generalised coordinates  $q_1$  and  $q_{r+1}$  of the finite element test-case with bar elements

This is an important assumption because the order of magnitude of the different generalised coordinates has a direct impact on the identification of the reduced tensors. In section 5.2.2.5, which treats the correct identification of the tensors, the important point is made that, due to the evaluation of the nonlinear forces, the relation between the  $\Delta q_k$  and the  $[\tilde{A}_k^{(1)}]$ , the  $[\tilde{A}_{kp}^{(2)}]$  and the  $[\tilde{A}_{kps}^{(3)}]$  is not linear. This has to be taken into account when the  $\Delta q_k$  are chosen and it is imperative that the  $\Delta q_k$  that are chosen reflect the actual order of magnitude of their corresponding generalised coordinate  $q_k$ . This imperative is also valid for the  $\Delta q_k$  with  $r+1 \leq k \leq r+3$  that correspond to the jumps  $\Delta \mathbf{u}$ ,  $\Delta \dot{\mathbf{u}}$  and  $\Delta \ddot{\mathbf{u}}$ . As figure 6.12 shows, it can be difficult to find a common order of magnitude for all  $\Delta q_k$ .

Thus, the approach that is taken is to identify the reduced tensors with different order of magnitude for the different reduced coordinate and to set

$$\mathcal{O}(\Delta q_k)_{(1 \leq k \leq r)} = \mathcal{O}(q_k)_{(1 \leq k \leq r)}, \quad (6.36)$$

and

$$\mathcal{O}(\Delta q_k)_{(r+1 \leq k \leq r+3)} = \mathcal{O}(q_k)_{(r+1 \leq k \leq r+3)}. \quad (6.37)$$

This may be done dynamically during each update from the second update onwards. The  $\mathcal{O}(q_{1 \leq k \leq r})$  is known from the preceding time history of the reduced solution and the  $\mathcal{O}(\Delta q_{r+1 \leq k \leq r+3})$  can also be determined because the jumps  $\Delta \mathbf{u}$ ,  $\Delta \dot{\mathbf{u}}$  and  $\Delta \ddot{\mathbf{u}}$  are known prior to the identification of the reduced

tensors  $\tilde{\mathbf{A}}^{(h)}$ . As a result of this approach it is possible that

$$\mathcal{O}(\Delta q_k)_{(r+1 \leq k \leq r+3)} \neq \mathcal{O}(\Delta q_k)_{(1 \leq k \leq r)}. \quad (6.38)$$

Thus the difference in the  $\mathcal{O}(\Delta q_k)$  reflects the difference in the order of the generalised coordinates  $\mathcal{O}(q_k)$  in equation (6.35).

With this improvement, the integrated method can use the indirect identification of the reduced tensors independently and correctly. With the correct distribution of the  $\mathcal{O}(\Delta q_k)$  as a function of the evolution of the order of magnitude  $\mathcal{O}(q_k)$  of the corresponding generalised coordinates the integrated method is finalised.

Being able to finalise the integrated method from section 6.1.1, by prescribing the incremental displacements during the indirect identification of the reduced tensors as a function of the evolution of the different generalised coordinates, also proves the value of the test-case with bar elements. It requires a relatively small numerical effort for the transient solution. While this does still not allow a meaningful determination of the possible computational gains due to the introduction of the reduction, it is highly practical for running a large number of solutions that can be adapted and that differ in every imaginable aspect, from the size of the time-step to the actual solution method. Thus it greatly helps in defining and finalising the integrated method on a representative problem.

**6.2.2.2.2 Inspecting time histories** The inspection of the time histories of differently solved reduced systems precedes the application of the score in the next section. Visualising the time histories of  $u_{100}$  at the tip of the finite element test-case with bar element from figure 6.7, allows gauging and interpreting the scores that are to be derived from these time histories.

The figure 6.13 shows the time histories of  $u_{100}$  that is obtained with several solution methods at  $r = 10$ . The reference solution is obtained with a full order HHT- $\alpha$ -method. Two solutions with constant reduced bases are obtained, one with the inflation formulation of the nonlinear terms and one with the polynomial expressions replacing the reduced nonlinear terms and rendering the system autonomous. Finally, two solutions with updated reduced bases are included, again one with the inflation formulation and one with the polynomial expression. This last solution that is obtained with the combination of an updated and augmented reduced basis with the polynomial expressions on the HHT- $\alpha$ -method is the result of the integrated method that is described in section 6.1.1.

The four reduced solutions and the reference solution are indistinguishable at the scale required to fit the entire solution in the figure. This is a first indicator for the very high quality that is obtained with the reduced models. The fact that the solutions do start at an  $u_{100} \neq 0$  shows that the prestressing and the adaptation of the initial reduced basis by interpolation are integrated with success.

In order to assess the actual quality of the reduced solutions, table 6.6 contains numerical values for the means of the R2MSE  $e_r$  and of the MAC  $e_a$ . The R2MSE is valuable source of information. It shows that introduction of the update has the most important impact on the quality of the reconstructed reduced solution. The two solutions that are obtained with the constant reduced basis produce the same error in the limits of rounding. The introduction of the polynomial expression with tensors that are indirectly identified at reduced level replaces the inflation formulation of the nonlinear terms without introducing an additional error in the two cases of a constant and of an updated and augmented reduced basis. The introduction of the update and augmentation decreases the R2MSE. The decrease is equally pronounced for the solution that is obtained with the inflation formulation and for the solution obtained with the polynomial expression. This shows again, that the introduction of the polynomial formulation for rendering the reduced model of the test-case with bar elements autonomous has no negative effect. The MAC confirms the impression gained from figure 6.13. The four solutions are of generally equal shape and differ only slightly in their quality.

During the following application of the score, it has to be kept in mind that the level of the differences in

## 6.2. APPLYING THE INTEGRATED METHOD TO GEOMETRICALLY NONLINEAR BAR ELEMENTS

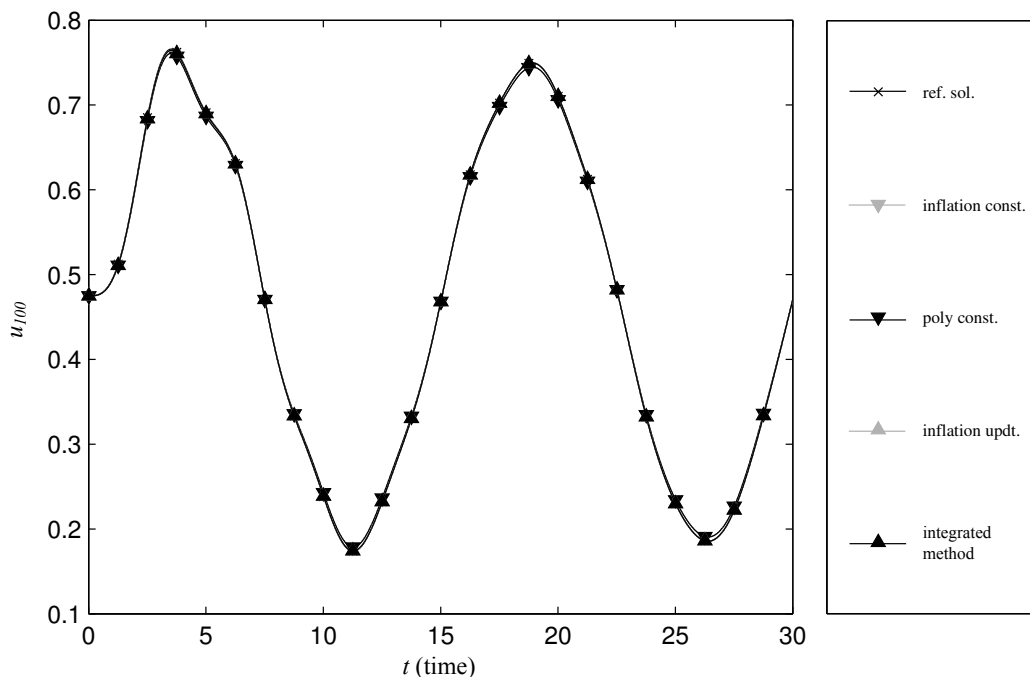


Figure 6.13: The time histories of  $u_{100}$  of the finite element test-case with bar elements for different reduced solution procedures

		constant inflation	constant polynomial	updated inflation	updated polynomial
R2MSE	$e_r$	$6.9066 \cdot 10^{-3}$	$6.9066 \cdot 10^{-3}$	$1.1122 \cdot 10^{-3}$	$1.1011 \cdot 10^{-3}$
MAC	$e_a$	1.0000	1.0000	1.0000	1.0000

Table 6.6: The error metrics for the transient solutions of the finite element test-case with bar elements obtained with different combinations of methods

the quality between the differently obtained solutions is comparable to the level of error that is presented in table 6.6. Thus the methods are giving rather delicate gains in quality.

**6.2.2.2.3 Applying the score** The score is developed in section 4.1.2.2 as a measure to compare different reduced basis amongst each other. To this effect pairs of a reduced basis method and of an order of the reduced system are ranked for different criteria. These rankings are then weighted and unified to build the score. Now the method for the creation of the reduced basis in the pair is replaced by the method used for obtaining the reduced transient solution. This tweak turns equation (4.11) into

$$\text{score}^{(\text{solution method}, r)} = \sum_i w_i \mathcal{R}_{e_i}^{(\text{solution method}, r)}. \quad (6.39)$$

and allows to compare different solution methods among each other. This can be done because the unique method for the creation of the reduced basis is the LNM at given displacements. Beyond that the score is applied as it is originally conceived, i.e. without any modification.

## 6.2. APPLYING THE INTEGRATED METHOD TO GEOMETRICALLY NONLINEAR BAR ELEMENTS

---

The methods for solving the reduced models are all based on the HHT- $\alpha$ -methods. They include approaches with

- a constant reduced basis and the inflation formulation,
- a constant reduced basis and the polynomial expression,
- an updated and augmented reduced basis and the inflation formulation and
- an updated and augmented reduced basis and the polynomial expression.

The last approach is the integrated method that is described in section 6.1.1. All reduced models are prestressed and the initial reduced basis is adapted by applying the interpolation of the reduced basis from section 5.3.2.

The figure 6.14 plots the scores for these four different solution methods against the order  $r$  of the reduced model. It is obvious that the quality of the reconstructed solution increases with an increasing order  $r$  of the reduced model. This is reflected by consistent distribution of the data points along the first diagonal of the plot.

Equally consistent is the distribution of the data points for each order  $r$  of the reduced model. The lowest scores are universally attributed to solutions with a constant reduced basis and the inflation formulation. Introducing the polynomial formulation of the nonlinear terms while maintaining a constant reduced basis gives the thus obtained solutions a slight edge over the solutions with inflation formulation. This slight advantage comes from the minuscule decrease in the computational time that is required by the polynomial formulation. There is no difference in error between these two solutions, as it is shown in table 6.6. For the test-case with bar elements the polynomial formulation can be used as a replacement on par with the exact inflation formulation.

The two solutions that are obtained with the approaches including an updated and augmented reduced basis stand apart from the solutions with constant reduced bases. With the only exception of the solution with the inflation formulation at  $r = 10$  they all attain scores higher than the solutions with constant bases at  $r = 16$ . As shown in table 6.6 there are only marginal differences in the quality between the two solutions. The slight underachievement of the solutions with the polynomial expression can thus possibly be explained with the increasing numerical cost required for the repeated identification of the reduced tensors. Due to the impossibility to derive meaningful information about the solution times from the numerical set-up of the test-case with bar elements this has to be accepted. It is not meaningful to draw a comparison with the time required for a full order reference solution. However, already at this point the inclusion of the solution time, albeit with a very small weight, in the score shows that a trade-off will be required between the gain in computational time and the gain in the quality of the solution.

In conclusion the results confirm the enormous gains in performance that can be achieved by applying the integrated method for solving a finite element test-case. The benefits for the quality of the solution are considerable. While the computational gains and numerical efforts remain inconsistent and impossible to judge because of the rather fast execution of all approaches for solving this test-case, the results foreshadow the requirement of a trade-off between quality and the performance of the reduced solution. This can only be resolved with the computationally much more expensive test-case with volume elements in the next section.

### 6.2.2.3 Demonstrating the superiority of updated and augmented reduced bases over equivalently sized constant reduced bases

The question if using a higher order reduced solution at  $r + 3$  from the beginning instead of updating and augmenting the reduced basis of order  $r$  does offer any advantages is already posed in section 5.1.3.6.2. There, the answer is that the update and augmentation of the reduced basis does deliver better results. Now it is to be demonstrated that this results also holds for the finite element test-case with bars.

To answer the initial question, the finite element test-case with bar elements with  $n = 100$  degrees of freedom is subjected to three reduced solutions for a simulated period of 30 s under prestress. These reduced

## 6.2. APPLYING THE INTEGRATED METHOD TO GEOMETRICALLY NONLINEAR BAR ELEMENTS

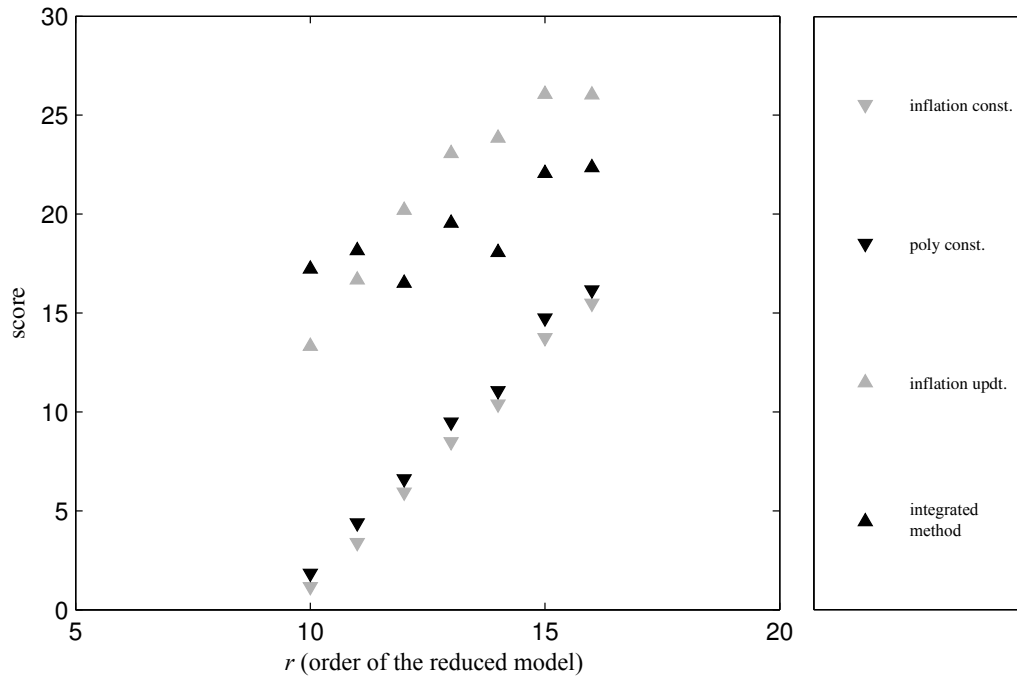


Figure 6.14: The score of different reduced solution procedures for the finite element test-case with bar elements

solutions are obtained with

- a constant reduced basis and an initial and constant order of  $r^{(t_0)} = 12$ ,
- a constant reduced basis and an initial and constant order of  $r^{(t_0)} = 15$ , and
- a reduced basis that is updated and augmented as described in section 5.1.3.1, and an initial order of  $r^{(t_0)} = 12$  that increases to  $r^{(t_0)} + 3 = 15$  during the first update of the reduced basis due to augmenting the reduced basis.

The solution with basis update is initialised at  $r^{(t_0)} = 12$ . After the first update, the order of the solution with basis update remains constant at  $r^{(t_0)} + 3 = 15$  and thus equal to the order of the solution with the constant basis at  $r^{(t_0)} = 15$ .

The three solutions are compared on the grounds of the displacements  $u_{100}$  of the free end of the bar in a comparison with the unreduced reference solution. In figure 6.15 the three solutions are barely distinguishable. Only the values of the error metrics in table 6.7 show clearly that the solution that is obtained with the updated and augmented reduced basis is considerably better than the two solutions that are obtained with a constant reduced basis. The R2MSE obtained from the updated solution is about five times smaller than the one obtained with the constant basis at  $r = 15$ . This demonstrates the overall value of the update.

A small additional investigation is required by the values of the MAC. These are all equal to one for all three solutions and stress the exceptional quality of all three solutions with respect to the shape of the time history of the displacements. Apparently only small differences in the amplitude are reflected in the different R2MSEs. However, this is not entirely the case. The enormous density of data due to a small time-step renders the MAC somewhat imprecise with respect to measuring the actual shape of the time histories. This becomes obvious when zooming in on the solutions around the time interval from 1.4 to 1.6 seconds in figure 6.16. In this interval an update of the reduced basis takes place and shows prominently due to small bump at around 1.525 seconds. Even though it appears as rather sharp, it is not a discontinuity

## 6.2. APPLYING THE INTEGRATED METHOD TO GEOMETRICALLY NONLINEAR BAR ELEMENTS

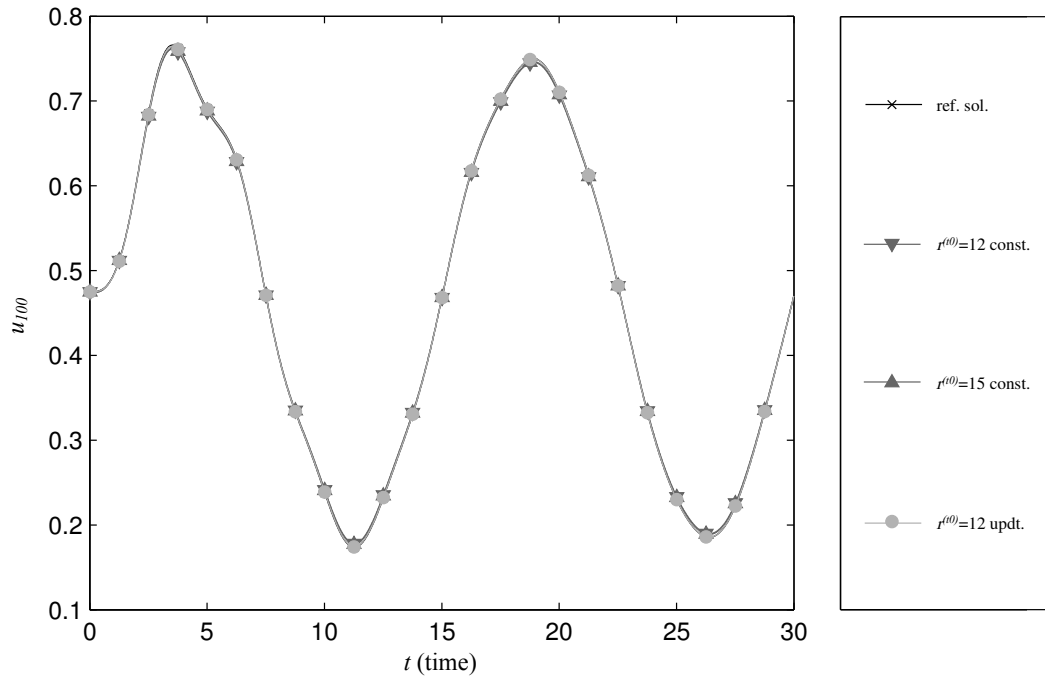


Figure 6.15: The time histories of the three reduced solutions and the reference solution of the finite element test-case with bar elements

		constant at $r^{(t_0)} = 12$	constant at $r^{(t_0)} = 15$	updated and augmented initialised with $r^{(t_0)} = 12$
R2MSE	$e_r$	$5.7152 \cdot 10^{-3}$	$4.5081 \cdot 10^{-3}$	$0.9206 \cdot 10^{-3}$
MAC	$e_a$	1.0000	1.0000	1.0000

Table 6.7: The error metrics for the transient solutions of the finite element test-case with bar elements with different constant reduced basis and with an updated and augmented reduced basis

in the displacements and not in the velocities. The apparently sharp bend is a product of the small time-step. These, and other, bumps are not captured by the MAC. They always bend the solution in the right direction towards the reference solution. The bumps do not destabilise the solution. In fact, they improve the solution and this demonstrates the value of the application of the basis update and augmentation.

This value is further demonstrated in figure 6.17, where an interval between 25 and 28 seconds is shown. While the two solutions with constant bases having visibly departed from the reference solution the solution with basis update and augmentation proves to be a perfect match. The solution with an updated and augmented basis is perfectly superposed to the reference position. The reference solution is not visible. In fact, the improvement observed in passing from  $r^{(t_0)} = 12$  to  $r^{(t_0)} = 15$  for the constant bases, is still less than the distance that is required to arrive at the reference solution starting from the constant basis solution at  $r_0 = 15$ . Naturally, this distance would have to be crossed by adding still more additional vectors to a constant basis and thus increasing the order of the reduced model considerably beyond the current value of  $r = 15$ .

This concludes the demonstration of the usefulness of the basis update. It can be shown that augmenting the reduced basis during the update process does not negate the advantages of a basis update facing equivalently sized constant reduced bases. Equivalently sized constant reduced basis still perform worse than

## 6.2. APPLYING THE INTEGRATED METHOD TO GEOMETRICALLY NONLINEAR BAR ELEMENTS

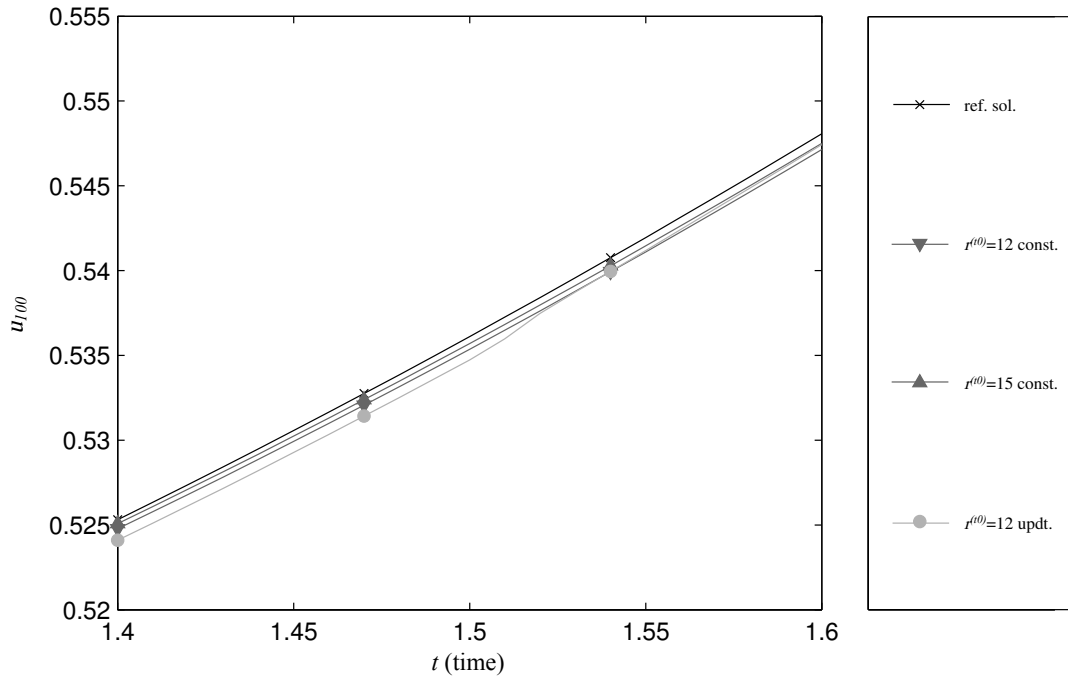


Figure 6.16: An early interval in the time histories of the three reduced solutions and the reference solution

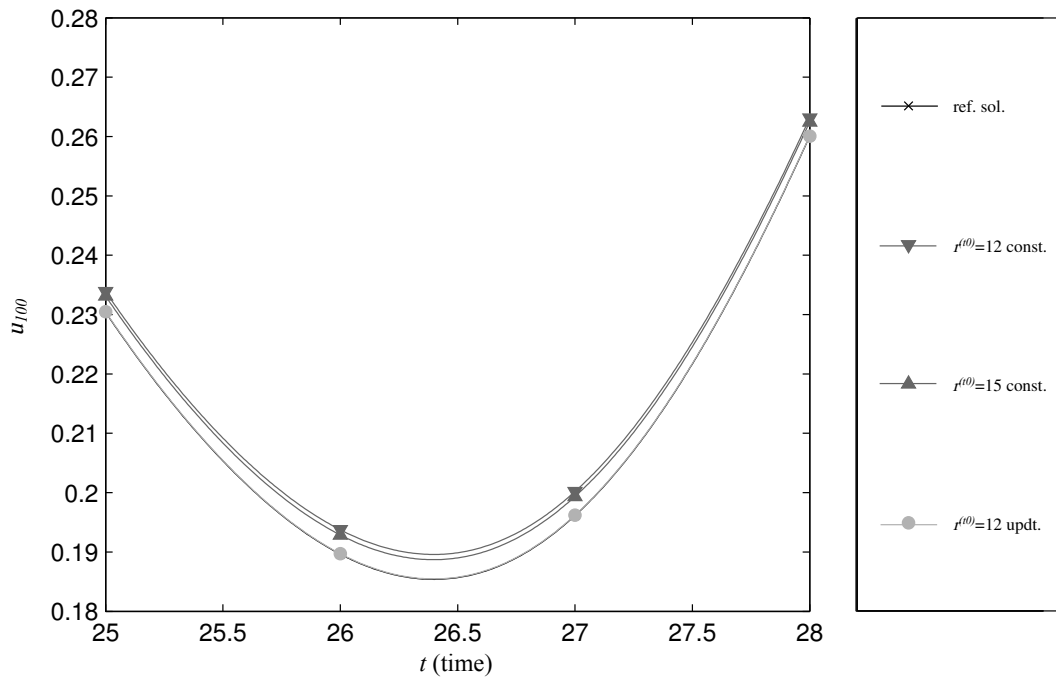


Figure 6.17: A late interval in the time histories of the three reduced solutions and the reference solution

updated and augmented reduced bases, even if these are of the same size after being augmented.

## 6.3 Applying the integrated method to geometrically nonlinear volume elements

The application of the integrated method from section 6.1 to the finite element test-case with volume elements consists of a characterisation of the test-case, the prestressing and the actual application. In this, it follows the general lines of the application of the integrated method to the test-case with bar elements in section 6.2.

The characterisation the test-case and its nonlinear behaviour is an important part of this section. Knowing the test-case and its nonlinear behaviour allows gauging the circumstances under which the integrated method can be applied with success. A fully characterised nonlinear test-case can thus serve as a blueprint for other, similar test-cases, which are to be solved with the integrated method. The characterisation starts with a sketch of the motivation for choosing and parameterising the finite element test-case with volume elements it is presented in the first part of this section. The second part covers the convergence and a comparison with the commercial finite element solver NASTRAN. This ensures a trustworthy environment for applying the integrated method.

It is continued to base the assessment of the quality of the solutions on the time-histories of the displacements. This follows foremost practical reasons because many criteria and tools for this kind of assessment are already developed and can be reapplied to the finite element test-case with volume elements without further modification. Furthermore the verification of the displacements is equivalent to the verification of internal stresses as the mainstay of engineering applications. This equivalence is ensured by using the linear material model from equation (2.58). Such a material allows accessing the internal stresses by a simple post-processing. Thus, knowing the displacements is sufficient.

The third, and most important, part of this section is taken by the solutions of the nonlinear test-case with finite volume elements. In a first step the results from the numerical studies in the chapter 4 are confirmed on the test-case with volume elements. This links the test-case with volume elements with the academic test-cases that are used in the previous studies of the comparison and robustness of the reduced bases. Confirming this direct link and the similarity of the results demonstrates the fact that the decisions with respect to the choice of the basis and the creation of the integrated method, and that have been, until now, based on the academic test-cases, remain valid for the finite element test-case with volume elements. This confirmation allows to continue the application of the already developed methods to the test-case with volume elements, because all previously made assessment do not have to be repeated and remain valid.

The prestressing is discussed briefly. It is neither intended to be strict in the theoretical sense nor comprehensive. It is simply a mean of introducing the external parameters  $\mu = [\Omega_a, r_a]$ , rotation frequency and radius, to test the interpolation of the reduced bases from section 5.3.2. Prestressing is already anticipated in the previous section for the test-case with bar elements. This section adds a more formalised reflection on the introduction of prestressing. The prestressing is discussed briefly. It is neither intended to be strict in the theoretical sense nor comprehensive. It is simply a mean of introducing the external parameters  $\mu = [\Omega_a, r_a]$ , rotation frequency and radius, to test the interpolation of the reduced bases from section 5.3.2. Prestressing is already anticipated in the previous section for the test-case with bar elements. This section adds a more formalised reflection on the introduction of prestressing.

In a final step the integrated method from section 6.1 is used to obtain the transient solution of the finite element test-case with volume elements. The results allow exploring the quality of the solution and, more importantly, the gains in computational performance. The test-case with volume elements is sufficiently complex to allow meaningful and significant conclusions with respect to the possible gains in computational performance. Its computational expensiveness is the main reason for the introduction of the test-case with volume elements.

#### 6.3.1 Describing and characterising the test-case with nonlinear volume elements

The finite element test-case with volume elements is a simplified model of a turbine blade. The use of volumetric nonlinear finite elements resembles much more closely the conditions encountered in real-world applications. It is expected to highlight specific challenges that are connected to the use of finite elements for obtaining reduced transient solutions of geometrically nonlinear system. The finite element test-case with volume elements is mainly used to verify and to integrate the methods of an update of the reduced basis, the autonomy of the formulation of the nonlinear terms and the parameterisation of the reduced model. These are introduced in chapter 5 to address the findings that have been observed with the academic test-cases in chapter 4 and are unified in the integrated method in section 6.1. To this effect this test-case works alongside the test-case with nonlinear bar elements in section 6.2 and many tests are carried over.

The test-case with volume element requires the massive computational efforts that are described during the introduction of the geometrically nonlinear finite element in section 2.2.3. These computational efforts finally allow for a viable investigation into the computational efforts and wall times that are required by the different solution methods.

##### 6.3.1.1 Considering the particularities of simulating structural dynamics of a turbine blade

One of the most comprehensive overviews on the integral numerical simulation of turbomachinery is given by Sayma et al. [200] and Vahdati et al. [230]. In addition to a very wide review of available literature, they cover the aspects of nonlinear equations for the formulation of the fluid problem, including the entire range of features, such as turbulence modelling, boundary conditions, meshing and purely numerical considerations, as well as the structural problem and coupling between the two physics. However, their structural problem is formulated in an almost exclusively linear fashion because, as they argue, even the mechanics of some of the worst sources of unwanted vibration in the engine are still poorly understood and the common remedy to such problems is the simple introduction of friction dampers at a very late stage of the design process. The introduction of damping in itself leads to some very advanced, nonlinear modelling (e.g. Sanliturk et al. [199]), which considerably complicates the necessary calculations, yet addresses solely the symptoms of a basically linear design, which favours unwanted vibrations.

The strictly nonlinear simulation of the structure of a turbine blade is the approach to be preferred if the occurrence of unwanted vibrations and resonances is to be discovered and dealt with as early in the design-process as possible. Unfortunately an early design stage inevitably means considerable uncertainty for many design-parameters. The highly sophisticated nonlinear formulations of structural problems require a great deal of specified information in order to yield meaningful results. For a nonlinear formulation of the structural problem in the context of turbomachinery to succeed, it is required to bridge that gap by being robust and easily adaptable. To add to the constraints of nonlinear simulation, the allocation of available computational resources clearly disfavours the early design stages, so that highly sophisticated nonlinear simulations are also required to be treated with a reasonable computational effort.

From all these considerations the requirements for a nonlinear solution emerge to be

- correctness: the nonlinear simulation has to correctly treat nonlinear phenomena and deliver results which are accurate to the required degree,
- flexibility: the nonlinear simulation has to accommodate changes in parameters that allow exploring possible directions of design, and,
- inexpensiveness : the nonlinear simulation has to include a mechanism which reduces the computational burden and makes feasible a relatively large number of repeated solutions.

As it is shown, there are well-proven approaches available that respond to each of the requirements. However, it also becomes obvious that the integration and the interaction of the different approaches poses its own challenges. These challenges are overcome with the integrated method in section 6.1, which is applied to the finite element test-case below.

### 6.3.1.2 Description of the test-case with geometrically nonlinear volume elements

The turbine blade test-case is introduced to apply the concepts and methods developed until now on a test-case which goes beyond the academic mass-spring systems in section 4.1.3.1. The aim of the introduction of the test-case is to expand the application of the reduction and adaptation methods to a more complex test-case which includes geometrically nonlinear elements.

The blade is modelled after a two-dimensional turbine blade used by Tran [228]. Its dimensions with respect to a global axis of rotation are

- $L_z = 4$  for the length of the blade in radial direction,
- $L_x = 2$  for the width of the blade in axial direction,
- $L_y = 1$  for the thickness of the blade in the perpendicular radial direction.

The curvature of the blade's faces at its tip and at its root is not taken into account. The blade's geometry describes a twisted cuboids, without taper. The twist is  $36^\circ$  in positive direction and linearly distributed in radial direction, i.e. zero at the untwisted root of the blade and maximum at the blade's tip.

The properties of the blade's material are

- $E = 7 \cdot 10^9$  for its Young's modulus,
- $\nu = 0.3$  for the Poisson's ratio,
- $\rho = 70$  for the density and
- $\epsilon = 0.04$  for the damping coefficient.

The blade is modelled with 2, 1 and 4 hexahedron elements in  $x$ ,  $y$  and  $z$  direction, respectively. Fully clamped at the root this leads to 24 free nodes with 3 translational degrees of freedom each and eventually to  $n = 72$  degrees of freedom for the entire system as it is shown in figure 6.18.

For the following tests the blade is subjected to a harmonic combined traction and flexion excitation along the  $[x, -y, z]$  diagonal of three-dimensional space. The excitation is concentrated and applied at the tip face of the blade. The oblique application is to approximate the aerodynamic conditions of the rotating blade in the wake downstream of a stator stage. The actual numerical values are chosen to be representative of an actual, high-speed rotation of modern turbo engines. The frequency is  $\frac{1}{5}$  per unit time. During the first quarter of the period the amplitude of the forcing is shaped with a  $\sin^2(t)$  in order to smooth the beginning of the forcing and to reduced numeric problems. After that initial period the forcing is continued with an  $\sin(t)$  as a classic harmonic excitation. The amplitude of the external forcing is tuned such that the resulting displacement is nonlinear.

The nonlinearity of the resulting displacements is verified by applying a rough approximation for a linear beam and observing the displacements. Schnell et al. [202] give for a static linear displacement

$$u_y = \frac{\hat{f}_E L_z^3}{3EI_y} \quad (6.40)$$

where the second moment of area of the beam is defined as  $I_y = \frac{L_x L_y^3}{12}$ . This is a very rough approximation because it does not take into account neither the twist of the test-case nor the oblique direction of the external force in the actual dynamic excitation. With all values for the geometry and the chosen amplitude injected, this approximation of the displacement yields

$$\epsilon = \frac{u_y}{L_z} = 0.2286. \quad (6.41)$$

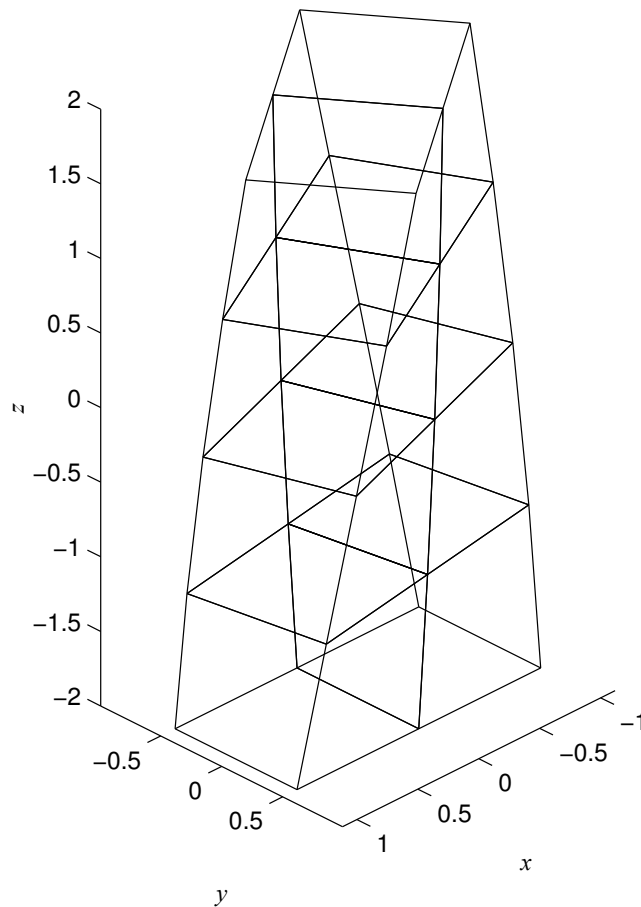


Figure 6.18: The finite element test-case with nonlinear volume elements

Such a value requires the application of nonlinear calculations.

In addition the entire blade is subjected to a rotation at a rate of  $\Omega_a = \frac{1}{300}$  per time unit around an axis that is parallel to the blade's  $y$  axis and at a distance of  $r_a = 5$  below the blade's centre of mass. This rotation is accounted for by including prestressing in the simulation. This prestressing is detailed in the section 6.3.2, below.

#### 6.3.1.3 Testing a single isolated nonlinear volume element under traction

The testing of a single volume element for its nonlinear behaviour is one of the standard tests that is available in structural dynamics. It allows characterising the behaviour of the elementary unit of the finite element problem. Confirming the nonlinear behaviour of one element allows to assemble the elements to a structure and the nonlinear behaviour of the single element is expected to transpire to the level of the assembly.

The finite element formulation developed in section 2.2.3, with a Total-Lagrangian description and a Saint Venant-Kirchhoff material model, is considered to be optimal for large displacements and small deforma-

### 6.3. APPLYING THE INTEGRATED METHOD TO GEOMETRICALLY NONLINEAR VOLUME ELEMENTS

---

tions. This constellation represents a specific type of nonlinearity. However, the developed formulation is also the standard approach if no specific information about the type of nonlinearity to be expected is available. Especially the use of the SVK material model avoids the complex and very specific knowledge required to apply a more sophisticated material model.

In order to test whether the developed formulation is sufficiently nonlinear a simple traction test is performed on a single element. The test is based on three indicators: the physical displacements, the norm of the involved stiffness matrices and the number of Newton-Raphson iterations required for the static solution. If the first two indicators differ considerably between the linear and the nonlinear solution, the test finite element can be considered to have a nonlinear behaviour. The number of Newton-Raphson iterations has no equivalent in the linear procedure and is included to illustrate the way in which the nonlinear solution procedure deals with the expected nonlinear behaviour. Also included is a visual inspection of the deformed configuration.

The test set-up comprises a perfect cuboid with a side length of 1. Referring to figure 2.2 the nodes are blocked and subjected to external forces as follows

- node 1 is blocked in  $x$ ,  $y$  and  $z$  direction,
- node 2 is blocked in  $x$  and  $z$  direction,
- node 3 is blocked in  $z$  direction,
- node 4 is blocked in  $y$  and  $z$  direction,
- node 5 is blocked in  $x$  and  $y$  direction and subjected to a force in positive  $z$  direction.
- node 6 is blocked in  $x$  direction and subjected to a force in positive  $z$  direction,
- node 7 is subjected to a force in positive  $z$  direction,
- node 8 is blocked in  $y$  direction and subjected to a force in positive  $z$  direction,

This set-up results in a pure traction in  $z$ -direction and allows a symmetric deformation of the element in the  $x$ - $y$ -plane.

To track the nonlinear behaviour of the element the amplitude of the force is varied and the problem subjected to a static solution. The static solutions are performed for the nonlinear element and, as a comparison, also for a linear element with the exact same test conditions. The resulting displacements, the norms of the stiffness matrix and the number of Newton-Raphson iterations are observed. The figure 6.19 traces the displacement in  $z$ -direction  $u_z$  as a function of the applied force for the nonlinear and the linear test. The displacement  $u_z$  is the same for all four nodes 5, 6, 7, and 8, on account of the symmetric nature of the test. It is apparent that the nonlinear solution differs considerably from the linear solution. The nonlinear behaviour of the element leads to a stiffening behaviour with an increasing force. Hence, the nonlinear element deforms less than its linear equivalent.

The stiffening behaviour, which was observed indirectly via the displacement  $u_z$ , is confirmed by the plot of the norm of the stiffness matrix  $\|\mathbf{K}\|$  against the force in figure 6.20. The norm is taken from the nonlinear stiffness matrix once the static equilibrium is reached. It is obvious that the nonlinear stiffness matrix evolves as a function of the displacements and hence the force. The norm of the linear stiffness matrix remains constant, regardless of the force or the displacement.

A final indicator for the increasing deviation of the nonlinear solution from the linear solution with an increasing force is the number of Newton-Raphson iterations that are required to converge on the static solution. These are traced in figure 6.21 against the force. They do not provide such a smooth indicator as the two other measures used until now, yet, their increase with the force demonstrates the increasing efforts by the algorithm to reach an equilibrium condition. For this test the external force is applied in a single step. The algorithm fails to converge beyond the maximum force applied in this test. So, should the extension to even higher forces become necessary, a pseudo dynamic solution, where the maximum force is applied gradually, would have been in order. Fortunately, the used maximum amplitude provides ample proof of the nonlinear behaviour of the element.

6.3. APPLYING THE INTEGRATED METHOD TO GEOMETRICALLY NONLINEAR VOLUME ELEMENTS

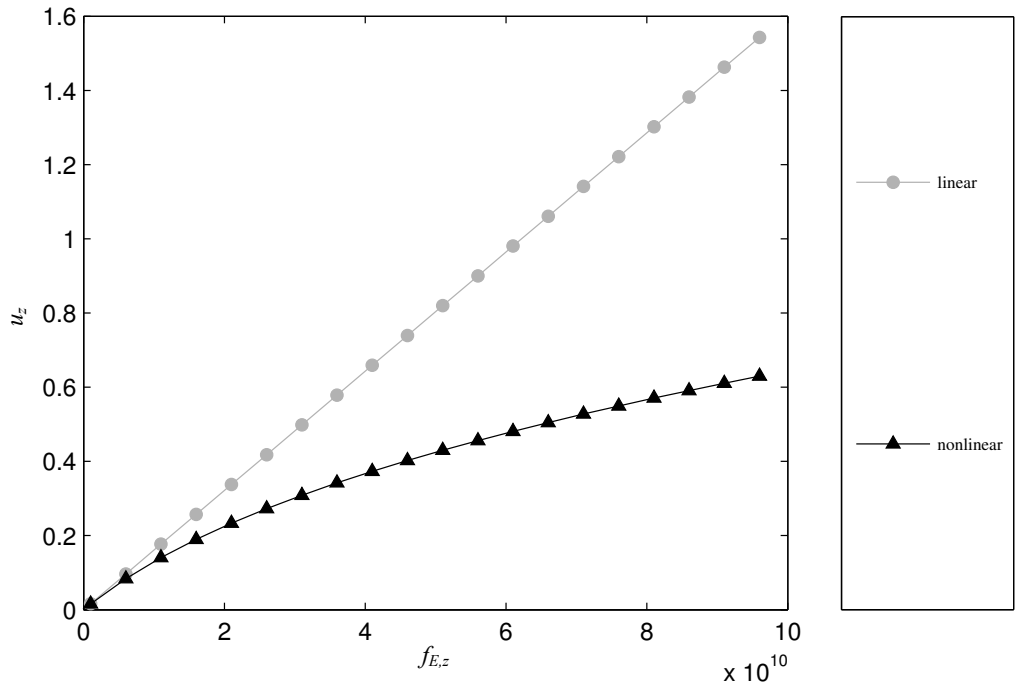


Figure 6.19: The maximum static deformations for the test with a single volume element

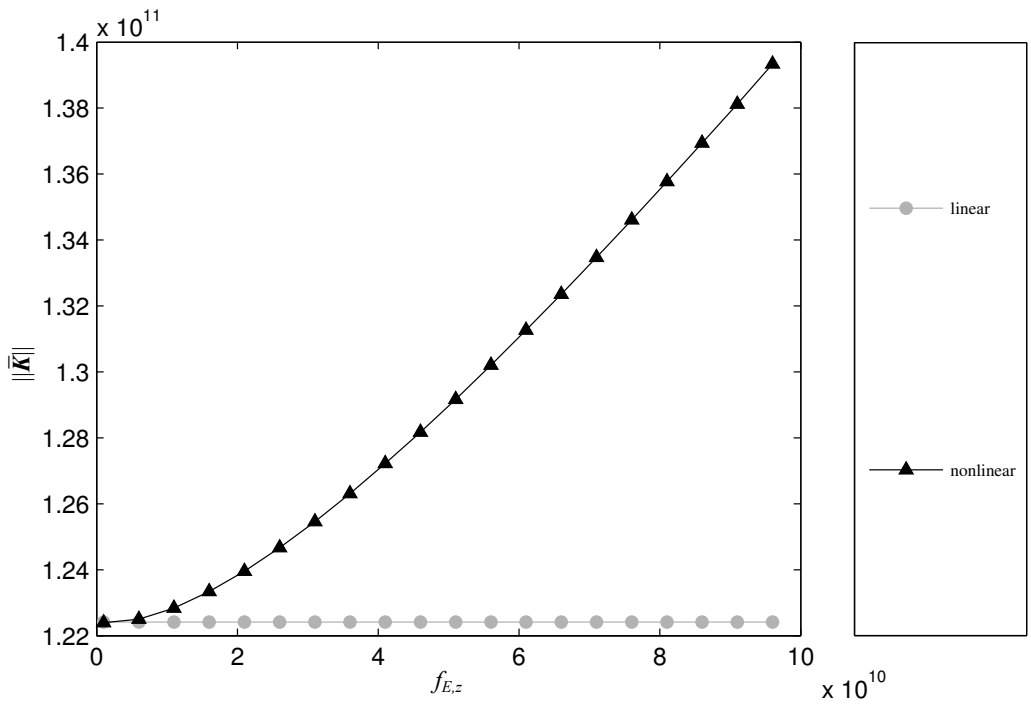


Figure 6.20: The norm of the nonlinear tangent stiffness matrix for the test with a single volume element

To give an impression of the extent of deformation and of the nonlinear behaviour, figure 6.22 presents

### 6.3. APPLYING THE INTEGRATED METHOD TO GEOMETRICALLY NONLINEAR VOLUME ELEMENTS

---

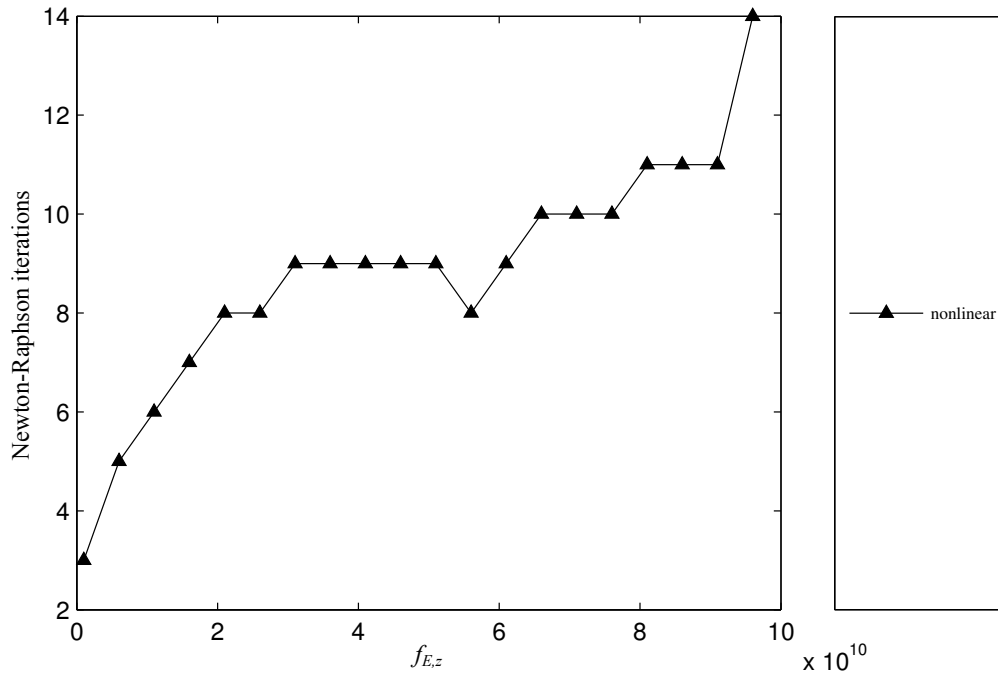


Figure 6.21: The number of Newton-Raphson iterations for the test with a single volume element

the nonlinear and the linear solution at the maximum amplitude of the force. The employed line styles are equivalent to those used in figures 6.19 to 6.20. In conclusion it can be stated that the developed nonlinear element is in fact nonlinear and can be used for building a test-case that is suitable for representing a geometrically nonlinear system.

A second conclusion, with a far greater impact, can also be drawn from this test. With respect to the characteristics of the nature, or shape, of the deformation there is no difference to be observed between the linear and the nonlinear solution. They differ only in amplitude. This implies that the nonlinear solution cannot be distinguished from the linear one by some sort of observable characteristic and thus the judgement of the quality of the results will be much more relying on the comparison of the values for the displacements than on the observation of its shape.

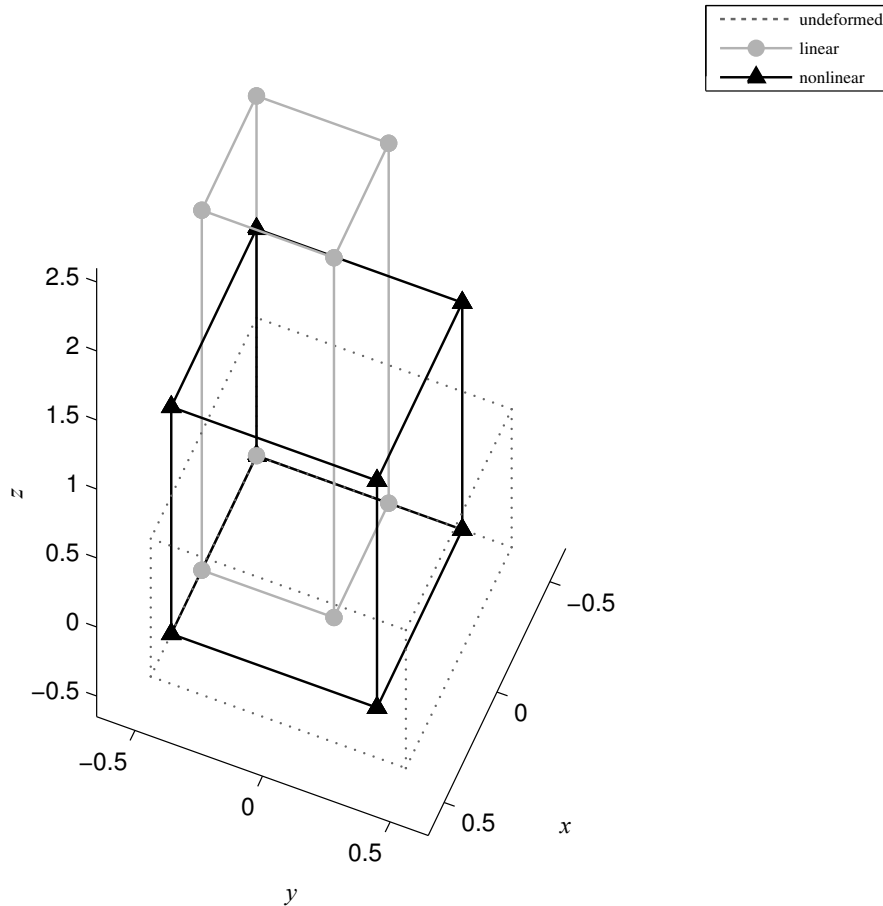


Figure 6.22: The maximum static nonlinear deformation for the test with a single volume element

#### 6.3.1.4 Testing the entire finite element test-case with multiple geometrically nonlinear volume elements

The tests above are now repeated with multiple nonlinear finite volume elements. The aim is to test if the nonlinear behaviour, which was identified during the single element test, transpires to an assembly of multiple elements. Also, the nonlinear characteristics of the assembly are tested. Characterising the nonlinear test-case with volume elements allows to characterise the conditions in which the integrated method of adapting the reduced basis, the autonomous formulation of the nonlinear terms and the parameterisation of the reduced model, that are developed in chapter 5, are and can be applied with success. To this effect static solutions with varying load levels are obtained with the nonlinear test-case with volume elements from figure 6.18 in section 6.3.1.2. The resulting static displacement, the norm of the stiffness matrix and the number of Newton-Raphson iterations, are the measures of nonlinearity traced as functions of the load level. Linear static solutions are also included, as a reference .

The blade is slightly twisted, fixed at its root and subjected to a combined flexing-traction force along the  $[x, -y, z]$  diagonal. The amplitude of the force is varied and the resulting displacements , the norm of the

### 6.3. APPLYING THE INTEGRATED METHOD TO GEOMETRICALLY NONLINEAR VOLUME ELEMENTS

---

stiffness matrix and the number of required Newton-Raphson iterations are traced. In order to concentrate the complex behaviour at the block's tip in a single scalar value, figure 6.23 traces the norm of the three-dimensional displacement vector of the 30<sup>th</sup> node. This node is placed on the maximum positive extent of the block on all axes. The observation of the norm of the nonlinear stiffness matrix in figure 6.24 remains unchanged with respect to the preceding study on the single element. The count of the Newton-Raphson iterations in figure 6.25 may seem high at first sight, but in order to ensure convergence, the external forces are applied in ten steps and the number of iterations is counted over all steps.

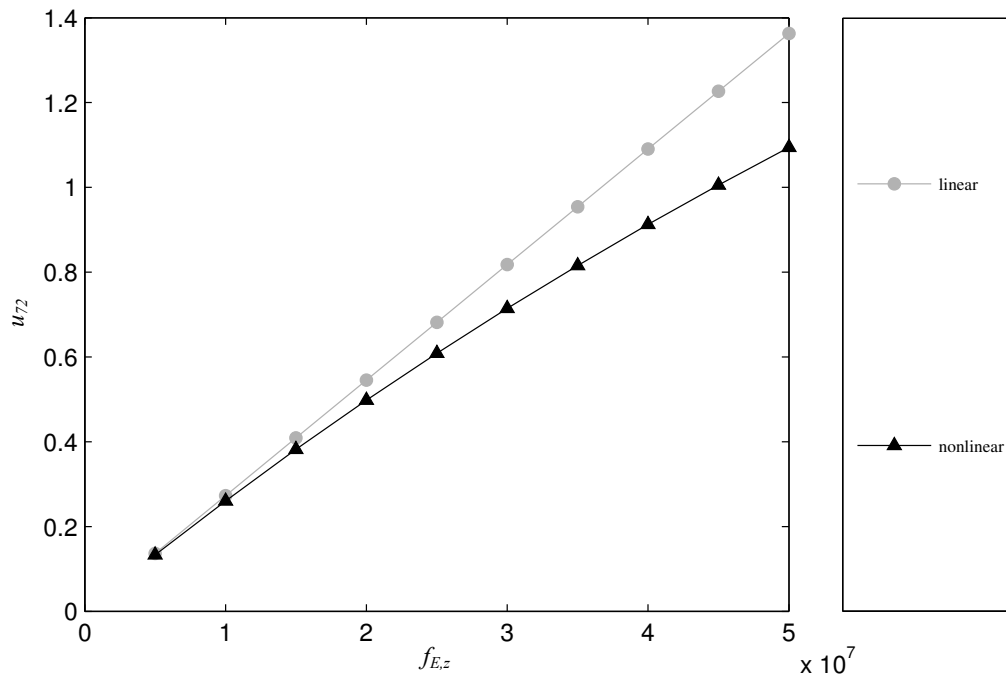


Figure 6.23: The resulting static displacements for the multiple elements test

The figure 6.26 displays the resulting displacements for the maximum applied amplitude. The vector of the applied forces is generally oriented towards the observer. The display reveals the considerable difference between the linear and the nonlinear solution.

In conclusion it can be stated that the nonlinear behaviour of the single element persists, if multiple elements are combined to a multi element structure. The developed nonlinear formulation can thus applied without further adaptation. Table 6.8 sums up the results by comparing the linear to the nonlinear solution with different error metrics. Again it has to be stressed that the linear and the nonlinear static solutions only differ in amplitude. There is no observable difference in shape or other characteristics. For the assembly this is even more the case than for the single element. In fact, for the assembly, the modal assurance criterion between the two solutions is 0.999, while the norm of the difference amounts to 18.8 % of the norm of the nonlinear solution at maximum amplitude. The fact that the difference between the linear and the nonlinear static solution is only a multiplicative factor is believed to be due to the simplicity of the test-case. It is however expected that this might change in the dynamic simulation, when the inertial effects of the twisted structure comes to bear.

6.3. APPLYING THE INTEGRATED METHOD TO GEOMETRICALLY NONLINEAR VOLUME ELEMENTS

---

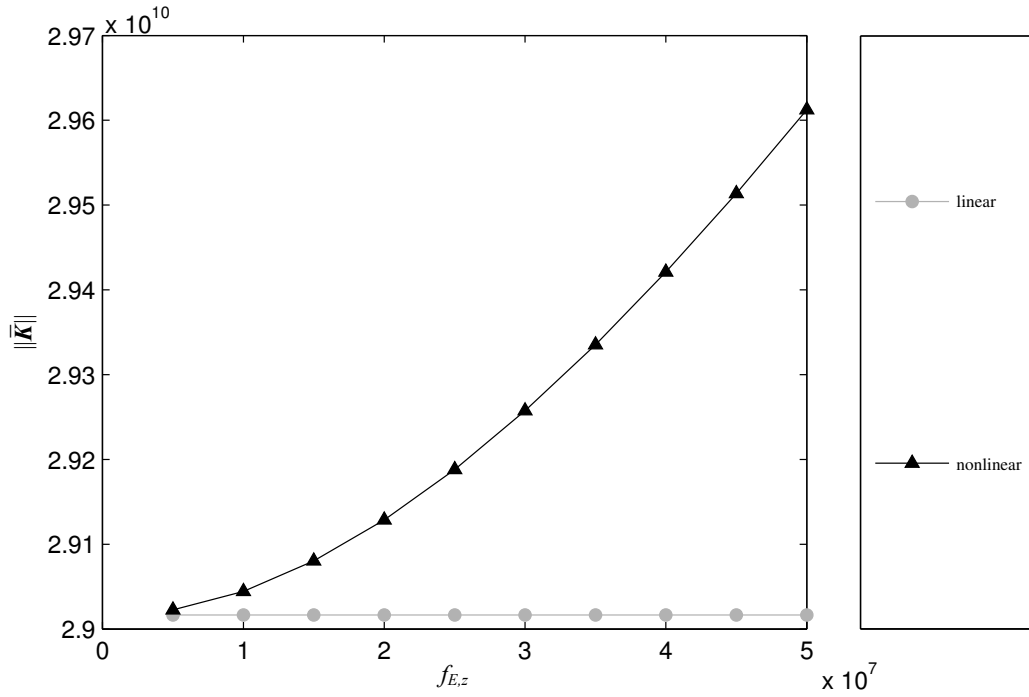


Figure 6.24: The norm of the nonlinear tangent stiffness matrix for the test with multiple volume elements

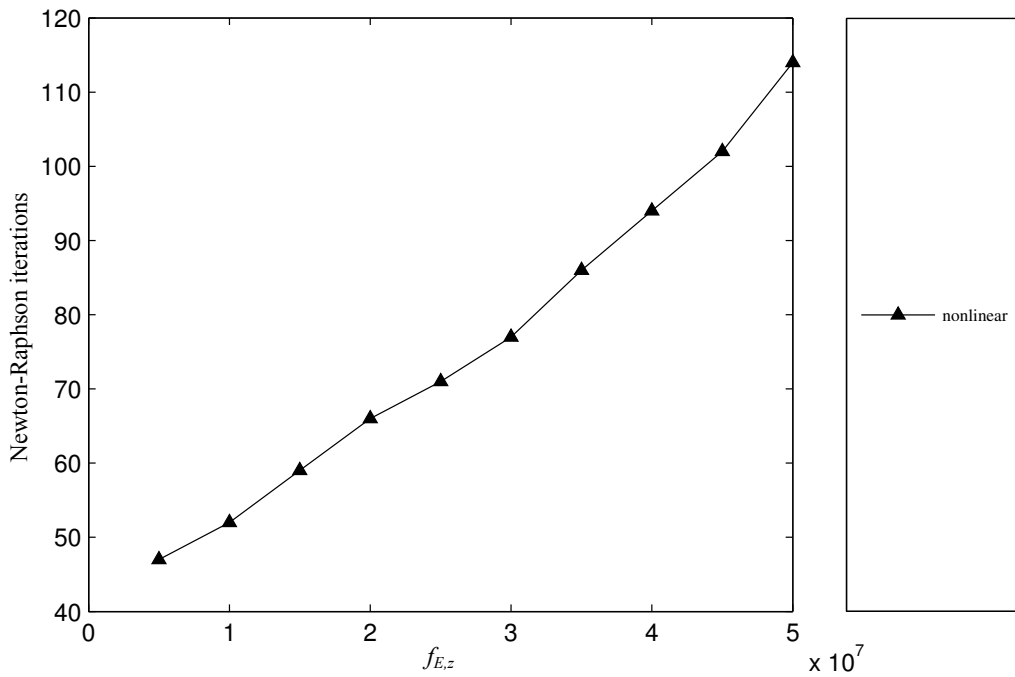


Figure 6.25: The number of Newton-Raphson iterations for the test with multiple volume elements

### 6.3. APPLYING THE INTEGRATED METHOD TO GEOMETRICALLY NONLINEAR VOLUME ELEMENTS

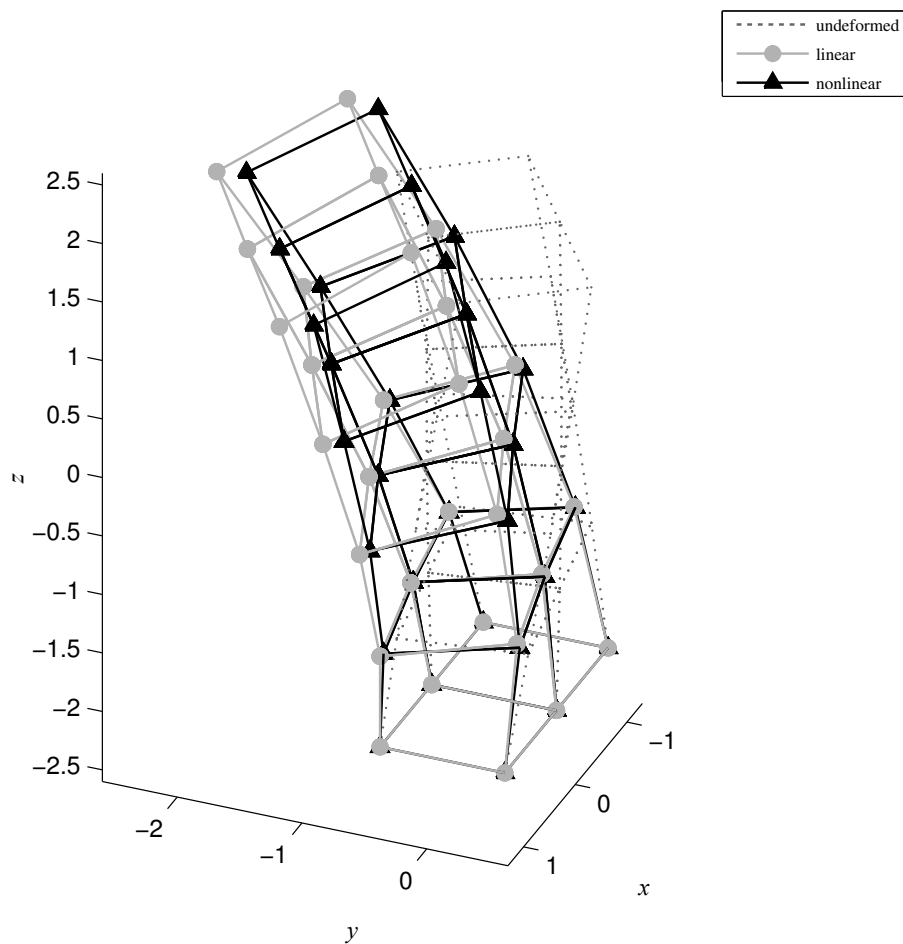


Figure 6.26: The maximum static nonlinear deformation for the test with multiple volume elements

FEM test-case		
R2MSE	$e_r$	0.6009
MAC	$e_a$	0.9988
$\left( \left  \bar{\mathbf{u}}_{tip}^{(linear)} \right  - \left  \bar{\mathbf{u}}_{tip}^{(nonlinear)} \right  \right) / \left  \bar{\mathbf{u}}_{tip}^{(linear)} \right $		18.8 %

Table 6.8: The comparison of the linear and the nonlinear static solution of the finite element test-case with volume elements obtained MatLab

### 6.3.1.5 Characterising the test-case with volume elements by testing its convergence properties

This section explores if the finite element test-case converges, how its convergence depends on the discretisation and on the material and if the convergence can be influenced positively with the derived knowledge. To this end static solutions are treated in the exact same manner as it has been done for the test-case with nonlinear bar elements in section 6.2.1.2. Again the three aspects discretisation, Young's modulus and reduction are investigated.

**6.3.1.5.1 Discretisation** The first aspect covers the number of finite elements. It represents the trade-off between a result, which is expected to be more correct as it is obtained with a more finely discretised system, and the required time for the solution, which increases considerably the finer the discretisation becomes.

The initial discretisation with 72 degrees of freedom is presented in figure 6.18. It consists of two elements in  $x$ -direction, one element in  $y$ -direction and four elements in  $z$  direction. For each consecutive refinement the number of elements in each direction is doubled. The next refinement with 360 degrees of freedom consists of four elements in  $x$ -direction, two elements in  $y$ -direction and eight elements in  $z$  direction and so on.

$n$	linear solution time in $s$	nonlinear solution time in $s$
72	0	24.0400
360	0.0200	177.3200
2160	1.2600	1.4178 $10^3$
14688	234.4500	1.2080 $10^4$

Table 6.9: The overall solution times for static solutions of the finite element test-case with volume elements

Table 6.9 shows that solution times become quickly prohibitive. This is not because several hundred or thousand seconds are much for a single static solution, but because this model is to be used for dynamic solutions, where the number of required similar operations has to be multiplied with several times the number of time-steps.

Tables 6.10 and 6.11 show that the solutions have not yet converged in the sense that an increase of the number of elements does no longer influence the solution. In other words, the degree of discretisation is not yet sufficient. In fact, the more nodes are used to discretise the system, the softer the discrete system becomes and the larger are the displacements.

$n$	$x$ -displacements	$y$ -displacements	$z$ -displacements
72	0.2760	-1.2347	0.1517
360	1.1059	-4.0558	0.4385
2160	4.4605	-15.7439	1.6403
14688	17.9140	-62.6475	6.4624

Table 6.10: The linear static displacements at the free end of the finite element test-case with volume elements for different discretisations

While the convergence behaviour is far less than satisfying, the time needed for the static solution dictates a rather coarse discretisation. This even more as the dynamic solutions with many time-steps and many more static solutions are to be performed several time to test the different solutions, reduced bases, algorithms and methods. Even with a coarse discretisation, the time needed for the dynamic solution of the full order model is still sufficiently long to allow the demonstration of the benefits of a reduction. The decision is hence made to discretise the system with 2, 1 and 4 elements in  $x$ ,  $y$  and  $z$  direction, respectively, which

### 6.3. APPLYING THE INTEGRATED METHOD TO GEOMETRICALLY NONLINEAR VOLUME ELEMENTS

$n$	$x$ -displacements	$y$ -displacements	$z$ -displacements
72	0.2760	-1.2345	0.1516
360	1.1057	-4.0543	0.4383
2160	4.4592	-15.7327	1.6385
14688	17.9032	-62.5587	6.4478

Table 6.11: The nonlinear static displacements at the free end of the finite element test-case with volume elements for different discretisations

amounts to 24 nodes with  $n = 72$  degrees of freedom. This is coarsest possible discretisation for a reliable convergence.

**6.3.1.5.2 Young's modulus** The material that is chosen can be modelled linearly with the isotropic Hooke-material introduced as early as in equation 2.3. While this is not strictly correct for a nonlinear solution it allows concentrating on the geometric nonlinearities. The isotropic Hooke-material is dominantly defined by the Young modulus  $E$ . This parameter is subjected to a variation and static linear and nonlinear solutions are performed. The results are shown in tables 6.12 and 6.13.

$E$	$x$ -displacements	$y$ -displacements	$z$ -displacements
$7 \cdot 10^4$	$0.2760 \cdot 10^6$	$-1.2347 \cdot 10^6$	$0.1517 \cdot 10^6$
$7 \cdot 10^6$	$0.2760 \cdot 10^4$	$-1.2347 \cdot 10^4$	$0.1517 \cdot 10^4$
$7 \cdot 10^8$	27.6031	-123.4724	15.1687
$7 \cdot 10^{10}$	0.2760	-1.2347	0.1517
$7 \cdot 10^{12}$	0.0028	-0.0123	0.0015
$7 \cdot 10^{14}$	$0.0276 \cdot 10^{-3}$	$-0.1235 \cdot 10^{-3}$	$0.0152 \cdot 10^{-3}$
$7 \cdot 10^{16}$	$0.0276 \cdot 10^{-5}$	$-0.1235 \cdot 10^{-5}$	$0.0152 \cdot 10^{-5}$

Table 6.12: The linear static displacements at the free end of the finite element test-case with volume elements for different values of Young's moduli

For the linear solutions the dependence between the Young's modulus  $E$  and the displacements is strictly linear. For the nonlinear case a too soft material leads to too large deformations and ultimately to the failure of the solution to converge. If convergence is established the dependence is nonlinear until the material becomes very stiff.

$E$	$x$ -displacements	$y$ -displacements	$z$ -displacements
$7 \cdot 10^4$	—	—	—
$7 \cdot 10^6$	—	—	—
$7 \cdot 10^8$	27.3354	-120.8083	14.7027
$7 \cdot 10^{10}$	0.2760	-1.2345	0.1516
$7 \cdot 10^{12}$	0.0028	-0.0123	0.0015
$7 \cdot 10^{14}$	$0.0276 \cdot 10^{-3}$	$-0.1235 \cdot 10^{-3}$	$0.0152 \cdot 10^{-3}$
$7 \cdot 10^{16}$	$0.0276 \cdot 10^{-5}$	$-0.1235 \cdot 10^{-5}$	$0.0152 \cdot 10^{-5}$

Table 6.13: The nonlinear static displacements at the free end of the finite element test-case with volume elements for different values of Young's modulus

The decision is made to continue the study with  $E = 7 \cdot 10^9$  because this rather low value ensures a

### 6.3. APPLYING THE INTEGRATED METHOD TO GEOMETRICALLY NONLINEAR VOLUME ELEMENTS

geometrically nonlinear behaviour of the elements while offering enough margin from convergence problems. It does not bear a physical unit because it is chosen for the purely numerical reason of obtaining a representative geometrically nonlinear finite element test-case.

**6.3.1.5.3 Reduction** The final test of convergence for the finite element test-case with geometrically nonlinear volume elements is its behaviour as a reduced model. Similar to the study of the convergence of the test-case with bar elements, in section 6.2.1.2.3, a number of reduced transient solutions is established at different orders  $r$  and the time histories of the displacements are compared to a reference solution.

The figure 6.27 traces the mean  $e_r$  and the variance  $v_r$  of the R2MSE from equation (4.5) against the order  $r$  of the reduced system. The values for the mean and the variance are obtained from transient solutions that are reduced at the given order  $r$ . The current reduced solutions are compared to a reference solution at full order. The test-case is established at  $n = 72$  with 24 nodes and a Young's modulus of  $E = 7 \cdot 10^9$ . All solutions are obtained with the LNM as reduced basis and with the inflation formulation of the non-linear terms. Therefore, no meaningful evidence of the possible gains in computational time can be derived and included in the study.

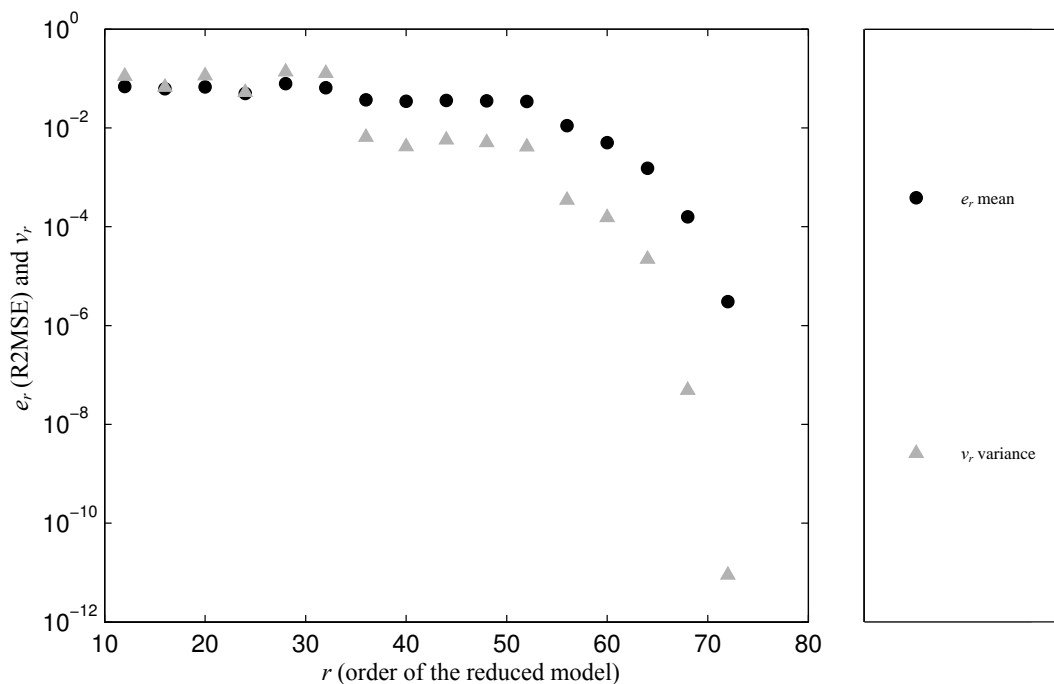


Figure 6.27: The mean and the variance of the R2MSE as a function of the order  $r$  of the reduced model of the finite element test-case with volume elements

The mean  $e_r$  and the variance  $v_r$  of the R2MSE of the time histories decrease with an increasing order of the reduced model  $r$ . Because  $r \rightarrow n$  leads to  $e_r \rightarrow 0$ , the test-case converges also with the order of the reduction. However, the convergence is rather slow and shows two pronounced discontinuities between  $r = 32$  and  $r = 36$  and between  $r = 52$  and  $r = 56$  where modes, which contribute significantly to the solution, are incorporated into the reduced basis. Given the lack of speed of the convergence any reduced model with  $12 \leq r \leq 56$  can be used interchangeably under considerations of the quality of the recreated solution. Remaining errors, at  $r \geq 60$ , are mainly due to the specific nonlinear behaviour of the reference solution which is resolved incompletely by the LNM. In conclusion it can be stated that the test-case also convergence as a function of the order  $r$  of the reduced model which is chosen for a transient solution. This

convergence comes in addition to the convergence as a function of the discretisation, which has already been determined above, and concludes the investigation of convergence of the test-case with volume elements.

**6.3.1.6 Characterising the test-case with volume elements by comparing the nonlinear static solutions with NASTRAN**

The finite element test-cases are implemented in a custom test rig for the integrated method under the MatLab environment (The Mathworks [221]). This implementation allows an accessible code which is close to the actual mathematical formulation of the elements but which is not optimised for performance.

In order to verify the developed nonlinear finite element formulation, the test-case is also solved by a commercial finite element solver. In this case NASTRAN by the vendor MSC in its version V2011.1 is applied because it is a well proven, industry standard tool and readily available (MSC Software [151, 152, 153]). The NASTRAN analysis is set up to reproduce the finite element test-case exactly, i.e. with nonlinear elements, a linear material law and rigged for large displacements. Also all boundary conditions for displacements and forces are mirrored exactly. The same goes naturally for the geometric and material properties. A performance comparison between the MatLab code and NASTRAN is not possible because these two codes are installed on different workstations with different specifications. However, even the nonlinear NASTRAN job takes only several seconds to finish, which underlines the high degree of sophistication and performance optimisation of this solver, which cannot, and should not, be compared to a simple solver in MatLab.

For the linear and the nonlinear case the resulting error metrics between the initial solution and the solution obtained with NASTRAN are shown in table 6.14. It appears that there a distinct difference between the solutions that exist both for the linear and the nonlinear case. An inspection of the corresponding figures 6.28 and 6.29 is in order. The NASTRAN solutions are displayed with black triangles. The inspection reveals that the in the solutions obtained with NASTRAN the tip surface is inclined around the  $y$ -axis.

		linear	nonlinear
R2MSE	$e_r$	0.6549	0.7100
MAC	$e_a$	0.9533	0.9251

Table 6.14: The comparison of the linear and the nonlinear static solutions obtained with NASTRAN and MatLab

The differences between the initial solutions and those obtained with NASTRAN are not as large in the final displacements plots as they may appear from table 6.14. The observed differences are most probably due to differences in the solution procedures itself that cannot always be controlled directly and whose exact influence on the solution cannot be determined from the technical documentation of the NASTRAN software. In particular this concerns the number of steps that are used to apply the external force gradually, the criterion that is used to determine if the Newton-Raphson iterations have converged and the number of time the nonlinear tangent stiffness matrix is updated. However, these factors are considered to be only minor influences because the convergence criterion is rather strict in both cases. The most prominent influence is observed to stem from the type of method that is used to integrate the finite elements. While the initial test-case uses exclusively complete integrations with Gauss-points, as introduced in section 2.2.3.4, this is not always possible for the NASTRAN solver, which places several restrictions on the use of complete integrations. Actually, the nonlinear solution has to be under-integrated with an approximation.

Table 6.15 compares the linear and the nonlinear solution, as they are obtained by NASTRAN, on the grounds of different error metrics. It is the equivalent to table 6.8. By comparing the two tables it becomes again obvious that the difference between the linear and the nonlinear solution is expressed mainly in amplitude and only to a lesser extent in the shape of the deformation.

### 6.3. APPLYING THE INTEGRATED METHOD TO GEOMETRICALLY NONLINEAR VOLUME ELEMENTS

---

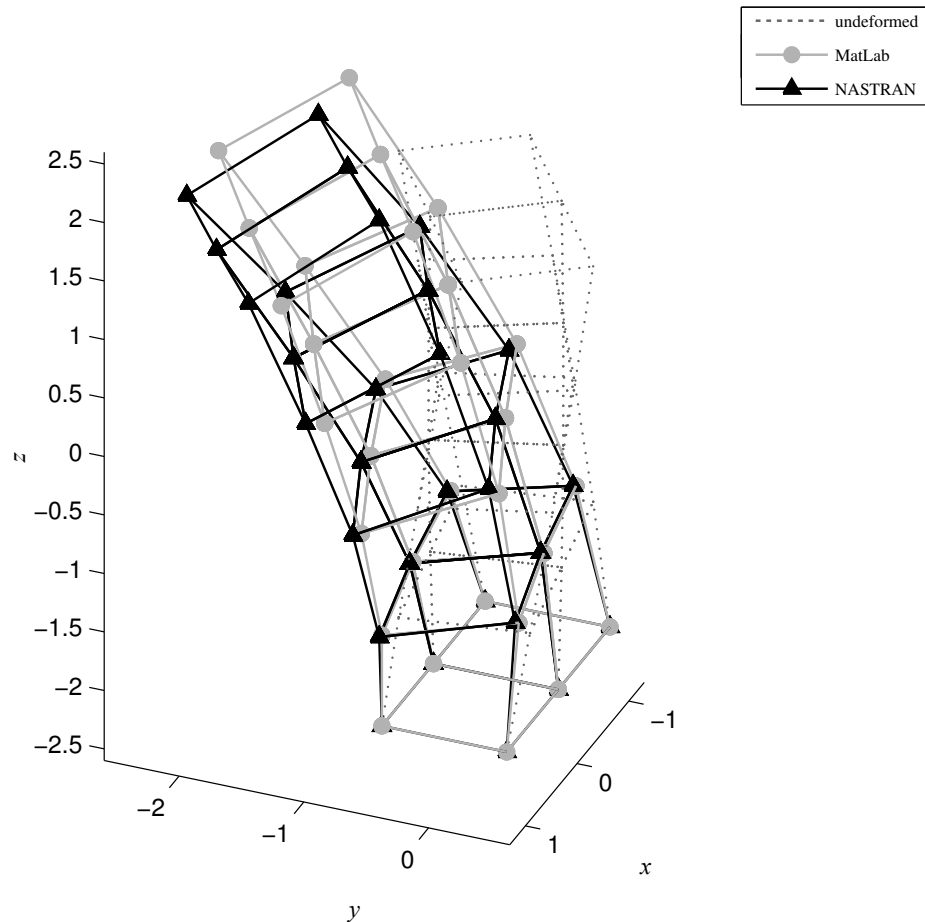


Figure 6.28: The comparison of the linear static deformations obtained with MatLab and NASTRAN

In fact there is a considerable difference in shape between the linear solutions obtained with the two codes and also between the nonlinear solutions obtained with the two codes. But within the codes the linear and the nonlinear are largely equal in shape. This is an expression and a confirmation of the weak nature of the present nonlinearities.

This confirms that the developed test-case can be used as a typical example of a geometrically nonlinear solution.

This conclusion can be made despite the remaining differences between the initial solutions and the solutions obtained with NASTRAN because the following research is not preoccupied with the correctness of the nonlinear solution but with its reproduction from a reduced order model. The developed nonlinear finite element test-case, which is confirmed to be typical and reliable, is a more than adequate tool.

Comparisons of dynamic transient solutions with NASTRAN are not performed because the study above, with static solutions, sufficiently demonstrates the suitability of the developed test-case. In a dynamic solution the inertial terms are simply reduced in size in order to not domineer over the nonlinear stiffness effects. This should give ample margin for a nonlinear dynamic analysis.

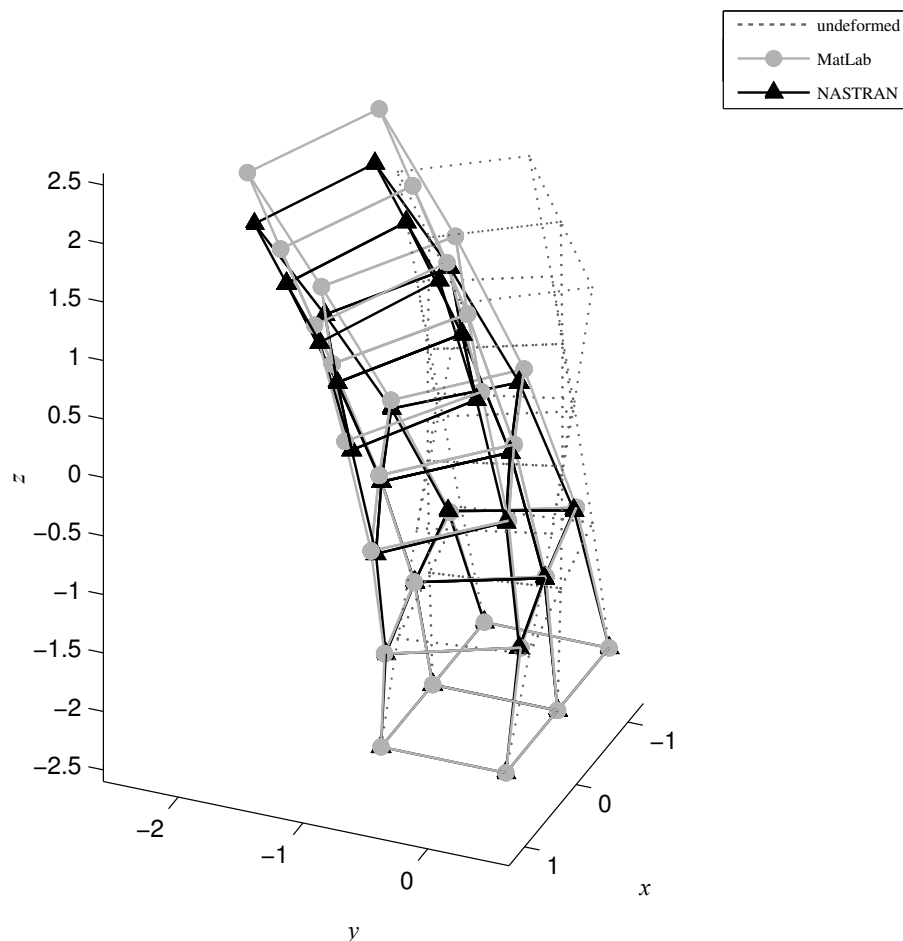


Figure 6.29: The comparison of the nonlinear static deformations obtained with MatLab and NASTRAN

### 6.3.2 Prestressing the finite element test-case with volume elements

One of the most constraining environmental variables with an impact on the structural dynamic of a turbine blade is the prestressing resulting from the centrifugal loads induced by the rotating motion of the engine's spools. The rotational speed of the engine is also expected to be one of the major parameters influencing the reduced basis to be applied.

Sternchüss et al. [215] provides a framework for the reduction of multistage turbine disks. While the evoked problems of coupling reduced substructures is not in the focus of the present work, the work gives considerable insight into the specific problems of simulating the structural dynamics of turbine engines.

In Sternchüss and Balmès [217], and in the underlying dissertation Sternchüss [216], an extensive and detailed framework is developed for the prestressing of turbine disks and blades. Most notably this concerns the effects, e.g. gyroscopic coupling and Coriolis-forces, that arise in a structure revolving with a rotational frequency  $\Omega_a$ . All resulting matrices that are representing these effects are developed. The quasistatic, prestressed equilibrium of a structure rotating in a stationary manner is calculated non-linearly. The non-

### 6.3. APPLYING THE INTEGRATED METHOD TO GEOMETRICALLY NONLINEAR VOLUME ELEMENTS

error metric		value
R2MSE	$e_r$	0.6454
MAC	$e_a$	0.9770
$\left( \left  \bar{\mathbf{u}}_{tip}^{(linear)} \right  - \left  \bar{\mathbf{u}}_{tip}^{(nonlinear)} \right  \right) / \left  \bar{\mathbf{u}}_{tip}^{(linear)} \right $		29.6 %

Table 6.15: The comparison of the linear and the nonlinear static solution of the finite element test-case with volume elements obtained NASTRAN

linearity is supposed due to the following nature of some of the forces and due to finite displacements of an otherwise linear material. The system is linearised around the quasistatic equilibrium displacements and all further calculations are performed with the linearised system. While this assumption does not hold for the systems used in the present work, it allows, under the additional assumptions of stationarity and others, the possibility to express the linearised tangent stiffness matrix for the prestressed configuration as a second order polynomial approximation in  $\Omega_a^2$ . This greatly simplifies the follow-on calculations for the linearised system if the external parameter of the rotational frequency is changed.

The present work requires the prestressing of the system foremost as a source of external parameters that have an influence on reduced basis. Furthermore, all simplifications available from linearising the system at the prestressed configuration are to be avoided to have an exclusively non-linear description of the system. This would require the integration of a full-fledged nonlinear description of all the terms due to the introduction of rotation into the geometrically non-linear description of the finite elements. A task that is as complex as it is obscuring the aim of simply having an external parameter available that is not completely artificial and has a remote resemblance to a real world equivalent.

With this objective in sight, the prestressing is considerably simplified. Even to a point where the intention of simply having a parameter available for follow-on studies is used to justify physically deficient descriptions. Most notably among these simplifications are the modelisation of the prestressing forces, which result from the centrifugal forces, as non-following forces during the initial, quasistatic prestressing, and the disregard of all additional forces, mainly the Coriolis-forces, during the following transient solutions. This allows to describe the prestress simply as an additional external force that depends on  $\Omega_a$  and the radius of rotation  $r_a$ . The prestress is then introduced by simply imposing different initial conditions for the transient solution.

The final justification for a considerably simplified inclusion of prestressing is its ultimate purpose. The prestressing is introduced to act as a parameter that affects foremost the reduced basis with which the solution of the reduced basis is initiated. This renders all deeper intrusions into the formulation of the non-linear system unnecessary.

The ultimate aim of the prestress is to introduce a set of parameters with a certain physical meaning that can be used to test the interpolation method that is described in section 5.3 with the intention to adapt the reduced basis to external parameters. The resulting vector of parameters is  $\boldsymbol{\mu} = [\Omega_a, r_a]$ , with the rotational frequency and the radius of the rotating motion. These external parameters act exclusively on the initial reduced basis, the initial conditions of the transient solution and the external forcing. The process of prestressing, which is described in the following, is already applied in its one-dimensional form to the finite element test-case with bar elements in section 6.2.2.1.

### 6.3.2.1 Generating the prestressing force

Taking the development of Sternchüss [216] the initial equation (2.82), which is only valid in an inertial reference frame, has to be extended to

$$M\ddot{\mathbf{u}} + (\mathbf{D} + \mathbf{C})\dot{\mathbf{u}} + (\mathbf{K}_c + \mathbf{K}_a)\mathbf{u} + \mathbf{g}(\mathbf{u}) = \mathbf{f}_E(t) \quad (6.42)$$

in a rotating frame.

The additional terms are

- $\mathbf{D}$  the skew-symmetric matrix of gyroscopic coupling,
- $\mathbf{K}_c$  the skew-symmetric matrix of centrifugal acceleration, and,
- $\mathbf{K}_a$  the SPD matrix of centrifugal softening.

The matrix  $\mathbf{K}_c$  for the centrifugal acceleration is proportional to  $\frac{\partial \Omega_a}{\partial t}$ . Hence, it can be dismissed directly, because the frequency of the rotation  $\Omega_a$  is constant. The fact that the remaining additional terms can be dismissed is discussed in section 6.3.2.2. In fact, all additional terms are dismissed, so that equation (6.42) returns to the description given with equation (2.82). The only remaining term is an additional external force that represents the centrifugal forces due to the rotation. This is achieved by shifting the centrifugal softening terms, which are proportional to  $\Omega_a^2$ , to the right-hand side of equation (6.42) and to treat them as an additional static, external force. This is detailed in below. Naturally this approach is not exact and maybe not even correct. It is dictated by the simple requirement of the prestressing as a source of parameters that have an influence on the reduced basis. As such, the emphasis is put on a simple and direct implementation instead of a theoretically sound and correct treatment.

The introduction of the prestressing force is shown on the test-case with volume elements from section 6.3.1. This approach is justified because the prestressing is only introduced to provide external parameters  $\boldsymbol{\mu}$  and therefore a detailed or generalised discussion of prestressing on theoretical level is not sought. For the test-case with volume elements the blade is supposed to spin around an axis that is parallel to  $x$ -axis and placed at  $y = 0$  at a distance of  $z = -r_a$  below the origin of the coordinate system in which the blade is described. The rotational frequency is defined to be  $\Omega_a$ . This is a scalar value, indicating that the rotation axis is fixed.

The prestressing force is transferred to the right hand side of equation (6.42). In this equation the matrix  $\mathbf{K}_a$  accounts for the presence of the prestressing forces as a softening. However, for a non-linear problem they can be transferred to the right-hand side and expressed there as an additional, static external force  $\mathbf{f}_{E,a}$ , defined in equation (6.44). As the problem in equation (2.82) is nonlinear the external forces due to the prestressing are linked to nonlinear internal forces by the requirement of a static equilibrium at the beginning of the transient solution. Therefore it is easier to obtain  $\mathbf{f}_{E,a}$  directly from the centrifugal accelerations than by constructing the matrix  $\mathbf{K}_a$  and multiplying it with a displacement.

For each node of the mesh the components of the nodal accelerations, resulting from the rotation are calculated as

$$\mathbf{a}_N = \begin{bmatrix} 0 \\ y \\ r_a + z \end{bmatrix} \Omega_a^2, \quad (6.43)$$

where  $y$  and  $z$  are the coordinates of the node in question. The nodal  $\mathbf{a}_N$  are then assembled to a global acceleration vector  $\mathbf{a}$  that is multiplied with the mass matrix of the blade in order to obtain a corresponding

### 6.3. APPLYING THE INTEGRATED METHOD TO GEOMETRICALLY NONLINEAR VOLUME ELEMENTS

---

force

$$\mathbf{f}_{E,a} = \mathbf{M}\mathbf{a}. \quad (6.44)$$

The resulting forces  $\mathbf{f}_{E,a}$  are then applied as external loading for a static nonlinear Newmark solution. This yields the displacements  $\mathbf{u}_a$  as the solution of

$$\mathbf{g}(\mathbf{u}_a) = \mathbf{f}_{E,a} \quad (6.45)$$

and the linear tangent stiffness matrix

$$\bar{\mathbf{K}}_a = \left. \frac{\partial \mathbf{g}(\mathbf{u})}{\partial \mathbf{u}} \right|_{\mathbf{u}_a}. \quad (6.46)$$

The displacements  $\mathbf{u}_a$  and the linear stiffness matrix  $\bar{\mathbf{K}}_a$  are used to generate the initial reduced basis  $\Phi_0$  at  $t_0$  of the simulated period. This can be achieved by using the interpolation approach from section 5.3.2.2. The  $\mathbf{u}_a$  and the  $\dot{\mathbf{u}}_a = \mathbf{0}$  are fed into the nonlinear Newmark scheme as initial conditions.

If the reduced system is to be prestressed, the initial conditions  $\mathbf{q}_a$  have to be created specifically. A simple least-squares projection with  $\mathbf{q}_a = (\Phi^T \Phi)^{-1} \Phi^T \mathbf{u}_a$  is not sufficient. Instead, an iterative reduced static solution is applied. This approach yields directly the  $\mathbf{q}_a$  and also the associated reduced basis  $\Phi$ . It only works with the reduced bases from section 3.3 that require a single displacement. Methods for the creation of the reduced basis that require more information, notably the orthogonal decompositions in section 3.3.3, which require a time history of the displacements, are not compatible with this iterative reduced static solution.

Once the simulation is initialised with the respective initial conditions and the corresponding reduced basis is established, a transient solution can be started. In the next step it is shown that this approach to introducing the prestressing is sufficient, and especially that the Coriolis-forces can be dismissed.

#### 6.3.2.2 Dismissing the Coriolis-forces

While simulating the rotation of the blade around the fixed axis of the engine, the pre-stress resulting from the centrifugal forces can be easily accounted for. However, rotation induces additional forces, namely the Coriolis-forces resulting from the Euler-equations, which have to be carefully studied before being treated.

The second major additional force is the Euler-forces. However, this fictitious force would depend on  $\frac{d\Omega_a}{dt}$ , implying a non-uniform rotation. This is not the case, as  $\Omega_a$  is constant over time, and the Euler-forces can thus be dismissed directly.

This is taken into account by dismissing the matrix  $\mathbf{K}_c$  in equation (6.42).

The Coriolis-forces are represented by the matrix  $\mathbf{D}$  in equation (6.42).

A measure for the influence of the Coriolis-forces is the Rossby-number  $\mathcal{R}o$ . It is widely used in fluid dynamics for e.g. atmosphere applications (e.g. Warn et al. [239]). It gives the proportion between inertial and Coriolis-forces. The Rossby-number is defined as

$$\mathcal{R}o = \frac{v}{fL} \quad (6.47)$$

where the  $v$  states a characteristic velocity and  $L$  a characteristic length scale of the problem. The Coriolis parameter  $f = 2\Omega \sin(\phi)$  is closely related to the origins of the discovery of the Coriolis-force on planet

### 6.3. APPLYING THE INTEGRATED METHOD TO GEOMETRICALLY NONLINEAR VOLUME ELEMENTS

---

Earth, where it accounts for the revolution of the planet  $\Omega$  and the geographical latitude  $\phi$ . It is somewhat adapted in order to fit the particularities necessary for its application in the context of a revolving turbine blade.

For the interpretation of the Rossby-number there are three cases to be considered :

- $\mathcal{R}o \gg 1$ , the inertial forces are predominating and the Coriolis-forces can be dismissed
- $\mathcal{R}o \approx 1$ , inertial and Coriolis-forces are equally important and neither can be dismissed
- $\mathcal{R}o \ll 1$ , the Coriolis-forces are predominating and the inertial forces can be dismissed.

For the numerical evaluation of the Rossby-number the following values are taken, each representing a worst-case estimate of the possible values

- $v = 1.473$ , as the maximum absolute value of any velocity during a simulation without Coriolis-forces,
- $L = r_a = 5$ , as the mean radius of the blade on its rotation around the engine's axis and
- $\Omega_a = \frac{1}{300}$ , as the blade's rotational speed around the engine's axis.

The term  $\sin(\phi)$  is evaluated by geometric considerations at the blade's root, where the maximum value for  $\sin(\phi)$  occurs

$$\sin(\phi) = \sqrt{\frac{\left(\frac{1}{2}L_x\right)^2 + \left(\frac{1}{2}L_y\right)^2}{\left(r_a \frac{1}{2}L_z\right)^2 + \left(\frac{1}{2}L_x\right)^2 + \left(\frac{1}{2}L_y\right)^2}}. \quad (6.48)$$

Inserting the numerical values into (6.47) yields the applicable Rossby-number

$$\mathcal{R}o = \frac{1.473}{2 \frac{1}{300} 0.3492 5} = 126.5. \quad (6.49)$$

This clearly states that the Coriolis-forces, and the matrix  $D$ , which is expressing them, can be dismissed for the test-case with volume elements.

#### 6.3.2.3 Introducing the prestressing in the solution algorithm

The introduction of the prestressing displacements into the non-linear systems, which are ultimately reduced, requires some attention. While not aiming at a deep theoretical foundation as accumulated by e.g. Sternchüss [216], an approach has to be developed that allows prestressing the system without interfering with the reduction.

The applied introduction of the prestressing is not a classic one. The classic theories of prestressing, especially for exclusively linear problems, introduce a shift of origin for the displacements by defining a new displacement coordinate by  $\check{u} = u - u_a$  (see e.g. Bathe [22]).

This is not done for the used approach because the non-linearity of the system prohibits such a simple transformation. To circumvent this limitation and to allow for an introduction of prestressing the proposed approach draws on the fact that the transient solutions under investigation are initialised from a static equilibrium and imposes this equilibrium prior to the dynamic solution.

To not change displacements of the system by shifting the origin offers the advantage to retain the absolute displacements  $u$ . This description of the system's dynamics does not interfere with the reduction. The approach only engages changes to the initial conditions and the external forces. This approach is feasible under the supposition that the Coriolis-forces can be dismissed. This is the case as it has been demonstrated

### 6.3. APPLYING THE INTEGRATED METHOD TO GEOMETRICALLY NONLINEAR VOLUME ELEMENTS

---

above.

The justification for keeping the prestressing force on the right-hand side of the system in equation (2.82), i.e. to include it in the external forcing, is to have a formulation that is equivalent to altering the external forcing as it was exercised in section 4.2.2 for testing the robustness of the reduced bases. As stated in the introduction to this section, this approach is not common for linear systems because it does not shift the origin. However, it lends itself readily to a completely non-linear system as described below.

For a completely non-linear system, where notably the transient solution is calculated in a non-linear manner, it is impossible to achieve a shift in origin similar to the introduction of the  $\bar{\mathbf{K}}_a$  from equation (6.46) for the linear system. Should a shift in origin of the form  $\check{\mathbf{u}} = \mathbf{u} - \mathbf{u}_a$  be introduced, this would require the formulation of a dedicated expression for the non-linear forces of the type  $\check{\mathbf{g}}(\check{\mathbf{u}})$  that evolves around the new origin of the prestress displacements  $\mathbf{u}_a$ .

Therefore the following approach is proposed which does not alter the non-linear forces vector. It uses a non-linear static solution for establishing the prestress displacements  $\mathbf{u}_a$ . From there on these displacements are used as initial conditions for the non-linear transient solution and balanced by adding the constant prestressing forces to the external forces.

Beginning with equation (2.82)

$$\mathbf{M}\ddot{\mathbf{u}} + \mathbf{C}\dot{\mathbf{u}} + \mathbf{g}(\mathbf{u}) = \mathbf{f}_E(t), \quad (6.50)$$

the static prestressing displacements  $\mathbf{u}_a$  are found. They have to comply with the static equilibrium

$$\mathbf{g}(\mathbf{u}_a) = \mathbf{f}_{E,a}. \quad (6.51)$$

With these the new, prestressed system can be written directly as

$$\mathbf{M}\ddot{\mathbf{u}} + \mathbf{C}\dot{\mathbf{u}} + \mathbf{g}(\mathbf{u}) = \mathbf{f}_{E,a}(t), \quad (6.52)$$

with its external forces contracted to

$$\mathbf{f}_{E,a}(t) = \mathbf{f}_E(t) + \mathbf{f}_{E,a} \quad (6.53)$$

in order to have a consistent representation. It has to be initialised with

$$\mathbf{u}(t = t_0) = \mathbf{u}_a \quad (6.54)$$

$$\dot{\mathbf{u}}(t = t_0) = \dot{\mathbf{u}}^{(0)}. \quad (6.55)$$

This system allows introducing the prestressing to the solution procedure as a carrier for parameters without altering the structure of the system or interfering with the reduction.

If the prestressed system is reduced, an equally reduced static solution is required to prepare the  $\mathbf{q}_a$ . This has to be done to ensure a stable static equilibrium in the prestressed configuration. Such an equilibrium cannot be achieved by simply putting  $\mathbf{q}_a = (\mathbf{\Phi}^T \mathbf{\Phi})^{-1} \mathbf{\Phi}^T \mathbf{u}_a$  as a least-squares approximation. The reduced system is such sensitive to the initial conditions.

Furthermore, during the reduced static solution for determining the prestress, the reduced basis  $\mathbf{\Phi}$  has to be adapted if it depends on the displacements. Taking the archetypical example of the LNM at current displacement from section 3.3.1.2, the reduced basis has to be updated after each Newton-Raphson iteration

### 6.3. APPLYING THE INTEGRATED METHOD TO GEOMETRICALLY NONLINEAR VOLUME ELEMENTS

---

of the static solution. Naturally, the method for updating the reduced basis, that is developed in section 5.1.3 can be used. However, the reduced basis is not augmented because the update at every iteration does not introduce jumps.

The proposed approach inserts a non-linear static solution for prestress displacements. The non-linear transient solution is the superposed to the prestress displacements which are kept in a static equilibrium by adding the static prestressing forces to the external forces.

#### 6.3.2.4 Testing prestress and basis adaptation on the finite element test-case with volume elements

With all elements available for treating the prestressing of reduced nonlinear finite element systems the subject can be tested. They aim is to obtain a first characterisation of the behaviour of the system under prestress. The Campbell diagram of the test-case with volume element is established and analysed. This analysis allows determining that the results of that are obtained from the test-case with bar elements can be ported over to the test-case with volume elements and the test-case with volume elements is characterised. This limited study also augments the findings that have been obtained for the parameterisation of the academic test-cases in section 5.3.5.

**6.3.2.4.1 Establishing and analysing the Campbell diagram** The Campbell diagram plots the eigenfrequencies of the blade against its rotation frequency  $\Omega_a$ . It is a very common tool in engineering application and it can be calculated by simple brute force approaches, which is the case here. However, there are more elegant variants available, e.g. a modal approach by Genta [82]. If frequency crossing occur an adapted tracking method is prepared by Tran [227].

Executed for the non-linear finite element test-case with volume elements, the resulting Campbell diagram in figure 6.30 shows some mild frequency crossing with curve veering for higher eigenfrequencies for several ranges of the rotation frequency but no frequency crossing (Tran [227]) In summary the Campbell diagram reveals no particularities that require special attention or that are susceptible of posing major problems during a reduced solution.

**6.3.2.4.2 Testing the basis adaptation by prestressing the finite element test-case with volume elements** The interpolation of the reduced bases that is developed in section 5.3.2.2 is applied to the finite element test-case with nonlinear volume elements. The parameters  $\mu$  are the prestress radius  $r_a$  and the rotational frequency  $\Omega_a$  that are introduced in section 6.3.2. The reduced bases that are used for the interpolation are established with the LNM at the static displacements  $\mathbf{u}_a$  that result from the prestressing at the given operating point  $\mu_i = [\Omega_i, r_i]$ .

Table 6.16 contains the error metrics of the R2MSE  $e_r$  and the MAC  $e_a$  between the reference modes  $\phi_{0,\text{ref}}$  and the modes  $\phi_0$  that are obtained with the interpolation. The origin R2MSE  $e_r^{(\mu_k)}$  and the origin MAC  $e_a^{(\mu_k)}$  are the error metrics that are obtained between the interpolated modes  $\phi_0$  and the origin  $\phi_k$  at the operating point  $\mu_k$  that is closest to the operating point where the basis is interpolated. They serve as reference and demonstrate the gain in precision of the modes due to the interpolation.

In fact the interpolated modes  $\phi_0$  and the reference modes  $\phi_{0,\text{ref}}$  are visually indistinguishable. The is shown with the example of the first mode in figure 6.31. Together with the numerical results from table 6.16 this demonstrates the exceptional quality of the interpolated reduced basis. However, the origin error metrics also show that the modes at the origin of the interpolation are not significantly different from the modes at the interpolation point  $\mu_0$ . Yet, a slight improvement on their quality can take place by applying the interpolation algorithm.

The results of the application of the interpolation algorithm to the prestressed test-case with finite volume elements show that this approach is applicable to the complicated shapes of the finite element modes. Even though the prestressing has only a minor impact on the shape of the modes and all modes that are used in

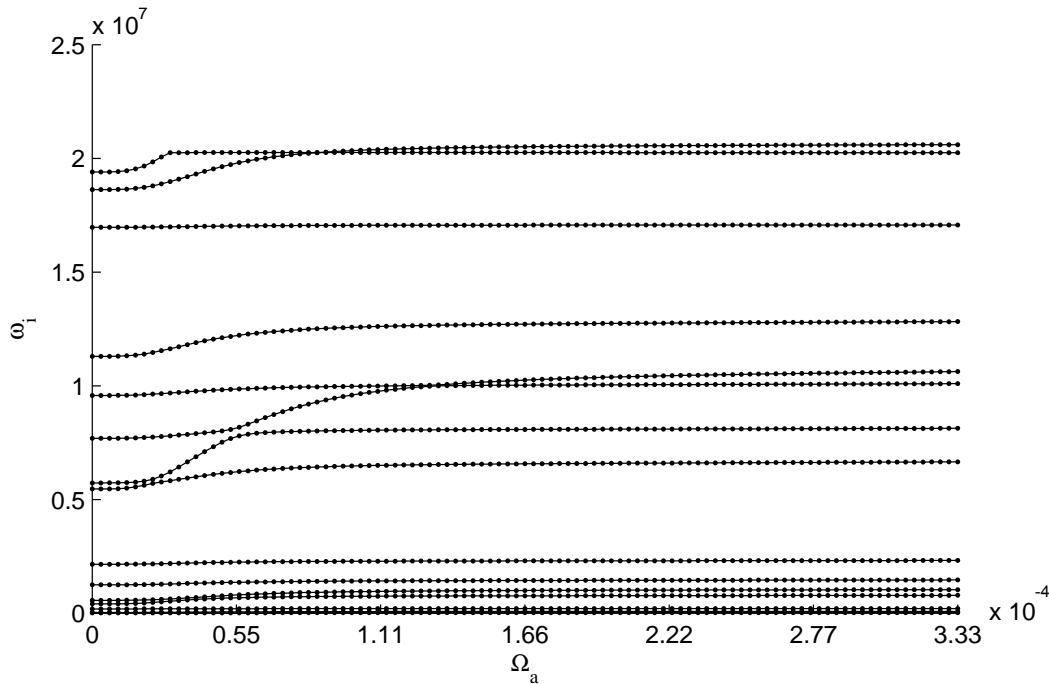


Figure 6.30: The Campbell diagram of the finite element test-case with volume elements under prestress

the database and at the origin of the interpolation are very similar, the interpolation approach still allows improvements. This study confirms the observations that have already been made for the test-case with bar elements in section 6.2.2.1 and adds the confidence that the interpolation method can also be applied to the much more complicated mode shapes of the three-dimensional nonlinear finite element test-case. The interpolation method can be used on the present test-case without restriction for preparing and initialising the transient solution.

**6.3.2.4.3 Outcome of the interpolation** In conclusion it can be stated that the interpolation algorithm from section 5.3.2 for adapting the reduced basis as a function of external parameters, can be used securely with the developed test-cases. The main reason for this is that the method performs well for moderately nonlinear systems if the parameters do not change excessively. This is proven with its application to the test-case with bar elements. This is an important result because it limits the range of safe application of the interpolation method to this type of nonlinear system. Going beyond this range, towards other categories of nonlinear systems with considerably different behaviour, would require additional efforts to extend the range of safe application to these categories.

Furthermore, the study of the Campbell diagram for the test-case with volume elements in section 6.3.2.4.1 above shows that the nonlinear test-case with volume element falls in this category of moderately nonlinear system. In particular, the low number of interactions between the modes assures that equal types of modes are interpolated. It can be considered as hardly probable that a traction mode from one precomputed operating point is interpolated with a torsion mode from another precomputed operating point. The main result remains valid. The interpolation method from section 5.3.2 can be applied without restrictions to the developed finite element test-cases.

### 6.3. APPLYING THE INTEGRATED METHOD TO GEOMETRICALLY NONLINEAR VOLUME ELEMENTS

mode	R2MSE $e_r$	origin R2MSE $e_r^{(\mu_k)}$	MAC $e_a$	origin MAC $e_a^{(\mu_k)}$
1	0.0139	0.0171	0.9998	0.9997
2	0.0104	0.0126	0.9999	0.9998
3	0.0322	0.0405	0.9990	0.9984
4	0.0208	2.0000	0.9996	0.9993
5	0.0092	0.0114	0.9999	0.9999
6	0.0161	0.0204	0.9997	0.9996
7	0.0271	0.0345	0.9993	0.9988
8	0.0231	0.0299	0.9995	0.9991
9	0.0246	0.0339	0.9994	0.9988
10	0.0242	0.0311	0.9994	0.9990
11	0.0249	0.0337	0.9994	0.9989
12	0.0478	0.0666	0.9977	0.9956

Table 6.16: The comparison of the interpolated modes with the reference modes for the finite element test-case with volume elements

#### 6.3.3 Applying the integrated method to the finite element test-case with volume elements

The application of the integrated method from section 6.1 to the finite element test-case with volume elements is straightforward. It does not require any additional modification of the developed methods. This allows revisiting all studies that have been performed until now while concentrating solely on the results. A situation that is exploited by first confirming the results from the comparison of the reduced bases from chapter 4 with selected reduced bases and only then applying the integrated method. This is done in several small steps, each with the introduction of one element at the time, and with a concentration on the aspects of accuracy and computational performance. These become highly visible with finite element test-case with volume elements.

##### 6.3.3.1 Confirming the numerical studies on the finite element test-case with volume elements

This section strives at confirming the results from the studies of comparing the reduced bases and to test their robustness, which are performed in chapter 4 with the academic test-cases. It follows the same approach as outlined in section 4.1.1.

**6.3.3.1.1 Comparison of the reduced bases** Included in the comparison of reduced bases on the non-linear finite element test-case are reduced bases created from

- Linear Normal Modes,
- Ritz-vectors, and
- Proper Orthogonal Decomposition.

These reduced bases have been chosen because there are the most promising directions of research for an entirely non-linear system under harmonic excitation. This follows the results obtained on the academic test-cases in section 4.2.1 and under the constraint of only a few simulations that can be executed. Included are reduced systems of order  $r \in \{1, 2, 5, 6, 12, 30\}$ . In order to highlight the different types of LNM modes that reflect basic deformations such as compression, bending and torsion, the test-case is subjected to a compressive load along the  $z$  axis. The obtained results are shown in figure 6.32.

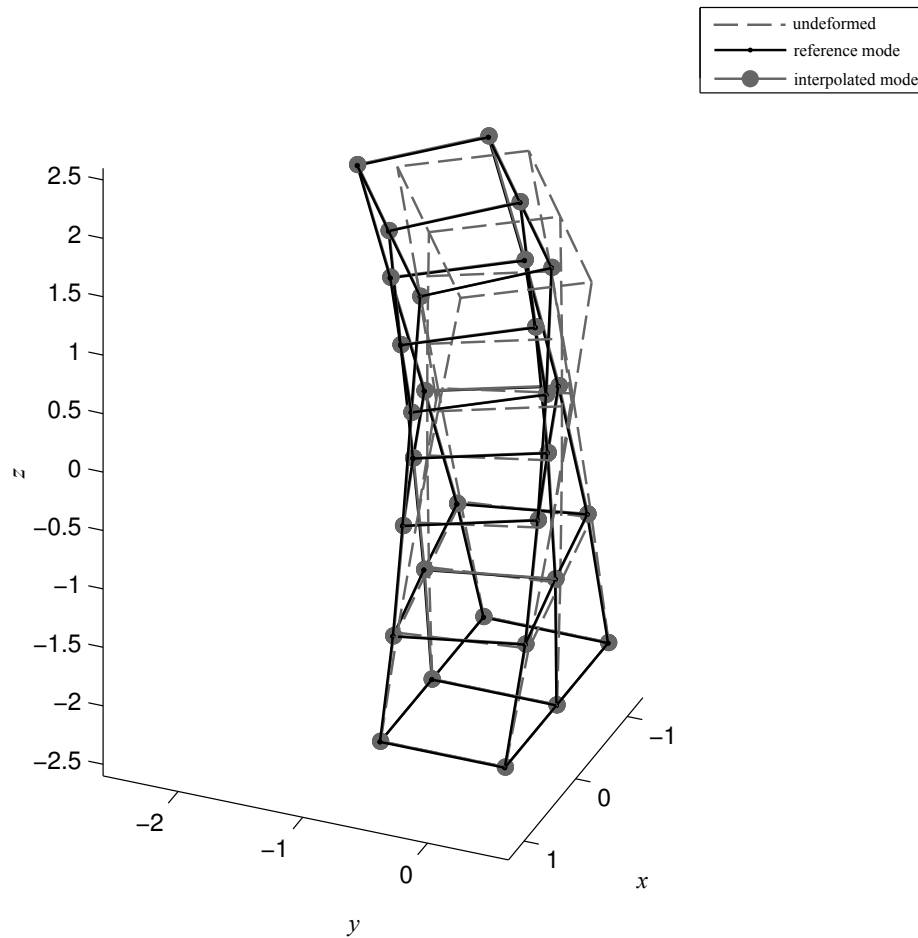


Figure 6.31: The interpolation of the first mode of the finite element test-case with volume elements

By closely inspecting the shape of the LNM it can be seen that the first five LNM of the underlying linear system are bending and torsion modes. The sixth LNM is the first compression mode to appear if the modes are arranged corresponding to the respective eigenfrequency in increasing order. This also becomes obvious in the large drop in error from  $r = 5$  to  $r = 6$ . The next such drop occurs at  $r = 12$ , where the twelfth LNM introduces the second compression mode. Adding more LNM to the reduced basis does not improve the result.

The LNM bases at  $r = 1$  and at  $r = 2$  are these two compression modes along the  $z$ -axis. These compression modes correspond to the sixth and twelfth mode in the LNM basis. The first and the second compression mode are selected by inspection of the mode shapes. Because of this selection of the modes, that is adapted to the deformations expected to result from the applied excitation, these two bases are not to be included directly into the comparison. Therefore they are marked with hollow circles. The inspection of these errors shows, that, for a pure compression excitation, these two modes are sufficient for the representation of the full order solution.

### 6.3. APPLYING THE INTEGRATED METHOD TO GEOMETRICALLY NONLINEAR VOLUME ELEMENTS

The Ritz-vectors are not very well suited to reduce the non-linear finite element system, because they tend to deliver inconsistent mode shapes.

The POD reduced bases immediately capture the correct deformation from  $r = 1$  on. Unlike the LNM they also include the forming of the belly at the root of the blade under compression. Secondary effects are then captured by the POD basis at  $r = 2$ . Increasing the order of the POD reduced model further does not contribute to the quality of the restored solution. This is most probably due to the fact that the response of the finite element test-case with volume elements is rather smooth and without any high frequency oscillations that would warrant a resolution with a high number of POD vectors. Between  $r = 5$  and  $r = 6$  POD and LNM are on par, and beyond that the POD perform worse than the LNM. In fact, the error obtained with the POD bases appears to increase with an increasing order  $r$  of the reduced basis. This contrary to the results obtained in section 4.2.1, during the comparative study and the expectation that is given by equation (3.133) for the energy ratio captured by the reduced system. However, this behaviour of the error seems to be a common experience during the numerical application of the POD. The numerical representation of the POD basis may be such that its rank is not full or that its rank lags behind the number of vectors, as the order of the basis is increased. This can lead to the observed adverse effect of increasing the order of the POD basis. From this point of view the finite element test-case is superior to the academic test-case introduced in section 4.1.3.1, because it brings forward this particularity of the POD bases.

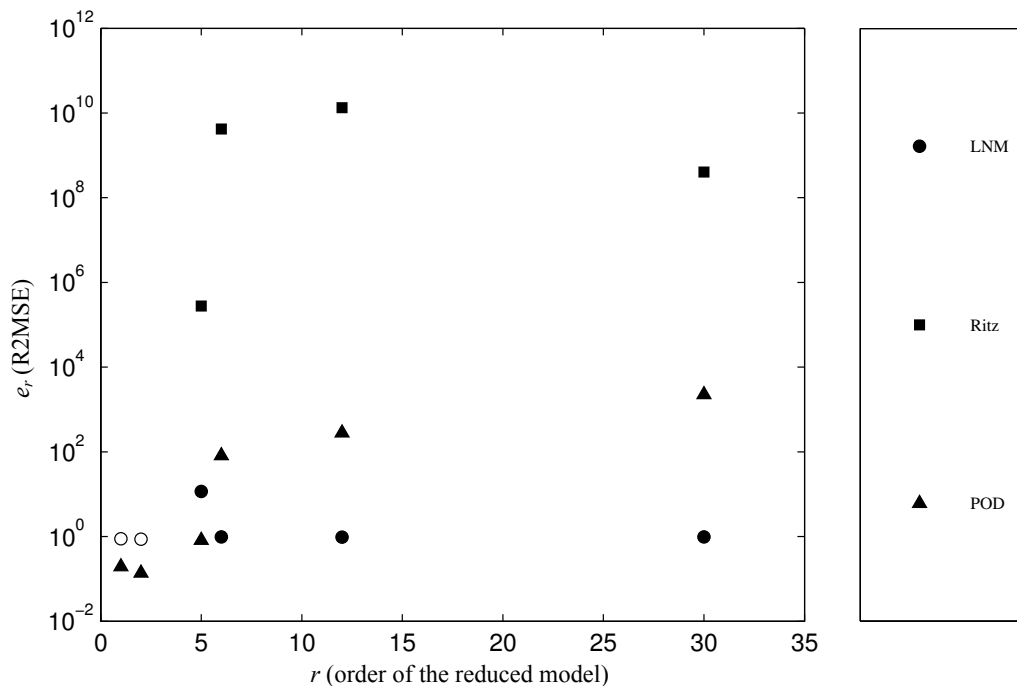


Figure 6.32: The R2MSE for the finite element test-case with volume element for different reduced bases

In conclusion it can be summarised that the LNM perform as well as the POD if the right modes are selected. In case of doubt it should be sufficient to include enough LNM in the reduced basis to cover all major components of the model's behaviour.

Additional studies, which cover excitations that lead to bending, yield comparable results yet are not documented. Combined excitations, which would lead to combinations of bending and compression with torsion, are not investigated, because the torsion modes have a high eigenfrequencies and are not covered by the rather small orders  $r$  of the reduced system. The study is continued with the initial external forcing from section 6.3.1.2, which oscillates in the  $[x, -y, z]$ -diagonal to circumvent the excitation of a single mode.

Such an excitation of a single mode might occur when only one frequency is excited.

**6.3.3.1.2 Robustness of reduced bases** The investigation into the robustness of the reduced bases is exercised only for the LNM and the POD reduced bases at  $r \in \{2, 5, 12\}$ . Only the amplitude  $\hat{f}_E$  and the frequency  $\Omega$  of the excitation are altered. Its point of application remains unchanged. The results are shown in figures 6.33 and 6.34.

For the LNM the general findings that are obtained for the academic systems in section 4.2.2 are well confirmed. Reducing the values for the amplitude and the frequency leads to better results. If the values are increased the quality of the solution deteriorates. However, for the finite element model, the frequency seems to have less influence than the amplitude. This is contradictory to the results obtained on the academic systems. For the POD bases, the results are much more ambiguous. A fact to which the sparse number of simulation only contributes. However, this mirrors the findings obtained with the academic systems.

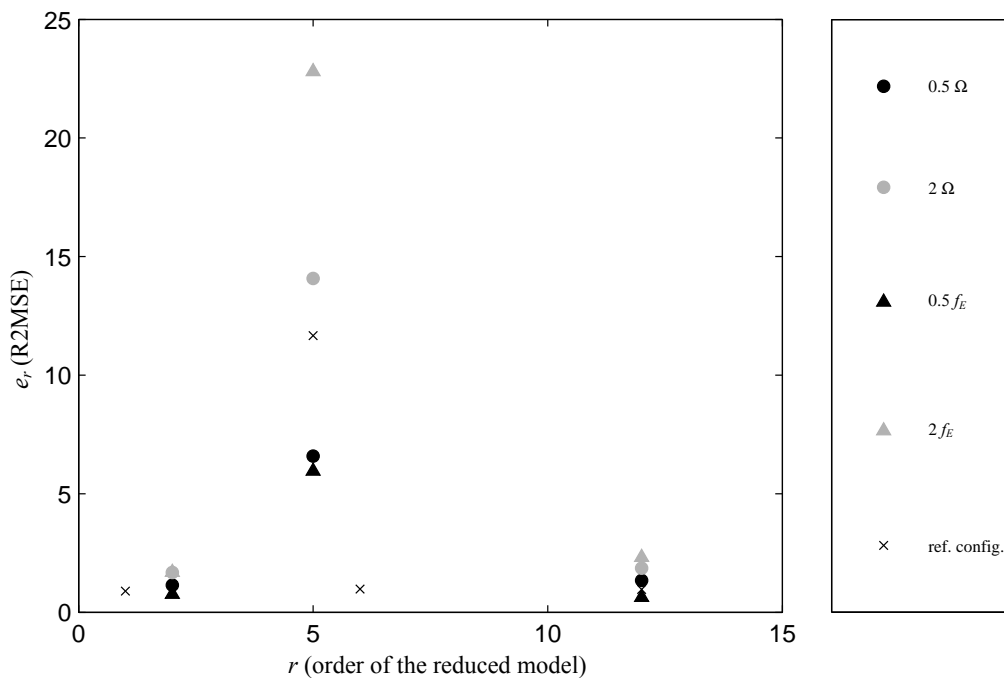


Figure 6.33: The R2MSE for the robustness of the Linear Normal Modes for the non-linear finite element system under harmonic excitation

**6.3.3.2 Evaluating the gain in computational performance by rendering the finite element test-case with volume element autonomous**

The preliminary results that are obtained with the FEM test-case highlight two of the main capabilities of the employed methods. The first one is the possibility of the recreation of the high-fidelity solution with an approximation and the second is the massive gain in computational performance by employing a reduced formulation while keeping a reasonable level of accuracy. These aspects of the polynomial formulation of the nonlinear terms is explored further in the following. For the time being, no update and augmentation of the reduced basis is performed and the study concentrates on the errors and computational gains due to the autonomous formulation of the finite element test-case with volume elements. Following the results from section 6.1.2, the variant of the polynomial formulation with indirect identification of the reduced tensors

### 6.3. APPLYING THE INTEGRATED METHOD TO GEOMETRICALLY NONLINEAR VOLUME ELEMENTS

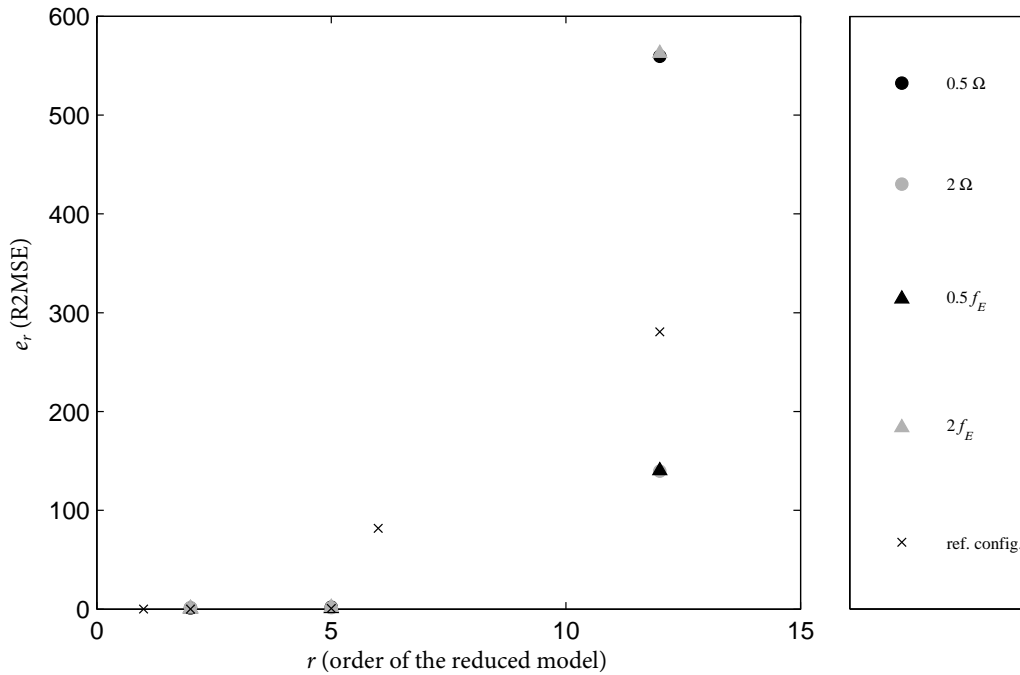


Figure 6.34: The R2MSE of the robustness of the Proper Orthogonal Decomposition for the non-linear finite element system under harmonic excitation

is applied to render the test-case autonomous. This variant of the polynomial formulation is described in section 5.2.2.2.

**6.3.3.2.1 Accuracy** Regarding the accuracy of the solutions that are obtained with different methods figure 6.35 shows an exemplary result. The physical displacements of a node at the blade's tip are obtained with

- the full order, high-fidelity solution using the non-linear volume finite elements,
- the full order solution, where the non-linear terms for the internal forces and the tangent stiffness matrix are replaced with a full order polynomial approximation, and
- a reduced solution, where the equation of the system's dynamics is projected on the LNM reduced basis with  $r = 10$  and the non-linear terms are replaced with reduced order a polynomial approximation that is identified indirectly.

It can be seen in figure 6.35 that the three solution match and the reduced solution is even conservative if judging by its established maximum amplitudes.

The corresponding errors are shown as means of the R2MSE  $e_r$  over all degrees of freedom and the time in figure 6.36. The reference solution is the full order solution with the finite element expressions for the nonlinear terms. The axes bear the indication of whether the system is reduced or not and whether the inflation or the polynomial formulation of the nonlinear terms is used. Only three of these four possible combinations of these properties are utilised, because the full order system with inflation serves as the reference solution.

It becomes obvious that the introduction of the polynomial formulation comes with a certain error. This is even the case for the full order solution. It is arguably the case that the identified full order tensors are

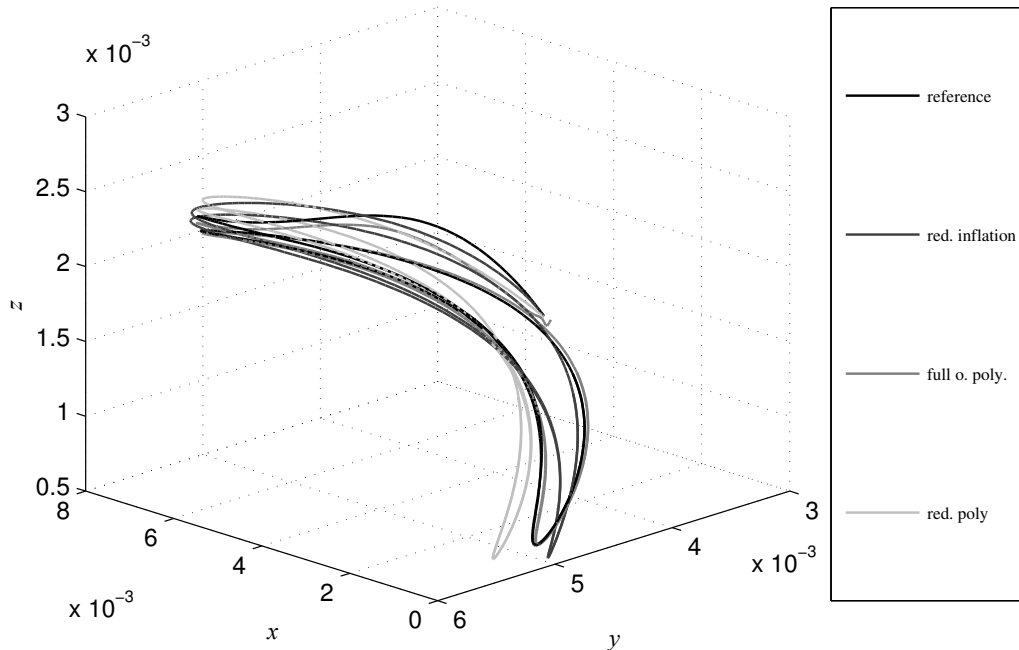


Figure 6.35: The time histories of the physical displacements of the node on the blade's tip for different solutions

not an exact description of the nonlinear terms. So, rendering the system autonomous comes at the cost of a loss in accuracy, if compared to the full order reference solution.

In fact, this error is lower than the error due to the introduction of the reduced basis. The highest error is naturally obtained with the introduction of the constant reduced basis to obtain a reduced system. It is stressed again that the error of the reduced autonomous system is a combination of the errors coming from the reduction and from the autonomy. Regarding these errors individually suggests how their contributions to the combined error of the reduced autonomous system are distributed. This justifies the special attention and considerable effort that has to be invested to obtain high-quality with the update and augmentation of the reduced basis, which ultimately leads to the integrated method. Other solutions with different reduced bases perform similarly.

**6.3.3.2.2 Polynomial formulation** The test-case with volume elements is also used to demonstrate a property of the polynomial approximation. The polynomial approximation from section 5.2.2 also includes quadratic terms in the form of the  $\mathbf{A}^{(2)}$  in equation 5.62 for the non-linear forces vector. If the tangential stiffness matrix is established in equation 5.95, these quadratic terms persist.

Naturally, a stiffness that depends quadratically on the displacements is not physical. This is even the reason for which the nonlinearities in the academic test-case in section 4.1.3.1 are to be cubic. The question to be posed is hence, whether these quadratic terms influence the solution and whether they can be neglected altogether.

Table 6.17 contains some values for the three tensors. Especially the last row, which contains the mean of all the values which are not zero, shows clearly that the quadratic terms cannot be neglected. They are in same order of magnitude as the terms of the tensor  $\mathbf{A}^{(1)}$ , which is the stiffness matrix of the underlying linear system. It is interesting to see that the tensors  $\mathbf{A}^{(1)}$  and  $\mathbf{A}^{(2)}$  share the same order of magnitude  $\mathcal{O}(10^8)$ . It has to be considered that the actual force values are obtained by multiplying the tensors with

### 6.3. APPLYING THE INTEGRATED METHOD TO GEOMETRICALLY NONLINEAR VOLUME ELEMENTS

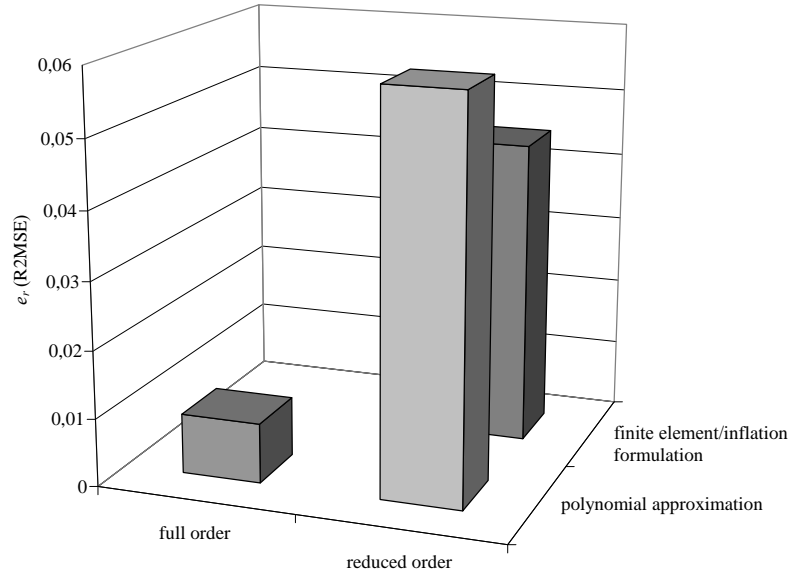


Figure 6.36: The mean of the R2MSE for different solutions of the finite element test-case with volume elements

increasing orders of the displacements. Seeing that the order of magnitude of  $\mathbf{A}^{(3)}$  is indeed  $\mathcal{O}(10^{10})$  it can be stated that  $\mathcal{O}(\mathbf{A}^{(1)}\mathbf{u}) = \mathcal{O}(\mathbf{A}^{(3)}\mathbf{u}^3)$  because the order of magnitude of the displacements  $\mathbf{u}$  is  $\mathcal{O}(10^{-1})$  for this specific case. From this observation it also follows that  $\mathcal{O}(\mathbf{A}^{(2)}\mathbf{u}^2) = 10^{-1}\mathcal{O}(\mathbf{A}^{(1)}\mathbf{u})$ . This translates to the fact that the contribution of the quadratic terms is only about 10 % of that of the linear and the cubic terms.

tensor		$\mathbf{A}^{(1)}$	$\mathbf{A}^{(2)}$	$\mathbf{A}^{(3)}$
the maximum absolute values	$\max(\ \mathbf{A}^{(i)}\ )$	$0.0001 \cdot 10^{14}$	$0.0001 \cdot 10^{14}$	$6.1149 \cdot 10^{14}$
the mean absolute values	$\ \bar{\mathbf{A}}^{(i)}\ $	$0.4276 \cdot 10^9$	$0.0965 \cdot 10^9$	$2.1752 \cdot 10^9$
the mean absolute values $\neq$ zero	$\ \bar{\mathbf{A}}^{(i)}\ _{\forall A_{ijlm}^{(i)} \neq 0}$	$0.0944 \cdot 10^{10}$	$0.0517 \cdot 10^{10}$	$1.7509 \cdot 10^{10}$

Table 6.17: The orders of magnitude in the polynomial approximation of the finite element test-case with volume elements

If this difference of one order of magnitude is sufficient to allow for neglecting the tensor  $\mathbf{A}^{(2)}$  has to be determined numerically. To this effect a solution at full order, for which the entries of  $\mathbf{A}^{(2)}$  are forced to be zero, is conducted. It reveals that this does not change the resulting displacements significantly. Yet it seems as if neglecting the quadratic terms might destabilise the solution and hinder convergence. The fact that the  $\mathbf{A}^{(2)}$  are required is established in section 5.2.2.5. Here this result is confirmed. The decision is made to continue keeping the quadratic terms to fulfil the required approach of completeness of the polynomial approximation. If this is justifiable, or even necessary, on theoretic grounds has to be determined outside

the scope of this numerical study.

**6.3.3.2.3 Performance** Matthies and Strang [145] stress that it is indeed very difficult to judge the computational performance of an algorithm based on measurements of times. This is confirmed by the authors experience expressed in section 4.1.2.4. Instead of measuring times, Matthies and Strang [145] propose to resort to counts of operations. These can be the number of evaluations of the nonlinear terms or the number required iterations for convergence. These numbers provide consistent measures that are independent from computational overhead and machine end implementation related influences. There is however, in the context of the current work, a loophole which may allow to use computational times equivalently with the number of evaluations of the nonlinear terms. The fact that the geometrically nonlinear volume elements, that are described in section 2.2.3, are implemented rather for understanding than for absolute computational performance, leads to the situation that their integration largely dwarfs the other operation required during the transient solution. This applies particularly to matrix operations, because the size of even the full order matrices is limited to the 72 degrees of freedom of the reference system. Thus, even the potentially costly inversion such a small matrix can hence basically be neglected against the evaluation of the nonlinear terms. Therefore, in the following, the measured times and the number of evaluations are used equally side by side.

Regarding the computational performance of the reduced solutions the results are plotted in figure 6.37. It plots the time needed for the actual solution of the respective system. The colours represent the same solutions as in figure 6.36 and the axis layout is the same. The full order reference solution is now also included in black. Its nonlinear terms are listed as inflation formulation event though, strictly speaking, a full order finite element formulation of the nonlinear terms cannot be inflated further.

The figure 6.37 clearly shows that the introduction of the polynomial approximation into the reduction is necessary in order to obtain a gain in computational time. Its introduction into the full order system has only a small effect on the computational time. The introduction of the reduction alone also has only a small influence. Only the parallel introduction of the reduction and the polynomial approximation yields a significant gain in computational effort. To fully grasp the gain in computational time it has to be stressed that in figure 6.37 the solution time is traced on a logarithmic axis. This a factor of gain of  $\mathcal{O}(10^3)$ . The introduction of the polynomial formulation on a test-case with finite volume elements, where the possible gains in computational effort are clearly visible and meaningful, highlights the tremendous gains that are possible.

At the same time the introduced error and its main source, the projection on a constant reduced basis, are exposed in figure 6.36. Adding the update and augmentation of the reduced basis to the solution procedure creates the integrated method as it is described in section 6.1. For the test-case with volume elements the integrated method promises a considerable improvement of the accuracy of the solution but it is also bound to eat into the gains in computational effort in figure 6.37. This requires a trade-off to be made between computational effort and the quality of the obtained solution. The following, complete integration of the basis update and augmentation may give hints to solve the contradiction that is lying under the trade-off. But already at this point it has to be made absolutely clear that no ultimate answer can be expected and the optimal trade-off always depends on the problem at hand and lies at the discretion of the user.

It is commonly accepted that for two-dimensional finite element problem the integration of the elements is the numerically most costly part of the solution, while the inversion of the matrices only comes second. For three-dimensional problems the larger number of degrees of freedom and the simpler elements, without rotational degrees of freedom, may lead to a reversal of this effect, i.e. the inversion of the matrices costs more numerical efforts than the integration of the elements. The results that are presented in figure 6.37 are not representing this particular aspect. The reduction of the matrices, while keeping an inflation formulation for the integration of the elements, does not seem to influence the solution time.

There is a possible explanation of these results. First, the used software, MatLab, is optimised and highly efficient for all kinds of matrix operations, so most certainly also for inversions. This should account for

### 6.3. APPLYING THE INTEGRATED METHOD TO GEOMETRICALLY NONLINEAR VOLUME ELEMENTS

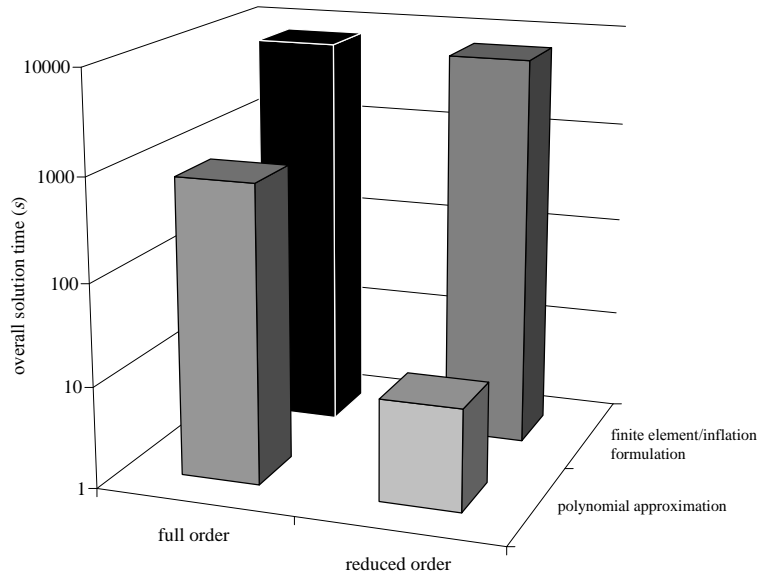


Figure 6.37: The overall solution times for different solutions of the finite element test-case with volume elements

the effect that there is no notable difference between the repeated inversion of the reduced matrices and the full order matrices. Especially if the full order matrices have already a rather limited size. Second, the implementation of the integration of the elements is far from being optimal. It is written rather for clarity and accessibility than for performance. The reason for this decision is the required access to the finite element formulation in order to obtain the direct identification of the tensors of the polynomial approximation in section 5.2.2.

The question of the performance has to be answered on an individual basis and depending on the problem at hand. A rough estimation for facilitating the decision can be given nonetheless. It hinges on the number of evaluations of the nonlinear terms at full order. The computational effort and the time that is required for these evaluations may be known or are supposed to be easily available.

For the full order solution the vector of the nonlinear internal forces  $\mathbf{g}(\mathbf{u})$  has to be evaluated at least twice per time-step. This is once for the calculation of the initial residual in equation (3.56) and once more for every iteration. Additionally, the tangent stiffness matrix from equation (3.57) has to be evaluated at least once per time-step and iteration. Depending on the severity of the threshold  $\epsilon$  in equation (3.64) these are optimal values and adding a factor in order to account for multiple iterations is prudent. A comparable number of evaluations would also be required for a solution obtained with the HHT- $\alpha$ -method. The number of required evaluations  $n_{\text{evaluations of } \mathbf{g}(\mathbf{u})}^{(\text{FOM})}$  of the full order nonlinear forces vector  $\mathbf{g}(\mathbf{u})$  can be expressed as

$$n_{\text{evaluations of } \mathbf{g}(\mathbf{u})}^{(\text{FOM})} \geq 2 \frac{t_e - t_0}{\Delta t}, \quad (6.56)$$

### 6.3. APPLYING THE INTEGRATED METHOD TO GEOMETRICALLY NONLINEAR VOLUME ELEMENTS

---

plus an equivalent number of evaluations of the full order stiffness matrix. This value for  $n_{\text{evaluations of } g(\mathbf{u})}^{(\text{FOM})}$  is a lower bound because there can be several iterations per time-step.

For the reduced solution with a constant reduced basis and the polynomial formulation as an approximation of the nonlinear terms the tensors of the polynomial formulation have to be identified. This requires

$$n_{\text{evaluations of } g(\mathbf{u})}^{(\text{ROM})} \geq \frac{1}{6} (r^3 + 6r^2 + 5r) \quad (6.57)$$

evaluations of the nonlinear forces vector. All other computations take place on reduced level.

#### 6.3.3.3 Integration of the autonomous formulation and the update and augmentation

The polynomial formulation of the nonlinear terms, which renders the reduced solution autonomous, is introduced in the previous section. It is thoroughly tested and it is demonstrated that its introduction and application in the context of geometrically nonlinear volume elements is perfectly feasible. The update and augmentation of the reduced basis is integrated as soon as the autonomy of the finite element test-case's autonomy is ensured. The introduction of the update and augmentation finalises the integrated method on the finite element test-case with volume elements after the interpolation of the initial reduced basis is proven to be feasible in section 6.3.2.

For the numerical results the transient solution of the finite element test case with volume elements from section 6.3.1 is obtained with different solutions methods. These methods are defined with respect to their nonlinear terms and with respect to the update of the reduced basis. In detail the reduced transient solutions procedures are

- an inflation formulation of the nonlinear terms and a constant reduced basis,
- a polynomial expression of the nonlinear terms and a constant reduced basis,
- an inflation formulation of the nonlinear terms and an updated and augmented reduced basis, and
- a polynomial expression of the nonlinear terms and an updated and augmented reduced basis, which is the integrated method.

The tensors for the reduced polynomial expression are obtained with the indirect reduced order identification as presented in figure 5.21. The reduced basis is constructed from the LNM as they are described in section 3.3.1. The formulation of the LNM at a given displacement is used for the update and augmentation of the reduced basis. The method made from a polynomial expression of the nonlinear terms and an updated and augmented reduced basis in the listing above is the integrated method as it is presented in section 6.1.1.

In the following the accuracy of the different solutions is treated first. Then the gains in performance are listed. These two properties of the solutions are treated independently in order to allow for well-informed trade-offs between them.

**6.3.3.3.1 Accuracy** The physical displacements of the different solutions at  $t = 1.5$  are shown in figure 6.38. This instant is chosen as being representative with large amplitude of the deformation, highlighting the differences between the solutions. This figure highlights especially the difference between solutions with a constant reduced basis and solutions with an update and augmented reduced basis. The integrated method belongs to the second type of solution. Both types of solutions are clearly distinguishable. At the tip of the blade these difference become most obvious. The two solutions that are obtained with a constant reduced basis display a larger deformation than the two solutions that are obtained with an updated and augmented reduced basis. The solutions with an updated and augmented reduced basis are nearly indistinguishable from the reference solution. This shows the considerable improvement that is possible by updating and augmenting the reduced basis. It also shows that for this case this improvement is independent from the

### 6.3. APPLYING THE INTEGRATED METHOD TO GEOMETRICALLY NONLINEAR VOLUME ELEMENTS

formulation of the reduced nonlinear terms. The solution with the inflation formulation and the solution with the polynomial formulation are basically indistinguishable. At the chosen instant two update and augmentation cycles took already place. Against the overall simulated period, the positive effect of the update and augmentation is visible almost immediately after the launch of the simulation.

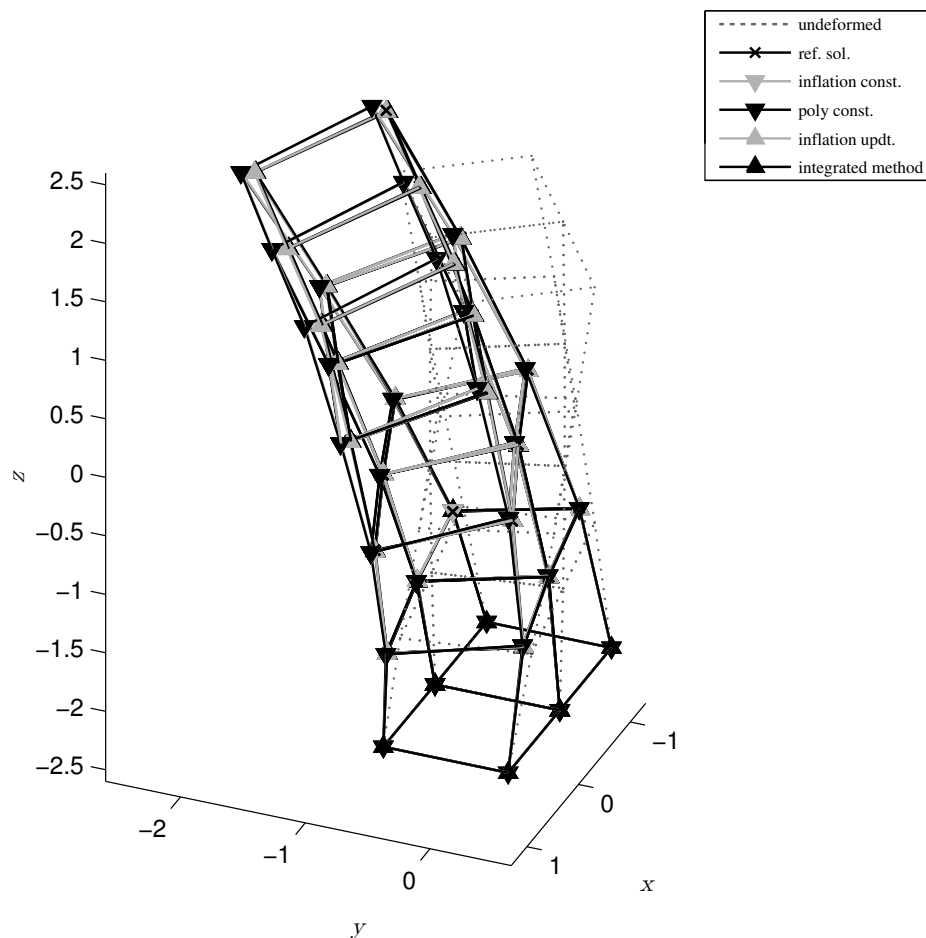


Figure 6.38: The physical displacements at  $t = 1.5$  of the finite element test-case with volume elements at  $r = 8$

The evolution of the R2MSE  $e_r$ , the MAC  $e_a$  and the relative energy  $\Delta E$  with time are traced in the figures 6.39, 6.40 and 6.41, respectively. The figures are shown exemplarily with  $r = 8$  as the order of the reduced model. All three error metrics from the figures 6.39 to 6.41 are shown with their mean and their variance of the entire simulated time in table 6.18. This table also contains different orders  $r$  of the reduced system.

All error metrics are taken between the actual reduced solution with the respective method and the full order reference solution. The R2MSE, as it is defined in equation (4.5), is used to judge the difference between the reduced solution and the full order solution at every time step. The MAC, defined in equation (4.10), allows to judge the similarity of the shapes of the displacements between the reduced solution and the reference solution. It may be the case that, even though the R2MSE indicates a large difference in

### 6.3. APPLYING THE INTEGRATED METHOD TO GEOMETRICALLY NONLINEAR VOLUME ELEMENTS

the values of the displacements, the resulting deformations are still remarkably similar. This is detected by discrepancies between the MAC and the R2MSE. Finally the relative energy difference is the sum of the kinetic and the potential energies in the inflated reduced solution normalised with the same sum from the full order reference solution. The energy difference is introduced in equation (4.8) in order to judge the amount of damping that is cut off by the introduction of the reduction. If there is more energy in the reduced system than there is in the full order system this might destabilise the solution.

The evolutions of the error metrics are generally smooth and follow the amplitude of the displacements of the solution. However, they display prominent spikes when then displacements cross zero. These spikes are purely numerical artefacts and due to the fact that the error metrics are relative ones.

In figure 6.39 it is remarkable how the R2MSE of the solution obtained with the integrated method evolves. At first rises with the other R2MSE as the simulation is started. But after the first update and augmentation at  $t \approx 0.75$  it drops sharply and is nearly eliminated shortly afterwards. Then, it continues to evolve with a maximum R2MSE of about one fourth of the maximum value of the R2MSE of the solutions with a constant reduced basis, i.e. the maximum value outside the spike artefact at the zero-crossing. After this first update and augmentation the solution obtained with the integrated method shows the characteristic flicker that is described in section 6.1.2.2. Every new update and augmentation cycle becomes visible as a sharp bend, which realigns the R2MSE with the abscissa, effectively reducing the error and ensuring the result's accuracy. The same behaviour is also displayed by the R2MSE of the solution obtained with the update and augmentation of the reduced basis and the inflation formulation of the nonlinear terms. This indicates that the update and augmentation of the reduced basis is the major reason for an increase of the accuracy for the reduced solution. However, applying the integrated method without the polynomial formulation, i.e. the update and augmentation alone, does not yield the performance increases shown in figure 6.37.

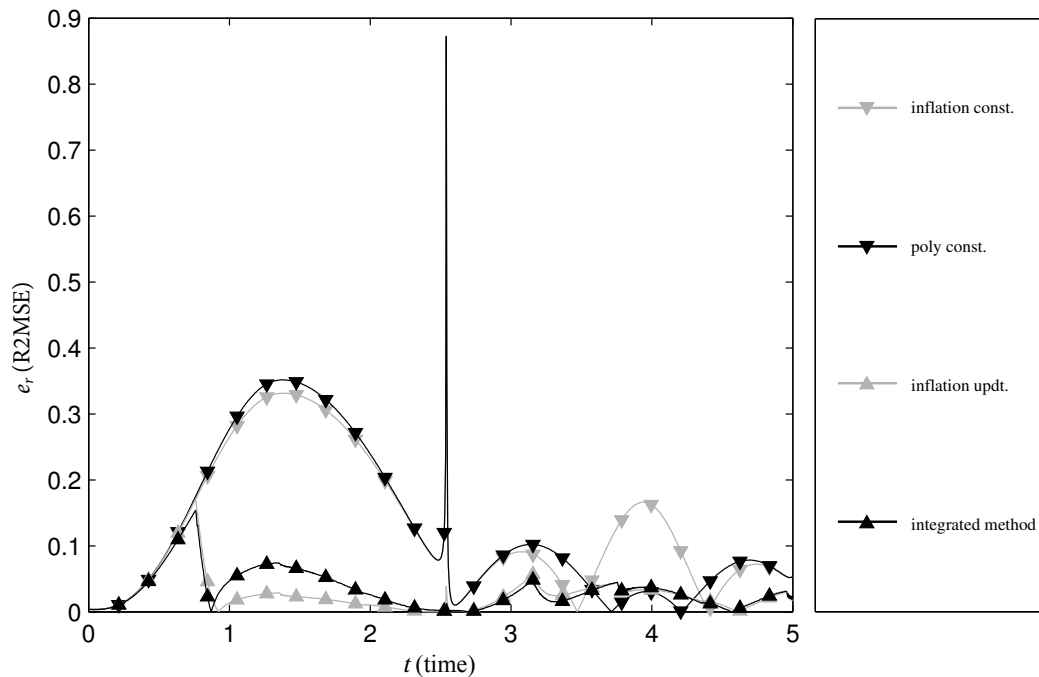


Figure 6.39: The evolution of the R2MSE for different solutions of the finite element test-case with volume elements at  $r = 8$

The study of the MAC in figure 6.40 confirms the results obtained from the study of the R2MSE. The

### 6.3. APPLYING THE INTEGRATED METHOD TO GEOMETRICALLY NONLINEAR VOLUME ELEMENTS

solutions with an updated and augmented reduced basis deliver higher values for the MAC. The shapes of their displacements resemble thus more the shape of the deformations of the reference solution. This confirms that the use of the integrated method yields an improvement in the amplitudes and the shapes of the deformation of the reduced solutions. However, the results for the shapes of the displacements are less pronounced than the ones for the R2MSE. All solutions deliver very high values for the MAC and the relative differences between the shapes of the different solutions are much less pronounced. This is in agreement with the second conclusion in section 6.3.1.3. There it is determined that the nature of the employed geometric nonlinearities leads to solutions that are basically only distinguishable in amplitude and does not offer any sort of special nonlinear observable characteristic.

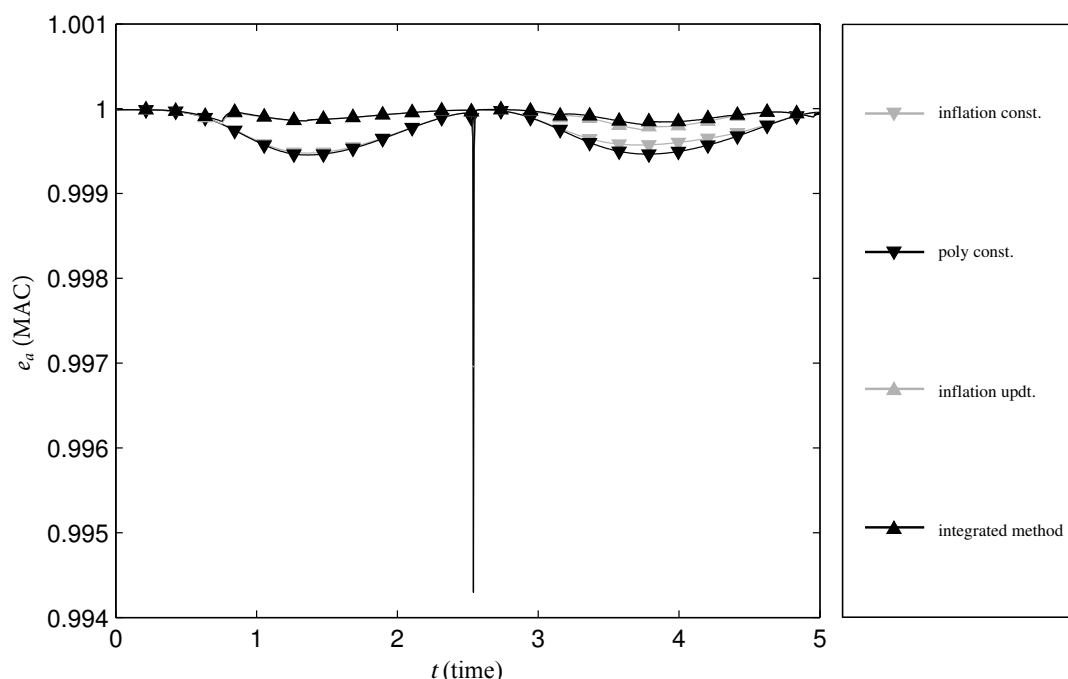


Figure 6.40: The evolution of the MAC for different solutions of the finite element test-case with volume elements at  $r = 8$

Finally, the study of the relative energy in figure 6.41 confirms the beneficial influence of the update and augmentation of the reduced basis in the integrated method. For the integrated method the oscillation of the relative energy is much lower than for the solutions with a constant reduced basis. Also, after the first update and augmentation cycle, the total energy in the reconstructed solution of the integrated method is lower than the energy in the full order reference solution. This shows that the update and augmentation presents a type of numerical damping that dissipates energy and stabilises the solution. In fact, it is shown in section 4.2.1.2.3 that the introduction of the reduced basis may cut off modes whose motion contributes considerably to the overall damping of the structure. By cutting off these modes there may be more energy present in the reconstructed reduced solution than in the reference solution. If compared with the solutions that are obtained with constant bases the update and augmentation of the reduced basis in the integrated method seems to counteract this tendency. Thus the integrated method introduces an artificial damping that counterbalances the removal of damping due to the cutting off of modes, albeit with a slight overreaction. Looking back at the R2MSE in figure 6.39 proves that this artificial damping does not come at the expense of wrong amplitudes.

The studies of all three error metrics unanimously confirm for all orders  $r$  that the use of the update and augmentation of the reduced basis boost the accuracy and the quality of the solution. It is interesting

### 6.3. APPLYING THE INTEGRATED METHOD TO GEOMETRICALLY NONLINEAR VOLUME ELEMENTS

---

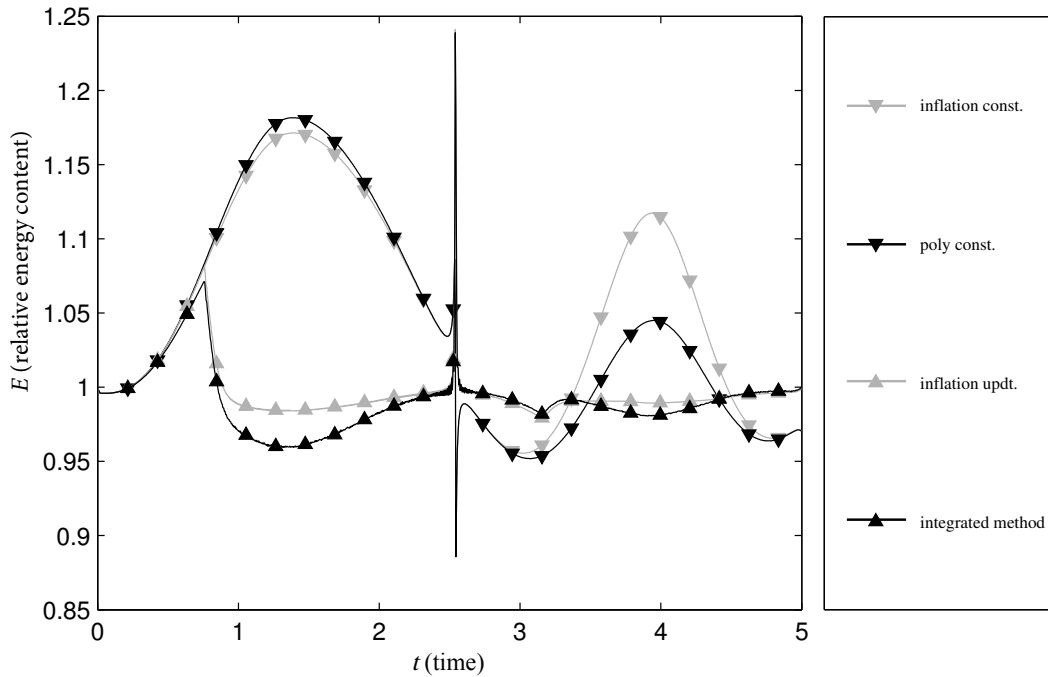


Figure 6.41: The evolution of the relative energy for different solutions of the finite element test-case with volume elements at  $r = 8$

so observe that the major contribution to the improvement of the accuracy of the reduced solutions comes from the introduction of the update and augmentation of the reduced basis and that the introduction of the polynomial expression of the nonlinear terms does not counteract this beneficial influence. This shows that the introduction of the polynomial formulation is mainly aimed at improving the numerical performance without overly deteriorating the result. The next step is to focus just on the computational performance of the different solutions so that an informed trade-off between speed and accuracy can be made.

### 6.3. APPLYING THE INTEGRATED METHOD TO GEOMETRICALLY NONLINEAR VOLUME ELEMENTS

solution	$r = 8$					
	R2MSE		MAC		relative energy	
	mean $e_r$	variance $v_r$	mean $e_a$	variance $v_a$	mean $\Delta E$	variance $v_{\Delta E}$
inflation const.	0.1324	0.0111	0.9997	$5.7218 \cdot 10^{-8}$	1.0538	0.0049
poly const.	0.1260	0.0134	0.9997	$6.5102 \cdot 10^{-8}$	1.0439	0.0054
inflation updt.	0.0267	0.0008	0.9999	$1.2680 \cdot 10^{-8}$	0.9971	0.0004
integrated method	0.0330	0.0008	0.9999	$1.1147 \cdot 10^{-8}$	0.9913	0.0001

solution	$r = 16$					
	R2MSE		MAC		relative energy	
	mean $e_r$	variance $v_r$	mean $e_a$	variance $v_a$	mean $\Delta E$	variance $v_{\Delta E}$
inflation const.	0.0665	0.0039	0.9998	$3.8145 \cdot 10^{-8}$	0.9774	0.0007
poly const.	0.0696	0.0059	0.9998	$4.4746 \cdot 10^{-8}$	0.9772	0.0012
inflation updt.	0.0182	0.0002	0.9999	$1.5898 \cdot 10^{-8}$	0.9944	0.0001
integrated method	0.0117	0.0001	0.9999	$1.3919 \cdot 10^{-8}$	0.9956	0.0001

Table 6.18: The numerical results for the application of the integrated method with LNM on the finite element test-case with volume elements

**6.3.3.3.2 Rapidity** For the use of the integrated method from 6.1.1 the full order vector of the nonlinear internal forces  $\mathbf{g}(\mathbf{u})$  is required by the identification of the reduced tensors  $\tilde{\mathbf{A}}^{(h)}$ . For the initial identification  $\frac{1}{6}(r^3 + 6r^2 + 5r)$  evaluations are required, as given in section 5.2.2.2. This number increases to  $\frac{1}{6}((r+3)^3 + 6(r+3)^2 + 5(r+3))$  for each update and augmentation of the reduced basis. The maximum possible number of updates is determined as  $\frac{t_e - t_0}{m_r \Delta t}$ , with  $m_r$  being the lower threshold of the retainer. The number of required evaluations  $n_{\text{evaluations of } \mathbf{g}(\mathbf{u})}^{(\text{ROM})}$  of the full order nonlinear forces vector  $\mathbf{g}(\mathbf{u})$  for the reduced solution is

$$n_{\text{evaluations of } \mathbf{g}(\mathbf{u})}^{(\text{ROM})} \leq \frac{1}{6}(r^3 + 6r^2 + 5r) + \frac{t_e - t_0}{m_r \Delta t} \left( \frac{1}{6}((r+3)^3 + 6(r+3)^2 + 5(r+3)) \right). \quad (6.58)$$

This is a maximum value because not all updates that are possible during the simulated period  $(t_0, t_e]$  are required to take place. It has to be compared to the number of evaluations  $n_{\text{evaluations of } \mathbf{g}(\mathbf{u})}^{(\text{FOM})}$  of the full order solution in equation (6.56).

Other factors, which are much more difficult to gauge and that depend heavily on the actual implementation of the problem, include the evaluation of the tensor evaluations for the generalised nonlinear forces vector  $\tilde{\mathbf{g}}(\mathbf{q})$  in equation (5.87) and for the generalised tangent stiffness matrix  $\tilde{\mathbf{K}}$  in equation (5.89). These evaluations tend to be numerically cheap. They have to be performed the same number of times than the evaluations of the full order terms during the full order solution.

Yet another factor that is difficult to gauge, but beneficial for the reduced system, is the requirement to inverse  $r \times r$  or  $(r+3) \times (r+3)$  matrices instead of  $n \times n$  matrices. For this standard problem of linear algebra many solution approaches exist (see e.g. Strang [218]) and have been implemented with high performance packages in codes as e.g. MatLab (The Mathworks [221]) or NASTRAN (MSC Software [151, 152, 153]). It has to be determined on a case-by-case basis to which extent the inversion of the smaller matrices unfolds its beneficial effect.

### 6.3. APPLYING THE INTEGRATED METHOD TO GEOMETRICALLY NONLINEAR VOLUME ELEMENTS

Ultimately it remains out of reach for this study to give a conclusive and always valid answer to the questions for the numerical performance of the integrated method.

The performance of the different solutions is measured with the overall solution time. This is possible because all solutions are implemented in the same way and calculated on the same workstation. However, there are still considerable uncertainties attached to the measurements due to network and parallel computing.

The reference solution requires 205430 *s*. This is the touchstone for the reduced solutions. The overall solution times of the solutions whose accuracy is examined in the previous paragraph are listed in the table 6.19.

$r = 8$				
solution	solution time	preparation time	total	% of ref. solution
inflation const.	210423.5 <i>s</i>	–	210423.5 <i>s</i>	102.4 %
poly const.	237.6 <i>s</i>	691.9 <i>s</i>	929.5 <i>s</i>	0.5 %
inflation updt.	293325.1 <i>s</i>	–	293325.1 <i>s</i>	142.8 %
integrated method	6928.6 <i>s</i>	–	6928.6 <i>s</i>	3.4 %

$r = 16$				
solution	solution time	preparation time	total	% of ref. solution
inflation const.	210718.8 <i>s</i>	–	210718.8 <i>s</i>	102.6 %
poly const.	1856.0 <i>s</i>	4237.8 <i>s</i>	6093.8 <i>s</i>	3.0 %
inflation updt.	292450.3 <i>s</i>	–	292450.3 <i>s</i>	142.4 %
integrated method	41420.6 <i>s</i>	–	41420.6 <i>s</i>	20.2 %

Table 6.19: The computational performance results for the application of the integrated method with LNM on the finite element test-case with volume elements

The values in table 6.19 show very clearly the cost associated with the identification of the polynomial approximation of the nonlinear terms. For the autonomous solution with a constant reduced basis at  $r = 8$  the identification of the tensors takes almost all of the overall solution time, while the actual solution time becomes negligible. The 0.5% percent are distributed as 0.49% for the identification and 0.01% for the actual solution among the stages of an autonomous solution with a constant basis. However, when several identifications are required during the updates and augmentations of the integrated method the times required for these identifications add up. The integrated solution requires six identifications, including the initial identification prior to the actual solution. Together, these identifications make the integrated solution take 3.0% the time of the full-order solution. This is still a gain in computational time, but the influence of the identifications becomes highly visible for  $r = 16$ . Here, the five required updates limit the gains due to the use of the polynomial formulation and the integrated solution takes one fifth of the full order solution. This highlights the computational costs of the identification of the reduced tensors, that are already put forward in section 5.2.2.2, and shows how important and difficult it is to make a trade-off between a rapid and an accurate reduced solution. To facilitate this trade-off some rough estimates for the required computational time are given in the following.

The preparation time for the solution with a constant reduced basis and the polynomial formulation of the nonlinear terms in table 6.19 is the time required for the identification of the tensors  $\mathbf{A}^{(h)}$ . It is important to have this time separated from the actual solution time, because it can be used to determine the value of the retainer  $m_r$  for the update and augmentation of the reduced basis. If the time that is required for the identification of the tensors is known to be  $t_{\text{ident}}$  and the time required for the full order reference solution

is  $t_{\text{ref}}$  than the condition

$$m_r \leq \frac{t_{\text{ident}}}{t_{\text{ref}}} \frac{t_e - t_0}{\Delta t} \quad (6.59)$$

has to be fulfilled for the integrated method may require less time than the full order solution. The fraction  $\frac{t_{\text{ident}}}{t_{\text{ref}}}$  determines the maximum number of update and augmentation cycles, each requiring an identification of the tensors  $\mathbf{A}^{(h)}$ , that can be performed before the identifications of the tensors requires more time than the full order reference solution. This information can be used in conjunction with equations (6.56) and (6.58) to determine the parameter  $m_r$  of the integrated method. This may become important when the values for the numbers  $n_{\text{evaluations of } g(\mathbf{u})}$  are not known, because the overall process is implemented in a proprietary code without the possibility to count the number of evaluations of the nonlinear forces vector.

For the solution obtained with the integrated method the identification of the initial tensors prior to the actual solution is not counted as preparation time. The identification of the tensors is considered an integral part of the integrated method. Therefore no distinction between the preparation of the solution and the solution itself is made for the identification of the tensors.

Against the overall required efforts of identifying the tensors for the autonomous solutions and of performing the evaluations of the nonlinear terms for the solutions with the inflation formulation the creation of the reduced basis is negligible. The reduced bases are created from the LNM and their only requirement is the establishment of a full order tangent stiffness matrix once for every update and augmentation cycle. The impact of the creation of the reduced basis may change for different reduced bases, but for the current test-case it is of no concern.

The study of the performance of the different solutions compares well to the initial assessment of the computational efforts in section 6.3.3.2. There, the influence of the introduction of the polynomial formulation is assessed. All results are confirmed here and especially the potential of the integrated method is again highlighted.

**6.3.3.3.3 Trade-off between accuracy and rapidity** In the two preceding paragraphs it is established that the rapidity of the reduced solution depends on the autonomy of the ROM, ensured with the polynomial formulation of the nonlinear terms. The accuracy of the reduced solution is ensured with the update and augmentation of the reduced basis. This update and augmentation entails an anewed identification of the tensors, a process that is rather costly. Its numerical effort scales with  $(r + 3)^3$  and the number of updates and augmentation cycles.

The requirements of a trade-off between a rapid and an accurate reduced solution, obtained with the integrated method, is investigated in figure 6.42. In this the figure the solution times from table 6.19 are plotted against the R2MSE from table 6.18 for the four different solutions. The order  $r$  of the ROM is colour-coded.

The solutions with a constant reduced basis and the inflation of the nonlinear terms only gain in rapidity from the treatment of the smaller matrices. these effects are barely noticeable for only 72 degrees of freedom in the full order system and therefore these solutions take constantly about 100% of the reference solution's time for all orders  $r$ . The same constancy can be observed for the solutions with an updated and augmented reduced basis and the inflation of the nonlinear terms. However, due to the additional effort of the update and augmentation cycle, these solutions require around 140% of the reference solution's time. Their error level is lower than for the solutions with the constant reduced basis. The solutions with a constant reduced basis and the polynomial formulation of the require constantly below 5% of the reference solution's time. However, their errors are comparable with the ones of the solutions with a constant reduced basis and the inflation of the nonlinear terms. This confirms that the polynomial formulation does only introduce a small additional error, while accelerating the solution process tremendously.

The solutions of the integrated method stand out, because they display a strong dependency of their solution time on the order  $r$  of the ROM. This dependency starts well below 5% at  $r = 4$  and reaches about 20% at  $r = 16$  exponentially. The errors of the solutions obtained with the integrated method are consistent with the other solutions obtained with an updated and augmented reduced basis. At this point it becomes obvious that for the integrated method a large order  $r$  of the ROM, which is chosen for accuracy, leads to the imminent danger of negating all possible gains in rapidity, because the numerical effort for the aneued identifications of the tensors scales over-proportionally.

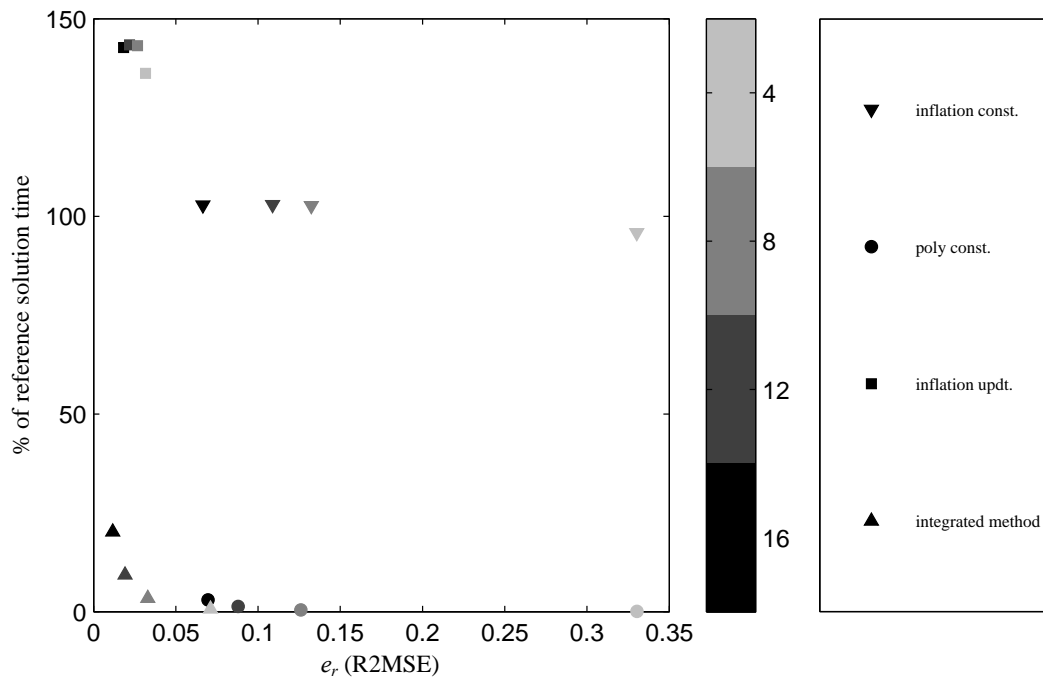


Figure 6.42: The R2MSE and solution times of the combinations of formulations of the reduced nonlinear forces vector and the reduced basis

The influence of the identifications becomes highly visible e.g. for  $r = 16$ . Here, the required updates limit the gains due to the use of the polynomial formulation and the integrated solution takes more and more time as the order of the reduced system increases. This highlights the computational costs of the identification of the reduced tensors, that are put forward in figure 6.37, and shows how important and difficult it is to make a trade-off between a rapid and an accurate reduced solution. To facilitate this trade-off it is referred to the rough estimates for the number of evaluations of the nonlinear forces above.

## 6.4 Outcome of the application of the integrated method

In the first of previous sections the integrated method is assembled from the different elements that are described in the chapter 5. The update and augmentation of the reduced basis ensures the accuracy of the reduced solution, the polynomial formulation renders the reduced order model autonomous from the full order model and the interpolation of the reduced basis ensure that external parameters are taken into account. These three approaches are assembled around a Newmark-type time-marching algorithm for a transient solution and the resulting integrated method is described in detail.

The integrated method is then successively applied to academic test-cases, a finite element test-case

with bar elements and a finite element test-case with volume elements. The different test-cases are used to highlight different aspects of the integrated method, e.g. the gain in computational time due to the introduction of the polynomial formulation. Each finite element test-case is extensively studied in order to characterise the environment in which the integrated method is applied. The most important characteristic is the behaviour of the geometric nonlinearity.

All applications of the integrated method are successful. Transient solutions of the academic test-case, the finite element test-case with bar elements and the finite element test-case with volume elements are obtained with considerable accuracy and a significant acceleration of the numerical calculations. In particular, the computationally heavy finite element test-case with volume elements allows making pertinent statements with respect to the gain in computational effort that can be derived from the application of the integrated method.

The costly identification of the tensors for the polynomial formulation is identified to pose the major risk to negate the gain in computational effort by the introduction of the polynomial formulation during the actual solution phase. Decision aids are given that help to balance these effects. These aids are based on the numbers of evaluations of the full order vector of internal nonlinear forces and the time required for the identification of the tensors, this allows to determine the frequency of the update and augmentation of the basis. The performance results are first presented independently from the results for the quality of the solutions, so that an unbiased trade-off between performance and accuracy can be made. Then they are combined to explore how the order of the reduced systems influences the performance.



## Chapter 7

# Conclusion

---

The conclusion centres on the discussion of the obtained results. The main focus is put on the developed methods and the formalised integrated method rather than the actual numerical results. The integrated method is presented as one possible realisation of a more general framework for obtaining a fast, high-quality and parameterisable transient solution of a geometrically nonlinear problem.

In the process the major decisions are reviewed in the light of the availability of all results. They turn out to be correct and some prove to be even anticipatory. The work eventually concludes with pointing out directions for further research. These future topics of research are aimed at enlarging and enhancing the application of the integrated method and its underlying framework.

### 7.1 Concluding the work

The central aim of this work is to provide a rapid, accurate and parameterisable transient solution of a geometrically nonlinear structure. This aim is achieved with the creation of the integrated method.

The process leading to this achievement is characterised by several major decisions. The most important one is certainly the choice of the projection on a reduced basis as the reduction method. This decision dictates the use of a nonlinear Newmark-type time-marching solution algorithm and imposes the choice of a method for creating the reduced basis. From this imposed choice the question arises which reduced basis may be particularly suited for the reduction of a geometrically nonlinear structure. Extensive numerical tests lead to the result that none of the reduced bases performs fully satisfactory and the meticulous inspection of the solution algorithm shows that the solution algorithm requires to be rendered autonomous.

It is the junction of these two findings that clearly shows that a successful reduction of a geometrically nonlinear structure by a projection on a reduced basis hinges crucially on the solution algorithm and only to a minor extent on the reduced basis itself. The application of the existing methods in an isolated manner is not sufficient. This discovery is followed up comprehensively by addressing the identified requirements of adapting the solution algorithm, of replacing the nonlinear terms with an autonomous expression and of adapting the reduced basis to external parameters.

For addressing these requirements more choices are required. For each of the requirements a selection of common methods is presented to provide a tool box of approaches. The actual choices are made after extensive numerical tests. For these tests the academic test-cases are used in order to provide a consistent testing environment throughout the entire study. All choices are based on conclusive numerical results. The update and augmentation of the reduced basis is chosen to adapt the solution algorithm in order to make the reduced basis follow the nonlinear evolution of the solution. The polynomial formulation is chosen to form the autonomous expression that replaces the reduced nonlinear terms. The interpolation in a tangent space is chosen to adapt the initial reduced basis to external parameters.

The three chosen approaches, of which each one addresses one identified requirement, are then united in the integrated method. By addressing the three identified requirements the integrated method allows for a rapid, accurate and parameterisable reduced transient solution.

#### 7.1.1 Discussing the obtained results

The results that are obtained during the study are not exclusively numerical results, as e.g. the results of the comparative study of the reduced bases. Thinking more in terms of products the results of this work may be algorithms, e.g. the update and augmentation of the reduced basis, or the framework of the integrated method.

##### 7.1.1.1 Results from the study of the reduced bases

The first major result is the limited suitability of the reduced bases in chapter 4. A large number of common reduced bases has been studied for their ability of delivering an accurate transient solution and for their robustness on differently parameterised test-cases.

Several common approaches for creating reduced bases are presented. All reduced bases are used to reduce academic test-cases built from combinations of two non-linear systems and two excitations. A comparative study, which determines the preferred applications of the reduced bases, and a study that determines the robustness of the bases by using them for differently parameterised configurations are performed. The performances of the reduced bases are assessed with a specifically designed multi-criteria decision analysis score and a metric for the relative performance. The results are condensed in concise tables. All procedures, which are used to obtain the results, are thoroughly verified by extensively studying the possible influences

of the applied bases and the solution procedure.

The conducted comparative study highlights that the choice of a specific reduced basis for a non-linear system should primarily be based on the type of excitation to which the system is subjected. The type of the non-linearity present in the system is only an additional criterion. The specifically constructed Proper Orthogonal Decomposition bases are constantly the best performing ones, explaining their widespread use. At the same time it has been shown that the Linear Normal Modes offer an alternative which avoids the requirement for the full order solution. While the Linear Normal Modes neglect the non-linear nature of the system they still perform as good as the Proper Orthogonal Decomposition bases or only slightly worse for non-linear structural dynamics. A more targeted study on large systems confirms the obtained results and showcases the possible gains in computational time through the application of a reduction.

Concerning the inherent robustness of the different bases, it can be stated that none of the studied bases possesses this particular property in sufficient measure, thus requiring the use of adaptation methods. However, the investigation also shows clearly that, should the use of a single constant basis on a system under differently parameterised excitations become necessary, this basis has to be established with the most critical values for the parameters.

The overall level of error beyond the individual performances of the different bases shows however that the simple projection of any non-linear system on a constant reduced basis is not sufficient to ensure a satisfying quality of the solution.

### 7.1.1.2 Updating and augmenting the reduced bases

The second major result is the process of updating and augmenting of the reduced basis. This highly modified common sense approach addresses the requirement of adapting the solution algorithm. This requirement is derived from the inability of the reduced bases to successfully reduce a nonlinear system. The update of the reduced basis seems to be a common sense approach, yet there is little literature that came to the attention of the author.

While the idea of the update of the reduced bases seems straightforward, maybe even simple, its actual implementation reveals that it requires an extensive modification in the form of the augmentation of the reduced basis in order to function properly. Updating the reduced basis in intervals requires the inclusion of the jumps in the physical displacements, the velocities and the accelerations in the update reduced basis, while properly initialising the new generalised coordinates after the update. This technique of augmentation is a novel approach and contributes considerably to the quality of the reduced transient solutions of the nonlinear systems. It is also a major component of the success of the integrated method

The update and augmentation of the reduced basis is formalised as a self-contained block in section 6.1.1.3. This block can be taken and applied as an addition to whichever solution algorithm requiring it.

### 7.1.1.3 Creation and application of the integrated method

The central result of this work is the integrated method. Starting with the requirement of a rapid, accurate and parameterisable transient solution of a geometrically nonlinear structure it is soon decided to base the framework for this transient solution on the reduction on a reduced basis. From inspection of the solution algorithm and the obtained numerical results the three requirements for adapting the solution algorithm, rendering it autonomous from the full order system and adapting the reduced basis to external parameters are identified. Addressing all three requirements with specialised methods and unifying these specialised methods in a framework is identified as the approach that ensures rapid, accurate and parameterisable transient solutions of a geometrically nonlinear structure. This framework and the choices that are made for each identified requirement are formalised in the integrated method.

The integrated method is applied with success to academic and finite element test-cases. The application to the finite element test-cases can be considered ground-breaking, even though they are performed under

## 7.1. CONCLUDING THE WORK

---

semi-realistic conditions. Due to the available numerical resources, only a limited number of degrees of freedom is used to discretised the finite element test-cases. However, the finite element test-cases give a meticulously correct representation of geometric nonlinearities. This is exactly the type of nonlinearity that is expected during industrial applications. It is painstakingly recreated with full-blown geometrically nonlinear finite bar and volume elements and verified by means of a comparison with a commercial finite element solver. This gives great confidence in the application of the integrated method.

### 7.1.1.4 Understanding the integrated method as a framework

The integrated method, as it is described in section 6.1.1, is the unification of three different methods on the common backbone of a Newmark-type solution algorithm. Each of the three methods addresses a specific requirement that has been identified and that is commanded by the overall aim of a rapid, accurate and parameterisable transient solution of a geometrically nonlinear structure. Each of the three methods is an example of different common methods that also address the same identified requirement. The method that is actually present in the integrated method is chosen based solely on numerical results. However, any other method that addresses the same identified requirement can replace it in the integrated method.

Therefore, the integrated method can be seen as an exemplary realisation of an integrated framework. This framework allows for a rapid, accurate and parameterisable transient solutions of a geometrically nonlinear structure and requires the following parts

- a solution algorithm that provides the overall structure of the integrated method,
- an adaptation of the solution algorithm that allows for the nonlinear evolution of the transient solution, thus ensuring its accuracy,
- an autonomous formulation that renders the reduced order model independent from the full order structure, thus ensuring its rapid calculation, and,
- a method for adapting the reduced model to external parameters.

Different members of the family of Newmark-type time-marching algorithms can be used as the backbone of the integrated method. While the academic test-cases are solved with the reduced nonlinear Newmark scheme in its standard representation, the test-cases built with nonlinear finite elements are solved with the HHT- $\alpha$ -method. The inclusion of the HHT- $\alpha$ -method had become necessary in order to stabilise the solutions of the finite element test-cases early on. Its successful application demonstrates that different time-marching algorithms of Newmark-type can serve as the backbone of the integrated method. If a structural dynamic problem would require another breed of Newmark-type solution algorithm, there seem no conceptual contradictions to extend the integrated method to this solution algorithm.

Along the presented candidate methods for each of these requirements, the choices are made on the grounds of numerical results. The consistent behaviour of the test-cases allows transferring results from the academic test-cases to the finite element test-cases. This makes the choices specific for the test-cases at hand. It does not guarantee the successful reduced solution of a different type of nonlinear problems. The integrated method, as it presented here, is by no means definitive and all of its elements can be adapted and exchanged as required.

Looking beyond the integrated method, as it is presented throughout this work, allows to see the obtained results as a framework that allows integrating different methods.

### 7.1.1.5 Communications originating from this study

This thesis represents the central dissemination of the results. In addition there are several other communications of different types that originated from the presented research work. They are listed in the following.

The results of the numerical studies of the performance and the robustness of the reduced bases are published in Lülff et al. [141] and presented in the conference contribution Lülff et al. [140]. The fundamentals of

## 7.1. CONCLUDING THE WORK

---

the integrated method, especially the autonomous formulation, are presented in LülF et al. [142]. A journal publication on this topic is being prepared at the time of redacting this thesis.

Also, this work has been the topic of three seminary presentations at universities. Two presentations were made by the author on the 12.1.2012 and the 10.12.2012 at the *Institut für wissenschaftliches Rechnen* of the *Technische Universität Braunschweig* on invitation of the director of the institute Prof. Dr. Herrmann G. Matthies. One presentation was made on the 20.9.2013 at the graduate school *MUSIC Multiscale Methods for Interface Coupling* of the *Leibniz Universität Hannover's Institut für Kontinuumsmechanik* on invitation of its director Prof. Dr.-Ing.habil. P. Wriggers.

The author participated in the annual ONERA in-house doctorands' conference *Journées des Doctorants* three times during his research work. The author participated in a four month research stay at the *Institut für wissenschaftliches Rechnen* under the tutelage of Prof. Dr. Herrmann G. Matthies.

### 7.1.2 Critical review of the major decisions

The obtained results and the developed integrated method hinge on at least three major decisions. Foremost this is the decision to use the projection on a reduced basis as the reduction approach. Another, major decision is the selection of the academic test-cases. The impact of this decision on the overall study is only implicit through the obtained results, but very important nonetheless because the obtained results drive the follow-on studies. A decision that is already discussed and justified on the basis of numerical results is the augmentation of the reduced basis. It is reviewed here as an example of a decision with the intention to demonstrate the reasoning leading to it.

These three decisions are reviewed below. They are justified in their respective chapters based in the information available at that time. In light of the overall results and with the integrated method becoming available their justification has to be reviewed.

#### 7.1.2.1 The decision for the reduction by projection on a reduced basis

The decision to create the reduction around the projection on a reduced basis is the result of a choice between different approaches in section 3.1. The Nonlinear Normal Modes, the Truncated Harmonic Balance Method and the Proper Generalised Decomposition are the other major possibilities. The Nonlinear Normal Modes are quickly dismissed on the grounds that they are rather in a tool for analysis than a full-fledged reduction approach in their own right. Also the Truncated Harmonic Balance Method is not suited as the aim of the study is a transient solution.

The Proper Generalised Decomposition is an emerging approach and much research is happening on the time-scale of this work. The recent rapid extension of the PGD to nonlinear problems and its possibility to embrace parameters simply as additional dimensions are strong arguments in its favour.

However, there are also strong arguments in favour of the projection on a reduced basis. Most notable among these are the large amount of additional methods available through an unequally longer history of research and the high degree of pervasiveness of this reduction approach. Also, as shown in section 3.2.2.1, the existing and widely diffused solution schemes of Newmark-type can be continued to be used as backbones of the integrated method. This is a strong argument and might ensure a quick proliferation of the integrated method, because all of its ingredients are also available.

It may seem overly un-progressive to base the integrated method on the projection on a reduced basis instead of embracing the emerging and vivid field of research of the PGD. However, it has to be stressed again that the reduction by a projection of a reduced basis has a long-standing history of research that produced confirmed methods, e.g. the many approaches for creating reduced bases, and also continues to deliver highly driving methods, such as e.g. the Least-Squares Petrov-Galerkin method. Thus the potential of the reduction by projection on a reduced basis is certainly not maxed out. From this perspective the projection and the PGD become comparable.

## 7.1. CONCLUDING THE WORK

---

Furthermore, the entire study, which ultimately leads to the creation of the integrated method, is, from the beginning, strictly geared towards a direct applicability of the used and developed methods. In this spirit it is only natural to favour an already well developed field of research with a tremendous pervasiveness in industrial applications. Especially the latter should boost the proliferation of the integrated method.

An effort for integrating different methods for obtaining steady state solution is made by Grolet and Thouverez [85]. They use the Harmonic Balance Method in conjunction with the Proper Generalised Decomposition and obtain the result that their method can deliver displacement based errors that are less than errors obtained with a POD reduced basis. This is a remarkable result, because the POD basis is shown to be optimal in the R2MSE sense, but regarding the actual displacements their method performs better. However the authors of Grolet and Thouverez [85] also acknowledge a remaining potential for performance of their method.

### 7.1.2.2 Choice of the academic test-cases

The academic test-cases are chosen in and defined in section 4.1.3. The main motivation for their choice is to have a common scenario for testing the reduced bases. This implicates the test-cases' commonality and adaptability and allows to provide the locally and the entirely nonlinear variant. Another major reason for the choice of these test-cases is the fact that they are based on an example that is provided in literature by AL-Shudeifat et al. [3] and proven.

In hindsight this choice proves highly advantageous. The behaviour of the nonlinear system is largely comparable to the finite element test-cases, especially the one with bar elements. This becomes obvious if the respective time histories are compared. The time history of the entirely nonlinear academic test-case is shown in figure 4.9 and the time history of for the nonlinear finite element test-case with bar elements is shown in figure 6.13. This situation allows to carry the results over and to confirm them on both types of test-case. Therefore the choice of the academic test-cases proves to be highly anticipatory.

### 7.1.2.3 The decision to augment the reduced basis

The decision of augmenting the reduced basis by appending the three jumps is made after a brief numerical study in section 5.1.3.5. This study is solved with the inflation formulation of the nonlinear terms and on the academic systems. This combination denies any meaningful assessment of computational performances and the decision is based on the obtained errors.

With the introduction and the decision in favour of the polynomial expressions as the autonomous formulation of the nonlinear terms this choice becomes questionable. The additional three vectors might have considerable performance repercussions for the polynomial expressions of the nonlinear terms. In section 5.2.2 it is shown that the required number of operations increases overproportionally with the order of the reduced system. From this perspective replacing the three least significant vectors of the reduced basis with the jumps might be the better choice under performance considerations.

At the same time the argument is repeated that only three additional vectors that augment the updated reduced basis offer a considerable increase in the quality of the transient solutions. For the locally and the entirely nonlinear academic test-cases this is shown in section 5.1.3.6.2 and for the finite element test-case with bar elements this is shown in section 6.2.2.3. Furthermore, adding only three additional vectors can be considered negligible for real applications of reduced models and the additional computational effort for actually solving the reduced model of order  $r + 3$  is overshadowed by the numerical effort required for identifying the reduced tensors.

## 7.2 Outlook for further research directions

The performed work is a comprehensive study that unifies several available and proven methods with newly formalised approaches, e.g. the update and the augmentation of the reduced bases, in the integrated method. As such, it is a self-contained work.

Against the background of the defining decision to base the integrated method on the reduction on a reduced basis it would be of highest interest to conduct a comparison of the integrated method with other reduction methods, especially the PGD. This comparison has to take into account the overall reduction times for the tested applications because the creation of the nucleus functions has to be counted in the overall efforts to obtain a reduced model. Furthermore the PDG offers the highly interesting property of integrating a large number of external parameters easily. Therefore a way has to be found to use the PDG method for all aspects of a reduced solution that concern parameters while retaining e.g. a reduced basis for the reduction of the structure itself.

The use of reduced bases, especially the Linear Normal Modes, implies that some sort of low-frequency hypothesis holds for the problem at hand. The response of the structure is supposed to be well characterized by the modal approach. Should this not be the case, because the frequency of the response increases and the modal density becomes too large, the integrated method breaks down because the reduction by projection on a reduced basis is no longer possible. In the high-frequency range other approaches, like e.g., energy methods (Le Guennec [131]), are required for the solution of the transient response. A possible direction of future research might hence be the creation of an integrated method on the basis of solution approaches that are geared for high-frequency range. If the reduction of these approaches is not necessary or impractical, at least the integration of an approach for the parameterization of such methods should be integrated. This could be done in much the same way as the proposed use of the PDG above.

The solutions are obtained with the classic nonlinear Newmark scheme. This is done with the aim of providing optimum conditions for the integrated methods. However, the use of this variant of this time-marching solution algorithm is virtually extinct in current finite element applications. Therefore a major axis of research to be expected to materialise in the future is the choice of another backbone for the integrated method. Replacing the classic nonlinear Newmark algorithm or the HHT- $\alpha$ -method with a state of the art solution procedure is bound to boost the performance of the integrated method considerably<sup>1</sup>.

Given the wide variety of methods for the creation of the reduced basis in section 3.3, it might become possible in a future iteration of the integrated method to switch from one reduced basis generation algorithm to another one during the update. A possible scenario would include initialising the reduced transient solution with the LNM and updating and augmenting this LNM basis several times until a number of characteristic snapshots is obtained. These snapshots are then used in one of the following updates to produce a POD basis that replaces the LNM basis.

A point that has to be made regarding the test-cases is that they consist exclusively of translational degrees of freedom. While they are well described and characterised they do only represent one particular type of nonlinear formulations. Many methods that are used during this study are originally conceived for test-case with rotational degrees of freedom, e.g. beams or shells. They are applied successfully to test-cases with exclusively translational degrees of freedom. However, the application of the integrated method in the opposite direction, on test-cases that contain also rotational degrees of freedom, has not been shown. This has to be proven in a dedicated study.

The three methods that address the three identified requirements are selected independently in this work. Each method that is ultimately selected for use in the integrated method is selected as the best against certain criteria among other methods that address the same identified requirement. However, the combination of these selected methods, the integrated method, is not bound to be the optimal combination for a given scenario. The question if there is a better performing combination available and if additional methods have

---

<sup>1</sup>A first tentative look in this direction is made in the annex section A.3, where the use of a constant tangent stiffness matrix is explored.

## 7.2. OUTLOOK FOR FURTHER RESEARCH DIRECTIONS

---

to be integrated in order to boost the performance of the integrated method even further, has to be answered by future research.

Finally, this work provides a basic framework for an integrated method. On the grounds of the chosen test-cases, selected criteria and obtained results the majority of the examined approaches for the various requirements are eventually rejected. These are not absolute determinations. Every user of the framework is expected to adapt the integrated method to her or his specific problems by replacing any of the used methods by an equivalent one, depending on the nature of the problem, the available tools and experience.

# Bibliography

- [1] P. J. Acklam.  
MATLAB array manipulation tips and tricks.  
online, 2003.  
<http://home.online.no/~pjacklam/matlab/doc/mtt/doc/mtt.pdf> - retrieved 13.12.2011.  
296
- [2] M. A. AL-Shudeifat and E. Butcher.  
Order reduction of forced nonlinear systems using updated LELSM modes with new Ritz vectors.  
*Nonlinear Dynamics*, 62:821–840, 2010.  
ISSN 0924-090X.  
DOI: 10.1007/s11071-010-9765-8.  
40, 62, 78, 80, 81, 82, 366
- [3] M. A. AL-Shudeifat, E. A. Butcher, and T. D. Burton.  
Enhanced order reduction of forced nonlinear systems using new Ritz vectors.  
In *Conference Proceedings of the Society for Experimental Mechanics Series*, volume 11 of *Nonlinear Modeling and Applications*, pages 41–52, Jacksonville, FL, 2011.  
40, 67, 94, 100, 294, 394
- [4] E. Allen, Z. Girouard, P. Goswami, and B. Leary.  
Centroidal Voronoi Tessellations.  
online, 2007.  
<ftp://202.38.75.156/upload/third/mathlover/voronoi-gpu/cvt.PDF> - retrieved 28.08.2012.  
77
- [5] M. Amabili, A. Sarkar, and M. Païdoussis.  
Chaotic vibrations of circular cylindrical shells: Galerkin versus reduced-order models via the Proper Orthogonal Decomposition method.  
*Journal of Sound and Vibration*, 290(3-5):736–762, 2006.  
ISSN 0022-460X.  
DOI: 10.1016/j.jsv.2005.04.034.  
69
- [6] M. Amabili.  
*Nonlinear Vibrations and Stability of Shells and Plates*.  
Cambridge University Press, 2008.  
12, 59
- [7] A. Ammar, B. Mokdad, F. Chinesta, and R. Keunings.  
A new family of solvers for some classes of multidimensional partial differential equations encountered in kinetic theory modeling of complex fluids.  
*Journal of Non-Newtonian Fluid Mechanics*, 139(3):153–176, 2006.

## BIBLIOGRAPHY

---

- ISSN 0377-0257.  
DOI: 10.1016/j.jnnfm.2006.07.007.  
4, 37, 47, 366, 368
- [8] A. Ammar, D. Ryckelynck, F. Chinesta, and R. Keunings.  
On the reduction of kinetic theory models related to finitely extensible dumbbells.  
*Journal of Non-Newtonian Fluid Mechanics*, 134(1-3):136–147, 2006.  
ISSN 0377-0257.  
DOI: 10.1016/j.jnnfm.2006.01.007.  
40, 75
- [9] A. Ammar, B. Mokdad, F. Chinesta, and R. Keunings.  
A new family of solvers for some classes of multidimensional partial differential equations encountered in kinetic theory modelling of complex fluids. Part II: Transient simulation using space-time separated representations.  
*Journal of Non-Newtonian Fluid Mechanics*, 144(2-3):98–121, 2007.  
ISSN 0377-0257.  
DOI: 10.1016/j.jnnfm.2007.03.009.  
4, 37, 47, 366, 368
- [10] D. Amsallem and C. Farhat.  
Interpolation method for the adaptation of reduced-order models to parameter changes and its application to aeroelasticity.  
*AIAA Journal*, 46:1803–1813, 2008.  
4, 5, 192
- [11] D. Amsallem, J. Cortial, K. Carlberg, and C. Farhat.  
A method for interpolating on manifolds structural dynamics reduced-order models.  
*International Journal for Numerical Methods in Engineering*, 80:1241–1258, 2009.  
133, 192, 376
- [12] D. Amsallem.  
*Interpolation on manifolds of CFD-based fluid and finite element-based structural reduced-order models for on-line aeroelastic predictions*.  
PhD thesis, Stanford University, 2010.  
40, 69, 70, 73, 194, 195, 196, 200, 214, 385, 388
- [13] D. Amsallem and C. Farhat.  
An online method for interpolating linear parametric reduced-order models.  
*SIAM Journal on Scientific Computing*, 33:2169–2198, 2011.  
37, 194, 197, 198, 385
- [14] D. Amsallem and C. Farhat.  
Stabilization of projection-based reduced-order models.  
*International Journal for Numerical Methods in Engineering*, 91(4):358–377, 2012.  
ISSN 1097-0207.  
DOI: 10.1002/nme.4274.  
113
- [15] D. Amsallem, M. J. Zahr, and C. Farhat.  
Nonlinear model order reduction based on local reduced-order bases.  
*International Journal for Numerical Methods in Engineering*, 92(10):891–916, 2012.  
59, 193

## BIBLIOGRAPHY

---

- [16] W. Aquino.  
An object-oriented framework for reduced-order models using Proper Orthogonal Decomposition (POD).  
*Computer Methods in Applied Mechanics and Engineering*, 196(41-44):4375–4390, 2007.  
ISSN 0045-7825.  
DOI: 10.1016/j.cma.2007.05.009.  
56, 93
- [17] N. Aubry.  
On the hidden beauty of the Proper Orthogonal Decomposition.  
*Theoretical and Computational Fluid Dynamics*, 2:339–352, 1991.  
ISSN 0935-4964.  
DOI: 10.1007/BF00271473.  
68
- [18] E. Bailey.  
*Steady state harmonic analysis of nonlinear networks*.  
PhD thesis, Stanford University, 1968.  
42, 367
- [19] O. Balci.  
Guidelines for successful simulation studies.  
In *Winter Simulation Conference (WSC)*, pages 25–32, 1990.  
DOI: 10.1109/WSC.1990.129482.  
2
- [20] M. C. C. Bampton and R. R. Craig, Jr.  
Coupling of substructures for dynamic analyses.  
*AIAA Journal*, 6(7):1313–1319, July 1968.  
ISSN 0001-1452.  
DOI: 10.2514/3.4741.  
41, 367
- [21] H.-J. Bartsch.  
*Taschenbuch mathematischer Formeln*.  
Fachbuchverlag Leipzig, 2001.  
99, 173, 175
- [22] K.-J. Bathe.  
*Finite Element Procedures*.  
Prentice-Hall, 1996.  
3, 12, 13, 16, 17, 23, 28, 32, 40, 59, 61, 62, 186, 265, 339, 366
- [23] J.-L. Batoz and G. Dhatt.  
Incremental displacement algorithms for nonlinear problems.  
*International Journal for Numerical Methods in Engineering*, 14(8):1262–1267, 1979.  
ISSN 1097-0207.  
DOI: 10.1002/nme.1620140811.  
51
- [24] M. H. Beale, M. T. Hagan, and H. B. Demuth.  
*Neural Network Toolbox User's Guide*.  
Mathworks, 2012.  
189

## BIBLIOGRAPHY

---

- [25] A. Beléndez, A. Hernández, A. Marquez, and C. Neip.  
Analytical approximation for the period of a nonlinear pendulum.  
*European Journal of Physics*, 27:539–551, 2006.  
79
- [26] A. Beléndez, E. Gimeno, M. Alvarez, and D. Méndez.  
Nonlinear oscillator with discontinuity by generalized harmonic balance method.  
*Computers & Mathematics with Applications*, 58(11-12):2117–2123, 2009.  
ISSN 0898-1221.  
DOI: 10.1016/j.camwa.2009.03.004.  
42
- [27] A. Beléndez, E. Gimeno, T. Beléndez, and A. Hernández.  
Rational harmonic balance based method for conservative nonlinear oscillators: Application to the duffing equation.  
*Mechanics Research Communications*, 36(6):728–734, 2009.  
ISSN 0093-6413.  
DOI: 10.1016/j.mechrescom.2009.03.001.  
42, 367
- [28] S. Bellizzi and R. Bouc.  
Analysis of multi-degree of freedom strongly non-linear mechanical systems with random input. Part I: non-linear modes and stochastic averaging.  
*Probabilistic Engineering Mechanics*, 14(3):229–244, 1999.  
ISSN 0266-8920.  
DOI: 10.1016/S0266-8920(98)00007-1.  
355
- [29] S. Bellizzi and R. Bouc.  
Analysis of multi-degree of freedom strongly non-linear mechanical systems with random input. Part II: equivalent linear system with random matrices and power spectral density matrix.  
*Probabilistic Engineering Mechanics*, 14(3):245–256, 1999.  
ISSN 0266-8920.  
DOI: 10.1016/S0266-8920(98)00010-1.  
355
- [30] S. Bellizzi and R. Sampaio.  
Karhunen-Loève modes obtained from displacement and velocity fields: assessments and comparisons.  
*Mechanical Systems and Signal Processing*, 23(4):1218–1222, 2009.  
ISSN 0888-3270.  
DOI: 10.1016/j.ymsp.2008.10.005.  
40, 69, 73
- [31] S. Bellizzi and R. Sampaio.  
Smooth Karhunen-Loève decomposition to analyze randomly vibrating systems.  
*Journal of Sound and Vibration*, 325(3):491–498, 2009.  
ISSN 0022-460X.  
DOI: 10.1016/j.jsv.2009.03.044.  
3, 74
- [32] S. Bellizzi, P. Guillemain, and R. Kronland-Martinet.  
Identification of coupled non-linear modes from free vibration using time-frequency representations.  
*Journal of Sound and Vibration*, 243(2):191–213, 2001.

## BIBLIOGRAPHY

---

- ISSN 0022-460X.  
DOI: 10.1006/jsvi.2000.3407.  
354
- [33] S. Bellizzi and R. Bouc.  
A new formulation for the existence and calculation of nonlinear normal modes.  
*Journal of Sound and Vibration*, 287(3):545–569, 2005.  
ISSN 0022-460X.  
DOI: 10.1016/j.jsv.2004.11.014.  
45, 368
- [34] T. Belytschko, W. K. Liu, and B. Moran.  
*Nonlinear Finite Elements for Continua and Structures*.  
John Wiley & Sons, 2000.  
18
- [35] P. Benner.  
Model reduction using center and inertial manifolds.  
In *Berlin-Braunschweig-Chemnitz Workshop Recent Advances in Model Reduction*, 2006.  
354
- [36] M. Bergmann and L. Cordier.  
Optimal control of the cylinder wake in the laminar regime by trust-region methods and POD  
reduced-order models.  
*Journal of Computational Physics*, 227(16):7813–7840, 2008.  
ISSN 0021-9991.  
DOI: 10.1016/j.jcp.2008.04.034.  
72, 133, 376
- [37] B. Besselink, U. Tabak, A. Lutowska, N. van de Wouw, H. Nijmeijer, D. Rixen, M. Hochstenbach,  
and W. Schilders.  
A comparison of model reduction techniques from structural dynamics, numerical mathematics and  
systems and control.  
*Journal of Sound and Vibration*, 332(19):4403 – 4422, 2013.  
ISSN 0022-460X.  
DOI: <http://dx.doi.org/10.1016/j.jsv.2013.03.025>.  
37, 50
- [38] F. Blanc, C. Touzé, J.-F. Mercier, K. Ege, and A.-S. B. Ben-Dhia.  
On the numerical computation of nonlinear normal modes for reduced-order modelling of conserva-  
tive vibratory systems.  
*Mechanical Systems and Signal Processing*, 36(2):520–539, 2013.  
ISSN 0888-3270.  
DOI: 10.1016/j.ymssp.2012.10.016.  
355
- [39] N. Boivin, C. Pierre, and S. W. Shaw.  
Non-linear modal analysis of structural systems featuring internal resonances.  
*Journal of Sound and Vibration*, 182(2):336–341, 1995.  
ISSN 0022-460X.  
DOI: 10.1006/jsvi.1995.0201.  
354
- [40] J. Bonet and R. Wood.

## BIBLIOGRAPHY

---

- Non-linear Continuum Mechanics for Finite Element Analysis.*  
Cambridge University Press, 2008.  
13, 14, 21
- [41] S. Browne, J. Dongarra, N. Garner, K. London, and P. Mucci.  
A scalable cross-platform infrastructure for application performance tuning using hardware counters.  
In *ACM/IEEE 2000 Conference Supercomputing*, ACM/IEEE 2000 Conference, Los Alamitos, CA, USA, 2000. IEEE Computer Society.  
DOI: <http://doi.ieeeecomputersociety.org/10.1109/SC.2000.10029>.  
93
- [42] T. Buhl, C. B. W. Pedersen, and O. Sigmund.  
Stiffness design of geometrically nonlinear structures using topology optimization.  
*Structural and Multidisciplinary Optimization*, 19:93–104, 2000.  
3
- [43] T. Bui-Thanh, K. Willcox, O. Ghattas, and B. van Bloemen Waanders.  
Goal-oriented, model-constrained optimization for reduction of large-scale systems.  
*Journal of Computational Physics*, 224(2):880–896, 2007.  
ISSN 0021-9991.  
DOI: 10.1016/j.jcp.2006.10.026.  
36, 47
- [44] T. Bui-Thanh, K. Willcox, and O. Ghattas.  
Model reduction for large-scale systems with high-dimensional parametric input space.  
*SIAM Journal on Scientific Computing*, 30(6):3270–3288, 2008.  
146, 379
- [45] J. Burkardt.  
timestamp.  
online, 2006.  
[http://people.sc.fsu.edu/~jburkardt/m\\_src/timestamp/timestamp.html](http://people.sc.fsu.edu/~jburkardt/m_src/timestamp/timestamp.html) - retrieved 11.03.2011.  
296
- [46] J. Burkardt, M. Gunzburger, and H.-C. Lee.  
POD and CVT-based reduced-order modeling of Navier-Stokes flows.  
*Computer Methods in Applied Mechanics and Engineering*, 196(1-3):337–355, 2006.  
ISSN 0045-7825.  
DOI: 10.1016/j.cma.2006.04.004.  
77
- [47] T. Burton and W. Rhee.  
On the reduction of nonlinear structural dynamics models.  
*Journal of Vibration and Control*, 6:531–556, 2000.  
40, 67, 355
- [48] E. Butcher and R. Lu.  
Order reduction of structural dynamic systems with static piecewise linear nonlinearities.  
*Nonlinear Dynamics*, 49:375–399, 2007.  
ISSN 0924-090X.  
DOI: 10.1007/s11071-006-9129-6.  
78
- [49] E. A. Butcher and M. A. AL-Shudeifat.

## BIBLIOGRAPHY

---

- An efficient mode-based alternative to principal orthogonal modes in the order reduction of structural dynamic systems with grounded nonlinearities.  
*Mechanical Systems and Signal Processing*, 25(5):1527–1549, 2011.  
ISSN 0888-3270.  
DOI: 10.1016/j.ymssp.2010.11.017.  
78, 79
- [50] T. M. Cameron and J. H. Griffin.  
An alternating frequency/time domain method for calculating the steady-state response of nonlinear dynamic systems.  
*Journal of Applied Mechanics*, 56:149–154, 1989.  
42
- [51] R. Camillacci, N. S. Ferguson, and P. R. White.  
Simulation and experimental validation of modal analysis for non-linear symmetric systems.  
*Mechanical Systems and Signal Processing*, 19(1):21–41, 2005.  
ISSN 0888-3270.  
DOI: 10.1016/j.ymssp.2004.05.002.  
354, 357
- [52] T. T. Cao and D. C. Zimmerman.  
Application of load-dependent Ritz vectors in structural damage detection.  
In *Proceedings of the 15th International Modal Analysis Conference*, pages 1319–1324, 1997.  
68
- [53] E. Capiez-Lernout and C. Soize.  
Robust updating of uncertain damping models in structural dynamics for low- and medium-frequency ranges.  
*Mechanical Systems and Signal Processing*, 22(8):1774–1792, 2008.  
ISSN 0888-3270.  
DOI: 10.1016/j.ymssp.2008.02.005.  
73
- [54] K. Carlberg and C. Farhat.  
A compact Proper Orthogonal Decomposition basis for optimization-oriented reduced-order models.  
In *12th AIAA/ISSMO Multidisciplinary Analysis and Optimization Conference*, 2008.  
200
- [55] K. Carlberg, C. Bou-Mosleh, and C. Farhat.  
Efficient non-linear model reduction via a Least-Squares Petrov-Galerkin projection and compressive tensor approximations.  
*International Journal for Numerical Methods in Engineering*, 86(2):155–181, 2011.  
ISSN 1097-0207.  
DOI: 10.1002/nme.3050.  
4, 5, 36, 137, 146, 147, 148, 149, 378, 379
- [56] K. Carlberg, C. Farhat, J. Cortial, and D. Amsallem.  
The GNAT method for nonlinear model reduction: effective implementation and application to computational fluid dynamics and turbulent flows.  
*Journal of Computational Physics*, 242:623–647, 2013.  
146, 147, 379
- [57] C. Chang and J. J. Engblom.  
Nonlinear dynamical response of impulsively loaded structures : a reduced basis approach.

## BIBLIOGRAPHY

---

- AIAA Journal*, 29(4):613–618, 1991.  
68, 114, 343
- [58] Y.-W. Chang, X. Wang, E. Capiiez-Lernout, M. P. Mignolet, and C. Soize.  
Reduced order modeling for the nonlinear geometric response of some curved structures.  
In *International Forum of Aeroelasticity & Structural Dynamics (IFASD)*, 2011.  
173, 174, 177, 180, 186, 382
- [59] D. Chelidze and W. Zhou.  
Smooth Orthogonal Decomposition-based vibration mode identification.  
*Journal of Sound and Vibration*, 292(3-5):461–473, 2006.  
ISSN 0022-460X.  
DOI: 10.1016/j.jsv.2005.08.006.  
73, 74
- [60] Y. Chen and J. White.  
A quadratic method for nonlinear model order reduction.  
In *2000 International Conference on Modeling and Simulation of Microsystems*, pages 477–480,  
2000.  
2
- [61] F. Chinesta, A. Ammar, A. Leygue, and R. Keunings.  
An overview of the Proper Generalized Decomposition with applications in computational rheology.  
*Journal of Non-Newtonian Fluid Mechanics*, 166(11):578–592, 2011.  
ISSN 0377-0257.  
DOI: 10.1016/j.jnnfm.2010.12.012.  
72, 326
- [62] F. Chinesta, A. Ammar, and E. Cueto.  
Recent advances and new challenges in the use of the Proper Generalized Decomposition for solving  
multidimensional models.  
*Archives of Computational Methods in Engineering*, 17:327–350, 2010.  
ISSN 1134-3060.  
DOI: 10.1007/s11831-010-9049-y.  
4
- [63] J. Chung and G. M. Hulbert.  
A time integration algorithm for structural dynamics with improved numerical dissipation: the  
generalized- $\alpha$  method.  
*Journal of Applied Mechanics*, 60:371–375, 1993.  
55
- [64] C. De Boor and A. Ron.  
Computational aspects of polynomial interpolation in several variables.  
*Mathematics of Computation*, 58:705–727, 1992.  
196
- [65] A. E. Deane, I. G. Kevrekidis, G. E. Karniadakis, and S. A. Orszag.  
Low dimensional models for complex geometry flows: Application to grooved channels and circular  
cylinders.  
*Physics of Fluids A*, 3(10):2337–2354, 1991.  
ISSN 08998213.  
DOI: 10.1063/1.857881.  
71

## BIBLIOGRAPHY

---

- [66] J. Dennis and R. B. Schnabel.  
*Numerical Methods for Unconstrained Optimization and Nonlinear Equations*.  
Society for Industrial and Applied Mathematics, 1996.  
51
- [67] J. D'Errico.  
mvgstd.m.  
online, 2009.  
<http://www.mathworks.com/matlabcentral/fileexchange/authors/679> - retrieved 25.06.2013.  
296
- [68] J. D'Errico.  
gradest.m automatic numerical differentiation.  
online, 2006.  
<http://www.mathworks.com/matlabcentral/fileexchange/13490-automatic-numerical-differentiation>  
- retrieved 18.02.2011.  
296
- [69] J. Dickens, J. Nakagawa, and M. Wittbrodt.  
A critique of mode acceleration and modal truncation augmentation methods for modal response  
analysis.  
*Computers & Structures*, 62(6):985 – 998, 1997.  
ISSN 0045-7949.  
DOI: [http://dx.doi.org/10.1016/S0045-7949\(96\)00315-X](http://dx.doi.org/10.1016/S0045-7949(96)00315-X).  
139, 164
- [70] D. Dinkler.  
Reduction methods in structural dynamics.  
In K. Meskouris and U. Wittek, editors, *Aspects in Modern Computational Structural Analysis*, pages  
19–31. Balkema Publishers, 1997.  
38
- [71] Q. Du, V. Faber, and M. Gunzburger.  
Centroidal Voronoi Tessellations: Applications and algorithms.  
*SIAM Review*, 41(4):637–676, 12 1999.  
40, 62, 77, 78, 366
- [72] K. Ekici, K. C. Hall, and E. H. Dowell.  
Computationally fast harmonic balance methods for unsteady aerodynamic predictions of helicopter  
rotors.  
*Journal of Computational Physics*, 227(12):6206–6225, 2008.  
ISSN 0021-9991.  
DOI: 10.1016/j.jcp.2008.02.028.  
42, 367
- [73] S. El-Rabaie, V. Fusco, and C. Stewart.  
Harmonic balance evaluation of nonlinear microwave circuits - a tutorial approach.  
*IEEE Transactions on Education*, 31(3):181 –192, aug 1988.  
ISSN 0018-9359.  
DOI: 10.1109/13.2310.  
42, 367
- [74] C. W. Emory and M. J. Patil.  
Prediction of limit cycle oscillation using nonlinear normal modes: Galerkin and collocation solu-  
tions.

## BIBLIOGRAPHY

---

- In *International Forum of Aeroelasticity & Structural Dynamics (IFASD)*, 2011.  
355
- [75] C. W. Emory.  
*Prediction of Limit Cycle Oscillation in an Aeroelastic System using Nonlinear Normal Modes.*  
PhD thesis, Virginia Polytechnic Institute and State University, 2010.  
355
- [76] U. Farooq and B. Feeny.  
Smooth Orthogonal Decomposition for modal analysis of randomly excited systems.  
*Journal of Sound and Vibration*, 316(1-5):137–146, 2008.  
ISSN 0022-460X.  
DOI: 10.1016/j.jsv.2008.02.052.  
73
- [77] B. F. Feeny.  
On proper orthogonal co-ordinates as indicators of modal activity.  
*Journal of Sound and Vibration*, 255(5):805–817, 2002.  
ISSN 0022-460X.  
DOI: 10.1006/jsvi.2001.4120.  
237
- [78] B. F. Feeny and R. Kappagantu.  
On the physical interpretation of Proper Orthogonal Modes in vibrations.  
*Journal of Sound and Vibration*, 211(4):607–616, 1998.  
ISSN 0022-460X.  
DOI: 10.1006/jsvi.1997.1386.  
69, 74, 203
- [79] B. F. Feeny and Y. Liang.  
Interpreting Proper Orthogonal Modes of randomly excited vibration systems.  
*Journal of Sound and Vibration*, 265(5):953–966, 2003.  
ISSN 0022-460X.  
DOI: 10.1016/S0022-460X(02)01265-8.  
62, 69, 74, 203
- [80] C. Felippa and K. Park.  
Direct time integration methods in nonlinear structural dynamics.  
*Computer Methods in Applied Mechanics and Engineering*, 17-18(Part 2):277–313, 1979.  
ISSN 0045-7825.  
DOI: 10.1016/0045-7825(79)90023-9.  
51
- [81] D. Galbally, K. Fidkowski, K. Willcox, and O. Ghattas.  
Non-linear model reduction for uncertainty quantification in large-scale inverse problems.  
*International Journal for Numerical Methods in Engineering*, 81(12):1581–1608, 2010.  
DOI: 10.1002/nme.2746.  
154, 380
- [82] G. Genta.  
A fast modal technique for the computation of the campbell diagram of multi-degree-of-freedom rotors.  
*Journal of Sound and Vibration*, 155(3):385–402, 1992.  
ISSN 0022-460X.

## BIBLIOGRAPHY

---

- DOI: 10.1016/0022-460X(92)90708-6.  
267
- [83] F. Georgiades, M. Peeters, G. Kerschen, and J. C. Golinval.  
Modal analysis of a nonlinear periodic structure with cyclic symmetry.  
*AIAA Journal*, 47:1014–1025, 2009.  
356
- [84] J. H. Griffin.  
A review of friction damping of turbine blade vibration.  
*International Journal of Turbo and Jet Engines*, 7:297–307, 1990.  
2
- [85] A. Grolet and F. Thouverez.  
On the use of the Proper Generalised Decomposition for solving nonlinear vibration problems.  
In *ASME 2012 International Mechanical Engineering Congress & Exposition, IMECE*, 2012.  
5, 44, 174, 294
- [86] G. V. Groll and D. J. Ewins.  
The harmonic balance method with arc-length continuation in rotor/stator contact problems.  
*Journal of Sound and Vibration*, 241(2):223–233, 2001.  
ISSN 0022-460X.  
DOI: 10.1006/jsvi.2000.3298.  
42, 367
- [87] D. Gross, W. Hauger, W. Schnell, and J. Schröder.  
*Technische Mechanik 1*.  
Springer, 2004.  
296
- [88] D. Gross, W. Hauger, W. Schnell, and J. Schröder.  
*Technische Mechanik 3*.  
Springer, 2004.  
296
- [89] D. Gross, W. Hauger, W. Schnell, and P. Wriggers.  
*Technische Mechanik 4*.  
Springer, 2004.  
296
- [90] R. J. Guyan.  
Reduction of stiffness and mass matrices.  
*AIAA Journal*, 3(2):380, 1965.  
40, 367
- [91] S. Han and B. Feeny.  
Application of Proper Orthogonal Decomposition to structural vibration analysis.  
*Mechanical Systems and Signal Processing*, 17(5):989–1001, 2003.  
ISSN 0888-3270.  
DOI: 10.1006/mssp.2002.1570.  
62, 69
- [92] O. E. Hansteen and K. Bell.  
On the accuracy of mode superposition analysis in structural dynamics.  
*Earthquake Engineering and Structural Dynamics*, 7:405–411, 1979.  
4, 137, 378, 379

## BIBLIOGRAPHY

---

- [93] J. Har and K. K. Tamma.  
*Advances in Computational Dynamics*.  
John Wiley & Sons, 2012.  
51, 60
- [94] A. Hay, J. Borggaard, I. Akhtar, and D. Pelletier.  
Reduced-order models for parameter dependent geometries based on shape sensitivity analysis.  
*Journal of Computational Physics*, 229(4):1327–1352, 2010.  
ISSN 0021-9991.  
DOI: 10.1016/j.jcp.2009.10.033.  
193
- [95] A. Hay, J. T. Borggaard, and D. Pelletier.  
Local improvements to reduced-order models using sensitivity analysis of the Proper Orthogonal  
Decomposition.  
*Journal of Fluid Mechanics*, 629:41–72, 2009.  
4, 73, 133, 193, 198, 199, 200, 376
- [96] F. M. Hemez and S. W. Doebling.  
Review and assessment of model updating for non-linear, transient dynamics.  
*Mechanical Systems and Signal Processing*, 15(1):45–74, 2001.  
ISSN 0888-3270.  
DOI: 10.1006/mssp.2000.1351.  
154, 380
- [97] H. M. Hilber, T. J. R. Hughes, and R. L. Taylor.  
Improved numerical dissipation for time integration algorithms in structural dynamics.  
*Earthquake Engineering and Structural Dynamics*, 5:283–292, 1977.  
55, 60
- [98] S. J. Hollister.  
BME/ME 506 Computational modeling of biological tissues.  
online, 2013.  
<http://www.umich.edu/~bme506/> - retrieved 17.09.2013.  
296
- [99] J. J. Hollkamp, R. W. Gordon, and S. M. Spottswood.  
Nonlinear modal models for sonic fatigue response prediction: a comparison of methods.  
*Journal of Sound and Vibration*, 284(3-5):1145–1163, 2005.  
ISSN 0022-460X.  
DOI: 10.1016/j.jsv.2004.08.036.  
173, 174, 181, 382
- [100] G. A. Holzapfel.  
*Nonlinear Solid Mechanics: A Continuum Approach for Engineering*.  
John Wiley & Sons, 2000.  
12
- [101] J. C. Houbolt.  
A recurrence matrix solution for the dynamic response of aircraft in gusts.  
Technical Report 1010, Langley Aeronautical Laboratory, 1950.  
51
- [102] S. R. Idelsohn and A. Cardona.  
A load-dependent basis for reduced nonlinear structural dynamics.

## BIBLIOGRAPHY

---

- Computers & Structures*, 20(1-3):203–210, 1985.  
ISSN 0045-7949.  
DOI: 10.1016/0045-7949(85)90069-0.  
65, 68, 114, 154, 343, 380
- [103] F. Ihlenburg.  
*Finite Element Analysis of Acoustic Scattering*.  
Springer, 1998.  
21
- [104] F. Ihlenburg.  
Nichtlineares Stabelement.  
online, 2010.  
<http://www.mp.haw-hamburg.de/pers/Ihl/HTML/fem1.html> - retrieved 10.11.2010.  
21
- [105] K. Ito and S. S. Ravindran.  
A reduced-order method for simulation and control of fluid flows.  
*Journal of Computational Physics*, 143(2):403–425, 1998.  
ISSN 0021-9991.  
DOI: 10.1006/jcph.1998.5943.  
73, 133, 199, 376
- [106] JabRef Development Team.  
*JabRef*.  
JabRef Development Team, 2010.  
296
- [107] K. E. Jansen, C. H. Whiting, and G. M. Hulbert.  
A generalized- $\alpha$  method for integrating the filtered Navier-Stokes equations with a stabilized finite element method.  
*Computer Methods in Applied Mechanics and Engineering*, 190(3-4):305–319, 2000.  
ISSN 0045-7825.  
DOI: 10.1016/S0045-7825(00)00203-6.  
55
- [108] D. Jiang, C. Pierre, and S. W. Shaw.  
Large-amplitude Non-linear Normal Modes of piecewise linear systems.  
*Journal of Sound and Vibration*, 272(3-5):869–891, 2004.  
ISSN 0022-460X.  
DOI: 10.1016/S0022-460X(03)00497-8.  
354
- [109] D. Jiang, C. Pierre, and S. Shaw.  
The construction of Non-linear Normal Modes for systems with internal resonance.  
*International Journal of Non-Linear Mechanics*, 40(5):729–746, 2005.  
ISSN 0020-7462.  
DOI: 10.1016/j.ijnonlinmec.2004.08.010.  
356
- [110] D. Jiang, C. Pierre, and S. Shaw.  
Nonlinear Normal Modes for vibratory systems under harmonic excitation.  
*Journal of Sound and Vibration*, 288(4-5):791–812, 2005.  
ISSN 0022-460X.

## BIBLIOGRAPHY

---

- DOI: 10.1016/j.jsv.2005.01.009.  
355
- [111] V. John and J. Rang.  
Adaptive time step control for the incompressible Navier-Stokes equations.  
*Computer Methods in Applied Mechanics and Engineering*, 199(9-12):514–524, 2010.  
ISSN 0045-7825.  
DOI: 10.1016/j.cma.2009.10.005.  
51
- [112] D. Jung and H. C. Gea.  
Topology optimization of nonlinear structures.  
*Finite Elements in Analysis and Design*, 40:1417–1427, 2004.  
3
- [113] R. K. Kapania and C. Byun.  
Reduction methods based on eigenvectors and Ritz vectors for nonlinear transient analysis.  
*Computational Mechanics*, 11:65–82, 1993.  
40, 66, 67, 68, 114
- [114] A. J. Keane and P. B. Nair.  
*Computational Approaches for Aerospace Design*.  
John Wiley & Sons, 2005.  
ISBN 9780470855485.  
DOI: 10.1002/0470855487.fmatter.  
2, 72, 73, 199, 200
- [115] M. I. Kellner, R. J. Madachy, and D. M. Raffo.  
Software process simulation modeling: Why? What? How?  
*Journal of Systems and Software*, 46(2-3):91–105, 1999.  
ISSN 0164-1212.  
DOI: 10.1016/S0164-1212(99)00003-5.  
2
- [116] G. Kerschen and J. C. Golinval.  
Physical interpretation of the Proper Orthogonal modes using the Singular Value Dcomposition.  
*Journal of Sound and Vibration*, 249(5):849–865, 2002.  
69
- [117] G. Kerschen, M. Peeters, J. C. Golinval, and A. F. Vakakis.  
Nonlinear Normal Modes Part I : A useful frame work for the structural dynamicist.  
*Mechanical Systems and Signal Processing*, 23:170–194, 2009.  
3, 37, 44, 353, 354, 355, 366, 368
- [118] G. Kerschen, K. Worden, A. F. Vakakis, and J.-C. Golinval.  
Past, present and future of nonlinear system identification in structural dynamics.  
*Mechanical Systems and Signal Processing*, 20:505–592, 2006.  
2, 3
- [119] D. Kim and R. B. Langley.  
An optimized least-squares technique for improving ambiguity resolution and computational efficiency.  
online, 1999.  
147, 379

## BIBLIOGRAPHY

---

- [120] M. Kirby, J. P. Boris, and L. Sirovich.  
A Proper Orthogonal Decomposition of a simulated supersonic shear layer.  
*International Journal for Numerical Methods in Fluids*, 10:411–428, 1990.  
71, 189
- [121] M. Kirby.  
Minimal dynamical systems from PDEs using Sobolev eigenfunctions.  
*Physica D: Nonlinear Phenomena*, 57(3-4):466–475, 1992.  
ISSN 0167-2789.  
DOI: 10.1016/0167-2789(92)90014-E.  
189
- [122] M. Kirby and R. Miranda.  
Nonlinear reduction of high-dimensional dynamical systems via neural networks.  
*Physical Review Letters*, 72(12):1822–1825, 1994.  
189
- [123] S. Krenk.  
*Non-linear Modeling and Analysis of Solids and Structures*.  
Cambridge University Press, 2009.  
16, 21, 29, 51
- [124] D. Kuhl and E. Ramm.  
Constraint energy momentum algorithm and its application to non-linear dynamics of shells.  
*Computer Methods in Applied Mechanics and Engineering*, 136:293–315, 1996.  
55
- [125] N. Kumar and T. D. Burton.  
On combined use of POD modes and Ritz vectors for model reduction in nonlinear structural dynamics.  
In *International Design Engineering Technical Conferences and Computers and Information in Engineering Conference (IDETC/CIE)*, volume 2009, pages 637–649. ASME, 2009.  
DOI: 10.1115/DETC2009-87416.  
73, 199
- [126] W. Lacarbonara and G. Rega.  
Resonant Non-linear Normal Modes. Part II: activation/orthogonality conditions for shallow structural systems.  
*International Journal of Non-Linear Mechanics*, 38(6):873–887, 2003.  
ISSN 0020-7462.  
DOI: 10.1016/S0020-7462(02)00034-3.  
355
- [127] W. Lacarbonara, G. Rega, and A. H. Nayfeh.  
Resonant Non-linear Normal Modes. Part I: analytical treatment for structural one-dimensional systems.  
*International Journal of Non-Linear Mechanics*, 38(6):851–872, 2003.  
ISSN 0020-7462.  
DOI: 10.1016/S0020-7462(02)00033-1.  
355
- [128] W. Lacarbonara and R. Camillacci.  
Nonlinear Normal Modes of structural systems via asymptotic approach.  
*International Journal of Solids and Structures*, 41:5565–5594, 2004.  
354, 355

## BIBLIOGRAPHY

---

- [129] M. Lalanne, P. Berthier, and J. der Hagopian.  
*Mécanique des vibrations linéaires*.  
Masson, Paris, 1980.  
340
- [130] C. Lanczos.  
An iteration method for the solution of the eigenvalue problem of linear differential and integral operators.  
*Journal of Research of the National Bureau of Standards*, 45(4):255–282, 1950.  
40, 66
- [131] Y. Le Guennec.  
*Transient dynamics of beam trusses under impulse loads*.  
PhD thesis, École Centrale Paris, 2013.  
295
- [132] V. Lenaerts, G. Kerschen, and J. C. Golinval.  
Identification of a continuous structure with a geometrical non-linearity. Part II: Proper Orthogonal Decomposition.  
*Journal of Sound and Vibration*, 262(4):907–919, 2003.  
ISSN 0022-460X.  
DOI: 10.1016/S0022-460X(02)01132-X.  
69
- [133] R. Lewandowski.  
Computational formulation for periodic vibration of geometrically nonlinear structures - Part 1: Theoretical background.  
*International Journal of Solids and Structures*, 34(15):1925–1947, 1997.  
ISSN 0020-7683.  
DOI: 10.1016/S0020-7683(96)00127-8.  
354
- [134] R. Lewandowski.  
Computational formulation for periodic vibration of geometrically nonlinear structures - Part 2: Numerical strategy and examples.  
*International Journal of Solids and Structures*, 34(15):1949–1964, 1997.  
ISSN 0020-7683.  
DOI: 10.1016/S0020-7683(96)00126-6.  
354
- [135] A. Leygue and E. Verron.  
A first step towards the use of Proper General Decomposition method for structural optimization.  
*Archives of Computational Methods in Engineering*, 17:465–472, 2010.  
ISSN 1134-3060.  
DOI: 10.1007/s11831-010-9052-3.  
47
- [136] X. Li, J. Ji, and C. H. Hansen.  
Non-linear normal modes and their bifurcation of a two DOF system with quadratic and cubic non-linearity.  
*International Journal of Non-Linear Mechanics*, 41(9):1028–1038, 2006.  
ISSN 0020-7462.  
DOI: 10.1016/j.ijnonlinmec.2005.12.005.  
356

## BIBLIOGRAPHY

---

- [137] E. Liberge and A. Hamdouni.  
Reduced order modelling method via Proper Orthogonal Decomposition (POD) for flow around an oscillating cylinder.  
*Journal of Fluids and Structures*, 26(2):292–311, 2010.  
ISSN 0889-9746.  
DOI: 10.1016/j.jfluidstructs.2009.10.006.  
71, 72
- [138] T. Lieu and M. Lesoinne.  
Parameter adaptation of reduced order models for three-dimensional flutter analysis.  
In *AIAA Aerospace Sciences Meeting and Exhibit*, Reno, Nevada, 2004.  
194, 385
- [139] L. Liu and T. Kalmár-Nagy.  
High-dimensional harmonic balance analysis for second-order delay-differential equations.  
*Journal of Vibration and Control*, 16(7-8):1189–1208, June July 2010.  
DOI: 10.1177/1077546309341134.  
42, 43, 44
- [140] F. A. Lülfi, D.-M. Tran, and R. Ohayon.  
Comparison of some reduction bases approaches for non-linear structural dynamic systems under different excitations.  
In *6th European Congress on Computational Methods in Applied Sciences and Engineering. ECCO-MAS*, September 2012.  
292, 393
- [141] F. A. Lülfi, D.-M. Tran, and R. Ohayon.  
Reduced bases for nonlinear structural dynamic systems: A comparative study.  
*Journal of Sound and Vibration*, 332:3897–3921, 2013.  
292, 393
- [142] F. A. Lülfi, D.-M. Tran, and R. Ohayon.  
Approaches for the construction of an autonomous reduced model of a non-linear structure for transient dynamic solution.  
In *CSMA 2013 11e Colloque National en Calcul des Structures*, 2013.  
293, 393
- [143] C. Mansoux, D. Gysling, J. Setiawan, and J. Paduano.  
Distributed nonlinear modeling and stability analysis of axial compressor stall and surge.  
In *American Control Conference*, volume 2, pages 2305–2316, june-1 july 1994.  
DOI: 10.1109/ACC.1994.752492.  
2
- [144] J. Marsden and T. Hughes.  
*Mathematical foundations of elasticity*.  
Dover Publications, 1983.  
296
- [145] H. G. Matthies and G. Strang.  
The solution of nonlinear finite element equations.  
*International Journal for Numerical Methods in Engineering*, 14:1613–1626, 1979.  
276
- [146] M. Meyer and H. G. Matthies.

## BIBLIOGRAPHY

---

- Efficient model reduction in non-linear dynamics using the Karhunen-Loève expansion and dual-weighted-residual methods.  
*Computational Mechanics*, 31:179–191, 2003.  
ISSN 0178-7675.  
DOI: 10.1007/s00466-002-0404-1.  
3
- [147] M. Meyer and H. G. Matthies.  
State-space representation of instationary two-dimensional airfoil aerodynamics.  
*Journal of Wind Engineering and Industrial Aerodynamics*, 92:263–274, 2004.  
ISSN 0167-6105.  
DOI: 10.1016/j.jweia.2003.11.004.  
3
- [148] M. P. Mignolet and C. Soize.  
Stochastic reduced order models for uncertain geometrically nonlinear dynamical systems.  
*Computer Methods in Applied Mechanics and Engineering*, 197:3951–3963, 2008.  
ISSN 0045-7825.  
DOI: 10.1016/j.cma.2008.03.032.  
174, 175, 382
- [149] M. P. Mignolet, A. Przekop, S. A. Rizzi, and S. M. Spottswood.  
A review of indirect/non-intrusive reduced order modeling of nonlinear geometric structures.  
*Journal of Sound and Vibration*, 332(10):2437–2460, 2013.  
ISSN 0022-460X.  
DOI: 10.1016/j.jsv.2012.10.017.  
6, 47, 49, 56
- [150] B. C. Moore.  
Principal component analysis in linear systems: Controllability, observability, and model reduction.  
*IEEE Transactions on Automatic Control.*, 26:17–32, 1981.  
70
- [151] MSC Software.  
*MD Nastran & MSC Nastran 2011 Quick Reference Guide*, 2011.  
259, 283
- [152] MSC Software.  
*MD Nastran & MSC Nastran 2011 Dynamic Analysis User's Guide*, 2011.  
259, 283
- [153] MSC Software.  
*MSC Nastran 2011 Implicit Nonlinear User's Guide*, 2011.  
259, 283
- [154] C.-D. Munz and T. Westermann.  
*Numerische Behandlung gewöhnlicher und partieller Differenzialgleichungen*.  
Springer, 2006.  
296
- [155] A. A. Muravyov and S. A. Rizzi.  
Determination of nonlinear stiffness with application to random vibration of geometrically nonlinear structures.  
*Computers & Structures*, 81(15):1513–1523, 2003.  
ISSN 0045-7949.

## BIBLIOGRAPHY

---

- DOI: 10.1016/S0045-7949(03)00145-7.  
173, 174, 177, 180, 186, 187, 189, 192, 215, 221, 382, 383, 384
- [156] A. H. Nayfeh and S. A. Nayfeh.  
On nonlinear modes of continuous systems.  
*Journal of Vibration and Acoustics*, 116(1):129–136, 1994.  
DOI: 10.1115/1.2930388.  
354
- [157] A. H. Nayfeh and S. A. Nayfeh.  
Nonlinear Normal Modes of a continuous system with quadratic nonlinearities.  
*Journal of Vibration and Acoustics*, 117(2):199–205, 1995.  
DOI: 10.1115/1.2873898.  
354
- [158] A. H. Nayfeh, C. Chin, and S. A. Nayfeh.  
On Nonlinear Normal Modes of systems with internal resonance.  
*Journal of Vibration and Acoustics*, 118(3):340–345, 1996.  
DOI: 10.1115/1.2888188.  
354
- [159] A. Nayfeh.  
*Non-linear interactions*.  
Wiley Interscience, 2000.  
45, 368
- [160] N. M. Newmark.  
A method of computation for structural dynamics.  
*Transactions of the American Society of Civil Engineers*, 127(1):1406–1432, 1962.  
50
- [161] R. Nickell.  
Nonlinear dynamics by mode superposition.  
*Computer Methods in Applied Mechanics and Engineering*, 7(1):107–129, 1976.  
ISSN 0045-7825.  
DOI: 10.1016/0045-7825(76)90008-6.  
3, 62, 339
- [162] B. R. Noack, K. Afanasiev, M. Morzyński, G. Tadmor, and F. Thiele.  
A hierarchy of low-dimensional models for the transient and post-transient cylinder wake.  
*Journal of Fluid Mechanics*, 497:335–363, 2003.  
DOI: 10.1017/S0022112003006694.  
72, 133, 376
- [163] A. K. Noor.  
Recent advances in reduction methods for nonlinear problems.  
*Computers & Structures*, 13(1-3):31–44, 1981.  
ISSN 0045-7949.  
DOI: 10.1016/0045-7949(81)90106-1.  
6
- [164] S. Novak and R. G. Frehlich.  
Transition to chaos in the Duffing oscillator.  
*Physical Review A*, 26:3660–3663, Dec 1982.  
DOI: 10.1103/PhysRevA.26.3660.  
94

## BIBLIOGRAPHY

---

- [165] T. Özis and A. Yildirim.  
Determination of the frequency-amplitude relation for a Duffing-harmonic oscillator by the energy balance method.  
*Computers & Mathematics with Applications*, 54(7-8):1184–1187, 2007.  
ISSN 0898-1221.  
DOI: 10.1016/j.camwa.2006.12.064.  
42, 367
- [166] C. Pak.  
Synge’s concept of stability applied to non-linear normal modes.  
*International Journal of Non-Linear Mechanics*, 41(5):657–664, 2006.  
ISSN 0020-7462.  
DOI: 10.1016/j.ijnonlinmec.2006.01.007.  
356
- [167] C. Pak.  
On the coupling of Non-linear Normal Modes.  
*International Journal of Non-Linear Mechanics*, 41(5):716–725, 2006.  
ISSN 0020-7462.  
DOI: 10.1016/j.ijnonlinmec.2006.04.003.  
356
- [168] T. Palau, A. Kuhn, S. Nogales, H. Böhm, and A. Rauh.  
A neural network based elasto-plasticity material model.  
In *6th European Congress on Computational Methods in Applied Sciences and Engineering*, 2012.  
189
- [169] M. Peeters, R. Viguie, G. Serandour, G. Kerschen, and J. Golinval.  
Computation of Nonlinear Normal Modes. Part I : Numerical continuation in Matlab.  
In *6th EUROMECH Nonlinear Dynamics Conference (ENOC)*, 2008.  
37, 360, 362, 366
- [170] M. Peeters, R. Viguie, G. Serandour, G. Kerschen, and J.-C. Golinval.  
Nonlinear Normal Modes Part II : Toward a practical computation using numerical continuation techniques.  
*Mechanical Systems and Signal Processing*, 23:195–216, 2009.  
3, 353, 354, 355, 357, 359, 361
- [171] M. Peeters.  
*Theoretical and Experimental Modal Analysis of Nonlinear Vibrating Structures using Nonlinear Normal Modes*.  
PhD thesis, University of Liège, 2010.  
Structural Dynamics Research Group, Aerospace and Mechanical Engineering Department.  
90
- [172] Z. Peng, Z. Lang, S. Billings, and G. Tomlinson.  
Comparisons between harmonic balance and nonlinear output frequency response function in non-linear system analysis.  
*Journal of Sound and Vibration*, 311(1-2):56–73, 2008.  
ISSN 0022-460X.  
DOI: 10.1016/j.jsv.2007.08.035.  
44
- [173] L. Perret, E. Collin, and J. Delville.

## BIBLIOGRAPHY

---

- Polynomial identification of POD based low-order dynamical system.  
*Journal of Turbulence*, 7(17):1–15, 2006.  
DOI: 10.1080/14685240600559665.  
174
- [174] E. Pesheck, C. Pierre, and S. W. Shaw.  
Accurate reduced-order models for a simple rotor blade model using Nonlinear Normal Modes.  
*Mathematical and Computer Modelling*, 33(10-11):1085–1097, 2001.  
ISSN 0895-7177.  
DOI: 10.1016/S0895-7177(00)00301-0.  
354
- [175] E. Pesheck, C. C. Pierre, and S. W. Shaw.  
A new Galerkin-based approach for accurate Non-linear Normal Modes through invariant manifolds.  
*Journal of Sound and Vibration*, 249(5):971–993, 2002.  
ISSN 0022-460X.  
DOI: 10.1006/jsvi.2001.3914.  
354
- [176] E. Pesheck.  
*Reduced order modeling of nonlinear structural systems using Nonlinear Normal Modes and invariant manifolds*.  
PhD thesis, University of Michigan, 2000.  
353, 354, 356, 357, 358
- [177] C. S. Peskin.  
Flow patterns around heart valves : a digital computer method for solving the equations of motion.  
*IEEE Transactionson Biomedical Engineering*, 30(4):316–317, 1973.  
72
- [178] J. S. Peterson.  
The reduced basis method for incompressible viscous flow calculations.  
*SIAM Journal on Scientific and Statistical Computing*, 10(4):777–786, 1989.  
ISSN 10648275.  
DOI: 10.1137/0910047.  
72
- [179] J. R. Phillips.  
Projection-based approaches for model reduction of weakly nonlinear, time-varying systems.  
*IEEE Transactions on computer-aided design of integrated circuits and systems*, 22(2):171–187,  
2003.  
173, 175, 176, 184, 187, 215, 382, 383
- [180] C. Pierre, D. Jiang, and S. Shaw.  
Nonlinear Normal Modes and their application in structural dynamics.  
*Mathematical Problems in Engineering*, Volume 2006:1–15, 2006.  
DOI: 10.1155/MPE/2006/10847.  
354
- [181] A. Placzek.  
*Construction de modèles d'ordre réduit non-linéaires basés sur la décomposition orthogonale propre pour l'aéroélasticité*.  
PhD thesis, Conservatoire National des Arts et Métiers, 2010.  
69, 72, 76, 113

## BIBLIOGRAPHY

---

- [182] C. Price.  
Sort eigenvectors and eigenvalues sortem.  
online, 2011.  
<http://www.mathworks.com/matlabcentral/fileexchange/18904-sort-eigenvectors-eigenvalues/content/sortem.m> - retrieved 04.05.2011.  
296
- [183] R. Rand, C. Pak, and A. Vakakis.  
Bifurcation of Nonlinear Normal Modes in a class of two degree of freedom systems.  
*Acta Mechanica*, 3:192–145, 1992.  
354
- [184] R. H. Rand.  
A direct method for Non-linear Normal Modes.  
*International Journal for Non-Linear Mechanics*, 9:363–368, 1974.  
45, 354, 368
- [185] R. V. Rao and V. J. Savsani.  
*Mechanical Design Optimization Using Advanced Optimization Techniques*.  
Springer, 2012.  
2
- [186] M. Rathinam and L. R. Petzold.  
A new look at Proper Orthogonal Decomposition.  
*SIAM Journal on Numerical Analysis*, 41:1893–1925, 2003.  
70
- [187] G. Recktenwald.  
readcoldata.m.  
online, 2009.  
<http://web.cecs.pdx.edu/~gerry/MATLAB/plotting/examples/readColData.m> - retrieved 25.06.2013.  
296
- [188] W. Rhee.  
*Linear and nonlinear model reduction in structural dynamics with application to model updating*.  
PhD thesis, Graduate Faculty of Texas Tech University, 2000.  
62, 67
- [189] S. A. Rizzi and A. Muravyov.  
Improved equivalent linearization implementations using nonlinear stiffness evaluation.  
Technical report, NASA/TM-2001-210838, 2001.  
177
- [190] R. M. Rosenberg.  
Normal modes of nonlinear dual-mode systems.  
*Journal of Applied Mechanics*, 27(2):268–263, 1960.  
3, 37, 45, 354, 366
- [191] R. M. Rosenberg.  
The normal modes of nonlinear n-degree-of-freedom systems.  
*Journal of Applied Mechanics*, pages 7–14, 1962.  
45, 354
- [192] R. M. Rosenberg.  
On nonlinear vibrations of systems with many degrees of freedom.

## BIBLIOGRAPHY

---

- Advances in Applied Mechanics*, 9:155–242, 1966.  
44, 45, 94, 95, 354, 368
- [193] T. Ross, V. Kreinovich, and C. Joslyn.  
Assessing the predictive accuracy of complex simulation models.  
In *Joint 9th IFSA World Congress and 20th NAFIPS International Conference*, volume 4, pages  
2008–2012, 2001.  
87
- [194] A. Russo.  
Gram-Schmidt process.  
online, 2008.  
<http://www.mathworks.com/matlabcentral/fileexchange/18843-gram-schmidt-process> - retrieved  
14.10.2011.  
296
- [195] D. Ryckelynck and D. M. Benziane.  
Multi-level a priori hyper-reduction of mechanical models involving internal variables.  
*Computer Methods in Applied Mechanics and Engineering*, 199(17-20):1134–1142, 2010.  
ISSN 0045-7825.  
DOI: 10.1016/j.cma.2009.12.003.  
75
- [196] D. Ryckelynck, L. Hermanns, F. Chinesta, and E. Alarcón.  
An efficient a priori model reduction for boundary element models.  
*Engineering Analysis with Boundary Elements*, 29(8):796–801, 2005.  
ISSN 0955-7997.  
DOI: 10.1016/j.enganabound.2005.04.003.  
40, 62, 75, 76
- [197] D. Ryckelynck.  
Réduction a priori de modèles thermomécaniques.  
*Comptes Rendus Mécanique*, 330(7):499–505, 2002.  
ISSN 1631-0721.  
DOI: 10.1016/S1631-0721(02)01487-0.  
40, 75, 366
- [198] R. Sampaio and C. Soize.  
Remarks on the efficiency of POD for model reduction in non-linear dynamics of continuous elastic  
systems.  
*International Journal for Numerical Methods in Engineering*, 72(1):22–45, 2007.  
ISSN 1097-0207.  
DOI: 10.1002/nme.1991.  
118, 374
- [199] K. Y. Sanliturk, D. J. Ewins, and A. B. Stanbridge.  
Underplatform dampers for turbine blades: theoretical modeling, analysis, and comparison with ex-  
perimental data.  
*Journal of Engineering for Gas Turbines and Power*, 123:919–929, 2001.  
2, 246
- [200] A. Sayma, M. Vahdati, and M. Imregun.  
An integrated nonlinear approach for turbomachinery forced response prediction. Part I: Formulation.  
*Journal of Fluids and Structures*, 14(1):87–101, 2000.

## BIBLIOGRAPHY

---

- ISSN 0889-9746.  
DOI: 10.1006/jfls.1999.0253.  
5, 246
- [201] R. Schmit and M. Glauser.  
Improvements in low dimensional tools for flow-structure interaction problems: Using Global POD.  
In *American Physical Society, Division of Fluid Dynamics 56th Annual Meeting*, November 2003.  
73, 199
- [202] W. Schnell, D. Gross, and W. Hauger.  
*Technische Mechanik 2*.  
Springer, 2002.  
231, 247
- [203] A. Sénéchal.  
*Réduction de vibrations de structure complexe par shunts piézoélectriques; Application aux turbo-machines*.  
PhD thesis, Conservatoire National des Arts et Métiers, 2011.  
174, 175, 176, 382
- [204] S. W. Shaw and C. Pierre.  
Non-linear Normal Modes and invariant manifolds.  
*Journal of Sound and Vibration*, 150(1):170–173, 1991.  
ISSN 0022-460X.  
DOI: 10.1016/0022-460X(91)90412-D.  
44, 354, 368
- [205] S. W. Shaw and C. Pierre.  
Normal modes of vibration for non-linear continuous systems.  
*Journal of Sound and Vibration*, 169(3):319–347, 1994.  
ISSN 0022-460X.  
DOI: 10.1006/jsvi.1994.1021.  
354
- [206] H. R. E. Siller.  
*Non-linear modal analysis methods for engineering structures*.  
PhD thesis, Imperial College London, 2004.  
229
- [207] L. Sirovich.  
Turbulence and the dynamics of coherent structures. Part I: Coherent structures.  
*Quarterly of Applied Mathematics*, 45:561–571, 1987.  
3, 40, 69, 71, 366
- [208] L. Sirovich.  
Turbulence and the dynamics of coherent structures. Part II symmetries and transformations.  
*Quarterly of Applied Mathematics*, 45:573–582, 1987.  
3
- [209] L. Sirovich.  
Turbulence and the dynamics of coherent structures. Part III: Dynamics and scaling.  
*Quarterly of Applied Mathematics*, 45:583–590, 1987.  
3

## BIBLIOGRAPHY

---

- [210] P. M. A. Slaats, J. de Jongh, and A. A. H. J. Sauren.  
Model reduction tools for nonlinear structural dynamics.  
*Computers & Structures*, 54(6):1155–1171, 1995.  
DOI: 10.1016/0045-7949(94)00389-K.  
4, 40, 65, 66, 87, 342, 343
- [211] J. C. Slater.  
A numerical method for determining Nonlinear Normal Modes.  
*Nonlinear Dynamics*, 10:19–30, 1996.  
ISSN 0924-090X.  
DOI: 10.1007/BF00114796.  
360
- [212] H. Sohn and K. H. Law.  
Extraction of Ritz vectors from vibration test data.  
*Mechanical Systems and Signal Processing*, 15(1):213–226, 2001.  
68
- [213] H. Späth.  
*Two dimensional spline interpolation algorithms*.  
Wellesley, 1995.  
196, 197
- [214] S. Spottswood and R. Allemang.  
Identification of nonlinear parameters for reduced order models.  
*Journal of Sound and Vibration*, 295(1-2):226–245, 2006.  
ISSN 0022-460X.  
DOI: 10.1016/j.jsv.2006.01.009.  
173, 382
- [215] A. Sternchüss, E. Balmès, P. Jean, and J.-P. Lombard.  
Reduction of multi-stage disk models: Application to an industrial rotor.  
*ASME Journal of Engineering for Gas Turbines and Power*, 131:98–111, 2009.  
261
- [216] A. Sternchüss.  
*Multi-level parametric reduced models of rotating bladed disk assemblies*.  
PhD thesis, École Centrale des Arts et Manufactures, 2009.  
261, 263, 265
- [217] A. Sternchüss and E. Balmès.  
On the reduction of quasi-cyclic disk models with variable rotation speeds.  
In *International Conference on Advanced Acoustics and Vibration Engineering (ISMA)*, pages 3925–  
3939, 2006.  
261
- [218] G. Strang.  
*Linear Algebra and Its Applications*.  
Thomson, 2nd edition, 2006.  
41, 67, 80, 148, 163, 172, 196, 203, 283, 335
- [219] E. Taciroglu.  
NewmarkIntegrator.  
online, 2003.  
<http://nees.ucla.edu/Assignments/NewmarkIntegrator.m> - retrieved 23.08.2013.  
59

## BIBLIOGRAPHY

---

- [220] J. A. Taylor and M. N. Glauser.  
Towards practical flow sensing and control via POD and LSE based low-dimensional tools.  
*Journal of Fluids Engineering*, 126(3):337–345, 2004.  
DOI: 10.1115/1.1760540.  
4, 73, 133, 199, 376
- [221] The Mathworks.  
*MATLAB R2013a Documentation*.  
The Mathworks, 6 2013.  
<http://www.mathworks.fr/fr/help/index.html> - retrieved 25.06.2013.  
259, 283
- [222] The Mathworks.  
*Code Vectorization Guide*.  
The Mathworks, 2011.  
<http://www.mathworks.com/support/tech-notes/1100/1109.html> - retrieved 18.02.2011.  
296
- [223] O. Thomas.  
Projection modale d'un problème éléments finis en non-linéaire géométrique.  
Technical report, Conservatoire National des Arts et Métiers, 2009.  
174, 382
- [224] O. Thomas, S. Nezamabadi, and J.-F. Deü.  
Calcul de vibrations non linéaires de micro/nano structures piézoélectriques stratifiées par modèles réduits avec correction quasi-statique.  
In *CSMA 2013 11e Colloque National en Calcul des Structures*, 2013.  
137, 379
- [225] C. Touzé, M. Vidrascu, and D. Chapelle.  
Calcul direct de la raideur non linéaire géométrique pour la réduction de modèles de coques en éléments finis.  
In *CSMA 2013 11e Colloque National en Calcul des Structures*, 2013.  
174, 382
- [226] D.-M. Tran.  
Multi-parameter aerodynamic modeling for aeroelastic coupling in turbomachinery.  
*Journal of Fluids and Structures*, 25:519–534, 2009.  
2
- [227] D.-M. Tran.  
Frequency and mode follow-up for evolutive structures.  
In *The Second International Conference on Dynamics, Vibration and Control (ICDVC-2006)*, 2006.  
23-26 August 2006, Beijing, China.  
267
- [228] D.-M. Tran.  
Component mode synthesis methods using partial interface modes: Application to tuned and mis-tuned structures with cyclic symmetry.  
*Computers & Structures*, 87:1141–1153, 2009.  
247
- [229] D.-M. Tran, C. Liauzun, and C. Labaste.  
Methods of fluid-structure coupling in frequency and time domains using linearized aerodynamics for turbomachinery.

## BIBLIOGRAPHY

---

- Journal of Fluids and Structures*, 17:1161–1180, 2003.  
172
- [230] M. Vahdati, A. I. Sayma, and M. Imregun.  
An integrated nonlinear approach for turbomachinery forced response prediction. Part II: Case studies.  
*Journal of Fluids and Structures*, 14(1):103–125, 2000.  
ISSN 0889-9746.  
DOI: 10.1006/jfls.1999.0254.  
5, 246
- [231] A. F. Vakakis.  
Non-linear Normal Modes (NNMs) and their applications in vibration theory: an overview.  
*Mechanical Systems and Signal Processing*, 11(1):3–22, 1997.  
ISSN 0888-3270.  
DOI: 10.1006/mssp.1996.9999.  
354, 355
- [232] A. Vakakis and R. Rand.  
Normal modes and global dynamics of a two-degree-of-freedom non-linear system II. High energies.  
*International Journal of Non-Linear Mechanics*, 27(5):875–888, 1992.  
ISSN 0020-7462.  
DOI: 10.1016/0020-7462(92)90041-5.  
354
- [233] A. Vakakis and R. Rand.  
Normal modes and global dynamics of a two-degree-of-freedom non-linear system I. Low energies.  
*International Journal of Non-Linear Mechanics*, 27(5):861–874, 1992.  
ISSN 0020-7462.  
DOI: 10.1016/0020-7462(92)90040-E.  
354, 356
- [234] J. van der Geest.  
Allcomb - all combinations.  
online, 2010.  
<http://www.mathworks.com/matlabcentral/fileexchange/10064> - retrieved 12.11.2012.  
296
- [235] N. Verdon.  
*Un système dynamique d'ordre réduit basé sur une approche APR-POD pour l'étude de l'interaction écoulement turbulent-particules.*  
PhD thesis, Université de la Rochelle, 2007.  
69, 75, 76
- [236] N. Verdon, C. Allery, D. Ryckelynck, and A. Hamdouni.  
An adaptive ROM approach for solving transfer equations.  
*Revue Européenne de Mécanique Numérique*, 15:589–605, 2006.  
76
- [237] F. Vetrano, C. L. Garrec, G. D. Mortchelewicz, and R. Ohayon.  
Assessment of strategies for interpolating POD based reduced order model and application to aeroelasticity.  
*ASD Journal*, 2(2):85–104, 2011.  
193

- [238] G. Vigo.  
*Méthodes de décomposition orthogonale aux valeurs propres appliquées aux écoulements intationnaires compressibles complexes.*  
PhD thesis, Université Paris IX, 2000.  
71, 73, 92, 193, 199, 200, 373
- [239] T. Warn, O. Bokhove, T. G. Shepherd, and G. K. Vallis.  
Rossby number expansions, slaving principles, and balance dynamics.  
*Quarterly Journal of the Royal Meteorological Society*, 121:723–739, 1995.  
264
- [240] E. L. Wilson.  
*Three-dimensional static and dynamic analysis of structures.*  
Computers and Structures, Inc., 2004.  
33
- [241] E. L. Wilson, M.-W. Yuan, and J. M. Dickens.  
Dynamic analysis by direct superposition of Ritz vectors.  
*Earthquake Engineering and Structural Dynamics*, 10(6):813–821, 1982.  
DOI: 10.1002/eqe.4290100606.  
3, 40, 61, 66, 366
- [242] W. L. Wood, M. Bossak, and O. C. Zienkiewicz.  
An alpha modification of Newmark’s method.  
*International Journal for Numerical Methods in Engineering*, 15(10):1562–1566, 1980.  
ISSN 1097-0207.  
DOI: 10.1002/nme.1620151011.  
55
- [243] O. Woodford.  
export\_fig.  
online, 2010.  
<http://www.mathworks.com/matlabcentral/fileexchange/23629-exportfig> - retrieved 11.03.2011.  
296
- [244] K. Worden and G. R. Tomlinson.  
*Nonlinearity in structural dynamics.*  
Institute of Physics Publishing, 2001.  
94
- [245] P. Wriggers.  
*Nonlinear Finite Element Methods.*  
Springer, 2008.  
12, 23
- [246] C. Yassouridis.  
Isogeometric modelling and simulation in railway technology.  
Master’s thesis, Technische Universität München, October 2010.  
99
- [247] O. Zienkiewicz, R. Taylor, and J. Zhu.  
*The Finite Element Method: Its Basis and Fundamentals.*  
McGraw-Hill, 2005.  
12, 13, 23, 27, 28, 31

## Appendix A

# Performing auxiliary studies to enhance the comparison of the reduced bases

---

This annex chapter bolsters the results of the studies in the chapter 4 and its sections 4.2.1 and 4.2.2. It contains certain practical considerations that are preceding the two comprehensive studies. These considerations are necessary in order to apply the reduction techniques to a numerical example because these techniques have been, until now, only regarded from the theoretical point of view. Additional considerations concerning specific sub-variants and oddities are strewn in as they arise from the results of the main studies. These considerations highlight several aspects or inquire deeper into certain directions.

## A.1 Performing additional work on reduced bases

The additional work that is performed on reduced bases covers a large spectrum of specific tasks that are required prior to the application of the reduced bases during the numerical studies in chapter 4. The additional work defines the basis.

The most important part of this section is the calibration of the Orthogonal Decomposition methods. The POD, the enhanced POD and the SOD require snapshots from a full order solution. It is determined how the choice of the snapshots influences the quality of the POD basis.

### A.1.1 Calibrating the Orthogonal Decomposition methods

The POD snapshots  $\tilde{u}(t_j)$  that are building the correlation matrix  $\tilde{U}$  in equation (3.128) are taken from solutions of the full order system. Naturally it is favourable to reduce the number of snapshots and with it the computational effort necessary to obtain them as far as possible. The period from which the snapshots for the Proper Orthogonal Decomposition reduction are taken is parameterised in the code and can be adjusted to explore the balance between precision and computation effort.

The parameters used for the configuration of the snapshot generation are

- $t_p$  the fraction of the overall simulated period  $t_e$ , which is actually computed in the course of the POD reduction procedure,
- $t_1$  the lower boundary of the period that is actually used to obtain the snapshots,
- $t_2$  the upper boundary of the period that is actually used to obtain the snapshots and
- $n_{\text{sna}}$  the number of snapshots taken from the period between  $t_1$  and  $t_2$ .

The algorithm computes the solution of the full order system between  $t_0$  and  $t_p \leq t_e$ . Then, a number of  $n_{\text{sna}}$  snapshots, equally repartitioned between  $t_1$  and  $t_2$  is selected. The instants  $t_p$  and  $t_2$  are identical. The time  $t_1$  is not necessarily equal to zero because it may be of interest to ignore the first time-steps of the solution as they do not necessarily contribute characteristic displacements to the basis.

The number of snapshots used for the creation of the covariance matrix is one of the primary concerns for this method and first discussed at the end of section 3.3.3.1. A non-empirical manner of determining the number of used snapshots could follow the propositions by Chinesta et al. [61], who argue that the decrease of the ordered eigenvalues of the correlation matrices indicates the smoothness of the evolution of the solution. This interrelation could be inverted to construct the correlation matrices in a way that they yield the steepest decrease of their eigenvalues by using the parameters from the listing above in an optimisation. This should result in taking the smoothest part of the time history as basis for the creation of the correlation matrices. But albeit this theoretical approach to this problem may yield optimised correlation bases it is much too specific for the problem at hand and not generic enough to cope with the four different test-cases. It is hence opted to address the assembly of the correlation matrices heuristically. This section summarises some of the findings during the ensuing determination of the local parameters above.

The initial set-up for this test is  $t_1 = 10$  and  $t_2 = t_p = 25$ , for an overall simulated time period of  $t_e = 100$ . The impact of a significant reduction of snapshots is studied by choosing  $n_{\text{sna}} = 15000$  for the first test run and  $n_{\text{sna}} = 50$  for the second. All other parameters are in line with the preliminary full study above. The figures A.1 and A.2 show the gain in reduction time from going from 1500 to only 50 snapshots. this loss is barely remarkable because only the eigenproblem in equation (3.129) is sped up. The figures A.3 and A.4 show the relative oscillation deviation for the solutions with the two different numbers of snapshots. The solution with  $n_{\text{sna}}$  delivers relative oscillation deviations on a slightly lower level than the solution with  $n_{\text{sna}}$ . A qualitative difference is barely remarkable. This is a good indicator for the excellent behaviour of the POD reduction method.

Further investigation into the time necessary for faithfully representing the full order system through a

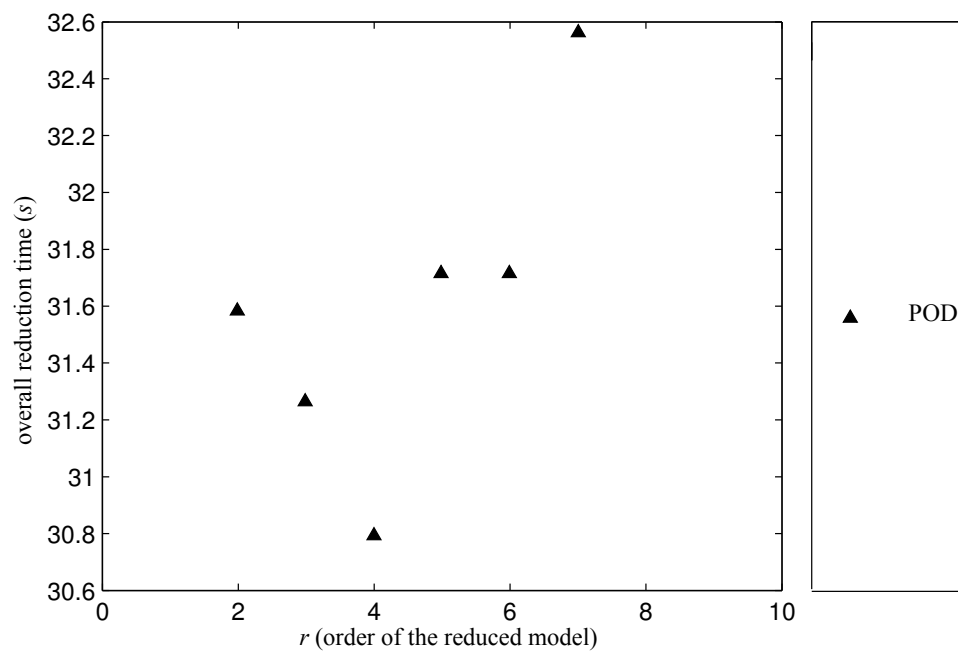


Figure A.1: The overall reduction time for  $n_{\text{sna}} = 1500$

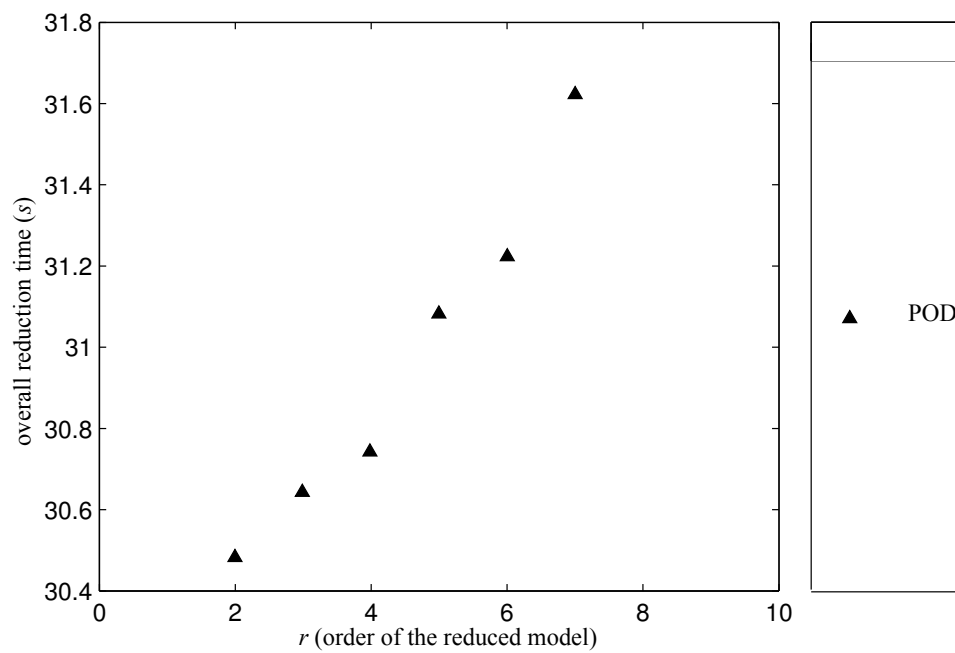


Figure A.2: The overall reduction time for  $n_{\text{sna}} = 50$

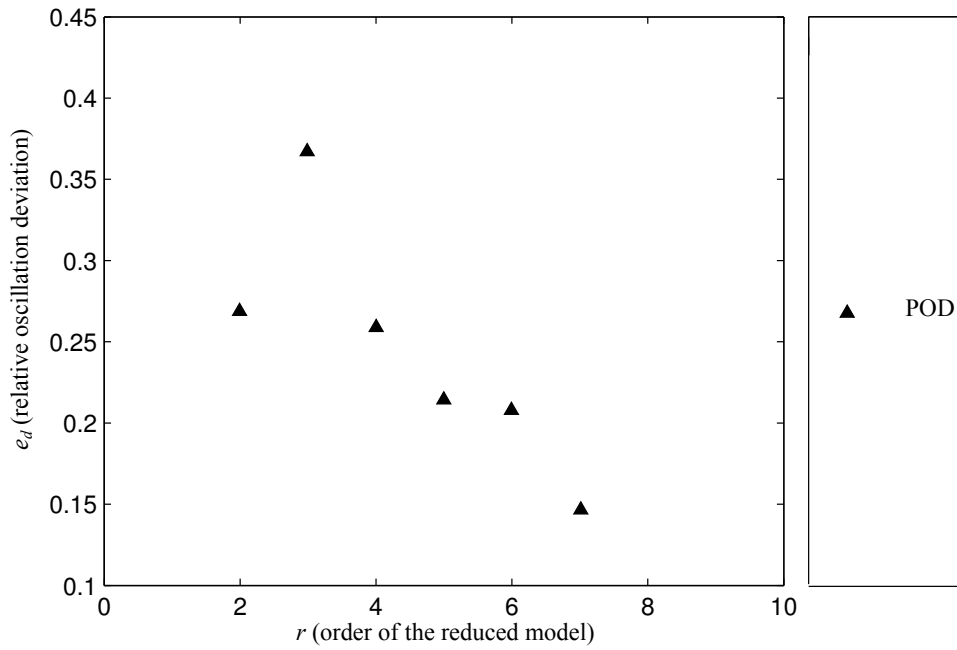


Figure A.3: The relative oscillation deviation  $n_{\text{sna}} = 1500$

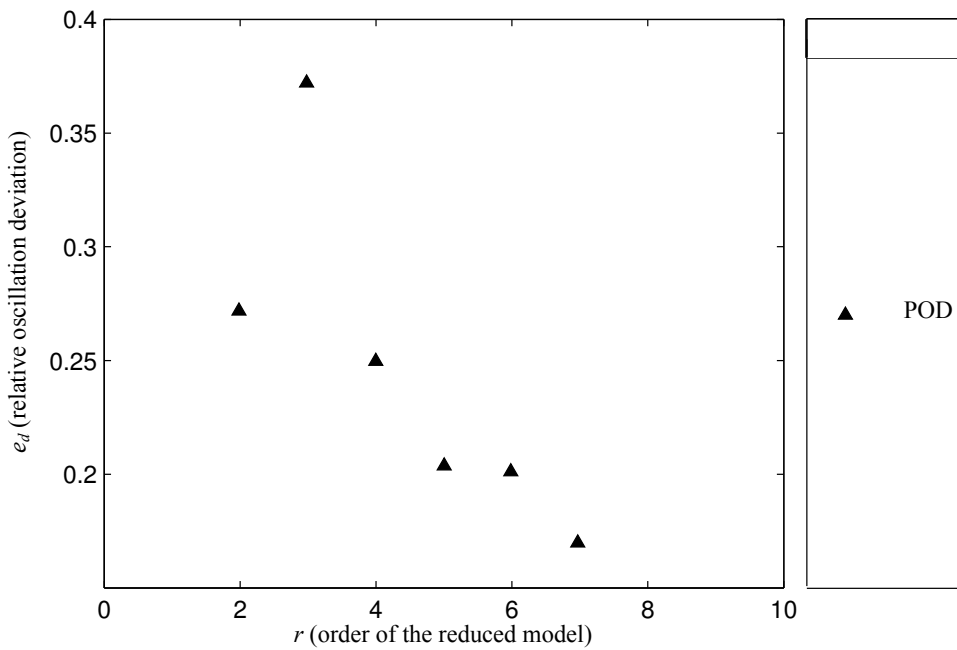


Figure A.4: The relative oscillation deviation  $n_{\text{sna}} = 50$

POD basis gives evidence that, at least for the current set-up, the time period between  $t_1$  and  $t_2$ , the one form which the snapshots are taken, has to cover a minimum of about one third of the overall simulated time, to obtain all necessary information from the snapshots and a meaningful reduction. Once this criterion is met, the actual number of snapshots can be reduced significantly, as proved above, in order to alleviate the computational burden of the eigenproblem.

It proved even more advantageous to place the window of the period between  $t_1$  and  $t_2$  on an especially interesting period, further inside the simulated period. This helps to extract the characteristics of the solution, which in turn optimises the POD-basis, but comes at the price that the time history of the full order system between  $t_0 = 0$  and  $t_1$  is calculated in vain.

Because of its availability and due to the fact that no contraindication concerning its use as the best basis of an Orthogonal Decomposition has been found, the entire raw reference solution is used as input for the two POD procedures as well as for the SOD procedure.

### A.1.2 Exploring similarities between the mode shapes of the LELSM-vectors and the LNM

The section 3.3.6.2 provides an overview of how the LELSM can be applied to systems with coupling nonlinearities and even the extension of this application to entirely nonlinear systems. The figure 4.5 suggests that, if this method is applied to the entirely nonlinear system from section 4.1.3.1.2, the resulting LELSM-vectors are closely resembling to the LNMs. This is confirmed in table A.1, where the MAC between the LNM and the LELSM-vectors for the first 10 modes is listed. The resulting first modes are traced in figure A.5 as an illustrative example. In fact, in this figure, the difference between the LNM and the LELSM-vector cannot be seen because the two vectors are virtually identical.

$r$	MAC
1	1.0000
2	1.0000
3	1.0000
4	1.0000
5	1.0000
6	1.0000
7	1.0000
8	0.9999
9	0.9997
10	0.9978

Table A.1: The modal assurance criterion for the different LELSM-vectors compared to the LNM for the entirely nonlinear system

It is strongly possible that is resemblance is due to the fact that the coupling cubic nonlinearities of the used entirely nonlinear system are all equal, i.e. the same  $k_{NL}$  for all coupling cubic nonlinearities. If such a system is reduced, there is obviously no interest in using the LELSM instead of the LNM to create a reduced basis because the two method result in the same basis yet with the LELSM requiring several solutions of eigenproblems due to its iterative nature. However, this is expected to change, when the coupling cubic nonlinearities are different.

To verify this a variation of the entirely nonlinear system is investigated, in which the nonlinear stiffnesses  $k_{NL}$  of the coupling cubic nonlinearities are distributed in a parabolic fashion of the degrees of freedom. This results in the coupling between the pairs of degrees of freedom 1 and 2 and  $n-1$  and  $n$  becoming purely linear. The maximum nonlinear coupling occurs between the degrees of freedom around  $\frac{n}{2}$ . If the LELSM

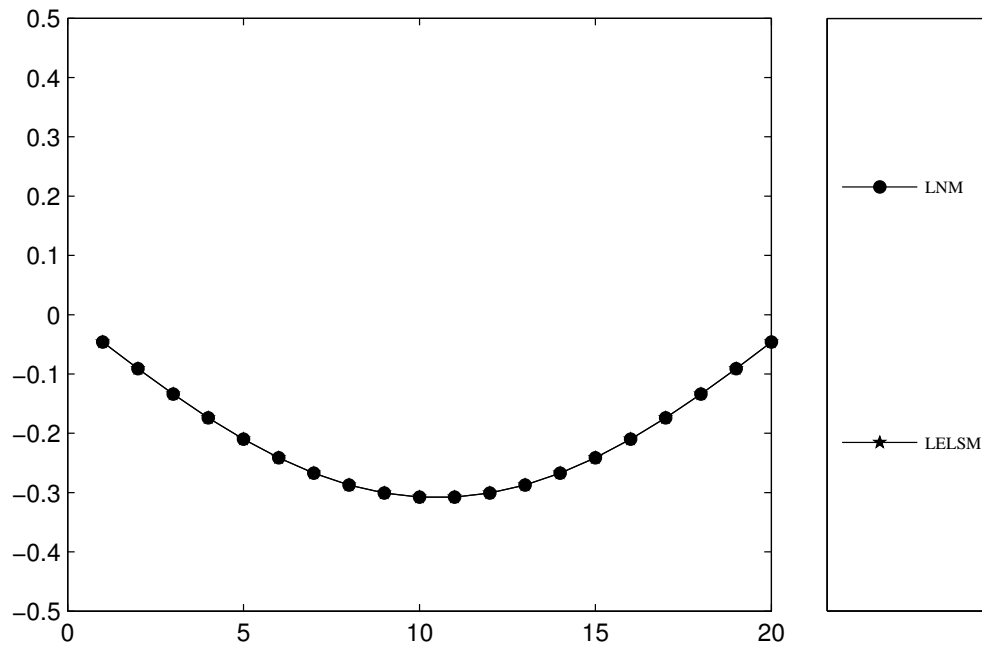


Figure A.5: The first LNM and the first LELSM-vector for the entirely nonlinear system

is applied to this specific system, the LELSM-vectors become different from the LNM. The resulting values of the MAC  $e_a$  are listed in table A.2 and the resulting first  $e$  modes are presented as an illustrative example in figure A.6. For higher modes, the differences are even more pronounced. Table A.2, if compared to table A.1, proves that the LELSM-vectors indeed become different from the LNM if the LELSM is applied to an entirely nonlinear system with unequally distributed coupling cubic nonlinearities.

The development is not pursued further at this point and it is not determined if the LELSM-vectors actually provide a better reduced basis for reducing the entirely nonlinear system with unequally distributed coupling cubic nonlinearities. This is because the results of the survey eventually show that it is not a specific reduced basis that is to be preferred, but that flaws in the reduction of a nonlinear system can be much more efficiently tackled on the level of solution procedures in section 5.1. Nevertheless, the results above warrant the application of the LELSM to entirely nonlinear systems, even if neither original intentions of the developers of this method nor its rather unfortunate application to the entirely nonlinear system with equally distributed coupling cubic nonlinearities at hand seem to herald this.

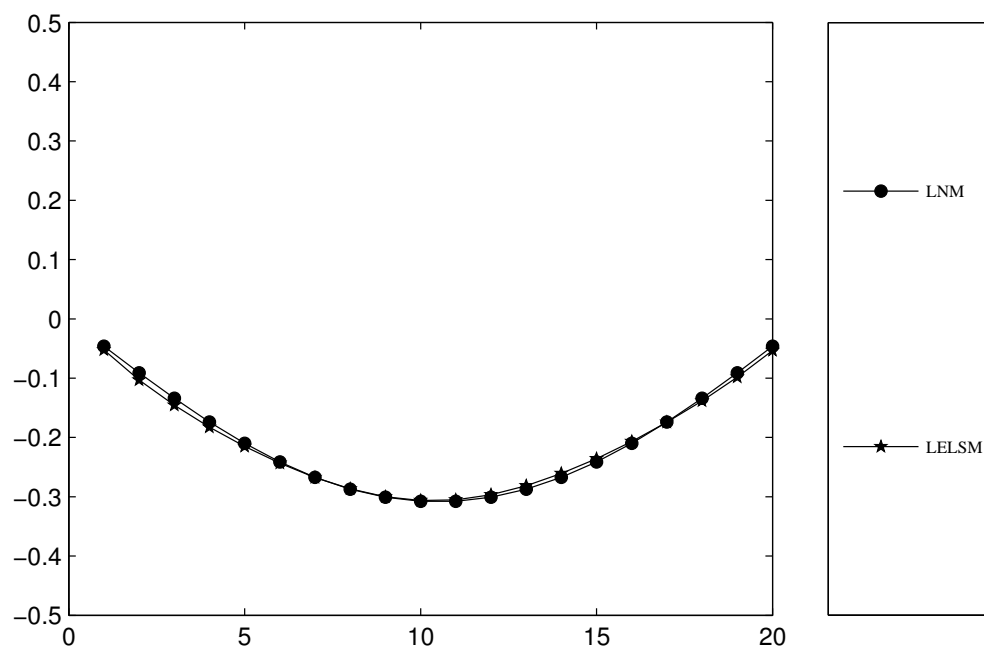


Figure A.6: The first LNM and the first LELSM-vector for an entirely nonlinear system with unequally distributed coupling cubic nonlinearities

$r$	MAC
1	0.9993
2	0.9681
3	0.8882
4	0.6873
5	0.5497
6	0.0501
7	0.3779
8	0.3282
9	0.0034
10	0.1165

Table A.2: The modal assurance criterion for the different LELSM-vectors compared to the LNM for an entirely nonlinear system with unequally distributed coupling cubic nonlinearities

## A.2 Performing long-running simulations to explore computational performance and algorithmic dissipation

The small academic test-cases in section 4.1.3 are too small to allow a meaningful study of the computational performance. The actual solution time is overshadowed by the computational overhead which is required to manage the simulations. These academic systems are of a very limited size and allow for analytical expressions of their nonlinear internal forces and their tangential stiffness matrix. This makes it impossible to derive meaningful information on the numerical performance of the tests.

The long-running simulations are conceived to circumvent this major shortcoming of the academic systems. The long-running solutions are performed over a much longer simulated time interval and with significantly enlarged variants of the nonlinear systems. These enlarged variants impose a considerable numerical effort for their solution. This makes it possible to neglect the numerical effort for automatising and managing the reduced solutions before the actual solution effort. The significant differences between the reduced solutions of the enlarged variants of the academic systems with different reduced bases are explored in the following.

### A.2.1 Exploring the computational performance

The findings of the sections of th chapter 4 allow to increasingly focus the search for the most adapted projection based reduction methods but they also reveal serious shortcomings of the employed exemplary test-case. The most important one is the dominance of the computational overhead which makes the gain in computation time due to the application of a reduction virtually inaccessible. The obvious remedy to this is a larger system whose actual solution effort dwarfs the computational overhead. In the process the insight gained during the studies above is used to further confine the application for which the reduction method has to be optimal. This is also a necessity because the large system in itself requires greater computational efforts and an accompanying reduction in the overall number of simulations in order to meet time constraints.

In a first step the large variants of the academic systems are defined. Then a comparative study, similar to the one in section 4.2.1 is conducted with these large systems with the aim of gaining insight into how well the different reduced bases perform. An additional focus is placed on the computational performance.

#### A.2.1.1 Defining the parameters of the large variants of the systems

The systems included in this study are the locally nonlinear system and the entirely nonlinear system. These two systems are based on equation (4.15) and their nonlinear terms are defined in equations (4.16) and (4.17), respectively.

However, they are differently parameterised than the small systems used in the preceding studies, which rely on the values defined in section 4.1.3.4. The new values describing the large systems are:

- $n$ , the order of the overall system is set to  $n = 500$ ,
- $j$ , the degree of freedom where the nonlinearity is localised is set to  $j = 400$ ,
- $p$ , the degree of freedom subjected to the external forcing is  $p = 100$ ,
- $\epsilon$ , the damping parameter, which defines the linear damping matrix  $C$ , is unchanged  $\epsilon = 0.04$ .

These two systems are subjected to an harmonic excitation, as it defined in equation (4.22), and to the impulse excitation, as it is defined in equation (4.24). The harmonic forcing is chosen in anticipation of the application of the reduction to turbomachinery, where the usual excitations are naturally ones that repeat itself after a given amount of time needed to complete a revolution. To provoke notable displacements in

the two Large Systems the amplitude  $\hat{f}_E$  has been increased tenfold and frequency  $\Omega$  reduced by the same factor:

- $\hat{f}_E$ , the amplitude of the external forcing is now  $\hat{f}_E = 30$  and
- $\Omega$ , the frequency of the external forcing is reduced to  $\Omega = 0.02289$ .

The choice of including only these nonlinear systems has been made because they resemble the actual application, which will include geometric nonlinearities, more closely than the entirely nonlinear system with its distributed nonlinearities. The same argumentation leads to the exclusion of the impulse excitation.

Another major factor is the extensive computational effort necessary for the solution of the full order and the reduced order systems alike, which is prohibitive to achieving the same completeness as during preceding studies. Closely linked with these computational consideration is the question of robustness, which poses extensive problems for most of the now excluded test-cases during the initial studies.

Finally it has to be mentioned that the two Smooth Orthogonal Decomposition variants are not included. They showed no promising behaviour in the preceding studies and are omitted with the aim of saving computational effort.

### A.2.1.2 Exploring the overall reduction time

The performance of a solution obtained from a reduced system implies a trade-off between the gain in computational speed and the ensuing loss of quality. This is discussed at length in section 4.1.2.

Compared to the study in section 4.2.1, which was executed on systems with  $n = 20$  and where the computational overhead, needed for initialising and managing the solution, rendered the consideration of the times needed for the solution of the reduced system in comparison to the time needed for the solution of the full order system practically senseless, now, with the large systems of  $n = 500$  degrees of freedom, the computational overhead becomes less influential and this in turn allows for a meaningful analysis of the Overall Reduction Time.

The Overall Reduction Time includes the time needed for the establishment of the respective basis and the time needed for the solution of the reduced system. It hence is a measure for the total effort needed to obtain a full order solution by means of a reduction procedure.

**A.2.1.2.1 Small variant** For comparison the plot of the Overall Reduction Time is made in figure A.7 for the initial, small variant of the same test-case.

The times for the different reduction methods have to be compared against the 5.18 s needed by the reference solution of the full order system. Against this information it is worth noting that evidently no significant gains in computation time can be expected with a system that comprises only  $n = 20$  degrees of freedom in total. This is due to the fact that the computational overhead, used e.g. for initialising the variables and calling the different routines, is much more important than the computational effort actually allocated to the solution of the reduced system. As this overhead remains constant disregarding the order  $r$  of the reduced system, the actual impact of the changing order of the reduced system is not very extended.

However, for all reduction methods there is a small, yet observable increase in overall reduction time as the order  $r$  of the reduced system is increased. And for all reduction methods, except the A Priori Reduction, the overall reduction time evolves in the same order of magnitude as the reference solution of the full order system. With slight gains if  $r$  is below a value of around 5, which corresponds to one fourth of the size of the full order system, and a continuous increase as the order of the reduced system increases. The differences between the different methods are barely distinguishable, only the two Smooth Orthogonal Decomposition variants offer noticeable gains in overall time in the order of about 10% up to the point at which the reduced system has about the half the size of the full order system, i.e.  $r = 10$ .

The A Priori Reduction method distinguishes itself from the other reduction methods and the rather

## A.2. PERFORMING LONG-RUNNING SIMULATIONS TO EXPLORE COMPUTATIONAL PERFORMANCE AND ALGORITHMIC DISSIPATION

foreseeable evolution of their overall reduction times by requiring considerably more time than the reference solution, about as twice as much. And also by a nearly twofold increase in overall reduction time while passing from  $r = 10$  to  $r = 12$ , against which the overall reduction times below and above these values appear nearly constant. Due to the special procedure, which is necessary to construct the APR reduced basis, requiring several consecutive solutions of lower order reduced systems, the considerably more overall reduction time for this method can be easily explained. For now it is however unclear which factor causes the step in overall time from  $r = 10$  to  $r = 12$ .

Foremost, the results obtained from the figure A.7, showing the overall reduction time for the treated test-case, indicate that a detailed study of the time needed for construction of the reduced basis and solving the reduced system and the ration between this time and the time used for the solution of the reference solution is not suited for yielding informative results. Because of the numerical overhead and a reduction that does not encompass the vector of internal forces, thus introducing additional transformation effort into the solution of the reduced system, the overall reduction time evolves around the time needed for establishing the reference solution. This matter is particularly compounded by the already relatively small size of the full order system. The investigation into the Overall Reduction Time is hence dropped from further studies in this chapter.

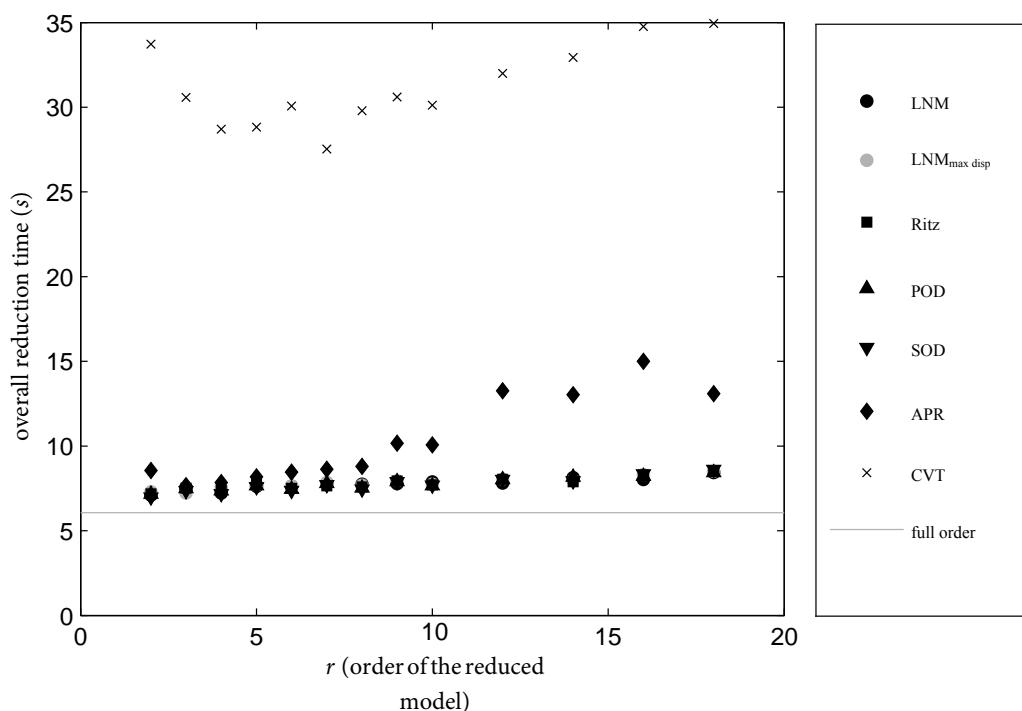


Figure A.7: The overall reduction time of the small variant of the entirely nonlinear system under harmonic excitation

**A.2.1.2.2 Large variant** The figure A.8 shows the overall reduction time for the large variant of the entirely nonlinear system and different reduction methods as a function of the order  $r$  of the reduced model. For the most methods the Overall Reduction time does not extend beyond about 4000 s, which has to be compared to the solution of the full order system, which requires just shy of 26000 s.

The first observations to be made are that, at large scale, there are two branches. One is made by the A Priori Reduction alone and skyrockets with considerable increments in overall reduction time, while the other branch is formed by the remaining methods included in this study, i.e. the classic Linear Normal

Modes , the LNM obtained at maximum displacement, the Ritz-vectors, the classic Proper Orthogonal Decomposition and the enriched Proper Orthogonal Decomposition. The most noticeable feature of this branch is that it is basically linear. In fact it suggests a proportional increase in the solution time of the reduced system, except for a noticeable leap between  $r = 5$  and  $r = 6$ . The proportional increase is however expected to change if the order  $r$  of the reduced system would be increased even further because the involved matrix operations' calculation requirements scale with higher exponents of their size.

This conclusion can be drawn because, for all reduction methods except the APR, the establishment of the basis is virtually instantaneous if compared to the time needed for the actual solution. Only the procedure used for establishing the basis of the A Priori Reduction takes significantly more time and here the ratio of the actual solution time and the overall reduction time can drop as low as 0.1. Which means that about 99 % of the Overall Reduction Time is allocated to the construction of the basis. This explains the considerable difference between the A Priori Reduction and the other methods.

Among the remaining methods in the lower branch the classic Linear Normal Modes stand apart, by having a slightly steeper increase in the Overall Reduction Time than the other methods in this branch. No evident explanation as to the why of this behaviour can be given.

Apart from this particularity there is no observable persistent difference between the remaining methods of the lower branch, thus ruling out a clear favourite. But this in turn means that all these methods offer remarkable gains in computational speed because even at  $r = 87$ , which corresponds to reduced systems with about one fifth of the size of the full order system, the Overall Reduction Time does not amount to more than about 15 % of the computation time of the full order system. For smaller reduced system is gain is even more pronounced.

In conclusion these observations can be made for the large variant of the systems, whose plots of the overall reduction time do look alike with respect to these points.

The over proportionality is already explained above, also for the remaining methods, by taking into account the number of elementary calculus operations per matrix operation, which scales nonlinearly with the size of the matrix, see e.g. Strang [218] for details. The steps and plateaus for the first system can however not be explained easily.

The most important result of this study is that it confirms and bolsters the findings of its sister study, which was conducted on the small system. Even more, which, during the first study on the small system, remained, to a certain extent, guesswork, is now clearly visible as it is amplified and explicitly exposed by the large systems.

This amplification helps foremost the understanding of the differences in quality of the bases obtained by the different methods. The most potent ones remain the POD variants and the classic LNM and modifying the, which leads to the LNM at maximum displacements, does not ameliorate this method's performance. The bad performance of the APR method remains.

Furthermore the insight into the computational gains is very valuable as it shows results that are no longer rendered insignificant by a dominating computational overhead and which clearly justify the usefulness of a reduction, even though the exemplarily used system, with its  $n = 500$  degrees of freedom, is far from what is to be expected during an application on a real-world application.

### A.2.1.3 Relative Root Mean Square Error

The figure A.10 plots the R2MSE  $e_r$ , originally defined in equation 4.5, for the large variant of the entirely nonlinear system. The plot of the relative root mean square error has again as its major property the distinction between the APR and the other reduction methods. This striking feature has been anticipated throughout the beforehand studies and reveals that the A Priori Reduction method fails to create a basis, which succeeds in recreating the solution to these specific systems.

To have comparable relative sizes of the full order and the reduced order systems for the studies performed

A.2. PERFORMING LONG-RUNNING SIMULATIONS TO EXPLORE COMPUTATIONAL PERFORMANCE AND ALGORITHMIC DISSIPATION

---

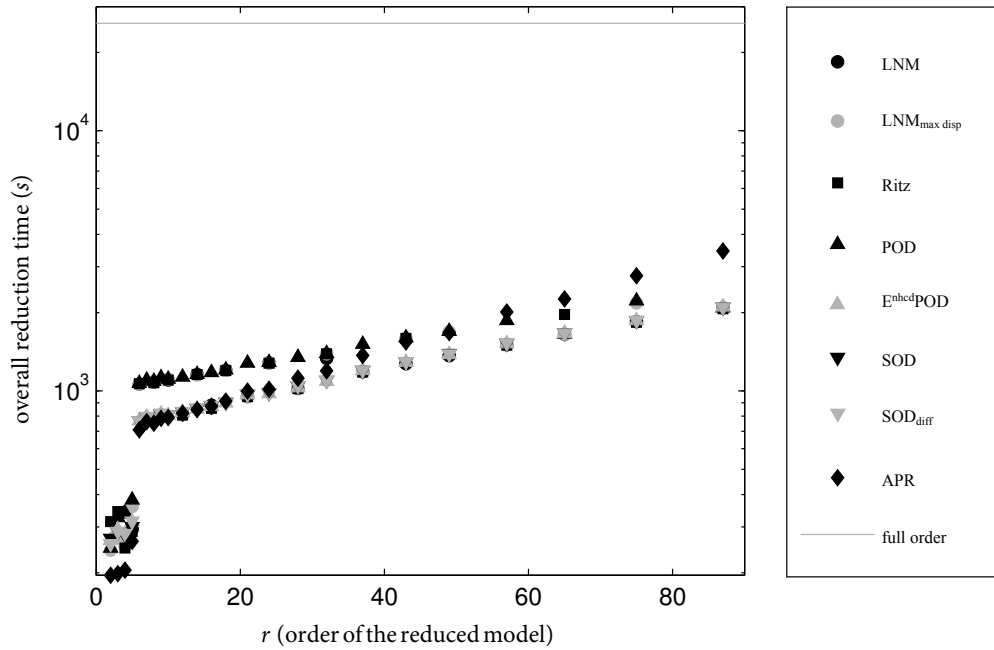


Figure A.8: The overall reduction time of the large variant of the entirely nonlinear system under harmonic excitation

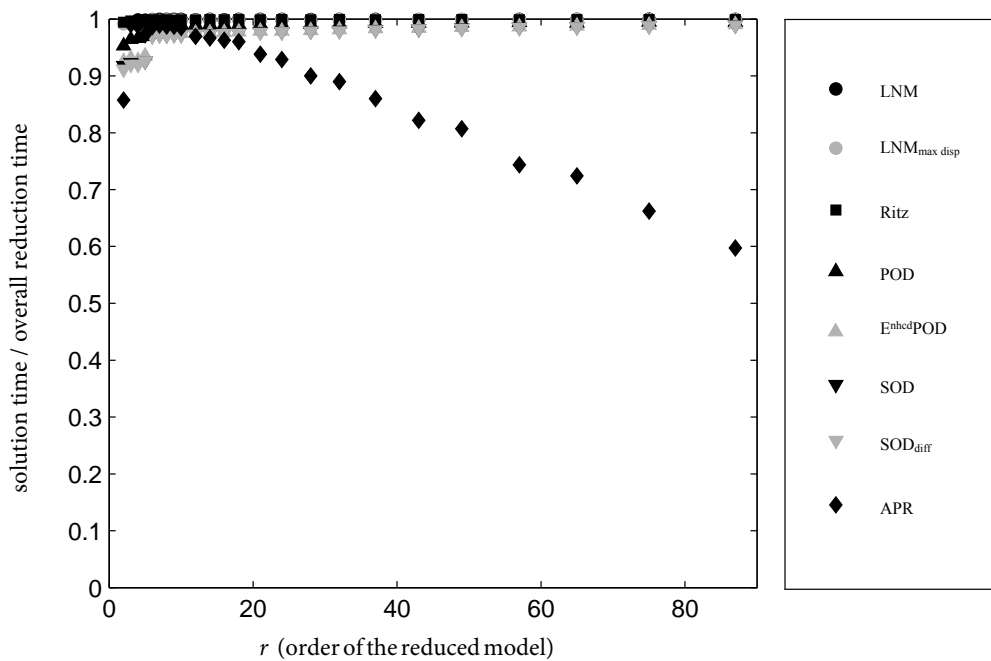


Figure A.9: The time ratio for the large variant of the entirely nonlinear system under harmonic excitation

on the small and on the large systems, regarding the results from  $r = 50$  onwards seems appropriate. This corresponds to a size of the reduced system of 10 % of the size of the full order system with  $n = 500$ , as it was practised with  $r = 2$  and  $n = 20$  in the studies on small systems. However, now the values below  $r = 50$  are certainly not dropped from the analysis, they are simply a little less established, yet still provide valuable information.

For all three systems the plots of the relative root mean square error are not well established below  $r = 30$ , with many methods' error metric converging more or less quickly on the respective branches. Above  $r = 30$  the different methods are easily distinguishable and well ordered.

For the first system the ranking of the reduction methods with increasing quality has the LNMs at maximum displacements at the beginning, with nearly constant and unacceptably high errors. It is followed by the APR, which also struggles considerably to yield good results, and then the Ritz-vectors, which still have a considerable error of more than 0.4. With errors between 0.15 and 0.05 the classic LNM and the two POD variants occupy a second branch of the plot, which has the two POD variants slightly below the LNMs. The difference between the two former is however not noticeable.

In the plot for the second system, the same order is repeated, with the exception that now the LNMs at maximum displacement perform largely on par with their classic counterparts. This time the two LNM variants, the Ritz-vectors and the two POD variants form a dense band, which slowly converges from 0.8 at  $r = 30$  to 0.3 at  $r = 87$ . Within this band a clear order can not positively be distinguished, but the Ritz-vectors are constantly placed towards the upper edge, while the POD variants tend to lower values. At the same time the APR results remain largely constant, which is consistent with an observation made on the small system. For the small system the APR errors remains constant for a considerable number of reduced systems until it finally started to converge on the correct solution. So again its results are expected to converge beyond  $r = 87$ , which is currently the limit of the present study.

For the third system the LNMs at maximum displacements and the APR modes, produce both relatively constant error slightly above 0.6, while the POD variants remain between 0.4 and 0.3. The Ritz-vectors and the classic LNM perform the transition between these two strings between  $r = 30$  and  $r = 87$ .

In conclusion it can be said that the orders of the reductions' qualities is preserved when going from a small to a large system. With the advantage that the large systems expose the difference between the different methods even further.

#### A.2.1.4 Comparing the reduced basis on the test-cases with the large variants of the systems

The table A.3 shows entire evaluation of the bases' performance as they are obtained with the large variants of the academic systems. It matches the table 4.2 in section 4.2.1.4 that condenses the evaluation of the bases tested on the small variants of the systems. The table for the large variants of the nonlinear systems below is obtained in exactly the same way as the table 4.2.

The two tables are largely identical. Not all reduced bases are used to reduce the large variants of the nonlinear systems due to constraints of the computers' availability. The results that are obtained with the large variants of the nonlinear system confirm the results from table 4.2.

This allows the conclusion that the results of the academic test-cases may not change with the size of the system.

A.2. PERFORMING LONG-RUNNING SIMULATIONS TO EXPLORE COMPUTATIONAL PERFORMANCE AND ALGORITHMIC DISSIPATION

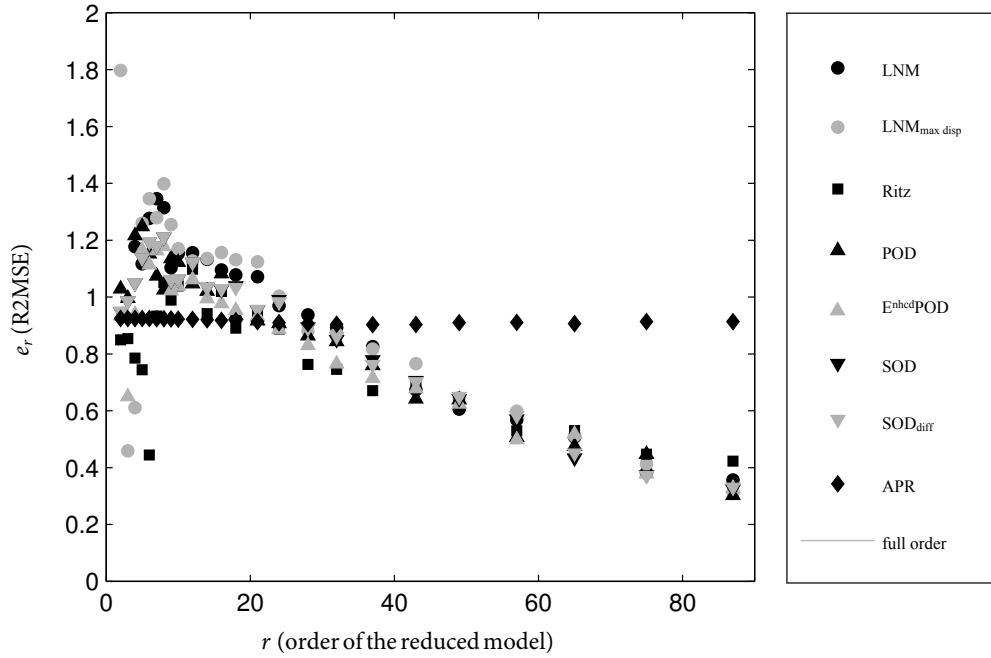


Figure A.10: The R2MSE of the large variant of the entirely nonlinear system under harmonic excitation

	$f_{E,har}$		$f_{E,imp}$	
	$g_{loc}$	$g_{ent}$	$g_{loc}$	$g_{ent}$
LNM	-	+	++	++
LNM <sub>max dsp</sub>	-	-	++	++
Ritz	+	+	+	-
POD	++	++	++	++
E <sup>nhcd</sup> POD	++	+	+	+
SOD	++	++	++	++
APR	-	-	--	--
CVT	+	-	--	--
LELSM	-	n.a.	++	n.a.

Table A.3: The comparison of the reduced bases for the test-cases with the large variants of the systems

## A.2.2 Exploring the algorithmic dissipation

The used nonlinear Newmark scheme allows to adjust algorithmic damping via the two parameters  $\gamma$  and  $\beta$ , which define the amount of forward or backward weighting, in equation (3.59). For these parameters proven standard values exist, it is however advisable to verify their possible influence in the case of a nonlinear study.

Currently the values for  $\gamma$  and  $\beta$  are set to  $\frac{1}{2}$  and  $\frac{1}{4}$ , respectively. These correspond to the constant average acceleration formulation of the nonlinear Newmark scheme (Nickell [161]). In order to find out if and when, how, these values influence the solution, long-running simulations have been executed. A theoretical overview over possible values for  $\beta$  and  $\gamma$ , together with their implications with respect to the stability of the solution, is given in the table 3.1.

The result is that an increased algorithmic dissipation has no qualitative influence on the results in terms of the employed error metrics. All reduction methods perform only marginally better if long running simulations at  $t_e = 700$  are compared at  $\gamma = 0.5$  and  $\beta = 0.25$  and at  $\gamma = 0.6$  and  $\beta = 0.4$  and no other parameters are changed. There is however considerable energy fluctuation to be observed for the chosen parameterisation of the nonlinear Newmark algorithm.

The time-step  $\Delta t$  itself can be changed without influencing the performance of the reduction method. However, during all solution activity, the condition  $\Delta t \leq \frac{2\pi}{\omega_{max}}$ , with  $\omega_{max}$  as the highest eigenfrequency of the underlying linear system, as given by Bathe [22], is strictly respected.

If damping terms are included in the formulation of the full order system, i.e.  $\mathbf{g} = \mathbf{g}(\mathbf{u}, \dot{\mathbf{u}})$ , these have to be recreated accurately by the reduced order system. This evidence is however difficult to proof in particular in the context of a limited scope numerical analysis.

This section reviews to approaches for gauging the damping of a transient solution and demonstrates that these are not very useful for the current setting. To obtain estimations for an equivalent linear damping coefficient  $c$  corresponding to the formulation of the non-linear forces vector  $\mathbf{g}$  for a single degree of freedom  $u_i$  of a large system there are two approaches: one working on the time history of  $u_i$  and one working on its spectrum. These two are applied to the single degree of freedom  $u_i$  albeit they are originally defined for a linear single degree of freedom system. Accordingly their usefulness has to be regarded as more than questionable.

### A.2.2.1 Time history method

The time history method would take an explicit portion of the time history of the displacements and try to find a formulation of the type

$$\hat{u}_i^{(t_1 \rightarrow t_2)} = \hat{u}_i e^{\frac{c}{2\sqrt{m_i k_i}} \sqrt{\frac{k_i}{m_i}} t} \quad (\text{A.1})$$

as an envelope of the oscillations of  $u_i$  by fitting the parameters  $\hat{u}_i$  and  $c$  numerically in order to obtain information on the equivalent linear damping coefficient  $c$ .

The times  $t_1$  and  $t_2$  have to be carefully placed between the initial transient phase, where little useful information can be gained from the time history, and the final stable phase, where an equilibrium between energy feeding from the external forcing and energy dissipation through the damping is established and  $u_i$  oscillates with a constant amplitude.

### A.2.2.2 Spectrum method

The spectrum method relies on the Fourier transformation of the time history of  $u_i$  and determines the *broadness* of a portion of the spectrum around the resonance-frequency  $\omega_{0i}$  to obtain an equivalent linear damping factor  $c$ . Its representation below follows Lalanne et al. [129].

Starting from the resonance-frequency  $\omega_{0i}$  with the associated amplitude  $\hat{u}_{0i}$  the two surrounding amplitudes  $\omega_{1i}$  and  $\omega_{2i}$  are determined with:

$$\hat{u}_{1i} = \hat{u}_{2i} = \frac{1}{2}\hat{u}_{0i} \quad (\text{A.2})$$

$$\omega_{1i} < \omega_{0i} < \omega_{2i}. \quad (\text{A.3})$$

The equivalent linear damping factor  $c$  is then obtained via an energy consideration

$$c = \frac{\omega_{2i} - \omega_{1i}}{\omega_{0i}} \sqrt{k_i m_i}. \quad (\text{A.4})$$

It is obvious that the two equations (A.1) and (A.4) reside on many hypotheses that can not be met by a multi-degree of freedom non-linear system and it was shown in their actual application that they deliver no useful information. It is believed that this is, in addition to their intrinsic shortcomings, due to the facts that

- the distances between the solution obtained from the full order system and the solution obtained from the reduced order system may escalate long before the damping can have a measurable influence on the system's response and
- the damping is mainly introduced for numerical reasons and as such too small to be correctly resolved by the two approximation methods presented above.

As such the two approaches are only presented for the sake of completeness, but without being actually applied on the solutions in order to obtain information on its stability and damping.

## A.3 Solving with a constant tangent stiffness matrix

The aim of this study is to investigate the possible gains in computational effort and to assess the resulting increase in error, resulting from not constantly updating the tangent stiffness matrix, which is necessary to execute a nonlinear Newmark scheme.

Keeping the tangent stiffness matrix  $\bar{\mathbf{K}}$  can be done in two ways. It can be established once, prior to the solution and be kept constant for the entire procedure in much the same way as it is done with the reduced bases in the preceding studies. This approach is however certain to produce convergence problems or, at least, would require a absurdly small time-step.

To remedy these obvious problems, the second approach has the tangent stiffness matrix calculated once per time-step and kept constant only during the inner iteration of the nonlinear Newmark scheme, which is described in equations (3.53) to (3.65).

But the results show that this approach has no impact. Neither on the quality nor on the performance of the solutions.

## Appendix B

# Testing LNM and Ritz-vectors with Second Order Terms

---

The second order terms are introduced for the Linear Normal Modes and the Ritz-vectors in sections 3.3.1.3 and 3.3.2.2, respectively. The SOT are not included in the numerical studies in chapter 4. The decision to exclude them is made on the basis of the numerical results that are obtained with the same test-cases as the ones used for the numerical studies. These results of the application of the SOT are presented and discussed in this annex chapter.

## B.1 Recalling the main methods

Two of the methods for the creation of the reduced basis that are described in section 3.3 are

- the classic Linear Normal Modes, which are the eigenvectors of the eigenproblem of the underlying linear system obtained at the equilibrium configuration,
- the classic Ritz-vectors.

For both there is an approach for the introduction of Second Order Terms (SOT) available. Second Order Terms are combined partial derivatives of the column vectors of the basis with respect to generalised coordinates. They are introduced to include the sensitivities of the column vectors of the reduced basis with respect to the generalised coordinates in the reduced basis.

The approach of the Second Order Terms applied to the various cases, in much the same way as during the initial comparison of the reduction methods, described in section 4.2.1. The parameters defining the systems, the excitations and the time solution are not altered, so that the results obtained in this study of the Second Order Terms can be directly compared to the results from the comparison. Only the two other Linear Normal Mode variants are included in the overview, as they the methods which are related the closest to the combination of classic Linear Normal Modes and Second Order Terms.

### B.1.1 Linear Normal Modes with Second Order Terms

If the Linear Normal Modes are enriched with second order terms (SOT), a certain number  $r_{\text{SOT}}$  of vectors  $\bar{\phi}$  is added as columns to the basis  $\Phi$  of  $r_{\text{LNM}}$  Linear Normal Modes from equation (3.114), yielding a reduced model of order  $r = r_{\text{LNM}} + r_{\text{SOT}}$ .

Following Slaats et al. [210], second order terms<sup>1</sup>  $\bar{\phi}_{i,k}$  are defined as the combined partial derivatives of Linear Normal Modes  $\phi_i$  with respect to reduced displacements  $q_k$

$$\bar{\phi}_{i,k} = \left( \frac{\partial \phi_k}{\partial q_i} + \frac{\partial \phi_i}{\partial q_k} \right) \quad i \in \{1, \dots, r_{\text{SOT}}\}, \quad (\text{B.1})$$

giving

$$\bar{\Phi} = [\phi_1, \dots, \phi_{r_{\text{LNM}}}, \bar{\phi}_{1,1}, \bar{\phi}_{2,2}, \dots, \bar{\phi}_{r_{\text{SOT}}, r_{\text{SOT}}}], \quad (\text{B.2})$$

for the entire reduction base and under the assumption of  $i = k$ , which is by no means a necessity.

In fact, the proper selection of  $r_{\text{SOT}}$  and of the values for  $i$  and  $k$  for the reduced displacements would certainly justify a dedicated study in its own right. Within the limits of the present study the approach has been taken to choose equal numbers for the contributing second order terms, i.e.  $\bar{\phi}_{i,i}$ , and for  $r_{\text{SOT}}$  to be not more than half the overall size  $r$  of the reduced system, i.e.  $r_{\text{SOT}} \leq \frac{r}{2}$ . Slaats et al. [210] compare several combinations of linear normal modes and second order terms and find only barely noticeable differences for different combinations of  $i$  and  $k$ . They also investigate the inclusion of static modes, i.e. characteristic displacements, an approach which is pursued in this study for the enriched Proper Orthogonal Decomposition below.

The usual approach for obtaining the second order terms is by altering the generalised coordinate  $q_k$  by a  $\Delta q_k$ , introducing this into the displacements  $\mathbf{u}_k = \Phi \mathbf{q} + \phi_k \Delta q_k$  and using this new displacement for a new tangent stiffness matrix  $\mathbf{K}_k = \frac{\partial \mathbf{g}(\mathbf{u})}{\partial \mathbf{u}} \Big|_{\mathbf{u}_k}$  in order to obtain a new set of eigenvector  $\Phi_k$  from the

<sup>1</sup>the index  $_{,k}$  does not imply a partial derivation with respect to  $k$ . Neither do the repeated indices  $i$  and  $k$  in equation (3.116) imply a summation as stipulated by the Einstein notation.

eigenproblem in equation (3.113). The  $i$ -th column of  $\Phi_k$  is then used with the  $i$ -th column of the original LNM  $\Phi$  in a finite difference divided by  $\Delta q_k$  to obtain the second order term  $\bar{\phi}_{i,k}$  numerically.

An alternative approach for constructing the second order terms  $\bar{\phi}_{i,k}$  relies on deriving equation (3.113) with respect to the generalised coordinate  $q_k$  and is presented for the second order terms of Ritz-vectors below.

### B.1.2 Ritz-vectors with Second Order Terms

Idelsohn and Cardona [102] and Chang and Engblom [57], among others, applied the concept of adding second order terms to the reduced basis, as it is introduced in section B.1.1 for the LNM, to Ritz-vectors. This activity enjoyed some attention and spawned a certain interest at that time, yet, it is now rarely to be found in publications.

Finding the derivative  $\bar{\phi}_{i,k}$  as per equation (B.1) of a Ritz vector could be achieved by applying the direct numerical way via a finite difference as taken for the LNM. This would lead to establishing the Ritz-vectors with different tangent stiffness matrices following the entire procedure formalised in equations (3.119) to (3.125) and subjecting the resulting Ritz-vectors to a finite difference over  $\Delta q_k$ , in order to approximate the derivation.

However, as shown later, an alternative approach, originally developed for the second order terms of LNM, yields better results. It relies on deriving equation (3.113) directly with respect to the generalised coordinate  $q_k$ , which is implicitly contained in the stiffness matrix  $\mathbf{K}$  and neglecting the inertial terms, ultimately leading to

$$\frac{\partial \phi_i}{\partial q_k} = -\mathbf{K}^{-1} \frac{\Delta \mathbf{K}}{\Delta q_k} \phi_i. \quad (\text{B.3})$$

This equation (B.3) can be readily applied to the already established Ritz-vectors, albeit it was originally conceived for LNM and applied successfully to several simple systems by e.g. Idelsohn and Cardona [102] and Chang and Engblom [57].

The difference between the numerical finite difference and the analytic approach in equation (B.3) is believed to be due to the requirement for neglecting the inertial term. This condition is mostly applicable to real systems, but for the academic systems studied below, the mass matrix  $\mathbf{M}$  and the stiffness matrix  $\mathbf{K}$  are of equal order.

## B.2 Choice of modes to be included

The choice of consecutive indices  $i$  and  $k$  is, for the moment, to be considered as arbitrary as every other because, as stated above, no experience or insight as to which pairs of  $\{i, k\}$  are best is available. Slaats et al. [210] report great gains in precision through the integration of Second Order Terms with only marginal or even barely distinguishable differences between the actual pairings of the  $i$  and  $k$ . Their results are thus heralding further investigation because the combination of which mode shape derived with respect to which reduced coordinate could be expected to have a greater influence.

In fact, the proper selection of  $r_{\text{SOT}}$  and of the values for  $i$  and  $k$  for the reduced displacements would certainly justify a dedicated study in its own right. Within the limits of the present study the approach has been taken to choose equal numbers for the contributing second order terms, i.e.  $\bar{\phi}_{i,i}$ , and for  $r_{\text{SOT}}$  to be not more than half the overall size  $r$  of the reduced system, i.e.  $r_{\text{SOT}} \leq \frac{r}{2}$ . Slaats et al. [210] compare several combinations of linear normal modes and second order terms and find only barely noticeable differences for different combinations of  $i$  and  $k$ . They also investigate the inclusion of static modes, i.e. characteristic dis-

placements, an approach which is pursued in this study for the enriched Proper Orthogonal Decomposition below.

It has been chosen to demonstrate the possibility of the Second Order Terms to contribute to a modal decomposition in the manner described beforehand because this manner offers an organised framework to select the mode shapes and the reduced coordinates to be used. A dedicated study and optimisation of the  $\{i, k\}$  is certain to yield better results, but far beyond the scope of this study.

### B.3 Applying the SOT

The approach of the SOT  $\bar{\Phi}_{i,k}$  is applied to the four test cases. The parameters defining the systems, the excitations and the time solution are not altered. The comparison is based on the score. The two LNM variants and the Ritz-vectors are included in the overview, because they are the two methods that provide the basis for SOT.

The figure B.2 shows the results for the locally non-linear system under harmonic excitation. The indicated overall order  $r$  of the reduced system is the sum of the indicated number  $r_{\text{SOT}}$  of SOT and  $r - r_{\text{SOT}}$  vectors stemming from either of the original basis.

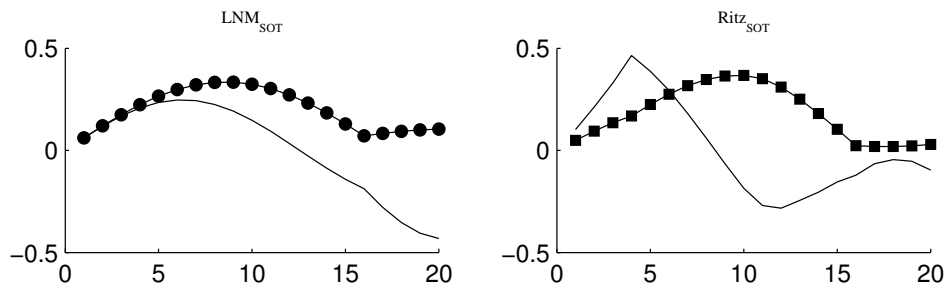


Figure B.1: The first two SOT of the different reduced bases for the locally non-linear system under harmonic excitation

The first two SOT based on the LNM are shown in figure B.1. They incorporate the features of the locally non-linear system and can thus, as the results show, actually improve the performance of a pure LNM basis. The inclusion of more SOT does not further improve upon this encouraging result when the overall size  $r$  of the system allows for that many SOT to be included. This becomes obvious from the LNM with  $r_{\text{SOT}} = 3$ .

The SOT from the Ritz-vectors do severely lessen the performance of the original reduced basis.

For the entirely non-linear system under harmonic excitation the improvements are negligible. For both systems under impulse excitations a slight degradation of the performance of both reduced bases can be observed.

In conclusion the SOT represent a promising expansion of the LNM only for locally non-linear systems if their number  $r_{\text{SOT}}$  is correctly chosen. For the other test cases the additional effort and necessary fine-tuning are overly demanding compared to possible ameliorations.

#### B.3.1 Overall Reduction Time

The plots of the overall reduction time, the time measure combining the time needed for creating the basis and solving the reduced system, reveal that the inclusion of the Second Order Terms at least doubles the time needed for the solution. It has been confirmed that the time needed for the actual creation of the basis, and thus also for calculating the Second Order Terms, remains negligible and almost instantaneous. The

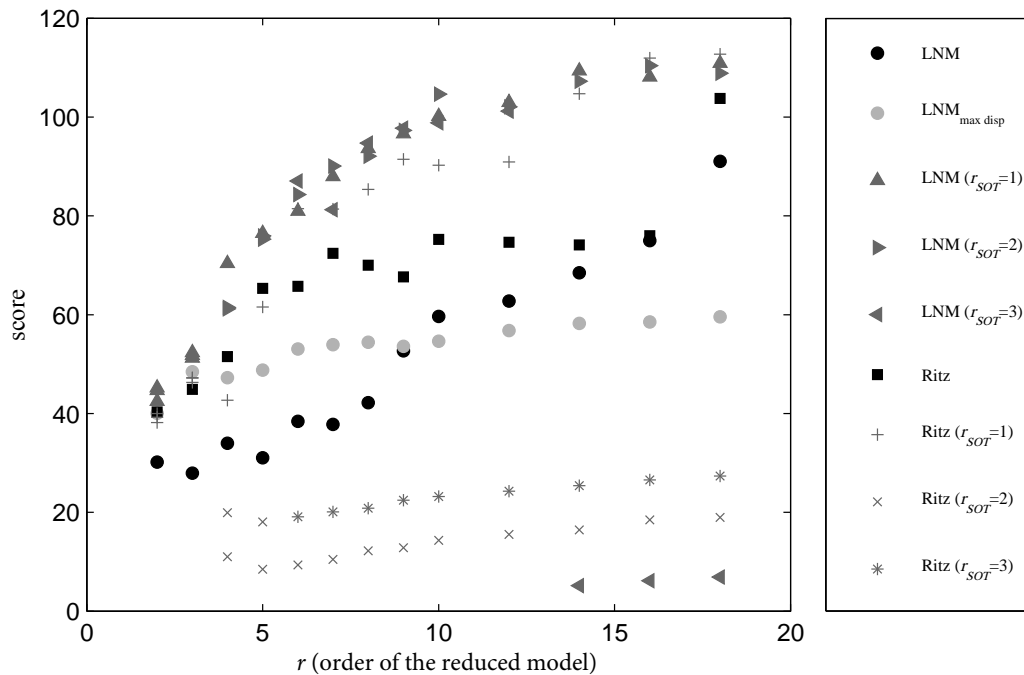


Figure B.2: The score for different SOT variants reducing the locally non-linear system under harmonic excitation

increase is hence exclusively attributed to the actual solution of the system. Because of the fact that there is no noticeable difference in overall solution time between the reduced system and the full order system, a fact identified in section 4.2.1 and attributed to the computational overhead, this a rather limiting factor for the usefulness of Second Order Terms.

### B.3.2 Harmonic Excitation

With respect to the relative root mean square errors, the locally nonlinear system is the most remarkable one because it is the only test-case for which the Second Order Terms added to the performance of the classic Linear Normal Modes.

For all sizes of the reduced system between  $r = 2$  and  $r = 7$  the adding of  $r_t = 1$  or  $r_t = 3$  Second Order Terms improves the reproduction of the full order solution and, within this range, the bases with that include Second Order Terms, perform better than any other LNM variant. The decisive contribution of the Second Order Terms in this case is their very fine spatial resolution. They resemble much the very high order classic Linear Normal Modes and help thus to resolve the secondary ripples which are visible in the plot of the reference solution in figure 4.7.

For the entirely nonlinear system the inclusion of only one Second Order Term reduces the quality of the recreated solution, while the addition of 3 and 5 Second Order Terms does have no noticeable influence. Adding seven Second Order Terms and thus creating a reduced system of an overall order of  $r+r_t = 9+7 = 16$  seems obviously to improve the solutions quality, but with only one point available, this conclusion is possibly not maintainable.

### B.3.3 Impulse Excitation

For all systems under impulse excitation the addition of Second Order Terms does not significantly alter the performance of the classic Linear Normal Modes. Only for  $r = 2$  there is a certain improvement present in all systems.

In summary it can be retained that the addition of Second Order Terms does not influence the reduction of systems under impulse excitation.

## B.4 Outcome of the study on Second Order Terms

The results of the study into the possibility of gains in precision through the addition of Second Order Terms shows benefits only for the locally nonlinear system I under harmonic excitation,. For the other systems and especially for all systems under impulse excitation the Second Order Terms do not really influence the performance of the reduced basis, if compared to classic Linear Normal Modes and the Linear Normal Modes obtained at maximum displacement.

The observed difference in quality between SOT to the Ritz-basis obtained from the numerical finite difference and the ones from the analytic approach in equation (B.3) is believed to come from the requirement for neglecting the inertial term. This condition is in most cases fulfilled for real systems, but for the academic systems studied below, the mass matrix  $\mathbf{M}$  and the stiffness matrix  $\mathbf{K}$  are of equal order.

The explication for the gain in precision through the addition of Second Order Terms for the locally nonlinear system under harmonic excitation, comes from the fact that the Second Order Terms are modes with a high spatial density. These small scale vibrations would only be obtained with high order classic Linear Normal Modes and help to resolve the characteristic superposed high frequency oscillation that is typical for the first test-case, consisting of the locally nonlinear system and the harmonic excitation.

As these high frequency oscillations are not present in the other systems' solutions the addition of Second Order Terms does neither help nor hamper their reduction.

A problem that remains to be discussed is, whether the chosen combinations of the  $i$  and  $k$  in equation (B.2) contribute to the encountered repartition of success and failure of the contribution of Second Order Terms among the test-cases and if the performance of bases including Second Order Terms can be increased by specifically adapting selection of the modes and the reduced coordinates, with respect to which the former are derived. Another possible direction of research presents itself in the combination of the Linear Normal Modes obtained at maximum displacement with the Second Order Terms, where the former would replace the classic Linear Normal Modes used in the study above.

However the optimisation of Second Order Term does not coincide with the overall direction of this research and the effort, expectedly to be invested into it, does not warrant performing this optimisation as a side-branch of the overall study. Especially as the obtained results do give no hint as to in which direction such an optimisation could be directed.

## Appendix C

# Improving the Centroidal Voronoi Tessellation

---

The Centroidal Voronoi Tessellation, as it is introduced in section 3.3.5, has been improved in several ways. This annex section provides background information and numerical results that justify the choices that are made.

In particular the replacement of the Euclidian norm with the modal assurance criterion is treated. Numerical results to underline this improvement are presented. Also an improvement for the application of the CVT to systems under impulse excitations is treated.

## C.1 General improvements and considerations of the CVT

The CVT, introduced in section 3.3.5, is now used as an iterative approach for refining a basis, while operating on the snapshots of the solution of the full order system. This is certainly an abuse of this method, which could also be initialised with a random basis. However, this deliberate contortion is interesting especially for LNM and Ritz-vectors, where improvements of the initial bases can be expected.

### C.1.1 Classic Formulation

For the moment the initial basis is taken from the LNM, the Ritz-vectors, the POD, the SOD and the APR. Hoping for a possible amelioration of for at least some of them. All these bases are used to initialise a CVT procedure.

Unfortunately the aspired improvement does not take place.

Firstly the figures for the overall reduction time in the annex section C show that significantly more time is needed for the CVT bases, and that is without the creation of the initial basis  $\Phi^{(0)}$ , which are just loaded from a file. This obviously partly due to the inefficient programming of the CVT algorithm and there are certainly more elegant and efficient ways to construct a CVT basis. However the additional effort over the creation of the initial basis cannot be neglected and has to be taken into account. Let alone the need for obtaining a full order solution for the snapshots.

Secondly the quality of the reconstructed solutions does not improve, except for the APR if applied to both systems under harmonic excitations. For all other methods on all test-cases the application of a CVT procedure actually deteriorates the quality of the solution. And even the improvement on the APR is no huge exploit because this method already performs the worst.

Taking the sum of a significantly higher effort and a not too satisfying result does not make the CVT a strong candidate for a possible reduced basis.

In fact, there seems currently no known application, on which the CVT performs better than the POD. Yet the two of them require the snapshots from the full order solution and it is thus the quality of the reduced solution which swings the favour towards the POD.

### C.1.2 Distance determination with Modal Assurance Criterion

In order determine the affiliation of a snapshot  $\tilde{\mathbf{u}}(t_j)$  to a region  $V_k$  equation (3.150) requires a measure of the distances between the snapshot and the generator  $\phi_k$ . As defined in section 3.3.5 this is commonly the Euclidian norm of the resulting vector  $\tilde{\mathbf{u}}(t_j) - \phi_k$ .

Another possibility of defining the distance between two vectors is the Modal Assurance Criterion, defined in section 4.1.2.1.5. It requires the reformulation of equation (3.150) as

$$\frac{|(\tilde{\mathbf{u}}(t_j))^T \phi_k|}{|(\tilde{\mathbf{u}}(t_j))^T \tilde{\mathbf{u}}(t_j)| |(\phi_k)^T \phi_k|} \geq \frac{|(\tilde{\mathbf{u}}(t_j))^T \phi_l|}{|(\tilde{\mathbf{u}}(t_j))^T \tilde{\mathbf{u}}(t_j)| |(\phi_l)^T \phi_l|} \quad \forall k \neq l \text{ and } \{k, l\} \in \{1, \dots, r\}, \quad (\text{C.1})$$

because the  $\leq$ -sign turns into a  $\geq$ -sign, due to the MAC being a measure of closeness and not of distance.

If the four-step procedure for constructing the CVT-basis from section 3.3.5 is now applied with equation (3.154) instead of equation (3.150) as a measure of the distance for the snapshots within each region  $V_k$ , naturally, the results change.

These results show considerable improvement for the two systems under harmonic excitation. Especially the completely nonlinear system, with its rather smooth and regular response, profits from the now distance

## C.2. PRESENTING THE NUMERICAL RESULTS JUSTIFYING THE REPLACEMENT OF THE EUCLIDIAN NORM WITH THE MAC

---

measure. However, these improvements do not put the CVT variants on par with e.g. the POD bases, which are considered to be the best performing ones.

For the two systems under impulse excitation the results worsen with the introduction of the MAC into the CVT procedure. A result which can only be documented because a rigorous explanation is yet to be found.

### C.1.3 Adapting the CVT for systems under impulse excitation

The CVT algorithm, as it is defined in section 3.3.5, is not necessarily adapted for systems under impulse excitation. This limitation can be circumvented by altering the third step of the three step procedure. Instead of simply defining the current generator  $\phi_k^{(j)}$  as the mean of the displacements in the region  $V_k^{(j)}$  it can be continuously updated with the current displacement and appropriately normalised. This approach yields

$$\phi_k^{(j)} = \frac{\phi_k^{(j-1)} + \frac{\tilde{\mathbf{u}}(t_j)}{|\tilde{\mathbf{u}}(t_j)|}}{|\phi_k^{(j-1)} + \frac{\tilde{\mathbf{u}}(t_j)}{|\tilde{\mathbf{u}}(t_j)|}|}. \quad (\text{C.2})$$

The errors obtained with this approach are much reduced for the two systems under impulse excitation. However, this comes at the price of having to accept higher levels of error for the test-cases with harmonic excitation.

The influences of the variant on the robustness of the CVT bases is, in general, negative.

Studying the vectors of this variant's bases reveals that the first vectors basically remain the LNM, which were used to initialise the bases. Only higher modes are changed and have an impact on the reduced solution.

## C.2 Presenting the numerical results justifying the replacement of the Euclidian norm with the MAC

This annex section lists the results that lead to the replacement of the Euclidian norm with the modal assurance criterion for grouping the snapshots into the Voronoi regions. This is explained in detail between equations (3.150) and (3.154) in section 3.3.5.

To verify if improvements take place due to the introduction of the MAC, the test-case defined in section 4.1.3.1 are reduced with either variant of the CVT.

The following figures C.1 to C.4 compare the differently initialized CVT bases as they are obtained either with the Euclidian norm (3.150) or with the modal assurance criterion (3.154). The comparison is performed on the grounds of the mean of the R2MSE. This error metric is chosen because a global score would imply a comparison between the differently initialized variants. Such a comparison is not helpful if studying the impact of the use of either the Euclidian norm or the MAC.

The results show that the introduction of the MAC reduces the error considerably and especially for the systems under impulse excitation. Also for the systems under harmonic excitation an improvement is observable in the range of  $4 \leq r \leq 8$ .

C.2. PRESENTING THE NUMERICAL RESULTS JUSTIFYING THE REPLACEMENT OF THE EUCLIDIAN NORM WITH THE MAC

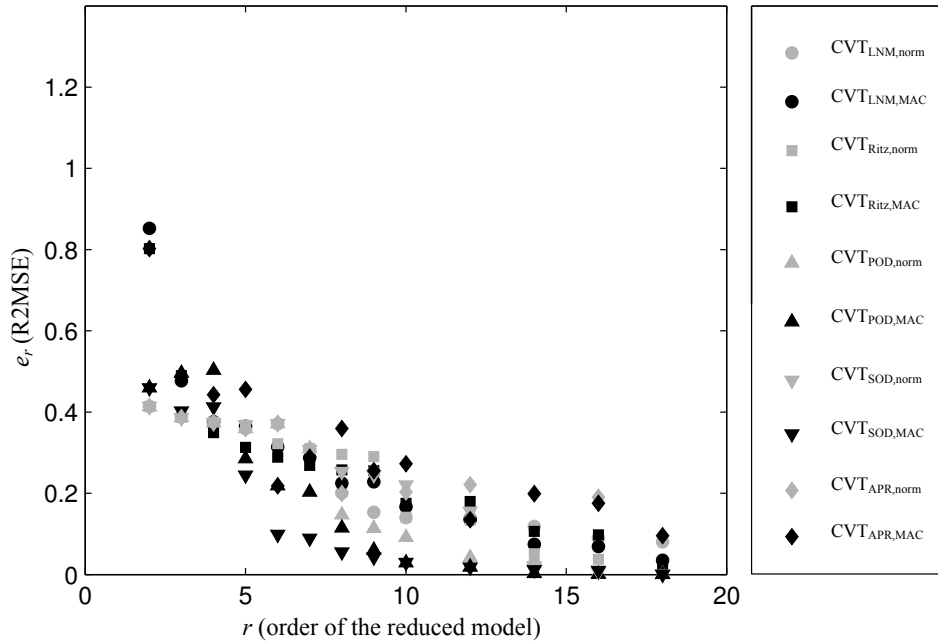


Figure C.1: The R2MSE for the locally nonlinear system under harmonic excitation: comparison of Euclidian norm and MAC

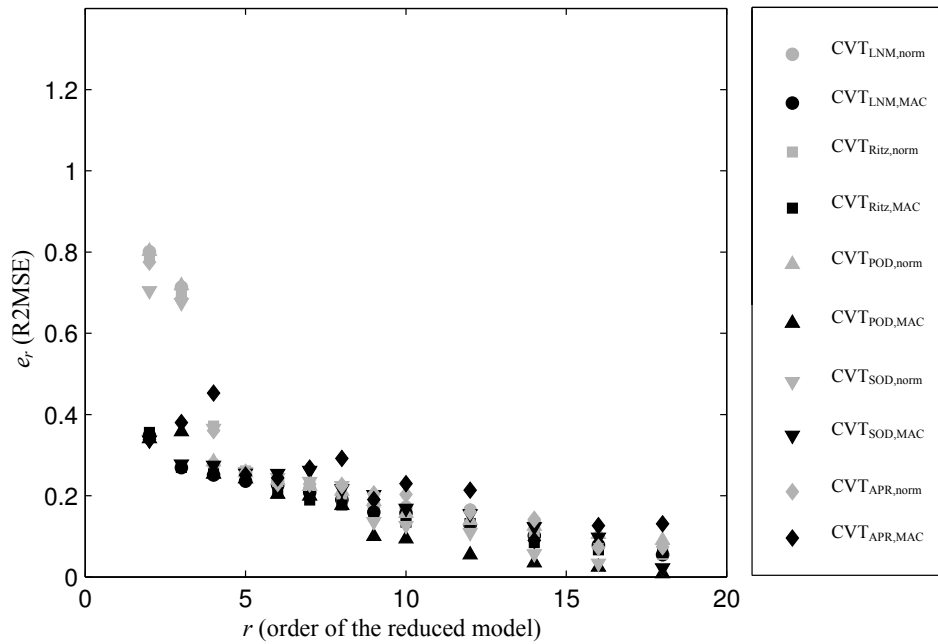


Figure C.2: The R2MSE for the entirely nonlinear system under harmonic excitation: comparison of Euclidian norm and MAC

C.2. PRESENTING THE NUMERICAL RESULTS JUSTIFYING THE REPLACEMENT OF THE EUCLIDIAN NORM WITH THE MAC

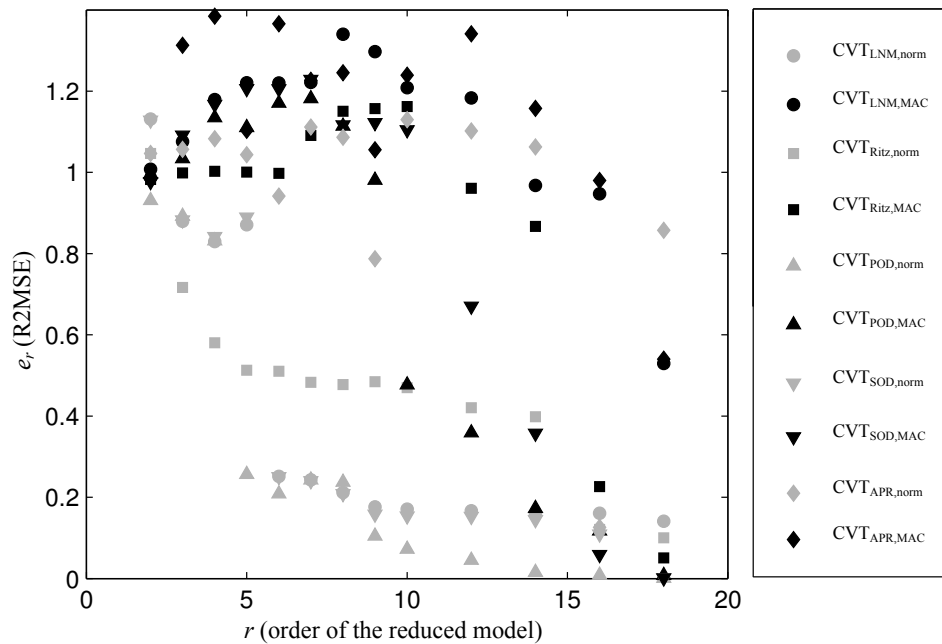


Figure C.3: The R2MSE for the locally nonlinear system under impulse excitation: comparison of Euclidian norm and MAC

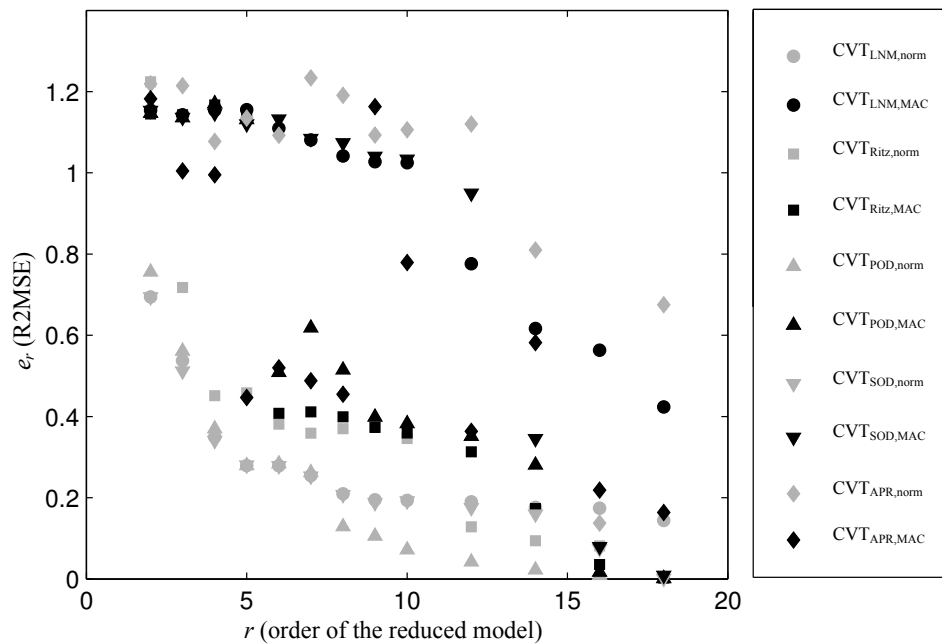


Figure C.4: The R2MSE for the entirely nonlinear system under impulse excitation: comparison of Euclidian norm and MAC



## Appendix D

# Broadening the description of the Non-linear Normal Modes

---

This annex section is an addendum to the section 3.1.2.4. It broadens the scope of the presentation of the Nonlinear Normal Modes. Basically, there are two approaches for the determination of nonlinear normal modes. The analytical computation as pursued by Pesheck [176] and the numerical continuation as proposed by Kerschen et al. [117] and Peeters et al. [170]. Both approaches are presented in a dedicated section. These sections are preceded by a small historical review of the development of the NNM along major published works and a brief discussion of the interaction of NNM. No calculations are performed and no results are obtained. This chapter is purely informational.

## D.1 Surveying the historical development of the Nonlinear Normal Modes

From the initial works of Rosenberg [190, 191, 192] on, the theory of NNMs is further expanded by Rand [184], who propose a direct method for the establishment of NNMs, and Rand et al. [183] and Vakakis and Rand [233, 232], who contribute to the theoretical definition and the analytical construction of NNMs. Shaw and Pierre [204, 205] establish the definition of the NNM we know today, as a low-dimensional, invariant manifold in the phase space, which is tangent to the corresponding linear mode. This approach is inspired by the use of inertial and central manifolds, as they are reviewed by e.g. Benner [35]. The stability of NNMs has been investigated by e.g. Vakakis and Rand [233] who used Poincaré-maps to identify bifurcating modes and a computational investigation of stability and bifurcations is made by Rand et al. [183].

Nayfeh and Nayfeh [156, 157] extend the invariant manifold approach to a complex-formulation, which has not yet found a widespread use and which is later expanded to cases with internal resonance by Nayfeh et al. [158].

Lewandowski [133, 134] proposed an adaptation of the continuation method for the analysis of the free and steady-state response of geometrically nonlinear systems and gave numerical examples.

Vakakis [231] insists on the usefulness of the nonlinear normal modes' capacity of allowing for energy localisation of vibrations. He states that a differentiation between spatially extended and spatially confined nonlinear normal modes can be very advantageous if localised phenomena such as shock and impact are studied.

Kerschen et al. [117] and Peeters et al. [170] compile a very comprehensive state-of-the-art with respect to NNMs and summarised several features of nonlinear systems that hampered their widespread solution until now. Among these features are internal resonance, bifurcating modes, saturation and, generally speaking, an extremely complex behaviour which can extend as far as chaotic movements. By weighting the respective advantages and shortfalls of analytical and numerical approaches for the establishment of NNMs, they propose several possible solutions that may point towards a future application of NNMs to large-scale nonlinear systems. These are, at least until now, still hampered by their intrinsic complexity, the lack of a proper orthogonality condition and the fact that the expansion theorem, which allows the superposition of modes in the linear case, is not applicable to NNMs. Their numeric continuation approach is presented later in this chapter. Finally they propose a frequency-energy plot that reflects the relationship between modal frequencies and modal amplitudes, as a suitable presentation for the understanding of the behaviour of the system under consideration.

Pesheck [176] achieve an analytical access to the manifold-formulation of the NNM, which is also presented in this chapter and Pesheck et al. [174] applied this formulation successfully to a rotor-blade as an example of a real world structure.

An asymptotic approach, going back to Lacarbonara and Camillacci [128], is replaced with a projection by Pierre et al. [180], as first proposed by Pesheck et al. [175], in their attempt to propose a solution technique for NNMs. Likewise Jiang et al. [108] adapt a combination of the concept of invariant manifolds, as the representation of choice of NNMs, and the projection approach to the simulation of piece-wise linear systems that exhibit large amplitudes.

Camillacci et al. [51] use adapted identification techniques, as developed by himself and Bellizzi et al. [32], to establish NNMs for a system with third-order nonlinearities and in order to construct an analytical relationship between the modal frequencies and the modal amplitudes. Furthermore he conducted numerical simulations with the NNMs and obtained results in reasonably good correspondence with an experiment that replicated the system chosen as an exemplary test-case.

Boivin et al. [39] use polynomial expansion to construct the modal relations between master and slave coordinates for weakly nonlinear systems. An approach that is expanded to systems with nonlinearities of third order by Nayfeh et al. [158].

To capture the response of a nonlinear system, subjected to random excitation, Bellizzi and Bouc [28, 29] introduce a stochastic averaging component into the construction of the NNMs, in order to capture the amplitude-frequency-interdependence of nonlinear systems. Their method results in an estimation of the power spectral density of the system's steady-state response.

Jiang et al. [110] develop a formulation for the free response, established by the same authors, further to a forced system with harmonic excitation. The external excitation is treated as an additional degree of freedom, which response is known, and which is conveniently integrated into the projection approach for the construction of the invariant manifold.

Peeters et al. [170] present a numerical algorithm for the construction of NNMs that is reproduced in this chapter, after the analytical approach directly hereunder. More information on numerical approaches for obtaining NNMs is given by Blanc et al. [38]

Concerning the applications of NNMs to solve actual problems in structural dynamics and thus the anticipation of ending their status as a curious and purely research topic some first examples are emerging. It is Emory [75], who, in his dissertation and the ensuing publication (Emory and Patil [74]), uses NNMs to solve a limit cycle problem in aeroelasticity on an academic wing model and proposes and compares different methods for solving the NNMs.

## D.2 Exploring the interaction of Nonlinear Normal Modes

It is Vakakis [231] who, in his very comprehensive overview paper, named nonlinear normal modes as a self-contradictory denomination because of their lack of an orthogonality relation. This lack of an orthogonality relation does not allow to completely decouple the NNMs from each other, as it is possible with linear normal modes, and it has as a direct consequence that there has to occur an interaction between different nonlinear modes. This interaction treads coupling and internal resonance and it has spawned a considerable research activity in the search of the conditions of its appearance and its impact on the system.

In this context it is crucial to understand that, as Kerschen et al. [117] put it, in a nonlinear system there can be more nonlinear normal modes than degrees of freedom. A situation, which results from possible bifurcations of the energy-dependent NNMs and which is not present for linear systems and linear normal modes.

Lacarbonara et al. [127] and Lacarbonara and Rega [126] attempt a solution to the problem of the possible interaction between two NNMs, which results from the lack of an overall orthogonality, in the case of internal resonance. For a certain class of nonlinear systems, the necessary condition of similar frequencies of the two modes together with the sufficient condition of the presence of a coupling term, which can activate the internal resonance, has been established. They develop conditions for one:one, two:one and three:one internal resonance in the case of flat structures with nonlinearities of up to third order. The necessary condition is the equality of the frequencies of two different NNMs and the sufficient condition is based on a low-order activation factor resulting from the nonlinear coupling, which activates the internal resonance if the two modes, susceptible of resonance, are no longer nonlinearly orthogonal.

Lacarbonara and Camillacci [128] propose an analytical asymptotic approach, based on the method of multiple scales, to construct the manifolds of individual NNMs away from and close to internal resonance. Their formulation allows studying the work done by one NNM on another NNM in the case of internal resonance, which reflects the energy transfer between the two resonant modes. The approach is however limited to a certain class of nonlinear systems.

Burton and Rhee [47] show that, in the vicinity of internal resonance, linear-based reduced models of nonlinear systems, exhibit more accuracy than NNMs. This suggests that for internal resonance the recourse to linear-based reduction may still be necessary, while the research on a NNM-formulation for internal resonance progresses.

The study of internal resonance conditions was followed up by Jiang et al. [109], who constructs multi-mode invariant manifolds from several master or seed variables that act as a basis for the NNM. As explained later in this chapter, these multi-mode manifolds are no longer based on a single set of kinematic configuration variables which act as master, but several pairs of kinematic configuration variables  $\{u_k, \dot{u}_k\}$  with  $k \in [1, \dots, r < n]$ , which are suspected to interact in internal resonance, are chosen as master variables.

Georgiades et al. [83] however stress that modal interaction, with the transfer of energy between the driving and the driven mode, can occur, even if the natural frequencies of the two involved modes, as they are derived from the underlying linear system, are not commensurate.

Li et al. [136] use the comparison of analytical and numerical results to track the reciprocal connection between modal interaction in the form of coupling and the occurrence of internal resonance. They find that modal coupling always exists, if internal resonance is possible.

Pak [166, 167] perform further studies on the coupling of nonlinear normal modes. Like Vakakis and Rand [233] they use Poincaré-maps to investigate interactions, energy exchanges and conceives stability criteria for nonlinear normal modes interacting with each other. His result is that every change in the stability of a mode results in a pitchfork or a period-doubling bifurcation.

So at this stage a complete understanding of the mutual interaction of nonlinear normal modes has yet to be established and although major directions for future insight have been established, the current state of research has to be considered as incomplete if not even inconclusive.

### D.3 Sketching the analytical approach for obtaining Nonlinear Normal Modes

Pesheck [176] pursue an analytical approach for the establishment of NNMs. Starting with a homogeneous and inertia-normalised formulation of equation (2.82), which now reads

$$\ddot{\mathbf{u}} - \mathbf{g}(\mathbf{u}, \dot{\mathbf{u}}) = 0 \quad (\text{D.1})$$

it is assumed that this relation between the accelerations  $\ddot{\mathbf{u}}$  and the kinematic configuration variables  $\mathbf{u}$  and  $\dot{\mathbf{u}}$  can be transformed into a system of first order differential equations:

$$\begin{cases} \dot{\mathbf{u}} = \mathbf{v} \\ \dot{\mathbf{v}} = \mathbf{g}(\mathbf{u}, \mathbf{v}) \end{cases} \quad (\text{D.2})$$

The vectors  $\mathbf{u} = [u_1, \dots, u_i, \dots, u_n]^T$  and  $\mathbf{v} = [\dot{u}_1, \dots, \dot{u}_i, \dots, \dot{u}_n]^T$  represent generalised positions in the phase space, which can be either physical or modal, while the forces acting on the system are regrouped in an adapted formulation of the vector of nonlinear internal forces  $\mathbf{g}$ .

From this system of first order differential equations (D.2) the nonlinear normal modes are constructed by choosing master coordinates and expressing the system's remaining degrees of freedom dependent on the master coordinates. Having selected a pair of kinematic configuration variables  $\{u_k, v_k\}$  as master coordinates for that specific NNM, all other slave coordinates can be written as functions of the master coordinates:

$$\begin{cases} u_i = X_i(u_k, v_k) \\ v_i = Y_i(u_k, v_k) \end{cases} \quad \forall i \in \{1, \dots, k-1, k+1, \dots, n\} \Leftrightarrow i \neq k. \quad (\text{D.3})$$

#### D.4. SKETCHING THE NUMERICAL APPROACH FOR OBTAINING NONLINEAR NORMAL MODES

---

The determination of the NNMs now corresponds to the determination of the functions  $X_i$  and  $Y_i$ . To this end, the equations of (D.3) are derived with respect to time

$$\begin{cases} \dot{u}_i = \frac{\partial X_i}{\partial u_k} \dot{u}_k + \frac{\partial X_i}{\partial v_k} \dot{v}_k \\ \dot{v}_i = \frac{\partial Y_i}{\partial u_k} \dot{u}_k + \frac{\partial Y_i}{\partial v_k} \dot{v}_k \end{cases} \quad \forall i \in \{1, \dots, k-1, k+1, \dots, n\} \Leftrightarrow i \neq k. \quad (\text{D.4})$$

Using the equalities of  $\dot{u}_i = v_i$  and  $\dot{v}_i = g_i$  equations (D.4) can be transformed into

$$\begin{cases} Y_i = \frac{\partial X_i}{\partial u_k} v_k + \frac{\partial X_i}{\partial v_k} v_k \\ g_i = \frac{\partial Y_i}{\partial u_k} v_k + \frac{\partial Y_i}{\partial v_k} g_k \end{cases} \quad \forall i \in \{1, \dots, k-1, k+1, \dots, n\} \Leftrightarrow i \neq k. \quad (\text{D.5})$$

These  $2n - 2$  equations for the  $X_i$  and the  $Y_i$ , which are describing the manifold of the NNM under consideration, do not included any assumptions beyond the scope of the ones used to establish equation (D.1) and, by reason of their generality, it may be impossible to find exact solutions for the  $X_i$  and the  $Y_i$ .

By limiting the order of the nonlinearities and introducing a polynomial expansion of the functions  $X_i(u_k, \dot{u}_k)$  and  $Y_i(u_k, \dot{u}_k)$  Pesheck [176] obtains a set of linear equations for the expansion coefficients of the NNM, which can be solved for a local expression of the nonlinear normal mode expressed in  $u_k$  and  $\dot{u}_k$ .

In this way equations (D.5) describe the manifold in the  $2n - 2$ -dimensional phase state for the nonlinear normal mode based on the master coordinates  $u_k$  and  $\dot{u}_k$ . With suitable expressions for the  $X_i$  and the  $Y_i$  the system is reduced completely to a single degree of freedom system, expressed in  $u_k$ .

## D.4 Sketching the numerical approach for obtaining Nonlinear Normal Modes

Peeters et al. [170] exploit the invariance of the manifold, which describes the NNM in the  $2n - 2$ -dimensional phase space, in order to obtain the nonlinear normal mode by means of time integration. The property of invariance states that all motions initiated on the manifold of the NNM under consideration remain on that manifold and it can be used to identify points in the phase-space, which provide initial conditions suitable of leading to orbits contained on the manifold of the NNM under consideration. This technique also takes advantage of the fact that the NNMs are energy-dependent, which is used by Camillacci et al. [51] in an expansion of the NNM from the point, where it has the corresponding linear normal mode as a tangent plane. This energy dependence is used to force the Nonlinear Normal Mode to depart from the tangent Linear Normal Mode.

The basic equation (2.82) for a nonlinear system, which is now considered homogeneous

$$M\ddot{u} + g(u, \dot{u}) = 0 \quad (\text{D.6})$$

is written in a state space form with

$$z = \begin{bmatrix} u \\ \dot{u} \end{bmatrix} \quad (\text{D.7})$$

#### D.4. SKETCHING THE NUMERICAL APPROACH FOR OBTAINING NONLINEAR NORMAL MODES

---

which, in turn, yields

$$\dot{\mathbf{z}} = \begin{bmatrix} \dot{\mathbf{u}} \\ \dot{\mathbf{u}} \end{bmatrix} = \begin{bmatrix} \dot{\mathbf{u}} \\ -\mathbf{M}^{-1}(\mathbf{g}(\mathbf{u}, \dot{\mathbf{u}})) \end{bmatrix}. \quad (\text{D.8})$$

This is basically the same transformation that is used by Pesheck [176] for the analytical approach in equations (D.1) and (D.2). Another commonality between the analytical and the numerical approach is the division of the displacements  $\mathbf{u}$  and velocities  $\dot{\mathbf{u}}$  in master and slave coordinates, which was extensively discussed for the analytical approach.

Beyond these two commonalities, the numerical approach takes a significantly different course of action: From a known and confirmed point of initial conditions for the kinematic configuration variables  $\mathbf{b}_{(i)} = \mathbf{z}_{0,(i)} = [\mathbf{u}_0, \dot{\mathbf{u}}_0]_{(i)}^T$  and the confirmed period  $T_{(i)}$  of that motion originating from these initial conditions the numerical approach augments the energy-level of the NNM under consideration by defining the new initial conditions  $\mathbf{b}_{(i+1)}^{(0)}$  in a distance  $\Delta\mathbf{z}_{(i)}$  from  $\mathbf{b}_{(i)}$ . The same is done for the period, whose predictive value is also based on the final value of the preceding iteration and is now augmented by an incremental step  $T_{(i+1)}^{(0)} = T_{(i)} + \Delta T_{(i)}$ . These new initial conditions  $\mathbf{b}_{(i+1)}^{(0)}$  and  $T_{(i+1)}^{(0)}$  act as initial values for search of a closed loop in the state-space, which complies with the manifold's characteristic of invariance. To this end a shooting procedure is used, which, based on equation (D.6), calculates the systems behaviour in physical displacements, with the aim of refining the predictive, initial values of  $\mathbf{b}_{(i+1)}^{(0)}$  and  $T_{(i+1)}^{(0)}$ , until they yield a periodic motion of the system, which finds its equivalence in the presence of a closed loop in the state space.

In detail the numerical approach takes the following steps to obtain the NNM in the state space. Knowing initial conditions  $\mathbf{b}_{(i)}$  that are confirmed to lie on the manifold of the NNM under consideration, together with the confirmed period  $T_{(i)}$  of that motion, the predictive values for the next point of the NNM  $\mathbf{b}_{(i+1)}^{(0)}$  and  $T_{(i+1)}^{(0)}$  are determined, by advancing on a tangential plane in the predetermined direction of  $\Delta\mathbf{b}_{(i)}$  for the kinematic configuration variables:

$$\mathbf{b}_{(i+1)}^{(0)} = \mathbf{b}_{(i)} + \Delta\mathbf{b}_{(i)} \quad (\text{D.9})$$

and

$$T_{(i+1)}^{(0)} = T_{(i)} + \Delta T_{(i)} \quad (\text{D.10})$$

for the period. In both cases the subscript  $(i + 1)$  indicates the next step on the NNM's manifold while the superscript  $(0)$  implies its property as the initial value for the following correction. This advancement on the tangential plane corresponds to an augmentation of energy, as it was introduced with the constant  $h$ , which expresses the dependence of the NNM on the energy, in equation (3.36). Proceeding like this, allows to cover the manifold of the NNM at different energy levels and so the states  $(i)$  can be interpreted as different energy levels.

Following these considerations and equations (D.9) and (D.10), the final values of the energy level  $(i)$ ,  $\mathbf{b}_{(i)}$  and  $T_{(i)}$ , have become the basis of the initial values,  $\mathbf{b}_{(i+1)}^{(0)}$  and  $T_{(i+1)}^{(0)}$ , of the next step  $(i + 1)$ , where the correct initial conditions  $\mathbf{b}_{(i+1)}$  and the correct period  $T_{(i+1)}$  are yet to be found.

Having new predictive initial values  $\mathbf{b}_{(i)}^{(0)}$  through equation (D.9) and a predictive value for the period  $T_{(i)}^{(0)}$  of the oscillation associated with these predictive values available through equation (D.10) allows for

the necessary calculations to be performed to solve the periodicity condition  $\mathbf{H}$ :

$$\mathbf{H}(\mathbf{b}_{(i)}, T_{(i)}) = \mathbf{z}(\mathbf{b}_{(i)}, T_{(i)}) - \mathbf{z}(\mathbf{b}_{(i)}, 0), \quad (\text{D.11})$$

which states that the physical displacements of the system  $\mathbf{z} = [\mathbf{u} \quad \dot{\mathbf{u}}]^\text{T}$ , as they were defined in equation (D.7), repeat each other after one period  $T_{(i)}$  of the oscillation. The physical displacements  $\mathbf{z}$  depend on the initial conditions  $\mathbf{b}_{(i)}^{(0)}$ , while the period  $T_{(i)}$  has a direct influence on the periodicity condition.

The periodicity conditions indicates how far the most recent guess is from the initial conditions that lead to a periodic movement on the NNM's invariant manifold. If its value is zero, the chosen initial conditions lead to a periodic movement with the chosen period. The aim of the correction step is to adapt the initial conditions and the period with the intention of driving the periodicity condition towards zero.

Hence an iteration has to be initiated from the predictive values  $\mathbf{b}_{(i)}^{(0)}$  and  $T_{(i)}^{(0)}$  to calculate the exact initial conditions  $\mathbf{b}_{(i)}$  and  $T_{(i)}$ . To this end Peeters et al. [170] propose a shooting procedure and a Newton-Raphson algorithm for a quick convergence of the periodicity condition  $\mathbf{H}(\mathbf{b}_{(i)}^{(j)}, T_{(i)}^{(j)})$ , which requires one complete simulation of the system via e.g. direct time integration in a nonlinear Newmark scheme, for each iteration step.

Once the exact values for the initial conditions  $\mathbf{b}_{(i)}$  and for the period  $T_{(i)}$  are obtained, the calculation of the NNM can return to the state-space. From these confirmed initial conditions  $\mathbf{b}_{(i)}$  of the  $i$ -th iteration step, the new initial conditions  $\mathbf{b}_{(i+1)}^{(0)}$  and the next period  $T_{(i+1)}^{(0)}$  are determined by returning to equations (D.9) and (D.10) and proceed with the pseudo arc-length continuation.

With these new initial values a new shooting-procedure can be initiated to converge the periodicity condition from equation (D.11).

For the very first step, the procedure is initiated with the initial conditions and the period of the underlying linear-normal mode. The increment  $\Delta\mathbf{b}_{(i)}$  is generated along the tangent vector to the NNM at the point  $\mathbf{b}_{(i)}$  for the first iteration and both this increment  $\Delta\mathbf{b}_{(i)}$  as well as the period's increment  $\Delta T_{(i)}$  are adapted by a step-size-control.

By successively marching the prediction steps away from the tangent point and performing iterative corrections on them the complete NNM is eventually computed.

## D.5 Describing the actual implementation of the numeric algorithm

For the numerical calculation of an NNM equation (2.82), which is, for now, considered to be homogenous

$$M\ddot{\mathbf{u}} + \mathbf{g}(\mathbf{u}, \dot{\mathbf{u}}) = 0 \quad (\text{D.12})$$

is cast into state space with the state variable

$$\mathbf{z} = \begin{bmatrix} \mathbf{u} \\ \dot{\mathbf{u}} \end{bmatrix} \quad (\text{D.13})$$

regrouping the kinematic configuration variables. This establishes the entire system as

$$\dot{z} = \begin{bmatrix} \dot{\mathbf{u}} \\ -\mathbf{M}^{-1}(\mathbf{g}(\mathbf{u}, \dot{\mathbf{u}})) \end{bmatrix}. \quad (\text{D.14})$$

The solution of this system depends on the initial conditions for the displacements and the velocities that are regrouped in the vector

$$\mathbf{b} = z_{(0)} = \begin{bmatrix} \mathbf{u}_0 \\ \dot{\mathbf{u}}_0 \end{bmatrix} \quad (\text{D.15})$$

that has the dimension  $2n$ .

Establishing the manifold of a NNM requires to find initial conditions  $\mathbf{b}$  that lead to a solution of the system that repeats itself with a period  $T$  that is not known prior to the solution. In order to find a set of such initial conditions and the corresponding periods a prediction-correction method, initialised from the underlying linear normal mode, is applied.

As stated in section 3.1.2.4 the linear normal modes of the underlying linear system can be represented as planes, tangent to the corresponding nonlinear normal mode in the equilibrium state. It is therefore obvious to initialise the iterative search for the shape of the invariant manifold describing the NNM with the conditions of equilibrium and the period of the linear normal mode.

According to equation (3.113) the frequency of a linear eigenmode  $\omega_i$  is related to the corresponding eigenvalue  $\lambda_i$ , coming from the eigenproblem (3.102). This can be used to calculate the period  $T = 2\pi \frac{1}{\sqrt{\lambda}}$  which serves as the starting point for the iterative solution of the nonlinear normal mode under consideration. This period  $T$  of the underlying linear normal mode becomes the zero-th period which initialises the iteration of the nonlinear mode. To complete the initial values for the subsequent iterations the initial conditions for the displacements and velocities, combined in the state space parameter  $z = [\mathbf{u}, \dot{\mathbf{u}}]^T$ , defined in equation (D.7), are set to zero, to reflect the equilibrium state of the system. Together these two initial conditions read:

$$\mathbf{b}_0 = \begin{bmatrix} \mathbf{0} \\ \mathbf{0} \end{bmatrix} \quad (\text{D.16})$$

and

$$T_0 = 2\pi \frac{1}{\sqrt{\lambda}}. \quad (\text{D.17})$$

From this point on, the stepwise expansion of the NNM's manifold takes the form of a predictive step followed by a successive iteration using a correction procedure, represented by the indices  $(i)$  and  $(j)$  respectively. This approach was initially proposed by Slater [211] and then refined by Peeters et al. [169], from where it is reproduced hereunder.

The calculation of the predictive values for the initial conditions  $\mathbf{b}_{(i+1)}^{(0)}$  for the correction procedure is based on a pseudo arc-length continuation

$$\mathbf{b}_{(i+1)}^{(0)} = \mathbf{b}_{(i)} + s_{(i)} \Delta \mathbf{b}_{(i)} \quad (\text{D.18})$$

with the difference that the step in initial conditions  $\Delta \mathbf{b}_{(i)}$  in equation (D.9) is now accompanied by a scalar parameter  $s_{(i)}$ . The same scalar parameter  $s_{(i)}$  is also introduced into equation (D.19), where it scales the incremental period:

$$T_{(i+1)}^{(0)} = T_{(i)} + s_{(i)} \Delta T_{(i)}. \quad (\text{D.19})$$

While the scaling factor  $s_{(i)}$  is controlled by the number of steps of the different solutions, refer to Peeters et al. [170], the incremental values  $\Delta \mathbf{b}_{(i)}$  and  $\Delta T_{(i)}$  are readily computed, using

$$\begin{bmatrix} \frac{\partial \mathbf{H}}{\partial \mathbf{b}} |_{\mathbf{b}_{(i)}, T_{(i)}} & \frac{\partial \mathbf{H}}{\partial T} |_{\mathbf{b}_{(i)}, T_{(i)}} \\ \frac{\partial h}{\partial \mathbf{b}} |_{\mathbf{b}_{(i)}}^T & 0 \end{bmatrix} \begin{bmatrix} \Delta \mathbf{z}_{(i)} \\ \Delta T_{(i)} \end{bmatrix} = \begin{bmatrix} \mathbf{0} \\ 0 \end{bmatrix}. \quad (\text{D.20})$$

In this equation  $\mathbf{H}$  is the periodicity condition and  $h$  the phase condition.

The periodicity condition  $\mathbf{H}(\mathbf{b}, T)$  depends on the initial conditions  $\mathbf{b}$  and the period  $T$ . Its objective is to ensure that the solution to the system repeats itself after the period  $T$  of the oscillation. To this end and by expanding equation (D.11) it can be written as:

$$\mathbf{H}(\mathbf{b}) = \mathbf{z}(\mathbf{b}, T) - \mathbf{z}(\mathbf{b}, 0) = \begin{bmatrix} \mathbf{u}(\mathbf{b}, T) \\ \dot{\mathbf{u}}(\mathbf{b}, T) \end{bmatrix} - \begin{bmatrix} \mathbf{u}(\mathbf{b}, 0) \\ \dot{\mathbf{u}}(\mathbf{b}, 0) \end{bmatrix} = \mathbf{0}. \quad (\text{D.21})$$

A slight modification for numerical purposes of the periodicity condition reduces the necessary simulation time by a factor of nearly two by putting  $\mathbf{H} = \mathbf{z}(\mathbf{b}, 0) + \mathbf{z}(\mathbf{b}, \frac{T}{2})$ , which has the same effect as the original periodicity condition, but exploits the recurrence of the values of the kinematic configuration variables with opposing signs after a half-period. In either formulation it is the aim of the correction procedure to drive the periodicity conditions towards zero.

The phase condition fixes the phase of the solution which would be otherwise left arbitrary. With the all zero initial conditions from equation (D.16) in view it is common to force all kinetic to be zero energy in the system for  $t = 0$ . An approach which yields:

$$h = \dot{\mathbf{u}}(0)^T \dot{\mathbf{u}}(0) = 0. \quad (\text{D.22})$$

In the actual implementation equation (D.20) is solved for the incremental predictor step  $\Delta \mathbf{b}_{(i)}$  by setting one of its components to one and applying the Moore-Penrose inverse of the thus reduced left-hand side. This is instrumental in forcing the algorithm to depart from the all zero initial conditions imposed through equation (D.15). Prior to using the incremental predictor step  $\Delta \mathbf{z}_{(i)}$  to its intended application in equation (D.18) it is normalised to obtain the full effect of the scaling parameter  $s_{(i)}$ .

Having thus established the predictive values  $\mathbf{z}_{(i+1)}^{(0)}$  and  $T_{(i+1)}^{(0)}$  at the index  $(i+1)$  for the initial conditions and the period respectively by means of equations (D.18) and (D.19), the iterative optimisation process can be launched on the index  $(j)$  in order to refine these initial conditions and the period from their respective predictive values. This is done through a shooting procedure which relies on a Newton-Raphson method to converge the residual of the periodicity condition  $\mathbf{H}$  to zero.

During this shooting procedure the lower index  $(i+1)$ , which indicates the predictor steps, is fixed and the iterative correction of the available initial conditions and the period is done over the upper index  $(j)$ , which was set to zero until now, marking the available values as initial values for the iteration.

In an implementable matrix formulation this reads:

$$\begin{bmatrix} \frac{\partial \mathbf{H}}{\partial \mathbf{b}} \big|_{\mathbf{b}^{(j)}, T^{(j)}} & \frac{\partial \mathbf{H}}{\partial T} \big|_{\mathbf{b}^{(j)}, T^{(j)}} \\ \frac{\partial \dot{h}}{\partial \mathbf{b}} \big|_{\mathbf{b}^{(j)}} & 0 \\ \Delta \mathbf{z}_{(i)}^T & \Delta T_{(i)} \end{bmatrix} \begin{bmatrix} \Delta \mathbf{z}_{(i+1)}^{(j)} \\ \Delta T_{(i+1)}^{(j)} \end{bmatrix} = \begin{bmatrix} -\mathbf{H} \left( \mathbf{b}^{(j)}, T^{(j)} \right) \\ -h \left( \mathbf{b}^{(j)} \right) \\ 0 \end{bmatrix}. \quad (\text{D.23})$$

The last row of the equation above, which forces  $\left[ \Delta \mathbf{z}_{(i)}^T, \Delta T_{(i)} \right] \left[ \Delta \mathbf{z}_{(i+1)}^{(j)}, \Delta T_{(i+1)}^{(j)} \right]^T = 0$  enforces the orthogonality of the incremental corrector steps with respect to the incremental predictor step, as they were established in equation (D.20). A feature that ensures a rapid convergence of the iteration.

The solutions  $\Delta \mathbf{z}_{(i+1)}^{(j)}$  and  $\Delta T_{(i+1)}^{(j)}$  for the alteration of the initial conditions and the period respectively are then added to the preceding values through equations similar to equations (D.18) and (D.19), but omitting the scaling factor  $s_{(i)}$  :

$$\mathbf{z}_{(i+1)}^{(j+1)} = \mathbf{z}_{(i+1)}^{(j)} + \Delta \mathbf{z}_{(i+1)}^{(j)} \quad (\text{D.24})$$

$$T_{(i+1)}^{(j+1)} = T_{(i+1)}^{(j)} + \Delta T_{(i+1)}^{(j)}. \quad (\text{D.25})$$

With these new values the convergence is verified by the comparison of the formulation of the periodicity condition  $\mathbf{H} \left( \mathbf{z}_{(i+1)}^{(j+1)}, T_{(i+1)}^{(j+1)} \right)$ , normalised with the initial conditions  $\mathbf{z}_{(i+1)}^{(j+1)}$ , with a predetermined threshold  $\epsilon$ :

$$\frac{\left| \mathbf{H} \left( \mathbf{z}_{(i+1)}^{(j+1)}, T_{(i+1)}^{(j+1)} \right) \right|}{\left| \mathbf{z}_{(i+1)}^{(j+1)} \right|} < \epsilon. \quad (\text{D.26})$$

This is in fact the most computationally costly part of the establishment of a Nonlinear Normal Mode, as it requires a time history of at least one half-period of the full order system.

If this condition in equation (D.26) is met, the initial values for the kinematic configuration variables and the period are considered to have converged on usable values and the NNM can be further expanded with a predictor step on the index  $(i)$  from equation (D.20) using the newly established results as starting point, while the index  $(j)$  is set to zero.

If this condition is however not met, the iteration is pursued by returning to equation (D.23) and continuing on the index  $(j)$  while remaining on the level  $(i + 1)$ .

Eventually, by finding all initial conditions and periods that lead to a periodic oscillation of the system and expanding them from the underlying linear normal mode, the entire nonlinear normal mode's manifold is constructed.

This concludes the numerical establishment of a nonlinear normal mode. Numerical results are not presented. They are available from e.g. Peeters et al. [169].

**Une méthode intégrée pour les réponses  
transitoires des modèles d'ordre réduit de structures en  
dynamique nonlinéaire géométrique**

Dipl.-Ing. **Fritz Adrian LÜLF**

## Introduction

Le but de ce travail est le développement d'une méthode numérique pour la construction d'un modèle réduit, autonome et paramétrable d'une structure dynamique géométriquement non linéaire et pour résoudre ce modèle réduit afin d'obtenir une solution transitoire avec un effort numérique qui est moindre que l'effort requis par la solution transitoire du modèle grand ordre.

L'introduction commence avec une brève motivation de construction d'un modèle réduit. L'intérêt central d'un modèle réduit est l'effort numérique faible qui en découle et qui permet ensuite une variété des applications comme par exemple des optimisations. La construction d'un modèle réduit permet de définir les trois exigences centrales de vitesse, précision et paramétrisation et de les identifier comme étant essentielles pour une solution réduite avec succès. Pour chacune de ces exigences l'état de l'art des approches et méthodes disponibles est évalué. Une grande variété d'approches sophistiquées et spécifiques est disponible, dont chacune répond à une des exigences demandées. La recherche bibliographique démontre aussi l'absence d'une méthode intégrée, combinant des approches pour chacune des trois exigences. Le développement d'une telle méthode intégrée qui répond aux trois exigences simultanément est déclaré le but principal de cette étude.

L'introduction met en avant que ce travail vise d'être une étude exploratrice qui se base uniquement sur des expériences numériques. La concentration exclusive sur des problèmes déjà discrétisés permet l'intégration sans couture des différentes méthodes spécifiques au niveau des équations matricielles. Cette approche est poursuivie et ses différentes étapes sont présentées dans la conclusion de l'introduction.

## Préparer les fondations de la dynamique des structures géométriquement non linéaires

Les formulations de l'équilibre dynamique des structures géométriquement non linéaires sont introduites dans cette section. Cette introduction est d'abord faite dans le milieu continu et ensuite d'une manière discrète. Les non linéarités sont distribuées sur toute la structure et elles sont modérées, permettant la description du comportement de la structure avec l'hypothèse des déplacements finis. Au delà de cette assumption des déplacements finis aucun type supplémentaire de non linéarité est considéré.

L'expansion graduelle des termes de la formulation continue vise la formulation *Total-Lagrangian*. Le choix d'exprimer la formulation continue dans la formulation *Total-Lagrangian* avec une loi de comportement linéaire est déterminé par l'exigence d'un système uniquement géométriquement non linéaire qui est sensé de servir comme cas-test.

La formulation discrète est développée pour permettre un traitement numérique de la formulation continue et pour aboutir à une équation matricielle qui décrit l'équilibre dynamique. Les descriptions détaillées des éléments finis non linéaires du type bar et volume suivent. Ces éléments sont requis pour les cas-test en éléments finis auquel la méthode qui est développée sera appliquée. Ils sont également utilisés pour démontrer comment la formulation continue est transformée dans la formulation discrète.

Finalement tous termes non linéaires de l'équilibre sont condensés dans une seule équation matricielle. Cette équation est le point de départ et le pivot pour le choix imminent d'une méthode de réduction et une procédure compatible pour obtenir une solution transitoire.

## Choix d'une approche de réduction et une procédure compatible pour obtenir une solution transitoire

Avec l'équation matricielle, décrivant l'équilibre dynamique d'un système géométriquement non linéaire discrétisé, disponible le choix d'une approche de réduction doit être fait. La sélection d'une procédure d'intégration dans le temps compatible pour obtenir des solutions transitoires du système complet de du modèle réduit dépend fortement de ce choix.

Dans un premier pas des approches différentes pour la réduction sont évaluées, quelques-unes sont des réductions pures, d'autres sont des approches combinées pour une réduction et une solution. Sur la base des critères définis l'approche de réduction par projection sur une base réduite est choisie. Parce que la projection sur une base réduite ne permet que la réduction, cette approche demande aussi le choix supplémentaire d'une procédure d'intégration dans le temps. Avec le schéma de Newmark une procédure commune et robuste est présentée. Il est également démontré que cette procédure de solution est aveugle face à la taille de système qu'elle résout. Ceci est très important parce que la description matricielle du système dynamique réduit, tel qu'il est créé par la projection sur une base réduite, à exactement la même structure que l'équation matricielle du système grand ordre. Ainsi, le schéma de Newmark peut obtenir des solutions transitoires pour le système grand ordre et le système d'ordre réduit.

A partir de cette possibilité l'introduction d'une formulation autonome des termes non linéaires du système d'ordre réduit s'avère nécessaire. Néanmoins, cet introduction est sautée pour l'instant parce qu'elle altère les tests entendus dans le chapitre 4. La section courante se termine avec présentations des bases réduites pour conclure la présentation de la réduction par projection sur une base réduite et pour préparer des bases candidates pour les tests à venir.

Le chapitre 2 traite la discrétisation de la formulation continue de l'équilibre dynamique (2.1), avec un nombre infini de degrés de liberté, vers l'équation matricielle (2.82) avec le nombre fini  $n$  de degrés de liberté. Néanmoins, le nombre  $n$  reste encore très grand pour des application en ingénierie.

Ce nombre très grand de degrés de liberté impose toujours des limites sur l'application du modèle grand ordre avec haute fidélité pour certaines applications comme, p.ex. optimisation ou contrôle  $\frac{1}{2}$  le, et ceci malgré l'accroissement continu de la puissance de calcul disponible. En même temps une discrétisation grossière avec un nombre faible  $n$  de degrés de liberté discrètes est contradictoire à l'esprit de discrétisation et donne des mauvais résultats. Pour éviter le choix considérable entre des mauvais résultats mauvais et une solution trop coûteuse le nombre  $n$  de degrés de liberté peut être réduit sur le nombre  $r$ , qui est beaucoup plus petite, tout en gardant les caractéristiques dominantes du système. Ceci est fait avec un réduction de modèle.

Ces techniques s'introduisent dans la séquence de travail après la discrétisation et avant la solution en soi, p.ex. une intégration dans le temps. A ce point les propriétés du système grand ordre (2.82) sont connues et les techniques de réduction peuvent les exploiter et peuvent être adaptées d'une manière optimale au système courant. Ceci évite les inconvénients d'une discrétisation grossière.

### Evaluer quelques approches de réduction

Le point de départ de la solution transitoire réduite d'un système dynamique, non linéaire, non-conservatif, grand ordre et entièrement discrétisée dans l'espace est l'équation (2.82).

L'enjeu de chaque technique de réduction de modèle est de trouver un moyen adéquate pour établir le modèle réduit du système avec seulement  $r$  degrés de liberté. Le modèle réduit est construit en appliquant des relations à définir d'une telle façon que ces relations décrivent les  $n$  degrés de liberté du système grand ordre  $u_i$  en fonction des  $r$  coordonnées généralisées  $q_k$  du système d'ordre réduit avec  $k \in \{1, \dots, r\}$  et  $r \ll n$ .

En utilisant ces relations le système grand ordre est réduit pour obtenir le modèle réduit, puis résolu et ensuite gonflé à grand ordre pour permettre une interprétation physique. L'étape de l'inflation est nécessaire

pour au moins quelques degrés de liberté physiques d'intérêt parce que les coordonnées généralisées du modèle d'ordre réduit peuvent être sans signification physique.

Pour obtenir un modèle réduit ils existent des méthodes qui sont indépendantes de l'algorithme d'intégration dans le temps choisi et des méthodes qui effectuent la réduction et la solution du système réduit de manière monolithique et interdépendante. Comme les principaux représentants du premier type de méthodes la projection sur une base réduite et la réduction de Guyan sont inclus dans la présentation des approches de réduction communs. Ces méthodes basées sur la projection définissent une base réduite sur laquelle le système (2.82) est projeté. Cela introduit une séparation claire de la réduction et de la solution.

Le deuxième type de méthode, dont la plupart a émergé récemment, ne s'appuie pas sur une projection, mais aspire à d'autres moyens de mettre en relation degrés de liberté grand ordre  $bm_u$  avec les déplacements généralisés  $bm_q$ . Les plus méthodes les notables parmi ce deuxième type sont la décomposition généralisée propre, décrit par exemple par Ammar et al. [7, 9], et les modes non-linéaire normal, introduits par Rosenberg [190] et récemment redécouvert avec succès par Peeters et al. [169] et Kerschen et al. [117]. Ces méthodes directes sont des techniques monolithiques parce que leur approche comprend et prévoit un certain algorithme pour obtenir la solution transitoire. Leur approche différente rend la comparabilité avec les techniques de réduction par projection quelque difficile.

### Projection sur une base réduite

Les méthodes basées sur la projection ont en commun qu'elles définissent un sous-espace, représentée par la matrice de réduction  $\Phi$ , qui est utilisé comme une base sur laquelle les équations discrètes décrivant le système dynamique non linéaire sont projetées.

Pour les méthodes de réduction en fonction de projection du modèle d'ordre réduit est introduit par le moyen de projeter les déplacements physiques  $u$  du système grand ordre sur la base  $\Phi$ , ce qui donne equation 3.1 avec  $q$  comme le vecteur des déplacements généralisés. L'introduction de cette relation dans l'équation (2.82) donne son homologue respectifs dans déplacements généralisés par l'équation 3.2. Ceci, à son tour, les donne  $n$  équations pour les  $r$  degrés de la liberté généralisés et donc un système sur-déterminé.

Pour contrer cette sur-détermination, des séparateurs supplémentaires peuvent être introduits par la définition d'une matrice  $\Psi$  de sorte que, si l'équation (3.2) est multipliée à gauche par la transposée de  $\Psi$ , elle devient equation (3.3). Cela donne un système d'ordre  $r$  qui peut être résolu plus facilement par un algorithme approprié que les équations du système haute-fidélité grand ordre  $n$ .

Avec l'introduction des matrices réduites  $\tilde{M}$ ,  $\tilde{C}$  et les vecteurs  $\tilde{g}$  et  $\tilde{f}_E$ , il est possible d'écrire l'équation (2.82) sous sa forme réduite (3.11).

Il est évident que les structures de l'équation (2.82), décrivant le système grand ordre, et l'équation (3.11) du système d'ordre réduit sont identiques. Cela implique que les mêmes techniques de solution peuvent être utilisées pour un système grand ordre ainsi que d'un système complètement réduit.

Pour la création des bases réduites pour la technique de réduction par projection il y a une multitude de variétés disponibles. La sélection utilisée dans cette étude est loin d'être exhaustive et comprend

- les LNM (Bathe [22]),
- les vecteurs de Ritz (Wilson et al. [241]),
- la POD (Sirovich [207]),
- l'APR (Ryckelynck [197]),
- la CVT (Du et al. [71]), et
- la LELSM (AL-Shudeifat and Butcher [2]).

De la revue de la littérature, il devient évident que la plupart des techniques et des progrès dans les techniques de réduction proviennent du domaine de la dynamique des fluides, où la recherche et l'innovation

ont été et restent vives, et que les méthodes qui en résultent sont seulement consécutivement transférés à des applications en dynamique des structures.

## Guyan Reduction

La réduction de Guyan a été proposée par Guyan [90] et se situe entre une réduction pure par projection sur une base réduite et le concept d'introduire les coordonnées de maître et de l'esclave, comme il sera présenté en détail dans la section 3.1.2.4. Dans la section 3.1.2.2 la réduction de Guyan est présentée dans son intention initiale comme une approche de réduction pour les systèmes linéaires. Depuis sa création, elle a toutefois subi une transformation énorme en devenant la base des techniques de sous-structuration, par exemple la méthode de Craig-Bampton (Bampton and Craig [20]). Cette branche de développement n'est pas considérée parce que l'idée de sous-structuration, le couplage des structures différentes à leurs interfaces mutuelles, ne se prête pas à la réduction d'une structure unique et uniforme.

Etant donné  $n$  déplacements physiques  $u_i$ , la réduction de Guyan les divise en  $r$  coordonnées maître  $q_k$  et  $n - r$  coordonnées esclaves  $\tilde{u}_l$ , qui sont pas contraint par l'excitation. Ensuite, les coordonnées esclaves  $\tilde{u}$  sont exprimées en fonctions des coordonnées maîtres  $q$  avec une transformation de coordonnées utilisant des renseignements de la formulation d'équilibre, c'est à dire la matrice de masse et la matrice de rigidité. Les coordonnées généralisées  $q$  sont un sous-ensemble des déplacements physiques  $u$ .

En raison du fait que les coordonnées maîtres  $q$  conservent leur signification physique, la réduction de Guyan est particulièrement adaptée pour coupler des physiques différents. Si par exemple une structure est noyée dans un fluide, et les deux domaines sont discrétisés dans l'espace, les déplacements de l'interface de la structure devient les coordonnées maîtres  $q$ . Les déplacements internes de la structure, qui n'interagissent pas avec le fluide, deviennent les coordonnées esclaves  $\tilde{u}$ . En outre, comme la partie de la force externe qui correspond aux coordonnées esclaves  $f_{E,q}$  doit être tous égaux à zéro, les déplacements soumis à une force provenant du fluide environnant sont conservés. Cela permet de réduire efficacement le modèle structurel aux déplacements qui sont d'intérêt pour la simulation de fluide et d'alléger le code couplée de la nécessité de calculer les déplacements internes de la structure.

## Balance harmonique trancée

La méthode de la balance harmonique trancée est présenté dans la section 3.1.2.3. La méthode de la balance harmonique trancée suppose l'historique en temps des déplacements  $u(t)$  à être représenté par une série de Fourier et présente les formulations ainsi obtenues dans l'équation du système. Cette idée apparemment simple exige néanmoins de nombreux calculs et est simple uniquement pour les systèmes linéaires. On suppose que la réponse soit de la même fréquence que l'excitation mais avec une amplitude et une phase à déterminer.

La création de cette méthode est attribuée à Bailey [18] et depuis a été largement appliquée aux réseaux électriques, par exemple, El-Rabaie et al. [73], et des systèmes tels que l'oscillateur Duffing par Beléndez et al. [27] et Özis and Yildirim [165]. Pour les applications en aérodynamique, la méthode de la balance harmonique trancée se prête naturellement à des problèmes essentiellement harmoniques tels que les rotors d'hélicoptères, comme le prouve Ekici et al. [72]. Applications en dynamique des structures non linéaires comprennent par exemple problèmes de contact rotor-stator, comme une enquête par Groll and Ewins [86].

Le résultat de la méthode de la balance harmonique trancée est la solution de l'état d'équilibre. Une solution qui ne peut être atteint qu'imparfaitement avec les techniques de solutions transitoires présentées dans la section 3.2.

## Nonlinear Normal Modes

Modes normaux non linéaires (NNM) sont une extension conceptuelle des modes normaux linéaires connus (LNM), car ils ont été introduits dans la section 3.3.1, mais leur construction est basée sur un concept tout à fait différent. Ils décrivent la dépendance de tous les degrés de liberté c'est le système sur un ensemble de coordonnées maître, qui doivent être choisis parmi les degrés de liberté du système. De cette façon, modes normaux non linéaires réduisent systèmes complexes à un degré multiple simple ou faible du système de liberté sans projection.

NNMS s'efforcent de trouver des relations explicites entre les  $u_i$  et le  $q_k$ , de sorte que les  $q_k$  restent des déplacements physiques  $u_k$  qui ne coïncident pas avec les autres  $u_i$  et  $i \neq k$ . Au lieu d'utiliser une projection comme dans l'équation (3.1) la relation entre les déplacements du système haute-fidélité et les déplacements du système d'ordre réduit est désormais rédigé comme équation (3.29). Par opposition à l'équation (3.12), où les  $q_k$  sont des coordonnées modales, au cours d'une réduction de mode normal non linéaire du  $u_k$  rester déplacements physiques et sont maître libellés coordonnées en raison de leur semence en fonction de la réduction.

Du point de vue historique, il est à noter que Rosenberg [192] décrit NNMS pour les systèmes conservateurs comme une "vibration en unisson" de degrés de liberté du système. Cette première description graphique de NNMS a ensuite été étendu à l'approche de la variété invariante soi-disant par Shaw and Pierre [204], qui sera élargi plus tard dans cette section.

Si un système discrétisé a  $n$  degrés de de liberté en déplacement  $u_i$  avec les  $n$  vitesses correspondantes  $\dot{u}_i$ , l'espace des phases du système est de dimension  $2n$ . Parmi ces  $n$  degrés de liberté d'un déplacement-vitesse-pair  $\{u_k, \dot{u}_k\}$  peuvent être choisis sous forme de coordonnées de base. Le NNM est maintenant le  $2n -$  collecteur dimensions 2 dans l'espace des phases dimensions du système qui exprime tout esclave coordonne  $\{u_i, \dot{u}_i\}$  par  $1 \leq i \leq n$  et  $i \neq k$  sous forme de coordonnées en fonction du maître  $\{u_k, \dot{u}_k\}$ , ce qui réduit efficacement le système à un seul degré de système de liberté. Ce collecteur est appelé non linéaire invariante car chaque mouvement du système initié dans le collecteur reste à l'intérieur du collecteur. C'est une propriété qui est partagée par les deux modes normaux linéaires et non linéaires. Kerschen et al. [117] soulignent que le lien entre les modes normaux non linéaires et les modes normaux classiques, linéaires réside dans le fait que les LNMs, qui représentent des surfaces planes dans l'espace des phases, sont tangents aux collecteurs courbe des NNMS dans le point d'équilibre du système.

Opposé à leurs homologues linéaires, non linéaires modes normaux présentent deux différences décisives:

- NNMs ne peuvent pas être superposés
- NNMS n'ont pas de relation d'orthogonalité stricte - ce qui signifie qu'ils ne sont pas linéairement indépendants.

Dans le cadre de cette section, l'examen des techniques de résolution est limitée aux exigences des systèmes discrétisés. Pour une revue exhaustive des techniques analytiques directes pour la construction de modes normaux non linéaires des systèmes continus on peut se référer à Nayfeh [159] et, d'autre exemple, pour Rand [184] ou Bellizzi and Bouc [33]. L'ensemble de la théorie et de la formulation numérique de NNM, comme il a été utilisé pour les expérimentations numériques, est présentée dans la section annexe D.

## Proper Generalised Decomposition

La brève expansion de la décomposition généralisée correcte (PDG) dans la section 3.1.2.5 suit le travail de Ammar et al. [7] et Ammar et al. [9], qui, dans leur mise en page complète de la méthode PGD, donnent une très aperçu complet. La portée de l'aperçu ci-dessous est toutefois limitée dans le détail parce que, dans la section suivante, le principal centre d'intérêt se situe sur la formulation discrète.

Le PDG est une approche qui sépare les variables d'un problème et cherche des solutions isolées pour chaque variable tout en imposant des conditions pour que les différentes solutions dans leur ensemble répon-

dent au problème initial. En tant que tel, cette approche de variables séparées est applicable à presque tous les problèmes et il ne se limite pas au domaine de la dynamique des structures. Il a cependant un équivalent très proche en dynamique des structures classiques, par exemple, où les théories de plaques et coques fournissent une illustration de cette approche. La contraction de l'enveloppe ou de propriétés de la plaque sur la description de la fibre neutre est une telle réduction. Elle illustre la séparation des trois variables de l'espace dans une partie orthogonale au plan neutre, et dans le plan de la fibre neutre lui-même. Ces pièces sont résolues séparément et les conditions sont données pour connecter ces parties de telle sorte que leur totalité décrit le comportement de la coque ou de la plaque.

L'idée de base du PGD consiste à exprimer la quantité recherchée  $u$  en tant que produit indépendant, les fonctions du noyau mono-dimensionnelles de ses variables. Comme les déplacements dynamiques d'une structure tridimensionnelle  $u = u(x_1, x_2, x_3, t)$  dépendent de l'espace à trois coordonnées  $x_1, x_2$  et  $x_3$  et le temps  $t$ , ils peuvent être exprimés dans le sens d'un PGD comme dans l'équation (3.43) si un nombre égal  $r$  de fonctions de réduction pour les trois dimensions de l'espace est utilisé. La même notion d'assemblage d'une fonction de fonctions du noyau est également appliquée aux déplacements virtuels pour l'équation (3.44). La puissance de cette approche de variables séparées, c'est que l'équation (3.43) peut être étendu si nécessaire. Si par exemple les déplacements dépendent également un paramètre externe  $\mu$ , cela poserait pas de problème pour développer l'équation (3.43) avec les fonctions du noyau supplémentaires  $F_{\mu,k}(\mu)$  pour prendre pied la dépendance de la solution sur le paramètre en compte. S'il ya plusieurs paramètres, une fonction de noyau supplémentaire pour chaque paramètre peut être inclus sans complexifier le problème.

Même si une discrétisation reste nécessaire, le mérite de la décomposition généralisée correcte réside dans la réduction considérable de l'effort de calcul de cette discrétisation et sa solution numérique. Cela est dû au fait que ce n'est plus le système physique qui est discrétisé mais sa représentation abstraite, réduite.

## Chosir une methode de reduction

Le choix d'une approche de réduction approprié est difficile. Les approches évaluées ci-dessus sont développées avec des objectifs différents et répondent à des exigences différentes.

Dans le cadre de cette étude, les approches de réduction doivent répondre à l'exigence de fournir un outil de calcul, qui doit recréer la solution transitoire de commande complète d'un système géométriquement non linéaire, non-conservateur, aussi fidèlement que possible, tout en réduisant considérablement le coût  $\frac{1}{2}t$  de calcul, comme indiqué dans la section 3.1.1.

C'est contre cette exigence que les approches de réduction sont jugées. Cependant, la plupart d'entre eux ne proposent également des caractéristiques spécifiques supplémentaires qui sont inclus dans l'évaluation.

La projection sur une base réduite de la section 3.1.2.1 est l'approche standard pour la réduction des problèmes dans les dynamiques structurelles de contexte. Cette est compréhensible, car certaines bases réduites ont un sens physique et ainsi contribuent non seulement à la solution, mais aussi à l'interprétation du problème. Il s'agit d'une approche modulaire avec une séparation claire de la réduction, par projection sur une base réduite, et la solution du système réduit. Cela implique que, d'abord, un système d'intégration adapté peut probablement être trouvé pour un problème donné et, si elle est formulée correctement, ce système d'intégration ne fait pas de distinction entre l'réduit et le système de commande complet. Par ailleurs, et d'autre part, une base réduite peut être choisie, qui fournit une performance optimale pour le problème à la main, et qui peut être facilement adapté à la taille. Son caractère modulaire permet également de focaliser les adaptations nécessaires, sur la base réduite ou sur l'algorithme pour obtenir la solution transitoire.

La réduction de Guyan, présenté dans la section 3.1.2.2, est une technique monolithique. Il offre quelques points de départ pour les extensions. En outre, il est conçu pour des problèmes linéaires et a subi aucune évolution significative depuis ses commencements. Il peut donc être considéré comme un bien développé et stable, la méthode et la conversion de la solution des systèmes non linéaires ne semble pas montrer beaucoup de promesses.

La méthode de la balance harmonique tronquée, section 3.1.2.3, est également une approche monolithique. Il est conçu pour les solutions stationnaires. Là encore, les modifications nécessaires à l'obtention de solutions transitoires sont jugés comme n'étant pas trop prometteur. Ceux-ci seraient encore plus compliquée par le fait que la réduction et la solution ne sont pas clairement séparées au sein de l'approche de la méthode d'équilibre harmonique tronqué.

Les modes normaux non linéaires, section 3.1.2.4, ont été conçues comme un outil d'analyse pour étudier les orbites stationnaires déjà, des systèmes simples de basse dimensionnalité. Ce n'est que récemment que leur application a été étendu à la réduction de modèle. Cependant, pour la réduction des grands systèmes dynamiques structurelles, elles semblent encore limitée par l'intention originale de leur création. Leurs propriétés, en particulier l'impossibilité de superposer les modes, et donc de changer facilement l'ordre du système réduit, si nécessaire, des arguments solides contre leur application sur un problème aussi vaste que la solution transitoire de l'équation (2.82), ce qui est pas encore défini en détail. Enfin, les NNMS sont déjà une approche monolithique, dans lequel la réduction et la solution sont intimement fusionnés, ce qui rend toutes les extensions possibles difficile.

La décomposition généralisée correcte, section 3.1.2.5, est le plus récemment développé l'une des approches étudiées le. Il a donc l'avantage d'être encore une approche ouverte qui pourrait facilement extensible au besoin. D'autre part, il est certainement encore aux prises avec des problèmes de dentition et ne donc pas offrir une plate-forme éprouvée pour d'autres extensions, qui pourrait s'appuyer sur sa robustesse inhérente. Enfin, le PDG commence au niveau d'une description continue du problème, et cela est en contradiction avec les objectifs déclarés de cette étude, ce qui suppose le problème sous-jacent déjà discrétisé.

Contre l'exigence donnée et avec un fort accent sur les besoins prévus pour adapter l'approche de la réduction la plus modulaire de la projection sur une base réduite est choisie.

La première des éventualités suivantes à des sections est consacrée à l'introduction du régime Newmark, un schéma d'intégration temporelle de la solution transitoire de la pleine commande et systèmes de commande réduits ressemblent. Dans la deuxième partie d'une sélection de base réduite commune est présenté, qui sera finalement testés pour leur aptitude à réduire un système géométriquement non linéaire.

## **Comparer les bases réduites et tester leur robustesse**

La préparation de la méthode pour décrire, résoudre et réduire un système géométriquement non linéaire est terminée. Les méthodes qui sont choisies sont le schéma non linéaire du Newmark pour la solution transitoire et la projection sur une base réduite pour la réduction. Maintenant des expériences numériques sont effectuées dans le but de déterminer laquelle parmi les bases réduites présentées est particulièrement apte pour la réduction d'un système non linéaire et si une base réduite est particulièrement robuste face a un changement des paramètres. Ce objectif double définit la structure de cette section.

La section commence avec la préparation des éléments nécessaires pour les expériences numériques. Ces éléments sont un description détaillée des objectifs et de l'étendue de l'étude face a son objectif double de comparer les bases et d'étudier leur robustesse. L'élément suivant est la définition des cas-test, qui sont définis comme les combinaisons de deux systèmes non linéaires différentes et deux excitations transitoires différentes, et leurs paramètres. Ensuite, le développement des critères adaptés, qui permettent de juger la performance des bases réduites face au but de cette étude, est détaillé.

Dans sa partie majeure, cette section contient deux études complètes. La première étude compare les bases réduites entre elles en les appliquant aux quatre cas-test. La deuxième étude prend les bases de projection telles qu'elles étaient construites lors de la première étude et teste leur performance si elles sont appliquées sur un système avec une excitation différente. Ces études démontrent que la décision pour la sélection d'une base réduite dépend, avant tout, sur le type d'excitation auquel le système non linéaire est soumis.

En outre il est démontré qu'aucune base réduite n'est capable de reproduire la solution complète avec la précision requise. Aussi, aucune des bases réduites testées ne donne une robustesse suffisante sous les critères appliqués.

Ces deux résultats demandent une approche beaucoup plus large qui va au delà de l'introduction d'une base réduite. Cette approche doit inclure l'algorithme de solution et aussi modifier la base réduite d'une manière adaptée. Elle conduit au chapitre 5, qui répond à ces deux points

## Preparer les études

La préparation des études en section 4.1 couvre les aspects de la définition de ses objectifs, et mettre en place les cas-tests et les critères conformément à ces objectifs.

La définition des objectifs de ces études distingue clairement les deux aspects de la comparaison des bases réduites et l'enquête de leur robustesse. Cette distinction se poursuit dans la définition des critères. Là, plusieurs critères couramment utilisés sont présentés et ils sont rassemblés dans deux métriques d'erreur simples: le score pour la comparaison et la performance relative de la robustesse. Enfin, les cas-tests sont définis. Encore une fois en conformité avec les objectifs des études, ils sont mis en place pour couvrir les différents scénarios de solutions transitoires des systèmes non linéaires.

Comparé à déjà publié fonctionne l'originalité de cette étude réside dans le fait qu'il examine rigoureusement les applications à privilégier pour la réduction des bases les plus couramment utilisés, tout en se limitant à des types génériques de systèmes non linéaires. L'étude vise à consolider la compréhension globale des domaines d'application des différentes bases réduites.

## Definir les buts de l'étude

Pour établir une base réduite toutes les méthodes pour la création d'une base réduite  $\Phi$  qui sont énumérés dans la section 3.3, les modes normaux linéaires, le Ritz-vecteurs, les différentes décompositions orthogonales, l'Une réduction Priori, la partition de Voronoï centres de gravité et la méthode de rigidité linéaire équivalent local, ont des façons très spécifiques de l'utilisation des informations du système, de l'excitation, et dans certains cas également de la solution. Les différentes méthodes donnent des résultats différents selon les types de non-linéarités et des excitations. La première partie de l'étude à entreprendre étudie précisément cette aptitude des bases différentes pour les différents cas-tests. Cette première partie est appelée la comparaison car il compare la réduction des bases entre eux.

Le but de cette étude comparative est double dans la mesure où, d'abord, elle permet de mieux comprendre la façon dont une certaine méthode de réduction joue sur une certaine combinaison de la non-linéarité et d'excitation, et que, d'autre part, cette présentation permet de comparer les différentes méthodes de réduction entre eux.

La deuxième partie de l'étude porte sur la robustesse inhérente des bases différentes. Toutes ces méthodes reposent sur les propriétés et les paramètres de la combinaison distincte de système non linéaire et excitation à l'étude, qui sont contenues dans les matrices et les vecteurs décrivant le système discret. Le fait que les modes linéaire normal, le Ritz-vecteurs, l'une diminution priori et la méthode de rigidité linéaire équivalent local ne nécessitent pas d'informations à partir de la solution du système de commandes bien rempli, leur permet d'être classés comme une des méthodes a priori. Face d'eux sont les soi-disant une des méthodes posteriori, la décomposition Proper Orthogonal, la décomposition orthogonale de la lisse et la partition de Voronoï centres de gravité, qui nécessitent des informations à partir d'une réelle, quoique solution d'ordre peut-être que partiel, complet. Aucune de ces deux catégories de bases peut être simplement s'appliquer à d'autres cas-tests comme ceux qu'ils ont conçus. Cette deuxième partie est appelée l'enquête de robustesse.

Cette étude de la robustesse détermine la robustesse des différentes méthodes de réduction s'ils sont confrontés à un cas-test paramétré différemment. Il prend les bases réduits qui sont établis pendant l'étude comparative et les utilise pour réduire les mêmes cas-tests avec excitations différemment paramétrées. Le

résultat de cette deuxième étude est un aperçu de la méthode doit être prévu pour être particulièrement robuste si elle est appliquée à un système en vertu d'une excitation qui n'a pas été utilisé pour le créer.

Un objectif souhaitable est certainement une procédure utilisant des bases optimales, pour construire un cadre robuste pour les simulations de différents et différemment paramétré structures non linéaires réduits.

Dans les limites de la sélection des méthodes et procédés solution pour générer les bases réduites qui en est faite dans le chapitre précédent 3, la présente étude est complète car elle couvre toutes les méthodes sélectionnées. Les bases réduites sont construits à partir de modes linéaire normal, le Ritz-vecteurs, propre et lisse décomposition orthogonale, soit une réduction Priori, tessellation de Voronoi centres de gravité et local méthode de rigidité linéaire équivalente, ainsi que de plusieurs variantes.

Ces deux objectifs sont conformes de l'exigence d'explorer l'application des bases réduites à des systèmes géométriquement non linéaires et d'étudier leur comportement dans différents paramétrages telles qu'elles sont énoncées dans l'introduction. D'autres essais avec d'autres objectifs ou autre ne sont pas menées.

### **L'évaluation des performances de comparaison en définissant le score**

L'objectif du système de notation par rapport à la section 4.1.2.2 est d'avoir accès à une classification complète des bases réduites. Il utilise un maximum d'abstraction pour la prise en compte de critères différents et permet d'évaluer la performance de la réduction des bases avec un maximum de distance conceptuelle à partir du moment-histoires réelles des solutions transitoires.

Pour faire face au nombre considérable de solutions réduit la performance des bases réduites est évaluée en appliquant un modèle de somme pondérée pour l'analyse de décision multi-critères. S'appuyant sur cette inspiration dans les multi-critères techniques d'analyse décisionnelle permet de combiner un ensemble de critères. Ce sont par exemple des moyens, à la racine par rapport l'erreur quadratique moyenne, la différence d'énergie et autres.

La théorie de l'analyse de décision multi-critères introduit la notion d'alternatives, qui correspondent à des choix possibles qui peuvent être faites. Ici, les alternatives sont des paires de base réduite et un ordre  $r$  du système réduite, par exemple le LNM à  $r = 4$  ou les vecteurs POD à  $r = 8$ . En incluant la commande du système réduit les alternatives permet par exemple qu'une base réduite à un moment donné  $r$  peut faire mieux que l'autre à une plus  $r$ . Pour chaque critère  $e$  un classement est établi dans lequel les paires sont placées à un rang  $\mathcal{R}_e^{(base,r)}$ .

Pour chaque paire d'une approche de base réduite et une commande du système réduite  $r$  les valeurs requises pour les paramètres sont extraits. Etant donné un cas-test les paires sont désormais évalués indépendamment pour chaque critère, soit un 1 est affecté à la paire pire performance de l'approche et  $r$ , un 2 est affecté à la deuxième pire rendement et le processus est répété jusqu'à ce que la meilleure paire performante reçoit le score le plus élevé.

Les classements sont alors réunis en une somme pondérée qui donne un score pour la paire. Ceci est illustré dans l'équation [eq: scoredifinition](#). La pondération favorise les valeurs moyennes des critères sur leurs écarts. Ces scores sont ensuite tracés par rapport à l'ordre du modèle réduit pour chaque base réduite pour permettre une évaluation de la performance des bases. Le score est également utilisé pour évaluer la pertinence des termes de second ordre.

A pointage  $\mathcal{R}_e^{(base,r)}$  plus élevé indique une paire plus performante.

Une valeur inférieure à aucun de ces critères donne un meilleur classement parce que tous ces critères doivent être réduites au minimum. Pour chaque paire les scores pour les différentes métriques d'erreur sont ensuite pondérées correspondant à l'importance qui est attribué à la métrique d'erreur individuel et un score intégré unique peut être affectée à chaque paire étant constituée d'une approche et un  $r$ .

Le temps global de réduction, c'est à dire le temps global du processeur pour établir la base réduite, la résolution du système réduite et revenant à une solution d'ordre complet, ce qui est une mesure de l'effort

total nécessaire pour obtenir le temps historique des déplacements par l'intermédiaire d'une procédure de réduction, est fourni uniquement avec une très faible poids. Cela est dû à des raisons numériques qui ne permettent pas une exploitation précise de ce critère. Il fait l'objet d'une étude spécifique dans la section annexe A.2.1. Le MAC de l'équation (4.10) n'est pas inclus dans le score car il est défini pour comparer les vecteurs colonnes de la base réduite et non le temps-histoires des solutions.

Le  $Note^{(base,r)}$  est alors tracée en face l'ordre  $r$  du système réduite. Les méthodes de création de la base réduite ajoutent une dimension supplémentaire à l'intrigue et sont traités par les différents symboles et couleurs. Cela permet d'évaluer les performances des bases d'un seul coup. En outre, en traitant les classifications pour les critères distincts comme les colonnes d'une base de données, des observations complémentaires peuvent être obtenues, par exemple, la variance des classifications pour une paire spécifique ou classification maximale de la paire.

### **L'évaluation du rendement de la robustesse en définissant la performance relative**

Vigo [238] définit dans sa robustesse de mémoire dans le cadre de la dynamique des fluides comme " la capacité de la POD [procédé] pour recréer correctement un flux similaire à, mais distinct de l'écoulement initial, utilisé pour la création de la base. Cette définition est basée sur une méthode de réduction POD, mais que le système de commandes bien rempli sous-jacente est le facteur dominant dans la détermination des bases différentes  $\Phi$  pour les différentes méthodes basées sur la réduction discutés dans les sections 3.3.1 à 3.3.4.1 elle peut être étendue à toutes les méthodes de réduction à base de projection aussi bien, si l'adaptation nécessaire de la dynamique des structures sont faites ainsi.

Dans le cadre de cette étude, la robustesse de la méthode de réduction à base de projection est défini comme la capacité de la méthode de recréer correctement une solution transitoire d'un système similaire, mais distinct du système initial, utilisé pour la création de la base. Une telle similitude pourrait signifier des différences de paramètres externes  $\mu$ . En tant que tel de la robustesse d'une méthode, ou l'absence de celui-ci, sera un critère pour la qualité de la base réduite. Une base solide réduit est considéré comme positif, car il peut être utilisé pour réduire systèmes avec des valeurs différentes pour les paramètres extérieurs. L'application d'une méthode moins robuste aux systèmes avec différents ensembles de paramètres extérieurs  $\{\mu_1, \dots, \mu_m\}$  conduirait à une solution transitoire réduite à des niveaux trop élevés d'erreur. Dans un tel cas, une nouvelle base réduite est nécessaire pour être construit spécifiquement pour le jeu actuel de paramètres externes ou la base réduite existante doit être adaptée pour fonctionner correctement avec la configuration actuelle des paramètres.

avec leur associé, bases précalculées devront être explorées que pour une méthode plus robuste.

Une autre approche importante pour juger de la robustesse d'une méthode est sa capacité à gérer les perturbations. La robustesse de la méthode indique sa capacité à traiter des perturbations d'origine physique et numérique qui peuvent avoir une influence sur l'exactitude ou même sur la stabilité de la solution.

Suivant ce raisonnement, il peut être nécessaire de sacrifier la vitesse de robustesse dans un compromis afin d'obtenir une méthode qui est stable.

Pour évaluer la robustesse de la base de leur performance doit être évaluée par rapport à une configuration de référence. Le rendement relatif est introduit en tant que l'inverse de la somme pondérée de l'écart moyen par rapport, l'écart d'oscillation relative, la moyenne de la racine par rapport l'erreur quadratique moyenne et la variance de la racine par rapport l'erreur quadratique moyenne de la solution réduite, à part, tous normalisé avec les valeurs respectives de la configuration de référence. Il couvre plusieurs aspects du comportement de la solution dans le but de capturer des améliorations dans le comportement qualitatif qui n'est pas pris en compte par le R2MSE seul. Ceci est fait dans l'équation (4.12) La performance relative utilise les mêmes poids que le score et il est écrit que l'inverse de la somme pondérée afin d'avoir la même orientation que le score. Pour une performance relative égale à une réduction de la base fonctionne aussi bien pour l', configuration réelle paramétrée différemment que pour la configuration de référence. Une performance relative supérieure à un indique une meilleure performance pour la configuration paramétrée

différemment. Les valeurs inférieures à un indiquent une diminution des performances.

## Observations de l'étude comparative

Outre les avantages et les inconvénients respectifs de chaque méthode et ses variantes possibles, il semble que les résultats les plus importants à tirer de cette étude dans la section 4.2.1.4 sont que le bien-fondé d'une méthode de réduction est principalement déterminée par l'excitation du système et les propriétés de l'historique de déplacement qui en résulte, et seulement dans une moindre mesure par la nature de la non-linéarité dans le système. Surtout en ce qui concerne la réponse plus lisse et régulier des deux systèmes sous excitation harmonique, ceux-ci semblent être les propriétés qui permettent une réduction réussie si toute méthode appropriée est sélectionnée. Toutes les bases sont moins adaptés pour les excitations d'impulsions, où même les bases POD ne sont pas plus performants que les bases LNM. Toutefois, pour les deux méthodes, ce qui se passe à un niveau d'erreur plus élevé que pour les cas-tests avec excitation harmonique. La performance globale similaire de LNM et POD bases appuie les conclusions de Sampaio and Soize [198], qui affirment que les bases LNM sont aussi efficaces que les bases POD pour leurs applications.

Parmi les méthodes étudiés, la qualité de la solution reconstituée varie grandement selon le cas-test. Les conclusions générales peuvent être tirées de l'inspection des figures 4.13 à 4.16 sont:

- les modes normaux linéaires sont parmi les meilleures méthodes de réduction performants pour le local et le système entièrement non-linéaire sous excitation d'impulsion et demeurent applicables malgré les non-linéarités présentes dans le système. Si une excitation harmonique est appliquée, leur performance se dégrade. Leur mise en place au déplacement maximum a une influence positive seulement pour le système non linéaire localement sous excitation harmonique. La même chose s'applique pour l'inclusion de deuxième ordre Conditions.
- le Ritz-vecteurs Excel pour le système non linéaire localement sous excitation harmonique, où ils montrent un grand avantage sur les variantes LNM.
- la base de décomposition Proper Orthogonal classique est constamment parmi les meilleures bases performants quel que soit le système ou l'excitation. Son enrichissement avec les déplacements maximaux se détériore toutefois légèrement l'excellente performance et est donc inacceptable, pour un ordre fixe  $r$  du système réduite. Sur le plan négatif, il nécessite la connaissance de la solution complète de la commande.
- La décomposition orthogonale lisse peut être considéré comme méthode de réduction utile, étant à égalité avec le POD classique, mais nécessitant beaucoup plus d'effort.
- la Une réduction Priori effectue pas aussi bien que d'autres méthodes et surtout s'ils sont liés à l'effort nécessaire pour calculer sa base. Si son application s'avère nécessaire, il est mieux adapté pour des excitations harmoniques sur les systèmes localement et entièrement non-linéaires. Son application à des systèmes sous une excitation d'impulsion doit être évitée car cette méthode n'a pas à faire face ainsi à l'évolution rapide déplacements résultant de l'impulsion.
- la partition de Voronoï centres de gravité permet des résultats raisonnables, en particulier pour le système non linéaire localement sous excitation harmonique. Pour excitations d'impulsions, il est comparable à l'APR.
- l'approche de la méthode de rigidité linéaire équivalent local donne des bases qui effectuent similaire au LNM, avec toutefois une légère amélioration pour le système non linéaire localement sous excitation harmonique.

L'évaluation complète de la performance des bases est condensée dans le tableau 4.2. Il montre la préférence relative des bases pour une combinaison donnée de non-linéarité et d'excitation. Les niveaux d'erreurs absolues des cas-tests ne sont pas inclus.

## Observations de l'étude de la robustesse

Les résultats détaillés dans la section 4.2.2.3 certainement permettent de conclure qu'aucune des méthodes étudiées est constamment robuste par rapport aux variations du forçage externe. Et cette conclusion hérauts et l'enquête sur l'utilisation des techniques d'adaptation qui sont discutés dans la section 5.3. Mais un examen attentif des résultats de cette étude permet de décider quels paramètres sont quand à être utilisé dans le cadre d'une telle adaptation.

Parmi les lacunes de toutes les méthodes le plus récurrent autre pour toutes les méthodes est l'extrême sensibilité par rapport aux variations du point d'application de l'excitation pour le système non linéaire entièrement soumis à une excitation  $\delta$  Dirac. Si l'amplitude de la force est modifiée, toutes les bases réduites reproduire approximativement les niveaux d'erreurs qu'ils produisent au cours de l'étude précédente pour cette combinaison de la constitution du système et d'excitation sous la configuration de référence. Changer le point d'application se détériore gravement les performances des bases. Même l'APR, qui ne parvient pas à recréer la solution de référence pour la configuration de référence des cas-tests avec excitation d'impulsion en premier lieu, se détériore davantage dans la performance.

Pour les essais des cas sous excitation harmonique doubler la fréquence pose des problèmes majeurs à toutes les méthodes, mais la configuration avec l'autre point d'application, qui déplace le point d'application, détériore les performances de la plupart des méthodes d'.

En conclusion, on peut affirmer que, comme dans l'étude précédente, les performances des méthodes en ce qui concerne le critère choisi dépend essentiellement du cas-test, à savoir la nature de la force et du système. Et, si certaines configurations aucun test-case et aucune méthode de réduction est sujette à présenter suffisamment de robustesse pour contourner les techniques d'adaptation. Mais cette étude a révélé que la fréquence de l'harmonique de forçage est inévitablement à établir des priorités parmi les paramètres qui sont traités par la technique d'adaptation.

Ces observations peuvent être concentrés dans les tableaux 4.5 et 4.6, où les signes mathématiques indiquent différents degrés d'altération de la performance des bases POD en fonction de l'évolution du paramétrage de l'excitation et le cas-test (+ + la qualité de la solution de ROM augmente de manière significative, + la qualité s'améliore, o la qualité ne change pas, - la qualité diminue, - - de la qualité diminue significativement, paramètre non applicable na, × la solution ne converge pas, \* la solution dans la configuration de référence a déjà une qualité considérablement diminué ou il ne converge pas).

Un double et représente une part relativement importante amélioration et cette amélioration est censé diminuer si elle est consécutivement caractérisé par une simple plus ou encore un cercle, ce qui veut dire pas de différence entre les deux solutions. Les dégradations progressives de la solution sont caractérisés par un ou deux points négatifs.

Si déjà la solution de référence montrent une très faible qualité tous les symboles dans la ligne respective sont marqués d'un astérisque et ne sont pas pris en compte dans les considérations finales. Ceux-ci correspondent aux cas où la méthode respective ne parvient pas à recréer correctement une solution dans la configuration de référence en premier lieu. Ces cas sont identifiés lors de l'étude comparative dans la section 4.2.1.

En conclusion, on peut affirmer que, comme dans l'étude comparative, les performances des méthodes en ce qui concerne le critère choisi dépendent essentiellement de la nature de la force et seulement dans une moindre mesure du système. L'étude révèle une extrême sensibilité par rapport aux variations du point d'application  $p$  pour presque toutes les méthodes. Il provoque la détérioration la plus grave dans l'exécution. Deuxième à-dire le doublement de la fréquence, ce qui pose de graves problèmes à toutes les méthodes sur tous les cas-tests.

Il ya moins de problèmes apparaissant pour presque toutes les méthodes si l'amplitude de l'excitation harmonique est modifié. La même observation peut être faite pour les deux systèmes si l'amplitude de la  $\delta$  excitation Dirac est doublé.

Si un changement dans l'un des deux paramètres de l'excitation, de l'amplitude  $\hat{f}_E$  ou fréquence  $\Omega$ , provoque l'exécution d'une méthode de se détériorer, cette diminution pourrait être moins prononcée si la respectue paramètre est réduite, c'est à dire si le système est forcé à osciller avec une amplitude plus faible ou plus lentement, en raison d'une diminution de la fréquence d'excitation. Si l'amélioration des performances d'une base déjà existante peuvent être attendus, ils sont plus susceptibles de se produire si la base est appliqué à un cas où les valeurs de ces deux paramètres sont revus à la baisse. La recommandation de cette observation est d'établir les bases sur les valeurs les plus critiques pour le forçage externe avant de les réutiliser sur excitations moins exigeants.

Sauf pour certaines configurations, aucune base réduite présente suffisamment robuste pour contourner les techniques d'adaptation. Le point d'application d'une excitation et la fréquence d'un harmonique de forçage sont inévitablement à établir des priorités parmi les paramètres qui sont traités par une technique d'adaptation.

Les trois principales conclusions à tirer de cette étude de la robustesse des bases sont les suivantes:

- changements d'amplitude ont beaucoup moins, et parfois quasiment aucun impact, que les changements dans la fréquence et surtout changer le point d'application car elle ne modifie pas la structure des déplacements, qui sont prélevées dans les vecteurs de la base.
- les performances d'une base appliquée à un système différent de celui qu'il a été construit avec des baisses beaucoup moins si le système original fonctionne à une valeur plus critique du paramètre respectif.
- chaque méthode simple manque de robustesse et nécessitera donc l'utilisation de techniques d'adaptation si elles doivent être appliquées à différents systèmes. Les différences de performances sont plus marquées entre les cas-tests qu'entre les méthodes elles-mêmes.

Comme un remède possible pour le manque de robustesse établi, Amsallem et al. [11] propose une approche beaucoup évolué pour l'interpolation entre des bases réduites, qui repose sur une interpolation dans un espace prévu, tangente à la une des bases réduites. Une autre approche, proposée par Hay et al. [95], repose sur la sensibilité de la base de projection par rapport aux paramètres extérieurs. Une méthode d'instantanés entrelacés de modèles paramétrés différemment est disponible, mais limitée aux méthodes de décomposition orthogonale. Ces approches peuvent être trouvés parmi les méthodes de sous-espace Lagrange ou la décomposition Proper Orthogonal composite pour la mécanique des fluides, par exemple Ito and Ravindran [105] et Taylor and Glauser [220], respectivement. Une autre approche liée à POD sont les modes dits décalage, ou des modes non-équilibre, proposés par exemple par Noack et al. [162] et Bergmann and Cordier [36], qui ajoutent un vecteur pointant d'une configuration à une autre à la base POD, qui devrait être prometteur si les deux excitations ont des moyens différents. En ajoutant simplement un vecteur, cette approche présente une certaine similitude avec la technique de POD améliorée, discuté à la section 3.3.3.3.

## Discussion des résultats de l'étude numérique

En utilisant quatre combinaisons différentes de systèmes non linéaires et les excitations d'une étude comparative et une étude sur la robustesse de plusieurs bases réduites communes est entrepris.

Les résultats de l'étude comparative permettent indentifying l'application préférée en termes de type de non-linéarité et le type d'excitation pour chaque base réduite. Ils mettent en valeur que le choix d'une base de réduction spécifique pour un système non linéaire doit être basée essentiellement sur le type d'excitation à laquelle est soumis le système. La constitution de la non-linéarité est seulement un critère supplémentaire. La base la plus adaptée doit être choisi avec soin parmi ceux présentés sur une base de cas par cas et en suivant les lignes directrices établies. Bases POD spécialement construits sont constamment les meilleurs de la scène, expliquant leur utilisation généralisée. Pourtant, il est surprenant de constater que les modes normaux linéaires sont, en général, l'exécution aussi bien que les bases de décomposition orthogonale appropriée ou seulement légèrement pire.

Les résultats de l'étude de la robustesse permet de juger de la solidité des bases réduites si elles sont appliquées à un cas-test paramétré différemment et d'identifier les paramètres de l'excitation qui ont le plus d'impact sur les performances d'une base réduite. Le point d'application de toute excitation et la fréquence d'un harmonique forçant sont inévitablement à établir des priorités parmi les paramètres qui sont traités. En outre, l'enquête montre aussi clairement que, si l'utilisation d'une seule base sur un système sous excitations différemment paramétrées devenu nécessaire, cette base doit être établie avec les valeurs les plus critiques pour les paramètres.

Cependant, les résultats révèlent également un certain nombre de lacunes.

En ce qui concerne l'attente formulée initialement d'identifier une base unique, qui est particulièrement bien adapté pour le traitement de structures non linéaires, il doit être précisé que, en fait, aucune base est largement adapté à tous les types de non-linéarités et pour chaque cas spécifique.

En ce qui concerne la robustesse inhérente aux différentes bases, on peut affirmer qu'aucun des bases étudiées possède cette propriété particulière dans une mesure souhaitable suffisante.

Pas de base est assez bon avant que les critères appliqués. Ce résultat est un peu décevant, car un grand nombre de bases réduites commun a été étudiée dans des conditions quasi-optimales. Cela inclut par exemple le POD, qui pourrait utiliser tous les clichés disponibles. Et aussi les modifications qui ont été spécifiquement ajoutés à certaines bases réduites n'ont, malgré certaines améliorations, ne contribuent façon substantielle à la qualité de la solution. Des exemples de telles modifications sont par exemple l'utilisation de la MAC pour la CVT dans la section 3.3.5, ou l'extension de la LELSM aux systèmes entièrement non-linéaires dans la section 3.3.6.2.

Des efforts supplémentaires sont donc pas destinés à proposer une autre base réduite. Au lieu de cela, la recherche doit se concentrer sur d'autres éléments du processus de résolution de systèmes réduits.

En particulier, les besoins qui sont identifiés dans cette étude et qui restent sont

1. adaptation du procédé en solution temps-marche de sorte qu'il tienne compte de l'évolution non linéaire de la solution,
2. qui rend le système autonome à nouveau réduite, et
3. ajout d'une méthode qui permet le paramétrage du procédé en solution réduite.

Ces exigences doivent être respectées pendant la tenue de l'algorithme global applicable aux structures de taille industrielle.

## **Répondre aux exigences identifiées d'un algorithme de solution adapté, de l'autonomie des termes nonlinéaires et du paramétrage**

Cette section réponds aux résultats de l'étude numérique. Les résultats du chapitre 4 ont l'air d'indiquer qu'aucune de bases réduites étudiées ne répond aux critères de qualité et de robustesse d'une manière satisfaisante. En regardant les efforts considérables nécessaires pour construire certaines bases réduites il est décevant de voir les bases courir à l'échec. Alors, la proposition d'encore une nouvelle base réduite ne semble pas être un chemin très prometteur à suivre pour le traitement des systèmes nonlinéaires réduits.

La plupart des méthodes présentées est illustrée et testée indépendamment l'une de l'autre avec une application sur les cas-test de l'étude numérique du chapitre 4. La décision est prise de présenter une sélection des méthodes communes pour chaque exigence dans le but de préparer une boîte à outils. A partir de cette sélection de différentes méthodes le choix peut alors être fait selon les besoins du cas-test.

Le résultat principal de cette section est le choix d'une méthode en réponse pour chacune des trios exigence identifiées.

Pour l'adaptation de l'algorithme de solution l mise-a-jour et augmentation de la base réduite est dévelop-

pée et choisie. D'autres approches qui sont testées sont la correction quasi-statique et la méthode Least-Squares Petrov-Galerkin.

L'autonomie des termes nonlinéaires est assurée avec le choix de la formulation polynomiale. La propriété décisive de la formulation polynomiale est qu'elle peut être rendue indépendante de la base réduite. Cette exigence cruciale est une conséquence directe de choix de l'approche mise-à-jour et augmentation de la base réduite.

Pour l'adaptation des bases réduites en fonction des paramètres une approche élégante d'interpolation dans un espace tangent est choisie de la littérature.

Ces trois éléments forment la réponse triple qui répond aux trois exigences identifiées comme étant des points clés pour le succès d'une réduction d'un système géométriquement nonlinéaire parameterisable dans le but d'obtenir une solution transitoire. Dans la prochaine étape ces trois méthodes sont combinées et appliquées à des cas-test en éléments finis.

## Adaptation de l'algorithme de solution

Les résultats de l'étude comparative dans la section 4.2.1.4 montrent que l'introduction d'une base réduite seule n'est pas suffisante pour réduire avec succès un système non-linéaire. En outre, il semble avoir été prouvé que cela est vrai pour toutes les bases réduites appliquées et que la plupart peut-être il n'y a pas de base réduite qui est adaptée aux systèmes non linéaires de manière satisfaisante. Par conséquent, dans la section 4.3, la décision a été prise à diriger des efforts supplémentaires dans le but de réduire un système non linéaire doivent être adressées à l'adaptation de l'algorithme de solution plutôt que sur la base réduite.

Cette section examine comment les algorithmes de résolution peuvent être adaptés pour résoudre des systèmes non linéaires réduits avec une erreur inférieure à celle obtenue avec l'introduction de la base réduite seul.

L'adaptation de l'algorithme de résolution doit parvenir à des limites relativement étroites. Il doit être compatible avec le schéma de Newmark non linéaire (section 3.2.2) et la HHT- $\alpha$ -méthode parce que ces algorithmes de résolution ont été choisis dans la section 3.1.3 pour fonctionner avec l'approche de bases réduites. De plus, une adaptation intrusive minimale des systèmes existants est souhaitable pour des raisons pratiques telles que le codage et la vérification.

Heureusement, il existe déjà un certain nombre d'approches disponibles dans la littérature qui permettent d'adapter le schéma de Newmark non-linéaire à la réduction des solutions de systèmes non linéaires. Une fois l'équivalent réduit du régime réduit non linéaire Newmark est adapté de résoudre avec succès des systèmes non linéaires réduits, cette adaptation peut simplement être reportée à l'approche HHT- $\alpha$ .

Les approches communes qui sont sélectionnées pour être testées et qui sont présentées dans ce qui suit sont

- la correction quasi-statique, car il est élargi par exemple Hansteen and Bell [92],
- la méthode des moindres carrés Petrov-Galerkin, comme il est proposé par Carlberg et al. [55], et
- la mise à jour de la base réduite, ce qui est perçu comme une idée commune.

La correction quasi-statique et moindres carrés Petrov-Galerkin ont en commun qu'ils ont construit sur le schéma de Newmark non linéaire et sont spécialement conçus pour la solution transitoire des systèmes réduits. La mise à jour de la base réduite est plutôt un prolongement du régime réduit non linéaire Newmark et vise à rendre la base réduite suivre l'évolution non linéaire de la solution réduite.

Les trois approches sont comparées à la norme schéma non linéaire Newmark avec l'inflation comme une référence afin de déterminer s'ils donnent des avantages pour la qualité de la solution.

## Description et test de la correction quasi-statique

La correction quasi-statique est une amélioration possible du système non linéaire réduit Newmark. Il vise à re-y compris les déplacements dus à la part des forces extérieures, qui est coupée par la projection, c'est à dire qui sont perpendiculaires à la base.

La projection habituelle du vecteur des forces externes  $f_e$  est présentée dans l'équation (5.1) comme il est indiqué plus tôt dans l'équation (3.93). Mais cette simple projection du vecteur des forces externes a un prix, qui est très bien développé par Hansteen and Bell [92], avec un recours possible. L'utilisation de la correction quasi-statique a récemment augmenté dans l'intérêt nouveau par le travail de Thomas et al. [224].

Dans l'équation (5.1) forces extérieures réduites  $\tilde{f}_E$  ne contient termes de  $f_E$ , ce qui est normal  $\Phi$ . C'est bien sûr dans la nature d'une projection, qui a pour but la génération du vecteur dimensions  $r$   $\tilde{f}_E$  pour les forces extérieures réduites. Pourtant, du point de vue mécanique, on peut se demander si les composantes de  $f_E$  qui sont normales à  $\Phi$ , peut être négligé sans mettre en danger un résultat correct. Et c'est là que la correction quasi-statique se branche en trouvant les composantes de  $f_E$ , ce qui est normal  $\Phi$ , et la construction d'un terme de correction statique d'eux. L'objectif est donc de décomposer l'ordre complet des forces extérieures vecteur  $f_E$  dans une partie  $f_e^\perp$ , ce qui en l'espace de  $\Phi$ , et une partie complémentaire  $f_e^\parallel$ , ce qui est orthogonale à l'espace de  $\Phi$ .

## Présentation et discussion des méthode des moindres carrés Petrov-Galerkin

Les méthode des moindres carrés Petrov-Galerkin (LSPG) dans la section 5.1.2 est une variante du schéma de Newmark non linéaire original et remplace l'intérieur itération de Newton-Raphson, représentée par des équations (3.80) pour (3.83).

L'idée principale de la technique de réduction Petrov-Galerkin moindres carrés, est d'appliquer une projection sur la base  $\Psi$  de la valeur résiduelle  $r$  de la solution d'un système dynamique et d'adapter cette projection base que les déplacements évoluent. A cet effet, le  $\Psi = \Phi$ , tel qu'il est utilisé dans la section 3.2.2.1, est remplacé par le produit de la base réduite original et Jacobien du système  $\Psi = S\Phi$ . Avec cette approche, les crochets de technique LSPG au sein du schéma de Newmark non linéaire et modifie la manière, le résiduel  $r$  dans l'équation (3.81) est entraîné vers zéro. Parce que l'approche LSPG nécessite l'évaluation de la valeur résiduelle  $r$  et le Jacobien  $S$ , c'est à dire à savoir la matrice de rigidité tangente non linéaire  $K$ , à l'ordre complet, Carlberg et al. [55] conçu approximations de ces deux termes. Dans Carlberg et al. [56] c'est hyper réduction libellée, car il introduit une deuxième couche de réduction dans le processus.

La méthode a été introduite par Carlberg et al. [55], dont l'approche est esquissée ci-dessous. Leur approche est basée en partie sur les travaux de Bui-Thanh et al. [44], qui utilise une approche simple des moindres carrés avec un accent sur l'adaptation de la réduction pour différents paramètres externes. Une présentation générale de la méthode des moindres carrés est omis dans le champ d'application de la présente section. Kim and Langley [119] donner un bref aperçu et de montrer que les applications réussies de cette gamme de technique générique autant que la résolution des ambiguïtés de signaux GPS. Plus récemment, Carlberg et al. [56] a développé la méthode LSPG plus loin dans le Gauss-Newton avec tenseurs approchées (GNAT) méthode. La deuxième couche de réduction est formalisé comme hyper-réduction et la méthode est étendue aux calculs de volumes finis pour les applications en CFD. Cependant, l'hyper-réduction ne s'applique pas ici parce que ces approximations supplémentaires pourraient introduire des erreurs supplémentaires. Cet argument est similaire à celle faite pour justifier l'utilisation de la formulation de l'inflation pour les études numériques des bases réduites au chapitre 4.

Carlberg et al. [55] écrire sur les moindres carrés de projection Petrov-Galerkin que cette approche " peut capturer en principe les effets non-linéaires, mais est pratique surtout lorsque la réduction de modèle non linéaire est effectuée au niveau totalement discret." Cette affirmation est d'être vérifié par la suite, en

l'appliquant aux mêmes cas-tests que ceux utilisés pour les études numériques dans le chapitre 4.

### Mise à jour de la base réduite

La mise à jour de la base réduite dans la section 5.1.3 est une procédure qui rend la base réduite suivre l'évolution non linéaire de la solution transitoire. Une telle approche semble en ordre, car les résultats de l'étude comparative dans la section 4.2.1 montrent qu'aucune base réduite constante est satisfaisant pour une réduction réussie d'un système non linéaire pour une solution transitoire.

Pour la procédure de mise à jour d'un mécanisme doit être mis au point qui détermine la nécessité de mettre à jour la base sur le terrain d'une erreur qui mesure la qualité de la solution réduite et la mise à jour elle-même doit être défini. Ceci est exprimé par le paramètre de la fréquence d'actualisation  $m$  et la position au sein du régime Newmark, où les robinets de l'algorithme de mise à jour dans la totalité des déplacements de l'ordre  $u^{(t)}$  pour créer la nouvelle base. La mise à jour de la base réduite est moins intrusive sur le régime non linéaire réduit Newmark, de la correction quasi-statique et la méthode LSPG. Ces deux méthodes donnent des résultats plutôt décourageants dans leurs sections respectives 5.1.1 et 5.1.2 ci-dessus.

Si la base réduite, qui est mis à jour, est composé de la LNM l'approche est communément dénommés modes tangente, comme cela se fait par exemple Idelsohn and Cardona [102]. C'est parce que le LNM sont formés avec la commande complète matrice de rigidité tangente courant  $\bar{K}$  du régime Newmark non linéaire. Une telle approche est comparable à la création du LNM au courant de déplacement  $u(t)$  et utilise la technique décrite dans la section 3.3.1.2, mais avec le courant de déplacement au lieu de la déplacement maximal. Mais au-delà de la LNM des bases réduites peuvent être mis à jour au cours de la solution transitoire.

La mise à jour de la base réduite ne doit pas être confondue avec la mise à jour de l'ensemble du modèle, qui est un défi problématique commune dans le domaine de la résolution des problèmes inverses (par exemple Hemez and Doebling [96] et Galbally et al. [81]).

Dans ce qui suit, il sera explorée où et comment la mise à jour de la base réduite est introduit dans le système non linéaire réduit Newmark de la section 3.2.1.1. La mise à jour de la base réduite est facilement logé par le régime non linéaire réduit Newmark. Une caractéristique originale de la méthode de mise à jour proposée est l'augmentation de la base mise à jour avec des quantités physiques pour égaliser apparaissant sauts dans les déplacements, vitesses et accélérations. Une fois la mise à jour est introduit, un critère de roman est proposé qui déclenche la mise à jour basée sur une métrique d'erreur de la solution réduite.

### Résultats de l'adaptation de l'algorithme de solution

Le choix d'une adaptation de l'algorithme de solution, dans le but d'améliorer la qualité de la solution réduite, est principalement basée sur les résultats numériques qui ont été obtenus avec les trois méthodes de correction quasi-statique, méthode des moindres carrés Petrov-Galerkin et la mise à jour et l'augmentation de la base réduite. La limitation de cette étude qu'il n'y a aucune comparaison directe entre les solutions des trois méthodes demeure. Il s'agit d'un choix délibéré, car les différentes méthodes sont conceptuellement très différent au niveau algorithmique et il n'y a pas de solution de référence commun. Solutions de référence différents ont été choisis parce qu'ils sont nécessaires pour démontrer les différents aspects des trois méthodes aussi clairement que possible. En comparant les méthodes indirectement entre eux au moyen de comparaisons avec des solutions de référence respectifs suffisamment d'informations sont disponibles pour décider d'une méthode d'adaptation qui est poursuivie.

La correction quasi-statique, en particulier sa variante sans retour, n'offre un potentiel pour une amélioration. Cependant, elle nécessite la solution de problèmes statiques complets de commande et est donc désavantagés sur le plan de la performance.

Le LSPG ne cède aucune amélioration. En outre, il faudrait une hyper-réduction supplémentaire de

remédier à ses lacunes de performance. En outre, l'approche LSPG est très intrusive dans le régime non linéaire réduit Newmark.

La mise à jour et la méthode d'augmentation présente un concept complexe de plusieurs sous-méthodes, mais il est aussi autonome et peuvent être introduites à tout moment dans l'algorithme de Newmark non linéaire réduite. Elle offre des améliorations raisonnables pour un effort raisonnable.

La mise à jour et la méthode d'augmentation est choisie pour être poursuivi et développé, pour une application à l'élément fini cas-tests dans le chapitre suivant.

## Remplacement de l'inflation des termes non linéaires avec une formulation autonome

L'obligation pour l'élaboration autonome des termes non linéaires est identifiée dans la section 3.2.3. Cette exigence de l'inspection des procédures proposées non linéaires de type Newmark de solution dans la section ref sec: reducedordertransientsolution et ne sont pas identifiées de toute forme de résultats numériques. Il est donc une exigence qui est entraîné par le processus d'obtention de solutions transitoires non linéaires réduits plutôt que par la qualité des résultats. Au cours de l'étude comparative et l'étude de la robustesse, dans les sections 4.2.1 et 4.2.2, respectivement, la formulation de la réduction de l'algorithme de solution de commande sans une formulation autonome s'avère avantageuse. Là, elle permet de limiter la source d'erreur exclusivement à l'introduction des bases réduites. Cependant, pour avoir un système vraiment réduit, formulations autonomes pour les termes non linéaires doivent être trouvées.

L'équation générique d'un système non linéaire (2.82) contient la fonction  $\mathbf{g}(\mathbf{u})$ , qui regroupe tous les non-linéarités présentes dans le système. La propriété intrinsèque de cette fonction est qu'elle ne peut pas être facilement réduite à une forme  $\tilde{\mathbf{g}}(\mathbf{q})$ . La même chose vaut pour la matrice de rigidité tangente réduite  $\tilde{\mathbf{K}}$ . Cependant, pour avoir un système vraiment réduit, tous les liens avec la formulation complète de la commande doit être coupée pendant la phase de solution transitoire. En outre, les calculs sont dans le besoin pour une telle réduction des termes non linéaires car la formulation du vecteur des forces non linéaires de type inflation est de calcul beaucoup trop coûteux. Aussi, avoir un système vraiment réduit aborde les questions de portabilité, qui est la possibilité de se lancer, et de l'exécuter sans connexion au logiciel éventuellement sous licence.

Les formulations autonomes des termes non linéaires doivent répondre à ces exigences et de rendre le système réduit autonome de toutes les entités de commandes plein à l'extérieur de la création de la base réduite.

Une exigence supplémentaire qui doit être imposée est que les formulations autonomes doivent accueillir l'une des bases réduits qui sont proposés dans la section 3.3. Cette exigence supplémentaire est imposée parce que les résultats de l'étude comparative dans la section 4.2.1 montrent que la sélection correcte de la base réduite le plus prometteur pour une donnée cas-test est très important pour une réduction réussie. En outre, la mise à jour de la base réduite, qui est choisie comme l'adaptation de l'algorithme de solution dans la section 5.1, nécessite une indépendance des formulations autonomes à partir d'une base spécifique réduite.

Cette section est consacrée à explorer différentes approches pour parvenir à une formulation réduite des forces non linéaire vecteur et la matrice de rigidité tangente non linéaire et donc de contourner une formulation de l'inflation. Celles-ci comprennent les approches communes de l'interpolation linéaire, linéarisation directe et une approximation polynomiale qui sont disponibles dans la littérature. Pour l'approximation polynomiale une nouvelle formulation est proposée qui rend cette approche indépendante de la base réduite et s'appuie fortement sur la mise en œuvre algorithmique pour obtenir un maximum de performances numérique.

## Présentation de l'interpolation linéaire et de la linéarisation directe

L'interpolation linéaire est peut-être l'approche la plus brute d'exprimer les forces non-linéaires des vecteurs  $\mathbf{g}(\mathbf{u})$ . Il se décompose le déplacement courant  $\mathbf{u}$  en une somme de déplacements prédéterminés  $\tilde{\mathbf{u}}_j$ , chacune multipliée par un facteur  $\alpha_j$ . Les facteurs sont ensuite utilisés pour assembler le recherché pour non linéaire vecteur de forces en additionnant les forces non linéaires correspondant aux déplacements prédéterminés.

La linéarisation directe est l'équivalent de la réduction de l'interpolation linéaire. Il utilise la même approche pour exprimer les forces non linéaires réduits vecteur  $\tilde{\mathbf{g}}(\mathbf{q})$ .

Les deux approches sont brièvement présentés. L'interpolation linéaire est présentée d'abord parce que la directe

## Développer la formulation polynomiale de la réduction de vecteur de forces non linéaire

La formulation polynomiale et surtout l'algorithme d'identification suivent les lignes proposées par Muravyov and Rizzi [155], avec quelques améliorations par Chang et al. [58], qui a proposé un changement de l'origine de l'identification. La réduction des tenseurs suit les développements de Phillips [179].

L'utilisation de la formulation polynomiale pour la reconstruction de la matrice de rigidité non linéaire tangente est une contribution originale de ce travail. Toutefois, les travaux précédents dans ce sens comprennent l'application de la méthode de poutres serrées par Hollkamp et al. [99] et Spottswood and Allemang [214] pour la prédiction des réponses fatigue sonores. Une nouvelle approche est aussi la tentative d'appliquer une technique d'identification indirecte des solutions complètes de commande avec une réduction supplémentaire des tenseurs.

La formulation polynomiale de la non-linéaire forces vecteur  $\mathbf{g}(\mathbf{u})$  suppose simplement qu'il est de la forme d'un polynôme d'ordre  $d$  en termes de déplacements dans l'équation (5.58) où les  $\mathbf{A}^{(h)}$  sont des tenseurs d'ordre  $\mathbb{R}^{n \times n^h}$ . Cette formulation provient d'un développement de Taylor des composantes du vecteur des forces internes non linéaires  $\mathbf{g}(\mathbf{u})$ . Pour chaque élément  $i \in \{1, \dots, n\}$  ce qui peut être écrit comme l'équation (5.59) si la sommation d'Einstein sur l'égalité des indices est utilisé.

Cette représentation de  $\mathbf{g}(\mathbf{u})$  comme un polynôme est très puissant pour au moins trois raisons.

Tout d'abord, il semble être communément accepté dans la littérature (Mignolet and Soize [148], Muravyov and Rizzi [155], Thomas [223], Touzé et al. [225]) qu'une limitation du degré du polynôme de  $d = 3$  est suffisant pour les structures géométriquement non linéaires. Notamment Mignolet and Soize [148] réclamation dans leur travail que les forces internes non linéaires de " arbitraire élastique linéaire [...] la structure subit d'importantes déformations", qui s'applique sans restrictions dans le cadre de ce travail, peut être exprimé analytiquement comme un polynôme de troisième ordre dans les dérivations des fonctions de base par rapport aux coordonnées spatiales. Les charnières de développement sur une formulation Total-Lagrange générale du problème et n'est pas limitée à un type particulier d'éléments finis non linéaire.

Deuxièmement, il ya plusieurs approches possibles pour identifier les composants des tenseurs  $\mathbf{A}^{(1)}$ ,  $\mathbf{A}^{(2)}$  et  $\mathbf{A}^{(3)}$  sans vraiment faire les dérivations qui sont la définition des tenseurs dans les équations (5.61) pour (5.63). Mignolet and Soize [148] distinction entre les approches directes et indirectes. Approches directes s'appuient sur les formulations éléments finis et d'obtenir les tenseurs  $\mathbf{A}^{(h)}$  par intégration. Ils sont développés par Touzé et al. [225], Thomas [223] et Sénéchal [203]. L'inconvénient des approches directes, c'est qu'ils doivent avoir accès à des formulations des éléments finis et sont donc spécifiques pour un type donné d'éléments finis non linéaire. Approches indirectes identifier les tenseurs  $\mathbf{A}^{(h)}$  au moyen de la combinaison de différentes évaluations statiques de  $\mathbf{g}(\mathbf{u})$  avec imposé déplacements. Une approche indirecte est proposé par Muravyov and Rizzi [155] et développé par Chang et al. [58]. L'avantage d'une approche indirecte est qu'il ne nécessite pas de connaissances sur les éléments et peut être utilisé avec n'importe quel, même, un code d'éléments finis exclusifs. Cependant, elle nécessite un nombre considérable d'évaluations statiques du vecteur de forces internes non linéaire.

Troisièmement, bien que la définition de la formulation polynomiale des forces internes non linéaires dans l'équation (5.58) est écrit sur le niveau de commandes bien rempli, il peut être facilement réduite. La formulation polynomiale pour vecteur réduite des forces internes non linéaires peut tout aussi bien être écrit en coordonnées généralisées dans l'équation (5.64) où les  $\tilde{\mathbf{A}}^{(h)}$  sont des tenseurs d'ordre  $\mathbb{R}^{r \times r^h}$ . En fait, toutes les approches directes et indirectes, qui ont été proposées jusqu'à ce que le savez, ne traitent que l'identification des tenseurs réduits  $\tilde{\mathbf{A}}^{(h)}$ . C'est parce que la technologie informatique actuelle ne permet même pas de stocker toutes les pleines tenseurs d'ordre  $\mathbf{A}^{(h)}$ . Cependant, il est montré dans la suite que, lorsque la totalité des tenseurs d'ordre  $\mathbf{A}^{(h)}$  sont connus, ils peuvent être facilement réduits par une base réduite avec une approche de Phillips [179].

Les colonnes de la figure 5.21 représentent les deux niveaux de systèmes, la commande complète et celle réduite. Le point de départ de l'identification des tenseurs  $\mathbf{A}^{(h)}$  ou  $\tilde{\mathbf{A}}^{(h)}$ , respectivement, peuvent être réalisé sur deux niveaux. Une fois l'identification des tenseurs est terminée, ils peuvent être utilisés dans deux applications: reconstruire le vecteur des forces non linéaire et la reconstruction de la matrice de rigidité tangente non linéaire, encore une fois sur deux niveaux. Une procédure de réduction pour les tenseurs permet à tout moment de réduire les tenseurs et de continuer les opérations au niveau du système réduite.

La figure 5.21 résume les différentes possibilités et les applications d'une formulation polynomiale du vecteur des forces non linéaires, qui sont présentés ci-dessus, à la fois pour la commande complète et le système réduit. Elle indique que, suite à une identification des  $\mathbf{A}^{(h)}$ , ou  $\tilde{\mathbf{A}}^{(h)}$  respectivement, une formulation polynomiale comme équation (5.58) peut être utilisé pour

- reconstruire les forces vecteur non linéaire lui-même avec l'équation de calcul optimisé (5.94) et
- reconstruire la matrice de rigidité tangente non linéaire  $\tilde{\mathbf{K}}$  en appliquant l'équation (5.95).

Si le vecteur réduit de forces non-linéaires  $\tilde{\mathbf{g}}$  est exprimée comme un polynôme, il peut tout aussi facilement être exprimé par l'utilisation de l'équation (5.108). Dans le cas de la réduction de la matrice de rigidité tangente est exprimée par l'équation (5.90).

L'algorithme proposé par Muravyov and Rizzi [155] prévoit une détermination indirecte des tenseurs réduits  $\tilde{\mathbf{A}}^{(h)}$  et pourrait être également appliquée à une identification complète de l'ordre dans cas de besoin. Si la totalité des tenseurs d'ordre  $\mathbf{A}^{(h)}$  sont connus, le passage au système réduite est possible à tout moment en appliquant l'équation (5.104), tel que proposé par Phillips [179]

Pour obtenir les conditions réduites des forces non linéaires internes  $\tilde{\mathbf{g}}$  et de la matrice de raideur tangentielle  $\tilde{\mathbf{K}}$  il existe trois variantes de l'approximation polynomiale possible. Ils diffèrent quant à savoir si l'identification a lieu sur ordre complet ou sur le niveau réduit, et, dans le premier cas, lorsque la réduction a lieu. Ces variantes sont shwon dans la figure 5.21. Dans le détail les variantes sont les suivantes:

1. l'identification complète de la commande à la réduction de fuite
2. l'identification de commandes bien rempli avec réduction inclus
3. la réduction d'identification d'ordre

La première variante présente pas d'avantage par rapport à une formulation de gonflage des termes non linéaires car il remplace les termes non linéaires sur pleine commande et non sur ordre réduit. Il est donc tombé de nouvelles investigations.

La troisième variante correspond à la formulation originale de Muravyov and Rizzi [155]. Il présente l'inconvénient d'être spécifique à une base réduite donné. Ce n'est pas le cas pour la première et la deuxième variante, qui sont à la fois indépendant de toute façon réduite. Ils exigent un effort considérable pour l'identification initiale à la commande complète. Cet effort considérable doit être investi pour identifier les éléments de l' $\mathbf{A}^{(h)}$  présente l'inconvénient majeur de cette approche, même si elle a été considérablement atténué par l'exploitation de la rareté de l' Pour toute matrice de rigidité linéaire. Au prix de ne plus avoir de séparation entre les tenseurs  $\mathbf{A}^{(h)}$  et la base réduite  $\Phi$ , cet effort peut être contournée si le correspondant termes réduits  $\tilde{\mathbf{A}}^{(h)}$  sont indirectement identifiés.

## Choix d'une formulation autonome en effectuant une étude numérique

Les techniques qui sont présentés comme candidats possibles pour remplacer la formulation d'inflation des termes non linéaires sont mis à l'épreuve numérique bref. Ce test numérique vise à contribuer à l'information de la décision sur laquelle de ces techniques doit être sélectionné. Entrée supplémentaire pour cette décision sera tiré d'inspecter les propriétés respectives, notamment en ce qui concerne l'exigence d'être indépendant de la base réduite, de chacune de ces techniques.

Les tests sont effectués avec le set-up qui a été développé dans la section 4.1 pour l'étude comparative numérique et l'étude de la robustesse. Le même cas-tests, l'algorithme de solution et les mesures d'erreur sont utilisées ici.

## Résultats de la nécessité de remplacer l'inflation des termes non linéaires avec une formulation autonome

Le travail présenté prend un nouveau regard sur la solution des systèmes d'ordre réduit dans le cadre de la dynamique transitoire de structure non-linéaire et met en évidence à qui pointe dans la procédure de résolution des formulations des termes non linéaires apparaissent. Il démontre que ces points sont des points d'articulation pour la solution réussie du modèle réduit et nécessitent donc une attention particulière. Un certain nombre de candidats pour une telle formulation autonome sont passés en revue. Une première application de ces formulations sur un système universitaire conduit à la concentration sur l'approximation polynomiale. Dans le prolongement de la demande suivante de cette formulation particulière à un élément fini de cas de test, l'approximation polynomiale est appliqué à la commande complète et pour le système non linéaire réduite. Les solutions ainsi obtenues se révéler acceptable correct si on le compare à une solution de commandes bien rempli avec des éléments finis. En outre, un gain considérable en temps de calcul est prouvé avoir lieu que si la solution est obtenue avec la formulation polynomiale réduite.

Cependant, l'exigence spécifique de l'approximation polynomiale pour un nombre considérable de solutions statiques est révéler. Cela peut éventuellement être un obstacle majeur à l'application de cette méthode sur des systèmes de commande complets. En réponse, le raccourci numérique de sous-réglage de l'indice est conçu pour permettre une application réussie. Avec l'approche sous-paramètre index un roman raccourci numérique est présentée, qui pourrait permettre l'application de l'approximation polynomiale de Muravyov and Rizzi [155], et celui-ci en particulier l'identification, aux systèmes de commande complets. Il s'agit d'une étape importante vers une formulation autonome des termes non-linéaires qui est indépendant de la base réduite. Une telle formulation est nécessaire pour la réduction des systèmes qui réduisent les changements de base au cours de la solution. Une telle base réduite non constante est nécessaire si les paramètres changement externe, tel que le point de fonctionnement, qui apparaît sous la forme de la précontrainte dans l'élément fini utilisé de cas de test, ou, si au cours du processus de solution de base réduit est mis à jour en réponse à l'évolution non linéaire de la solution.

La formulation polynomiale est choisi pour être poursuivi et développé pour une application à l'élément fini cas-tests dans le prochain chapitre 6.

## Adaptation base réduite aux paramètres extérieurs

Le fait qu'aucune déclaration explicite quant à la dépendance des propriétés du système dynamique,  $M$ ,  $g(u, \dot{u})$  et  $f_E$ , à partir de paramètres extérieurs ont été réalisés jusqu'à présent, ne signifie pas que cette dépendance n'existe pas. Ces paramètres extérieurs  $\mu$  sont définis comme non directement liées au système, mais ayant un impact sur le système. Ils peuvent être de nature physique, en définissant par exemple un point de fonctionnement par une température, ce qui affecte l'équation constitutionnel de la matière, ou une vitesse de rotation pour faire tourner un système stationnaire, qui induit différentes précontraintes. Ils peuvent aussi être liés à un problème d'optimisation, comme par exemple différents matériaux de densités

différentes ou des changements de géométrie ou ayant un impact implicitement le processus de modélisation, comme par exemple un changement dans les paramètres des algorithmes de résolution.

L'objectif de cette section est d'étudier les approches possibles pour comprendre cette dépendance dans l'analyse.

Malgré le fait que d'une interpolation linéaire entre les deux bases  $\Phi_1$  et  $\Phi_2$  pour le cas particulier d'un seul paramètre externe scalaire  $\mu$ , peut sembler réalisable, il n'est en effet pas parce que l'interpolation ne conserve pas la condition d'orthogonalité pour le interpolée de base  $\Phi_0$ .

être conscient de cela, Lieu and Lesoinne [138] proposé une approche par interpolation non les vecteurs des bases, mais les angles entre eux. Cette approche a ensuite été généralisé par Amsallem [12], qui a choisi l'une des bases précalculées  $\Phi_i$  comme origine d'un collecteur Grassmann et exécuté l'interpolation dans une tangente de l'espace pour que collecteur, qui donne le point final d'une géodésique comme recherché nouvelle base  $\Phi_0$ . Au Amsallem and Farhat [13] le choix approprié de l'origine est encore une question ouverte. L'ensemble du procédé est esquissé le long de ses équations centrales ci-dessous.

Quoique cette procédure nécessite une quantité considérable de transformations, il est toujours considéré comme moins coûteux par ses auteurs, que la reconstruction d'un modèle dédié d'ordre réduit sur le point de fonctionnement  $\mu_0$  à partir d'un modèle haute fidélité. Toutefois, elle exige d'établir et de gérer une base de données de modèles approximatifs pour différents points de fonctionnement avant l'initialisation d'une approche qui nécessite différents points de fonctionnement. Mais une fois cette base de données est établi sur une large gamme de conditions d'exploitation, il permet la construction de modèles dédiés ordre réduit dans la même gamme.

L'approche proposée par interpolation Amsallem [12], décrite dans cette section, prend les quatre étapes de

1. le choix de l'origine de l'interpolation,
2. la transformation dans l'espace tangent,
3. l'interpolation elle-même,
4. la transformation inverse dans le collecteur d'origine.

Bien que cette approche et l'interpolation se sont universels, les transformations nécessaires sont spécifiques au type de matrice qui doit être interpolé. Amsallem [12] contient une liste exhaustive des transformations possibles pour une multitude de types de matrices. Limité à la portée de ce travail, il ya deux types de matrices, qui sont d'intérêt:

Le principal inconvénient de cette approche est qu'elle est nécessite une base constante réduite ou les déplacements importants ont être maintenu en coordonnées physiques et les bases de données doivent être mises à jour à chaque changement de base.

## **Intégrer les méthodes qui répondent aux exigences identifiées et appliquer les a des cas-test en éléments finis**

La mise-a-jour de la base réduite, la formulation polynomiale des termes nonlinéaires et l'interpolation en fonction des paramètres externes sont les méthodes qui sont sélectionnées pour répondre aux défauts identifiées de la procédure initiale utilisée précédemment pour obtenir des solutions transitoires des systèmes nonlinéaires. Dans le chapitre 5 ces trios méthodes sont testées amplement et adaptées et améliorées ou nécessaire. Elles sont maintenant appliqués a des cas-test en éléments finis. Les cas-test en éléments finis sont construit avec les éléments finis qui sont développés dans le chapitre 2.

Dans une première étape la méthode intégrée est assemble a partir des éléments de l'interpolation de la base réduite en fonction des paramètres externes, de l'introduction de la base réduite, du remplacement de

l'expression en éléments finis des termes nonlinéaires par la formulation polynomiale et de la mise-à-jour et augmentation de la base réduite. La méthode intégrée est formalisée et testée sur les cas-test académiques.

Dans une deuxième étape la méthode intégrée est appliquée à deux cas-test en éléments finis. Le premier cas-test en éléments finis est construit avec des éléments bar et le deuxième cas-test est construit avec des éléments volumiques. Un effort considérable est investi pour définir, caractériser et explorer les cas-test en éléments finis parce que leur comportement nonlinéaire et les solutions transitoires qui en découlent définissent les limites de la validité confirmée pour l'application de la méthode intégrée.

L'intégration des trois éléments de l'adaptation de l'algorithme de la solution en mettant à jour la base réduite, ce qui rend le système de réduction autonome avec la formulation polynomiale des termes non linéaires et en adaptant la base réduite initiale en fonction des paramètres extérieurs à la méthode d'interpolation marque le centre de aspect de la recherche effectuée. L'approche intégrée de ces trois aspects permet le traitement de réduction des systèmes de géométrie et les structures paramétrées.

Ces trois aspects sont testés isolés dans leur section respective 5.1, 5.2 et 5.3. Chacun d'entre eux répond à une exigence spécifique qui a été identifiée lors de l'introduction de la base réduite dans l'algorithme de solution dans la section 3.2.3 ou pendant les études numériques détaillées dans le chapitre 4.

L'interpolation des bases réduites en fonction de paramètres externes  $\mu$  est considérée comme étant légèrement écartés et ne sont pas directement intégrés avec les deux autres aspects, car il ne fournit que la base réduite initiale  $\Phi_0$  à  $t_0$  des solutions transitoires. Les bases suivantes sont adaptées par l'algorithme de mise à jour et l'augmentation qui prend en compte le paramétrage. En outre, l'adaptation de la base réduite de l'élément fini cas-tests est déjà étudié lors de l'introduction de la précontrainte dans la section 6.3.2. Il est prouvé que la précontrainte peut être introduit dans une structure non linéaire par ajout d'une composante statique au forçage externe et en choisissant des conditions initiales correspondantes.

La tâche la plus critique est donc à l'intégration de la formulation autonome avec la mise à jour et le mode d'augmentation. Ces deux éléments sont intégrés dans le procédé HHT- $\alpha$  que l'ossature générale de la méthode intégrée de manière explicite. Intégrations dans la réduction linéaire Newmark-régime sont également effectuées et considérées comme équivalentes.

La formulation autonome et la méthode de mise à jour et l'augmentation sont d'abord intégrés et appliqués sur l'enseignement de cas de test à partir de la section 4.1.3. Cette approche prudente est nécessaire parce que l'expression polynomiale de la section 5.2.2, qui constitue la formulation autonome des termes non linéaires, propose plusieurs variantes qui peuvent être combinés avec la mise à jour et la méthode d'augmentation. Toutes ces variantes donnent de bons résultats dans les tests numériques de la formulation autonome seul dans la section 5.2.4 mais à ce stade il n'est pas encore connu la variante qui s'intègre mieux avec la mise à jour et la méthode d'augmentation. Ceci est déterminé par l'application de la méthode intégrée pour les cas-tests académiques, de sorte que, dans une seconde étape, seule la variante la plus prometteuse de l'expression polynomiale est utilisée pour le rendu de l'élément fini cas-tests autonome.

## **Description de la méthode intégrée**

L'approche de la solution intégrée est le fruit central du travail effectué. Il s'agit d'une nouvelle combinaison de méthodes existantes et originales qui sont combinées pour obtenir la solution transitoire du modèle réduit d'une structure paramétrée et géométriquement non linéaire.

Pour l'élément fini de cas de test de la structure sous-jacente de base de l'approche est fourni par la méthode HHT- $\alpha$  qui est décrit dans la section 3.2.2.2. Cette méthode de solution est choisie pour démontrer que l'approche peut être construite au-dessus de tous les régimes de solutions de type Newmark et qu'il ne se limite pas à la non-linéaire Newmark-schéma classique de la section 3.2.2.1.

La réduction du système complet de commande est réalisée par la projection sur une base réduite. Les principaux avantages de cette approche sont sa modularité et la possibilité d'utiliser un système commun de la solution de base pour des problèmes d'ordre réduit et complet. Cette question est examinée en détail

dans la section 3.1.

Le paramétrage de la base réduite initiale est assurée par la méthode d'interpolation de la section 5.3.2. Il s'agit d'une méthode tirée de la littérature sans adaptation car il se comporte bien sur les problèmes donnés. Son introduction est identifié comme étant nécessaire après l'inspection des résultats du test de la robustesse de certaines bases réduites dans la section 4.2.2.

La solution réduite est rendu autonome par l'introduction de l'expression polynomiale pour les termes non linéaires. Cette exigence est identifiée à partir de l'inspection de l'algorithme de solution sous-jacente dans la section ref sec: identifyingtheneedforautonomy. Encore une fois, l'utilisation de la HHT- $\alpha$ -méthode au lieu de la classique réduit non linéaire Newmark-plan, montre que cette exigence est universelle pour les membres des algorithmes de résolution Newmark-type et que la réponse choisie en forme de l' formulation polynomiale est universel et portable. La formulation polynomiale est discuté en détail et adapté aux besoins spécifiques de la faisabilité des calculs et l'indépendance d'une base réduite spécifique dans la section 5.2.2.

L'ingrédient principal de l'approche solution intégrée est la mise à jour et l'augmentation de la base réduite de la section 5.1.3. Cette méthode permet de faire la base réduite suivre l'évolution de la solution transitoire non linéaire et augmente considérablement la qualité sur une solution qui a été obtenu avec une base réduite constante. Cette nécessité est identifié avec les études numériques pour la comparaison de la réduction des bases dans la section 4.2.1 et l'apparition de sauts est contré avec succès par l'inclusion de l'augmentation de la base réduite à jour. L'approche de la mise à jour et l'augmentation s'appuie sur la modularité du concept de la réduction par projection sur une base réduite et peut donc être facilement intégré dans le schéma-Newmark ainsi que dans le répertoire de la méthode HHT- $\alpha$ . Il est indépendant du choix particulier de la méthode qui fournit en fait la base réduite, quelques méthodes courantes sont présentées dans la section 3.3, et il est compatible avec l'expression polynomiale des termes non linéaires, après que ce dernier a été rendu indépendant à partir d'une base spécifique réduite.

L'approche de la solution intégrée avec ces trois ingrédients sont présentés ci-dessous selon les lignes générales. Les sections qui sont référencés ci-dessus dans cette introduction servent de source d'information détaillée. Les choix particuliers qui doivent être prises dans le cas particulier d'un système d'éléments finis par rapport à la variante réelle de chaque méthode sont examinés dans les sections suivantes. La description de l'approche de la solution intégrée est présenté ci-dessous en trois étapes. Dans la première, la solution est préparée en fournissant les bases de données nécessaires, par exemple pour l'interpolation de la base initiale réduite. Dans une deuxième étape, la solution transitoire réduite est initialisé et s'est poursuivie jusqu'à la base réduite est augmentée pour la première fois. La troisième étape concerne la mise à jour et l'augmentation de la base réduite et le maintien de la solution transitoire réduite à base mise à jour répétée jusqu'à ce que la fin de la période simulée.

## **Préparation de la solution transitoire réduite et interpolation de la base réduite initial**

La préparation de la solution transitoire réduite se déroule avant tout dans le domaine classique de pré-traitement. La masse et la matrice d'amortissement  $\mathbf{M}$  et  $\mathbf{C}$  sont nécessaires ainsi que l'expression de  $\mathbf{g}(\mathbf{u})$ . De plus, le temps histoire des forces extérieures  $bm.f_e(t)$  est à définir. Il est rappelé à cet égard que la définition de la non-linéarité géométrique tel qu'il est utilisé dans ce travail exclut l'apparition de forces de contact, de sorte que le temps toute l'histoire des forces extérieures est connu avant la solution. Toutes ces tâches de pré-traitement ont lieu lors de la commande complète et peuvent être obtenus à partir d'un solveur éléments finis commercial.

Si la variante de l'expression polynomiale de l'identification de commandes bien rempli avec réduction incluse est choisie, les tenseurs nécessaires  $\mathbf{A}^{(1)}$ ,  $\mathbf{A}^{(2)}$  et  $\mathbf{A}^{(3)}$  doivent être identifiés dès maintenant en utilisant l'expression de  $\mathbf{g}(\mathbf{u})$  et la procédure d'identification de la section 5.2.2.4.

Pour le paramétrage d'un certain nombre de points de fonctionnement représentatifs  $\{\boldsymbol{\mu}_1, \dots, \boldsymbol{\mu}_m\}$

doivent être stockés ou récupérés à partir d'une base de données soit disponible dès le début de la solution transitoire. Le point de fonctionnement réel  $\mu_0$ , à laquelle la solution transitoire réduite est censée avoir lieu, doit également être défini. On suppose que  $\mu_0 \notin \{\mu_1, \dots, \mu_m\}$ . En outre, il est supposé que le point de fonctionnement influe seulement sur la base réduite et peut-être les conditions initiales, aussi. Toutes les autres quantités qui sont décrivant le système, notamment  $M$ ,  $C$  et  $f_e(t)$ , sont censés être indépendants à partir du point de fonctionnement.

Si les conditions initiales  $u_0 = u(t_0)$  et  $\dot{u}_0 = \dot{u}(t_0)$  ne sont pas en fonction du point de fonctionnement, ils sont également donnés à ce stade.

Enfin, l'ordonnance du modèle réduit  $r$  doit être déterminée avec un choix de la méthode de génération de la base réduite. Ces décisions sont difficiles à faire parce que, d'abord, ils ont besoin de connaître le comportement de la structure et, d'autre part, ils ne sont pas indépendants. Par exemple, si une structure est soumise à une charge externe qui provoque une torsion avant tout et cette structure doit être réduite avec le LNM, l' $r$  doit choisie de telle sorte que aussi des modes de torsion sont inclus dans l'assiette réduite. D'autres approches de la section 3.3 pour la création de la base, comme par exemple le POD, ne fournissent des critères de décision, comme par exemple la ration énergétique, qui sont un peu plus ciblée. Dans tous les cas, ces décisions difficiles restent à l'ingénieur et son expérience.

Une décision de difficulté comparable est le choix des valeurs pour les paramètres de la procédure de solution, en particulier le pas de temps  $\Delta t$ , les paramètres  $\alpha$  et le seuil de convergence  $\epsilon$ , ainsi que le paramètres pour la mise à jour et l'augmentation, notamment le seuil de déclenchement de la mise à jour  $\epsilon_r$  et le dispositif de retenue  $m_r$ .

## Initialisation et le calcul de la solution transitoire réduite avec mise à jour de base et l'augmentation

L'algorithme de solution temps-marche est l'épine dorsale du processus de solution. Il est initialisé avec la base réduit interpolés et toutes les autres variables, qui sont préparés dans la section ci-dessus. Dans la méthode après la réduction HHT- $\alpha$  de la section 3.2.2.2 est développé dans toute son extension. Cela inclut l'introduction de la formulation polynomiale de la section 5.2.2 pour assurer l'autonomie des termes non linéaires réduits et l'introduction de deux mesures de la dérivée de la première réduction résiduel  $|\frac{d\|\tilde{r}_{(i=1)}\|}{dt}|$  et de la retenue  $m$ , qui régissent le processus de mise à jour, dans la réduite HHT- $\alpha$ -méthode. La mise à jour et l'augmentation elle-même est, pour l'instant, seulement mentionné comme un bloc autonome, qui est introduit dans l'algorithme temps-marche à une position donnée et uniquement appelée lorsque les deux métriques allo son Execution. Cela est possible parce que la mise à jour et l'algorithme d'augmentation dans la section 5.1.3 est construit explicitement un tel bloc autonome et la méthode réduit HHT- $\alpha$  qui entoure ce bloc autonome, est inconscient son precesence. Tout ce qui se passe à l'intérieur du bloc de la mise à jour et l'augmentation réelle est décrite dans la section suivante 6.1.1.3.

La première étape vers la réduction du système et d'utiliser le modèle réduit résultant d'une solution transitoire est de fournir la base réduite  $\Phi_0$ . Cette base initial réduit est de servir jusqu'à la première mise à jour et d'augmentation. Il est obtenu au niveau du point de fonctionnement réel  $\mu_0$  avec la méthode d'interpolation de la section 5.3.2.

Pour préparer l'interpolation d'une base de données des bases réduites  $\{\Phi_1, \dots, \Phi_m\}$  aux points de fonctionnement données  $\{\mu_1, \dots, \mu_m\}$  est établie. La base initiale  $\Phi_0$  est établie en suivant la démarche en quatre étapes à partir de Amsallem [12], dans la section 5.3.2.2. Une origine de l'interpolation  $\mu_k$  est choisi parmi les points de fonctionnement données dans la base de données. La base de données de la base réduite est transformée en la tangente avec des équations (5.112) et (5.113). L'interpolation a lieu avec l'interpolation multiparamétrique de la section 5.3.2.3. La base interpolée est retransformé par les équations (5.114) et (5.114).

## Effectuer la mise à jour de base et l'augmentation et la poursuite de la solution transitoire réduite

Avec l'équation ci-dessus (6.6) et (6.7) à deux mesures  $\left| \frac{d\|\tilde{\mathbf{r}}_{(i=1)}\|}{dt} \right|$  et  $m$ , ainsi que leurs seuils  $\epsilon_r$  et  $m_r$ , qui régissent le déclenchement de la mise à jour et l'augmentation de la base réduite, sont intégrés dans le méthode autonome réduite HHT- $\alpha$ . Si ces mesures déclenchent une mise à jour de l'approche qui est développé dans la section ref sec: UPDT peut être inséré comme un bloc autonome entre l'équation (6.11) et (6.12) de l'autonomie réduite HHT- $\alpha$ -méthode ci-dessus. Le bloc autonome de la mise à jour et l'augmentation est inséré à la position un, au début du pas de temps courant et basé sur la solution du pas de temps précédent, tel qu'il est déterminé dans la section 5.1.3.2. La séquence de la méthode autonome réduite HHT- $\alpha$  reste insensible à la mise en place de la nouvelle base.

Dans le détail le processus de mise à jour et l'augmentation prend les dix étapes suivantes

1. A l'instant de la mise à jour de la solution est gonflé à l'ordre complet avec la base réduite de courant. Pour les déplacements à l'inflation lit  $\mathbf{u}^{(t)} = \Phi^{(t-m\Delta t)} \mathbf{q}^{(t)}$  et il est fait d'une manière analogue pour les vitesses et les accélérations.
2. L'état généralisé courant est stocké sous forme  $\mathbf{q}_{\text{avant}}^{(t)}$ ,  $\dot{\mathbf{q}}_{\text{avant}}^{(t)}$  et  $\ddot{\mathbf{q}}_{\text{avant}}^{(t)}$ .
3. Le nouveau titre préliminaire  $\check{\Phi}^{(t)}$  devient disponible gr̃i  $\frac{1}{2}$  ce à l'application de la méthode de création de la base réduite qui est choisie avant la solution. Pour l'exemple de la LNM à un déplacement donné de la section 3.3.1.2 cela devient
  - la commande complète raideur tangente matrice  $\mathbf{K}^{(t)} = \left. \frac{\partial \mathbf{g}(\mathbf{u})}{\partial \mathbf{u}} \right|_{\mathbf{u}^{(t)}}$  est établie avec la solution gonflé de commandes bien rempli
  - il est ensuite utilisé dans les équations (3.113) et (3.114) pour obtenir la base réduite à jour  $\check{\Phi}^{(t)}$
  - cette base réduite préliminaire  $\check{\Phi}^{(t)}$  est d'ordre  $r$
4. Les coordonnées préliminaires sont généralisées établi que l'équation (6.22) On fait de même pour obtenir les vitesses généralisées préliminaires  $\check{\dot{\mathbf{q}}}^{(t)}$  et accélérations  $\check{\ddot{\mathbf{q}}}^{(t)}$ . Item Les sauts sont calculées en appliquant l'équation (5.38) pour les coordonnées généralisées dans les équations (6.23) et les équations (5.39) et (5.40) pour l' vitesses et les accélérations, respectivement.
5. La base réduite à jour et augmentée est fourni par l'équation (5.41) que l'équation (6.24). Cette base est actuellement de l'ordre  $r+3$ , où  $r$  est l'ordre qui est choisie initialement avant la solution. L'ordre de  $\Phi^{(t)}$  de l'équation (6.24) ne change pas avec le nombre de mises à jour qui ont déjà eu lieu depuis l'initialisation de la solution réduite à  $t_0$ .
6. Les nouvelles coordonnées généralisées sont adaptés par des équations (5.42) pour (5.44). Pour l'exemple des coordonnées généralisées ce lit comme indiqué dans l'équation (6.25). La même augmentation est appliqué à des vitesses dans l'équation (6.26) et aux accélérations dans l'équation (6.27) Ces trois vecteurs sont agumented de les relier avec les sauts de la base réduite augmentée de l'équation (6.24).
7. La base réduite de gauche est défini comme  $\Psi = (\Phi^{(t)})^T$ .
8. Les deux matrices statiques  $\mathbf{M}$  et  $\mathbf{C}$  sont réduits à la base réduite à jour et augmentée  $\Phi^{(t)}$  pour afin de correspondre aux nouvelles coordonnées généralisées.
9. Le compteur de la retenue est remis à  $m = 0$  pour indiquer qu'une mise à jour a eu lieu et de bloquer la mise à jour qui suit:  $m_r$ -étapes temps.

Une fois la nouvelle base réduite  $\Phi^{(t)}$  est disponible, les tenseurs  $\tilde{\mathbf{A}}^{(1)}$ ,  $\tilde{\mathbf{A}}^{(2)}$  et  $\tilde{\mathbf{A}}^{(3)}$  doivent être adaptés en fonction du variante de l'algorithme d'identification choisie. Soit par la réduction renouvelée de la totalité des tenseurs d'ordre ou par une identification directe renouvelée des tenseurs réduits. Cette étape promet de devenir la partie la plus cõi  $\frac{1}{2}$  teuse de calcul de la mise à jour de la base réduite, et une étude

consacrée est effectuée pour décider de la variante de la formulation polynomiale qui est la plus adaptée.

Une fois les dix étapes ainsi que l'adaptation supplémentaire des tenseurs ont été effectuées, le HHT- $\alpha$ -méthode peut continuer sans être encore au courant de la base mise à jour et augmentée.

## Conclusion

La conclusion est centrée sur la discussion des résultats obtenus. L'accent est plutôt mis sur les méthodes qui ont été développées et la méthode intégrée formalisée et moins sur les résultats numériques. La méthode intégrée est présentée comme une réalisation possible d'un *framework* plus général qui permet d'obtenir des solutions transitoires rapides, d'une qualité haute et paramétrables d'une structure géométriquement non linéaire.

En passant les décisions les plus importantes sont soumises à une revue critique suite à la disponibilité de tous les résultats. Ces décisions sont prouvées comme correctes et quelques-unes sont même prévisionnelles. Finalement le travail se termine avec la présentation des futures voies pour la recherche. Ces voies de recherche visent l'agrandissement et l'extension de l'application de la méthode intégrée et de son *framework* sous-jacent.

### Conclusion du travail

L'objectif principal de ce travail est de fournir une solution transitoire rapide, précise et paramétrable d'une structure géométriquement non linéaire. Ce but est atteint avec la construction de la méthode intégrée.

Le processus menant à cette réalisation est caractérisé par plusieurs décisions importantes. La plus importante est certainement le choix de la projection sur une base réduite comme la méthode de réduction. Cette décision impose l'utilisation d'un algorithme de résolution en temps de marche de type Newmark non linéaire et elle impose le choix d'une méthode pour créer la base réduite. De ce choix la question se pose quelle base réduite peut être particulièrement adaptée pour la réduction d'une structure géométriquement non linéaire. Essais numériques complètes conduisent à des résultats qu'aucun des bases réduites réalise pleinement satisfaisante les exigences et l'examen minutieux de l'algorithme de solution montre que l'algorithme de solution nécessite d'être rendu autonome.

La jonction de ces deux résultats montre clairement qu'une réduction réussie d'une structure géométriquement non linéaire par une projection sur une base réduite dépend de façon cruciale de l'algorithme de solution et seulement dans une moindre mesure de la base réduite elle-même. L'application des méthodes existantes de manière isolée n'est pas suffisante. Ce constat est suivi en répondant aux besoins identifiés de l'adaptation de l'algorithme de solution, du remplacement des termes non linéaires avec une formulation autonome et de l'adaptation de la base réduite en fonction de paramètres externes.

Pour répondre à ces exigences plusieurs choix sont nécessaires. Pour chacune des exigences d'une sélection de méthodes communes est présentée afin de fournir une boîte à outils d'approches. Les choix actuels sont effectués après de nombreux tests numériques. Pour ces tests, les cas-tests académiques sont utilisés afin de fournir un environnement de test cohérent dans toute l'étude.

La mise à jour et l'augmentation de la base réduite est choisie pour adapter l'algorithme de la solution afin de faire la base réduite suivre l'évolution non linéaire de la solution. La formulation polynomiale est choisie pour former la formulation autonome qui remplace les termes non linéaires réduits. L'interpolation sur un espace tangent est choisie pour adapter la base réduite initiale à des paramètres extérieurs. Tous ces choix sont basés sur les résultats numériques concluants.

Les trois approches choisies, dont chacune répond un besoin identifié, sont ensuite réunies dans la méthode intégrée. En répondant aux trois besoins identifiés, la méthode intégrée permet une solution transitoire réduite rapide, de haute qualité et paramétrable.

## Discussion des résultats obtenus

Les résultats obtenus lors de l'étude ne sont pas exclusivement résultats numériques, comme par exemple les résultats de l'étude comparative des bases réduites. Pensant davantage en termes de produits, les résultats de ce travail peuvent être algorithmes, comme par exemple, la mise à jour et l'augmentation de la base réduite, ou le cadre de la méthode intégrée.

**Les résultats de l'étude des bases réduites** Le résultat principal est l'aptitude limitée des bases réduites. Un grand nombre de bases réduites communes a été étudié pour sa capacité de fournir une solution transitoire précise et pour leur robustesse sur des cas-tests paramétrés différemment.

Plusieurs approches communes pour la création de bases réduites sont présentés. Toutes les bases réduites sont utilisés pour réduire les combinaisons de deux systèmes non-linéaires et deux excitations dans une étude comparative qui détermine les applications préférées des bases réduites, et une étude qui détermine la robustesse des bases en les utilisant pour des configurations paramétrées différemment. Les performances des bases réduites sont évalués avec une analyse décision multi-critères spécialement conçu et une mesure de la performance relative. Les résultats sont condensés dans les tableaux concis. Toutes les procédures qui ont été utilisées pour obtenir les résultats ont été soigneusement vérifiées par l'étude approfondie des influences possibles des bases appliquées et la procédure de solution.

L'étude comparative menée met en évidence que le choix d'une base réduite spécifique pour un système non-linéaire doit être basé essentiellement sur le type d'excitation à laquelle est soumis le système. La constitution de la non-linéarité est seulement un critère supplémentaire. Les bases de décomposition orthogonale propre spécifiquement construites sont constamment les meilleures, ce qui explique leur utilisation généralisée. Dans le même temps, il a été montré que les modes normaux linéaires offrent une alternative qui évite la nécessité d'une solution d'ordre complète. Alors que les modes normaux linéaires négligent le caractère non linéaire du système, ils effectuent toujours aussi bon que les bases de décomposition orthogonale propre ou seulement légèrement moins bons pour la dynamique des structures non-linéaires. Une étude plus ciblée sur les grands systèmes confirme les résultats obtenus et met en valeur les gains possibles grâce à l'application d'une réduction.

En ce qui concerne la robustesse inhérente aux différentes bases, on peut affirmer qu'aucune des bases étudiées ne possède cette propriété particulière dans une mesure suffisante, ce qui nécessite l'utilisation de méthodes d'adaptation. Toutefois, l'étude comparative montre aussi clairement que, si l'utilisation d'une seule base sur un système sous excitations différemment paramétrées devient nécessaire, cette base doit être établie avec les valeurs les plus critiques pour les paramètres.

Toutefois, le niveau global d'erreur au-delà des performances individuelles des différentes bases montre que la simple projection d'un système non-linéaire sur une base réduite constante n'est pas suffisant pour assurer une qualité satisfaisante de la solution.

**Mise à jour et augmenter les bases réduites** Le deuxième résultat important est le processus de mise à jour et de l'augmentation de la base réduite. Cette approche de bon sens fortement modifié répond à l'exigence d'adapter l'algorithme de solution qui est dérivé de l'incapacité des bases réduites pour réduire avec succès un système non linéaire. La mise à jour de la base réduite semble être une approche de bon sens, mais il y a peu de littérature qui est venu à l'attention de l'auteur.

Bien que l'idée de la mise à jour des bases réduites semble simple, peut-être même simpliste, sa mise en œuvre effective révèle qu'elle nécessite une vaste modification de la forme de l'augmentation de la base réduite afin de fonctionner correctement. La mise à jour de la base réduite à intervalles exige l'inclusion des sauts dans les déplacements physiques, les vitesses et les accélérations dans la base réduite mise à jour, tandis que l'initialisation correcte des nouvelles coordonnées généralisées. Cette technique d'augmentation est une nouvelle approche et contribue considérablement à la qualité des solutions transitoires réduites des systèmes non linéaires. Il est également un élément important du succès de la méthode intégrée

La mise à jour et l'augmentation de la base réduite sont formalisées comme un bloc autonome dans la section 6.1.1.3. Ce bloc peut être prise et appliquée comme un complément à n'importe quel algorithme de solution.

**La création et l'application de la méthode intégrée** Le résultat central de ce travail est la méthode intégrée. En commençant par l'exigence d'une solution transitoire rapide, de haute qualité et paramétrable d'une structure géométriquement non linéaire, il est rapidement décidé de fonder le cadre de cette solution transitoire sur la réduction avec une base réduite. De l'inspection de l'algorithme de solution et des résultats numériques obtenus aux trois exigences d'adaptation de l'algorithme de solution, de rendre autonome le système d'ordre réduit et d'adapter la base réduite à des paramètres externes sont identifiés. De répondre aux trois exigences avec des méthodes spécialisées et d'unifier ces méthodes spécialisées dans un cadre est identifié comme l'approche qui assure des solutions transitoires rapides, de haute qualité et paramétrables d'une structure géométriquement non linéaire. Ce cadre et les choix qui sont faits pour chaque besoin identifié sont formalisées dans la méthode intégrée.

La méthode intégrée est appliquée avec succès à des cas-tests académiques et en éléments finis. L'application aux cas-tests en éléments finis peut être considéré comme révolutionnaire, même si elles sont réalisées dans des conditions semi-réalistes. En raison des ressources numériques disponibles, seul un nombre limité de degrés de liberté est utilisé pour discrétisées par éléments finis les cas-tests. Toutefois, les cas-tests en élément fini donnent une représentation méticuleusement correcte des non-linéarités géométriques. C'est exactement le type de non-linéarité qui est prévu au cours des applications industrielles. Il est soigneusement recréé avec des éléments finis non linéaires de type barre et de type volume et vérifiée au moyen d'une comparaison avec un solveur éléments finis commercial. Cela donne une grande confiance dans l'application de la méthode intégrée.

**Comprendre la méthode intégrée comme un cadre** La méthode intégrée, telle qu'elle est décrite dans la section 6.1.1, est l'unification des trois méthodes différentes sur le squelette commun d'un algorithme de solution de type Newmark. Chacune des trois méthodes répond à une exigence spécifique qui a été identifié et qui est commandée par l'objectif global d'une solution transitoire rapide, précise et paramétrable d'une structure géométriquement non linéaire. Chacune des trois méthodes est un exemple de différentes méthodes communes qui traitent également de la même exigence identifié. La méthode qui est effectivement présente est choisie sur la seule base des résultats numériques. Cependant, toute autre méthode qui traite de la même exigence identifiée peut le remplacer dans la méthode intégrée.

Par conséquent, la méthode intégrée peut être vu comme une réalisation exemplaire d'un cadre intégré. Ce cadre permet de solutions transitoires rapides, précises et paramétrable d'une structure géométriquement non linéaire et nécessite les pièces suivantes

- un algorithme de solution qui fournit la structure globale de la méthode intégrée,
- une adaptation de l'algorithme de solution qui permet suivre de l'évolution non linéaire de la solution transitoire, assurant ainsi sa précision,
- une formulation autonome qui rend le modèle d'ordre réduit indépendant de la structure complète d'ordre élevé, assurant ainsi son calcul rapide, et,
- un procédé pour l'adaptation du modèle réduit à des paramètres extérieurs.

Différents membres de la famille algorithmes d'intégration dans le temps de type Newmark peuvent être utilisés comme l'épine dorsale de la méthode intégrée. Alors que les cas-tests académiques sont résolus avec le schéma non linéaire réduit Newmark dans sa représentation standard, les cas-tests construits avec des éléments finis non linéaires sont résolus avec la HHT- $\alpha$ -méthode. L'inclusion de la HHT- $\alpha$ -méthode était devenu nécessaire afin de stabiliser les solutions des cas-tests en éléments finis dès le début. Son application réussie démontre que les différents algorithmes d'intégration dans le temps de type Newmark peut servir comme l'épine dorsale de la méthode intégrée.

Sur les candidats de méthode présentés pour chacune de ces exigences, les choix sont faits sur la base de résultats numériques. Le comportement cohérent des cas-tests permet de transférer les résultats des cas-tests académiques et des cas-tests en éléments finis. Cela rend les choix spécifique pour le test-cas. Il ne garantit pas la solution réduite réussie d'un autre type de problèmes non linéaires.

Au-delà de la méthode intégrée, telle qu'elle est présentée tout au long de ce travail, permet de voir les résultats obtenus comme un cadre qui permet d'intégrer des méthodes différentes.

**Communications provenant de cette étude** Cette thèse représente la diffusion centrale des résultats. En outre, il existent plusieurs autres communications de différents types qui proviennent de travaux de recherche présentés. Ils sont énumérés ci-après.

Les résultats des études numériques de la performance et la robustesse des bases réduites sont publiés dans Lülff et al. [141] et présentés dans la contribution de la conférence Lülff et al. [140].

Les principes fondamentaux de la méthode intégrée, en particulier la formulation autonome, sont présentés dans Lülff et al. [142]. Une publication dans une revue sur ce sujet est en cours de préparation au moment de la finalisation de cette thèse.

L'auteur a participé à la conférence annuelle interne des doctorants de l'ONERA Journées des Doctorands trois fois au cours de ses travaux de recherche.

L'auteur a participé à un stage de recherche de quatre mois à l'*Institut fuer Wissenschaftliches Rechnen* sous la tutelle du Professeur G. Herrmann Matthies.

### **Analyse critique des principales décisions**

Les résultats obtenus et la méthode intégrée développée charnière sur au moins trois décisions majeures. Tout d'abord il s'agit de la décision d'utiliser la projection sur une base réduite comme l'approche de réduction. Une autre décision importante est la sélection des cas-tests académiques. L'impact de cette décision sur l'étude d'ensemble est seulement implicite à travers les résultats obtenus, mais néanmoins très important parce que les résultats obtenus conduisent les études suivantes. Une décision qui est déjà discutée et justifiée sur la base des résultats numériques est l'augmentation de la base réduite. Elle est examinée ici comme exemple d'une décision dans le but de démontrer le raisonnement qui y conduit.

Ces trois décisions sont examinées ci-dessous. Elles sont justifiées dans leurs chapitres respectifs sur la base des informations disponibles à ce moment. À la lumière des résultats globaux et la méthode intégrée deviennent disponibles leur justification doit être revue.

**La décision pour la réduction par projection sur une base réduite** La décision de créer la réduction autour de la projection sur une base réduite est le résultat d'un choix entre différentes approches dans la section 3.1. Les modes normaux non linéaires, la méthode de la balance harmonique tronquée et la décomposition généralisée propre (PGD) sont les autres possibilités majeures. Les modes normaux non linéaires sont rapidement rejetées au motif qu'ils sont plutôt un outil d'analyse qu'une approche de réduction à part entière dans leur propre droit. Aussi la méthode de la balance harmonique tronquée ne convient pas que le but de l'étude est une solution transitoire.

La décomposition généralisée propre est une nouvelle approche et de nombreuses recherches se passent sur l'échelle de temps de ce travail. La récente extension rapide de la PGD à des problèmes non linéaires et sa possibilité d'embrasser paramètres simplement comme des dimensions supplémentaires sont des solides arguments en sa faveur.

Cependant, il y a aussi des arguments forts en faveur de la projection sur une base réduite. Parmi les plus notables sont la grande quantité de méthodes supplémentaires disponibles avec une histoire plus ou moins long de la recherche et un haut degré de généralisation de cette approche de réduction. En outre, comme

indiqué dans la section 3.2.2.1, les algorithmes de solution existante et largement diffusé de type Newmark peuvent être continués à être utilisés en tant que piliers de la méthode intégrée. C'est un argument fort et assure une prolifération rapide de la méthode intégrée, parce que tous ses ingrédients sont également disponibles.

Il peut sembler trop non progressive de fonder la méthode intégrée sur la projection sur une base réduite au lieu d'embrasser le domaine émergent de la recherche et vivante de la PGD. Toutefois, il convient de souligner à nouveau que la réduction par la projection sur une base réduite a une longue histoire de recherche qui a produit des méthodes confirmées, par exemple, les nombreuses approches pour la création de bases réduites, et continue également d'offrir des méthodes hautement conduisant, comme par exemple la méthode de Petrov-Galerkin au moindres carrés. Ainsi, le potentiel de la réduction par projection sur une base réduite est certainement pas maximisé. Dans cette perspective, la projection et le PGD deviennent comparables.

En outre, toute l'étude, ce qui conduit finalement à la création de la méthode intégrée, est strictement orientée vers une application directe des méthodes utilisées et développées depuis le début. Dans cet esprit, il est naturel de privilégier un domaine de recherche déjà bien développé avec un énorme omniprésence dans les applications industrielles. Surtout celui-ci devrait stimuler la prolifération de la méthode intégrée.

**Choix des cas-tests académiques** Les cas-tests académiques sont choisis et définis dans la section 4.1.3. La motivation principale de leur choix est d'avoir un scénario commun pour tester les bases réduites. Cela implique la standardisation et l'adaptabilité des cas-tests et permet de fournir les variantes localement et entièrement non-linéaires. Une autre raison majeure pour le choix de ces cas-tests, c'est le fait qu'ils sont basés sur un exemple qui est fourni dans la littérature par AL-Shudeifat et al. [3] et éprouvée.

Avec le recul, ce choix s'avère très avantageux. Le comportement du système non linéaire est largement comparable aux cas-tests en éléments finis, en particulier celle des éléments de barre. Cela devient évident si les temps-histoires respectives sont comparés. La temps-histoire du cas-test académique entièrement non-linéaire est illustrée dans la figure 4.9 et la temps-histoire du cas-test en éléments finis non-linéaire finis avec des éléments de barres est illustré dans la figure 6.13.

Cette situation permet de réaliser des résultats supplémentaires et de les confirmer sur les deux types de cas de test.

**La décision d'augmenter la base réduite** La décision d'augmenter la base réduite en ajoutant les trois sauts est faite après une brève étude numérique dans la section 5.1.3.5. Cette étude est résolu avec la formulation de l'inflation des termes non linéaires et sur les systèmes académiques. Cette combinaison nie toute évaluation significative des performances de calcul et la décision est fondée sur les erreurs obtenues.

Avec l'introduction des et la décision en faveur des polynômes comme la formulation autonome des termes non linéaires ce choix devient discutable. Les trois vecteurs supplémentaires pourraient avoir des répercussions considérables sur le rendement des polynômes des termes non linéaires. Dans la section 5.2.2 il est démontré que le nombre requis d'opérations augmente proportionnellement avec la taille du système réduite. De ce point de vue de remplacer les trois vecteurs de poids faible de la base réduite avec les sauts pourrait être le meilleur choix en fonction de considérations de performance.

Dans le même temps l'argument est répété qu'uniquement trois vecteurs supplémentaires augmentent la base réduite mise à jour et offrent une diminution considérable de l'erreur. Pour le niveau local et les cas-tests académiques entièrement non linéaires cela est montré dans la section 5.1.3.6.2 et pour le cas-test en 'éléments finis avec des éléments barre ceci est montré dans la section 6.2.2.3. En outre, ajouter seulement trois vecteurs supplémentaires peut être considéré comme négligeable pour les applications réelles de modèles réduits et l'effort de calcul supplémentaire pour réellement résoudre le modèle réduit de l'ordre  $r + 3$  est éclipsé par l'effort numérique nécessaire pour identifier les tenseurs réduits.

## Perspectives pour des nouvelles orientations de recherche

Le travail accompli est une étude exhaustive qui unifie plusieurs méthodes disponibles et éprouvées avec des approches nouvellement formalisées, par exemple la mise à jour et de l'augmentation de la réduction des bases, dans le procédé intégré. En tant que tel, il s'agit d'un travail autonome.

Dans le contexte de la décision de fonder la définition de la méthode intégrée sur la réduction avec une base réduite, il serait d'intérêt le plus élevé de procéder à une comparaison de la méthode intégrée avec d'autres méthodes de réduction, en particulier la PGD. Cette comparaison doit prendre en compte les temps globaux de réduction pour les applications testées parce que la création des fonctions du noyau doit être pris en compte dans les efforts globaux visant à obtenir un modèle réduit.

Les solutions sont obtenues avec le schéma non-linéaire classique Newmark. Ceci est fait dans le but d'offrir des conditions optimales pour les méthodes intégrées. Cependant, l'utilisation de cette variante de cet algorithme de solution d'intégration en temps marche est pratiquement disparu dans les applications d'éléments finis actuels. Par conséquent, un axe majeur de la recherche qui peut à se matérialiser dans l'avenir est le choix d'une autre épine dorsale de la méthode intégrée. Remplacer l'algorithme classique non linéaire Newmark ou le HHT- $\alpha$ -méthode avec une procédure de solution de l'état l'art est lié à améliorer les performances de la méthode intégrée considérablement <sup>1</sup>.

Compte tenu de la grande variété de méthodes pour la création de la base réduite dans la section 3.3, il pourrait devenir possible dans une version future de la méthode intégrée de passer d'un algorithme de génération de la base réduite à un autre au cours de la mise à jour. Un scénario possible serait inclure l'initialisation de la solution transitoire réduite avec le LNM et la mise à jour et en augmentant cette base LNM plusieurs fois jusqu'à ce qu'un certain nombre de clichés caractéristique est obtenue. Ces clichés sont ensuite utilisées dans l'une des mises à jour suivantes pour produire une base POD qui remplace la base LNM.

Un point qui doit être fait en ce qui concerne les cas-tests est qu'ils sont constitués exclusivement de degrés de liberté en translation. Alors qu'ils sont bien décrits et caractérisés, ils ne représentent que ce type particulier de formulations non linéaires. De nombreuses méthodes qui sont utilisées lors de cette étude sont conçus à l'origine pour les cas de test avec des degrés de liberté de rotation, par exemple, des poutres ou des coquilles. Elles sont appliquées avec succès à des cas-tests avec des degrés de liberté de translation exclusivement. Toutefois, l'application de la méthode intégrée dans la direction opposée, sur des cas-tests qui contiennent également des degrés de liberté de rotation, n'a pas été démontré. Ceci doit être prouvé dans une étude dédiée.

Les trois méthodes qui répondent aux trois exigences identifiés sont choisis indépendamment dans ce travail. Chaque méthode qui est finalement choisi pour être utilisée dans la méthode intégrée est sélectionnée comme la meilleure selon certains critères parmi d'autres méthodes qui répondent aux mêmes exigences identifiées. Cependant, la combinaison de ces méthodes sélectionnées, la méthode intégrée, n'est pas forcément la meilleure combinaison pour le scénario donné. La question à savoir est, s'il ya une combinaison plus performante disponible et si d'autres méthodes doivent être intégrés afin d'améliorer les performances de la méthode intégrée encore plus loin. Il faut y répondre par la recherche future.

Enfin, ce travail fournit un cadre de base pour une méthode intégrée. Sur le terrain des cas-tests choisis, les critères retenus et des résultats obtenus la majorité des approches examinées pour les différentes exigences sont finalement rejetées. Ce ne sont pas des déterminations absolues. On s'attend à que chaque utilisateur du cadre d'adapter la méthode intégrée à son ou ses problèmes spécifiques en remplaçant l'une des méthodes utilisées par une méthode équivalente, selon la nature du problème, les outils et l'expérience disponibles.

---

<sup>1</sup>Un premier coup d'oeil tentative dans ce sens est faite dans l'annexe section A.3, où l'utilisation d'une matrice de rigidité tangente constant est explorée

**Résumé :**

Pour les solutions transitoires répétées des structures géométriquement nonlinéaires l'effort numérique présente souvent une contrainte importante. Ainsi, l'introduction d'un modèle d'ordre réduit, qui prend en compte les effets nonlinéaires et qui accélère considérablement les calculs, s'avère souvent nécessaire.

Ce travail aboutit à une méthode qui permet des solutions transitoires accélérée, fidèles et paramétrables, à travers d'un modèle réduit de la structure initiale. La structure est discrétisée et son équilibre dynamique décrit par une équation matricielle.

La projection sur une base réduite est introduite afin d'obtenir un modèle réduit. Une étude numérique complète sur plusieurs bases communes démontre que la simple introduction d'une base constante ne suffit pas pour prendre en compte le comportement nonlinéaire. Trois exigences sont déduites pour une solution transitoire accélérée, fidèle et paramétrable. L'algorithme de solution doit permettre un suivi de l'évolution nonlinéaire de la solution transitoire, la solution doit être autonome des termes nonlinéaires en éléments finis et la base doit être adaptée à des paramètres externes.

Trois approches sont mises en place, chacune répondant à une exigence. Elles sont assemblées dans la méthode intégrée. Les approches sont la mise-à-jour et augmentation de la base, la formulation polynomiale des termes nonlinéaires et l'interpolation de la base. Un algorithme de type Newmark forme le cadre de la méthode intégrée. L'application de la méthode intégrée sur des cas test en élément finis géométriquement nonlinéaires confirme qu'elle répond au but initial d'obtenir des solutions transitoires accélérée, fidèles et paramétrables.

**Mots clés :**

dynamique de structures, nonlinéarités géométriques, réduction du model, bases réduites, modes propres, décomposition orthogonal propre, mise-à-jour de la base réduite, paramètres

**Abstract :**

For repeated transient solutions of geometrically nonlinear structures the numerical effort often poses a major obstacle. Thus, the introduction of a reduced order model, which takes the nonlinear effects into account and accelerates the calculations considerably, is often necessary.

This work yields a method that allows for rapid, accurate and parameterisable solutions by means of a reduced model of the original structure. The structure is discretised and its dynamic equilibrium described by a matrix equation.

The projection on a reduced basis is introduced to obtain the reduced model. A comprehensive numerical study on several common reduced bases shows that the simple introduction of a constant basis is not sufficient to account for the nonlinear behaviour. Three requirements for an rapid, accurate and parameterisable solution are derived. The solution algorithm has to take into account the nonlinear evolution of the solution, the solution has to be independent of the nonlinear finite element terms and the basis has to be adapted to external parameters.

Three approaches are provided, each responding to one requirement. They are assembled to the integrated method. The approaches are the update and augmentation of the basis, the polynomial formulation of the nonlinear terms and the interpolation of the basis. A Newmark-type algorithm provides the frame of the integrated method. The application of the integrated method on test-cases with geometrically nonlinear finite elements confirms that this method leads to the initial aim of a rapid, accurate and parameterisable transient solution.

**Keywords :**

structural dynamics, geometric nonlinearities, model reduction, reduced bases, linear normal modes, proper orthogonal decomposition, basis update, parameters